# BRAIN NETWORKS IN AGING: REORGANIZATION AND MODULATION BY INTERVENTIONS

EDITED BY: Junfeng Sun and Chunbo Li
PUBLISHED IN: Frontiers in Aging Neuroscience

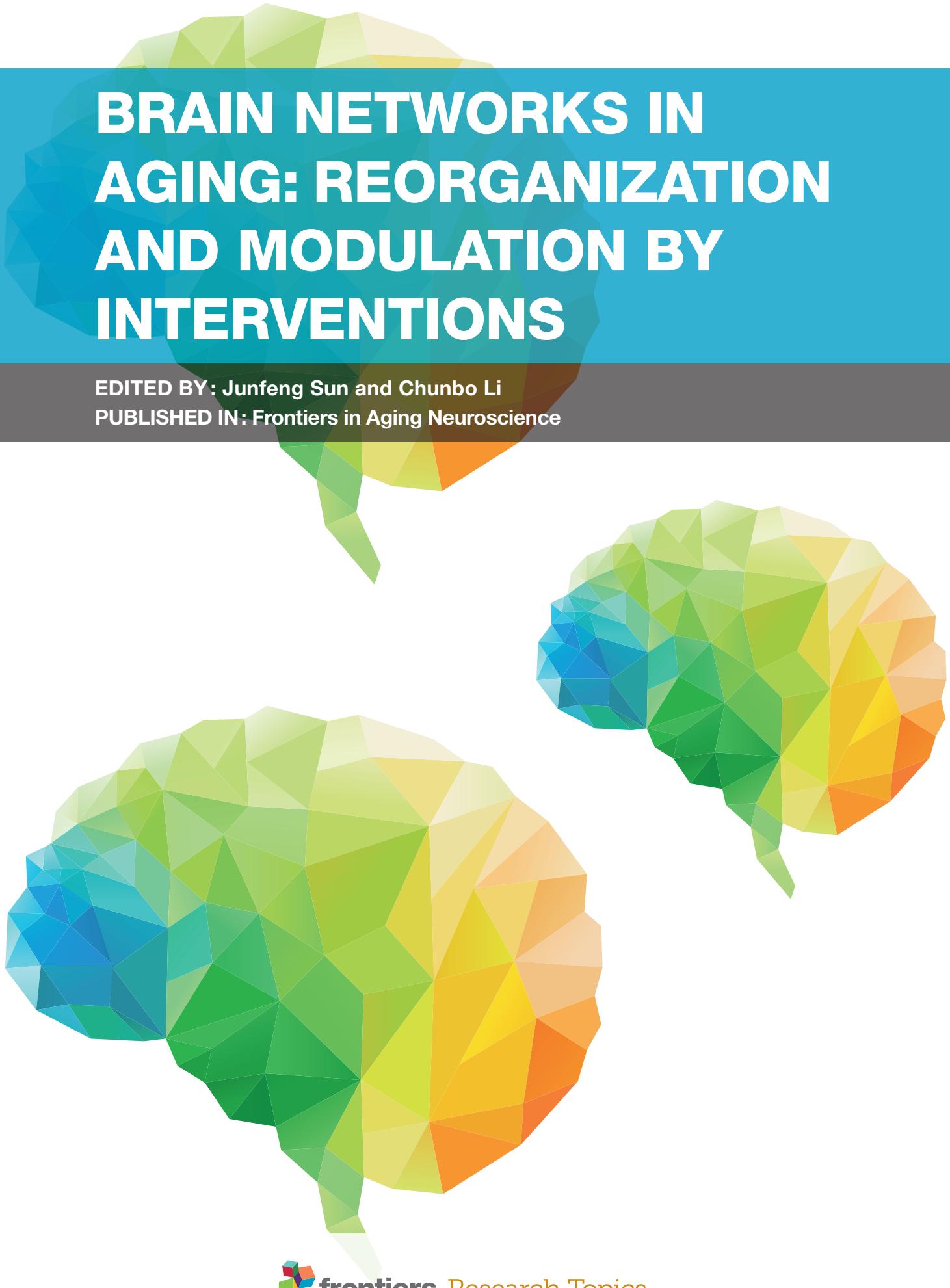

frontiers Research Topics

frontiers



**ISSN 1664-8714**
**ISBN 978-2-88945-416-7**
**DOI 10.3389/978-2-88945-416-7**

## About Frontiers

Frontiers is more than just an open-access publisher of scholarly articles: it is a pioneering approach to the world of academia, radically improving the way scholarly research is managed. The grand vision of Frontiers is a world where all people have an equal opportunity to seek, share and generate knowledge. Frontiers provides immediate and permanent online open access to all its publications, but this alone is not enough to realize our grand goals.

## Frontiers Journal Series

The Frontiers Journal Series is a multi-tier and interdisciplinary set of open-access, online journals, promising a paradigm shift from the current review, selection and dissemination processes in academic publishing. All Frontiers journals are driven by researchers for researchers; therefore, they constitute a service to the scholarly community. At the same time, the Frontiers Journal Series operates on a revolutionary invention, the tiered publishing system, initially addressing specific communities of scholars, and gradually climbing up to broader public understanding, thus serving the interests of the lay society, too.

## Dedication to Quality

Each Frontiers article is a landmark of the highest quality, thanks to genuinely collaborative interactions between authors and review editors, who include some of the world's best academicians. Research must be certified by peers before entering a stream of knowledge that may eventually reach the public - and shape society; therefore, Frontiers only applies the most rigorous and unbiased reviews.

Frontiers revolutionizes research publishing by freely delivering the most outstanding research, evaluated with no bias from both the academic and social point of view.

By applying the most advanced information technologies, Frontiers is catapulting scholarly publishing into a new generation.

## What are Frontiers Research Topics?

Frontiers Research Topics are very popular trademarks of the Frontiers Journals Series: they are collections of at least ten articles, all centered on a particular subject. With their unique mix of varied contributions from Original Research to Review Articles, Frontiers Research Topics unify the most influential researchers, the latest key findings and historical advances in a hot research area! Find out more on how to host your own Frontiers Research Topic or contribute to one as an author by contacting the Frontiers Editorial Office: **researchtopics@frontiersin.org**

# BRAIN NETWORKS IN AGING: REORGANIZATION AND MODULATION BY INTERVENTIONS

Topic Editors:
**Junfeng Sun,** Shanghai Jiao Tong University, China
**Chunbo Li,** Shanghai Mental Health Center, Shanghai Jiao Tong University School of Medicine, China

Old adults undertake reduced cognitive function in aging, accompanying brain reorganization in forms of brain activities, brain tissues, and both functional and structural brain networks. Compared with younger adults, the decreased brain activities in older adults are generally taken as a reflection of cognitive reduction, while the increased brain activities could be interpreted as compensation for reduced brain function or just dedifferentiation which refers to much less selective and less distinct activity in task-relevant brain regions for old adults. However, the interpretation of these brain reorganization is not easy. Actually, studies on only regional brain activities cannot fully elucidate the neural mechanisms of reduced cognitive abilities in aging, as multiple regions are generally integrated together to achieve advanced cognitive function in human brain. In recent years, brain connectivity/network, which targets how brain regions are integrated, have drawn increasing attention in neuroscience with the development of neuroimaging techniques and graph theoretical analysis. In addition to the understanding on the reorganization of brain networks, we also hope to find ways like cognitive training to retain or even enhance cognitive function of older adults. However, only few neuroimaging studies have examined the influence of interventions to old adult's brain activity, connectivity, and cognitive performance.

Focusing on the brain network in aging, this Research Topic mainly collected three set of studies. The first set of studies include six papers on the cognitive function of normal older subjects and mild cognitive impairment (MCI) patients in behavior and neural activities based on Electroencephalography (EEG). The second set of studies focus on the brain networks of MCI and Alzheimer's disease (AD) patients based on magnetic resonance imaging (MRI). The third set of studies are on the intervention effects to brain networks in aging. Several other papers on neuromodulation induced plasticity and the applications of sparse representation-based classification in cognitive impairment and other brain diseases have been enrolled to expand methods for exploring brain networks in aging. We wish these works would enrich our understanding of brain networks in aging and offer new insights for developing possible interventions to retain cognitive abilities in aging subjects.

**Citation:** Sun, J., Li, C., eds. (2018). Brain Networks in Aging: Reorganization and Modulation by Interventions. Lausanne: Frontiers Media. doi: 10.3389/978-2-88945-416-7

# Table of Contents

frontiers in Aging Neuroscience

EDITORIAL
published: 19 December 2017
doi: 10.3389/fnagi.2017.00425

# Editorial: Brain Networks in Aging: Reorganization and Modulation by Interventions

*Junfeng Sun*[1, 2*] *and Chunbo Li*[2, 3, 4*]

[1] School of Biomedical Engineering, Shanghai Jiao Tong University, Shanghai, China, [2] Brain Science and Technology Research Center, Shanghai Jiao Tong University, Shanghai, China, [3] Shanghai Key Laboratory of Psychotic Disorders, Shanghai Mental Health Center, Shanghai Jiao Tong University School of Medicine, Shanghai, China, [4] Center for Excellence in Brain Science and Intelligence Technology (CEBSIT), Chinese Academy of Sciences, Shanghai, China

**Keywords: brain network, aging, cognitive training, EEG, MRI**

## Editorial on the Research Topic

## Brain Networks in Aging: Reorganization and Modulation by Interventions

Older adults undertake reduction of cognitive function and brain reorganization in forms of regional brain activity, inter-region connectivity, and brain network topology in both function and structure during aging process. Various theories, such as compensation and dedifferentiation, have been proposed to explain the underlying mechanisms of these aging-related changes. As advanced cognitive function is generally achieved by the integration of multiple brain regions, brain network is used to characterize the integration and organization of brain regions that may be spatially far separated. Furthermore, interventions such as cognitive training and noninvasive neuromodulation have been demonstrated to be promising tools to maintain or even improve the cognitive function of older adults during specific aging states. Focusing on the brain network in aging, this Research Topic mainly collected three set of studies.

The first set of studies include six papers on the cognitive function of normal older subjects and mild cognitive impairment (MCI) patients in behavior and neural activities based on Electroencephalography (EEG). Hong et al. investigated the aging effects on brain networks during either response execution (Go) or response inhibition (NoGo) condition with graph theoretical analysis. Results showed that the functional brain networks of both young and old subjects had prominent but different small-world properties in Go and No-go tasks, and older adults showed stronger task-modulated effects on small-world properties than younger adults (Hong et al.). In another study, Hsieh et al. examined the older adults' inhibition strategies to irrelevant distraction and conflict distraction respectively in Go/NoGo tasks. Three studies investigated aging effects on attention. Kaufman et al. studied the aging effects on three attentional networks (alerting, orienting, and executive control) from both behavior performance and event-related potential (ERP), and showed that older adults had alerting deficits in attention compared with younger adults (Kaufman et al.). In another study based on an oddball task, Kaufman et al. demonstrated that older subjects had enhanced scalp signals during an early stage of visual processing, which correlated with neural activity in primary visual cortex as well as orbitofrontal cortex (Kaufman et al.). Furthermore, Li and Zhao examined the aging effects on inter-region functional connectivity during bottom-up and top-down attention. In addition, Li et al. showed that the amplitude of P2 and P300 of MCI patients were weaker than normal subjects during retrieval period, and the P2 amplitude in retrieval period was positively correlated to the scores of memory test and visual spatial examination (Li et al.).

The second set of studies focus on the brain networks of MCI and Alzheimer's disease (AD) patients based on magnetic resonance imaging (MRI). A bunch of studies have examined the

OPEN ACCESS

***Edited and reviewed by:***
*Hanting Zhang,*
*West Virginia University, United States*

***Correspondence:**
*Junfeng Sun*
*jfsun@sjtu.edu.cn*
*Chunbo Li*
*chunbo_li@163.com*

***Received:*** *04 May 2017*
***Accepted:*** *11 December 2017*
***Published:*** *19 December 2017*

***Citation:***
*Sun J and Li C (2017) Editorial: Brain Networks in Aging: Reorganization and Modulation by Interventions. Front. Aging Neurosci. 9:425. doi: 10.3389/fnagi.2017.00425*

alterations of resting-state functional connectivity (rsFC) of MCI and/or AD patients from normal controls. However, limited reproducibility has been shown across studies which may have different study protocols. Tam et al. analyzed four different resting state functional MRI (rs-fMRI) data together, and reported reduced rsFC within areas of the default mode network and cortico-striatal-thalamic loop in amnestic MCI (aMCI) compared to normal controls. In another study, Kim et al. investigated the network properties of subjects including normal controls, aMCI patients, and prodromal and intermediate stages of AD patients with rs-fMRI data, and demonstrated that an unexpected stage-specifically non-monotonic reorganization of brain networks in the progression to AD. Wei et al. proposed a classification framework based on support vector machine to identify MCI converters (patients that covert to AD) from the MCI non-converters, and demonstrated that short-term prediction (6 and 12 months) resulted in better performance than long-term prediction.

The third set of studies are on the intervention effects to brain networks in aging. Jiang et al. investigated the cognitive training effects on cortical thickness and cognitive function for normal older subjects received single-domain or multi-domain cognitive training of 24 sessions. They observed significant interaction effect between group and time in the cortical thickness of the left supramarginal and the left frontal pole cortical regions, and old subjects received more benefits from multi-domain cognitive training than single-domain cognitive training (Jiang et al.). Cao et al. reported maintained or increased functional connectivity within the default mode network, salience network, and central executive network in older subjects after multi-domain cognitive training. Furthermore, Luo et al. observed significant cognitive training effects on lateralization of brain activities: the lateralization of the left frontoparietal network was retained in the training group but decreased in the control group. These studies accumulate new evidence for developing possible interventions to retain cognitive abilities in aging subjects.

Moreover, discussions on neuromodulation induced plasticity to in older adults (Shpektor et al., Puri and Hinder), MicroRNAs in pathologies of Alzheimer's disease (AD) (Ye et al.), and brief introduction on the applications of sparse representation-based classification in cognitive impairment and other brain diseases (Wen et al.) have been enrolled in this research topic. We wish these works would expand the technologies and methods for exploring brain networks in aging.

In summary, this Research Topic gathered a group of studies mainly on brain networks in normal older subject as well as MCI and AD patients. Studies demonstrated that normal older adults undertook decay in response inhabitation, attention control, and memory, which were accompanied by altered ERP components or functional connectivity compared with younger adults. For MCI or AD patients, alteration of their brain networks compared to normal older controls were observed, and the alterations may serve as potential biomarker in predicting the conversion of MCI to AD. In addition, the three studies in the third set investigated the effects of cognitive training to normal older adults and provided new evidence for developing interventions to retain cognitive function of older adults in aging. All these studies would enrich our understanding of neural mechanisms underlying aging.

## AUTHOR CONTRIBUTIONS

JS drafted the manuscript, and CL revised the manuscript.

## ACKNOWLEDGMENTS

JS was supported by National Natural Science Foundation of China (No. 61673267) and Natural Science Foundation of Shanghai (No. 16ZR1446600), CL was supported by National Natural Science Foundation of China (No. 81371505, 30770769), the Science and Technology Commission of Shanghai Municipality, China (13dz2260500), and the SHSMU-ION Research Centre for Brain Disorders.

**Conflict of Interest Statement:** The authors declare that the research was conducted in the absence of any commercial or financial relationships that could be construed as a potential conflict of interest.

frontiers in Aging Neuroscience

ORIGINAL RESEARCH
published: 17 May 2016
doi: 10.3389/fnagi.2016.00100

# Age-Related Differences in the Modulation of Small-World Brain Networks during a Go/NoGo Task

*Xiangfei Hong[1,2], Yuelu Liu[3], Junfeng Sun[2] and Shanbao Tong[2]**

[1] Shanghai Key Laboratory of Psychotic Disorders, Shanghai Mental Health Center, Shanghai Jiao Tong University School of Medicine, Shanghai, China, [2] School of Biomedical Engineering, Shanghai Jiao Tong University, Shanghai, China, [3] Center for Mind and Brain, University of California, Davis, CA, USA

Although inter-regional phase synchrony of neural oscillations has been proposed as a plausible mechanism for response control, little is known about the possible effects due to normal aging. We recorded multi-channel electroencephalography (EEG) from healthy younger and older adults in a Go/NoGo task, and examined the aging effects on synchronous brain networks with graph theoretical analysis. We found that in both age groups, brain networks in theta, alpha or beta band for either response execution (Go) or response inhibition (NoGo) condition showed prominent small-world property. Furthermore, small-world property of brain networks showed significant differences between different task conditions. Further analyses of node degree suggested that frontal-central theta band phase synchrony was enhanced during response inhibition, whereas during response execution, increased phase synchrony was observed in beta band over central-parietal regions. More interestingly, these task-related modulations on brain networks were well preserved and even more robust in older adults compared with younger adults. Taken together, our findings not only suggest that response control involves synchronous brain networks in functionally-distinct frequency bands, but also indicate an increase in the recruitment of brain network resources due to normal aging.

**Keywords: aging, graph theory, induced activity, phase synchrony, response inhibition**

OPEN ACCESS

***Edited by:***
*Jean Mariani,*
*Université Pierre et Marie Curie, France*

***Reviewed by:***
*Tamer Demiralp,*
*Istanbul University, Turkey*
*Laura Lorenzo-López,*
*University of A Coruña, Spain*

****Correspondence:***
*Shanbao Tong*
*stong@sjtu.edu.cn*

***Received:*** *24 September 2015*
***Accepted:*** *18 April 2016*
***Published:*** *17 May 2016*

***Citation:***
*Hong X, Liu Y, Sun J and Tong S (2016) Age-Related Differences in the Modulation of Small-World Brain Networks during a Go/NoGo Task. Front. Aging Neurosci. 8:100. doi: 10.3389/fnagi.2016.00100*

## INTRODUCTION

Response inhibition, the ability to inhibit a prepotent tendency of behavioral response, is a core component of human cognitive control functions (Diamond, 2013). Previous electroencephalography (EEG) studies regularly focused on the event-related potentials (ERPs) evoked by Go and NoGo (or Stop) stimuli in Go/NoGo (or Stop-Signal) response control paradigm. Two ERP components, i.e., N2 and P3, were consistently identified in the ERP waves elicited by the NoGo (or Stop) stimuli compared with the Go stimuli, typically observed over frontal-central cortex after ∼200 ms and ∼300 ms post-stimulus onset, respectively. Such ERP components were usually interpreted as the neural markers of response inhibition (Falkenstein et al., 1999; Albert et al., 2013; Huster et al., 2013), and were also shown to be sensitive to normal aging (Hong et al., 2014).

Besides the analysis of ERP, frequency or time-frequency domain analysis on oscillatory EEG power during Go/NoGo tasks has also been reported in several studies. For example,

states or tasks that require an increased level of cognitive control, i.e., NoGo condition, always evoked higher power of theta oscillations during 200–600 ms post-stimulus period over the frontal-central scalp (Kirmizi-Alsan et al., 2006; Huster et al., 2013; Ergen et al., 2014). As a widely replicated finding, frontal theta activity was recently proposed to be a plausible mechanism for cognitive control functions (Cavanagh and Frank, 2014). While during movement execution tasks (Go condition), decreased power of alpha and beta oscillations over the sensorimotor areas was a common finding in the literature (Leocani et al., 1997; Pfurtscheller and Lopes da Silva, 1999).

Although ERP and frequency-domain analyses have been the dominating techniques in previous EEG research on Go/NoGo tasks, recent studies began to focus on the neural oscillations from the perspective of inter-regional phase synchrony in different frequency bands, and suggested an important role of large-scale neural synchrony in response inhibition (Serrien et al., 2005; Moore et al., 2008; Tallet et al., 2009; Brier et al., 2010; Muller and Anokhin, 2012; Anguera et al., 2013b; Cavanagh and Frank, 2014). For example, one recent study suggested that the effective inhibition of a prepotent response should be associated with an increase of the theta-band phase synchrony between the frontal and parietal cortices in a Go/NoGo task (Muller and Anokhin, 2012), and another study reported inhibition-specific changes in beta-band phase coherence between cerebral motor areas in a stop task (Tallet et al., 2009).

In spite of accumulating studies reporting the role of phase synchrony among healthy young adults, the influences of normal aging during an active inhibitory state have been scarce in the literature. Nonetheless, there have been phase synchrony studies that mainly focused on the pathological aging population, i.e., Alzheimer's disease, showing the reduced phase synchrony during either the resting state (Uhlhaas and Singer, 2006; Stam et al., 2007, 2009; Knyazeva et al., 2010) or task states such as working memory (Pijnenburg et al., 2004) compared with normal elders. More interestingly, a recent study showed an increase of frontal-posterior theta-band phase coherence in healthy older adults following cognitive training that resulted in performance benefits (Anguera et al., 2013a). However, although such findings consistently implied a close relationship between cognitive control and neural synchrony during cognitive aging, a comprehensive and direct comparison of neural synchrony between healthy young and old adults from the perspective of large-scale neural synchrony is still lacking.

We inferred that there might be different possibilities on the results. On one hand, inspired by previous findings that the decline in cognitive ability was always accompanied with reduced neural synchrony during pathological aging (Uhlhaas and Singer, 2006), one may infer that the cognitive decline during normal aging would implicate a reduction in the ability to modulate neural synchrony for older adults compared with younger adults. Yet alternatively, from the perspective of compensatory mechanisms of cognitive aging, older adults might recruit additional brain activation to partially compensate the cognitive decline (Cabeza et al., 2002; Rajah and D'Esposito, 2005; Park and Reuter-Lorenz, 2009; Grady, 2012), which would lead to the enhancement of the neural synchrony in older adults. Nonetheless, in either case, investigating the effects of normal aging on neural synchrony during a cognitive control tasks would provide valuable insights for understanding the age-related changes in neural mechanisms of cognitive control functions.

In this study, we aimed to study the influence of normal aging on neural synchrony during response control. To this end, we recorded multi-channel EEG from healthy younger and older adults in a Go/NoGo response control task. Frequency-domain analysis was performed to examine task-related modulations on oscillatory EEG power, which could provide useful information for the comparison with existing literature. After that, functional brain networks were constructed based on phase synchrony analysis (Sun et al., 2012). Graph theory was then used to analyze the topological organizations of oscillatory brain networks during Go and NoGo conditions (Bullmore and Sporns, 2009; Rubinov and Sporns, 2010). We expected to observe the task-related modulations on brain networks between response execution (Go) and response inhibition (NoGo) conditions in functionally-distinct frequency bands, i.e., theta, alpha and beta bands (Tallet et al., 2009; Brier et al., 2010; Muller and Anokhin, 2012; Anguera et al., 2013b). Furthermore, we compared the task-modulated brain networks between younger and older adults to investigate age-related differences in neural synchrony during response inhibition and execution.

# MATERIALS AND METHODS

## Participants

We recruited 23 healthy younger (mean ± standard deviation; age: 21.4 ± 2 years; range: 18–25 years; 7 females; all right-handed) and 18 healthy older adults (mean ± standard deviation; age: 61 ± 6 years; range: 50–70 years; 11 females; all right-handed) as participants. All participants reported normal or corrected-to-normal vision, without a history of neurological or psychiatric disorders. All older participants went through the Mini-Mental Status Examination (mean score: 28/30; range: ≥26; Folstein et al., 1975) with normal cognition. A minimum of 9 years of school education was required for each participant. All participants gave their written informed consents before the experiment, and were financially compensated for the experiment regardless of their performance. The experimental protocols were approved by the institutional Ethical Committee of Shanghai Jiao Tong University, complying with the Declaration of Helsinki.

## Stimuli and Procedures

A modified visual Go/NoGo task was adopted in this study. Before each trial, a black central crosshair (1.38° by 1.38°) and two lateral black location markers (2.39° by 2.39°, located 9.05° from the vertical meridian, and 7.2° below the horizontal meridian) were constantly presented on a white background. Participants were instructed to always maintain

fixation on the crosshair whenever it was displayed. Each trial began with a 200 ms central black arrow cue pointing to either the left (50%) or the right (50%). Subjects were required to covertly attend the left or the right location according to the cue and ignore the other location. The target stimulus (1.67° by 1.67°), either a plus sign (50%) or the letter "x" (50%), was presented for 200 ms inside either the left (50%) or the right (50%) location marker after a random cue-target interval (CTI: jittered between 1000–1200 ms). Subjects were required to respond only to the plus sign presented in the attended location (Go trials) as quickly and accurately as possible with the right index finger, and refrain from responding to the letter "x" presented in the attended location marker (NoGo trials). Targets presented in the unattended location marker were to be ignored completely. A fixed inter-trial interval of 2600 ms was presented between the target offset and the cue onset of the next trial. For the Go trials, responses within 1600 ms after the target offset were recorded as valid trials.

Participants were comfortably seated in a sound attenuated room during the experiment. All stimuli were presented on a 19 inch LCD display (Dell: P190SB) placed 60 cm in front of the participant. The experimental paradigm was implemented in E-Prime (Version: 2.0, Psychology Software Tools, Inc., Sharpsburg, PA, USA), and behavioral responses were recorded with the Serial Response Box$^{TM}$ included in the E-Prime toolkit. Each block consisted of 60 trials lasting for about 5 min. To minimize subject fatigue, a short (2–3 min) break was included between two successive blocks. All subjects went through a training block to get familiar with the experimental procedures. After the training, all younger subjects completed eight blocks of formal experiment trials and older subjects completed six blocks, considering the fact that the elders are more likely to develop mental fatigue that could affect the brain activity (Sun et al., 2014). To eliminate potential differences due to unequal trial numbers in the two groups, further EEG analyses only included data from the first six blocks in the younger group.

## EEG Recording and Preprocessing

Continuous EEG signals were recorded from 32 scalp electrodes (30 recording channels: Fp1, Fp2, F3, F4, F7, F8, Fz, FC1, FC2, FC5, FC6, C3, C4, Cz, T7, T8, CP1, CP2, CP5, CP6, P3, P4, P7, P8, 171 Pz, O1, O2, Oz, TP9, TP10; recording reference: FCz; ground: AFz) using the BrainAmp MR Plus amplifier and EasyCap$^{TM}$ (Brain Products GmbH, Gilching, Germany). Two additional electrodes were placed on the outer left canthus and above the right eye to record horizontal electrooculogram (HEOG) and vertical electrooculogram (VEOG), respectively. EEG signals were amplified and sampled at 1000 Hz with 0.016–100 Hz online band-pass filtering. Impedance of each electrode was maintained below 10 kΩ during the recording.

EEG preprocessing was performed in the Matlab-based (MathWorks, MA, USA) EEGLAB (Delorme and Makeig, 2004) and ERPLAB toolboxes (Lopez-Calderon and Luck, 2014). Raw continuous EEG data first went through a two-way, zero phase shift, Butterworth filter (band-pass: 0.1–40 Hz; roll-off slope: 12 dB/oct), followed by a Parks McClellan notch filter to eliminate remaining noise at 50 Hz. Independent component analysis was performed to remove the ocular artifacts (Jung et al., 2000). Continuous EEG data were then re-referenced to the average of bilateral mastoid electrodes (TP9 and TP10), and segmented into epochs from −200 to 800 ms referring to the target onsets. Epochs with physical artifact in any EEG channel were marked as bad epochs according to the following criteria: (1) the maximal absolute value of voltage difference within a moving window (width: 200 ms; step: 50 ms) exceeding 150 μV; and (2) the maximal absolute value of voltage at any time point exceeding 100 μV. Furthermore, EEG epochs with overt eye movements or blinks that might prevent subjects from recognizing the targets were marked as bad epochs according to the following criteria: (1) the maximal absolute value of voltage difference in the HEOG channel within a moving window (width: 400 ms; step: 10 ms) exceeding 40 μV; and (2) the maximal absolute value of voltage difference in the VEOG channel at any time point around the target (−200 to 200 ms post-stimulus) exceeding 50 μV. After that, all EEG epochs were further visually inspected and all bad epochs were excluded in subsequent analyses.

In this study, the 200–700 ms post-stimulus period was chosen for the following analysis of EEG spectral power and phase synchrony, considering that: (1) our previous study has shown that this window covers the processes related to response inhibition, as suggested by the ERP components (N2 and P3) observed during this window (Hong et al., 2014); (2) from the computational perspective, our previous research based on surrogate tests has shown that an epoch of 500 ms yields optimal results for phase synchrony analysis in EEG theta, alpha and beta bands (Sun et al., 2012). For the sake of comparison, the last 500 ms of inter-trial interval (−500 to 0 pre-cue) was selected as the Baseline condition, which was included in the following analysis as reference.

It has been widely agreed that the event-related EEG includes both evoked and induced activities (Pfurtscheller and Lopes da Silva, 1999; Bastiaansen and Hagoort, 2003). The evoked activity, directly driven by the stimulus and both time- and phase-locked to it, can be extracted from the ongoing EEG by a straightforward averaging of EEG epochs, resulting in the ERP. The induced activity, on the other hand, is largely rhythmic (oscillatory) in nature, refers to oscillations caused or modulated by stimuli or state changes that do not directly drive the rhythm, so that they are time-locked, but not necessarily phase-locked, to the eliciting event. Moreover, previous studies have suggested to remove evoked activity when analyzing induced activity (Dietl et al., 1999; Doppelmayr et al., 2000; Gruber et al., 2002; Deiber et al., 2009). In this study, we are only interested in induced activity, because evoked activity (ERP, N2 and P3 components) has been analyzed and reported in our previous study (Hong et al., 2014). Therefore, ERP activity from each task condition (Go, NoGo) was subtracted from EEG epochs of the same condition for each subject to eliminate the contributions from evoked activity before subsequent analyses of

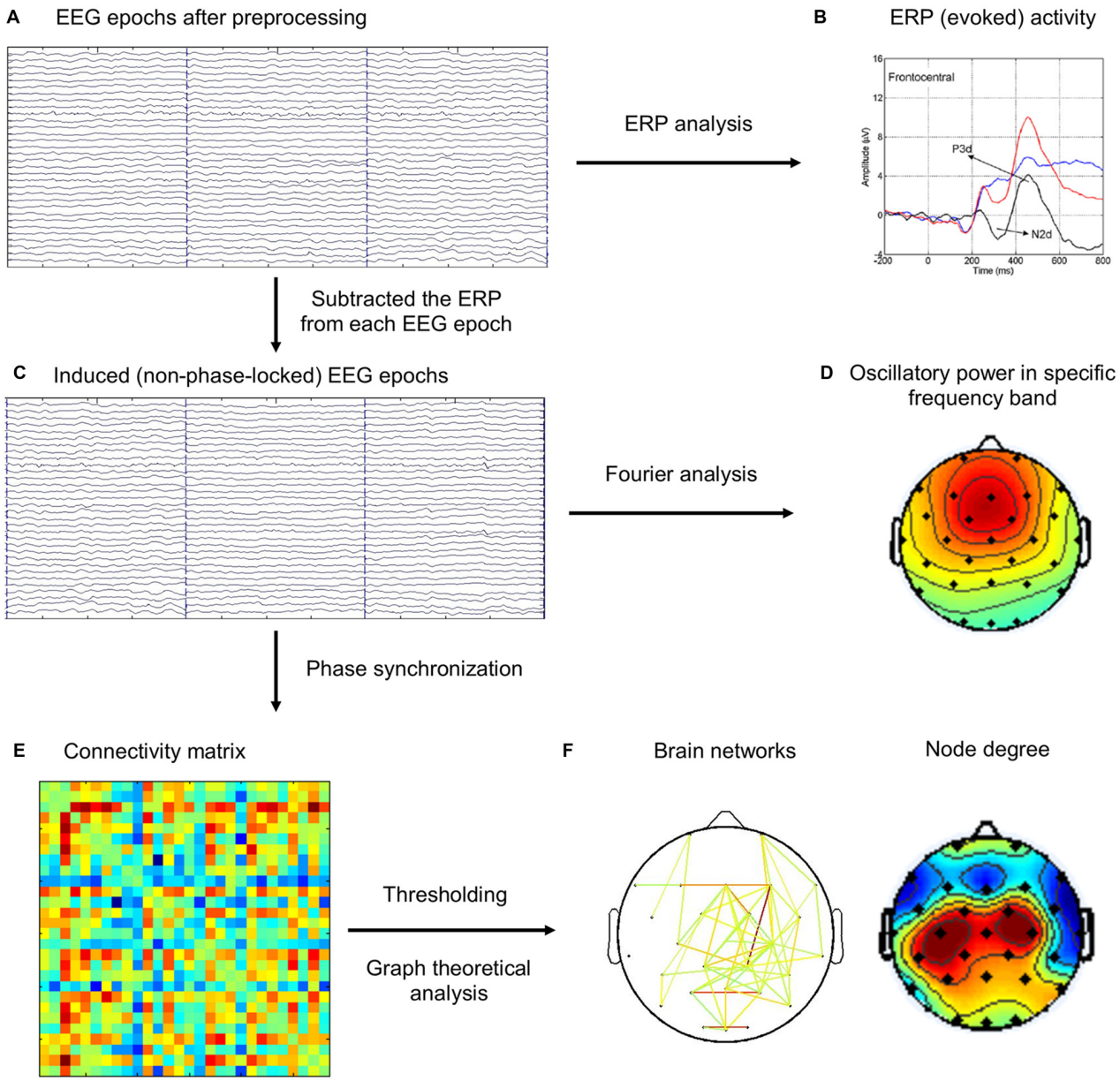


**FIGURE 1 | The schematic diagram for the brain network analysis. (A)** Electroencephalography (EEG) epochs after preprocessing steps. **(B)** The event-related potentials (ERPs) were computed by averaging the same type of EEG epochs (Go, NoGo), which was reported in our previous study (Hong et al., 2014). **(C)** ERP activity was subtracted from EEG epochs. **(D)** Frequency-domain analysis of oscillatory power using Fourier analysis. **(E)** Phase synchronization (PS) index was computed for each pair of channels in each trial, and the connectivity matrix was averaged across the same type of EEG epochs (Baseline, Go, NoGo). **(F)** Different thresholds were applied on the connectivity matrix to construct brain networks, which were then analyzed using graph theoretical metrics.

induced activity. The flowchart of EEG analysis was illustrated in **Figure 1**.

## EEG Spectral Power Analysis

To analyze the modulation of EEG band power during the Go/NoGo task, we computed fast Fourier transform for the 200–700 ms post-stimulus period with Hamming window for each electrode, and then averaged the spectra across all trials of the same experimental condition (Baseline, NoGo, Go). To eliminate the inter-subject variance, task-related power change was computed as the percentage change of spectral power between different task conditions (Hong et al., 2013).

## Phase Synchronization Analysis

Phase synchronization (PS) has been successfully used to analyze rhythmic synchrony in oscillatory neural signals (Sun et al., 2012; Hong et al., 2013; Yan et al., 2013). The strength of phase

synchrony can be quantified by PS index (PSI), which is based on the instantaneous phase (IP) of oscillations. For an epoch of real-value narrow-band EEG signal $s(t)$, its IP can be defined as:

$$\phi(t) = \arg[z(t)] = arctan\frac{\tilde{s}(t)}{s(t)} \quad (1)$$

where,

$$z(t) = s(t) + j\tilde{s}(t) \quad (2)$$

is the analytic signal of $s(t)$, and

$$\tilde{s}(t) = \frac{1}{\pi}\text{P.V.}\int_{-\infty}^{\infty}\frac{s(\tau)}{t-\tau}\text{d}\tau \quad (3)$$

is the Hilbert transform of $s(t)$ (P.V. denotes that the integral is taken in the sense of Cauchy principal value). Let $\phi_1(t)$ and $\phi_2(t)$ denote the IPs of two narrow-band EEG waves from two EEG channels during the same period. If the IP difference, i.e., $|m\phi_1(t) - n\phi_2(t)|$, is bounded by a constant, this pair of EEG waves are deemed to be in $m$:$n$ PS, where $m$ and $n$ are positive integers (Tass et al., 1998; Wacker and Witte, 2011). In this study, we followed the approach adopted in recent studies of phase synchrony and only focused on the 1:1 PS (Sun et al., 2012; Hong et al., 2013; Yan et al., 2013). In this case, the PSI ($\rho$) can be quantified as the mean phase coherence of the IP difference, i.e.,

$$\rho = \sqrt{\langle\cos[\phi_1(t) - \phi_2(t)]\rangle_t^2 + \langle\sin[\phi_1(t) - \phi_2(t)]\rangle_t^2} \quad (4)$$

where $\langle\cdot\rangle_t$ denotes the average over time. The value of PSI ($\rho$) is in the range of [0 1], with $\rho = 0$ indicating no PS at all and $\rho = 1$ indicating perfect PS.

In this study, the PS analysis for each EEG epoch was performed as follows: (1) filtering the EEG epochs into different frequency bands (theta: 4–8 Hz; alpha: 8–13 Hz; beta: 13–30 Hz); (2) computing the IP of the sub-band EEG signals according to Eq (1) for each epoch; (3) computing the PSI between each pair of electrodes using Eq (4); and (4) assigning the PSIs into an association matrix (28 × 28 in this study), with element in the $i^{th}$ row and $j^{th}$ column, $\rho_{ij}$, representing the PSI between channel $i$ and channel $j$. Finally, we averaged PSI matrices from all epochs under the same experimental conditions (Baseline, Go, NoGo) for each subject and obtained three PSI matrices (Baseline, Go, NoGo) in each frequency band for each subject.

## Graph Theoretical Analysis

In graph theoretical analysis, each channel is defined as a node, and the connectivity strength between two nodes is designated as the edge that connects them. The association matrix ($\{\rho_{ij}\}$) was converted into a weighted graph ($\{w_{ij}\}$) by applying a threshold ($T$) to eliminate those weak and spurious connections, i.e.,

$$w_{ij} = \begin{cases} \rho_{ij}, & \text{if} \geq T \\ 0, & \text{otherwise.} \end{cases} \quad (5)$$

where $w_{ij}$ denotes the connectivity strength between node $i$ and node $j$. The threshold value $T$ was determined via a commonly used approach which explores the brain graph as a function of the changing threshold (Bullmore and Bassett, 2011; Hong et al., 2013; Yan et al., 2013). Previous studies have shown that the efficient organization of brain networks is typically observed in relatively sparse networks with network densities (the ratio between the existing edge number and maximal possible edge number) being less than 0.5, and that the maximal cost-efficiency of brain networks are typically reached at a network density of around 0.3 (Achard and Bullmore, 2007; Bassett et al., 2009; Bullmore and Bassett, 2011; Bullmore and Sporns, 2012; Jin et al., 2012). Therefore, in this study, we constructed connectivity graphs under a series of edge numbers ($K$) ranging from 60–180 with a step of 20. Specifically, for a given edge number $K$, the threshold ($T$) was assigned as the $K^{th}$ largest value among all PSIs. The corresponding network density hence ranged approximately from 0.16 to 0.48.

The degree of a node, defined as the total connectivity strength of the corresponding node, was used to describe the importance of that node in the graph. Nodes with high degrees are regarded as hubs and are likely to play an important role in network communications (Bullmore and Sporns, 2009; Bullmore and Bassett, 2011). For weighted networks, the degree of node $i$ ($D_i$) is quantified as:

$$D_i = \sum_{j\in N} w_{ij} \quad (6)$$

where $N$ denotes the set of all nodes in the network.

Recent research has shown that brain networks typically exhibit the so-called "small-world" property, which is thought to reflect an efficient organization with an optimal compromise between local segregation and global integration (Bassett et al., 2006; Achard and Bullmore, 2007; Jin et al., 2012). In this study, we will compare the small-world property of functional brain networks between young and old adults within different frequency bands to explore age-related reorganizations during the response inhibition task. Generally, small-world networks are characterized as networks with significantly greater local segregation but approximately the same level of global integration compared with random networks (Watts and Strogatz, 1998; Rubinov and Sporns, 2010; Bullmore and Sporns, 2012). Clustering coefficient is a measure indicating the level of local segregation of a network (Rubinov and Sporns, 2010). For a weighted network, the clustering coefficient is defined as the average clustering coefficient between all nodes in the network (Onnela et al., 2005),

$$C = \frac{1}{n}\sum_{i\in N} C_i = \frac{1}{n}\sum_{i\in N}\left[\frac{1}{D_i(D_i-1)}\sum_{j,h\in N}\left(w_{ij}w_{ih}w_{jh}\right)^{1/3}\right] \quad (7)$$

where $n$ is number of nodes in the graph and $D_i$ is the degree for node $i$ as defined in Eq (6) Characteristic path length, on the

other hand, describes the level of global integration of a network (Rubinov and Sporns, 2010). It is defined as the average shortest path length between all pairs of nodes (Latora and Marchiori, 2001),

$$L = \frac{1}{\frac{1}{n(n-1)} \sum_{i \neq j \in N} \frac{1}{d_{ij}}} \quad (8)$$

where $d_{ij}$ denotes the shortest path length between node $i$ and node $j$.

To examine the small-world property of functional brain networks, the clustering coefficient and characteristic path length were compared with those from 20 size-matched random networks generated from randomly rewiring the original brain networks (Maslov and Sneppen, 2002). This procedure yielded the normalized clustering coefficient $\gamma = C/C_{\text{rand}}$ and characteristic path length $\lambda = L/L_{\text{rand}}$, where $C_{\text{rand}}$ and $L_{\text{rand}}$ denote the average clustering coefficient and characteristic path length of the 20 random networks, respectively. The small-world property can then be quantified by the small-worldness index (Humphries and Gurney, 2008),

$$\sigma = \frac{\gamma}{\lambda} \quad (9)$$

For a typical small-world network, $\sigma$ is greater than 1 ($\gamma > 1$, $\lambda \approx 1$). Note that the graph theoretical analysis was performed in Matlab with Brain Connectivity Toolbox (Rubinov and Sporns, 2010).

## Statistical Analysis

For the analysis of $C$ and $L$, we used the normalized values, i.e., $\gamma$ and $\lambda$, to eliminate possible influences from connectivity strength (Rubinov et al., 2009), and performed the statistical analysis under different network density levels. It should be noted that: (1) the purpose of constructing brain graphs under a series of network density levels was to cover the *real* network density level that has been suggested to be located in the pre-defined range as much as possible; (2) the brain graphs under different network density levels are far from independent graphs, and thus the correction for multiple comparisons, i.e., Bonferroni correction, is not appropriate here (Stam et al., 2007; Rubinov et al., 2009; Jin et al., 2012; Hong et al., 2013; Li et al., 2015). Instead of the correction for $p$-values, in this study, we did not treat the results as significant unless the $p < 0.05$ significance level was observed under at least 3 (out of 7) different network density levels. For the statistical analysis of node degree, we chose a specific threshold around the median edge density of 0.3 (120 edges; network density: 120/378 = 0.3175) that is typically regarded as the most economical network density level (Achard and Bullmore, 2007; Bassett et al., 2009; Bullmore and Bassett, 2011). Statistical significance of network measures were assessed by the repeated-measures analysis of variance (ANOVA), independent-samples $t$-test and paired-samples $t$-test (two-tailed). Statistical analysis was performed in SPSS 16.0.

# RESULTS

## Behavioral Performance

The behavioral results have been reported elsewhere (Hong et al., 2014). Briefly, the overall accuracy including both Go and NoGo trials was marginally higher for younger adults compared with older adults (younger: 99.52% ± 0.08% vs. older: 98.91% ± 0.31%; $t_{(18.027)} = 1.893$, $p = 0.074$). Older adults responded more slowly to Go targets than younger adults (younger: 477.56 ± 10.74 ms vs. older: 556.49 ± 28.46 ms; $t_{(20.582)} = -2.595$, $p = 0.017$). Furthermore, the analysis of false alarm rate (FAR) to NoGo-targets at the attended location showed no significant differences between the two groups (younger: 0.52% ± 0.13% vs. older: 1.17% ± 0.50%; $t_{(18.115)} = -1.250$, $p > 0.2$). Taken together, behavioral results suggested that although the response was slower due to aging, both younger and older adults showed satisfactory and comparable inhibitory performances in the Go/NoGo task.

## EEG Spectral Power Modulation

As shown in **Figure 2**, both younger and older adults showed increased frontal-central theta power during NoGo condition than Baseline condition and Go condition. In alpha and beta band, there were power decreases over central-parietal areas during Go condition than Baseline condition and NoGo condition, and such decreases were stronger in the older group than the younger group. Overall, our results replicated previous studies on EEG band power modulation during Go/NoGo tasks (Leocani et al., 1997; Pfurtscheller and Lopes da Silva, 1999; Kirmizi-Alsan et al., 2006; Huster et al., 2013; Cavanagh and Frank, 2014; Ergen et al., 2014).

## Brain Network Results

### Small-World Property

The normalized clustering coefficient ($\gamma$), characteristic path length ($\lambda$) and small-worldness index ($\sigma$) for younger and older adults within the theta, alpha and beta frequency bands are illustrated in **Figure 3**. Statistical significance was tested by two-way repeated-measures ANOVA with Task (Baseline, Go and NoGo) as a within-group factor and Age (younger, older) as a between-group factor. The statistical results for $\gamma$, $\lambda$ and $\sigma$ are included in **Tables 1–3**, respectively. The major findings include:

1. Theta band: Main effect of Task was observed for $\gamma$ ($p < 0.05$ under all 7 network density levels), $\lambda$ ($p < 0.05$ under 3 network density levels) and $\sigma$ ($p < 0.05$ under all 7 network density levels). Follow-up analysis suggested that both age groups showed larger $\gamma$ ($p < 0.05$ under all 7 network density levels), smaller $\lambda$ ($p < 0.05$ under 5 network density levels) and larger $\sigma$ ($p < 0.05$ under all 7 network density levels) during Go condition than NoGo condition. Furthermore, the difference in $\sigma$ between Go condition and NoGo condition was larger in older adults than that in younger adults, as indicated by significant interaction between

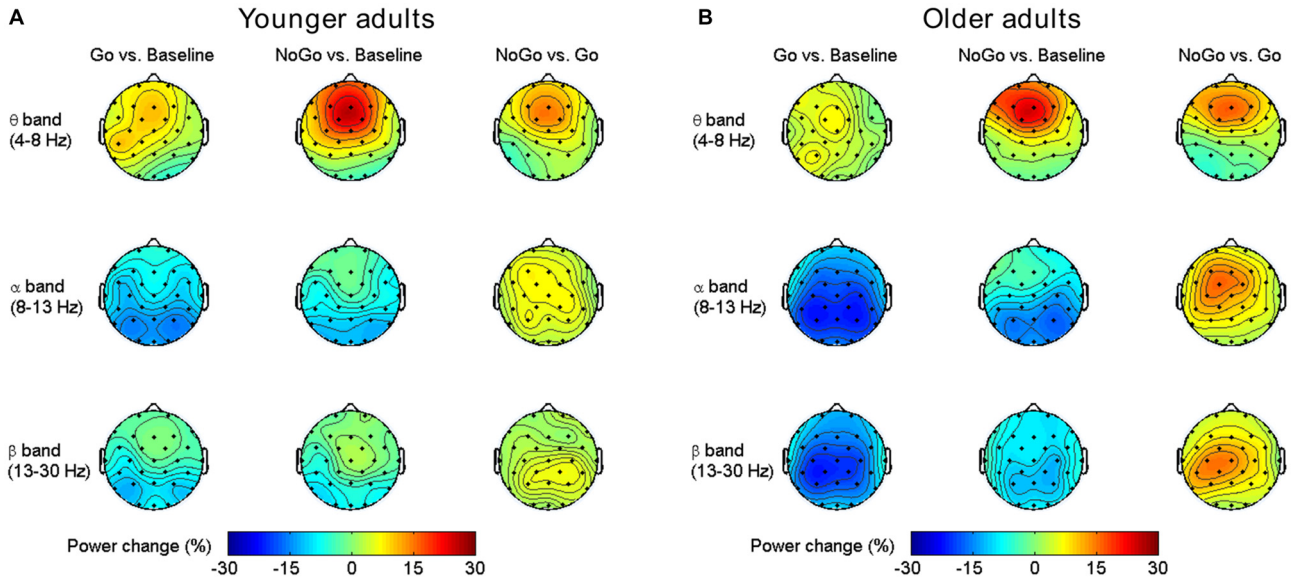


**FIGURE 2 | Group-averaged task-related oscillatory power changes in different frequency bands for the younger group (A) and older group (B).**

Task (Go, NoGo) and Age (younger, older; $p < 0.05$ under 4 network density levels). In addition, older adults showed larger $\gamma$ and $\sigma$ than younger adults during both Go and NoGo conditions ($p < 0.05$ under all 7 network density levels).

2. Alpha band: Main effect of Task was observed for $\gamma$ ($p < 0.05$ under all 7 network density levels) and $\sigma$ ($p < 0.05$ under all 7 network density levels). Follow-up analysis suggested that both age groups showed smaller $\gamma$ ($p < 0.05$ under 4 network density levels) and $\sigma$ ($p < 0.05$ under 3 network density levels) during Go condition than NoGo condition. However, there were no stable main effects or interactions related to Age under different network density levels in the alpha band.
3. Beta band: Main effect of Task was observed for $\gamma$ ($p < 0.05$ under all 7 network density levels) and $\sigma$ ($p < 0.05$ under all 7 network density levels). Follow-up analysis suggested that both age groups showed smaller $\gamma$ ($p < 0.05$ under all 7 network density levels) and smaller $\sigma$ (significant under 6 network density levels) during Go than NoGo condition. Furthermore, older adults showed smaller $\lambda$ than younger adults during both Go and NoGo conditions ($p < 0.05$ under all 7 network density levels).

In summary, both younger and older adults showed stable task-related modulations of functional brain networks in theta, alpha and beta bands during the Go/NoGo task. Furthermore, age-related differences were observed in both theta and beta band brain networks. Older adults showed stronger task-related modulations of theta band brain networks than younger adults. In alpha band, however, no stable age-related differences were observed between the two age groups.

## Node Degree Distribution

The differences in node degree between different task conditions (Baseline, Go, NoGo) were tested by paired-samples $t$-test in each age group separately. The statistical $t$-maps under the edge number of 120 (31.75% network density) are presented in **Figure 4**. Consistent with the small-world property, task-related modulations on node degree could also be clearly observed in theta, alpha and beta bands. In theta band, the frontal-central nodes showed an increase of degree during NoGo condition than Go condition. In beta band, higher node degree was observed during Go condition than NoGo condition among the central-parietal nodes. While in alpha band, such difference between Go condition and NoGo condition was much smaller than that in theta and beta bands.

To quantitatively analyze the task- and age-related effects on node degree in theta and beta band brain networks, we defined two regions of interest (ROIs) based on the $t$-maps in **Figure 4**: (1) the frontal-central ROI (channels Fp1, Fp2, F3, F4, C3, C4, F7, F8, Fz, Cz, FC1, FC2, FC5, FC6); and (2) the central-parietal ROI (channels C3, C4, P3, P4, Cz, Pz, CP1, CP2, CP5, CP6). The node degree within each ROI was averaged in theta and beta bands, respectively. The ROI-averaged node degree was then subject to a three-way ANOVA with Task (Baseline, Go, NoGo) as a within-group factor and Age (younger, older) as a between-group factor (**Figure 5A**). In theta band, we observed a main effect of Task ($F_{(2,76)} = 9.736$, $p < 0.001$) on frontal-central node degree. Follow-up analysis suggested that for younger adults, the task-modulated effects on frontal-central node degree were marginally significant (Go vs. NoGo: $t_{(22)} = -2.004$, $p = 0.058$). For the older adults, in contrast, such task-modulated effects were highly significant (Go vs. Baseline: $t_{(16)} = -2.725$, $p = 0.015$; Go vs. NoGo: $t_{(16)} = -5.174$,

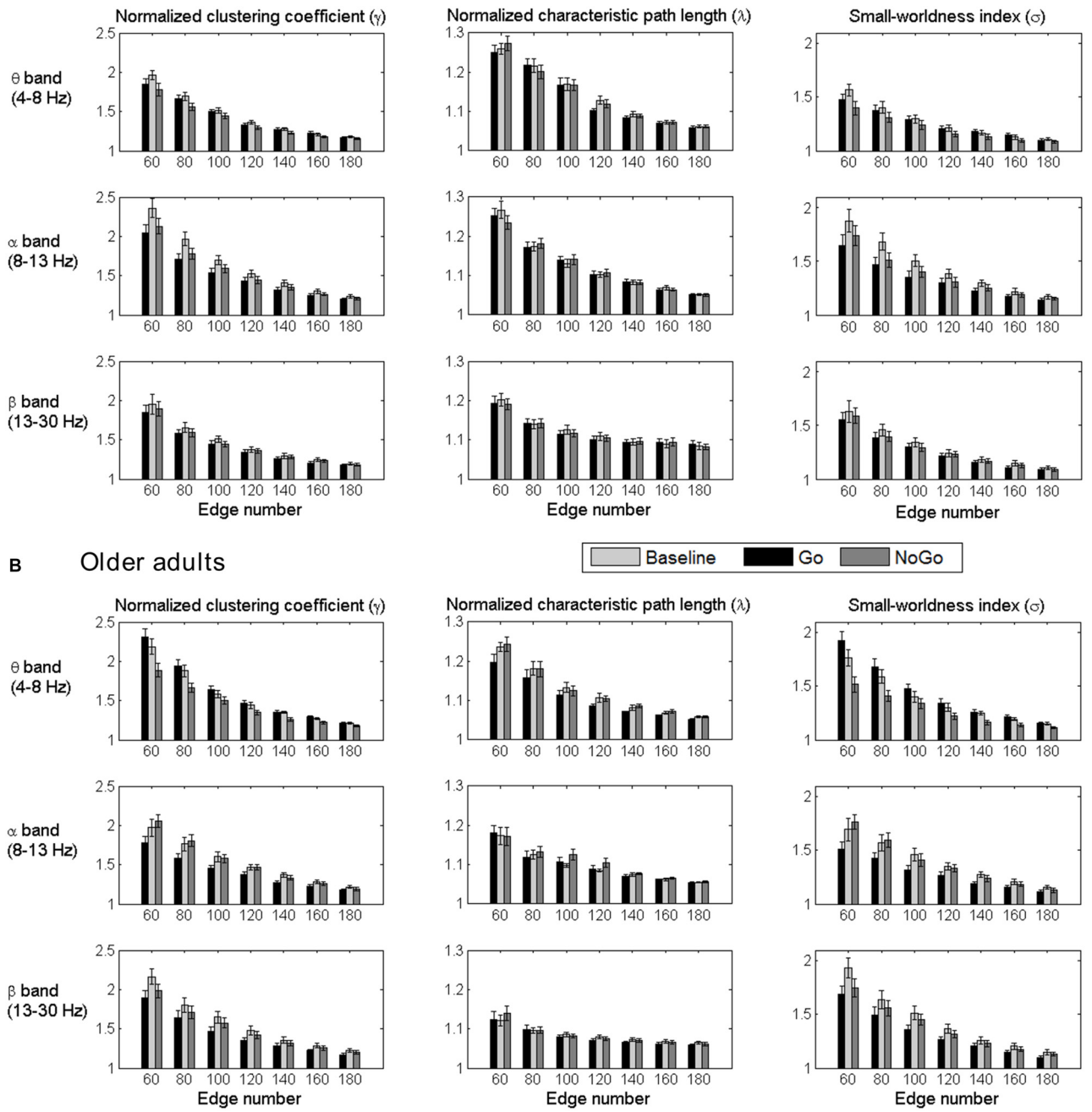


**FIGURE 3 | Group-averaged normalized clustering coefficient ($\gamma$), characteristic path length ($\lambda$) and small-worldness index ($\sigma$) of the brain networks for all task conditions (Baseline, Go, NoGo) in the younger group (A) and older group (B) under different network density levels.** Error bars indicate the standard error of the mean (SEM).

$p < 0.001$). In beta band, there was a main effect of Task ($F_{(2,76)} = 52.488$, $p < 0.001$) and a significant interaction of GNG × Age ($F_{(2,76)} = 10.217$, $p < 0.001$) on the central-parietal node degree. Follow-up analysis suggested that the task-modulated effects on central-parietal node degree were significant in either the younger (Go vs. Baseline: $t_{(22)} = 4.604$, $p < 0.001$; NoGo vs. Baseline: $t_{(22)} = 2.632$, $p = 0.015$; Go vs. NoGo: $t_{(22)} = 2.307$, $p = 0.031$) or the older (Go vs. Baseline: $t_{(16)} = 7.674$, $p < 0.001$; NoGo vs. Baseline: $t_{(16)} = 4.404$, $p < 0.001$; Go vs. NoGo: $t_{(16)} = 5.205$, $p < 0.001$) group.

To further characterize the age-related differences in task-modulated effects on node degree, we calculated

**TABLE 1 | Results of two-way repeated-measures ANOVA (Task: Baseline vs. Go vs. NoGo; Age: younger vs. older) on normalized clustering coefficient (observed/random).**

| Frequency band | Edge number | Factors | | |
|---|---|---|---|---|
| | | Task | Age | Task × Age |
| Theta (4–8 Hz) | 60 | **$F = 10.019$, $p < 0.001$** | **$F = 8.262$, $p = 0.007$** | **$F = 4.057$, $p = 0.021$** |
| | 80 | **$F = 11.458$, $p < 0.001$** | **$F = 8.367$, $p = 0.006$** | $F = 2.045$, $p = 0.136$ |
| | 100 | **$F = 4.609$, $p = 0.013$** | **$F = 4.258$, $p = 0.046$** | $F = 0.966$, $p = 0.385$ |
| | 120 | **$F = 8.959$, $p < 0.001$** | **$F = 7.485$, $p = 0.009$** | $F = 1.565$, $p = 0.216$ |
| | 140 | **$F = 11.839$, $p < 0.001$** | **$F = 6.873$, $p = 0.013$** | $F = 1.198$, $p = 0.307$ |
| | 160 | **$F = 10.436$, $p < 0.001$** | **$F = 11.981$, $p = 0.001$** | $F = 0.316$, $p = 0.730$ |
| | 180 | **$F = 5.444$, $p = 0.006$** | **$F = 12.504$, $p = 0.001$** | $F = 0.878$, $p = 0.420$ |
| Alpha (8–13 Hz) | 60 | **$F = 6.712$, $p = 0.002$** | $F = 3.883$, $p = 0.056$ | $F = 2.640$, $p = 0.078$ |
| | 80 | **$F = 9.112$, $p < 0.001$** | $F = 2.568$, $p = 0.083$ | $F = 1.182$, $p = 0.284$ |
| | 100 | **$F = 7.107$, $p = 0.003$** | $F = 0.940$, $p = 0.339$ | $F = 0.537$, $p = 0.587$ |
| | 120 | **$F = 4.966$, $p = 0.013$** | $F = 0.361$, $p = 0.551$ | $F = 1.402$, $p = 0.252$ |
| | 140 | **$F = 10.138$, $p < 0.001$** | $F = 0.832$, $p = 0.367$ | $F = 0.267$, $p = 0.767$ |
| | 160 | **$F = 7.474$, $p = 0.001$** | $F = 0.225$, $p = 0.638$ | $F = 0.185$, $p = 0.831$ |
| | 180 | **$F = 5.794$, $p = 0.007$** | $F = 0.671$, $p = 0.418$ | $F = 0.058$, $p = 0.944$ |
| Beta (13–30 Hz) | 60 | **$F = 9.988$, $p < 0.001$** | $F = 0.702$, $p = 0.407$ | $F = 2.320$, $p = 0.105$ |
| | 80 | **$F = 9.379$, $p = 0.001$** | $F = 1.363$ $p = 0.250$ | $F = 1.129$, $p = 0.329$ |
| | 100 | **$F = 18.344$, $p < 0.001$** | $F = 1.960$, $p = 0.170$ | **$F = 5.175$, $p = 0.008$** |
| | 120 | **$F = 14.281$, $p < 0.001$** | $F = 1.449$, $p = 0.236$ | **$F = 4.024$, $p = 0.022$** |
| | 140 | **$F = 14.111$, $p < 0.001$** | $F = 1.062$, $p = 0.309$ | $F = 1.502$, $p = 0.229$ |
| | 160 | **$F = 23.374$, $p < 0.001$** | $F = 0.588$, $p = 0.448$ | $F = 1.599$, $p = 0.209$ |
| | 180 | **$F = 16.803$, $p < 0.001$** | $F = 0.179$, $p = 0.675$ | **$F = 5.812$, $p = 0.004$** |

*Significant results are marked as bold.*

**TABLE 2 | Results of two-way repeated-measures ANOVA (Task: Baseline vs. Go vs. NoGo; Age: younger vs. older) on normalized characteristic path length (observed/random).**

| Frequency band | Edge number | Factors | | |
|---|---|---|---|---|
| | | Task | Age | Task × Age |
| Theta (4–8 Hz) | 60 | **$F = 3.390$, $p = 0.039$** | $F = 3.583$, $p = 0.066$ | $F = 0.746$, $p = 0.478$ |
| | 80 | $F = 0.435$, $p = 0.649$ | $F = 3.324$, $p = 0.076$ | $F = 1.175$, $p = 0.314$ |
| | 100 | $F = 0.472$, $p = 0.626$ | **$F = 6.299$, $p = 0.016$** | $F = 0.261$, $p = 0.771$ |
| | 120 | **$F = 6.260$, p = 0.003** | $F = 3.153$, $p = 0.084$ | $F = 0.195$, $p = 0.823$ |
| | 140 | $F = 3.030$, $p = 0.071$ | $F = 2.075$, $p = 0.158$ | $F = 0.757$, $p = 0.472$ |
| | 160 | $F = 2.570$, $p = 0.095$ | $F = 0.803$, $p = 0.376$ | $F = 1.145$, $p = 0.324$ |
| | 180 | **$F = 7.533$, $p = 0.002$** | $F = 0.944$, $p = 0.337$ | $F = 1.041$, $p = 0.358$ |
| Alpha(8-13 Hz) | 60 | $F = 0.510$, $p = 0.602$ | **$F = 13.099$, $p = 0.001$** | $F = 0.404$, $p = 0.669$ |
| | 80 | $F = 0.874$, $p = 0.421$ | **$F = 10.463$, $p = 0.003$** | $F = 0.038$, $p = 0.962$ |
| | 100 | $F = 3.224$, $p = 0.059$ | $F = 4.034$, $p = 0.052$ | $F = 0.886$, $p = 0.417$ |
| | 120 | $F = 2.228$, $p = 0.115$ | $F = 1.567$, $p = 0.218$ | $F = 0.889$, $p = 0.415$ |
| | 140 | $F = 0.241$, $p = 0.692$ | $F = 1.516$, $p = 0.226$ | $F = 0.504$, $p = 0.606$ |
| | 160 | $F = 0.499$, $p = 0.532$ | $F = 0.291$, $p = 0.592$ | $F = 1.344$, $p = 0.267$ |
| | 180 | $F = 0.044$, $p = 0.957$ | $F = 1.215$, $p = 0.277$ | $F = 1.061$, $p = 0.351$ |
| Beta (13–30 Hz) | 60 | $F = 0.151$, $p = 0.860$ | **$F = 11.322$, $p = 0.002$** | $F = 0.747$, $p = 0.477$ |
| | 80 | $F = 0.196$, $p = 0.822$ | **$F = 9.128$, $p = 0.004$** | $F = 0.014$, $p = 0.986$ |
| | 100 | $F = 2.905$, $p = 0.061$ | **$F = 8.689$, $p = 0.005$** | $F = 0.262$, $p = 0.770$ |
| | 120 | $F = 1.815$, $p = 0.170$ | **$F = 8.787$, $p = 0.005$** | $F = 0.017$, $p = 0.983$ |
| | 140 | **$F = 3.998$, $p = 0.039$** | **$F = 6.597$, $p = 0.014$** | $F = 2.248$, $p = 0.113$ |
| | 160 | $F = 0.480$, $p = 0.561$ | **$F = 5.083$, $p = 0.030$** | $F = 2.580$, $p = 0.082$ |
| | 180 | $F = 0.504$, $p = 0.579$ | **$F = 4.710$, $p = 0.036$** | $F = 1.525$, $p = 0.224$ |

*Significant results are marked as bold.*

the relative changes of ROI-averaged node degree between Go condition and NoGo condition, and then compared the relative changes between the two groups using independent-samples *t*-test. Older adults showed significantly larger relative changes of node degree than younger adults in both the theta (frontal-central ROI, $t_{(38)} = 2.228$, $p = 0.032$) and the beta (central-parietal ROI, $t_{(38)} = -2.540$, $p = 0.015$) bands. **Figure 5B** illustrates the main connections that have different strengths between different task conditions. Apparently, in theta band brain network, NoGo condition evoked stronger cortical connections than Go condition within

**TABLE 3 | Results of two-way repeated-measures ANOVA (Task: Baseline vs. Go vs. NoGo; Age: younger vs. older) on small-worldness index.**

| Frequency band | Edge number | Factors | | |
|---|---|---|---|---|
| | | Task | Age | Task × Age |
| Theta (4–8 Hz) | 60 | **$F = 13.507$, $p < 0.001$** | **$F = 13.344$, $p = 0.001$** | **$F = 5.809$, $p = 0.004$** |
| | 80 | **$F = 9.625$, $p < 0.001$** | **$F = 10.069$, $p = 0.003$** | **$F = 3.175$, $p = 0.047$** |
| | 100 | **$F = 4.505$, $p = 0.014$** | **$F = 6.705$, $p = 0.014$** | $F = 1.215$, $p = 0.302$ |
| | 120 | **$F = 9.402$, $p < 0.001$** | **$F = 7.839$, $p = 0.008$** | $F = 1.403$, $p = 0.252$ |
| | 140 | **$F = 12.770$, $p < 0.001$** | **$F = 7.145$, $p = 0.011$** | $F = 1.741$, $P = 0.182$ |
| | 160 | **$F = 11.397$, $p < 0.001$** | **$F = 10.748$, $p = 0.002$** | $F = 0.540$, $p = 0.585$ |
| | 180 | **$F = 5.956$, $p = 0.004$** | **$F = 12.059$, $p = 0.001$** | $F = 1.101$, $p = 0.338$ |
| Alpha (8–13 Hz) | 60 | **$F = 5.778$, $p = 0.005$** | $F = 0.787$, $p = 0.381$ | $F = 1.460$, $p = 0.239$ |
| | 80 | **$F = 7.094$, $p = 0.003$** | $F = 0.069$, $p = 0.794$ | $F = 2.152$, $p = 0.123$ |
| | 100 | **$F = 7.320$, $p = 0.002$** | $F = 0.140$, $p = 0.711$ | $F = 0.253$, $p = 0.777$ |
| | 120 | **$F = 4.774$, $p = 0.015$** | $F = 0.068$, $p = 0.796$ | $F = 0.823$, $p = 0.443$ |
| | 140 | **$F = 9.117$, $p = 0.001$** | $F = 0.357$, $p = 0.554$ | $F = 0.146$, $p = 0.865$ |
| | 160 | **$F = 6.219$, $p = 0.003$** | $F = 0.135$, $p = 0.716$ | $F = 0.048$, $p = 0.954$ |
| | 180 | **$F = 5.470$, $p = 0.010$** | $F = 0.874$, $p = 0.356$ | $F = 0.069$, $p = 0.934$ |
| Beta (13–30 Hz) | 60 | **$F = 9.399$, $p < 0.001$** | $F = 3.040$, $p = 0.089$ | $F = 2.955$, $p = 0.058$ |
| | 80 | **$F = 10.485$, $p < 0.001$** | $F = 3.289$, $p = 0.078$ | $F = 1.314$, $p = 0.275$ |
| | 100 | **$F = 15.622$, $p < 0.001$** | **$F = 4.638$, $p = 0.038$** | **$F = 5.972$, $p = 0.004$** |
| | 120 | **$F = 10.008$, $p < 0.001$** | $F = 4.010$, $p = 0.052$ | **$F = 3.300$, $p = 0.042$** |
| | 140 | **$F = 11.703$, $p < 0.001$** | $F = 3.106$, $p = 0.086$ | $F = 0.900$, $p = 0.411$ |
| | 160 | **$F = 20.484$, $p < 0.001$** | $F = 2.518$, $p = 0.121$ | $F = 0.520$, $p = 0.597$ |
| | 180 | **$F = 13.819$, $p < 0.001$** | $F = 2.815$, $p = 0.066$ | $F = 1.714$, $p = 0.198$ |

*Significant results are marked as bold.*

frontal-central area (**Figures 5Bk,l**), while in beta band brain network, Go condition evoked stronger cortical connections than NoGo condition within central-parietal area (**Figures 5Bm,n**).

## DISCUSSION

We present a thorough analysis on the task-related modulations on induced EEG activities as well as the effects caused by normal aging during a Go/NoGo task. Behaviorally, both younger and older adults showed high accuracy and negligible FARs in the Go/NoGo task, suggesting a sufficient level of inhibitory performance. Fourier analysis revealed an increase in frontal-central theta power during NoGo condition, and decreased central-parietal alpha and beta power during Go condition, which replicated previous findings in the literature. For the graph theoretical analysis on oscillatory brain networks, both age groups showed classic small-world brain networks in theta, alpha and beta bands, and older adults showed stronger task-modulated effects on small-world property than younger adults. Meanwhile, such frequency-specific modulation of brain networks were spatially segregated, indicating the differences of brain network between response inhibition and response execution. Specifically, theta-band brain network showed larger frontal-central node degree in NoGo condition than that in Go condition, whereas beta-band brain network showed larger central-parietal node degree in Go condition than that in NoGo condition. Moreover, these task-related modulations on node degree were also stronger in older adults than younger adults. Taken together, our findings indicate that the topological organization of oscillatory brain networks in theta and beta bands might serve as a hallmark for response inhibition and execution, which might become stronger and more robust due to normal aging.

### Task-Related Effects on Oscillatory Brain Networks

It is commonly agreed that small-worldness implies both high local clustering and short path length, which reflects an optimal balance between local segregation and global integration of brain networks (Watts and Strogatz, 1998; Bassett and Bullmore, 2006; Rubinov and Sporns, 2010). Several studies have documented the small-world organization of oscillatory brain networks in simple motor tasks, i.e., finger or foot movements, and resting state (Bassett et al., 2006; De Vico Fallani et al., 2008; Jin et al., 2012). In this study, we further demonstrated the small-worldness of brain networks in a Go/NoGo task that requires high-level cognitive computations. More importantly, we found that the index of small-worldness ($\sigma$) was significantly different between Go condition and NoGo condition. Although previous research failed to observe significantly different small-worldness index between simple motor tasks and the resting state, there seemed to be an overall trend of decreasing small-worldness indices during a finger-tapping task compared with resting state in the beta band network (Jin et al., 2012). These results were in line with our findings of the decreased small-worldness index in Go condition than Baseline condition and NoGo condition in beta band network. In theta band, however, we observed an increase of small-worldness index in Go condition than NoGo condition. These findings indicate that the theta and beta band brain networks play different functional roles in the Go/NoGo task, which is concordant with the literature, that is, the theta-band phase synchrony is more likely to be involved in inhibitory process (NoGo; Brier et al., 2010; Muller and Anokhin, 2012;

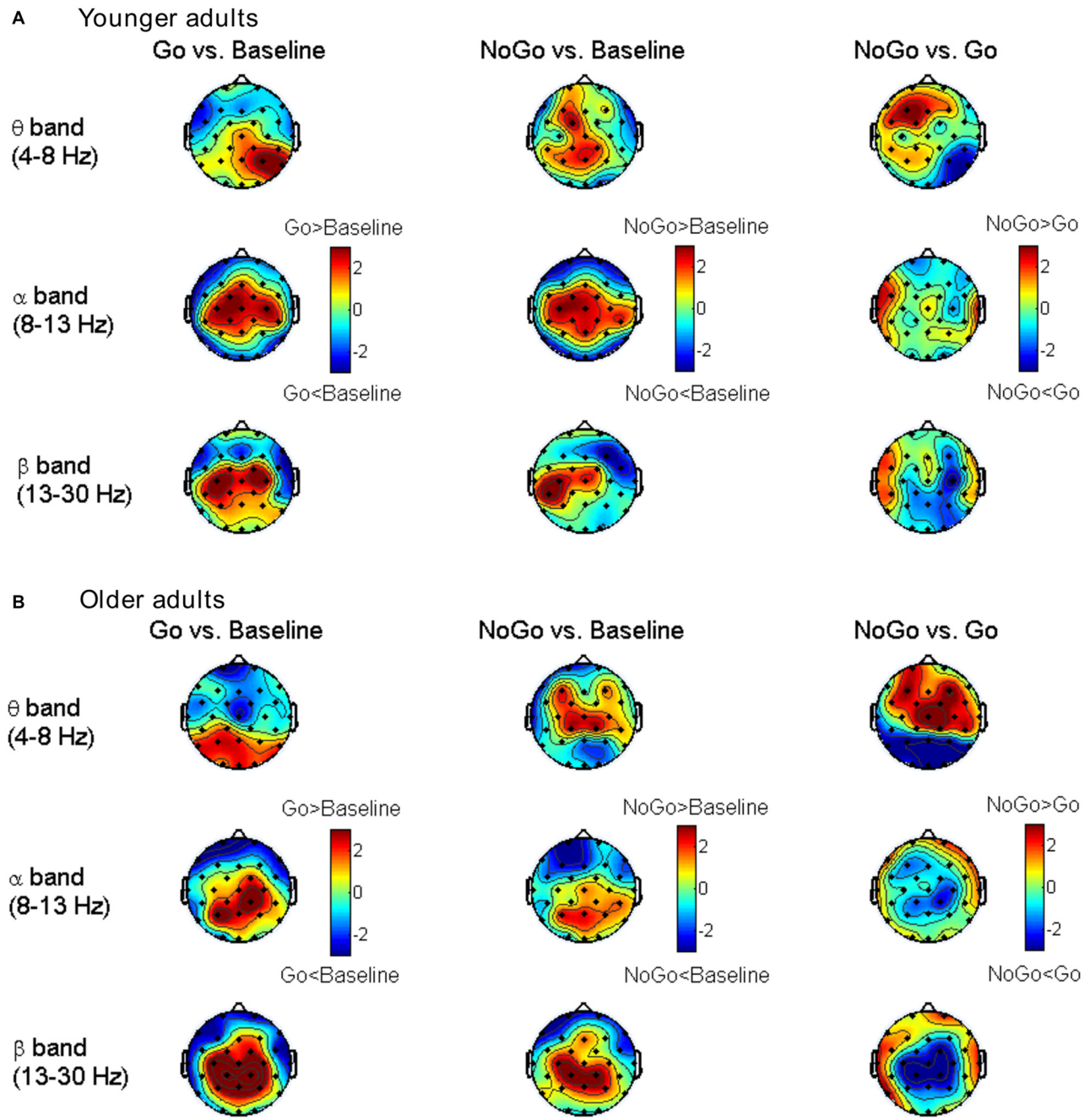


**FIGURE 4 | Topographic maps for *t*-values of the node degree between different task conditions for the younger group (A) and older group (B) in different frequency bands.** The results are illustrated under the network density level of 120 edges.

Anguera et al., 2013b), while the beta-band phase synchrony plays a major role in motor production (Go; Aoki et al., 2001; Brovelli et al., 2004; Jin et al., 2012).

The quantitative analysis of node degree further supported that theta- and beta-band phase synchrony played different functional roles in the Go/NoGo task. In theta band brain network, response inhibition significantly enhanced the frontal-central node degree (**Figure 5A**). This finding coincides well with the current understanding of theta oscillations, that is, frontal theta phase synchrony is commonly enhanced when more cognitive control is required (Cavanagh and Frank, 2014). On the other hand, in beta band brain network, response execution significantly enhanced the central-parietal node degree (**Figure 5B**), indicating that motor response is associated with the increase of beta-band synchrony which enhances

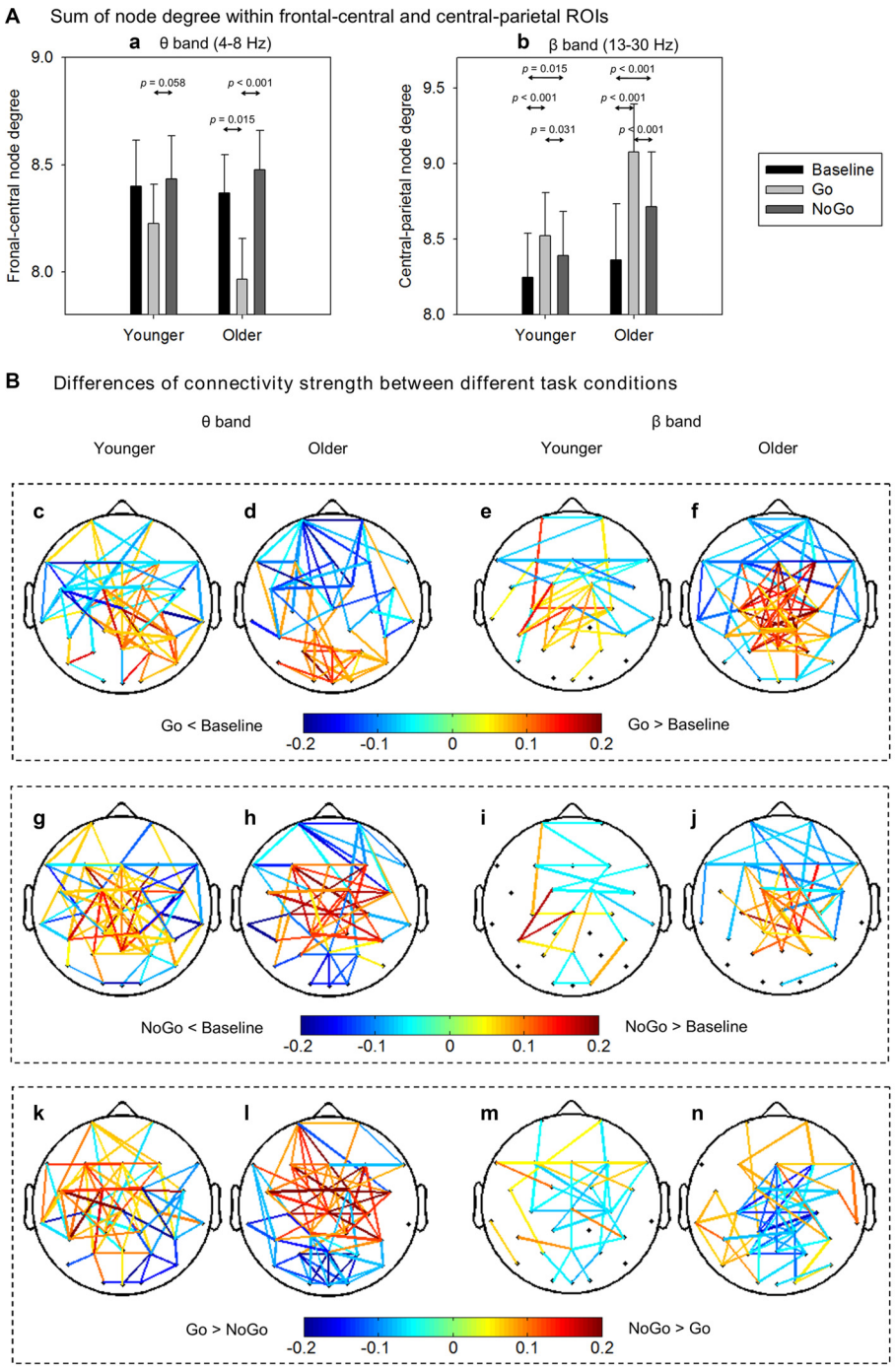


**FIGURE 5 | (A)** Group-averaged node degree within the frontal-central (theta band) and central-parietal (beta band) regions of interest (ROIs). Error bars indicate SEM. **(B)** Group-averaged differences of connectivity strength between different task conditions. Only the connections with absolute differences greater than 0.05 are shown in the figure. The results are illustrated under the network density level of 120 edges.

cortical connections with or within the sensorimotor areas (Mima et al., 2000; Bassett et al., 2006; Jin et al., 2012).

In theta band network, task-modulated effects on small-worldness manifested in significantly decreased clustering coefficient and increased characteristic path length in NoGo condition than that in Go condition. In the beta band network, however, the task-modulated effects on small-worldness index was only presented in the significant changes in clustering coefficient (**Figure 3**). Given that clustering

coefficient and characteristic path length represent local segregation and global integration of complex networks, respectively (Watts and Strogatz, 1998; Rubinov and Sporns, 2010; Bullmore and Bassett, 2011), our findings suggest that theta band brain network involved more distant cortical connections than beta band brain network. Furthermore, this inference was also supported by the differences in connectivity strength between Go condition and NoGo condition. Specifically, task-related changes (NoGo > Go) in theta band brain network involved relatively large-scale cortical connections, including the frontal, central and parietal areas (**Figures 5Bk,l**), whereas in beta band brain network, task-related changes (Go > NoGo) in cortical connections were primarily concentrated around the sensorimotor area (**Figures 5Bm,n**).

## Aging Effects on Oscillatory Brain Networks

Compared with younger adults, the small-worldness as well as task-modulated effects were well preserved in older adults. Furthermore, the task-modulated effects on node degree distribution in theta and beta band brain network were more prominent in older adults than younger adults (**Figure 5A**). There have been neuroimaging evidences that older adults could recruit more frontal activation than younger adults in cognitive control tasks, i.e., the Go/NoGo task, reflecting a functional compensation (Rajah and D'Esposito, 2005; Park and Reuter-Lorenz, 2009; Spreng et al., 2010; Heilbronner and Münte, 2013; Hong et al., 2014). Therefore, it could be inferred that normal aging not only increases the functional activation in specific regions, but also enhances the brain functional connections, which might indicate the recruitment of additional resources, and such findings are consistent with recent functional connectivity study based on functional magnetic resonance imaging (fMRI; Geerligs et al., 2014). Collectively, our findings clearly show that normal aging does not reduce, but rather enhances the neural synchrony during cognitively demanding tasks, which could shed new light on the neural mechanisms of cognitive aging when combined with the previously reported decrease in neural synchrony due to pathological aging (Pijnenburg et al., 2004; Uhlhaas and Singer, 2006; Stam et al., 2007, 2009; Knyazeva et al., 2010).

An attention-cueing Go/NoGo task with cue-target design, rather than a simple Go/NoGo task was used in this study. In such cue-target paradigm, Go/NoGo stimuli were always preceded by an instructive cue that led to increased response preparation in order to get a fast response to Go-stimulus. In this case, a prepared response had to be aborted when a NoGo-stimulus appeared at the cued location, which led to a robust response inhibition process (Bruin et al., 2001; Smith et al., 2006, 2007). Consistently, significant inhibition-related ERP components had been reported in our previous study (Hong et al., 2014). Moreover, since this study focused on response inhibition and execution, attention-related cognitive process and brain activity was not included here, which though, had been reported elsewhere (Hong et al., 2015).

In this study, the averaged ERP activity was subtracted from EEG signals before PS analysis to eliminate the effects from evoked activities that are phase-locked to the stimulus onset, i.e., N2 and P3 components. The N2 and P3 components have been widely reported to be the neural marker of response inhibition (Falkenstein et al., 1999; Albert et al., 2013; Huster et al., 2013; Hong et al., 2014). Since the ERP waves have subtracted before phase synchrony and brain network analysis, our findings suggest that task-modulated brain network constructed from induced (non-phase-locked) EEG activity could serve as another possible neural marker that is independent of conventional ERP markers. Moreover, such marker of brain network could be well preserved and even become stronger during normal aging.

One limitation in this study should be noted. Following a common approach in the literature (Dietl et al., 1999; Doppelmayr et al., 2000; Gruber et al., 2002; Deiber et al., 2009), we subtracted the averaged ERP from EEG epochs to eliminate the effects from evoked activity in this study. Such approach is based on the assumption that the same ERP is present in each single trial, which however, may be problematic. Unfortunately, extracting precise ERP activity at single trial level is still a highly challenging task, and currently there is still lack of widely accepted method in this field. Future work is required to address this limitation.

To conclude, by employing graph theoretical analysis, we thoroughly investigated the age-related differences in synchronous neural network within functionally-distinct frequency bands in a Go/NoGo task. This study explicitly demonstrated a close relationship between the frequency-specific neural synchrony and response inhibition as well as response execution. Our findings could also provide important implications into the current understanding of the neural mechanisms of cognitive aging from the perspective of synchronous brain networks.

## AUTHOR CONTRIBUTIONS

XH, YL, JS and ST designed research; XH performed research; XH, YL and JS analyzed data; XH, YL and ST wrote the article.

## ACKNOWLEDGMENTS

This work was supported by National Natural Science Foundation of China (No. 61571295) and Science and Technology Commission of the Shanghai Municipality (No. 13dz2260500). XH was supported by China Scholarship Council (201206230034). JS was supported in part by Med-X Research Fund of Shanghai Jiao Tong University (YG2012MS09). We thank Yixue Li for assistance with the data collection.

## REFERENCES


Achard, S., and Bullmore, E. (2007). Efficiency and cost of economical brain functional networks. *PLoS Comput. Biol.* 3:e17. doi: 10.1371/journal.pcbi.0030017

Albert, J., López-Martin, S., Hinojosa, J. A., and Carretiá, L. (2013). Spatiotemporal characterization of response inhibition. *Neuroimage* 76, 272–281. doi: 10.1016/j.neuroimage.2013.03.011

Anguera, J. A., Boccanfuso, J., Rintoul, J. L., Al-Hashimi, O., Faraji, F., Janowich, J., et al. (2013a). Video game training enhances cognitive control in older adults. *Nature* 501, 97–101. doi: 10.1038/nature12486

Anguera, J. A., Lyman, K., Zanto, T. P., Bollinger, J., and Gazzaley, A. (2013b). Reconciling the influence of task-set switching and motor inhibition processes on stop signal after-effects. *Front. Psychol.* 4:649. doi: 10.3389/fpsyg.2013.00649

Aoki, F., Fetz, E. E., Shupe, L., Lettich, E., and Ojemann, G. A. (2001). Changes in power and coherence of brain activity in human sensorimotor cortex during performance of visuomotor tasks. *Biosystems* 63, 89–99. doi: 10.1016/s0303-2647(01)00149-6

Bassett, D. S., and Bullmore, E. (2006). Small-world brain networks. *Neuroscientist* 12, 512–523. doi: 10.1177/1073858406293182

Bassett, D. S., Bullmore, E. T., Meyer-Lindenberg, A., Apud, J. A., Weinberger, D. R., and Coppola, R. (2009). Cognitive fitness of cost-efficient brain functional networks. *Proc. Natl. Acad. Sci. U S A* 106, 11747–11752. doi: 10.1073/pnas.0903641106

Bassett, D. S., Meyer-Lindenberg, A., Achard, S., Duke, T., and Bullmore, E. (2006). Adaptive reconfiguration of fractal small-world human brain functional networks. *Proc. Natl. Acad. Sci. U S A* 103, 19518–19523. doi: 10.1073/pnas.0606005103

Bastiaansen, M., and Hagoort, P. (2003). Event-induced theta responses as a window on the dynamics of memory. *Cortex* 39, 967–992. doi: 10.1016/s0010-9452(08)70873-6

Brier, M. R., Ferree, T. C., Maguire, M. J., Moore, P., Spence, J., Tillman, G. D., et al. (2010). Frontal theta and alpha power and coherence changes are modulated by semantic complexity in Go/NoGo tasks. *Int. J. Psychophysiol.* 78, 215–224. doi: 10.1016/j.ijpsycho.2010.07.011

Brovelli, A., Ding, M., Ledberg, A., Chen, Y., Nakamura, R., and Bressler, S. L. (2004). Beta oscillations in a large-scale sensorimotor cortical network: directional influences revealed by Granger causality. *Proc. Natl. Acad. Sci. U S A* 101, 9849–9854. doi: 10.1073/pnas.0308538101

Bruin, K. J., Wijers, A. A., and van Staveren, A. S. (2001). Response priming in a go/nogo task: do we have to explain the go/nogo N2 effect in terms of response activation instead of inhibition? *Clin. Neurophysiol.* 112, 1660–1671. doi: 10.1016/s1388-2457(01)00601-0

Bullmore, E. T., and Bassett, D. S. (2011). Brain graphs: graphical models of the human brain connectome. *Annu. Rev. Clin. Psychol.* 7, 113–140. doi: 10.1146/annurev-clinpsy-040510-143934

Bullmore, E., and Sporns, O. (2009). Complex brain networks: graph theoretical analysis of structural and functional systems. *Nat. Rev. Neurosci.* 10, 186–198. doi: 10.1038/nrn2575

Bullmore, E., and Sporns, O. (2012). The economy of brain network organization. *Nat. Rev. Neurosci.* 13, 336–349. doi: 10.1038/nrn3214

Cabeza, R., Anderson, N. D., Locantore, J. K., and McIntosh, A. R. (2002). Aging gracefully: compensatory brain activity in high-performing older adults. *Neuroimage* 17, 1394–1402. doi: 10.1006/nimg.2002.1280

Cavanagh, J. F., and Frank, M. J. (2014). Frontal theta as a mechanism for cognitive control. *Trends Cogn. Sci.* 18, 414–421. doi: 10.1016/j.tics.2014.04.012

De Vico Fallani, F., Astolfi, L., Cincotti, F., Mattia, D., Marciani, M. G., Tocci, A., et al. (2008). Cortical network dynamics during foot movements. *Neuroinformatics* 6, 23–34. doi: 10.1007/s12021-007-9006-6

Deiber, M. P., Ibañez, V., Missonnier, P., Herrmann, F., Fazio-Costa, L., Gold, G., et al. (2009). Abnormal-induced theta activity supports early directed-attention network deficits in progressive MCI. *Neurobiol. Aging* 30, 1444–1452. doi: 10.1016/j.neurobiolaging.2007.11.021

Delorme, A., and Makeig, S. (2004). EEGLAB: an open source toolbox for analysis of single-trial EEG dynamics including independent component analysis. *J. Neurosci. Methods* 134, 9–21. doi: 10.1016/j.jneumeth.2003.10.009

Diamond, A. (2013). Executive functions. *Annu. Rev. Psychol.* 64, 135–168. doi: 10.1146/annurev-psych-113011-143750

Dietl, T., Dirlich, G., Vogl, L., Lechner, C., and Strian, F. (1999). Orienting response and frontal midline theta activity: a somatosensory spectral perturbation study. *Clin. Neurophysiol.* 110, 1204–1209. doi: 10.1016/s1388-2457(99)00057-7

Doppelmayr, M., Klimesch, W., Schwaiger, J., Stadler, W., and Röhm, D. (2000). The time locked theta response reflects interindividual differences in human memory performance. *Neurosci. Lett.* 278, 141–144. doi: 10.1016/s0304-3940(99)00925-8

Ergen, M., Saban, S., Kirmizi-Alsan, E., Uslu, A., Keskin-Ergen, Y., and Demiralp, T. (2014). Time-frequency analysis of the event-related potentials associated with the Stroop test. *Int. J. Psychophysiol.* 94, 463–472. doi: 10.1016/j.ijpsycho.2014.08.177

Falkenstein, M., Hoormann, J., and Hohnsbein, J. (1999). ERP components in Go/Nogo tasks and their relation to inhibition. *Acta Psychol. (Amst)* 101, 267–291. doi: 10.1016/s0001-6918(99)00008-6

Folstein, M. F., Folstein, S. E., and McHugh, P. R. (1975). "Mini-mental state". A practical method for grading the cognitive state of patients for the clinician. *J. Psychiatr. Res.* 12, 189–198. doi: 10.1016/0022-3956(75)90026-6

Geerligs, L., Saliasi, E., Renken, R. J., Maurits, N. M., and Lorist, M. M. (2014). Flexible connectivity in the aging brain revealed by task modulations. *Hum. Brain Mapp.* 35, 3788–3804. doi: 10.1002/hbm.22437

Grady, C. (2012). The cognitive neuroscience of ageing. *Nat. Rev. Neurosci.* 13, 491–505. doi: 10.1038/nrn3256

Gruber, T., Müller, M. M., and Keil, A. (2002). Modulation of induced gamma band responses in a perceptual learning task in the human EEG. *J. Cogn. Neurosci.* 14, 732–744. doi: 10.1162/08989290260138636

Heilbronner, U., and Münte, T. F. (2013). Rapid event-related near-infrared spectroscopy detects age-related qualitative changes in the neural correlates of response inhibition. *Neuroimage* 65, 408–415. doi: 10.1016/j.neuroimage.2012.09.066

Hong, X., Sun, J., Bengson, J. J., Mangun, G. R., and Tong, S. (2015). Normal aging selectively diminishes alpha lateralization in visual spatial attention. *Neuroimage* 106, 353–363. doi: 10.1016/j.neuroimage.2014.11.019

Hong, X., Sun, J., Bengson, J. J., and Tong, S. (2014). Age-related spatiotemporal reorganization during response inhibition. *Int. J. Psychophysiol.* 93, 371–380. doi: 10.1016/j.ijpsycho.2014.05.013

Hong, X., Sun, J., and Tong, S. (2013). Functional brain networks for sensory maintenance in top-down selective attention to audiovisual inputs. *IEEE Trans. Neural Syst. Rehabil. Eng.* 21, 734–743. doi: 10.1109/TNSRE.2013.2272219

Humphries, M. D., and Gurney, K. (2008). Network 'small-world-ness': a quantitative method for determining canonical network equivalence. *PLoS One* 3:e0002051. doi: 10.1371/journal.pone.0002051

Huster, R. J., Enriquez-Geppert, S., Lavallee, C. F., Falkenstein, M., and Herrmann, C. S. (2013). Electroencephalography of response inhibition tasks: functional networks and cognitive contributions. *Int. J. Psychophysiol.* 87, 217–233. doi: 10.1016/j.ijpsycho.2012.08.001

Jin, S. H., Lin, P., and Hallett, M. (2012). Reorganization of brain functional small-world networks during finger movements. *Hum. Brain Mapp.* 33, 861–872. doi: 10.1002/hbm.21253

Jung, T. P., Makeig, S., Westerfield, M., Townsend, J., Courchesne, E., and Sejnowski, T. J. (2000). Removal of eye activity artifacts from visual event-related potentials in normal and clinical subjects. *Clin. Neurophysiol.* 111, 1745–1758. doi: 10.1016/s1388-2457(00)00386-2

Kirmizi-Alsan, E., Bayraktaroglu, Z., Gurvit, H., Keskin, Y. H., Emre, M., and Demiralp, T. (2006). Comparative analysis of event-related potentials during Go/NoGo and CPT: decomposition of electrophysiological markers of response inhibition and sustained attention. *Brain Res.* 1104, 114–128. doi: 10.1016/j.brainres.2006.03.010

Knyazeva, M. G., Jalili, M., Brioschi, A., Bourquin, I., Fornari, E., Hasler, M., et al. (2010). Topography of EEG multivariate phase synchronization in early Alzheimer's disease. *Neurobiol. Aging* 31, 1132–1144. doi: 10.1016/j.neurobiolaging.2008.07.019

Latora, V., and Marchiori, M. (2001). Efficient behavior of small-world networks. *Phys. Rev. Lett.* 87:198701. doi: 10.1103/physrevlett.87.198701

Leocani, L., Toro, C., Manganotti, P., Zhuang, P., and Hallett, M. (1997). Event-related coherence and event-related desynchronization/synchronization in the 10 Hz and 20 Hz EEG during self-paced movements. *Electroencephalogr. Clin. Neurophysiol.* 104, 199–206. doi: 10.1016/s0168-5597(96)96051-7

Li, Y., Cao, D., Wei, L., Tang, Y., and Wang, J. (2015). Abnormal functional connectivity of EEG gamma band in patients with depression during emotional face processing. *Clin. Neurophysiol.* 126, 2078–2089. doi: 10.1016/j.clinph.2014.12.026

Lopez-Calderon, J., and Luck, S. J. (2014). ERPLAB: an open-source toolbox for the analysis of event-related potentials. *Front. Hum. Neurosci.* 8:213. doi: 10.3389/fnhum.2014.00213

Maslov, S., and Sneppen, K. (2002). Specificity and stability in topology of protein networks. *Science* 296, 910–913. doi: 10.1016/j.ijpsycho.2014.05.013

Mima, T., Matsuoka, T., and Hallett, M. (2000). Functional coupling of human right and left cortical motor areas demonstrated with partial coherence analysis. *Neurosci. Lett.* 287, 93–96. doi: 10.1016/s0304-3940(00)01165-4

Moore, R. A., Gale, A., Morris, P. H., and Forrester, D. (2008). Alpha power and coherence primarily reflect neural activity related to stages of motor response during a continuous monitoring task. *Int. J. Psychophysiol.* 69, 79–89. doi: 10.1016/j.ijpsycho.2008.03.003

Muller, V., and Anokhin, A. P. (2012). Neural synchrony during response production and inhibition. *PLoS One* 7:e38931. doi: 10.1371/journal.pone.0038931

Onnela, J. P., Saramäki, J., Kertész, J., and Kaski, K. (2005). Intensity and coherence of motifs in weighted complex networks. *Phys. Rev. E Stat. Nonlin. Soft. Matter Phys.* 71:065103. doi: 10.1103/physreve.71.065103

Park, D. C., and Reuter-Lorenz, P. (2009). The adaptive brain: aging and neurocognitive scaffolding. *Annu. Rev. Psychol.* 60, 173–196. doi: 10.1146/annurev.psych.59.103006.093656

Pfurtscheller, G., and Lopes da Silva, F. H. (1999). Event-related EEG/MEG synchronization and desynchronization: basic principles. *Clin. Neurophysiol.* 110, 1842–1857. doi: 10.1016/s1388-2457(99)00141-8

Pijnenburg, Y. A., v d Made, Y., van Cappellen van Walsum, A. M., Knol, D. L., Scheltens, P., and Stam, C. J. (2004). EEG synchronization likelihood in mild cognitive impairment and Alzheimer's disease during a working memory task. *Clin. Neurophysiol.* 115, 1332–1339. doi: 10.1016/j.clinph.2003.12.029

Rajah, M. N., and D'Esposito, M. (2005). Region-specific changes in prefrontal function with age: a review of PET and fMRI studies on working and episodic memory. *Brain* 128, 1964–1983. doi: 10.1093/brain/awh608

Rubinov, M., Knock, S. A., Stam, C. J., Micheloyannis, S., Harris, A. W., Williams, L. M., et al. (2009). Small-world properties of nonlinear brain activity in schizophrenia. *Hum. Brain Mapp.* 30, 403–416. doi: 10.1002/hbm.20517

Rubinov, M., and Sporns, O. (2010). Complex network measures of brain connectivity: uses and interpretations. *Neuroimage* 52, 1059–1069. doi: 10.1016/j.neuroimage.2009.10.003

Serrien, D. J., Orth, M., Evans, A. H., Lees, A. J., and Brown, P. (2005). Motor inhibition in patients with Gilles de la Tourette syndrome: functional activation patterns as revealed by EEG coherence. *Brain* 128, 116–125. doi: 10.1093/brain/awh318

Smith, J. L., Johnstone, S. J., and Barry, R. J. (2006). Effects of pre-stimulus processing on subsequent events in a warned Go/NoGo paradigm: response preparation, execution and inhibition. *Int. J. Psychophysiol.* 61, 121–133. doi: 10.1016/j.ijpsycho.2005.07.013

Smith, J. L., Johnstone, S. J., and Barry, R. J. (2007). Response priming in the Go/NoGo task: the N2 reflects neither inhibition nor conflict. *Clin. Neurophysiol.* 118, 343–355. doi: 10.1016/j.clinph.2006.09.027

Spreng, R. N., Wojtowicz, M., and Grady, C. L. (2010). Reliable differences in brain activity between young and old adults: a quantitative meta-analysis across multiple cognitive domains. *Neurosci. Biobehav. Rev.* 34, 1178–1194. doi: 10.1016/j.neubiorev.2010.01.009

Stam, C. J., de Haan, W., Daffertshofer, A., Jones, B. F., Manshanden, I., van Cappellen van Walsum, A. M., et al. (2009). Graph theoretical analysis of magnetoencephalographic functional connectivity in Alzheimer's disease. *Brain* 132, 213–224. doi: 10.1093/brain/awn262

Stam, C. J., Jones, B. F., Nolte, G., Breakspear, M., and Scheltens, P. (2007). Small-world networks and functional connectivity in Alzheimer's disease. *Cereb. Cortex* 17, 92–99. doi: 10.1093/cercor/bhj127

Sun, J., Hong, X., and Tong, S. (2012). Phase synchronization analysis of EEG signals: an evaluation based on surrogate tests. *IEEE Trans. Biomed. Eng.* 59, 2254–2263. doi: 10.1109/TBME.2012.2199490

Sun, Y., Lim, J., Meng, J., Kwok, K., Thakor, N., and Bezerianos, A. (2014). Discriminative analysis of brain functional connectivity patterns for mental fatigue classification. *Ann. Biomed. Eng.* 42, 2084–2094. doi: 10.1007/s10439-014-1059-8

Tallet, J., Barral, J., and Hauert, C. A. (2009). Electro-cortical correlates of motor inhibition: a comparison between selective and non-selective stop tasks. *Brain Res.* 1284, 68–76. doi: 10.1016/j.brainres.2009.05.058

Tass, P., Rosenblum, M., Weule, J., Kurths, J., Pikovsky, A., Volkmann, J., et al. (1998). Detection of n:m phase locking from noisy data: application to magnetoencephalography. *Phys. Rev. Lett.* 81, 3291–3294. doi: 10.1142/9789812793782_0004

Uhlhaas, P. J., and Singer, W. (2006). Neural synchrony in brain disorders: relevance for cognitive dysfunctions and pathophysiology. *Neuron* 52, 155–168. doi: 10.1016/j.neuron.2006.09.020

Wacker, M., and Witte, H. (2011). On the stability of the n:m phase synchronization index. *IEEE Trans. Biomed. Eng.* 58, 332–338. doi: 10.1109/TBME.2010.2063028

Watts, D. J., and Strogatz, S. H. (1998). Collective dynamics of 'small-world' networks. *Nature* 393, 440–442. doi: 10.1038/30918

Yan, J., Sun, J., Guo, X., Jin, Z., Li, Y., Li, Z., et al. (2013). Motor imagery cognitive network after left ischemic stroke: study of the patients during mental rotation task. *PLoS One* 8:e77325. doi: 10.1371/journal.pone.0077325

**Conflict of Interest Statement**: The authors declare that the research was conducted in the absence of any commercial or financial relationships that could be construed as a potential conflict of interest.

frontiers in Aging Neuroscience

ORIGINAL RESEARCH
published: 06 January 2016
doi: 10.3389/fnagi.2015.00243

# Adaptive Strategies for the Elderly in Inhibiting Irrelevant and Conflict No-Go Trials while Performing the Go/No-Go Task

*Shulan Hsieh*[1,2]*, *Mengyao Wu*[1,3] *and Chien-Hui Tang*[1]

[1] Cognitive Electrophysiology Laboratory: Control, Aging, Sleep, and Emotion (CASE), Department of Psychology, National Cheng Kung University, Tainan, Taiwan, [2] Institute of Allied Health Sciences, National Cheng Kung University, Tainan, Taiwan, [3] Department of Occupational Therapy, Shu-Zen Junior College of Medicine and Management, Kaohsiung, Taiwan

This study aimed to differentiate whether or not older adults are more prone to distraction or conflict, as induced by irrelevant and conflict no-go stimuli (irNOGO and cfNOGO), respectively. This study also aimed to determine whether or not older adults would devote more effort to withholding a no-go trial in the higher-control demand condition (20% no-go trials' probability) as compared to the lower-control demand condition (50 and 80% no-go trials' probability). A total of 96 individuals were recruited, and each of the three no-go trials' probability conditions included 32 participants (16 younger adults and 16 older adults). Both behavioral and event-related potential (ERP) data were measured. The behavioral results showed that the older adults performed more poorly than the younger adults for the go trials, as reflected by slower reaction times (RTs) and higher numbers of omission errors in the go trials. In contrast, in the no-go trials, the older adults counter-intuitively exhibited similar behavioral performance (i.e., equivalent commission errors) as compared to the younger adults. The ERP data further showed that the older adults (but not the younger adults) exhibited larger P3 peak amplitudes for the irNOGO than cfNOGO trials. Yet, on the other hand, the older adults performed more poorly (i.e., had more commission errors) in the cfNOGO than irNOGO trials. These results seem to suggest that the older adults recruited more control processes in order to conquer the commitment of responses in the no-go trials, especially in the irNOGO trials. This age-related compensatory response of recruiting more control processes was specifically seen in the 20% no-go trial probability condition. This study therefore provides a deeper understanding into how older adults adopt strategies for performing the go/no-go task such as devoting more control processes to inhibiting the irNOGO trials compared to the cfNOGO trials in order to cope with their deficient inhibition ability.

**Keywords: event-related potential, distraction, inhibition, no-go, probability**

OPEN ACCESS

***Edited by:***
*Junfeng Sun,*
*Shanghai Jiao Tong University, China*

***Reviewed by:***
*Noa Fogelson,*
*Universidade da Coruña, Spain*
*Xiangfei Hong,*
*Philips Research, China*

***Correspondence:**
*Shulan Hsieh*
*psyhsl@mail.ncku.edu.tw*

***Received:*** *20 September 2015*
***Accepted:*** *10 December 2015*
***Published:*** *06 January 2016*

***Citation:***
*Hsieh S, Wu M and Tang C-H (2016) Adaptive Strategies for the Elderly in Inhibiting Irrelevant and Conflict No-Go Trials while Performing the Go/No-Go Task. Front. Aging Neurosci. 7:243. doi: 10.3389/fnagi.2015.00243*

## INTRODUCTION

Daily life often requires an individual to produce a certain behavior in an environment that is filled with irrelevant and often distracting information. Hence, to achieve the goal of acting adequately, one has to adaptively overcome the competition brought by the strong, yet inappropriate, momentary tendency to inhibit a prepotent yet unintentional response in order

to prevent negative consequences. These adaptive processes are broadly termed *inhibition* or *suppression*, and they have often been hypothesized to involve the frontal lobe functions (e.g., Rogers et al., 1998). Given the importance of inhibition in everyday life, several studies have attempted to address the issue of whether or not elderly people could successfully cope with brain degeneration, particularly in the frontal lobes (Dempster, 1992; Raz, 2000; West, 2000; Dennis and Cabeza, 2008), to achieve the goal of acting adequately in everyday life scenarios.

However, the findings regarding how capable an elderly person can be in performing an inhibition-related task are equivocal: some studies showed that the elderly suffered from generic inhibition deficit, hence, they were incapable of performing any inhibition-related task as compared to the younger adults (Hasher and Zacks, 1988; Bokura et al., 2002; Vallesi et al., 2009; Vallesi, 2011; Lucci et al., 2013; Pires et al., 2014), while some other studies have shown that the elderly could develop some strategies to compensate for their deficiency in achieving the task goal (Cabeza et al., 2002; Phillips and Andrés, 2010; Hsieh and Fang, 2012; Hsieh et al., 2012; Hsieh and Lin, 2014). Many factors such as different experimental settings, different populations, and different types of stimuli and requirements could potentially contribute to the discrepancies. Among these factors, we suggest that task parameters may play a critical role in older adults' performance strategies. Hence, in this study we manipulated two task parameters in a go/no-go task paradigm to address the inhibition proficiency of older adults. We focused specifically on a go/no-go task paradigm because such an inhibition task has been proven to be sensitive to aging (Bokura et al., 2002; Vallesi et al., 2009; Vallesi, 2011; Lucci et al., 2013; Pires et al., 2014). The two-task parameters we manipulated here include a no-go stimulus and a no-go stimulus probability. With regard to the type of no-go stimulus, we incorporated two types of no-go stimuli: irrelevant no-go (irNOGO) and conflict no-go (cfNOGO). The irNOGO stimuli belong to a different semantic category from that of the go stimuli (e.g., numbers vs. letters), which yields an obvious distinction between the target (go) and non-target (no-go) stimuli, even though the no-go stimuli may share a common feature with the go stimuli. For example, both the irNOGO and go stimuli could be either red or blue, but they belong to numbers and letters, respectively. In contrast, the cfNOGO stimuli share the same category (i.e., letters) as the go stimuli. The rationale for this manipulation is that the irNOGO stimuli should be easier to distinguish from the go stimuli; therefore, it is easier inhibit compared to the cfNOGO stimuli. On the other hand, some prior studies in the memory research domain have suggested that older adults were more vulnerable to internal distraction and weakening concentration skills due to their subtle changes in brain activity (e.g., Grady et al., 2006). It is therefore interesting to examine whether or not older adults are also susceptible to external distractions, such as those induced by the irNOGO stimuli in a go/no-go task.

With regard to no-go stimulus probability, we manipulated the probability of no-go trials in a block to be either 20, 50, or 80%. The rationale for the probability manipulation is that with a strong response bias towards go stimuli (20% no-go probability), one can maximize the engagement of executive control to inhibit no-go stimuli (Bruin and Wijers, 2002; Ford et al., 2004). Subsequently, the performance of a go/no-go task may be more sensitive to aging in the condition of this higher demand condition (20% of no-go probability).

With the manipulation of these two task parameters, we could examine whether or not aging results in a selective deficit in which task parameters are sensitive to the effect of aging in only some scenarios. Because no overt response can be recorded for no-go trials in a go/no-go paradigm, a neural imaging approach is needed to uncover the underlying processes of the no-go trials. In this study, we employed the event-related potential (ERP) method, which yields higher temporal resolution and uncovers the underlying neural activity for no-go trials.

Two ERP components are considered in this study that have been demonstrated to be sensitive to a go/no-go task, that is, the stimulus-locked P3 and N2 components (for a review, see Pires et al., 2014). Stimuli that trigger a tendency to make incorrect prepotent responses (e.g., incongruent or no-go stimuli) have been found to be associated with enhanced fronto-central N2 amplitude, which is thought to reflect inhibition (Van Boxtel et al., 2001; Roche et al., 2005) and/or response conflict control processes (Falkenstein et al., 2001; Van Veen and Carter, 2002a,b; Nieuwenhuis et al., 2003). Furthermore, Nieuwenhuis et al. (2003) observed that no-go N2 amplitudes were higher in the high go-prepotency (20% no-go) condition compared with medium (50%) and low go-prepotency (80% no-go) conditions, which supports the conflict theory of N2. Following the N2, there is a positive ERP component that peaks at approximately 250–500 ms for both go (known as the go P3) and no-go (known as the no-go P3) trials. Both go and no-go P3s may reflect context updating (Donchin and Coles, 1988), which is necessary for successful ongoing execution and inhibition of prepotency responses. Specifically, the no-go P3 has been shown to be closely related to inhibition (Roberts et al., 1994; Fallgatter and Strik, 1999; Tekok-Kilic et al., 2001; Smith et al., 2008). Hence, by observing how aging may modulate the no-go N2 and P3 components, we can uncover age-related inhibition and/or conflict processes.

## MATERIALS AND METHODS

### Participants

A total of 96 individuals were recruited through the internet and local community advertisements; each of the three no-go probability condition blocks included 32 participants (16 younger adults and 16 older adults). For the 20% no-go probability condition, 16 young adults (9 females) had a mean age of 21.31 $\pm$ 1.40 years (range 20–25 years) and an average of 15.69 $\pm$ 1.25 years of education; the 16 elderly adults (9 females) had a mean age of 66.38 $\pm$ 4.57 years (range 61–72 years) and an average of 12.69 $\pm$ 2.15 years of education. For the 50% no-go probability condition, the 16 young adults (8 females) had a mean

age of 21.31 ± 1.30 years (range 20–25 years) and an average of 15.00 ± 1.10 years of education; the 16 elderly adults (8 females) had a mean age of 67.25 ± 4.74 years (range 60–76 years) and an average of 12.56 ± 3.60 years of education. For the 80% no-go probability condition, the 16 young adults (9 females) had a mean age of 21.63 ± 1.54 years (range 19–24 years) and an average of 15.44 ± 1.21 years of education; the 16 elderly adults (9 females) had a mean age of 68.63 ± 6.08 years (range 61–80 years) and an average of 13.31 ± 2.75 years of education (see **Table 1**).

The 2-way analysis of variance (ANOVAs) on age with two between-subjects factors of age and no-go probability showed a significant main effect of age (young: 21.42 ± 1.38 years vs. old: 67.42 ± 5.09 years, $F_{(1,90)}$ = 3529.05, $p < 0.01$), but it did not show a significant main effect of no-go probability or a significant interaction between age and no-go probability (i.e., all *ps* > 0.05). The 2-way ANOVA on years of education showed a significant effect of age (young: 12.85 ± 2.82 years vs. old: 15.38 ± 1.18 years, $F_{(1,90)}$ = 31.18, $p < 0.01$). No significant effect of no-go probability or interaction between age and no-go probability was found (all *ps* > 0.05).

All participants provided their written informed consent, and the study protocol was approved by the Institutional Review Board (IRB) of the National Cheng Kung University Hospital, Taiwan. All participants were paid NT $500–1000 (US $15–30) for approximately 3 h of participation. All participants were right-handed, free of neurological and psychological disorders, and had normal or corrected-to-normal vision. The Mini-Mental State Examination (MMSE; Folstein et al., 1975) screened all participants for dementia based on the following screening criteria: 25–30 points = normal; 21–24 points = mild dementia; 14–20 points = moderate dementia; and ≤13 points = severe dementia. For the 20% no-go probability condition, the mean MMSE score was 28.63 ± 0.60 for the younger adults and 27.06 ± 1.14 for the older adults. For the 50% no-go probability condition, the mean MMSE score was 28.50 ± 0.71 for the younger adults and 26.68 ± 1.10 for the older adults. For the 80% no-go probability condition, the mean MMSE score was 28.18 ± 1.01 for the younger adults and 27.19 ± 0.73 for the older adults.

The 2-way ANOVA on the MMSE score showed a significant effect of age (young: 26.98 ± 1.03 vs. old: 28.44 ± 0.81, $F_{(1,90)}$ = 58.15, $p < 0.01$) but no significant effect of no-go probability; also, there was no significant interaction between age and no-go probability (all *ps* > 0.05). Since there was a significant effect of age on MMSE scores, this may be a potential confounding variable for the results, i.e., the changes may be due to cognitive decline rather than physiological aging. In order to preclude the possible contribution of cognitive decline in the older group, we have additionally run an analysis of covariance (ANCOVA) using MMSE as a covariate factor. The results of the ANCOVA showed the same patterns as those of the ANOVA reported here. Hence, although the older adults exhibited lower MMSE scores, they did not confound the current findings.

## Stimuli

The stimuli were generated using E-Prime software (Psychology Software Tools, Inc., Pittsburgh, PA, USA) and were presented in red or blue against a black background on the center of a computer screen that was placed at a distance of 90 cm from the participant. In this task, go stimuli were red or blue vowels ("A", "E", "I", "U") and no-go stimuli were either red or blue consonants ("L", "N", "P", "Z"; designed as cfNOGO stimuli) or red and blue numbers ("3", "4", "5", "6"; designed as irNOGO stimuli).

## Design and Procedure

Each trial began with the presentation of a white fixation cross "+" for a duration of 200 ms, followed by a go or no-go stimulus for a duration of 300 ms. This was then replaced by a black blank screen that awaited a response or until 1800 ms elapsed if no response was recorded. Also, there was an additional waiting duration that varied randomly between 1–1000 ms before the next trial commenced (see **Figure 1**). Participants were required to make (for a go stimulus) or withhold (for a no-go stimulus) a response as soon and as accurately as possible.

The total number of trials in the no-go probability condition block was 960. The probabilities of no-go stimuli were 20% (192 trials), 50% (480 trials), and 80% (768 trials), respectively. Among the no-go trials, cfNOGO and irNOGO stimuli comprised 50% each. There were at least 36 practice trials (more trials if necessary) before each condition block. During the practice session, feedback of "correct" or "incorrect" was given at the end of each trial

**TABLE 1 | The demographic information for all participants in all conditions.**

| | 20% no-go | | 50% no-go | | 80% no-go | |
|---|---|---|---|---|---|---|
| | Younger | Older | Younger | Older | Younger | Older |
| Gender (male/female) | 7/9 | 7/9 | 8/8 | 8/8 | 7/9 | 7/9 |
| Age (year) | 21.31 (1.36) | 66.38 (4.43) | 21.31 (1.26) | 67.25 (4.59) | 21.63 (1.49) | 68.63 (5.88) |
| Education (year) | 15.69 (1.21) | 12.69 (2.08) | 15.00 (1.06) | 12.56 (3.48) | 15.44 (1.17) | 13.31 (2.66) |
| BDI | 3.44 (2.06) | 5.25 (4.71) | 4.69 (3.58) | 6.69 (3.58) | 3.69 (2.17) | 4.25 (3.44) |
| MMSE | 28.63 (0.60) | 27.06 (1.14) | 28.50 (0.71) | 26.69 (1.10) | 28.19 (1.01) | 27.19 (0.73) |

*BDI, Beck Depression Inventory; MMSE, Mini-Mental State Examination; the value in each cell denotes the mean, and the value in each bracket denotes standard deviation.*

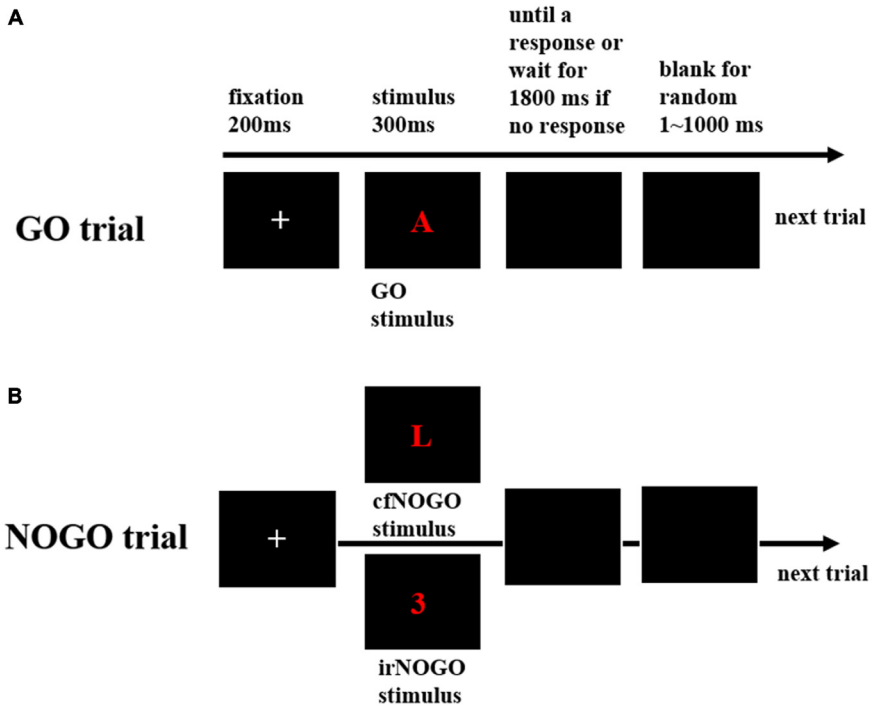


**FIGURE 1 | The behavioral paradigm. (A)** Schematic representation of the events in a go trial, including a fixation, followed by a go stimulus; **(B)** Schematic representation of the events in a no-go trial, including a fixation, followed by either of the two no-go stimuli, irrelevant (irNOGO) and conflict (cfNOGO).

to facilitate the participants' familiarization with the response rule.

## EEG Recording

The participants were seated in a comfortable chair in a sound-attenuated room during the experiment. Electroencephalography (EEG) activity was continuously recorded using Neuroscan SynAmp2 amplifier and Q-Cap (Neuroscan Q-Cap: AgCl-32 electrode cap; Neuroscan, Inc., El Paso, TX, USA) from 32 scalp electrodes. The vertical electrooculogram (EOG) was recorded by two electrodes 2 cm above and 2 cm below the left eye, and the horizontal EOG was recorded by two electrodes 1 cm external to the outer canthus of each eye. A ground electrode was placed on the forehead. The electrodes were initially referenced online to the left mastoid and offline to the average of the left and right mastoids. Electrode impedances were maintained below 5 kΩ. The EEG and EOG signals were amplified and digitized at a sampling rate of 500 Hz, with an online high-pass filter of 0.1 Hz and a low-pass filter of 30 Hz. Ocular artifacts associated with blinks were corrected by the ocular reduction command offered by the Neuroscan software (Neuroscan, Inc., El Paso, TX, USA) and were then further removed via an algorithm (Neuroscan software) that rejected any epoch if the signal was below $-50 \pm 50$ μV, if the drift of the EEG from baseline exceeded $-50 \pm 50$ μV, or if the A/D converts became saturated. The total rejection rate across the various conditions averaged approximately 23, 28 and 24% for each no-go probability condition block, respectively.

## Event-Related Potential (ERP) Analysis

We focused on the N2 and P3 components as they have been hypothesized to link inhibition and response conflict control processes. Moreover, because go and no-go trials involve different processes with respect to motor execution, we separated the ERP analyses of go trials from those of no-go trials. In each condition block, stimulus-locked epochs were taken from the continuous EEG signal and time-locked to the onset of the go/no-go stimulus from −50 ms to 800 ms for all recording channels. For each channel, all stimulus-locked epochs were baseline-corrected by obtaining the mean level of activity in the period from 50 ms before to 50 ms after target onset and then subtracting that average from the level of activity at the sample point. The N2 was found to be maximal at the FCz site, whereas the P3 was maximal at the Cz site in this study. Hence, we searched for the peak-to-peak amplitude at the FCz site during the time windows of 150–350 ms (positive dip) and 250–450 ms (negative peak) following the onset of the stimulus and then computed the voltage difference between the positive dip and negative peak as the stimulus-locked N2 peak-to-peak amplitude. Then, we searched for the peak latency and peak amplitude at the Cz site during the time window of 300–750 ms following the onset of the stimulus and then computed the voltage difference between the peak amplitude relative to the baseline as the stimulus-locked P3 peak amplitude and the time point at which the P3 peak amplitude occurred as the P3 peak latency.

## Statistical Analysis

The 2-way ANOVAs for the go trials were performed on the behavioral and ERP data, respectively, with two between-subject factors of age and no-go probability. The 3-way ANOVAs for the no-go trials were performed on the behavioral and ERP data, respectively, with two between-subjects factors of age and no-go probability and one within-subject factor of no-go stimulus types. *Post hoc* analysis following the significant effect of no-go probability (with three levels) was performed using Tukey tests. When two (or more) factors in the ANOVA showed a statistically significant interaction, we carried on analyzing the simple main effects which involve the examination of the effect of one factor at one level of the other factor. That is, the data were split for each level of one factor and one-way ANOVAs were conducted. Like any other one-way ANOVA with more than two levels, after the significant F, a *post hoc* Tukey test was conducted to find out which pair (or pairs) of means was (were) statistically different. To overcome the inflation of Type 1 error when a series of simple main effect analyses were conducted, we used the Bonferroni correction to adjust the $p$ value. In addition, in the choice of error term for simple main effect test, we followed the pooled error term approach advised by Howell (2010). That is, Mean Square Error (MSE) from the original factorial ANOVA was used as opposed to MSE from the follow-up one-way ANOVA in calculating the F for the simple main effects. The detailed steps for the calculation are described in Howell's (2010) book (e.g., ps. 483–488 in his book, "*Statistical Methods for Psychology*").

# RESULTS

## Behavioral Data Analysis

The first trial of each block and trials with RTs faster than 150 ms or slower than 1500 ms were discarded from further analysis. The behavioral results are shown in **Figure 2**, including the go trials' RT (**Figure 2A**) and omission rates (**Figure 2B**) and the no-go trials' commission errors (**Figure 2C**).

## Reaction Time (RT) on Go Trials

The 2-way ANOVA on the RTs of the go trials showed that the younger adults generally performed faster than the older adults, $F_{(1,90)} = 63.11$, $p < 0.001$, and that RTs were faster in the 20% no-go probability (high go-prepotency) and the 50% no-go probability (medium go-prepotency) conditions than in the 80% no-go probability (low go-prepotency) condition (no-go probability, $F_{(2,90)} = 21.42$, $p < 0.001$; all Tukey tests: $ps < 0.005$). There was no significant interaction between the two factors, $F_{(2,90)} = 2.61$, $p = 0.08$.

## Percentage of Error (PE) on Go Trials: Omission Errors

The 2-way ANOVA on the omission errors of the go trials showed that the younger adults generally performed better (fewer omission errors) than the older adults, $F_{(1,90)} = 15.20$, $p < 0.001$, and that omission errors were fewer in the 20 and 50% no-go probability conditions (3.46 and 3.04%) than in the 80% no-go probability condition (7.70%; $F_{(2,90)} = 4.92$, $p < 0.01$; all Tukey tests: $p < 0.05$). There was no significant interaction between the two factors, $F_{(2,90)} = 0.93$, $p = 0.40$.

## Percentage of Error (PE) on No-Go Trials: Commission Errors

The 3-way ANOVA on the commission errors of the no-go trials showed that there was no significant effect of age, $F_{(1,90)} = 2.14$, $p = 0.15$, but there was a significant effect of no-go probability, $F_{(2,90)} = 47.41$, $p < 0.0001$. Commission errors were more frequent in the 20% no-go probability condition (16.53%) than in the 50% (4.13%) and 80% no-go probability conditions (2.95%; all Tukey tests: $ps < 0.05$). There was also a significant effect of no-go stimulus type, $F_{(1,90)} = 88.31$, $p < 0.0001$, showing that irNOGO (4.78%) stimuli elicited fewer commission errors than cfNOGO (10.96%) stimuli. There was also a significant 2-way interaction between no-go probability and no-go stimulus type, $F_{(2,90)} = 26.52$, $p < 0.0001$. Follow-up tests for this interaction showed that the effect of no-go probability was significant on both cfNOGO trials ($F_{(2,90)} = 71.51$, $p < 0.0001$) and irNOGO trials ($F_{(2,90)} = 14.41$, $p < 0.001$), yet there was a larger effect on the cfNOGO trial type. In addition, the simple effect of the no-go stimulus type (fewer commission errors for the irNOGO than cfNOGO trials) was significant only in the 20 and 50% no-go probability conditions.

## Summary of Behavioral Data

To summarize, the older adults appeared to perform more poorly than the younger adults on go trials, as reflected by their slower go RTs and higher go omission errors; this age effect was not modulated by no-go probability. In contrast, the older adults counter-intuitively exhibited similar behavioral performance (i.e., equivalent commission errors) as compared to the younger adults. In addition, it appeared to be more difficult for both age groups to withhold a response to cfNOGO stimuli compared to irNOGO stimuli, based on the data of commission errors.

## Event-Related Potential (ERP) Data

ERPs associated with each condition and age group at the Fz, FCz, Cz, CPz, and Pz sites as well as topographic maps are shown in **Figures 3A,B** for go trials and **Figures 4A,B** for no-go trials.

## P3 Peak Latency on Go Trials

The 2-way ANOVA on the P3 peak latencies of go trials showed that the younger adults exhibited earlier P3 peak latencies than the older adults (young: 526.04 ms vs. old: 596.75 ms), $F_{(1,90)} = 26.63$, $p < 0.0001$, but there was no significant effect of no-go probability, $F_{(2,90)} = 0.81$, $p = 0.45$. There was also no significant 2-way interaction between age and no-go probability, $F_{(2,90)} = 1.11$, $p = 0.34$ (see **Figure 5A**).

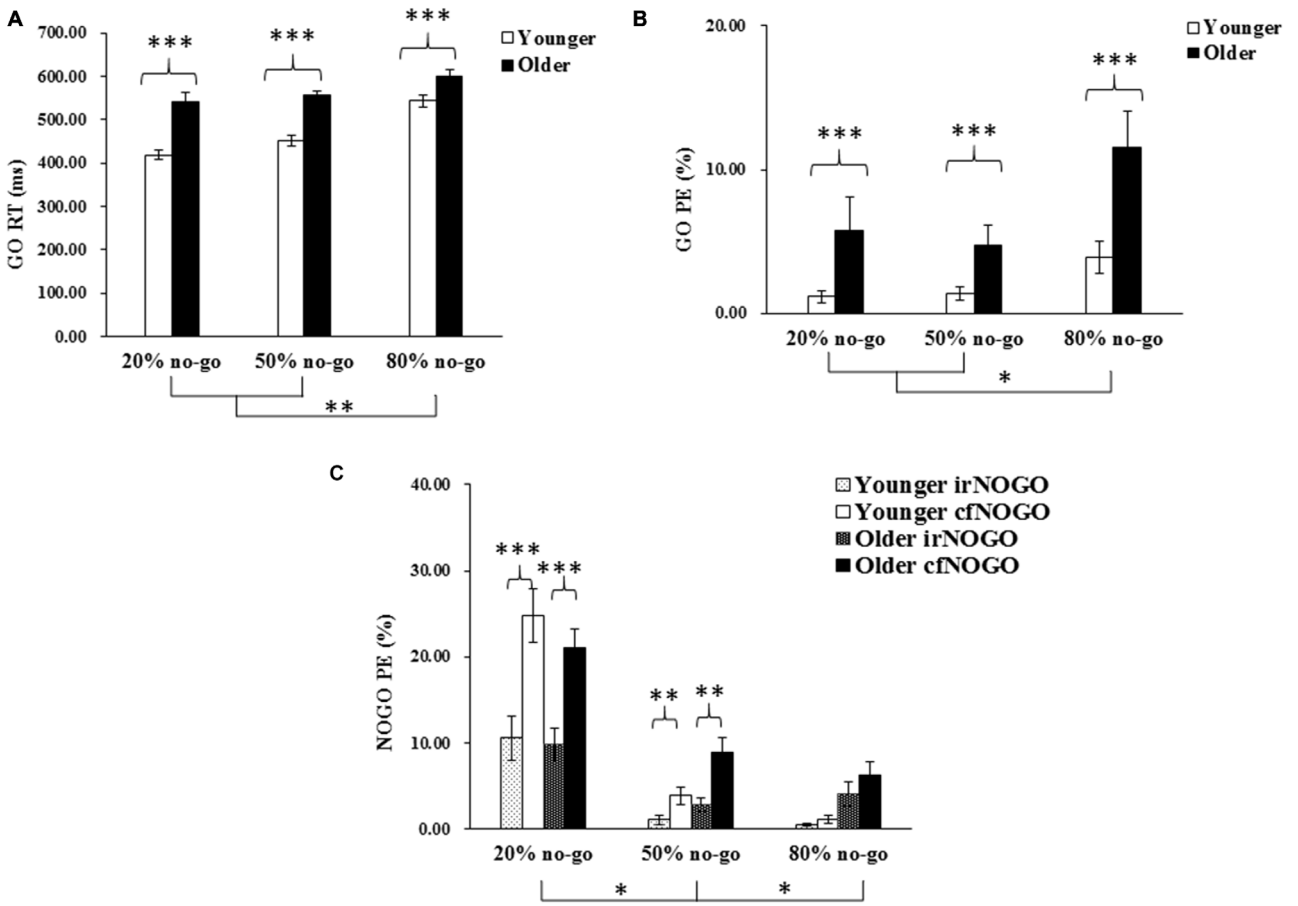


**FIGURE 2 | (A)** Mean response times (RTs; and standard errors of the mean) of correct responses (in milliseconds) to go stimuli as a function of age and no-go probability condition; **(B)** Mean percentage of errors (PE; and standard errors of the mean) of omitted responses to go stimuli as a function of age and no-go probability condition; **(C)** Mean percentage of errors (PE; and standard errors of the mean) of committed responses to no-go stimuli as a function of age and no-go probability condition. Significant effects are highlighted with $^{*}p < 0.05$, $^{**}p < 0.01$, or $^{***}p < 0.001$.

## P3 Peak Amplitude on Go Trials

The 2-way ANOVA on the P3 peak amplitudes of the go trials showed larger P3 peak amplitudes for the younger (12.53 μV) than older (7.01 μV) adults, $F_{(1,90)} = 34.58$, $p < 0.0001$, but no significant main effect of no-go probability, $F_{(2,90)} = 0.79$, $p = 0.46$. Yet, there was a significant 2-way interaction between age and no-go probability, $F_{(2,90)} = 4.94$, $p < 0.01$. A simple effect test following this interaction showed that the significant main effect of no-go probability occurred only for the younger adults, $F_{(2,90)} = 4.80$, $p < 0.05$, but not for the older adults, $F_{(2,90)} = 0.93$, $p = 0.40$, and that the significant effect of age occurred in the 50%, $F_{(1,90)} = 11.49$, $p < 0.005$, and 80%, $F_{(1,90)} = 31.59$, $p < 0.0001$, no-go probability conditions but not in the 20% no-go probability conditions, $F_{(1,90)} = 1.38$, $p = 0.24$ (see **Figure 5B**).

## P3 Peak Latency on No-Go Trials

The 3-way ANOVA on the P3 peak latencies of no-go trials showed that the younger adults exhibited earlier P3 peak latencies than the older adults (young: 516.35 ms vs. old: 641.46 ms), $F_{(1,90)} = 162.85$, $p < 0.001$, and that irNOGO stimuli elicited earlier P3 peak latencies than cfNOGO stimuli, $F_{(1,90)} = 30.42$, $p < 0.0001$. There were no significant effect of no-go probability and any interactions (age × type of no-go stimulus: $F_{(1,90)} = 2.03$, $p = 0.16$; no-go probability × type of no-go stimulus: $F_{(2,90)} = 0.08$, $p = 0.93$; age × type of no-go stimulus × no-go probability: $F_{(2,90)} = 0.922$, $p = 0.40$, see **Figure 6A**.

## P3 Peak Amplitude on No-Go Trials

The 3-way ANOVA on the P3 peak amplitudes of the no-go stimuli showed that P3 peak amplitudes for the no-go trials were larger in the 20% no-go probability condition than in the 50 and 80% no-go probability conditions, $F_{(2,90)} = 15.58$, $p < 0.0001$ (all Tukey tests: $ps < 0.01$). There was also a significant 2-way interaction between age and no-go stimulus type, $F_{(1,90)} = 13.49$, $p < 0.001$.

A simple effect test on the interaction between age and no-go stimulus type showed that only older adults exhibited larger P3 peak amplitudes for irNOGO stimuli than for cfNOGO stimuli but not for the younger adults (young: $F_{(1,90)} = 1.80$, $p = 0.19$; old: $F_{(1,90)} = 14.83$, $p < 0.001$; see **Figure 6B**).

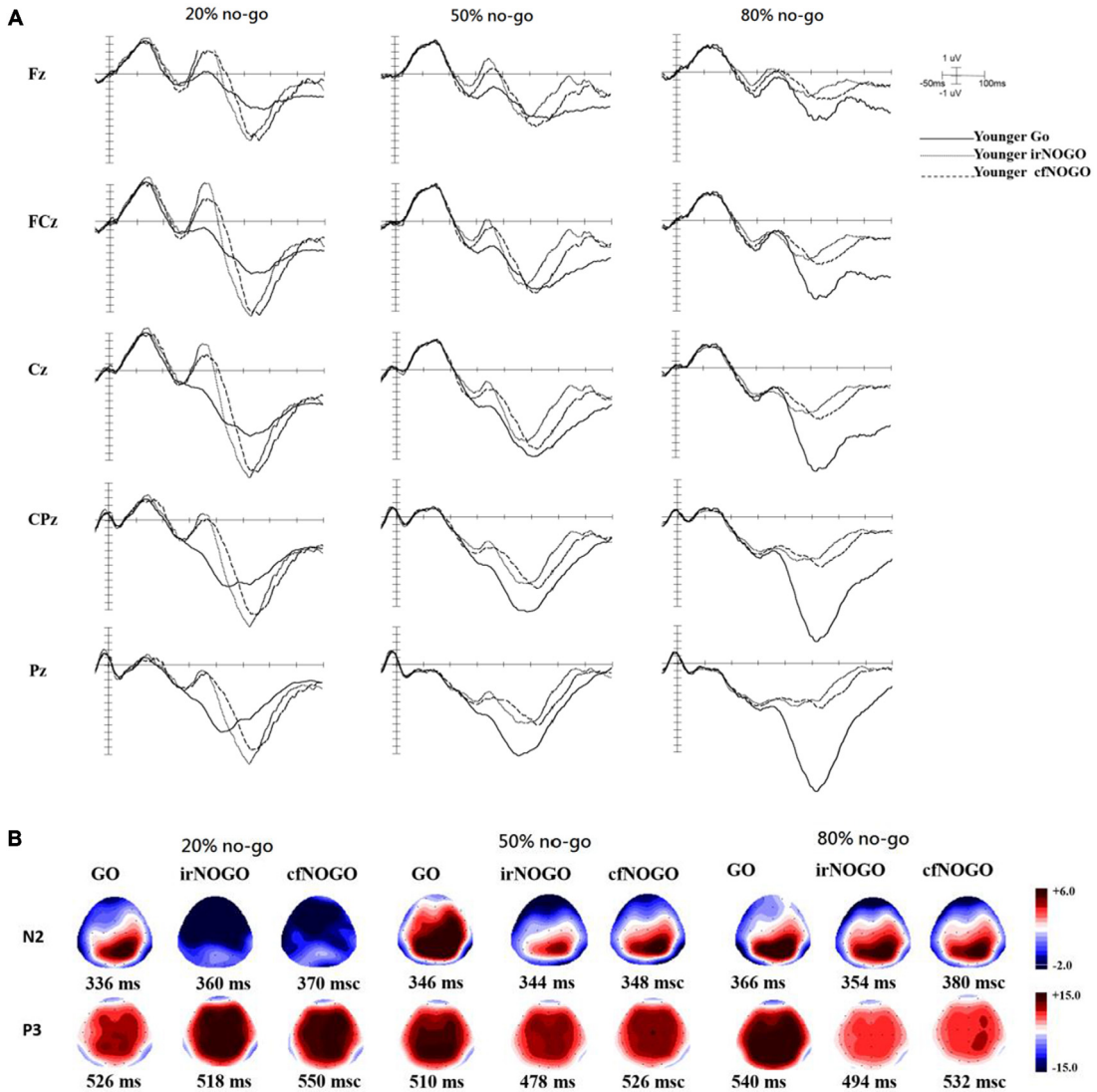


**FIGURE 3 | (A)** ERP waveforms as a function of no/no-go condition (GO, irNOGO, cfNOGO) and no-go probability condition at five representative electrodes of Fz, FCz, Cz, CPz, and Pz for the younger adults. **(B)** Topographic maps of the GO N2, irNOGO N2, cfNOGO N2, GO P3, irNOGO P3, and cfNOGO P3, separately for each no-go probability condition and for the younger adults. Each map describes the topographic distribution at the peak latency for each condition.

## Summary of the P3 Findings

### Go P3 Peak Latency and Amplitude

For the go P3 peak latency, there was a significant effect of age that showed an earlier P3 peak latency for the younger adults. As for the go P3 peak amplitude, the significant effect of aging (younger larger than older) occurred only in the 50 and 80% no-go probability conditions. In addition, the significant effect of no-go probability occurred only for the younger adults, i.e., showing smaller go P3 peak amplitudes in the 20% than 80% no-go probability condition but not for the older adults.

### No-Go P3 Peak Latency and Amplitude

The significant effect of age was found for the overall no-go P3 peak latency. In addition, both age groups exhibited earlier P3 peak latencies for the irNOGO trials compared to the cfNOGO trials. As for the no-go P3 peak amplitude, there was a significant effect of no-go probability for both age groups, showing larger no-go P3 peak amplitudes in the 20% no-go probability conditions compared to the 50 and 80% no-go probability conditions. More importantly, only the older adults exhibited larger P3 peak amplitudes for the irNOGO trials compared to the cfNOGO trials. These results suggested that while the younger adults exhibited similar no-go P3 peak amplitudes between the irNOGO and cfNOGO trials, the older adults exhibited more prominent P3 peak amplitudes for the irNOGO than cfNOGO trials. Subsequently, this phenomenon resulted in a significant effect of age for the cfNOGO trials but not for the irNOGO trials.

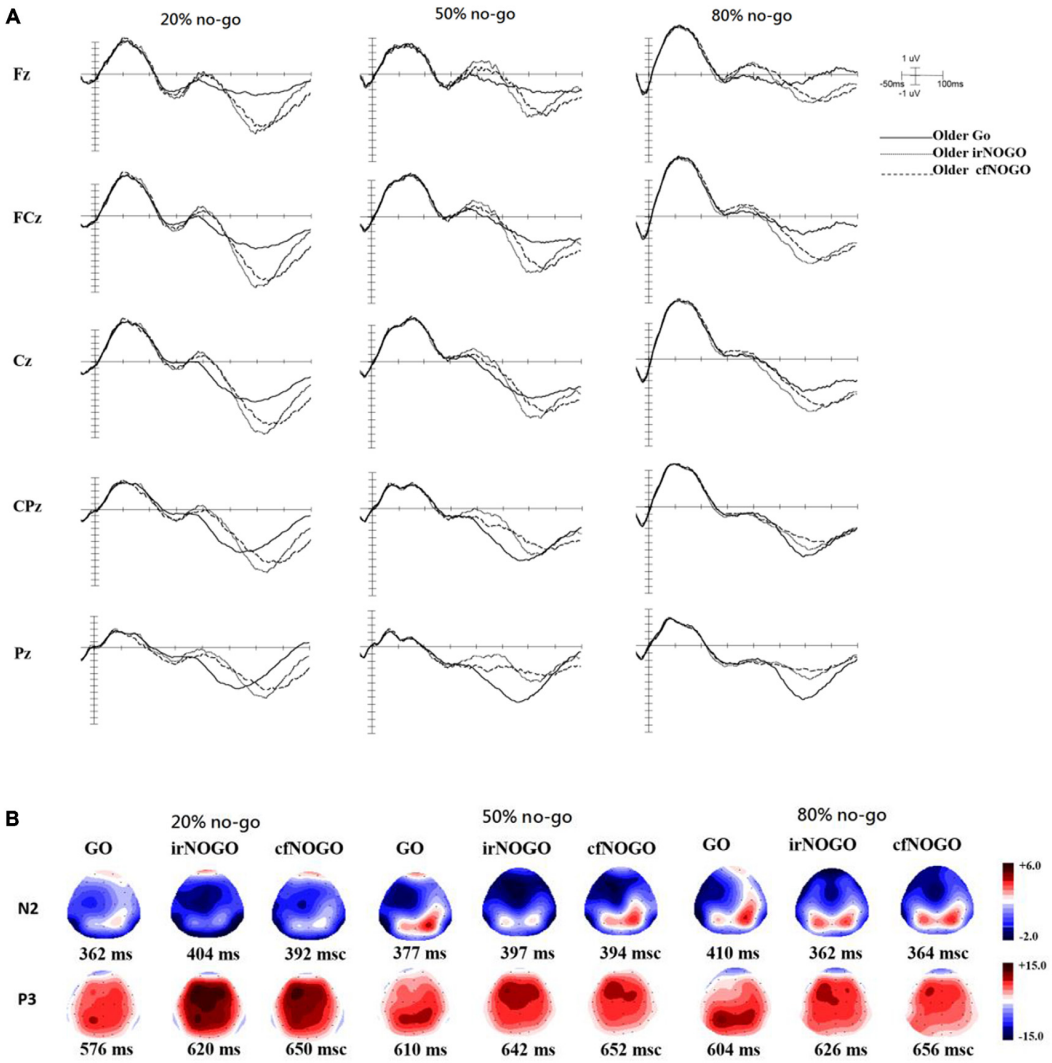


**FIGURE 4 | (A)** ERP waveforms as a function of no/no-go condition (GO, irNOGO, cfNOGO) and no-go probability condition at five representative electrodes of Fz, FCz, Cz, CPz, and Pz for the older adults. **(B)** Topographic maps of the GO N2, irNOGO N2, cfNOGO N2, GO P3, irNOGO P3, and cfNOGO P3, separately for each no-go probability condition and for the older adults. Each map describes the topographic distribution at the peak latency for each condition.

## N2 Peak-to-Peak Amplitude on Go Trials

The 2-way ANOVA on the N2 peak-to-peak amplitudes of the go trials showed no significant effects or interactions (age: $F_{(1,90)} = 1.24$, $p = 0.27$; no-go probability: $F_{(2,90)} = 1.35$, $p = 0.27$; age $x$ no-go probability: $F_{(2,90)} = 1.89$, $p = 0.19$; see **Figure 7**).

## N2 Peak-to-Peak Amplitude on No-Go Trials

The 3-way ANOVA on the N2 peak-to-peak amplitudes of no-go stimuli showed that the younger adults exhibited larger N2 peak-to-peak amplitudes (−5.97 μV) than the older adults (−4.52 μV), $F_{(1,90)} = 8.24$, $p < 0.01$. Also, N2 peak-to-peak amplitudes were larger in the 20% no-go probability condition compared to the 50% no-go probability condition and amplitudes in the latter condition were larger than amplitudes in the 80% no-go probability condition, $F_{(2,90)} = 33.87$, $p < 0.0001$ (all Tukey tests: $ps < 0.01$). There was also a significant effect of no-go stimulus type, $F_{(1,90)} = 7.61$, $p < 0.01$; this indicates that irNOGO stimuli elicited larger N2 peak-to-peak amplitudes than cfNOGO stimuli. There were significant 2-way interactions between age and no-go probability, $F_{(2,90)} = 3.78$, $p < 0.05$, and between no-go probability and no-go stimulus type, $F_{(2,90)} = 7.34$, $p < 0.005$.

The simple effect test for the interaction between age and no-go probability showed that the effect of age was only significant for the 20% no-go probability condition, where the younger adults exhibited larger N2 peak-to-peak amplitudes than older adults. On the other hand, both age groups exhibited significant effects for the no-go probability on the N2 peak-to-peak amplitude.

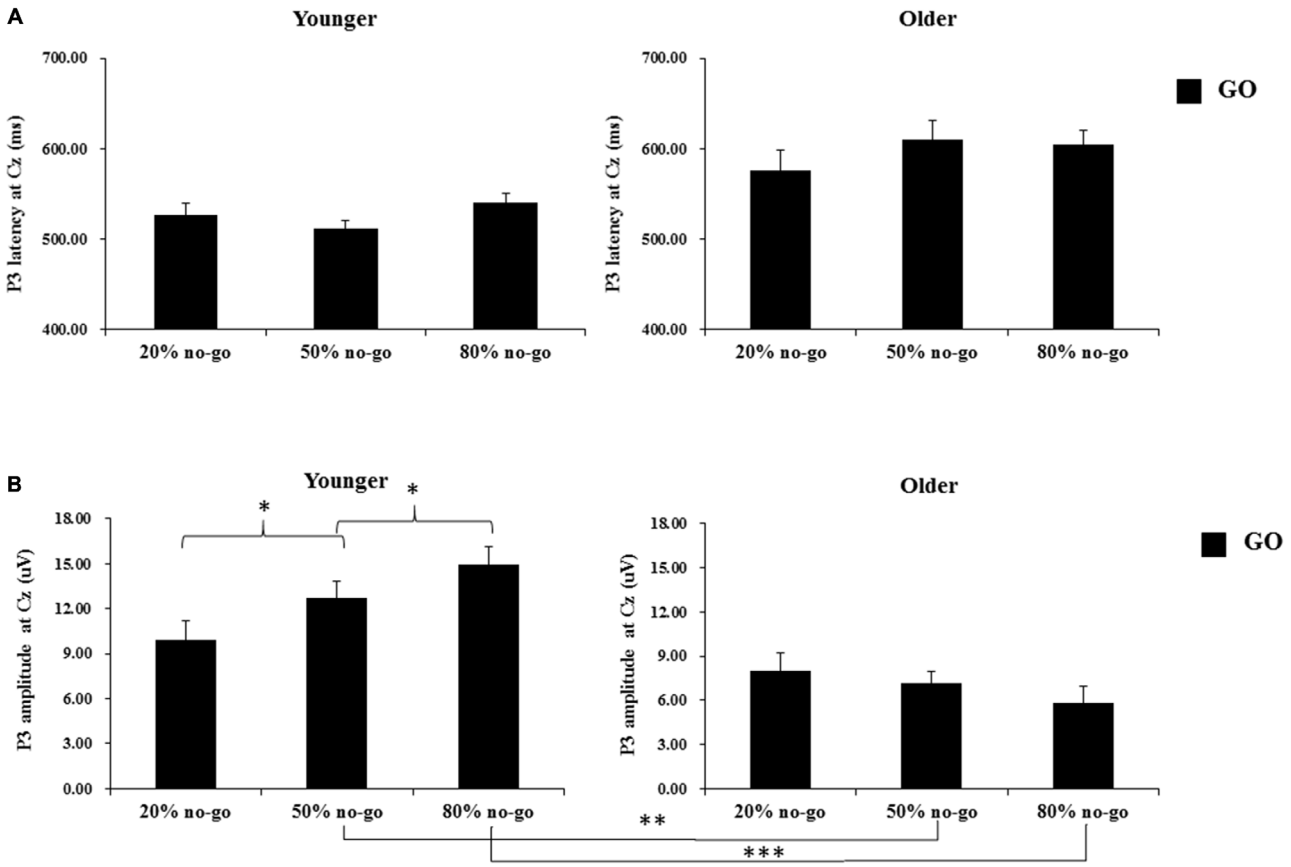


**FIGURE 5 | (A)** Grand mean P3 peak latencies (in milliseconds) at the Cz site as a function of no-go probability condition for GO trials and for the younger (upper left panel) and older (upper right panel) adults, respectively. Error bars represent standard errors; **(B)** Grand mean P3 peak amplitudes (in μV) at the Cz site as a function of no-go probability condition for GO trials and for the younger (lower left panel) and older (lower right panel) adults, respectively. Error bars represent standard errors. Significant effects are highlighted with $^{*}p < 0.05$, $^{**}p < 0.01$, or $^{***}p < 0.001$.

The simple effect test on the interaction of no-go probability and no-go stimulus type nevertheless showed a significant main effect of no-go stimulus type (i.e., the irNOGO trials elicited larger N2 amplitudes than cfNOGO trials) in the 20% no-go probability condition, $F_{(1,90)} = 20.03$, $p < 0.0001$, but not for the 50 and 80% no-go probability condition (50%: $F_{(1,90)} = 1.46$, $p = 0.23$; 80%: $F_{(1,90)} = 0.81$, $p = 0.37$). Furthermore, for both the irNOGO and cfNOGO stimuli, the amplitudes were larger in the 20% no-go probability condition than in the 50 and 80% no-go probability condition (all $ps < 0.05$; see **Figure 8**).

## Summary of the N2 Findings

### Go N2 Peak-to-Peak Amplitude

The significant effect of no-go probability on go N2s occurred only for the younger adults and between the 50 and 80% no-go probability conditions, whereas none of the significant main effects and interactions were found for the older adults.

### No-Go N2 Peak-to-Peak Amplitude

The significant effect of age (i.e., the younger adults exhibited larger N2 amplitudes than the older adults) on no-go N2s occurred mainly in the 20% no-go probability condition. In addition, the significant effect of no-go trial type (i.e., irNOGO trials exhibited larger N2 amplitudes than cfNOGO trials) was found only for the 20% no-go probability condition for both age groups. Furthermore, for both the irNOGO and cfNOGO stimuli, the amplitudes were larger in the 20% no-go probability condition than in the 50 and 80% no-go probability conditions.

## DISCUSSIONS

The aim of this study was to evaluate whether older adults exhibited selective inhibition deficit by using a go/no-go paradigm with the manipulation of no-go stimulus-type and no-go probability. The current behavioral results showed that the older adults performed more poorly than the younger adults as reflected from their slower RTs and their higher omission errors in the go trials. This age difference was not further modulated by no-go probability, despite the fact that there was a significant effect of no-go probability on both RTs and omission errors. Interestingly, in contrast to the inferior performance on go trials for the older adults compared to the younger adults, the older adults counter-intuitively exhibited similar behavioral

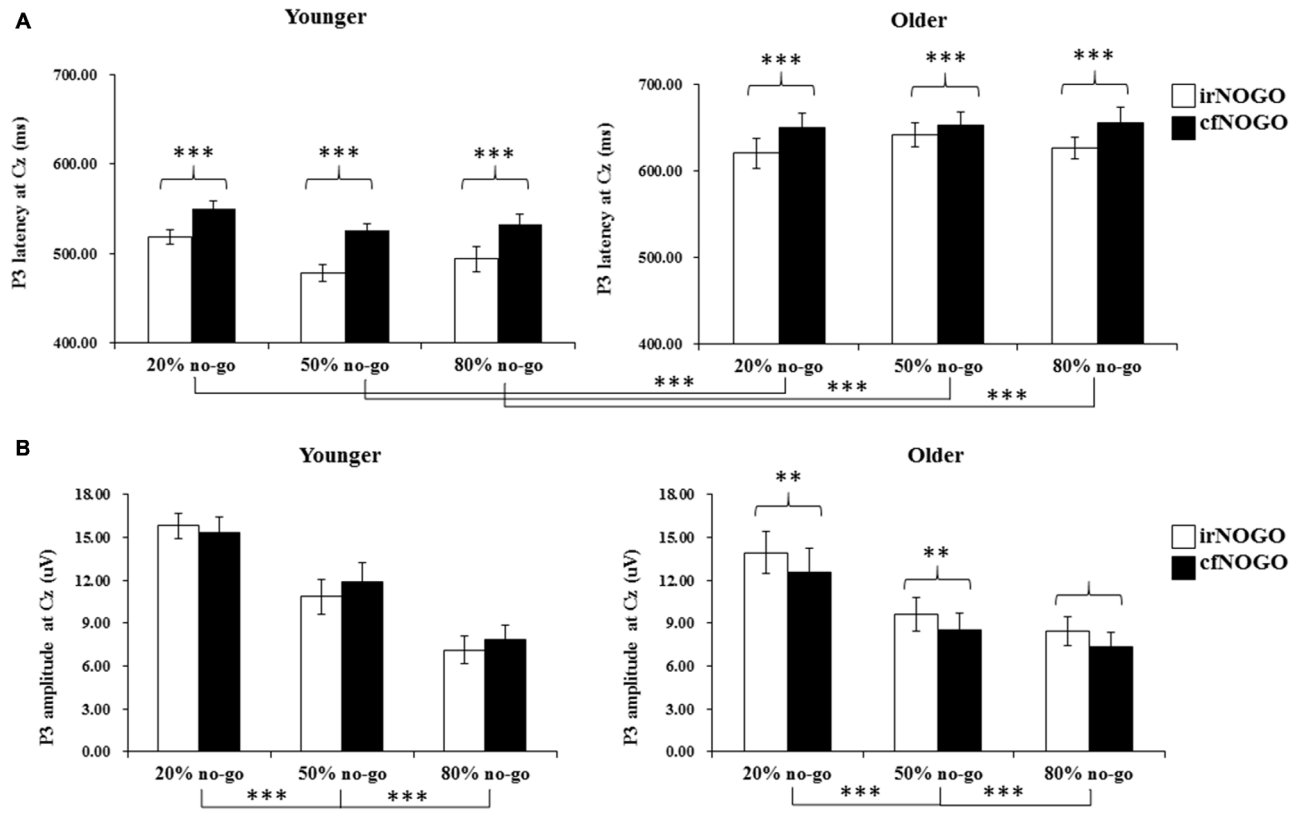


**FIGURE 6 | (A)** Grand mean P3 peak latencies (in milliseconds) at the Cz site as a function of no-go probability condition for NOGO (irNOGO and cfNOGO) trials and for the younger (upper left panel) and older (upper right panel) adults, respectively. Error bars represent standard errors; **(B)** Grand mean P3 peak amplitudes (in μV) at the Cz site as a function of no-go probability condition for NOGO (irNOGO and cfNOGO) trials and for the younger (lower left panel) and older (lower right panel) adults, respectively. Error bars represent standard errors. Significant effects are highlighted with $^{**}p < 0.01$, or $^{***}p < 0.001$.

performance on no-go trials (i.e., equivalent commission errors) as compared to the younger adults. These results seemed to suggest that the older adults were capable of inhibiting the no-go trials. In addition, based on the no-go commission error data, it appeared to be more difficult for both younger and older adults to withhold a response to cfNOGO stimuli compared to irNOGO stimuli. Yet, since the behavioral no-go performance can only be measured with commission errors, it is interesting to examine whether or not the underlying neural activity for the no-go trials, as reflected by the ERPs, would be also similar, as shown in the behavioral data between the two age groups.

The current ERP data showed that for the younger adults, the cfNOGO stimuli were associated with smaller N2 amplitudes than those of the irNOGO stimuli, specifically for the 20%

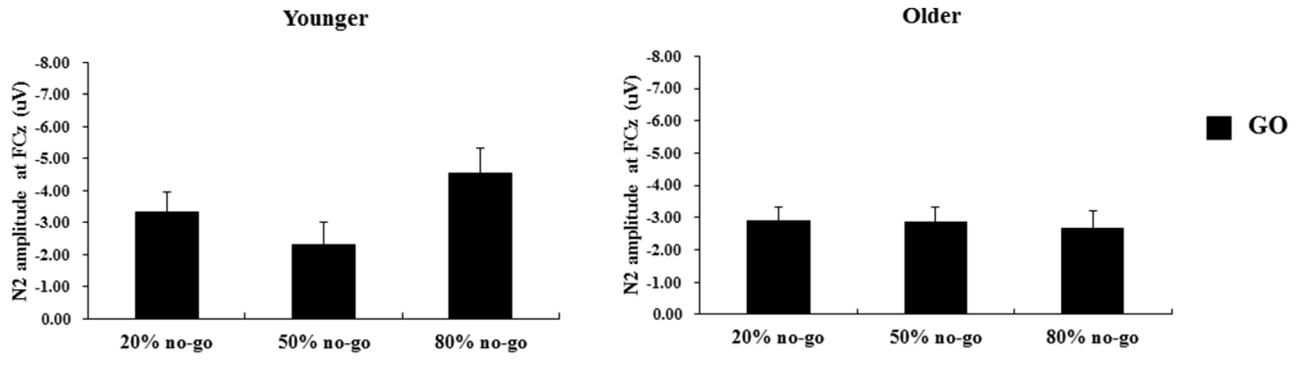


**FIGURE 7 | Grand mean N2 peak-to-peak amplitudes (in μV) at the FCz site as a function of no-go probability condition for GO trials and for the younger (left panel) and older (right panel) adults, respectively. Error bars represent standard errors.**

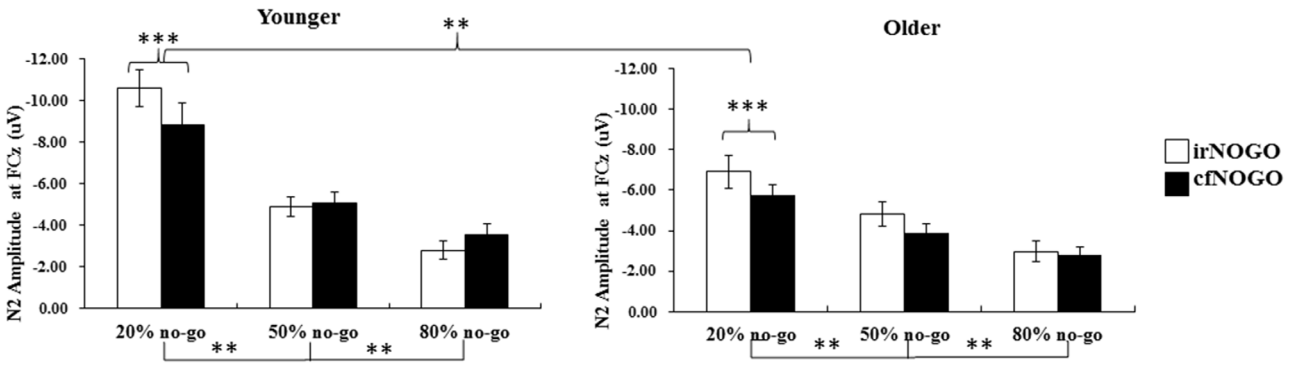


**FIGURE 8 | Grand mean N2 peak-to-peak amplitudes (in μV) at the FCz site as a function of no-go probability condition for NOGO (irNOGO and cfNOGO) trials and for the younger (left panel) and older (right panel) adults, respectively.** Error bars represent standard errors. Significant effects are highlighted with $^{**}p < 0.01$, or $^{***}p < 0.001$.

no-go probability condition. Previous research has argued that the N2 enhancement of the no-go trials either reflects the operation of a cognitive top-down inhibition mechanism needed to suppress the incorrect tendency to respond or reflects an electrophysiological correlate of conflict between go and no-go response representations that is detected in ACC (Nieuwenhuis et al., 2003). Since the current results showed that the cfNOGO trials were associated with smaller N2 amplitudes and were accompanied with more commission errors than the irNOGO trials (but only for the 20% no-go trial condition), this suggests that either the younger adults experienced less conflict and hence recruited less control processes for the cfNOGO trials than irNOGO trials based on the conflict hypothesis of N2 (Falkenstein et al., 2001; Van Veen and Carter, 2002a,b) or they were less able to inhibit the cfNOGO stimuli based on the inhibition account (Roche et al., 2005). Nevertheless, since we additionally observed that N2 peak-to-peak amplitudes were also modulated by the no-go stimulus probability for the younger adults, the results appeared to be more consistent with the results reported by Nieuwenhuis et al. (2003); see also Smith et al. (2008), who suggested that N2 may reflect response conflict rather than inhibition *per se*.

More importantly, in the current study, the older adults paradoxically exhibited larger P3 amplitudes for the irNOGO than cfNOGO trials, whereas behaviorally they committed more errors in the cfNOGO than irNOGO trials. This seems to suggest that the older adults recruited more control processes in order to conquer the commitment of responses for the no-go trials, especially for the irNOGO trials. The more direct evidence that supports this speculation comes from the correlational analysis between the behavioral performance and P3 amplitudes. The correlation was significant ($r = 0.51$, $p < 0.001$; see **Figure 9**) and showed that better performance (i.e., lower PE) inhibiting the no-go trials was associated with larger the P3 amplitudes in the no-go trials, relative to go trials. This finding was consistent with Vallesi et al. (2009), who showed that the irNOGO trials seemed to be more distracting (and hence cause a larger conflict N2) for the older adults to withhold the response; hence, the older adults needed to recruit more control processes in withholding the response towards the irNOGO trials than the cfNOGO trials, as reflected by their larger no-go P3 peak amplitudes for the irNOGO than cfNOGO trials. However, no such phenomenon was found for the younger adults. This age-related compensatory response (i.e., conquering the irNOGO stimuli with the price of poorer performance of the cfNOGO stimuli) were specifically seen in the 20% no-go trial probability condition. The manipulation of the low probability of no-go trials has proved successful in activating frontal lobe structures associated with executive control in other response inhibition tasks (MacDonald et al., 2000). Hence, in this scenario, the older adults might thus recruit more compensatory responses in withholding the responses towards the no-go trials. This might also explain why there was no age effect seen in the behavioral no-go commission errors due to the compensatory responses.

The current finding that the older adults were more distracted by the irNOGO stimuli than the cfNOGO stimuli appears to be consistent with previous reports in the memory research domain, which suggests that older adults (more pronounced after age 65) suffer from increasing vulnerability to internal distraction and weakening concentration skills due to subtle changes in brain activity (Grady et al., 2006). Grady et al. (2006) found that older adults have difficulty activating brain regions necessary for concentration (e.g., reading) and de-activating or tuning down other regions that are associated with internal thoughts (e.g., thinking about yourself, what you did yesterday). Two key regions of the brain that allow the mind to focus on a single task and tune out unwanted thoughts get out of kilter much earlier in life than previously suspected. When the mind pays strict attention, special neural circuits in the prefrontal cortex become more active, and at the same time, related brain areas in the medial frontal lobe (monitoring more general background activity) slack off. Conversely, when the mind is at rest, the level of brain activity in these two regions is then reversed. Such a seesaw activity pattern can begin to break down during memory tasks starting at about age 40.

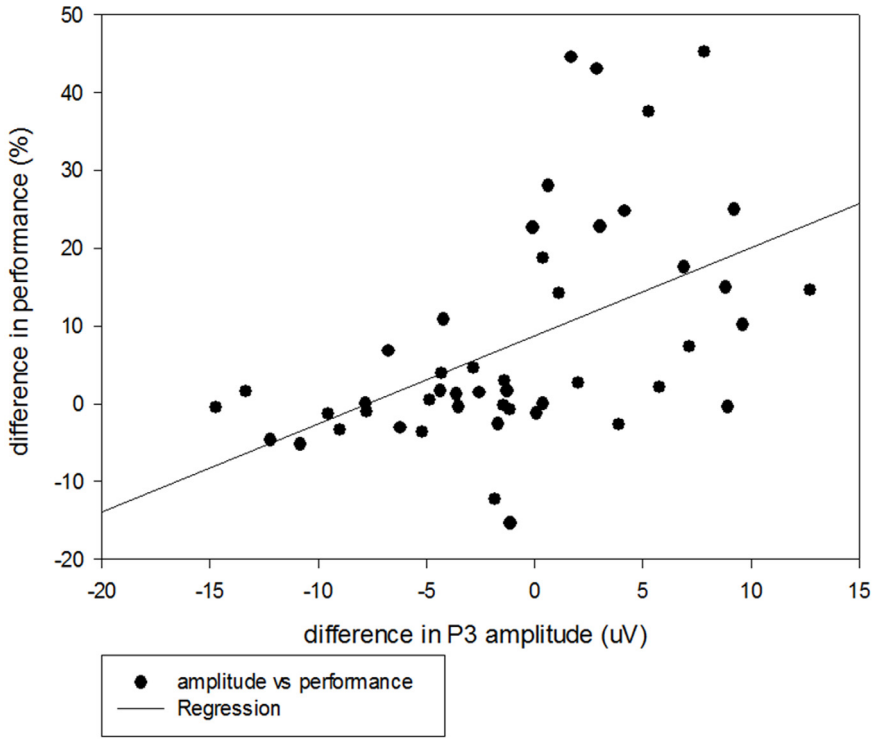


**FIGURE 9 | Scatterplot with regression line illustrating the correlation between P3 amplitudes (uV) and behavioral performance (%) for the irNOGO trials relative to GO trials across all three no-go probability conditions for the older adults.**

Another interesting finding of this study is that older adults seemed to devote more effort towards no-go trials, since the no-go probability effect was only seen significantly for the no-go trials, whereas the effect of no-go probability was significant for both the go and no-go trials for the younger adults. While the younger adults exhibited the conventional larger P3 amplitudes on go trials in the low go-prepotency condition than in the high go-prepotency condition, the older adults did not show such a pattern. It is therefore not surprising to observe a significant age effect on the go P3 amplitudes in the 50 and 80% no-go probability conditions rather than in the 20% no-go probability condition ($p = 0.24$). On the other hand, the amplitudes of both N2 and P3 on the no-go trials were found to vary significantly as a function of the relative frequency of no-go probability (20, 50 and 80%) conditions for both age groups. These results suggest that the older adults (similarly to the younger adults) when withholding the responses could be influenced by the no-go trials' probability. Given that the older adults were not influenced by the go trials' probability when executing the responses for the go trials but that they were influenced by the no-go trials' probability when withholding the responses on no-go trials, we could suspect that the older adults seemed to devote more effort to the no-go trials since it was more effortful for them to withhold the responses; hence, they were more sensitive to the no-go trials' probability.

Some final issues should be noted. First, this study used a between-subjects design for the factor of no-go probability which might underestimate the effect of no-go probability on the current results, and therefore the current interpretations regarding the interactions with the no-go probability should be treated with caution. Second, although the MMSE scores for the elderly participants in the current study were all within the normal range (on average 26–28), one may be still concerned that these elderly might exhibit an early sign of mild cognitive impairment. Nevertheless, since we have run ANCOVAs using MMSE as a covariate factor and the result patterns remained the same as reported here, we believe that although the older adults exhibited lower MMSE scores, they did not confound the current findings. Third, the topography of the no-go P3 in the older adults (**Figure 4B**) seems to be more frontally distributed compared with the younger adults who showed a more central distribution (**Figure 3B**). This might be a hint toward a posterior-anterior shift in aging (PASA, see Davis et al., 2008). In order to examine if the current findings were consistent with the theory of PASA, we re-ran ANOVAs for the P3 data with an additional factor of electrode sites of FCz, Fz, and Cz. The results of the 4-way ANOVAs showed no significant interactions of electrode sites with all other factors, except its own significant effect; hence, the current data did not seem to show a PASA effect for the elderly. Finally, it has been reported in previous studies that older adults showed similar (Falkenstein et al., 2002) and sometimes stronger no-go P3 amplitudes (Hong et al., 2014) compared with younger adults. However, in this study, it seems that older adults showed smaller no-go P3 amplitudes

(**Figure 6B**). Yet, it is important to note that Falkenstein et al. (2002) and Hong et al. (2014) used the P3 difference wave (P3d: no-go minus go ERPs) rather than the absolute no-go P3 amplitude, as reported in this study. When we subtracted go ERPs from no-go ERPs, we likewise observed similar P3d amplitudes (in 20% condition) and larger P3d amplitudes (in both 50 and 80% conditions) for the older adults compared with the younger adults. We decided to report go and no-go ERPs separately because of the following reasons: (1) go and no-go trials involve different processes with respect to motor execution and (2) we were more interested in contrasting irNOGO and cfNOGO trials.

To conclude, using ERP data the current study revealed that older adults were more prone to distraction induced by irNOGO stimuli, and therefore they exerted more control processes to conquer such distraction. Furthermore, older adults tended to devote more effort to withholding responses towards the no-go trials, especially in the condition where more control demand was needed (e.g., in the 20% no-go trials' probability in this study). This study provided a deeper understanding into how older adults adopted strategies in performing the go/no-go task (e.g., devoting attention to no-go trials in order to cope with their deficient inhibition ability). This interpretation appears to be contradictory to the well-known aging hypothesis of inhibition deficits (Hasher and Zacks, 1988). Yet, given that previous research has already demonstrated that older adults would develop a strategy to cope with some task scenarios, we suggest in the current study that older adults performing the go/no-go task adopted a compensating strategy of paying more attention to the no-go trials.

## ETHICS STATEMENT

The study was approved by the Ethical committee of the National Cheng Kung University in accordance with the Declaration of Helsinki. Written informed consent was obtained from all subjects before the experiment.

## AUTHOR CONTRIBUTIONS

SH designed the experiment, wrote the grant proposal, guided in executing the experiment, interpreted the data, and wrote the manuscript; MU analyzed the data, plotted the figures; C-HT conducted the experiment and collected the data.

## ACKNOWLEDGMENTS

We would like to thank the Ministry of Science Technology (MOST) of the Republic of China, Taiwan for financially supporting this research (Contract No. 101-2410-H-006-046-MY3 and No. 104-2410-H-006-021-MY2). In addition, this research was, in part, supported by the Ministry of Education, Taiwan, R.O.C., The Aim for the Top University Project to the National Cheng Kung University (NCKU). We also wish to thank American Manuscript Editors (AmericanManuscriptEditors.com) for English proofreading.

## REFERENCES

Bokura, H., Yamaguchi, S., Matsubara, M., and Kobayashi, S. (2002). Frontal lobe contribution to response inhibition process—an ERP study and aging effect. *Int. Congr. Ser.* 1232, 17–20. doi: 10.1016/s0531-5131(01)00677-x

Bruin, K., and Wijers, A. (2002). Inhibition, response mode and stimulus probability: a comparative event-related potential study. *Clin. Neurophysiol.* 113, 1172–1182. doi: 10.1016/s1388-2457(02)00141-4

Cabeza, R., Anderson, N. D., Locantore, J. K., and McIntosh, A. R. (2002). Aging gracefully: compensatory brain activity in high-performing older adults. *Neuroimage* 17, 1394–1402. doi: 10.1006/nimg.2002.1280

Davis, S. W., Dennis, N. A., Daselaar, S. M., Fleck, M. S., and Cabeza, R. (2008). Que PASA? The posterior-anterior shift in aging. *Cereb. Cortex* 18, 1201–1209. doi: 10.1093/cercor/bhm155

Dempster, F. N. (1992). The rise and fall of the inhibitory mechanism: toward a unified theory of cognitive development and aging. *Dev. Rev.* 12, 45–75. doi: 10.1016/0273-2297(92)90003-k

Dennis, N. A., and Cabeza, R. (2008). "Neuroimaging of healthy cognitive aging," in *The Handbook of Aging and Cognition*, Vol. 3, eds F. I. M. Craik and T. A. Salthouse (Mahwah, NJ: Lawrence Erlbaum Associates), 1–54.

Donchin, E., and Coles, M. G. (1988). Is the P300 component a manifestation of context updating? *Behav. Brain Sci.* 11, 357–374. doi: 10.1017/s0140525x00058027

Falkenstein, M., Hoormann, J., and Hohnsbein, J. (2001). Changes of error-related ERPs with age. *Exp. Brain Res.* 138, 258–262. doi: 10.1007/s002210100712

Falkenstein, M., Hoormann, J., and Hohnsbein, J. (2002). Inhibition-related ERP components: variation with modality, age and time-on-task. *J. Psychophysiol.* 16, 167–175. doi: 10.1027/0269-8803.16.3.167

Fallgatter, A. J., and Strik, W. K. (1999). The NoGo-anteriorization as a neurophysiological standard-index for cognitive response control. *Int. J. Psychophysiol.* 32, 233–238. doi: 10.1016/s0167-8760(99)00018-5

Folstein, M. F., Folstein, S. E., and McHugh, P. R. (1975). "Mini-mental state": a practical method for grading the cognitive state of patients for the clinician. *J. Psychiatr. Res.* 12, 189–198. doi: 10.1016/0022-3956(75)90026-6

Ford, J. M., Gray, M., Whitfield, S. L., Turken, U., Glover, G., Faustman, W. O., et al. (2004). Acquiring and inhibiting prepotent responses in schizophrenia: event-related brain potentials and functional magnetic resonanceimaging. *Arch. Gen. Psychiatry* 61, 119–129. doi: 10.1001/archpsyc.61.2.119

Grady, C. L., Springer, M. V., Hongwanishkul, D., McIntosh, A. R., and Winocur, G. (2006). Age-related changes in brain activity across the adult lifespan. *J. Cogn. Neurosci.* 18, 227–241. doi: 10.1162/jocn.2006.18.2.227

Hasher, L., and Zacks, R. T. (1988). Working memory, comprehension and aging: a review and new view. *Psychol. Learn. Motiv.* 30, 193–225. doi: 10.1016/s0079-7421(08)60041-9

Hong, X., Sun, J., Bengson, J. J., and Tong, S. (2014). Age-related spatiotemporal reorganization during response inhibition. *Int. J. Psychophysiol.* 93, 371–380. doi: 10.1016/j.ijpsycho.2014.05.013

Howell, D. C. (2010). *Statistical Methods for Psychology*. 7th Edn. Belmont, CA: Thomson Wadsworth.

Hsieh, S., and Fang, W. (2012). Elderly adults through compensatory responses can be just as capable as young adults in inhibiting the flanker influence. *Biol. Psychol.* 90, 113–126. doi: 10.1016/j.biopsycho.2012.03.006

Hsieh, S., and Lin, Y.-C. (2014). The boundary condition for observing compensatory responses by the elderly in a flanker-task paradigm. *Biol. Psychol.* 103, 69–82. doi: 10.1016/j.biopsycho.2014.08.008

Hsieh, S., Liang, Y.-C., and Tsai, Y.-C. (2012). Do age-related changes contribute to the flanker effect? *Clin. Neurophysiol.* 123, 960–972. doi: 10.1016/j.clinph.2011.09.013

Lucci, G., Berchicci, M., Spinelli, D., Taddei, F., and Di Russo, F. (2013). The effects of aging on conflict detection. *PLoS One* 8:e56566. doi: 10.1371/journal.pone.0056566

MacDonald, A. W., III, Cohen, J. D., Stenger, V. A., and Carter, C. S. (2000). Dissociating the role of the dorsolateral prefrontal and anterior cingulate cortex in cognitive control. *Science* 288, 1835–1838. doi: 10.1126/science.288.5472.1835

Nieuwenhuis, S., Yeung, N., van den Wildenberg, W., and Ridderinkhof, K. R. (2003). Electrophysiological correlates of anterior cingulate function in a go/no-go task: effects of response conflict and trial type frequency. *Cogn. Affect. Behav. Neurosci.* 3, 17–26. doi: 10.3758/cabn.3.1.17

Phillips, L. H., and Andrés, P. (2010). The cognitive neuroscience of aging: new findings on compensation and connectivity. *Cortex* 46, 421–424. doi: 10.1016/j.cortex.2010.01.005

Pires, L., Leitão, J., Guerrini, C., and Simões, M. R. (2014). Event-related brain potentials in the study of inhibition: cognitive control, source localization and age-related modulations. *Neuropsychol. Rev.* 24, 461–490. doi: 10.1007/s11065-014-9275-4

Raz, N. (2000). "Aging of the brain and its impact on cognitive performance: integration of structural and functional findings," in *Handbook of Aging and Cognition - II*, eds F. I. M. Craik and T. A. Salthouse (Mahwah, NJ: Lawrence Erlbaum Associates Publishers), 1–90.

Roberts, L. E., Rau, H., Lutzenberger, W., and Birbaumer, N. (1994). Mapping P300 waves onto inhibition: Go/No Go discrimination. *Electroencephalogr. Clin. Neurophysiol.* 92, 44–55. doi: 10.1016/0168-5597(94)90006-x

Roche, R. A., Garavan, H., Foxe, J. J., and O'Mara, S. M. (2005). Individual differences discriminate event-related potentials but not performance during response inhibition. *Exp. Brain Res.* 160, 60–70. doi: 10.1007/s00221-004-1985-z

Rogers, R. D., Sahakian, B. J., Hodges, J. R., Polkey, C. E., Kennard, C., and Robbins, T. W. (1998). Dissociating executive mechanisms of task control following frontal lobe damage and Parkinson's disease. *Brain* 121, 815–842. doi: 10.1093/brain/121.5.815

Smith, J. L., Johnstone, S. J., and Barry, R. J. (2008). Movement-related potentials in the Go/NoGo task: the P3 reflects both cognitive and motor inhibition. *Clin. Neurophysiol.* 119, 704–714. doi: 10.1016/j.clinph.2007.11.042

Tekok-Kilic, A., Shucard, J. L., and Shucard, D. W. (2001). Stimulus modality and Go/NoGo effects on P3 during parallel visual and auditory continuous performance tasks. *Psychophysiology* 38, 578–589. doi: 10.1017/s0048577201991279

Vallesi, A. (2011). Targets and non-targets in the aging brain: a go/nogo event-related potential study. *Neurosci. Lett.* 487, 313–317. doi: 10.1016/j.neulet.2010.10.046

Vallesi, A., Stuss, D. T., McIntosh, A. R., and Picton, T. W. (2009). Age-related differences in processing irrelevant information: evidence from event-related potentials. *Neuropsychologia* 47, 577–586. doi: 10.1016/j.neuropsychologia.2008.10.018

Van Boxtel, G. J. M., Van der Molen, M. W., Jennings, J. R., and Brunia, C. H. M. (2001). A psychophysiological analysis of inhibitory motor control in the stop-signal paradigm. *Biol. Psychol.* 58, 229–262. doi: 10.1016/s0301-0511(01)00117-x

Van Veen, V., and Carter, C. S. (2002a). The anterior cingulate as a conflict monitor: fMRI and ERP studies. *Physiol. Behav.* 77, 477–482. doi: 10.1016/s0031-9384(02)00930-7

Van Veen, V., and Carter, C. S. (2002b). The timing of action-monitoring processes in the anterior cingulate cortex. *J. Cogn. Neurosci.* 14, 593–602. doi: 10.1162/08989290260045837

West, R. (2000). In defense of the frontal lobe hypothesis of cognitive aging. *J. Int. Neuropsychol. Soc.* 6, 727–729. doi: 10.1017/s1355617700666109

**Conflict of Interest Statement**: The authors declare that the research was conducted in the absence of any commercial or financial relationships that could be construed as a potential conflict of interest.

frontiers in Aging Neuroscience

ORIGINAL RESEARCH
published: 09 May 2016
doi: 10.3389/fnagi.2016.00099

# An Event-Related Potential Investigation of the Effects of Age on Alerting, Orienting, and Executive Function

*David A. S. Kaufman*[1], *Christopher N. Sozda*[2,3], *Vonetta M. Dotson*[2] *and William M. Perlstein*[2,3,4,5,6]*

[1] Department of Psychology, Saint Louis University, St. Louis, MO, USA, [2] Department of Clinical and Health Psychology, University of Florida, Gainesville, FL, USA, [3] Malcom Randall Veterans Administration Medical Center, Gainesville, FL, USA, [4] McKnight Brain Institute, University of Florida, Gainesville, FL, USA, [5] Departments of Psychiatry, Saint Louis University, St. Louis, MO, USA, [6] VA RR&D Brain Rehabilitation Research Center of Excellence, Malcom Randall Veterans Administration Medical Center, Gainesville, FL, USA

The present study compared young and older adults on behavioral and neural correlates of three attentional networks (alerting, orienting, and executive control). Nineteen young and 16 older neurologically-healthy adults completed the Attention Network Test (ANT) while behavioral data (reaction time and error rates) and 64-channel event-related potentials (ERPs) were acquired. Significant age-related RT differences were observed across all three networks; however, after controlling for generalized slowing, only the alerting network remained significantly reduced in older compared with young adults. ERP data revealed that alerting cues led to enhanced posterior N1 responses for subsequent attentional targets in young adults, but this effect was weakened in older adults. As a result, it appears that older adults did not benefit fully from alerting cues, and their lack of subsequent attentional enhancements may compromise their ability to be as responsive and flexible as their younger counterparts. N1 alerting deficits were associated with several key neuropsychological tests of attention that were difficult for older adults. Orienting and executive attention networks were largely similar between groups. Taken together, older adults demonstrated behavioral and neural alterations in alerting, however, they appeared to compensate for this reduction, as they did not significantly differ in their abilities to use spatially informative cues to aid performance (e.g., orienting), or successfully resolve response conflict (e.g., executive control). These results have important implications for understanding the mechanisms of age-related changes in attentional networks.

**Keywords: ANT, attentional networks, alerting, N1, aging, ERPs**

OPEN ACCESS

***Edited by:***
*Junfeng Sun,*
*Shanghai Jiao Tong University, China*

***Reviewed by:***
*Yury (Juri) Kropotov,*
*The Institute of the Human Brain of Russian Academy of Sciences, Russia*
*Laura Lorenzo-López,*
*University of A Coruña, Spain*

***Correspondence:**
*William M. Perlstein*
*wmp@phhp.ufl.edu*

***Received:*** *04 February 2016*
***Accepted:*** *18 April 2016*
***Published:*** *09 May 2016*

***Citation:***
*Kaufman DAS, Sozda CN, Dotson VM and Perlstein WM (2016) An Event-Related Potential Investigation of the Effects of Age on Alerting, Orienting, and Executive Function. Front. Aging Neurosci. 8:99. doi: 10.3389/fnagi.2016.00099*

## INTRODUCTION

Intact attentional processes are vital for goal-directed behavior, as they guide the allocation of cognitive resources in accordance with changing environmental demands. Research from the past several decades has proposed that attention is comprised of dissociable yet interrelated anatomical and functional neural networks responsible for alerting, orienting, and executive control (Posner and Peterson, 1990; Posner and Fan, 2004). The alerting system helps

us to achieve and sustain an alert state (Fernandez-Duque and Posner, 1997), which is thought to facilitate response preparation via enhanced early attentional processing. The orienting system functions to select information from sensory input, and through spatial cuing, can be manipulated to covertly direct attention (Posner, 1980; Fan et al., 2002). Lastly, executive control of attention encompasses higher-order cognitive processes needed to resolve conflict associated with the need to override a prepotent, but contextually inappropriate response (Fan et al., 2002). These executive operations are particularly crucial when situations are novel or difficult, and require response monitoring or inhibition of strong prepotent response tendencies (Fan and Posner, 2004).

In order to probe these different attentional networks, Fan et al. (2002) developed a single-trial computerized task known as the Attention Network Test (ANT). The ANT combines aspects of Posner and Peterson (1990) spatial cuing task with features of the Eriksen Flanker task (Eriksen and Eriksen, 1974), such that target flankers are spatially and/or temporally cued. Moreover, the ANT has been used to characterize the three attentional networks in studies employing behavioral (e.g., Fan et al., 2002), electrophysiological (e.g., Fan et al., 2007; Neuhaus et al., 2007), and hemodynamic (e.g., Fan et al., 2005; Posner et al., 2006) methodologies. Despite the popularity of this task, cautions have been raised about its psychometric properties. A large meta-analysis found poor split-half reliabilities within alerting and orienting network effects, along with significant inter-network correlations between the various networks (MacLeod et al., 2010). Accordingly, these attentional networks may not be as reliable or independent as initially thought, and it is important for researchers to document these psychometric properties when reporting individual study findings.

Several studies have used the ANT to examine how attentional networks are affected by aging processes; however, findings have been mixed. After controlling for the effects of generalized cognitive slowing, older adults have demonstrated weakened alerting effects, relative to younger adults (Jennings et al., 2007; Gamboz et al., 2010). In contrast, when longer cue presentation was employed, Fernandez-Duque and Black (2006) found a significantly larger alerting effect in older compared to young adults. Recent findings did not reveal significantly differing orienting effects between young and older adults (Jennings et al., 2007), a result consistent with prior literature that spatial cueing benefits older adults as much as young adults (Hartley et al., 1990; Folk and Hoyer, 1992; Greenwood et al., 1993). Regarding executive control, no significant conflict-related effects have been observed in several studies comparing older and young adults (Fernandez-Duque and Black, 2006; Jennings et al., 2007). In contrast, a more recent study suggests age-related changes may occur in the executive control network (Zhou et al., 2011). Taken together, it remains unclear whether age-related attentional declines may be confounded by cognitive slowing (Verhaeghen and De Meersman, 1998; Verhaeghen and Cerella, 2002), or other cognitive disruptions beyond slowed speed of information processing (Hartley, 1993).

Electrophysiological methodologies have provided further insight about the underlying neural mechanisms of attentional networks. In particular, studies of attentional processes (e.g., Fan et al., 2007; Neuhaus et al., 2007, 2010) have employed scalp-recorded brain event-related potentials (ERPs), which provide unmatched temporal sensitivity for examining neural correlates. Despite recent electrophysiological investigations, the alerting network has received the least focus of the three attentional networks in the literature. With the goal of examining effects of alerting cues on subsequent attentional processing, one study reported significant increases in N1 amplitude evoked by targets that followed alerting cues (Neuhaus et al., 2010). This posterior N1 component is believed to reflect early attentional facilitation of target processing, which is enhanced by valid cues that reliably predict target location (Hillyard et al., 1998).

With respect to orienting of visual attention, researchers have also observed increased amplitude of posterior negativity beginning approximately 100 ms following validly cued target stimuli (Harter et al., 1989; Hopf and Mangun, 2000; Nobre et al., 2000; Talsma et al., 2005). These results have been replicated using the ANT (Neuhaus et al., 2010), and are presumed to reflect the successful shift of selective visual attention from one stimuli to another in response to validly cued stimuli (Mangun, 1995; Hillyard et al., 1998). Neuroimaging findings suggest activation within a dorsal fronto-parietal network is strongly associated with orienting of attention (e.g., Fan et al., 2005).

Executive aspects of attention can be measured many different ways, with researchers typically targeting higher-order cognitive processes involved in conflict processing, inhibition, or decision-making. One method that has been frequently studied is the flanker task, in which compatibility of stimuli surrounding target stimuli is manipulated to vary the level of response inhibition needed. ERP investigations using the ANT in healthy young adults have revealed attenuation of posterior positivity following incongruent target stimuli (Neuhaus et al., 2007, 2010). Although the P300 is commonly observed in paradigms that probe attentional resource allocation (see Polich, 2007), it is also susceptible to conflict effects. For example, incongruent Stroop stimuli have been associated with negative deflections occurring during the P300 response time window (approximately 450 ms following stimulus onset). Although these conflict-sensitive N450 components have been shown to exhibit a more frontocentral scalp distribution (van Veen and Carter, 2002; Larson et al., 2009), cognitive/response conflict also appears to affect the more parietal-maximal P300. Consistent with the literature on the N450 component, these negative deflections during the P300 likely reflect anterior cingulate cortex (ACC) mediated conflict-resolution associated with the inhibition of a strong pre-potent response tendency (Fan et al., 2005, 2007; Neuhaus et al., 2010).

While the above results demonstrate the utility of the ANT to elucidate the presence of the three neural attentional networks, no published studies to date have examined the neural correlates of the ANT in *older* adults. Additionally, although a growing body of behavioral literature suggests age-related

impairments in each attentional network, findings are mixed and often confounded by generalized slowing in older participants. Consequently, the primary aim of the current study was to use ERPs to supplement behavioral data to determine whether significant between-group neural differences are observed in the presence-and/or absence of significant behavioral deficits, as well as if neural correlates are more closely associated to behavioral findings that are corrected for generalized slowing than when uncorrected. Guided by prior electrophysiological findings of Neuhaus et al. (2007, 2010), ERP components of interest included the posterior N1 (for alerting and orienting networks), and parietal P300 (executive control network) components, which are presumed to reflect phasic alerting, orienting of attention, and processing of response conflict (executive control), respectively.

# MATERIALS AND METHODS

## Participants

Participants included 19 young (12 females, 7 males; mean age 22.9 ± 4.0 years) and 16 older (8 females, 8 males; mean age 64.8 ± 8.0 years) adults recruited from the community through local advertisements. All participants were right-handed, native-English speakers, and had normal or corrected-to-normal vision. Groups were matched for gender, $\chi 2_{(1)} = 0.62$, $ps > 0.43$. Although older adults reported a higher mean level of educational attainment than young adults, $t_{(33)} = -2.70$, $p < 0.02$, education did not correlate with ANT RT, error-rates, or ERP amplitudes collapsed across conditions ($p$'s $> 0.052$). Education was significantly correlated with Stroop performance, $r_{(34)} = 0.49$, $p < 0.003$, however, this measure is typically only corrected for age and not education in standard clinical practice. Exclusion criteria included presence of psychiatric illness, learning disability, probable dementia or global cognitive impairment (as determined by a MMSE score <25), neurological disorders, and motor difficulties that would interfere with task performance. All participants provided written informed consent in accordance with procedures established by the University of Florida Health Science Center Institutional Review Board, and received course credit or financial compensation for their study participation.

## Procedures

### Cognitive and Emotional Assessment

Participants completed the following neuropsychological tests: Mini-Mental State Exam (MMSE; Folstein et al., 1975), Trail Making Test A and B (TMT; Reitan and Wolfson, 1995), Digit-Symbol Coding from the Wechsler Adult Intelligence Scale, 3rd Edition (WAIS-III; Wechsler, 1997), and Stroop Color and Word Test (ST; Golden, 1978). The Beck Depression Inventory-Second Edition (BDI-II; Beck, 1996), Geriatric Depression Scale (GDS; Yesavage et al., 1983), State-Trait Anxiety Inventory (STAI; Speilberger et al., 1983), and modified Apathy Scale (AS; Starkstein et al., 1992), were used to measure symptoms of depression, anxiety, and apathy, respectively. Demographic and neuropsychological characteristics of participants are presented in **Table 1**.

### Cognitive Task and Stimuli

Participants completed a computerized experimental task identical to the procedure used by Fan et al. (2002), as depicted in **Figure 1**. Stimuli were programmed and presented using E-Prime (v.1.0, Psychology Software Tools, Inc.,). Briefly, individuals were instructed to focus on a centrally located fixation cross throughout the procedure, and to determine as

**TABLE 1 | Demographic and neuropsychological data for young and older participant groups.**

| | Young Adults | | Older Adults | | | Analysis | |
|---|---|---|---|---|---|---|---|
| | Mean | SD | Mean | SD | *t* | *p* | Cohen's *d* |
| Age (years) | 22.95 | 4.0 | 64.81 | 8.0 | −20.02 | <0.001 | 6.81 |
| Educational level (years) | 15.05 | 1.2 | 17.13 | 3.1 | −2.70 | 0.011 | 0.92 |
| BDI-II score | 3.05 | 3.2 | 2.88 | 3.0 | 0.16 | ns | 0.05 |
| f GDS score | 1.79 | 2.4 | 0.94 | 1.3 | 1.26 | ns | 0.43 |
| STAI—State score | 26.79 | 5.2 | 27.56 | 7.2 | −0.37 | ns | 0.12 |
| STAI –Trait score | 31.10 | 7.3 | 28.50 | 5.2 | 1.20 | ns | 0.40 |
| Apathy Scale score | 8.10 | 4.8 | 8.81 | 4.6 | −0.47 | ns | 0.15 |
| MMSE Score | 28.95 | 1.0 | 28.69 | 1.3 | 0.69 | ns | 0.23 |
| Stroop Test—Word-reading | 99.26 | 12.3 | 107.06 | 17.4 | −1.55 | ns | 0.53 |
| Stroop Test—Color-naming | 74.37 | 9.0 | 77.50 | 13.8 | −0.81 | ns | 0.27 |
| Stroop Test—Color-word | 45.31 | 10.1 | 46.19 | 13.4 | −0.22 | ns | 0.08 |
| Stroop Test—Interference | 2.99 | 8.8 | 1.51 | 9.3 | 0.48 | ns | 0.16 |
| Digit symbol coding (# correct) | 89.89 | 13.1 | 72.87 | 11.6 | 3.95 | <0.001 | 1.38 |
| TMT—Part A (sec) | 22.16 | 4.1 | 31.06 | 9.8 | −3.61 | 0.001 | 1.22 |
| TMT—Part B (sec) | 50.53 | 18.2 | 67.81 | 27.9 | −2.20 | 0.035 | 0.75 |
| TMT—Part B minus Part A (sec) | 28.37 | 16.9 | 36.75 | 22.2 | −1.27 | ns | 0.43 |

*BDI-II, Beck Depression Inventory—Second Edition; GDS, Geriatric Depression Scale; STAI, State-Trait Anxiety Inventory; MMSE, Mini-Mental State Exam; TMT, Trail Making Test.*

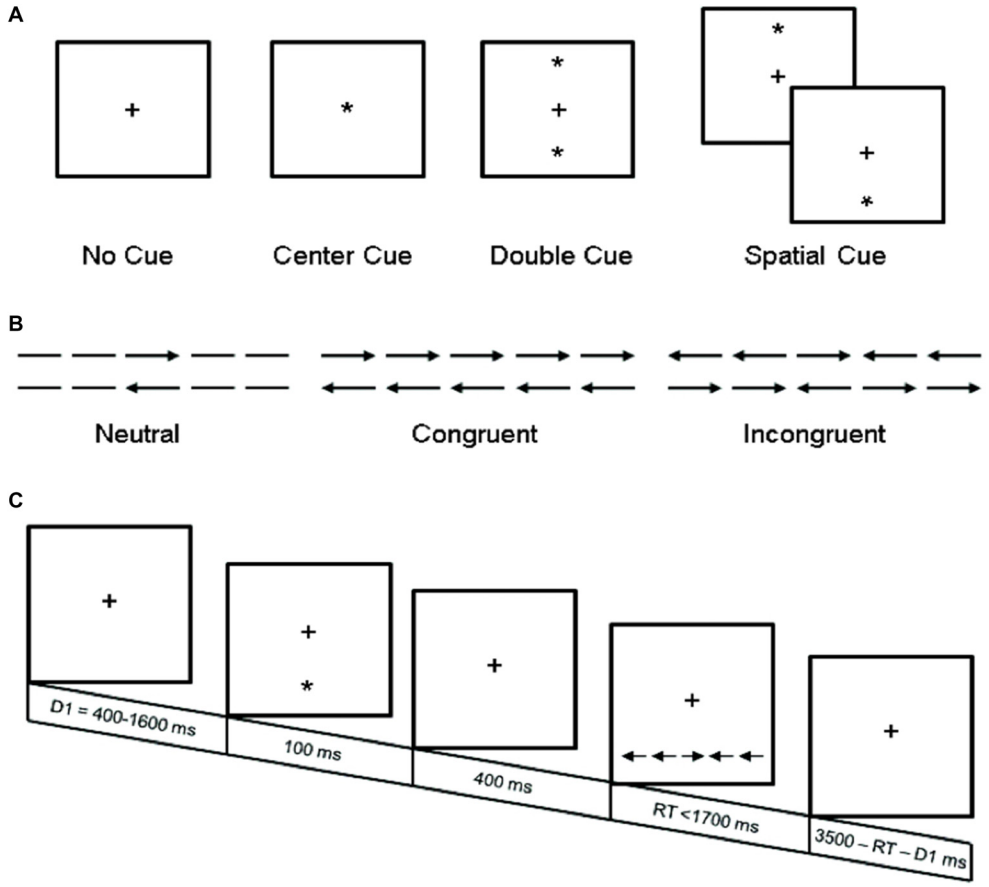


**FIGURE 1 | Experimental procedure. (A)** The four cue conditions, in which the asterisk cue (*) provides information about the presence (center and double cue) or location (spatial cue) of the upcoming target stimuli; **(B)** The six target stimuli used in the present experiment; and **(C)** An example trial (spatial cue—incongruent target stimuli). Adapted from Fan et al. (2002).

rapidly and accurately as possible whether the target probe, a central arrow, located above or below central fixation pointed left or right. In addition to varying target locations, on 75% of trials the target probe was preceded by different types of cues, and on 67% of trials the target probe was accompanied by congruent or incongruent flankers (which were equally frequent). The task utilized two target locations (above or below central fixation), two target directions (left or right), four cue conditions (no-cue, center-cue, double-cue and spatial-cue), and three flanker conditions (congruent, incongruent, or neutral), yielding 48 different types of trials. Each trial lasted ∼4000 ms and consisted of five events: (1) random variable pre-cue fixation (400–1600 ms); (2) warning cue presentation (100 ms); (3) post-cue fixation (400 ms); (4) target and flanker presentation (self-terminating up to 1700 ms); and (5) post-target fixation (3500 ms minus duration of pre-cue fixation minus RT). Participants completed a 24-trial practice block, followed by 3-experimental blocks of 96 pseudo-random trials (2 target locations × 2 target directions × 2 repetitions × 3 flanker conditions × 4 cue conditions). Accuracy and RT feedback were provided to participants only during the practice block.

## Electrophysiological Data Acquisition and Reduction

Electroencephalogram (EEG) was recorded from 64 scalp sites using a geodesic sensor net and Electrical Geodesics, Inc., (EGI; Eugene, Oregon) amplifier system (20 K gain, nominal bandpass = 0.10–100 Hz). Reported electrode sites have been renamed from the 64-channel geodesic sensor net to conform to the international 10–10 positions. Electrode placements enabled recording vertical and horizontal eye movements reflecting electro-oculographic (EOG) activity. EEG was digitized continuously at 250 Hz with a 16-bit analog-to-digital converter and referenced to Cz. A right posterior electrode served as common ground, and electrode impedances were maintained below 50 kΩ, consistent with manufacturer recommendations. Following recording, EEG data were adjusted for movement, electromyographic muscle artifact, electro-ocular eye movement, and blink artifacts using spatial filtering methods implemented through Brain Electric Source Analysis (BESA v5.1; Scherg, 1990). Single-trial EEG epochs were excluded from the averaging using threshold criteria that maximized the number of trials accepted from each individual, following the recommendations of Luck (2005). The average voltage threshold used for excluding trials was 113.86 μV

(*SD* = 16.89), and voltage threshold did not significantly differ between groups, $t_{(33)} = 1.46$, $p = 0.16$. Point-to-point transitions were not allowed to exceed 75 μV. Individual-subject per condition EEG epochs were separately extracted and averaged across trials from the continuous EEG recording, with epochs lasting 1600 ms (300 ms pre-cue to 800 ms post-probe including 400 ms cue-offset–probe-onset interval). Cue-locked target ERP components were examined to observe the sustained effects of cue on subsequent target processing, in replication of methods used previously (Neuhaus et al., 2010). All averaged ERP epochs were digitally filtered at 30 Hz low-pass and baseline-corrected using respective pre-stimulus windows. Peak voltage values for target-related N1 amplitude were measured bilaterally over posterior parietal scalp sites (10–10 system equivalents = P9, PO7, PO8, P10) between 176–216 ms post-target onset. Because of group-related latency differences apparent in P300 grand-average waveforms, ERPs were scored such that mean P300 amplitude was measured from 380–410 ms for young adults and 500–530 ms for older adults at central-posterior electrode sites (10–10 equivalents = CPz, Pz, and POz), averaged 30-ms symmetrically about the peak. The scoring windows for each group were determined by identifying the maximum peak amplitude of P300 within grand-averaged waveforms for each age group.

## Data Analyses

### Behavioral Performance Data

Statistical analyses were carried out with JMP 7.0.2 (SAS Institute Inc., Cary, NC, USA). Attention network effects and neuropsychological variables were analyzed using one-way mixed-model restricted maximum likelihood analyses of variance (REML ANOVAs; Wolfinger et al., 1994). Median correct-trial RT (Ratcliff, 1993) and arcsine transformed commission-error rates, excluding non-responses (Neter et al., 1985), were analyzed separately using 2-Group (young adults, older adults) × 3-Flanker type (incongruent, neutral, congruent) × 4-Cue type (no, spatial, double, and center) mixed-model REML ANOVAs. In order to follow up on these ANOVA results, attention network effects were calculated using the following cognitive subtractions: *alerting effect* = no-cue RT minus double-cue RT; *orienting effect* = center-cue RT minus spatial cue RT; *executive control (conflict) effect* = incongruent RT minus congruent RT. For ANOVA factors that differed by group, independent *t*-tests were used to compare attentional network effects between young and older adults. Additionally, to examine whether condition-related RT effects were artificially created due to generalized slowing experienced by older adults, we calculated a *z*-score transformation of each participant's RT by taking the mean over all conditions for a given individual, subtracting his/her condition mean from the overall mean, and dividing by the overall standard deviation across the overall mean. This method has been proven effective in identifying age-related cognitive effects independent of global slowing (Bush et al., 1993; Faust et al., 1999; Jennings et al., 2007). Finally, split-half reliabilities for each network effect were calculated by correlating data from the first and second halves of trials within each network.

### ERP Data

In a manner parallel to the behavioral data, ERP activity from attention networks was analyzed using REML ANOVAs, which included the following factors: Group × Channel (N1 analyses = 10–10 equivalents P9, PO7, PO8, P10; P3 analyses = 10–10 equivalents CPz, Pz, and POz), × Condition (either double cue and no cue, spatial cue and center cue, or congruent probe and incongruent probe, depending on the attention network being analyzed). Selection of electrode sites for analyses of electrophysiological data was based on evaluation of the scalp-distribution maps in which N1 and P300 amplitudes were maximal. Interaction effects were decomposed using least-square means contrasts; and Cohen's-*d* effect sizes (Cohen, 1988) were calculated using pooled standard deviations for group and/or condition-related effects. ANOVAs were then followed up with the calculation of attention network effects, using the same paired subtractions that were used to generate the behavioral attention network effects. ERP network effects were derived using the following cognitive comparisons: *alerting N1 effect* = double-cue amplitude − no-cue amplitude; *orienting N1 effect* = spatial cue amplitude − center-cue amplitude; *executive control P3 ("conflict") effect* = congruent amplitude − incongruent amplitude. Group differences on these ERP network effects were analyzed using independent *t*-tests. Mean amplitudes for ERP network effect were then correlated with neuropsychological measures that differentiated young and older adults.

## RESULTS

## ANT Behavioral Performance

A Group × Flanker type × Cue type ANOVA on correct-trial median RTs revealed a significant main effect of group, $F_{(1,33)} = 38.75$, $p < 0.0001$, reflecting the expected pattern of generalized slowing in older adult participants. As expected, a significant main effect of flanker type, $F_{(2,363)} = 832.73$, $p < 0.0001$, was also observed, reflecting increased slowing when faced with incongruent flankers. Participants responded more quickly as cue types became more informative (no cue RT < center cue RT < double cue RT < spatial cue RT), as evidence by a significant main effect of cue type, $F_{(3,363)} = 137.96$, $p < 0.0001$. Additionally, a significant Group × Flanker type interaction, $F_{(2,363)} = 4.59$, $p < 0.02$, indicated that older adult participants responded significantly more slowly compared to neutral trials for both congruent and incongruent stimuli, whereas young adults only displayed slowing compared to neutral stimuli for incongruent target conditions. A Group × Cue-type interaction, $F_{(3,363)} = 5.20$, $p < 0.002$, indicated that older adults did not benefit from center cues as much as young adults. Flanker type × Cue

type, $F_{(6,363)} = 1.47$, $p = 0.19$, and Group × Flanker type × Cue type, $F_{(6,363)} = 1.54$, $p = 0.16$, interactions were not significant.

Attention network difference scores revealed significant RT differences between groups for alerting (Young = 46 ± 25 ms; Older = 18 ± 32 ms), $F_{(1,33)} = 7.69$, $p < 0.01$, orienting (Young = 43 ± 27 ms; Older = 87 ± 32 ms), $F_{(1,33)} = 19.81$, $p < 0.0001$, and executive control (Young = 117 ± 22 ms; Older = 135 ± 29 ms), $F_{(1,33)} = 4.32$, $p < 0.05$, effects. However, after normalization of RT data to account for generalized slowing experienced by older adults using *z*-score transformations, significant group differences remained only for the alerting effect, $F_{(1,33)} = 8.02$, $p < 0.01$. In other words, young adults responded faster following alerting cues, but older adults did not—even after controlling for group differences in overall speed. Group differences in the orienting effect, $F_{(1,33)} = 0.39$, $ps > 0.53$, and conflict effect $F_{(1,33)} = 2.39$, $ps > 0.13$, were no longer significant following normalization to control for generalized slowing. Mean attention network effects, *z*-score transformed attention network effects, and correct-trial median RT data for both groups as a function of flanker type and cue type are summarized in **Table 2**.

Split-half reliabilities on RT data revealed that the conflict effect had the highest internal consistency ($r_{(33)} = 0.41$, $p < 0.05$), followed by alerting ($r_{(33)} = 0.37$, $p < 0.05$) and orienting ($r_{(33)} = 0.29$, $p = 0.09$) effects. When analyzed separately by group, network reliabilities were much lower for older adults than young. Young adults had significant split-half reliabilities for the conflict ($r_{(17)} = 0.54$, $p < 0.05$) and alerting ($r_{(17)} = 0.48$, $p < 0.05$) networks, while older adults had no significant reliabilities within networks. Alerting and conflict effects were significantly correlated in younger adults ($r_{(17)} = -0.50$, $p < 0.05$), but no other cross network correlations were significant for task RT.

Regarding task performance accuracy, a Group × Flanker type × Cue type ANOVA revealed a significant main effect of flanker type, $F_{(2,363)} = 36.56$, $p < 0.0001$, reflecting the expected larger error-rates on incongruent than congruent trials. A significant main effect of cue type $F_{(3,363)} = 4.26$, $p < 0.006$, was also observed, indicating greater accuracy to targets following spatial cues. The group main effect, $F_{(1,33)} = 0.30$, $p = 0.59$, and Group × Congruency interaction, $F_{(2,363)} = 2.84$, $ps > 0.06$, were not significant, suggesting equal task performance across groups regardless of task difficulty. Finally, a significant Group × Flanker type × Cue-type, $F_{(6,363)} = 2.17$, $p < 0.05$, revealed that spatial cuing improved accuracy on incongruent trials for young, but not older adults. This finding reveals that conflict processing is improved following spatial cues for young adults only, and may suggest that older adults fail to benefit fully from spatial cueing when increased conflict is present. With regard to task accuracy, attention network difference scores did not differ as a function of group, which is likely attributable to the low error rates seen in both groups. Of additional note, a negative correlation was observed between alerting effect RT and alerting effect error rate for young adults ($r_{(17)} = -0.61$, $p < 0.01$), suggesting that they exhibited a speed-accuracy tradeoff when engaging the alerting network. This effect was not seen in older adults ($r_{(14)} = -0.25$, $ps > 0.35$).

## ERP Components

As shown in **Table 3**, the average number of trials included in ERPs did not differ significantly between groups for target N1 alerting and orienting components. However, older adults had more trials included in the target P300 conflict component relative to younger adults.

## Target N1 Alerting Effect (Double-cue vs. No-cue)

Occipito-parietal waveforms illustrating grand average ERP waveforms for the alerting effect are shown in **Figure 2**. The Group × Condition × Channel ANOVA yielded significant main effects of group, $F_{(1,33)} = 10.20$, $p = 0.0031$, channel, $F_{(3,231)} = 6.47$, $p = 0.0003$, and condition, $F_{(1,231)} = 8.96$, $p = 0.0031$. A significant Group × Channel interaction,

**TABLE 2 | Mean (± SD) attention network effects (RT), *Z*-score transformations for attention network effects, and arcsine transformed error rates as a function of flanker-type and group**.

| | Young Adults | | Older Adults | | | Analysis | |
|---|---|---|---|---|---|---|---|
| | Mean | SD | Mean | SD | *t* | *p* | Cohen's *d* |
| Mean RT (ms) | 485.16 | 44.9 | 646.44 | 109.6 | −5.87 | <0.001 | 1.99 |
| Alerting effect (ms) | 46.29 | 24.9 | 17.78 | 32.1 | 2.77 | 0.009 | 1.00 |
| Orienting effect (ms) | 43.08 | 27.0 | 87.41 | 31.9 | −4.45 | <0.001 | 1.51 |
| Conflict effect (ms) | 117.29 | 22.3 | 135.41 | 29.2 | −2.08 | 0.050 | 0.71 |
| *Z*-score RT transformations | | | | | | | |
| Alerting effect | 0.68 | 0.34 | 0.27 | 0.50 | 2.83 | 0.008 | 0.98 |
| Orienting effect | 0.65 | 0.40 | 0.76 | 0.62 | −0.63 | 0.540 | 0.21 |
| Conflict effect | 1.64 | 0.36 | 1.39 | 0.58 | 1.54 | 0.140 | 0.53 |
| Mean error rates (%) | 6.20 | 12.4 | 5.40 | 10.5 | −0.73 | ns | 0.07 |
| Congruent | 1.90 | 6.0 | 2.40 | 7.0 | 0.46 | ns | 0.08 |
| Incongruent | 13.70 | 16.6 | 9.60 | 13.3 | −1.59 | ns | 0.27 |
| Neutral | 3.00 | 8.1 | 4.20 | 8.8 | 0.79 | ns | 0.14 |

*Alerting, no cue (RT) minus double cue (RT); Orienting, center cue (RT) minus spatial cue (RT); Conflict, incongruent (RT) minus congruent (RT).*

**TABLE 3 | Mean (± SD) number of ERP segments comprising each component, as a function of group.**

| | Young Adults | | Older Adults | | | Analysis | |
|---|---|---|---|---|---|---|---|
| | Mean | SD | Mean | SD | *t* | *p* | Cohen's *d* |
| ERP Component | | | | | | | |
| Target N1 Alerting | 43.82 | 10.24 | 49.66 | 9.87 | −1.71 | 0.10 | 0.59 |
| Target N1 Orienting | 44.50 | 10.97 | 49.53 | 9.73 | −1.42 | 0.16 | 0.49 |
| Target P300 Conflict | 57.95 | 13.04 | 68.63 | 11.62 | −2.53 | 0.02 | 0.88 |

$F_{(3,231)}$ = 4.04, $p$ = 0.0079, indicated that voltages did not significantly differ between any channels for older adults, however, young adults demonstrated significantly greater voltage fluctuations between channels. A Group × Condition interaction, $F_{(1,231)}$ = 15.07, $p < 0.0001$, revealed that young adults demonstrated larger N1 amplitude for double cues relative to no cue, $t_{(18)}$ = 1.90, $p$ = 0.001, $d$ = 0.90, while older adults showed no difference between these two cue conditions, $t_{(15)} = -0.25$, $p$s > 0.54. Attention network difference scores calculated from peak amplitudes supported these ANOVA results with significant N1 alerting amplitude differences between groups, Young = −2.58 ± 2.62 μV; Older = 0.17 ± 1.35 μV, $t_{(33)}$ = 3.99, $p < 0.001$, suggesting that young adults demonstrated a strong alerting effect on N1 amplitude, while older adults did not.

## Target N1 Orienting Effect (Spatial-cue vs. Center-cue)

Occipito-parietal waveforms illustrating grand average ERP waveforms for the orienting effect are shown in **Figure 3**. The Group × Condition × Channel ANOVA yielded significant main effects of group, $F_{(1,33)}$ = 14.22, $p$ = 0.0006, condition, $F_{(1,231)}$ = 8.35, $p$ = 0.0042, and channel, $F_{(3,231)}$ = 3.59, $p < 0.015$. The main effect of group reflected significantly smaller N1 amplitude in older compared to young adults, while increased amplitude to spatial vs. center cue was revealed in the main effect of condition. The effect of channel revealed greatest amplitude at PO7 and smallest amplitude at P10. No significant interactions were observed ($p$s > 0.09). Furthermore, attention network difference scores calculated from peak N1 orienting amplitudes revealed no group differences ($p > 0.09$).

## Target P300 Conflict Effect (Congruent vs. Incongruent)

Parietal waveforms illustrating conflict-related target processing are illustrated in **Figure 4**. The Group × Condition × Channel ANOVA yielded significant main effects of group, $F_{(1,33)}$ = 11.90, $p$ = 0.0016, condition, $F_{(1,165)}$ = 39.32, $p < 0.0001$, and channel, $F_{(2,165)}$ = 4.02, $p < 0.02$. The main effect of group reflected significantly smaller P300 amplitude collapsed across target conditions in older compared to young adults, while reduced amplitude to incongruent vs. congruent cue was revealed in the main effect of condition. The effect of channel revealed greatest amplitude at CPz and smallest amplitude at

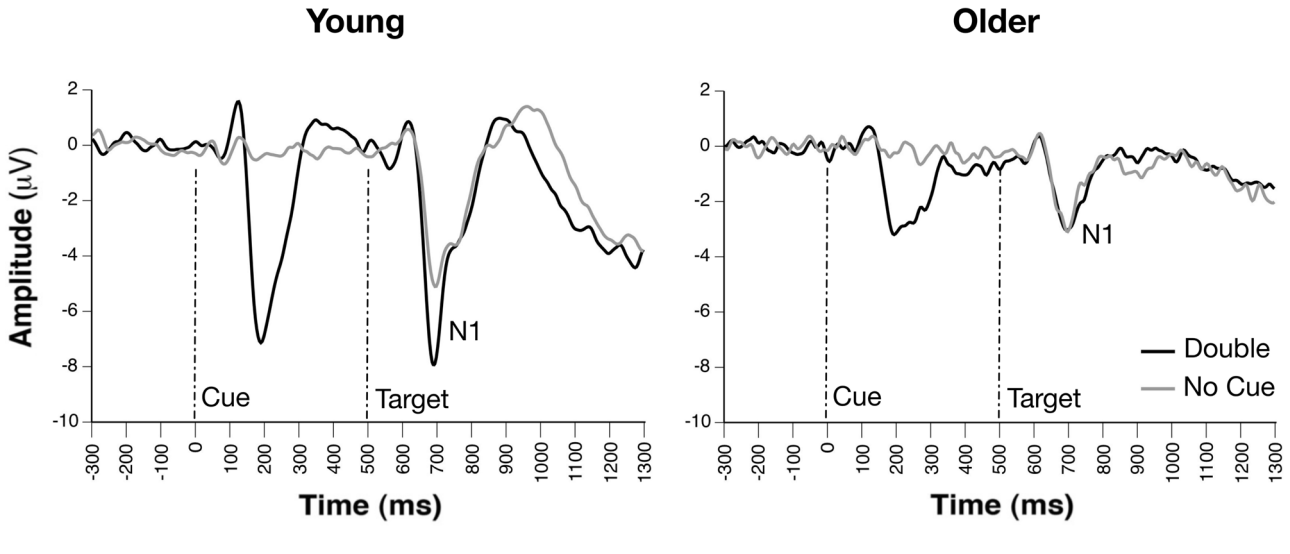


**FIGURE 2 | Grand average event-related potential (ERP), waveforms of cue- and probe-locked double and no cue trials, revealing group differences on alerting effects on target-related N1 amplitudes (channel PO7).**

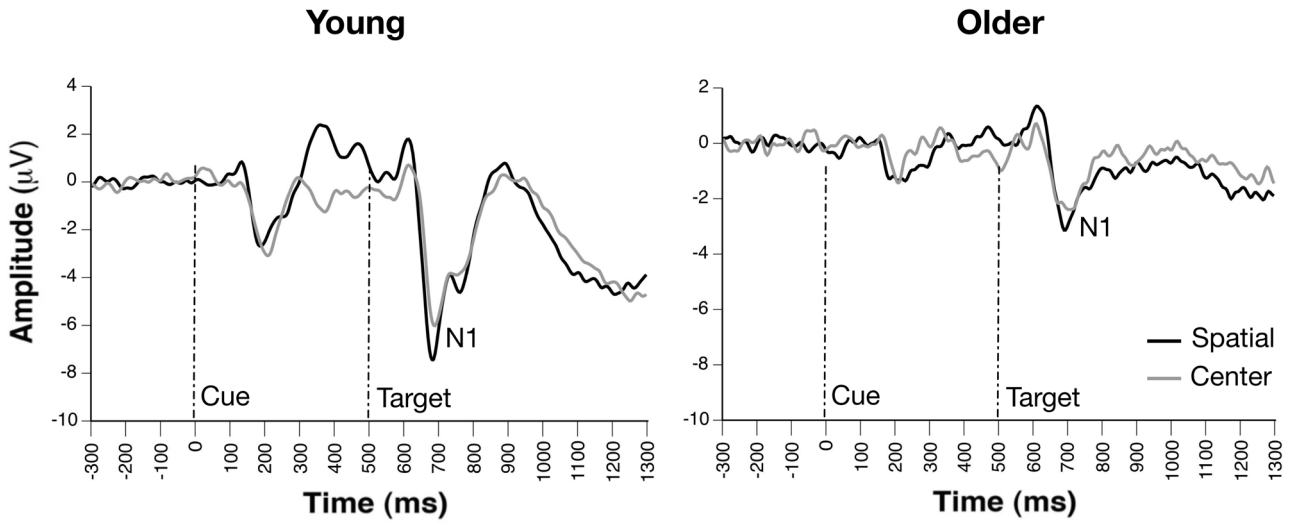


**FIGURE 3 | Grand average ERP waveforms of cue- and probe-locked spatial and center cue trials, revealing similar orienting effects on target-related N1 amplitudes between groups (channel PO7).**

POz. No significant interactions were observed ($ps > 0.37$). Additionally, attention network difference scores calculated from peak P300 conflict amplitudes revealed no group differences ($p > 0.90$).

## Relationships Between Behavioral and ERP Attention Network Effects

Mean N1 alerting amplitude taken from the channel with maximal amplitude (PO7) was not correlated with RT alerting effects (no cue − double cue), but N1 alerting amplitude was significantly correlated with performance on Digit Symbol Coding ($r_{(33)} = -0.50$, $p < 0.01$), Trails A ($r_{(33)} = 0.52$, $p = 0.001$), and Trails B ($r_{(33)} = 0.42$, $p = 0.01$). Mean N1 orienting amplitude (taken from PO7) was not correlated with RT orienting effects (center cue − spatial cue) or any other neuropsychological variables. Mean P300 conflict amplitude (taken from Pz) was not correlated with RT conflict effects (incongruent − congruent) or any other neuropsychological variables.

# DISCUSSION

This study employed behavioral measures and high-density ERPs to probe age-related changes in the functioning of three attentional networks (alerting, orienting, and executive control). After controlling for effects of generalized slowing, only the alerting network remained significantly different in older compared with young adults, as suggested by limited facilitation of RT when provided with a double cue compared to no cue. With respect to ERP correlates of alerting, double cues significantly enhanced target-related N1 amplitude relative to the no-cue condition in young adults, consistent with prior findings of enhanced early attentional processing of targets following alerting cues (Neuhaus et al., 2010). While this N1 alerting effect was pronounced in younger adults, it was completely absent in older adults. These results support prior findings that early attentional processes reflected in the N1 are attenuated in older adults (Ford et al., 1995; Golub et al., 2001). Even more importantly, N1 alerting amplitude during the ANT was correlated with performance on three neuropsychological measures of controlled attention (i.e., Digit-Symbol Coding, Trails A and B) that differentiated older and younger adults. These findings reveal a unique vulnerability of the alerting network in aging, and suggest that compromised alerting in older adults is associated with broader difficulties in controlled attention.

While older adults demonstrated difficulty in using alerting cues to prepare for subsequent events, they were not impaired in their ability to use spatially informative cues to aid performance (orienting), or in their ability to successfully resolve response conflict (executive control). These results parallel the findings of other studies (e.g., Jennings et al., 2007; Gamboz et al., 2010) that also found age-related declines in the alerting network but intact functioning in other networks, after generalized slowing was taken into account. With regard to performance accuracy, both young and older participants committed significantly more errors during the more difficult incongruent flanker condition vs. neutral and congruent conditions. However, error rates did not significantly differ between groups, suggesting that older adults successfully inhibited strong prepotent response tendencies as well as their younger peers. Despite this, there were group differences in the relationship between error rate and response time for the alerting effect. While young adults adopted a strong speed-accuracy tradeoff when engaging the alerting network, older adults did not show this tendency. This finding is consistent with prior research on the speed-accuracy tradeoff in aging (Forstmann et al., 2011), which has suggested that older adults

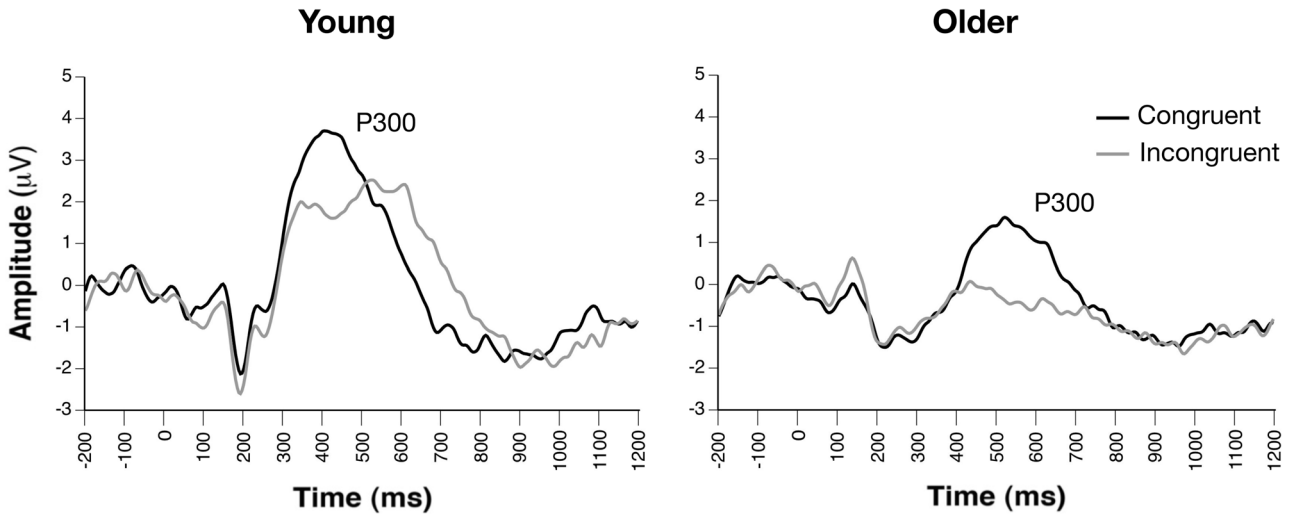


**FIGURE 4 | Grand average ERP waveforms of target-locked congruent and incongruent trials, revealing similar conflict effects on target-related P300 amplitudes between groups (channel Pz)**.

may have difficulty speeding up their response tendencies due to disrupted brain connections (particularly in corticostriatal pathways).

Regarding ERP correlates of visual orienting of attention, spatial cues were found to significantly enhance N1 amplitude vs. center cues in both young and older adult participants. Both groups appeared to engage neural processes underlying the orienting of attention and subsequent processing of target information equally well. These results also imply that valid cueing was beneficial and had a lasting effect on subsequent processing of target stimuli, a result consistent with other ERP examinations of the ANT demonstrating enhanced N1 during attentional orienting (Neuhaus et al., 2010), as well as studies of orienting of visual attention which found similar enhancements in N1-like posterior negativities following validly-cued target stimuli (Harter et al., 1989; Hopf and Mangun, 2000; Nobre et al., 2000; Talsma et al., 2005). Such results also suggest that although older adults may demonstrate less efficient response preparation as evidenced by reduced alerting, they are still able to shift attentional resources under the guidance of spatially informative cues.

Finally, examination of target-related conflict P300 revealed that both young and older adults showed significant and equivalent P300 amplitude reductions to incongruent vs. congruent target stimuli. Older adults did show reduced P300 amplitudes overall, as has been shown previously (e.g., Fjell and Walhovd, 2001); however, this group effect did not interact with target congruency. Thus, older adults engaged similar mechanisms of conflict processing and their cortical systems underlying inhibitory processes were relatively intact. Whereas this study is to the best of our knowledge the first to employ ERPs to examine the ANT in older adults, our young adult data support recent ERP studies of the ANT that have demonstrated P300 reductions to incongruent vs. congruent target stimuli (e.g., Neuhaus et al., 2007, 2010). Similar congruency effects have been observed in Stroop paradigms (Zurrón et al., 2009), which have been interpreted in the context of well-replicated reductions in posterior P300 amplitude as task difficulty increases (Polich, 1987; Katayama and Polich, 1998). Given these consistent findings across different paradigms, it appears that reductions in P300 amplitudes reflect a disrupted allocation of attention that is associated with processing incongruent stimuli relative to congruent stimuli. Importantly, our findings suggest that congruency effects on P300 amplitudes are present in both young and older adults.

Taken together, our findings revealed significant behavioral and neural alterations of the alerting network in older adults. Cues designed to facilitate an alerting response were less effective in older than young adults. While alerting cues enhanced subsequent ERP reflections of attentional processing in younger adults, older adults did not show this effect. In fact, reductions in the N1 alerting effect in older adults help to account for broader age-related neuropsychological declines in attention. By contrast, ERP correlates of orienting and executive control networks reflected generalized amplitude reductions consistent with normal aging. These novel findings reveal that aging does not impact all networks of attention equally, but is uniquely associated with impairments in attentional alerting.

With regard to study limitations, the version of the ANT used in this study did not include an "invalid" spatial cueing condition, which would have enabled us to examine the full complement of engagement *and* disengagement of attentional orienting. Thus, we cannot interpret our results in terms of potential age-related deficits in disengagement (c.f., Shulman et al., 2010). Recently, several investigators have included invalid cues in their ANT paradigms, and have noted both beneficial and detrimental effects on the ability to

overcome response conflict following valid and invalid cues, respectively (e.g., Fan et al., 2009). Specifically, whereas valid cues likely enhance prepotent stimulus processing and effective shifting (i.e., orienting) of attention, invalid cueing conditions likely require the re-direction of attentional processes and the use of additional resources for conflict resolution. Consequently, future studies should investigate the differential effects of cue-validity on early ERP components, which have been found to be differentially sensitive to the effects of valid and invalid cueing conditions (e.g., Wright et al., 1995; Talsma et al., 2005). Similarly, the use of vertical, rather than lateralized cueing may have obscured orienting effects, as evidenced by small N1 to the spatial vs. center-cue conditions. Future ERP studies of orienting may benefit from use of lateralized attention network paradigms used in previous behavioral studies (e.g., Greene et al., 2008).

A broader problem associated with the ANT is the use of cognitive subtractions. For example, the alerting effect is typically assumed to reflect a contrast between two similar cognitive states that are differentiated only by cues. However, the condition in which no cue is provided may create additional difficulty for participants, as they do not know which type of stimulus will be presented next (Galvao-Carmona et al., 2014). By contrast, the appearance of the double cue removes uncertainty about the upcoming stimulus, particularly when these cues are always valid. Thus, a differential cognitive load may develop and interact with participant expectations during these trials, rendering a simplistic cognitive subtraction inadequate. In the current study, the additional analysis of ERP correlates in a factorial design produced ANOVA results that supported the findings of the cognitive subtractions, suggesting that the observed alerting effects cannot be dismissed as a simplistic comparison of two conditions.

An additional limitation was that our sample size was relatively small, which may have introduced variability and influenced our ability to detect significant differences. Finally, both groups of participants performed the task with very high accuracy. The near-ceiling performance accuracy precludes our ability to examine task errors on the ANT more fully, given their low frequency and non-normal distribution. Insufficient numbers of trials also hindered our ability to separately examine the neural reflections of each congruency condition as a function of cue condition. Instead, target congruency had to be collapsed across conditions in order to observe the effects of cue, which may have masked potentially meaningful insights about the interactions between cues and subsequent attentional targets.

## SUMMARY AND CONCLUSIONS

The current study examined age-related differences on the behavioral and neural correlates of three attentional networks (alerting, orienting, and executive control). Results revealed significant behavioral and ERP alterations in the alerting system of healthy older adults, even after controlling for generalized slowing and amplitude reductions. It appears that older adults had selective difficulty engaging the alerting network of attention, which prevented efficient facilitation of attention and subsequent responding. However, there is good news for those feeling "antsy" about age effects on attentional networks, as older adults did not exhibit behavioral or neural differences in orienting and executive control networks. As such, older adults may not be as efficiently alerted to upcoming information, yet they are equally capable in other aspects of attentional function. As the world's population ages, these results have important implications for our understanding of healthy aging.

## ETHICS STATEMENT

The study was approved by the University of Florida, Health Sciences Institutional Review Board.

## AUTHOR CONTRIBUTIONS

DASK was responsible for experimental design, data collection, and manuscript preparation. CNS was responsible for data collection, data analysis, and manuscript preparation. VMD was responsible for manuscript preparation. WMP was responsible for manuscript preparation.

## FUNDING

This work was supported by Grants from the NIH (T32-AG020499 to DASK, R21-MH0737076 to WMP, and R21-NS079767).

## REFERENCES

Beck, A. T. (1996). *Beck Depression Inventory - Second Edition (BDI-II).* San Antonio, TX, USA: The Psychological Corporation.

Bush, L., Hess, U., and Wolford, G. (1993). Transformations for within-subject designs: a monte carlo investigation. *Psychol. Bull.* 113, 566–579. doi: 10.1037/0033-2909.113.3.566

Cohen, J. (1988). *Statistical Power Analysis for the Behavioral Sciences.* Hillsdale, NJ: Erlbaum Associates.

Eriksen, B. A., and Eriksen, C. W. (1974). Effects of noise letters upon the identification of a target letter in a nonsearch task. *Percept. Psychophys.* 16, 143–149. doi: 10.3758/bf03203267

Fan, J., Byrne, J., Worden, M. S., Guise, K. G., McCandliss, B. D., Fossella, J., et al. (2007). The relation of brain oscillations to attentional networks. *J. Neurosci.* 27, 6197–6206. doi: 10.1523/JNEUROSCI.1833-07.2007

Fan, J., Gu, X., Guise, K. G., Liu, X., Fossella, J., Wang, H., et al. (2009). Testing the behavioral interaction and integration of attentional networks. *Brain Cogn.* 70, 209–220. doi: 10.1016/j.bandc.2009.02.002

Fan, J., Hof, P. R., Guise, K. G., Fossella, J. A., and Posner, M. I. (2007). The functional integration of the anterior cingulate cortex during conflict processing. *Cereb. Cortex* 187, 796–805. doi: 10.1093/cercor/bhm125

Fan, J., McCandliss, B. D., Fossella, J., Flombaum, J. I., and Posner, M. I. (2005). The activation of attentional networks. *Neuroimage* 26, 471–479. doi: 10.1016/j.neuroimage.2005.02.004

Fan, J., McCandliss, B. D., Sommers, T., Raz, A., and Posner, M. I. (2002). Testing the efficiency and independence of attentional networks. *J. Cogn. Neurosci.* 14, 340–347. doi: 10.1162/0898929023173 61886

Fan, J., and Posner, M. (2004). Human attentional networks. *Psychiatr. Prax.* 31, S210–S214. doi: 10.1055/s-2004-828484

Faust, M. E., Balota, D. A., Spieler, D. H., and Ferraro, F. R. (1999). Individual differences in information processing rate and amount: implications for group differences in response latency. *Psychol. Bull.* 125, 777–799. doi: 10.1037/0033-2909.125.6.777

Fernandez-Duque, D., and Black, S. E. (2006). Attentional networks in normal aging and Alzheimer's disease. *Neuropsychology* 20, 133–143. doi: 10. 1037/0894-4105.20.2.133

Fernandez-Duque, D., and Posner, M. I. (1997). Relating the mechanisms of orienting and alerting. *Neuropsychologia* 35, 477–486. doi: 10.1016/s0028-3932(96)00103-0

Fjell, A. M., and Walhovd, K. B. (2001). P300 and neuropsychological tests as measures of aging: scalp topography and cognitive changes. *Brain Topogr.* 14, 25–40. doi: 10.1023/A:1012563605837

Folk, C. L., and Hoyer, W. J. (1992). Aging and shifts of visual spatial attention. *Psychol. Aging* 7, 453–465. doi: 10.1037/0882-7974.7.3.453

Folstein, M. F., Folstein, S. E., and McHugh, P. R. (1975). "Mini-mental state": a practical method for grading the cognitive state of patients for the clinician. *J. Psychiatr. Res.* 12, 189–198. doi: 10.1016/0022-3956(75)90026-6

Ford, J. M., Roth, W. T., Isaacks, B. G., White, P. M., Hood, S. H., and Pfefferbaum, A. (1995). Elderly men and women are less responsive to startling noises: N1, P3 and blink evidence. *Biol. Psychol.* 39, 57–80. doi: 10.1016/0301-0511(94)00959-2

Forstmann, B. U., Tittgemeyer, M., Wagenmakers, E. J., Derrfus, J., Imperait, E., and Brown, S. (2011). The speed-accuracy tradeoff in the elderly brain: a structural model-based approach. *J. Neurosci.* 31, 17242–17249. doi: 10. 1523/JNEUROSCI.0309-11.2011

Galvao-Carmona, A., González-Rosa, J. J., Hidalgo-Muñoz, A. R., Parámo, D., Benétez, M. L., Izquierdo, G., et al. (2014). Disentangling the attention network test: behavioral, event related potentials and neural source analysis. *Front. Hum. Neurosci.* 8:813. doi: 10.3389/fnhum.2014.00813

Gamboz, N., Zamarian, S., and Cavellero, C. (2010). Age-related differences in the attention network test (ANT). *Exp. Aging Res.* 36, 287–305. doi: 10. 1080/0361073X.2010.484729

Golden, C. J. (1978). *Stroop Color and Word Test.* Chicago: Stoelting.

Golub, E. J., Miranda, G. G., Johnson, J. K., and Starr, A. (2001). Sensory cortical interactions in aging, mild cognitive impairment and Alzheimer's disease. *Neurobiol. Aging* 22, 755–763. doi: 10.1016/s0197-4580(01) 00244-5

Greene, D. J., Barnea, A., Herzberg, K., Rassis, A., Neta, M., Raz, A., et al. (2008). Measuring attention in the hemispheres: the lateralized attention network test (LANT). *Brain Cogn.* 66, 21–31. doi: 10.1016/j.bandc.2007. 05.003

Greenwood, P. M., Parasuraman, R., and Haxby, J. V. (1993). Visuospatial attention across the adult lifespan. *Neuropsychologia* 31, 471–485. doi: 10. 1016/0028-3932(93)90061-4

Harter, M. R., Miller, S. L., Price, N. J., LaLonde, M. E., and Keyes, A. L. (1989). Neural processes involved in directing attention. *J. Cogn. Neurosci.* 1, 223–237. doi: 10.1162/jocn.1989.1.3.223

Hartley, A. A. (1993). Evidence for the selective preservation of spatial selective attention in old age. *Psychol. Aging* 8, 371–379. doi: 10.1037/0882-7974. 8.3.371

Hartley, A. A., Kieley, J. M., and Slabach, E. H. (1990). Age differences and similarities in the effects of cues and prompts. *J. Exp. Psychol. Hum. Percept. Perform.* 16, 523–537. doi: 10.1037/0096-1523.16.3.523

Hillyard, S. A., Vogel, E. K., and Luck, S. J. (1998). Sensory gain control (amplification) as a mechanism of selective attention: electrophysiological and neuroimaging evidence. *Philos. Trans. R. Soc. Lond. B Biol. Sci.* 353, 1257–1270. doi: 10.1098/rstb.1998.0281

Hopf, J. M., and Mangun, G. R. (2000). Shifting attention in space: an electrophysiological analysis using high spatial resolution mapping. *Clin. Neurophysiol.* 111, 1241–1257. doi: 10.1016/s1388-2457(00) 00313-8

Jennings, J. M., Dagenbach, D., Engle, C. M., and Funke, L. J. (2007). Age-related changes and the attention network task: an examination of alerting, orienting and executive function. *Neuropsychol. Dev. Cogn. B Aging Neuropsychol. Cogn.* 14, 353–369. doi: 10.1080/13825580600788837

Katayama, J., and Polich, J. (1998). Stimulus context determines P3a and P3b. *Psychophysiology* 35, 23–33. doi: 10.1111/1469-8986.35 10023

Larson, M. J., Kaufman, D. A., and Perlstein, W. M. (2009). Neural time course of conflict adaptation effects on the Stroop task. *Neuropsychologia* 47, 663–670. doi: 10.1016/j.neuropsychologia.2008.11.013

Luck, S. J. (2005). *An Introduction to the Event-Related Potential Technique* Cambridge, MA: MIT Press.

MacLeod, J. W., Lawrence, M. A., McConnell, M. M., Eskes, G. A., Klein, R. M., and Shore, D. I. (2010). Appraising the ANT: psychometric and theoretical considerations of the attention network test. *Neuropsychology* 24, 637–651. doi: 10.1037/a0019803

Mangun, G. R. (1995). Neural mechanisms of visual selective attention. *Psychophysiology* 32, 4–18. doi: 10.1111/j.1469-8986.1995. tb03400.x

Neter, J., Wasserman, W., and Kutner, M. H. (1985). *Applied Linear Statistical Models: Regression, Analysis of Variance and Experimental Designs.* 2nd Edn. Homewood, IL: R.D. Irwin.

Neuhaus, A. H., Koehler, S., Opgen-Rhein, C., Urbanek, C., Hahn, E., and Dettling, M. (2007). Selective anterior cingulate cortex deficit during conflict solution in schizophrenia: an event-related potential study. *J. Psychiatr. Res.* 41, 635–644. doi: 10.1016/j.jpsychires.2006.06.012

Neuhaus, A. H., Urbanek, C., Opgen-Rhein, C., Hahn, E., Ta, T. M. T., Koehler, S., et al. (2010). Event-related potentials associated with Attention Network Test. *Int. J. Psychophysiol.* 76, 72–79. doi: 10.1016/j.ijpsycho.2010. 02.005

Nobre, A. C., Sebestyen, G. N., and Miniussi, C. (2000). The dynamics of shifting visuospatial attention revealed by event-related potentials. *Neuropsychologia* 38, 964–974. doi: 10.1016/s0028-3932(00)00015-4

Polich, J. (1987). Task difficulty, probability and inter-stimulus interval as determinants of P300 from auditory stimuli. *Electroencephalogr. Clin. Neurophysiol.* 68, 311–320. doi: 10.1016/0168-5597(87)90052-9

Polich, J. (2007). Updating P300: an integrative theory of P3a and P3b. *Clin. Neurophysiol.* 118, 2128–2148. doi: 10.1016/j.clinph.2007. 04.019

Posner, M. I. (1980). Orienting of attention. *Q. J. Exp. Psychol.* 32, 3–25.

Posner, M. I., and Fan, J. (2004). "Attention as an organ system," in *Topics in Integrative Neuroscience: From Cells to Cognition*, eds J. R. Pomerantz and M. C. Crair (Cambridge: Cambridge University Press), 31–61.

Posner, M. I., and Peterson, S. E. (1990). The attention system of the human brain. *Annu. Rev. Neurosci.* 13, 25–42. doi: 10.1146/annurev.neuro. 13.1.25

Posner, M. I., Sheese, B. E., Odludaş, Y., and Tang, Y. (2006). Analyzing and shaping human attentional networks. *Neural Netw.* 19, 1422–1429. doi: 10. 1016/j.neunet.2006.08.004

Ratcliff, R. (1993). Methods for dealing with reaction time outliers. *Psychol. Bull.* 114, 510–532. doi: 10.1037/0033-2909.114.3.510

Reitan, R. M., and Wolfson, D. (1995). Category test and trail making test as measures of frontal lobe functions. *Clin. Neuropsychol.* 9, 50–56. doi: 10. 1080/13854049508402057

Scherg, M. (1990). "Fundamentals of dipole source potential analysis," in *Auditory Evoked Magnetic Fields and Electric Potentials. Advances in Audiology*, (Vol. 6) eds F. Grandori and M. Hoke (Basel: Karger), 65–78.

Shulman, G. L., Pope, D. L., Astafiev, S. V., McAvoy, M. P., Snyder, A. Z., and Corbetta, M. (2010). Right hemisphere dominance during spatial selective attention and target detection occurs outside the dorsal frontoparietal network. *J. Neurosci.* 30, 3640–3651. doi: 10.1523/JNEUROSCI.4085-09.2010

Speilberger, C. D., Gorusch, R. L., Lushene, R., Vagg, P. R., and Jacobs, G. A. (1983). *Manual for the State-Trait Anxiety Inventory.* Palo Alto, CA: Consulting Psychologists Press.

Starkstein, S. E., Mayberg, H. S., Preziosi, T. J., Andrezejewski, P., Leiguarda, R., and Robinson, R. G. (1992). Reliability, validity and clinical correlates of apathy in Parkinson's disease. *J. Neuropsychiatry Clin. Neurosci.* 4, 134–139. doi: 10. 1176/jnp.4.2.134

Talsma, D., Slagter, H. A., Nieuwenhuis, S., Hage, J., and Kok, A. (2005). The orienting of visuospatial attention: an event-related potential study. *Brain Res. Cogn. Brain Res.* 25, 117–129. doi: 10.1016/j.cogbrainres.2005.04.013

van Veen, V., and Carter, C. S. (2002). The anterior cingulate as a conflict monitor: fMRI and ERP studies. *Physiol. Behav.* 77, 477–482. doi: 10.1016/s0031-9384(02)00930-7

Verhaeghen, P., and Cerella, J. (2002). Aging, executive control and attention: a review of meta-analyses. *Neurosci. Biobehav. Rev.* 26, 849–857. doi: 10.1016/s0149-7634(02)00071-4

Verhaeghen, P., and De Meersman, L. (1998). Aging and the Stroop effect: a meta-analysis. *Psychol. Aging* 13, 120–126. doi: 10.1037/0882-7974.13.1.120

Wechsler, D. A. (1997). *Wechsler Adult Intelligence Scale.* 3rd Edn. San Antonio, TX: The Psychological Corporation.

Wolfinger, R., Tobias, R., and Sall, J. (1994). Computing gaussian likelihoods and their derivatives for general linear mixed models. *SIAM J. Sci. Comput.* 15, 1294–1310. doi: 10.1137/0915079

Wright, M. J., Geffen, G. M., and Geffen, L. B. (1995). Event-related potentials during covert orientation of visual-attention: effects of cue validity and directionality. *Biol. Psychol.* 41, 183–202. doi: 10.1016/0301-0511(95)05128-7

Yesavage, J. A., Brink, T. L., Rose, T. L., Lum, O., Huang, V., Adey, M., et al. (1983). Development and validation of a geriatric depression screening scale: a preliminary report. *J. Psychiatr. Res.* 17, 37–49. doi: 10.1016/0022-3956(82)90033-4

Zhou, S. S., Fan, J., Lee, T. M., Wang, C. Q., and Wang, K. (2011). Age-related differences in attentional networks of alerting and executive control in young, middle-aged, and older Chinese adults. *Brain Cogn.* 75, 205–210. doi: 10.1016/j.bandc.2010.12.003

Zurrón, M., Pousoa, M., Lindína, M., Galdoa, S., and Díaza, F. (2009). Event-related potentials with the Stroop colour-word task: timing of semantic conflict. *Int. J. Psychophysiol.* 72, 246–252. doi: 10.1016/j.ijpsycho.2009.01.002

**Conflict of Interest Statement**: The authors declare that the research was conducted in the absence of any commercial or financial relationships that could be construed as a potential conflict of interest.

frontiers in Aging Neuroscience

ORIGINAL RESEARCH
published: 02 May 2016
doi: 10.3389/fnagi.2016.00101

# Orbitofrontal Cortex and the Early Processing of Visual Novelty in Healthy Aging

*David A. S. Kaufman[1]*, Cierra M. Keith[1] and William M. Perlstein[2,3,4]*

*[1] Department of Psychology, Saint Louis University, St. Louis, MO, USA, [2] Department of Clinical and Health Psychology, University of Florida, Gainesville, FL, USA, [3] Department of Psychiatry, University of Florida, Gainesville, FL, USA, [4] VA RR&D Brain Rehabilitation Research Center of Excellence, Malcom Randall Veterans Administration Medical Center, Gainesville, FL, USA*

Event-related potential (ERP) studies have previously found that scalp topographies of attention-related ERP components show frontal shifts with age, suggesting an increased need for compensatory frontal activity to assist with top-down facilitation of attention. However, the precise neural time course of top-down attentional control in aging is not clear. In this study, 20 young (mean: 22 years) and 14 older (mean: 64 years) adults completed a three-stimulus visual oddball task while high-density ERPs were acquired. Colorful, novel distracters were presented to engage early visual processing. Relative to young controls, older participants exhibited elevations in occipital early posterior positivity (EPP), approximately 100 ms after viewing colorful distracters. Neural source models for older adults implicated unique patterns of orbitofrontal cortex (OFC; BA 11) activity during early visual novelty processing (100 ms), which was positively correlated with subsequent activations in primary visual cortex (BA 17). Older adult EPP amplitudes and OFC activity were associated with performance on tests of complex attention and executive function. These findings are suggestive of age-related, compensatory neural changes that may driven by a combination of weaker cortical efficiency and increased need for top-down control over attention. Accordingly, enhanced early OFC activity during visual attention may serve as an important indicator of frontal lobe integrity in healthy aging.

**Keywords: ERPs, aging, oddball, orbitofrontal cortex, attention, sLORETA**

OPEN ACCESS

***Edited by:***
*Junfeng Sun,*
*Shanghai Jiao Tong University, China*

***Reviewed by:***
*Shulan Hsieh,*
*National Cheng Kung University, Taiwan*
*Ling Li,*
*University of Electronic Science and Technology of China, China*

****Correspondence:***
*David A. S. Kaufman*
*dkaufma3@slu.edu*

***Received:*** *01 December 2015*
***Accepted:*** *18 April 2016*
***Published:*** *02 May 2016*

***Citation:***
*Kaufman DAS, Keith CM and Perlstein WM (2016) Orbitofrontal Cortex and the Early Processing of Visual Novelty in Healthy Aging. Front. Aging Neurosci. 8:101. doi: 10.3389/fnagi.2016.00101*

## INTRODUCTION

The ability to orient to new stimuli and respond with flexibility to a changing environment is a crucial skill (Barceló et al., 2002). One way to simulate environmental change and examine cognitive control involves the introduction of an unexpected novel stimulus, which intends to capture and divert attention (de Fockert et al., 2004; Barcelo et al., 2006). In cognitive neuroscience, the oddball paradigm has been frequently used to assess neural responses to irregularly occurring, novel stimuli (Friedman, 2003). Although it is a relatively simple task involving response to an infrequent target stimulus presented amongst more common standard stimuli, it has been interpreted as a probe for frontal cortex activity (Fabiani and Friedman, 1995). Huettel and McCarthy (2004) theorized that activation of the prefrontal cortex during the oddball paradigm can be associated with inhibition and modification of behavioral response strategies. Given the infrequency of targets, oddball tasks foster a predominantly passive response style that must

be overcome when targets are detected. Accordingly, optimization of attentional processing during these tasks requires synchronization between bottom-up and top-down processing systems.

Top-down processing assists in the voluntary discrimination of relevant stimuli from distractors (Gazzaley et al., 2005). Normal aging is associated with increases in distractibility, which may be due to increased difficulty filtering irrelevant sensory information during attentional processing (McDowd and Filion, 1992; Chao and Knight, 1997; Alain and Woods, 1999; Fabiani et al., 2006). This inhibitory deficit hypothesis is commonly cited as an influential factor driving age-related cognitive decline (Hasher and Zacks, 1988; Gazzaley and D'Esposito, 2007). Age-related changes in attentional control are often linked to frontal lobe structures, which undergo structural and functional compromise in healthy aging (Raz et al., 2005). However, older adults also exhibit declines with bottom-up sensory processing (Carp et al., 2011), which can also contribute to age-related declines in visual attention. While many studies have suggested that enhanced activity in frontal lobe structures helps to compensate for age-related declines in sensory processing (Reuter-Lorenz and Cappell, 2008; Li et al., 2013), it remains unclear exactly how top-down mechanisms of control are coordinated.

The neural time course of attentional processing can be examined with high temporal resolution using electrophysiological methods. Visual oddball studies have frequently reported event-related potentials (ERPs) that highlight age-related differences in attention. In particular, target-related P3 components (also referred to as P300 or P3b) demonstrate increased latency in older adults, while overall amplitudes decrease with age (Polich, 2007; Friedman, 2008). In young adults, target-related P3 amplitudes are typically maximal over parietal electrode sites, yet in older adults these amplitudes decrease at both parietal and central locations, while often preserving higher amplitudes over frontal sites. This has often been interpreted as an age-related "frontal shift" with regard to neural resources necessary for processing attentional targets (Fabiani and Friedman, 1995; Friedman et al., 1993). When infrequent distracters are incorporated into oddball paradigms, they evoke a different type of P3 response (often referred to as P3a or novelty P3), which reflects a more rapid detection of novel, task-irrelevant events (Simons and Perlstein, 1997). Distracter-related P3 amplitudes are maximal over frontocentral sites, and increase when the target recognition is more difficult (Katayama and Polich, 1999; Polich and Comerchero, 2003). Although the shift in target-related P3 amplitudes has often presumed a link with frontal lobe structures, imaging studies suggest that a broader network of neural sources give rise to this component, including prefrontal cortex, temporal-parietal junction, lateral parietal cortex, and anterior cingulate (Bedowski et al., 2004).

While many studies have investigated age-related frontal shifts in P3 potentials, effects of aging on early visual sensory (or "exogenous") ERPs have received less attention. This omission is important, as recent studies have revealed that frontal lobe structures may influence visual processing in very early time windows (80–150 ms). Using a combination of Magnetoencephalography (MEG) and Functional magnetic resonance imaging (fMRI) methods, Bar et al. (2006) found that the orbitofrontal cortex (OFC) exhibited differential activity that predicted successful recognition of visual objects, beginning approximately 80 ms after the object appeared. These authors took their findings to suggest that the OFC may receive coarse visual inputs following initial sensory processing which can then be used to make predictions that guide subsequent visual processing that is more specialized (Bar, 2009). Indeed, some cells in the OFC appear to be particularly sensitive to visual novelty, showing selective activation between 80–120 ms post-stimulus (Rolls et al., 2005). While few studies have reported age-related changes that occur in these early sensory processing stages, De Sanctis et al. (2008) observed increased N1 amplitude in older adults, along with enhanced early frontal cortical activation. These results suggest that older adults may enhance frontal activity during early visual processing in order increase their top-down control over visual attention.

In the current study, a three-stimulus oddball paradigm was used to examine early processing of visual novelty in young and older adults. Scalp ERP results were analyzed for early sensory processing and subjected to source localization. Distracter novelty was manipulated during the task, which presented either monochrome or colorful distractors in different trial blocks. Color distracters were presented in order to evoke early visual cortex activity associated with color feature selection, which can be observed as a large posterior negativity, beginning approximately 140 ms post-stimulus and localized to occipital cortex (Hillyard and Anllo-Vento, 1998). Given the proposed role of the OFC in novelty processing and top-down regulation of attention, it was hypothesized that this structure would become differentially involved during the early processing of distracters (80–120 ms). In particular, this early OFC activation was expected to precede visual cortex activations associated with color feature processing. In line with prior studies reporting age-related decline in visual attention, older adults were expected to rely on greater levels of OFC involvement during early processing of colorful distracters. In addition to the oddball paradigm, participants completed several neuropsychological tasks, so that age-related changes could be interpreted in the broader context of executive functioning.

# MATERIALS AND METHODS

## Participants

A total of 34 participants (20 younger, 14 older) were recruited from advertisements in the local community and undergraduate psychology courses. Demographic characteristics are presented in **Table 1**. Participants were matched across all characteristics except for age, in which younger participants had a mean age (± SD) of 22.1 years (± 3.1) and older participants had a mean age of 64.4 years (± 9.5). Neuropsychological

**TABLE 1 | Demographic and cognitive data for younger and older participants.**

| | Younger ($n$ = 20) | | Older ($n$ = 14) | | |
|---|---|---|---|---|---|
| | **Mean** | **(SD)** | **Mean** | **(SD)** | ***p*** |
| **Demographics** | | | | | |
| Age (years) | 22.1 | (3.1) | 64.4 | (9.5) | *<0.001* |
| Education (years) | 15.4 | (1.7) | 17.1 | (3.3) | ns |
| Female (%) | 50 | – | 43 | – | ns |
| Right-handed (%) | 85 | – | 86 | – | ns |
| **Cognitive functioning** | | | | | |
| MMSE | 28.9 | (1.1) | 28.7 | (1.3) | ns |
| Digit symbol coding (Total) | 87.7 | (12.2) | 77.4 | (11.7) | *0.02* |
| Stroop word reading (sec) | 101.4 | (15.0) | 99.5 | (13.5) | ns |
| Stroop color naming (sec) | 80.0 | (14.0) | 72.6 | (15.9) | ns |
| Stroop color word naming (sec) | 46.9 | (12.6) | 38.8 | (11.9) | ns |
| Trails A (sec) | 20.8 | (4.7) | 27.7 | (10.6) | *0.01* |
| Trails B (sec) | 47.0 | (15.4) | 63.8 | (28.7) | *0.03* |
| WCST Categories completed | 6.0 | 0.0 | 5.6 | (1.3) | ns |
| WCST Total errors | 15.1 | (9.6) | 17.6 | (16.7) | ns |
| WCST Perseverative responses | 8.6 | (4.3) | 10.3 | (10.4) | ns |
| WCST Perseverative errors | 7.9 | (3.8) | 9.8 | (8.9) | ns |
| WCST Set failure | 0.1 | (0.3) | 0.3 | (0.7) | ns |

*MMSE, Mini-Mental State Examination; WCST, Wisconsin Card Sorting Test.*

testing revealed that older adults had comparable levels of cognition (MMSE), inhibition (Stroop), and feedback-dependent problem solving (Wisconsin Card Sorting Test). However, older adults were significantly slower on tasks of complex attention and set-shifting (Digit Symbol Coding, Trails A and B). Potential participants (3 young, 1 older) were excluded from the study because they endorsed a history of substance abuse or dependence, acquired brain disorders (e.g., traumatic brain injury), neurological disorders, or color-blindness. Participants provided written informed consent according to procedures established by the University of Florida Health Science Center Institutional Review Board and were provided either $20 or course extra credit for study participation.

## Event-Related Potential Stimuli and Task

Stimuli and procedures for the three-stimulus oddball task were adapted from Polich and Comerchero (2003). Standard stimuli, to which the participants were told not to respond, consisted of small gray circles measuring 2" in diameter. Target stimuli were medium-sized gray circles, measuring 3", and participants were instructed to press a button when they saw these stimuli. Distracter stimuli, to which the participants were told not to respond, consisted of large squares measuring 4.5" in diameter. Because distracters were deviant from standards and targets in these two characteristics (size, shape), the amount of visual attention devoted to these distracters was optimized (Polich and Comerchero, 2003; Sawaki and Katayama, 2007). Distracter novelty was further manipulated by stimulus features contained within the large squares. Half of the distracters were gray, like the targets and standards, and were identical in appearance throughout the experiment. The other distracters contained colorful fractal designs that were unique and only occurred once over the course of the experiment (see **Figure 1** for an example). Mean (± SD) luminance intensity for the color distracter slides were 24.1 cd/m$^2$ (± 9.3), which did not deviate substantially from that of gray distracters (23.1 cd/m$^2$). Thus color and gray distracters had similar physical properties (size, luminance), despite their differences in chromatic features.

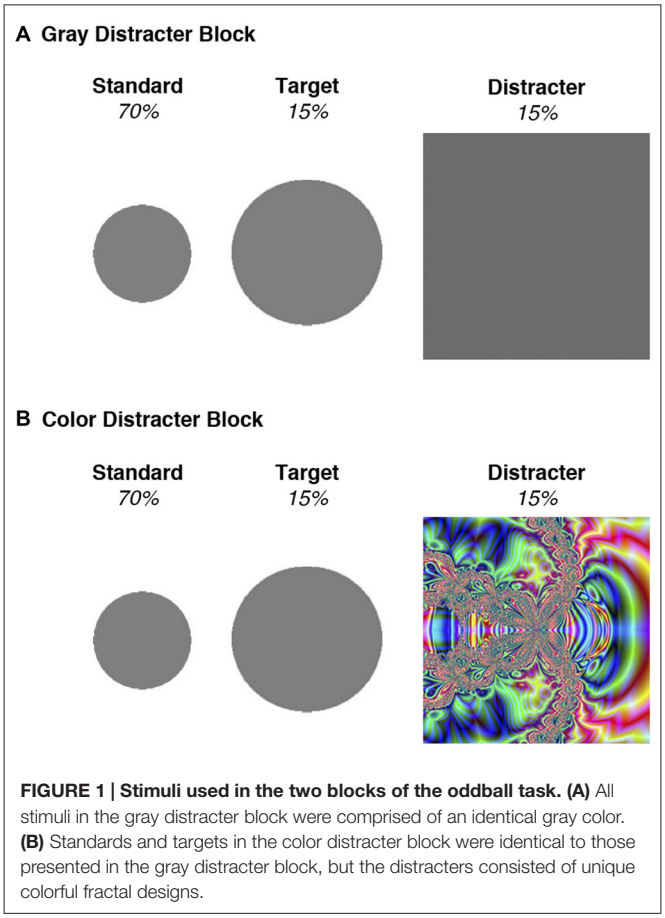


**FIGURE 1 | Stimuli used in the two blocks of the oddball task. (A)** All stimuli in the gray distracter block were comprised of an identical gray color. **(B)** Standards and targets in the color distracter block were identical to those presented in the gray distracter block, but the distracters consisted of unique colorful fractal designs.

A total of 600 stimuli were randomly presented in four blocks of 150. Seventy percentage were standard stimuli (small circles), 15% were targets (medium circles), and 15% were distracters (large squares). Each stimulus was presented for 75 ms, with a 2 s inter-stimulus interval. Color and gray distracters were presented in different trial blocks to examine the block-related effects of distracter type on behavioral and electrophysiological data. Presentation order of color and gray distracter blocks was counterbalanced across participants such that half of the participants completed the color distracter blocks first and third, while the other participants completed color distracter blocks second and fourth. A practice task consisting of 10 stimuli (6 standards, 2 targets, and 2 gray distracters) was presented in advance to ascertain that all participants were able to discriminate targets from standards. The practice task was repeated as needed until all participants achieved 8 out of 10 correct responses.

## Electrophysiological Data Recording, Reduction, and Measurement

Electroencephalographram data were recorded from the scalp using a 64-channel system (Electrical Geodesics, Inc., Eugene, Oregon) running Net Station Software. Impedance of electrodes was maintained below 50 kΩ. EEG was initially referenced to the vertex and recorded continuously at 250 Hz, with on-line band-pass filtering from 0.1 to 100 Hz. Electroencephalogram data were then re-referenced to an average reference off-line and digitally low-pass filtered at 30 Hz. Eye movement and blink artifacts were corrected using spatial filtering methods (Scherg, 1990). The mean (± SD) amplitude used for rejection was a lenient 110 μV (± 16), in order to maximize the number of trials that could be included in averaging without introducing artifacts. The maximum allowable amplitude settings for each trial were individualized for each participant (as recommended by Luck, 2005), but did not differ by group, $t_{(32)} = 0.25$, $p > 0.80$. Point-to-point transitions were not allowed to exceed 75 μV. Of the 64 electrodes used to collect data, less than 2% were interpolated during analysis in order to correct for artifacts.

Individual-subject stimulus-locked averages were derived separately for standard, target, and distracter stimuli in each of the two distracter blocks. Error trials were excluded from ERP analysis. Epochs were extracted from a window of 200 ms prior- to 800 ms post-stimulus presentation and baseline-corrected (200 ms prior to stimulus onset) before subject averaging and analysis. Four occipital electrodes corresponding with O1, O2, PO7, and PO8 were used to examine early posterior positivity (EPP; EGI sensors: 32, 37, 40, 45).

Early Posterior Negativity (EPN) was maximal over medial occipital sites, particularly for younger adults, so three medial occipital electrodes corresponding with O1, O2, and Oz were used to quantify this component (EGI sensors: 37, 40, 38). Four midline electrodes corresponding with FCz, Cz, CPz, Pz were chosen for measurement and analysis of P3 responses (EGI sensors: 4, 65, 30, 34). ERP components were analyzed using adaptive mean amplitude and peak latency scoring protocols in Net Station Software. The adaptive mean algorithm identified a peak within each selected time window and then defined a new time window around this peak for scoring the mean voltage. Time windows used for scoring the different ERP components were as follows: Lateral EPP: 80–130 ms (adaptive mean: 8 ms pre- to 8 ms post-peak), Midline EPN: 100–220 ms (adaptive mean: 8 ms pre- to 8 ms post-peak), and P3: 300–650 ms (adaptive mean: 120 ms pre- to 120 ms post-peak).

## Data Analysis

Visual inspection of the oddball task data for normality revealed a considerable positive skew. We, therefore, applied the arcsine correction for all error rate data (Neter et al., 1985) and subjected them to a 2-Distracter (gray, color) × 3-Stimulus (standard, target, distracter) repeated measures analysis of variance (ANOVA). For analyses of oddball task response time (RT), median RTs were employed for correct responses (Ratcliff, 1993) and compared between distracter conditions via dependent sample *t*-tests.

Because of their broad scalp distribution, P3 mean amplitudes and peak latencies were examined with 2-Distracter (gray, color) × 3-Stimulus (standard, target, distracter) × 4-Electrode Site (Fcz, Cz, Cpz, Pz) repeated measures ANOVAs. EPP and EPN components were subjected to 2-Distracter (gray, color) × 3-Stimulus (standard, target, distracter) repeated measures ANOVAs, using data from the average electrodes in which each ERP component showed maximal amplitude (Picton et al., 2000). Orthogonal ("Helmert") planned contrasts were used in these ANOVAs such that stimulus comparisons were made in the following order: (1) standards vs. targets and distracters; and (2) targets vs. distracters. When applicable, difference waves were calculated by subtracting one condition of interest from another (e.g., color distracters—gray distracters). In order to isolate scalp ERP signals associated with color distracter processing, difference waves were calculated for each stimulus type, such that trials from the gray distracter block were subtracted from trials in the color distracter block.

When necessary to decompose ANOVA results, follow-up *post hoc* comparisons were made using Bonferroni corrections for multiple comparisons. The Huynh-Feldt epsilon adjustment was used for all repeated measures ANOVAs with greater than 1 degree of freedom; uncorrected degrees of freedom and corrected *p*-values are reported.

## Neural Source Analysis

Source localization was examined using a realistic finite difference forward model of head conductivity (based on a typical adult head MRI from the Montreal Neurological Institute). A dense dipole set was used in GeoSource 2.0 Software (Electrical Geodesics Inc.), which includes 2447 source dipoles (*x*, *y*, *z* triples) in 7 $mm^3$ voxels of gray matter, following the method of Pascual-Marqui et al. (1994). The linear inverse solution was computed using the constraints of sLORETA.

Brodmann areas (BAs) were examined using "source montages" defined by the Talairach coordinates (Waters and Tucker, 2013). All dipoles in the brain were represented by a triple regional source, consisting of three dipoles in the *x*, *y*, and *z* orthogonal orientations. The net equivalent dipole for each BA source region was computed as the vector sum of the *x*, *y*, *z* triples for the voxels contained within that region. Particular BAs were selected for statistical analysis based on our predictions that OFC and visual cortex would both be active during the early time windows corresponding to scalp ERP components. Thus BA 11 and BA 17 were selected as *a priori* regions of interest, with neural time course activations for these two regions extracted as the root mean square (RMS) of the *x*, *y*, *z* orthogonal orientations. Consistent with other methods used to examine neural source effects (Lamm et al., 2013; Waters and Tucker, 2013), these two source regions were noted to exhibit changes in source intensity (above an arbitrary threshold) that was observably coincident with the temporal features of the scalp ERP. Mean amplitudes from these source waveforms were then calculated for particular time windows of interest (100 ms, 140 ms), and subjected to difference wave

calculation in a manner similar to scalp ERP components of interest.

# RESULTS

## Oddball Task Performance

Accuracy and RT data from the oddball task were subjected to separate 2-Distracter × 3-Stimulus ANOVAs. With regard to task accuracy, planned contrasts revealed a main effect of distracter type, such that participants made more errors to infrequent stimuli than standards, [$F_{(1,32)}$ = 47.8, $p < 0.001$, $\eta^2 = 0.60$], while distracters evoked more errors than targets [$F_{(1,32)}$ = 18.3, $p < 0.001$, $\eta^2 = 0.36$]. There was no main effect of group for accuracy. Errors were much more common for trials in the color distracter blocks than gray distracter blocks [$F_{(1,32)}$ = 69.4, $p < 0.001$, $\eta^2 = 0.69$], with high error rates for distracters (21.0%), followed by targets (6.1%), and standards (2.0%) in the color distracter block. With regard to target RT, there were no main effects of group or distracter type or Group × Distracter interaction.

## Event-Related Potential Data

Within the gray distracter block, standard stimuli waveforms contained an average (± SD) of 165.5 ± 22.9 trials, while target waveforms contained 35.5 ± 5.1 trials and distracter waveforms contained 34.0 ± 4.9. Within the color distracter block, standard stimuli waveforms contained an average (± SD) of 165.7 ± 23.9 trials, while target waveforms contained 34.8 ± 5.2 trials and distracter waveforms contained 34.6 ± 5.2. A Group (2) × Distracter (2) × Stimulus (3) ANOVA confirmed that younger and older participants did not differ in their number of trials that were acceptable for analysis. Furthermore, distracter type did not influence the number of trials comprising the waveforms (main effect and interaction with stimulus type were nonsignificant). Stimulus-locked ERP waveforms taken from lateral and medial occipital sites can be seen in **Figure 2**.

### Early Posterior Positivity (EPP)

EPP activity was maximal over lateral occipital sites. While there was no main effect of group, planned contrasts revealed that EPP amplitude exhibited a significant Group × Distracter × Stimulus interaction. Older adults exhibited larger EPP for color distracters than younger adults, even though other stimuli showed no group differences, $F_{(1,32)} = 8.9$, $p < 0.01$, $\eta^2 = 0.22$.

In order to better isolate scalp ERP signals associated with color distracter processing, difference waves were calculated for each stimulus type, such that trials from gray distracter blocks were subtracted from those with color distracters. This resulted in the following EPP difference wave categories: (1) standard color-gray; (2) target color-gray; and (3) distracter color-gray. A Group (2) × Stimulus (3) ANOVA confirmed that the color-related enhancement of distracter EPP was only seen in older adults, $F_{(1,32)} = 15.7$, $p < 0.001$, $\eta^2 = 0.33$. **Figure 3A** shows these effects by graphing the standardized EPP amplitudes (i.e., color-gray difference waves) for each stimulus across groups.

EPP latencies peaked between 100–112 ms across conditions. There was a significant main effect of group, such that EPP amplitudes peaked earlier for older adults, $F_{(1,32)} = 4.3$, $p < 0.05$, $\eta^2 = 0.12$. A Distracter × Stimulus interaction revealed that EPP peak latency was shorter for color distracters than gray, while other stimuli did not differ as a function of distracter block, $F_{(1,32)} = 6.1$, $p < 0.05$, $\eta^2 = 0.16$.

### Early Posterior Negativity (EPN)

EPN activity was maximal over medial occipital sites. There was a main effect of group, with older adults exhibiting larger EPN than younger adults, $F_{(1,32)} = 12.8$, $p = 0.001$, $\eta^2 = 0.29$. Planned contrasts revealed that EPN amplitude exhibited significant a distracter × stimulus type interaction, such that color distracters evoked larger EPN than gray distracters, $F_{(1,32)} = 25.1$, $p = 0.001$, $\eta^2 = 0.44$. However, this interaction did not differ as a function of group, and no other effects on EPN were significant.

EPN difference waves were calculated for each stimulus type, following the same procedures employed for EPP difference waves. A Group (2) × Stimulus (3) ANOVA confirmed a strong main effect of stimulus, such that color distracters evoked larger EPN amplitudes than targets or standards, $F_{(1,32)} = 43.3$, $p < 0.001$. This color-related enhancement of distracter EPN did not differ as a function of group, $F_{(1,32)} = 0.1$, $p > 0.72$. **Figure 3B** shows these effects by plotting the standardized EPN amplitudes (i.e., color-gray difference waves) for each stimulus across groups.

EPN latencies peaked between 140–160 ms across conditions. Planned contrasts revealed a Distracter × Stimulus interaction, such that EPN peak latency was shorter for distracters than targets and standards, but only in color distracter block, $F_{(1,32)} = 6.7$, $p < 0.05$, $\eta^2 = 0.17$. Thus EPN latency did not vary as a function of group.

### P3

P3 activity had a broad distribution and could be seen across multiple midline sites. Planned contrasts revealed a significant Group (2) × Distracter (2) × Stimulus (3) × Site (4) interaction, such that older patients exhibited larger centrofrontal P3 amplitude for targets and distracters relative standards in the color distracter block [$F_{(1,32)} = 10.0$, $p < 0.01$, $\eta^2 = 0.24$]. This effect can be visualized when comparing the P3 voltage distribution maps in **Figure 2**, which demonstrate enhanced centrofrontal P3 amplitude for older adults relative to younger controls.

Midline P3 latencies peaked between 380–450 ms across conditions. Planned contrasts of peak latencies revealed a main effect of stimulus, such that target P3 latencies were longer than those evoked by distracters [$F_{(1,32)} = 14.4$, $p = 0.001$, $\eta^2 = 0.29$], or standards [$F_{(1,32)} = 6.7$, $p < 0.05$, $\eta^2 = 0.17$]. While there was no main effect of group, group interacted with stimulus [$F_{(1,32)} = 13.1$, $p = 0.001$, $\eta^2 = 0.29$], such that older adults had P3 latencies that were longer for infrequent stimuli (targets and distracters) relative to young adults.

### Neural Source Modeling

In order to estimate neural sources associated with the early sensory effects of color distracters, difference waves for each stimulus were subjected to sLORETA analysis. Visual

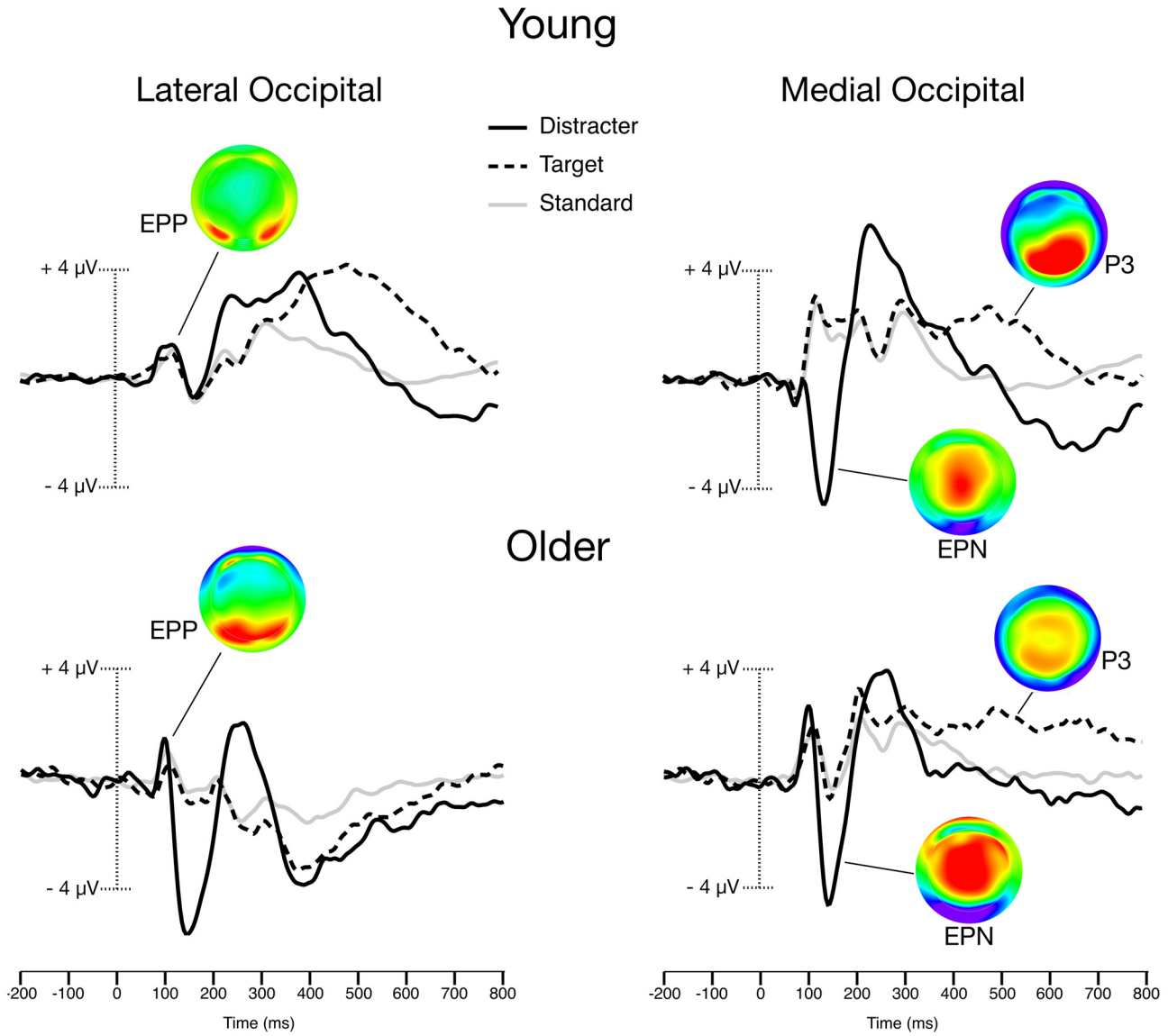


**FIGURE 2 | Grand-averaged Event-related potentials (ERPs) from the color distracter block trials.** Scalp maps illustrate the peak amplitudes of color distracter processing for early posterior positivity (EPP; 100 ms), Early Posterior Negativity (EPN; 140 ms), and P3 (400 ms). Lateral occipital waveforms were averaged from O1, O2, PO7, and PO8 electrodes. Medial occipital waveforms were averaged from O1, O2, and Oz electrodes.

examination of sLORETA source models revealed distracter-related activations in visual cortex (BA 17) and OFC (BA 11) regions within the first 200 ms post-stimulus. For each BA region of interest, the RMS of each dipole's three orientations was calculated, as shown in the source waveforms in **Figure 4**. For both age groups, activity began to increase in visual cortex regions approximately 80 ms post-stimulus, peaked around 140 ms, and then decreased back down to baseline around 200 ms post-stimulus. In order to quantify these activations, mean source amplitudes were scored for visual cortex ROIs during the beginning (100 ms) and peak activation (140 ms) portions of this time window. It should be noted that this early time window corresponds to the peak latency of the scalp EPP, while the later time window corresponds to the peak latency of the scalp EPN. Shortly after the initial increase in visual cortex activity, small activations can be seen in OFC between 90–110 ms post-stimulus. Accordingly, mean source amplitudes were scored for the OFC during the peak of this frontal activation (100 ms), which also overlaps in time with the scalp EPP. No distinct neural activations were evoked by color distracters during the P3 time window (350–600 ms); thus, no source models were generated for P3 components.

Cortical source activations for each stimulus were then subjected to difference wave contrasts (color-gray distracter), in a manner similar to EPP and EPN scalp waveforms.

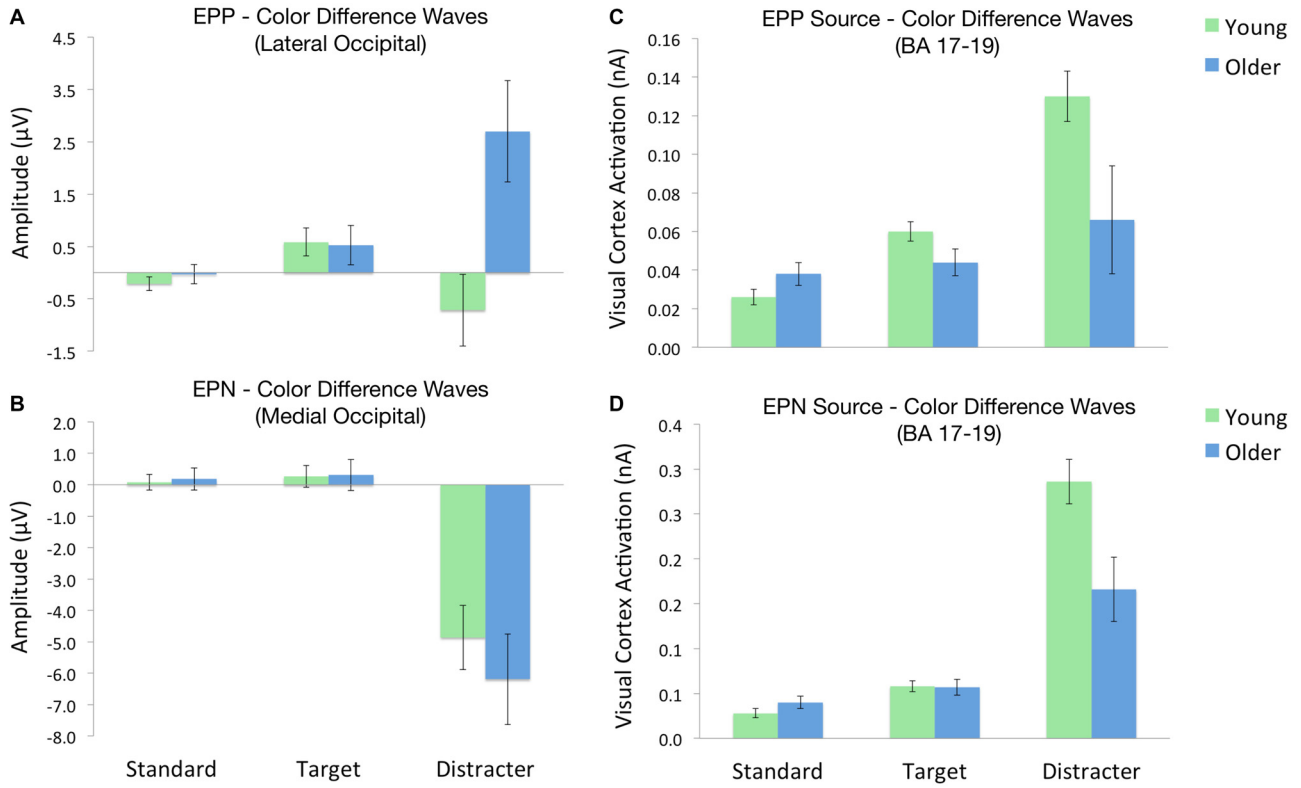


**FIGURE 3 | ERP amplitudes and source activations across each oddball stimulus.** Each value depicts the contrast between stimuli in the color and gray distracter blocks (i.e., color-gray difference waves). **(A)** EPP amplitudes across lateral occipital electrodes. **(B)** EPN amplitudes across medial occipital electrodes. **(C)** Visual cortex source activity during the EPP time window. **(D)** Visual cortex source activity during the EPN time window.

Activations from BA 17 were subjected to separate Group (2) × Stimulus (3) ANOVAs for the early (100 ms) and later (140 ms) time windows of visual processing. Visual source activations in the EPP time window (100 ms) revealed a Group × Stimulus interaction, such that older adults exhibited decreased visual cortex activity for color distracters relative to younger adults, despite the fact that standards and targets evoked equal activity between groups, $F_{(1,32)} = 8.1$, $p < 0.01$, $\eta^2 = 0.20$. Likewise, the EPN time window (140 ms) also showed this interaction, with younger adults exhibiting greater visual cortex activity for color distracters, $F_{(1,32)} = 5.5$, $p < 0.05$, $\eta^2 = 0.15$. Thus despite the fact that color distracters evoked larger scalp EPP amplitudes in older adults, visual cortex activations were stronger in younger adults during both EPP and EPN time windows, as shown in **Figures 3C,D**.

Neural source activations were found to be associated with scalp ERP components, but the relationships between EPP and source activity differed as a function of age. Older adults showed a positive correlation between early primary visual cortex activity (100 ms) and color distracter EPP ($r = 0.60$, $p < 0.05$), such that stronger visual cortex activity correlated with larger scalp signals for color distracters. Additionally, early OFC activation (100 ms) correlated with EPP amplitude in older adults ($r = 0.69$, $p < 0.01$). In this same time window, younger adults showed no relationships between EPP and neural sources in the visual cortex or OFC. EPN amplitude was correlated with visual cortex activations (140 ms) similarly for older ($r = -0.64$, $p < 0.05$) and younger adults ($r = -0.68$, $p = 0.001$).

Neural source activations from OFC were also subjected to Group (2) × Stimulus (3) ANOVA to examine the effects of color distracters. Unlike visual cortex regions, the strength of source signal in the OFC did not vary significantly as a function of group, $F_{(1,32)} = 0.54$, $p > 0.46$, and there were no Group × Stimulus interactions, $F_{(1,32)} = 0.16$, $p > 0.68$. However, older adults showed a significant relationship between early OFC and visual cortex activity, such that early (100 ms) OFC activations correlated with subsequent (140 ms) visual cortex activations ($r = 0.61$, $p < 0.05$). Young adults did not show this association. RMS source waveforms extracted from dipoles in these regions reveal the neural time course of OFC and visual cortex activity, as seen in **Figure 4**. Older adults exhibited an early peak of OFC activation approximately 100 ms post-stimulus, followed by a subsequent peak of visual cortex activation approximately 140 ms post-stimulus. Younger adults did not show this early OFC activation or any association between OFC and visual cortex during early visual processing.

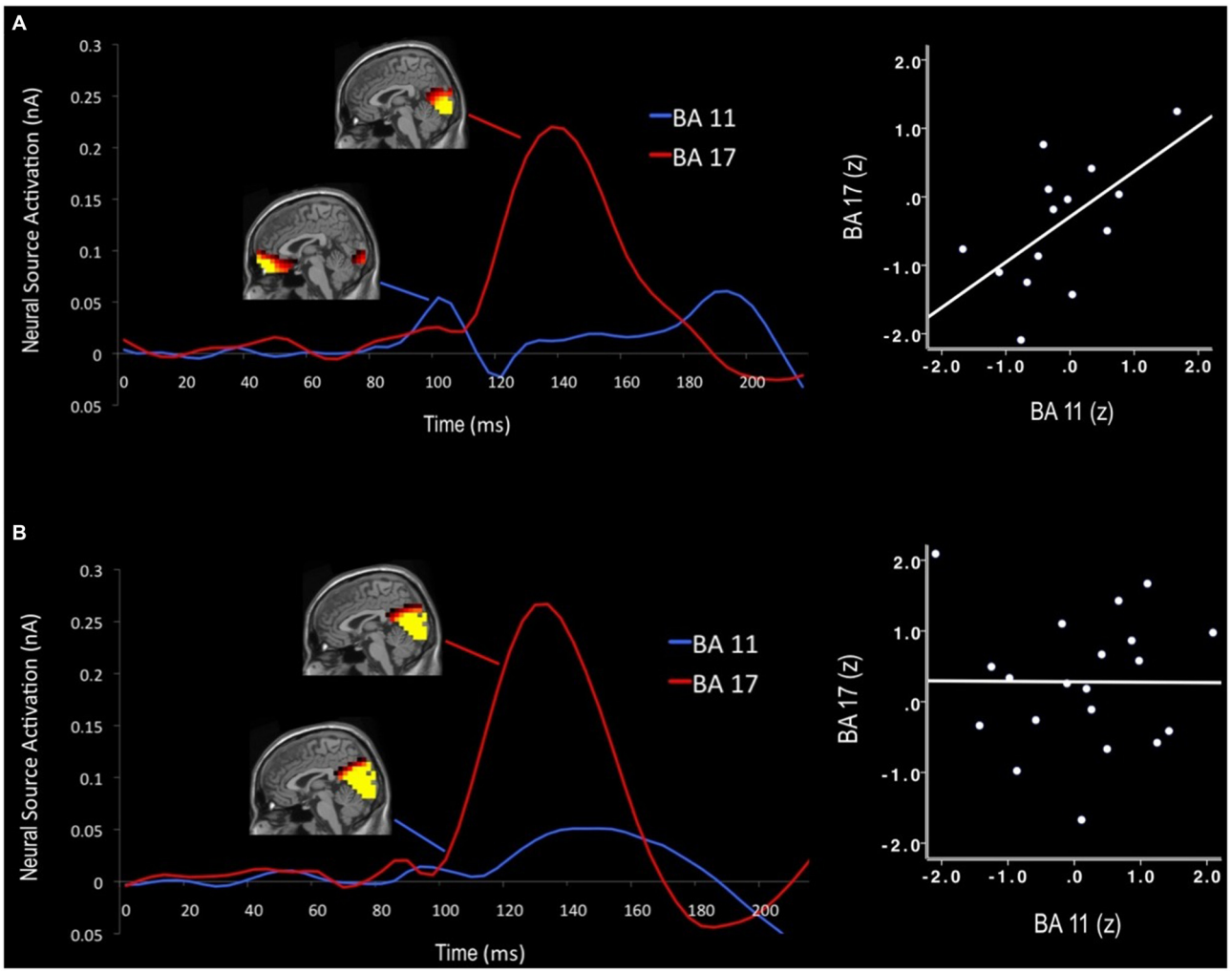


**FIGURE 4 | Neural time course of distracter color-gray difference waves for older (A) and younger adults (B).** Activation maps display cortical activity at 100 ms and 140 ms that was preferential for color-related distracter processing. Early orbitofrontal cortex (OFC; BA 11) activations predicted subsequent visual cortex activity (BA 17) in older adults, but not for younger adults. Note: Scales visible source activations differ for each time window (100 ms: visible range = 0.06–0.10 nA; 140 ms: visible range = 0.15–0.25 nA).

### Correlations with Executive Function

In older adults, several scores from several neuropsychological tests were associated with scalp ERPs and source activations. For older adults, the total number of errors on the WCST was positively correlated with color distracter EPP amplitude ($r = 0.60$, $p < 0.05$). Early OFC activations (100 ms) correlated with scores from Digit Symbol Coding ($r = 0.67$, $p < 0.01$) and Stroop Color Word Naming ($r = 0.54$, $p < 0.05$). Additionally, subsequent visual cortex activations (140 ms) correlated with Digit Symbol Coding ($r = 0.76$, $p < 0.01$). Thus better executive function in older adults was associated with enhanced early processing of color distracters—larger scalp EPP, enhanced OFC activations (100 ms), and enhanced visual cortex activations (140 ms).

Younger adults showed a different pattern of relationships between neuropsychological measures and color distracter processing. No tests were correlated with scalp ERPs in young adults. Early visual cortex activations (100 ms) correlated with scores from Stroop Color Word Naming ($r = 0.54$, $p < 0.05$), while subsequent visual cortex activations (140 ms) correlated with completion time from Trails B ($r = -0.45$, $p < 0.05$). OFC activations were not associated with any of the neuropsychological measures. Therefore, better executive function in younger adults was correlated with enhanced processing of color distracters in the visual cortex, but not the OFC.

## DISCUSSION

This study examined age-related differences in visual novelty processing. Occipital electrodes revealed two early sensory ERPs that were selectively enhanced by colorful distracters in the oddball task. An EPP peaked at 100 ms in lateral occipital electrodes, while an early posterior negativity (EPN) peaked at

140 ms in medial occipital electrodes. Enhancement of the EPN was expected, since this component is associated with color feature processing (Hillyard and Anllo-Vento, 1998). However, older adults also exhibited amplified sensory processing of colorful distracters prior to the EPN. This occurred during an earlier stage of visual attention (100 ms after stimulus onset), and was associated with increased activity in primary visual cortex and OFC. Older adults' OFC activity during this early time window was correlated with subsequent visual cortex activity (140 ms), suggesting that the OFC may have been engaged to help facilitate visual recognition of the colorful distracters. In contrast, young adults did not exhibit any early (100 ms) enhanced processing in scalp EPP or neural source activity. Cells in the OFC have been shown to respond selectively to novel visual stimuli, as early as 80 ms following stimulus onset (Rolls et al., 2005). The function of this early activity may be to direct attention toward unexpected or salient stimuli that require further processing (Petrides et al., 2002). When incoming sensory information is ambiguous, perceptual decisions may benefit from "predictive coding", in which the brain maintains an internal template in order to better anticipate forthcoming perceptions (Summerfield et al., 2006). Consistent with this view, the OFC appears to be synchronized with early (80 ms) and later (130 ms) visual cortex processing (Bar et al., 2006), in order to enhance processing in sensory cortex and improve recognition success. Until recently, the neuroanatomical connections necessary to explain this effect have not been clear. However, it appears that magnocellular pathways provide rapid feed-forward (occipital to OFC) and feed-backward (OFC to fusiform) pathways on a timescale that would facilitate object recognition (Kveraga et al., 2007). It has also been proposed that a subcortical route may project visual information to the OFC from the pulvinar complex, which receives input directly from the retina (Pessoa and Adolphs, 2010). With either pathway, it would appear that early projections reaching the OFC within 100 ms would provide only coarse visual information (e.g., limited spatial frequency and contrast). However, even this basic level of representation appears to be sufficient to activate a minimal set of perceptual expectations in the OFC, which can then influence subsequent bottom-up visual processing to facilitate recognition (Bar et al., 2006; Kveraga et al., 2007).

In the later stage of color feature processing (140 ms), EPN amplitude was amplified for both groups in response to colorful distracters, which appears to have been driven by broad increases throughout primary and secondary visual cortices (BA 17–19). Young adults had greater activation in visual cortex during this stage of processing than older adults. Weaker ERP correlates of visual processing have been observed in other visual detection studies (Czigler et al., 2006), and support a general notion that visual processing isless efficient in healthy aging. Thus the current findings support prior claims that healthy aging is associated with neural dedifferentiation of visual processing networks (Grady et al., 1994; Madden et al., 2004; Carp et al., 2011; Burianova et al., 2013).

In line with prior oddball studies focusing on P3 potentials, older adults demonstrated a "frontal shift" in their P3 responses to targets and distracters. In older adults, colorful distracters evoked larger P3 amplitudes in centrofrontal sites, even though their anterior P3 responses had longer latencies than young adults. This finding has been documented using ERP methods (e.g., Fabiani and Friedman, 1995), as well as functional neuroimaging (Davis et al., 2008). One implication of these findings is that the anterior shift in neural recruitment reflects compensation to offset age-related declines in posterior brain function. Frontal regions like the OFC may become active earlier in older adults in order to enhance top-down organization of sensory information, which becomes less efficient with age (Burianova et al., 2013).

The involvement of OFC in early processing of visual novelty has interesting implications for our understanding of cognitive aging. While generally appreciated for its role in emotional processing and decision-making (Bechara et al., 2000), the OFC plays a broader role in generating expectations about incoming information (Petrides et al., 2002). Additionally, such findings may be relevant to the inhibitory deficit hypothesis of cognitive aging. While often associated with emotional control over behavior, the OFC plays a prominent role in regulating inhibitory control (Bari and Robbins, 2013). Recent studies have supported a role for OFC in executive functions needed to dissociate between two perceptually similar actions during response conflict (Bryden and Roesch, 2015). In particular, dopamine regulation of OFC may play a critical role in facilitating proper inhibitory control when behavioral flexibility is required (Cheng and Li, 2013).

It is noteworthy that the older adults in the current study were not cognitively impaired. They did not differ from young adults in overall cognitive status or general levels of executive functioning, yet their early OFC activity appeared to influence subsequent bottom-up visual processing. Given the correlations between neural source activity and cognitive tests, it appears that greater OFC involvement in top-down regulation of attention was associated with broader neuropsychological benefits in healthy aging. Unlike the older group, young adults did not show relationships between early OFC activity and executive function, even though early visual cortex activations were associated with better executive function. Due to the greater activity of visual cortex in this group, it is likely that their visual recognition processing was more efficient and needed less compensatory assistance from the OFC. Older adults relied more on the OFC to provide predictive coding at the earliest stage of visual processing, such that they could perform the task successfully despite weaker visual cortex activations. Importantly, this tendency in our older adult sample appeared to be adaptive, as greater levels of this OFC activation was correlated with greater levels of executive function.

In summary, the current study revealed age-related differences in the early sensory processing of novel stimuli. Older adults had enhanced scalp signals corresponding to an early stage of visual processing (100 ms), which correlated with neural activity in both primary visual cortex and OFC. Consistent with prior findings on posterior cortex dedifferentiation, older adults

required enhanced OFC activation in order to compensate for reduced visual processing efficiency. This early compensatory OFC activity in older adults predicted subsequent feature processing in visual cortex (140 ms) and was associated with greater levels of complex attention and executive function. Thus older adults benefited from greater top-down control during visual processing. These findings lend support for models of cognitive aging that account for both neural dedifferentiation and compensatory neural reorganization. Future studies are needed to explore the underlying neural dynamics and connectivity between the OFC and visual cortex, and determine the degree to which these findings generalize to older individuals with more significant levels of neural dedifferentiation or cognitive decline.

## ETHICS STATEMENT

The study was approved by the University of Florida, Health Sciences Institutional Review Board.

## AUTHOR CONTRIBUTIONS

DASK, Data collection, analysis, manuscript writing; CMK, Manuscript writing; WMP, Manuscript writing and oversight.

## FUNDING

This work was supported by Grants from the NIH (T32-AG020499 and R21-NS079767).

## REFERENCES

Alain, C., and Woods, D. L. (1999). Age-related changes in processing auditory stimuli during visual attention: evidence for deficits in inhibitory control and sensory memory. *Psychol. Aging* 14, 507–519. doi: 10.1037/0882-7974.14.3.507

Bar, M. (2009). The proactive brain: memory for predictions. *Philos. Trans. R. Soc. Lond. B Biol. Sci.* 364, 1235–1243. doi: 10.1098/rstb.2008.0310

Bar, M., Kassam, K. S., Ghuman, A. S., Boshyan, J., Schmid, A. M., Dale, A. M., et al. (2006). Top-down facilitation of visual recognition. *Proc. Natl. Acad. Sci. U S A* 103, 449–454. doi: 10.1073/pnas.0507062103

Barcelo, F., Escera, C., Corral, M. J., and Periánez, J. A. (2006). Task switching and novelty processing activate a common neural network for cognitive control. *J. Cogn. Neurosci.* 18, 1734–1748. doi: 10.1162/jocn.2006.18.10.1734

Barceló, F., Periáñez, J. A., and Knight, R. T. (2002). Think differently: a brain orienting response to task novelty. *Neuroreport* 13, 1887–1892. doi: 10.1097/00001756-200210280-00011

Bari, A., and Robbins, T. W. (2013). Inhibition and impulsivity: behavioral and neural basis of response control. *Prog. Neurobiol.* 108, 44–79. doi: 10.1016/j.pneurobio.2013.06.005

Bechara, A., Damasio, H., and Damasio, A. R. (2000). Emotion, decision making and the orbitofrontal cortex. *Cereb. Cortex* 10, 295–307. doi: 10.1093/cercor/10.3.295

Bedowski, C., Prvulovic, D., Goebel, R., Zanella, F. E., and Linden, D. E. (2004). Attentional systems in target and distracter processing: a combined ERP and fMRI study. *Neuroimage* 22, 530–540. doi: 10.1016/j.neuroimage.2003.12.034

Bryden, D. W., and Roesch, M. R. (2015). Executive control signals in orbitofrontal cortex during response inhibition. *J. Neurosci.* 35, 3903–3914. doi: 10.1523/JNEUROSCI.3587-14.2015

Burianova, H., Lee, Y., Grady, C. L., and Moscovitch, M. (2013). Age-related dedifferentiation and compensatory changes in the functional network underlying face processing. *Neurobiol. Aging* 34, 2759–2767. doi: 10.1016/j.neurobiolaging.2013.06.016

Carp, J., Park, J., Polk, T. A., and Park, D. C. (2011). Age differences in neural distinctiveness revealed by multi-voxel pattern analysis. *Neuroimage* 56, 736–743. doi: 10.1016/j.neuroimage.2010.04.267

Chao, L. L., and Knight, R. T. (1997). Prefrontal deficits in attention and inhibitory control with aging. *Cereb. Cortex* 7, 63–69. doi: 10.1093/cercor/7.1.63

Cheng, J. T., and Li, J. S. (2013). Intra-orbitofrontal cortex injection of haloperidol removes the beneficial effect of methylphenidate on reversal learning of spontaneously hypertensive rats in an attentional set-shifting task. *Behav. Brain Res.* 15, 148–154. doi: 10.1016/j.bbr.2012.11.006

Czigler, I., Pató, L., Poszet, E., and Balázs, L. (2006). Age and novelty: event-related potentials to visual stimuli within an auditory oddball–visual detection task. *Int. J. Psychophysiol.* 62, 290–299. doi: 10.1016/j.ijpsycho.2006.05.008

Davis, S. W., Dennis, N. A., Daselaar, S. M., Fleck, M. S., and Cabeza, R. (2008). Que PASA? The posterior-anterior shift in aging. *Cereb. Cortex* 18, 1201–1209. doi: 10.1093/cercor/bhm155

de Fockert, J., Rees, G., Frith, C., and Lavie, N. (2004). Neural correlates of attentional capture in visual search. *J. Cogn. Neurosci.* 16, 751–759. doi: 10.1162/089892904970762

De Sanctis, P., Katz, R., Wylie, G. R., Sehatpour, P., Alexopoulos, G. S., and Foxe, J. J. (2008). Enhanced and bilateralized visual sensory processing in the ventral stream may be a feature of normal aging. *Neurobiol. Aging* 29, 1576–1586. doi: 10.1016/j.neurobiolaging.2007.03.021

Fabiani, M., and Friedman, D. (1995). Changes in brain activity patterns in aging: the novelty oddball. *Psychophysiology* 32, 579–594. doi: 10.1111/j.1469-8986.1995.tb01234.x

Fabiani, M., Low, K. A., Wee, E., Sable, J. J., and Gratton, G. (2006). Reduced suppression or labile memory? Mechanisms of inefficient filtering of irrelevant information in older adults. *J. Cogn. Neurosci.* 18, 637–650. doi: 10.1162/jocn.2006.18.4.637

Friedman, D. (2003). Cognition and aging: a highly selective overview of event-related potential (ERP) data. *J. Clin. Exp. Neuropsychol.* 25, 702–720. doi: 10.1076/jcen.25.5.702.14578

Friedman, D. (2008). "The components of aging," in *Oxford Handbook of Event-Related Potential Components*, eds S. L. Luck and E. S. Kappenman (New York, NY: Oxford University Press), 513–536.

Friedman, D., Simpson, G., and Hamberger, M. (1993). Age-related changes in scalp topography to novel and target stimuli. *Psychophysiology* 30, 383–396. doi: 10.1111/j.1469-8986.1993.tb02060.x

Gazzaley, A., Cooney, J. W., McEvoy, K., Knight, R. T., and D'Esposito, M. (2005). Top-down enhancement and suppression of the magnitude and speed of neural activity. *J. Cogn. Neurosci.* 17, 507–517. doi: 10.1162/0898929053279522

Gazzaley, A., and D'Esposito, M. (2007). Top–down modulation and normal aging. *Ann. N Y Acad. Sci.* 1097, 67–83. doi: 10.1196/annals.1379.010

Grady, C. L., Maisog, J. M., Horwitz, B., Ungerleider, L. G., Mentis, M. J., Salerno, J. A., et al. (1994). Age-related changes in cortical blood flow activation during visual processing of faces and location. *J. Neurosci.* 14, 1450–1462.

Hasher, L., and Zacks, R. T. (1988). "Working memory, comprehension and aging: a review and a new view," in *The Psychology of Learning and Motivation*, ed. G. H. Bower (New York, NY: Academic Press), 193–225.

Hillyard, S. A., and Anllo-Vento, L. (1998). Event-related brain potentials in the study of visual selective attention. *Proc. Natl. Acad. Sci. U S A* 95, 781–787. doi: 10.1073/pnas.95.3.781

Huettel, S. A., and McCarthy, G. (2004). What is odd in the oddball task? Prefrontal cortex is activated by dynamic changes in response strategy. *Neuropsychologia* 42, 379–386. doi: 10.1016/j.neuropsychologia.2003.07.009

Katayama, J., and Polich, J. (1999). Auditory and visual P300 topography from a 3 stimulus paradigm. *Clin. Neurophysiol.* 110, 463–468. doi: 10.1016/s1388-2457(98)00035-2

Kveraga, K., Boshyan, J., and Bar, M. (2007). Magnocellular projections as the trigger of top-down facilitation in recognition. *J. Neurosci.* 27, 13232–13240. doi: 10.1523/jneurosci.3481-07.2007

Lamm, C., Pine, D. S., and Fox, N. A. (2013). Impact of negative affectively charged stimuli and response style on cognitive-control-related neural activation: an ERP study. *Brain Cogn.* 83, 234–243. doi: 10.1016/j.bandc.2013.07.012

Li, L., Gratton, C., Fabiani, M., and Knight, R. T. (2013). Age-related frontoparietal changes during the control of bottom-up and top-down attention: an ERP study. *Neurobiol. Aging* 34, 477–488. doi: 10.1016/j.neurobiolaging.2012.02.025

Luck, S. J. (2005). *An Introduction to the Event-Related Potential Technique.* Cambridge, MA: The MIT Press.

Madden, D. J., Whiting, W. L., Provenzale, J. M., and Huettel, S. A. (2004). Age-related changes in neural activity during visual target detection measured by fMRI. *Cereb. Cortex* 14, 143–155. doi: 10.1093/cercor/bhg113

McDowd, J. M., and Filion, D. L. (1992). Aging, selective attention and inhibitory processes: a psychophysiological approach. *Psychol. Aging* 7, 65–71. doi: 10.1037/0882-7974.7.1.65

Neter, J., Wasserman, W., and Kutner, M. H. (1985). *Applied Linear Statistical Models: Regression, Analysis of Variance, and Experimental Designs*, 2nd Edn. Homewood, IL: R.D. Irwin.

Pascual-Marqui, R. D., Michel, C. M., and Lehmann, D. (1994). Low-resolution electromagnetic tomography: a new method for localizing activity in the brain. *Int. J. Psychophysiol.* 18, 49–65. doi: 10.1016/0167-8760(84)90014-x

Pessoa, L., and Adolphs, R. (2010). Emotion processing and the amygdala: from a 'low road' to 'many roads' of evaluating biological significance. *Nat. Rev. Neurosci.* 11, 773–783. doi: 10.1038/nrn2920

Petrides, M., Alivisatos, B., and Frey, S. (2002). Differential activation of the human orbital, mid-ventrolateral and mid-dorsolateral prefrontal cortex during the processing of visual stimuli. *Proc. Natl. Acad. Sci. U S A* 99, 5649–5654. doi: 10.1073/pnas.072092299

Picton, T. W., Bentin, S., Berg, P., Donchin, E., Hillyard, S. A., Johnson, R. Jr., et al. (2000). Guidelines for using human event-related potentials to study cognition: recording standards and publication criteria. *Psychophysiology* 37, 127–152. doi: 10.1017/s0048577200000305

Polich, J. (2007). Updating P300: an integrative theory of P3a and P3b. *Clin. Neurophysiol.* 118, 2128–2148. doi: 10.1016/j.clinph.2007.04.019

Polich, J., and Comerchero, M. D. (2003). P3a from visual stimuli: typicality, task and topography. *Brain Topogr.* 15, 141–152. doi: 10.1023/A:1022637732495

Ratcliff, R. (1993). Methods for dealing with reaction time outliers. *Psychol. Bull.* 114, 510–532. doi: 10.1037/0033-2909.114.3.510

Raz, N., Kindenberger, U., Rodrigue, K. M., Kennedy, K. M., Head, D., Williamson, A., et al. (2005). Regional brain changes in aging healthy adults: general trends, individual differences and modifiers. *Cereb. Cortex* 15, 1676–1689. doi: 10.1093/cercor/bhi044

Reuter-Lorenz, P. A., and Cappell, K. A. (2008). Neurocognitive aging and the compensation hypothesis. *Curr. Dir. Psychol. Sci.* 17, 177–182. doi: 10.1111/j.1467-8721.2008.00570.x

Rolls, E. T., Browning, A. S., Inoue, K., and Hernadi, I. (2005). Novel visual stimuli activat a population of neurons in the primate orbitofrontal cortex. *Neurobiol. Learn. Mem.* 84, 111–123. doi: 10.1016/j.nlm.2005.05.003

Sawaki, R., and Katayama, J. (2007). Difficulty of discrimination modulates attentional capture for deviant information. *Psychophysiology* 44, 374–382. doi: 10.1111/j.1469-8986.2007.00506.x

Scherg, M. (1990). "Fundamentals of dipole source potential analysis," in *Auditory Evoked Magnetic Fields and Electric Potentials. Advances in Audiology*, (Vol. 6) eds F. Grandori and M. Hoke (Basel: Karger), 65–78.

Simons, R. F., and Perlstein, W. M. (1997). "A tale of two reflexes: an ERP analysis of prepulse inhibition and orienting," in *Attention and Orienting: Sensory and Motivational Processes*, eds R. F. Simons and P. J. Lang (Mahwah, NJ: Lawrence Erlbaum Associates, Inc.), 229–255.

Summerfield, C., Enger, T., Greene, M., Koechlin, E., Mangels, J., and Hirsch, J. (2006). Predictive codes for forthcoming perception in the frontal cortex. *Science* 314, 1311–1314. doi: 10.1126/science.1132028

Waters, A. C., and Tucker, D. M. (2013). Positive and negative affect in adolescent self-evaluation: psychometric information in single trials used to generate dimension-specific ERPs and neural source models. *Psychophysiology* 50, 538–549. doi: 10.1111/psyp.12035

**Conflict of Interest Statement**: The authors declare that the research was conducted in the absence of any commercial or financial relationships that could be construed as a potential conflict of interest.

frontiers in Aging Neuroscience

ORIGINAL RESEARCH
published: 01 December 2015
doi: 10.3389/fnagi.2015.00223

# Age-Related Inter-Region EEG Coupling Changes During the Control of Bottom–Up and Top–Down Attention

*Ling Li* and Dandan Zhao*

*Key Laboratory for NeuroInformation of Ministry of Education, School of Life Science and Technology, University of Electronic Science and Technology of China, Chengdu, China*

We investigated age-related changes in electroencephalographic (EEG) coupling of theta-, alpha-, and beta-frequency bands during bottom–up and top–down attention. Arrays were presented with either automatic "pop-out" (bottom–up) or effortful "search" (top–down) behavior to younger and older participants. The phase-locking value was used to estimate coupling strength between scalp recordings. Behavioral performance decreased with age, with a greater age-related decline in accuracy for the search than for the pop-out condition. Aging was associated with a declined coupling strength of theta and alpha frequency bands, with a greater age-related decline in whole-brain coupling values for the search than for the pop-out condition. Specifically, prefronto-frontal coupling in theta- and alpha-bands, fronto-parietal and parieto-occipital couplings in beta-band for younger group showed a right hemispheric dominance, which was reduced with aging to compensate for the inhibitory dysfunction. While pop-out target detection was mainly associated with greater parieto-occipital beta-coupling strength compared to search condition regardless of aging. Furthermore, prefronto-frontal coupling in theta-, alpha-, and beta-bands, and parieto-occipital coupling in beta-band functioned as predictors of behavior for both groups. Taken together these findings provide evidence that prefronto-frontal coupling of theta-, alpha-, and beta-bands may serve as a possible basis of aging during visual attention, while parieto-occipital coupling in beta-band could serve for a bottom–up function and be vulnerable to top–down attention control for younger and older groups.

**Keywords: aging, electroencephalographic (EEG), visual pop-out, visual search, control of attention, inter-region phase coupling, theta, alpha**

OPEN ACCESS

***Edited by:***
*Junfeng Sun,*
*Shanghai Jiao Tong University, China*

***Reviewed by:***
*Yu (Aaron) Tang,*
*The University of Texas Southwestern Medical Center, USA*
*Jesse Jon Bengson,*
*Center for Mind and Brain, USA*

****Correspondence:***
*Ling Li*
*liling@uestc.edu.cn*

***Received:*** *09 October 2015*
***Accepted:*** *17 November 2015*
***Published:*** *01 December 2015*

***Citation:***
*Li L and Zhao D (2015) Age-Related Inter-Region EEG Coupling Changes During the Control of Bottom–Up and Top–Down Attention. Front. Aging Neurosci. 7:223. doi: 10.3389/fnagi.2015.00223*

## INTRODUCTION

Normal aging is associated with decline in the performance of a variety of cognitive functions, including effects observed in the visual search (Plude and Doussard-Roosevelt, 1989) and in the tasks involving both bottom–up attention and top–down attention, with a more prominent decline in tasks emphasizing top–down attention control (Greenwood et al., 1997; Kok, 2000; Madden et al., 2005; Madden, 2007; Lien et al., 2011; Li et al., 2013). Normal aging is correlated with changes in neural structure, including decline in brain volume (Scahill et al., 2003; Fotenos et al., 2008)

and gray and white matter volumes (Raz et al., 2005; Gordon et al., 2008). Age-related losses in gray and white matter in medial-temporal, parietal, and frontal areas were reported. Hypotheses of age-related brain functional changes mainly include Compensation Related Utilization of Neural Circuits Hypothesis (CRUNCH) (Reuter-Lorenz and Lustig, 2005; Grady, 2008; Reuter-Lorenz and Cappell, 2008) and dedifferentiation hypothesis (Madden et al., 2007).

A variety of functional imaging, neurophysiological and neuropsychological studies have provided compelling evidence that frontoparietal networks play important roles in both top–down cognitive and bottom–up sensory factors of attention control (Corbetta and Shulman, 2002; Giesbrecht et al., 2003; Bledowski et al., 2004a,b Buschman and Miller, 2007; Husain and Nachev, 2007; Knudsen, 2007; Li et al., 2010). An aging study of visual attention has reported that older adults showed increased magnitude and spread of activity in fronto-parietal regions compared with younger adults, suggesting a compensation for a decline in overall bottom–up sensory input (dedifferentiation; Madden et al., 2007; see reviews Reuter-Lorenz and Park, 2010). However, activity decreases with aging in frontal cortex (Anderson et al., 2000; Milham et al., 2002; Johnson et al., 2004) and occipital cortex (Madden et al., 2004) were also reported in attention studies, pointing to an age-related decline in allocation of attentional resources efficiency (Lorenzo-López et al., 2008) or reduction in inhibitory control functions in attention (Colcombe et al., 2003; Madden et al., 2004; Andrés et al., 2006; Hasher et al., 2008). Performance has been found associated with fronto-parietal activation for older adults and with occipital activation for younger adults in top–down attention (Madden et al., 2007), but with prefrontal activation for younger adults and with deep gray matter structures for older adults in visual target detection (Madden et al., 2004). Increased activities in frontal regions associated with improved performance (Grady et al., 2002; Madden et al., 2004; Lorenzo-López et al., 2008; Vallesi et al., 2010), or with decreased performance (Madden et al., 2005) in older adults have also been reported in certain tasks. The CRUNCH interprets these contradictory results at some degree, whereby older adults use more or new neural circuits to accomplish tasks compared to younger adults.

A functional imaging study shows that aging is associated with decreased connectivity between areas within the fronto-parietal control network and between areas within the somatomotor network in a selective attention task, but with increased connectivity between the fronto-parietal and somatomotor network (Geerligs et al., 2014). Functional connectivity decreases with aging within the fronto-parietal regions during cue processing under executive control was reported (Madden et al., 2010). There has been study showing both selective increases between visual attention regions and supplementary motor area and decreases between sensorimotor systems and supplementary motor area in resting-state functional connectivity with age (Roski et al., 2013). In summary, aging is associated with lower connectivity within task-relevant networks and greater connectivity between the task-relevant networks and outside networks by functional imaging studies (Madden et al., 2005, 2010; Dennis et al., 2008; St Jacques et al., 2009; Geerligs et al., 2014), supporting the CRUNCH that older adults use more or new neural circuits to compensate for age-related decline.

In electrocephalogram (EEG) studies, older adults show reduced frontal theta activity during sustained attentional processes, and reduced theta connectivity strength within frontal regions and between frontal midline and temporal cortices during working memory maintenance (Kardos et al., 2014). Decreased posterior alpha activation in an attention network test (Deiber et al., 2013) and reduced beta activation in a visual attentional task correlated to alertness and sustaining attentional processes (Gola et al., 2012, 2013) with aging were reported. Aging is associated with decreased modularity and clustering and increased connectedness of anterior nodes in beta-band network during resting condition, pointing to a compensation of the anterior atentional system (Knyazev et al., 2015). These findings provide evidence that aging modulates distinct neural circuits at different oscillatory frequencies during attention functions. There is, however, relatively little evidence directly investigating aging-related functional connectivity by EEG in bottom–up and top–down attention together.

We used a paradigm based on a study in non-human primates by Buschman and Miller (2007) to investigate age-related coupling of different frequency bands during top-down and bottom-up attention control. Arrays were presented with either automatic "pop-out" (bottom–up) or effortful "search" (top–down) behavior to younger and older participants. Buschman and Miller found that fronto-extrastriate coherences were greater in the search than in the pop-out condition at low gamma-band (22–34 Hz) and parietal–extrastriate coherences were greater in the pop-out than in the search condition at high gamma-band (35–55 Hz). In a human EEG study, a double dissociation was reported, with significantly increased power from 4 to 24 Hz in parietal areas for pop-out targets and increased power from 4 to 24 Hz in frontal regions for search targets (Li et al., 2010). Greater frontal-parietal synchrony at low gamma-band frequencies for inefficient than efficient visual search were reported (Phillips and Takeda, 2009). Based on above neuroimaging and electrophysiology literatures, as well as the results from our previous studies (Li et al., 2010, 2013), we expected the differential roles of fronto-parieto-occipital connectivity at different lower oscillatory frequencies under both types of attention for younger and older groups. The purpose of the present study was to examine the effects of aging on functional connectivity at different oscillatory frequencies during visual search and simultaneously compare the fronto-parieto-occipital connectivity during top–down and bottom–up attention. We hypothesized that (a) aging and search condition are associated with decreases in connectivity due to a slowing in performance, and (b) connectivity at different oscillatory frequencies plays a differential role contributing to group and attentional control.

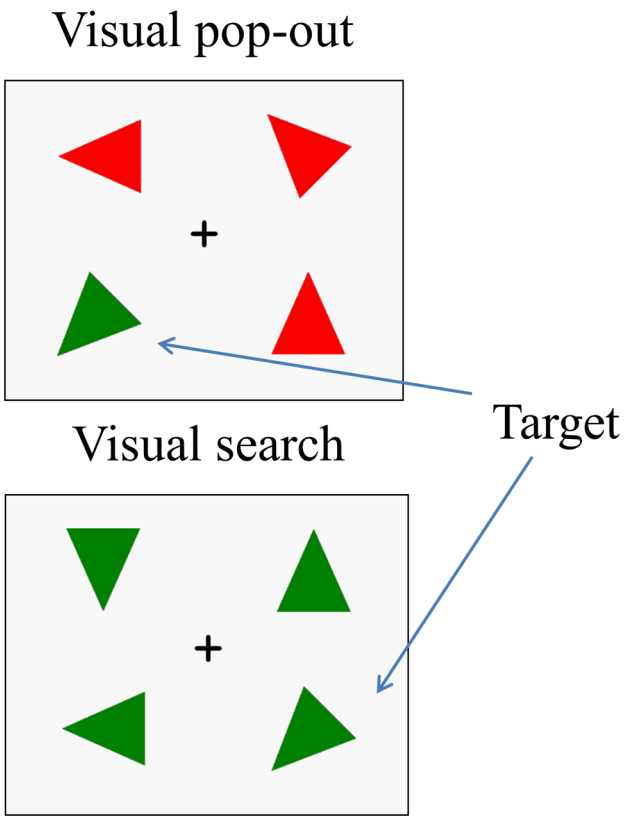


**FIGURE 1 | An example of the stimulus array in the two experimental conditions.** Each trial includes a target. In the **(up panel)**, the distractors differ from the target in both color and orientation, so that target detection is highly efficient and easy. In this pop-out condition, search is influenced primarily by the bottom–up attention. In the **(down panel)**, the distractors differ from the target only in orientation, so that target detection is less efficient and difficult. In this search condition, target detection is controlled mainly by top–down attention.

## MATERIALS AND METHODS

### Subjects

We utilized data reported in a previous study (Li et al., 2013) consisting of 13 younger subjects (6 females, mean age ± standard deviation = 23.9 ± 4.3 years, range from 18 to 35 years old) and 13 older subjects (6 females, mean age ± standard deviation = 63.1 ± 6.2 years, range from 52 to 75 years old). The mean numbers of years of education for the younger and older subjects were 15.9 ± 2.5 and 16.0 ± 2.2 years respectively. All the subjects were right-handed, had normal color vision, and had no history of neurological problems. None of the subjects were taking any psychotropic, neurological, or psychiatric medications at the time of testing. The experimental procedures were approved by the Committee for the Protection of Human Subjects for the University of California, Berkeley. Written Informed consent was obtained from all subjects prior to being tested.

### Stimuli and Procedure

The stimuli were made up of 16 acute isosceles triangles, each with a particular color (red or green) and orientation [one of eight, (i-1) × 45°, $i$ = 1, 2, 3, 4, 5, 6, 7, 8]. The triangles had two equal sides 6.5 cm in length and a third side 5.5 cm long, with an area of 16.20 cm × 16.20 cm. **Figure 1** illustrates an example of the stimulus sequence. After a 500 ms fixation cross, a target triangle (one of 16 triangles) appeared in the center of the screen for 1000 ms and was followed by a short 500 ms delay screen with a fixation cross. After the delay, a four stimulus array was presented, consisting of the target and three distracter triangles in the four quadrants of the screen. The target was randomly presented in one of these locations (upper-left, lower-left, upper-right, and lower-right). The center of each triangle was 6.2 cm vertical (either up or down) from the horizontal midline and 8.2 cm lateral (either right or left) from the vertical midline, resulting in stimuli at a visual angle of 5.34° from fixation. The array remained on the screen until a response and was followed by a 1000 ms fixation to show the end of the trial. Three distractor triangles were chosen to create the two main attention conditions in the experiment: "pop-out" and "search." The pop-out condition was created using distracters that differed from the target in both color and orientation (Treisman and Gelade, 1980), while the search condition was created by using distracters that differed from the target only in orientation. Half of the trials were in the pop-out condition and half were in the search condition. Half of the targets were presented in left visual field and half were in right visual field.

Subjects were asked to centrally fixate throughout the recording and to respond as quickly as possible whether the target was to the left or right of fixation. Participants used their right-hand for responding by pressing either button 1 for left or 2 for right from a computer key pad. Participants performed two practice blocks before starting the experiment and extra practice blocks were given as required until subjects were able to reach a mean accuracy of 80% in the task. After the practice, 12 experimental blocks comprising 32 trials each lasting about 2.5 min were run. There were 1–2 min breaks between blocks, with longer breaks every three blocks. E-prime (Psychology Software Tools, Pittsburgh, PA, USA) was used to present the stimuli and analyze the behavioral data.

### Data Recording and Preprocessing

EEG was recorded by an ActiveTwo system (Biosemi, The Netherlands) with a 64 channel electrode cap. Right and left earlobes and four electrooculogram (EOG) were simultaneously recorded. EEG data were off-line referenced to the average of the right and left earlobes. EOG was measured from an electrode above and below the right eye to record vertical eye movements and electrodes on the outer canthus of each eye to measure horizontal eye movements. All channels were amplified with an analog bandpass filter of 0.06–208 Hz and were digitized at 1024 Hz.

Matlab was used for all data processing. Re-referenced EEG signals were filtered from 0.5 to 55 Hz with a two-way FIR bandpass filter (eegfilt.m from EEGLAB toolbox, Delorme and

Makeig, 2004) and segmented from 200 ms before the onset of the stimulus (visual array) to 1000 ms after the stimulus. Trials were rejected if they had an incorrect response or lacked a button press between 200 and 1500 ms (younger adults) or 200–2000 ms (older adults) after the onset of the stimulus array. Epochs with EOG artifacts were removed if there was a difference in amplitude between the two vertical EOG or between the two horizontal EOG of greater than 100 μV, or if there was more than 3 standard deviations (SDs) from the mean of the EOG difference wave. For each epoch, the linear drift was removed and the data was baseline corrected using the 200 ms pre-stimulus period. Finally, any epoch with a channel containing amplitudes of more than four standard deviations from the epoch mean was rejected. After above preprocessing, 537 trials remained for left pop-out targets, 480 trials remained for right pop-out targets, 479 trials remained for left visual search targets, and 424 trials remained for right search targets for the younger participants. 417 trials remained for left pop-out targets, 402 trials remained for right pop-out targets, 332 trials remained for left visual search targets, and 344 trials remained for right search targets for the older participants. These trials were used for ERP analysis (see in Li et al., 2010, 2013) and for the current EEG coupling analysis. At least 25 trials were included in the average for each condition.

## EEG Cross-channel Coupling Analysis

To minimize the contribution of volume conduction and remove spurious coupling (Nunez et al., 1997; Lachaux et al., 1999), the following steps were applied to single trial of EEG data before the computation of the phase synchrony. Step 1: each single trial of 4 conditions (2 × 2, target condition and visual field) of every subject for both groups was filtered by the band-pass finite impulse response filters at 4 Hz intervals between 4 and 40 Hz. Totally signals of 9 frequency bands EEG were obtained. Step 2: we used a current source density (CSD) toolbox of MATLAB supplied by Kayser J. (http://psychophysiology.cpmc.columbia.edu/Software/CSDtoolbox/index.html) that implemented a spherical spline algorithm of Perrin et al. to estimate scalp current density (SCD) for EEG data (Perrin et al., 1989; Kayser and Tenke, 2006). The spline interpolation constant was set to 4.

After above SCD computation, the data from 200 ms before the onset of stimuli array to 1000 ms after the stimuli were used to estimate long-range neural phase synchrony in nine frequency bands by calculating phase-locking value (PLV). The PLV has been used to measure the bivariate phase synchronization in a number of EEG studies (Mormann et al., 2000; Quian Quiroga et al., 2002; Knyazev et al., 2015). The PLV between electrodes $j$ and $k$, at each sample time $t$, across the $N$ trials, were quantified as $PLV_{j,k,t}=\left|\frac{1}{N}\sum_{N} e^{i[\varphi_j(t)-\varphi_k(t)]}\right|$. Instantaneous phase $\varphi(t)$ of a signal was estimated by Hilbert transform.

The PLV takes on values between 0 and 1, but the PLV must first be normalized before it can be used as a metric of cross-electrode coupling strength. That is, we are interested in the properties of the distribution of phase difference between two electrodes. One way is to compare the actual mean PLV with a set of surrogate PLV created by offsetting phase of one signal by some large time lag. Two hundred surrogate PLV values for each frequency and time point were calculated, and the mean and standard deviation of surrogate PLV were estimated. Therefore, the normalized PLV [(real PLV – mean of surrogate PLV)/standard deviation of surrogate PLV] were defined as the modulation index used in this paper. For a given number of sample points, we can directly compare this normalized PLV for cross-electrode coupling strength across different pairs as well as different frequency bands which may have very different power levels. The normalized PLV index was computed for all pair-wise combinations of channels, generating 2016 (totally 64 channels) index values for each time point in 9 frequency bands in each condition for both groups. With $\alpha = 0.01$ and $N = 2016$ comparisons, an index value greater than 4.42 was required for significance by Bonferroni correction for multiple comparisons.

## Statistical Analysis

Behavioral data were analyzed with a repeated measure ANOVA with condition (pop-out and search) and target visual field (left and right) as the within-subject factors and age (young and old) as the between-subject factor, followed by Bonferroni corrected $t$-tests if necessary with $p$-value $<0.05$ as a significant threshold.

Mean normalized PLV values and mean numbers of connection were calculated first by the mean of whole-brain significant coupling values in 0–600 ms time-window. Then mean normalized PLV multiplied by mean numbers of connection to obtain total coupling values. Finally, the total coupling values were analyzed with a repeated measure ANOVA with condition (pop-out and search) and target visual field (left and right) as the within-subject factors and age (young and old) as the between-subject factor for 9 frequency bands.

Eight regions of interest (ROIs) were selected including left prefrontal (Fp1, AF7, AF3, F5, F3, F1), right prefrontal (Fp2, AF8, AF4, F6, F4, F2), left central-frontal (FC5, FC3, FC1, C5, C3, C1), right central-frontal (FC6, FC4, FC2, C6, C4, C2), left central-parietal (CP5, CP3, CP1, P5, P3, P1), right central-parietal (CP6, CP4, CP2, P6, P4, P2), left parietal-occipital (PO7, PO3, O1), and right parieto-occipital (PO8, PO4, O2) regions (see **Figure 2**). Max normalized PLV values for all pair-wise combinations of eight regions of interest were calculated, generating 28 (totally 8 ROIs) index values for frequency bands of interest in four conditions for both groups. With $\alpha = 0.05$ and $N = 28$ comparisons, an index value greater than 2.91 was required for significance by Bonferroni correction for multiple comparisons. Each significant connectivity between ROIs were then analyzed with a repeated measure ANOVA with condition (pop-out and search) and target visual field (left and right) as the within-subject factors and age (young and old) as the between-subject factor for frequency bands of interest.

Linear relationship between above coupling values and behaviors were then tested by Pearson correlation coefficient for four conditions in both groups in each frequency band, respectively.

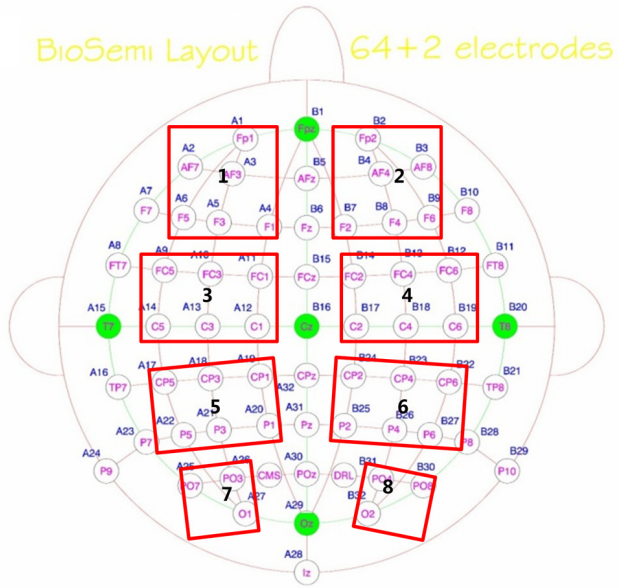


**FIGURE 2 | Eight regions of interest (ROIs, marked by red rectangles) for inter-region analysis were selected including left prefrontal (Fp1, AF7, AF3, F5, F3, F1), right prefrontal (Fp2, AF8, AF4, F6, F4, F2), Left central-frontal (FC5, FC3, FC1, C5, C3, C1), right central-frontal (FC6, FC4, FC2, C6, C4, C2), Left central-parietal (CP5, CP3, CP1, P5, P3, P1), right central-parietal (CP6, CP4, CP2, P6, P4, P2), Left parietal-occipital (PO7, PO3, O1), and right parieto-occipital (PO8, PO4, O2) regions.**

# RESULTS

## Behavioral Results

Mean reaction times (RTs) and accuracy rates are summarized in **Table 1** (mean ± standard deviation). There was a main effect of age (young and old), condition (pop-out and search), and target visual field (left and right) on mean RTs [age effect: $F(1,24) = 31.35$, $p < 0.001$; condition effect: $F(1,24) = 786.05$, $p < 0.001$; target visual field effect: $F(1,24) = 5.70$, $p = 0.025$, ANOVA], with slower RTs in the older subjects and in the search condition and in the left visual field target. However, there was no significant interaction in RTs among age, condition and target visual field. A main effect of age and condition was observed on accuracy rates [age effect: $F(1,24) = 19.75$, $p < 0.001$; condition effect: $F(1,24) = 88.55$, $p < 0.001$], with higher accuracy overall in the younger group and in the pop-out condition. There was a significant interaction in accuracy between age and condition [$F(1,24) = 14.28$, $p = 0.001$], showing an increased decline in accuracy for the older compared with the younger subjects in the search condition compared with the pop-out condition.

Reaction times and accuracy rates were assessed using a two-way repeated ANOVA with condition and target visual field for both groups, respectively. There was only a main effect of condition on mean RTs and accuracy rates for younger group [RTs: $F(1,12) = 449.51$, $p < 0.0001$; accuracy rates: $F(1,12) = 30.95$, $p < 0.001$], with quicker RTs and higher accuracy in the pop-out condition. For older group, there was a main effect of condition on mean RTs and accuracy rates [RTs: $F(1,12) = 355.06$, $p < 0.0001$; accuracy rates: $F(1,12) = 58.46$, $p < 0.001$], with quicker RTs and higher accuracy in the pop-out condition, and there was a main effect of target visual field only on RTs [$F(1,12) = 5.06$, $p = 0.044$], with slower RTs in the left visual field target.

## EEG Coupling Results

### Whole-brain Total Coupling Values

Supplementary Table S1 summarizes the statistical effects of three factors of age, condition, and target visual field and interaction on the total coupling values for 9 frequency bands. As can be seen in Supplementary Table S1, there was a main effect of age for total coupling values only in the theta and alpha bands [theta band: $F(1,24) = 9.28$, $p = 0.006$; alpha band: $F(1,24) = 5.89$, $p = 0.023$], and there was a main effect of condition in almost all frequency bands. Since there was not any effect of age or any interaction effect between age and other factors in the higher frequency bands (24–40 Hz), we did not report these results in the following analyses. In three beta bands (12–24 Hz) there was an interaction between age and target visual field, so that we averaged their coupling values as one beta band to analyze. Hence, the frequency bands of interest were theta (4–8 Hz), alpha (8–12 Hz), and beta (12–24 Hz) activities.

**Table 2** presents the total coupling values of whole-brain in the theta, alpha, and beta frequency bands of two target visual fields for the pop-out and search conditions in younger

**TABLE 1 | Behavioral results (mean ± SD).**

| Condition | Target visual field | RT (ms) | | Accuracy (%) | |
|---|---|---|---|---|---|
| | | Young | Old | Young | Old |
| Visual pop-out | Left | 487.74 ± 106.82 | 704.91 ± 97.57 | 99.03 ± 1.16 | 97.75 ± 1.64 |
| | Right | 476.44 ± 94.39 | 678.11 ± 96.20 | 99.20 ± 0.87 | 98.16 ± 1.60 |
| Visual search | Left | 775.67 ± 129.86 | 1025.53 ± 74.26 | 92.74 ± 4.75 | 81.15 ± 9.35 |
| | Right | 768.45 ± 106.63 | 979.53 ± 148.64 | 93.13 ± 3.88 | 85.80 ± 7.64 |

*Mean reaction times (RT, ms) and accurate rates (%) and their corresponding standard deviations as a function of condition and target visual field in younger and older subjects.*

and older participants. For theta frequency band, there was a main effect of age (young and old) and target visual field (left and right), with bigger coupling values in the younger subjects only for search condition [independent *t*-tests, pop-out and left: $t_{(24)} = 2.39$, Bonferroni corrected $p > 0.05$; pop-out and right: $t_{(24)} = 2.23$, corrected $p > 0.05$; search and left: $t_{(24)} = 3.57$, corrected $p < 0.05$; search and right: $t_{(24)} = 2.79$, corrected $p < 0.05$]. There was an interaction between age and visual target field [$F(1,24) = 6.50$, $p = 0.018$], so that we tested two-way repeated measure ANOVA for the total coupling values with condition (pop-out and search) and target visual field (left and right) as the within-subject factors for both groups, respectively. There was only a main effect of target visual field for younger group [$F(1,24) = 9.26$, $p = 0.01$], with bigger coupling values in the left visual field target for pop-out condition [Paired *t*-tests, pop-out: $t_{(12)} = 2.74$, corrected $p < 0.05$; search: $t_{(12)} = 2.18$, corrected $p > 0.05$], but no such effect was present for the elderly group.

For alpha frequency band, there was a main effect of age and a marginal effect of condition on the total coupling values (Supplementary Table S1), and there was no significant interaction among age, condition and target visual field. The total coupling values were smaller for older compared to younger adults only in search condition [independent *t*-tests, pop-out and left: $t_{(24)} = 1.81$, corrected $p > 0.05$; pop-out and right: $t_{(24)} = 1.74$, corrected $p > 0.05$; search and left: $t_{(24)} = 3.52$, corrected $p < 0.05$; search and right: $t_{(24)} = 2.63$, corrected $p < 0.05$].

For beta frequency band, there was a main effect of condition [$F(1,24) = 7.10$, $p = 0.014$] and target visual field [$F(1,24) = 4.52$, $p = 0.044$], but no main effect was present in age. There was an interaction between age and visual target field [$F(1,24) = 6.40$, $p = 0.018$], so that we tested two-way repeated measure ANOVA for the total coupling values with condition (pop-out and search) and target visual field (left and right) as the within-subject factors for both groups, respectively. There was only a main effect of target visual field for younger group [$F(1,24) = 9.20$, $p = 0.01$], with bigger coupling values in the left visual field target for search condition [Paried *t*-tests, pop-out: $t_{(12)} = 2.23$, corrected $p > 0.05$; search: $t_{(12)} = 2.40$, corrected $p < 0.05$], but no such effect was present for the elderly group.

**Supplementary Figure S1** illustrates the presence of significant positive linear relationship within the older adults between total coupling values and RTs in the pop-out condition with left visual field target in theta frequency band [Pearson correlation coefficient ($r$) = 0.588, $p = 0.035$]. A regression was used to test whether a quadratic relationship also contributed to the variance, but it was not significant [$r = 0.605$, $p = 0.103$]. All other correlation between total coupling values and RTs or accuracies was not significant ($p > 0.05$).

## ROIs Coupling Value in Theta Frequency Band

Max normalized PLV values for all pair-wise combinations of eight regions of interest were calculated, generating 28 (totally 8 ROIs) index values for theta band (4–8 Hz) in four conditions for both groups. **Figure 3A** summarizes the main effect of age (blue line) and condition (red line) among eight regions of interest. As can be seen in **Figure 3A**, there was a main effect of age for coupling values on five long range connections, including the connections between left prefrontal and left central-frontal regions [1 and 3, $F(1,24) = 6.14$, $p = 0.02$], between right prefrontal and right central-frontal regions [2 and 4, $F(1,24) = 4.73$, $p = 0.04$], between right central-frontal and right central-parietal regions [4 and 6, $F(1,24) = 5.43$, $p = 0.03$], between left central-parietal and left parietal-occipital [5 and 7, $F(1,24) = 11.47$, $p = 0.002$], between right central-parietal and right parieto-occipital regions [6 and 8, $F(1,24) = 5.60$, $p = 0.04$], with smaller coupling values in older subjects. There was a main effect of condition for coupling values between left central-frontal and left central-parietal regions [3 and 5, $F(1,24) = 6.64$, $p = 0.017$], with smaller coupling values in the search condition.

For the connection between left prefrontal and central-frontal regions, there was an interaction between age and target visual field [$F(1,24) = 7.88$, $p < 0.001$], and there was no significant effect of condition. Hence we averaged the coupling values of the pop-out and search conditions, and applied repeated measure ANOVA with target visual field (left and right) as the within-subject factor and age (young and old) as the between-subject factor. **Figure 3B** shows the coupling values in both groups for both target fields. There was a main effect of age [$F(1,24) = 6.14$, $p = 0.02$] and an interaction between age and target field [$F(1,24) = 16.63$, $p < 0.001$], with bigger coupling values in left target than in right target for younger subjects [Paried *t*-tests, $t_{(12)} = 3.28$, $p = 0.007$] and bigger coupling values in right target than in left target for older subjects [Paried *t*-tests, $t_{(12)} = 2.43$, $p = 0.032$].

**TABLE 2 | The total coupling values for all pair-wise combinations of electrodes in the theta, alpha, and beta frequency bands (mean ± SEM).**

| Condition | Target visual field | Theta band (4–8 Hz) | | Alpha band (8–12 Hz) | | Beta band (12–24 Hz) | |
|---|---|---|---|---|---|---|---|
| | | Young | Old | Young | Old | Young | Old |
| Pop-out | Left | 488.98 ± 64.69 | 270.28 ± 64.69 | 724.80 ± 130.16 | 391.14 ± 130.16 | 586.45 ± 81.01 | 433.29 ± 81.01 |
| | Right | 422.78 ± 55.43 | 248.36 ± 55.43 | 712.57 ± 137.41 | 375.45 ± 137.41 | 503.33 ± 74.08 | 410.13 ± 74.08 |
| Search | Left | 445.81 ± 52.71 | 179.77 ± 52.71 | 599.18 ± 70.38 | 249.36 ± 70.38 | 489.66 ± 56.17 | 277.76 ± 56.17 |
| | Right | 369.09 ± 43.39 | 198.13 ± 43.39 | 501.36 ± 60.03 | 278.36 ± 60.03 | 398.02 ± 54.24 | 316.03 ± 54.24 |

*The total coupling values and their corresponding standard error of mean as a function of condition and target visual field in younger and older subjects.*

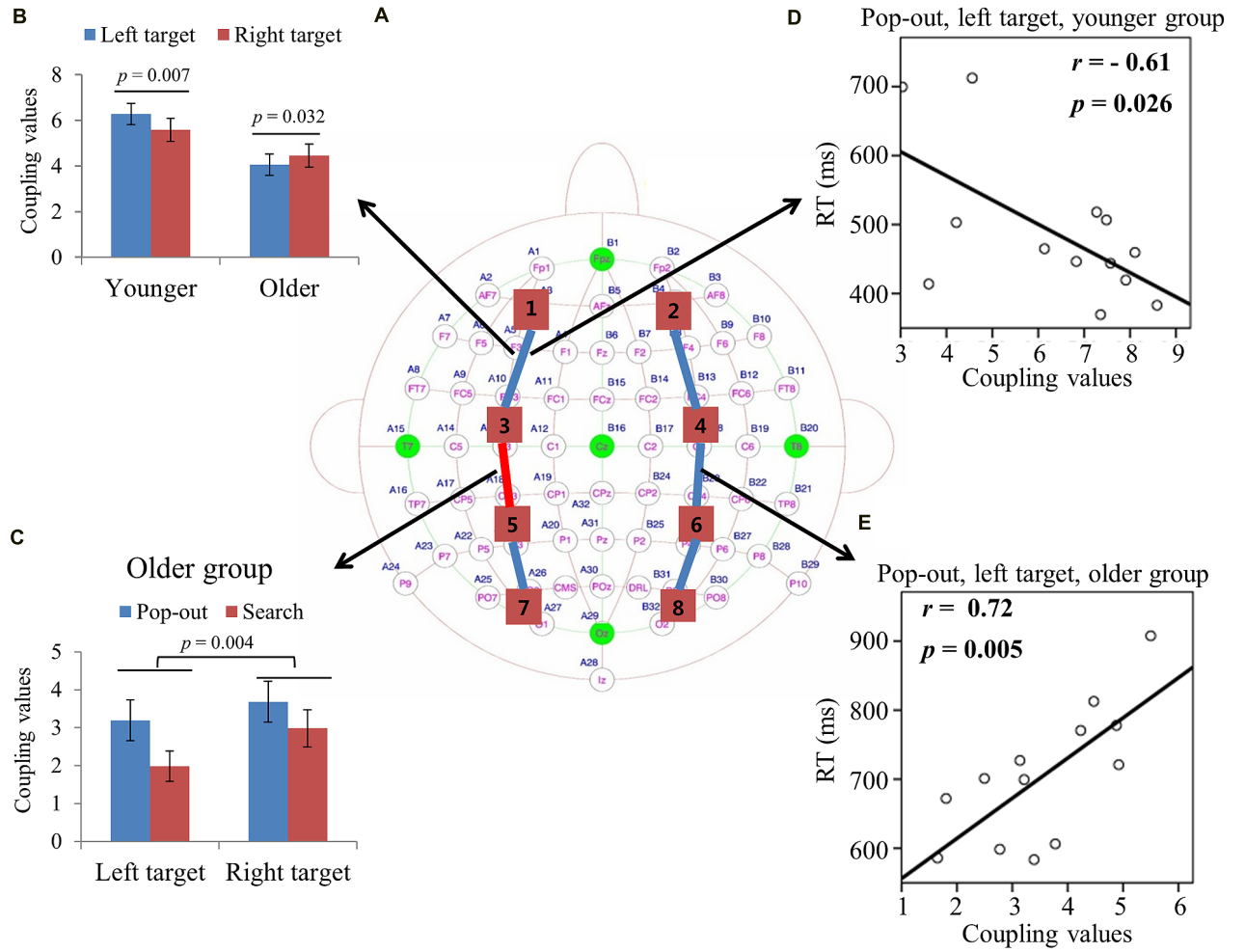


**FIGURE 3 | (A)** Inter-regions coupling in theta frequency band. Blue lines indicate main effect of age (younger > older) and red line indicates main effect of condition (pop-out > search). **(B)** Coupling values between left prefrontal and central-frontal regions as a function of target visual field in younger and older subjects, with greater coupling values in left target than in right target for younger subjects and greater coupling values in right target than in left target for old subjects. **(C)** Coupling values between left central-frontal and central-parietal regions as a function of target visual field in both conditions for older group, with greater values in pop-out condition and in right target, and no such effects for younger group. **(D)** Linear negative regression between mean RT and coupling value between left prefrontal and central-frontal regions for the pop-out condition with the left field target in the younger group. **(E)** Linear positive regression between mean RT and coupling value between right central-frontal and central-parietal regions for the pop-out condition with the left field target in the older group.

For the connection between left central-frontal and left central-parietal regions, there was an interaction between age and target visual field [$F(1,24) = 9.62$, $p = 0.005$]. Hence we divided the test into two repeated measure ANOVA with condition and target visual field as the within-subject factors for younger and older groups, respectively. There was a main effect of target field [$F(1,12) = 12.22$, $p = 0.004$] and condition [$F(1,12) = 5.69$, $p = 0.034$] for older group, with greater coupling values in the right field target and in the pop-out condition. There was no significant effect for the younger group. **Figure 3C** shows the coupling values in both conditions and target fields for older group. For the other four long range connections, there was no other significant effect.

**Figure 3D** illustrates the presence of significant negative linear relationship within the younger adults between coupling values of left prefrontal and central-frontal regions and RTs in the pop-out condition with left visual field target [$r = -0.61$, $p = 0.026$]. **Figure 3E** illustrates a significant positive linear relationship within the older adults between coupling values of right central-frontal and central-parietal and RTs in the pop-out condition with left visual field target [$r = 0.72$, $p = 0.005$]. All other correlation between coupling values and RTs or accuracies was not significant ($p > 0.05$).

## ROIs Coupling Value in Alpha Frequency Band

**Figure 4A** summarizes the main effect of age (blue) and condition (red) among eight regions of interest. As can be seen in **Figure 4A**, there was a main effect of age for coupling values on two long range connections, including the connections between left prefrontal and left central-frontal regions [1 and

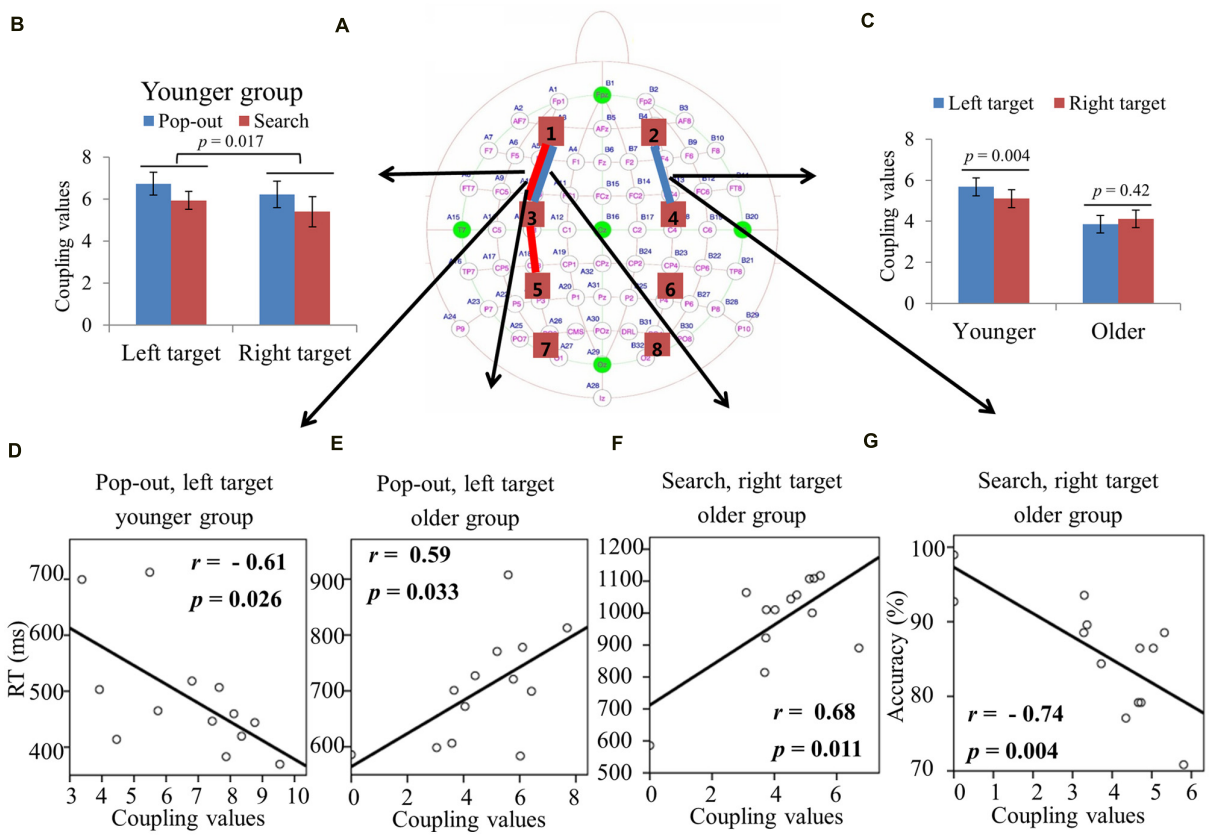


**FIGURE 4 | (A)** Inter-regions coupling in alpha frequency band. Blue lines indicate main effect of age (younger > older) and red line indicates main effect of condition (pop-out > search). **(B)** Coupling values between left prefrontal and central-frontal regions as a function of target field and condition in younger subjects, with greater coupling values in the left field target and in the pop-out condition. There was only a main effect of condition for the older group, with greater coupling values in the pop-out condition. **(C)** Coupling values between right prefrontal and central-frontal regions as a function of target field in younger and older subjects, with greater coupling values in left target than in right target for younger subjects and no difference between right and left targets for old subjects. **(D)** Linear negative regression between mean RT and coupling value between left prefrontal and central-frontal regions for the pop-out condition with the left field target in the younger group. Linear positive regression between mean RT and coupling value between left prefrontal and central-frontal regions for the pop-out condition with the left field target **(E)** and for the search condition with the right target **(F)** in the older group. **(G)** Linear negative regression between mean accuracy and coupling value between right prefrontal and central-frontal regions for the search condition with the right target in the older group.

3, $F(1,24) = 5.174$, $p = 0.03$], between right prefrontal and right central-frontal regions [2 and 4, $F(1,24) = 5.87$, $p = 0.02$], with smaller coupling values for older subjects. There was a main effect of condition for coupling values on connections between left prefrontal and left central-frontal regions [1 and 3, $F(1,24) = 14.03$, $p = 0.001$], between left central-frontal and left central-parietal regions [3 and 5, $F(1,24) = 5.87$, $p = 0.02$], with smaller coupling values in search condition.

For the connection between left prefrontal and central-frontal regions, there was an interaction between age and target visual field [$F(1,24) = 9.02$, $p = 0.006$]. Hence we divided the test into two repeated measure ANOVA with condition and target visual field as the within-subject factors for younger and older groups, respectively. There was a main effect of target field [$F(1,12) = 7.75$, $p = 0.017$] and condition [$F(1,12) = 5.09$, $p = 0.044$] for younger group, with greater coupling values in the left field target and in the pop-out condition. There was only a main effect of condition [$F(1,12) = 10.36$, $p = 0.007$] for the older group, with greater coupling values in the pop-out condition. **Figure 4B** shows the coupling values in both conditions and target fields for younger group.

For the connection between right prefrontal and central-frontal regions, there was an interaction between age and target visual field [$F(1,24) = 5.55$, $p = 0.03$], and there was no significant effect of condition. Hence we averaged the coupling values of the pop-out and search conditions, and applied repeated measure ANOVA with target visual field (left and right) as the within-subject factor and age (young and old) as the between-subject factor. **Figure 4C** shows the coupling values in both groups for both target fields. There was a main effect of age [$F(1,24) = 5.87$, $p = 0.02$] and an interaction between age and target field [$F(1,24) = 5.58$, $p = 0.03$], with bigger coupling values in left target than in right target for younger subjects [Paried $t$-tests, $t_{(12)} = 3.58$, $p = 0.004$]. Thus, greater bilateral prefronto-frontal coupling were shown in the left visual target for younger group.

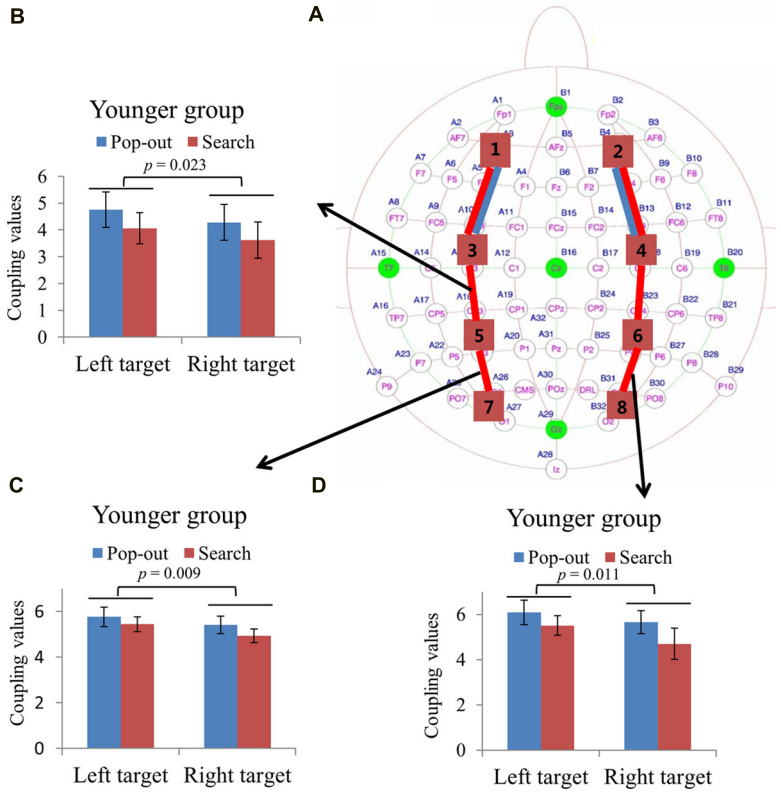


**FIGURE 5 | (A)** Inter-regions coupling in beta frequency band. Blue lines indicate main effect of age (younger > older) and red line indicates main effect of condition (pop-out > search). Coupling values between left central-frontal and central-parietal regions **(B)**, between left central-parietal and parietal-occipital regions **(C)**, and between right central-parietal and parietal-occipital regions **(D)** as a function of target field and condition in younger subjects, with bigger coupling values in left target than in right target, and no such effect was presented in the older group.

**Figure 4D** illustrates the presence of significant negative linear relationship within the younger adults between coupling values of left prefrontal and central-frontal regions and RTs in the pop-out condition with left visual field target [$r = -0.61$, $p = 0.026$]. **Figures 4E,F** illustrate the significant positive linear relationships within the older adults between coupling values of left prefrontal and central-frontal regions and RTs in the pop-out condition with left visual field target [$r = 0.59$, $p = 0.033$] and in the search condition with right visual field target [$r = 0.68$, $p = 0.011$], respectively. **Figure 4G** illustrates the significant negative linear relationship within the older adults between coupling values of right prefrontal and central-frontal regions and accuracies in the search condition with right visual field target [$r = -0.74$, $p = 0.004$]. All other correlation between coupling values and RTs or accuracies was not significant ($p > 0.05$).

## ROIs Coupling Value in Beta Frequency Band

**Figures 5A** and **6A** summarizes the main effect of age and condition among eight regions of interest. As can be seen in **Figure 5A** with blue lines, there was a main effect of age for coupling values on two long range connections, including the connections between left prefrontal and left central-frontal regions [1 and 3, $F(1,24) = 5.49$, $p = 0.03$], between right prefrontal and right central-frontal regions [2 and 4, $F(1,24) = 5.03$, $p = 0.03$], with smaller coupling values for older subjects. In addition, there was a main effect of condition for those two frontal connections [1 and 3, $F(1,24) = 4.46$, $p = 0.045$; 2 and 4, $F(1,24) = 7.26$, $p = 0.01$] marked with red lines in **Figure 5A**, with smaller coupling values in search condition. There was a main effect of condition for coupling values between left central-frontal and left central-parietal regions [3 and 5, $F(1,24) = 4.87$, $p = 0.04$], between right central-frontal and right central-parietal regions [4 and 6, $F(1,24) = 5.96$, $p = 0.02$], between left central-parietal and left parietal-occipital [5 and 7, $F(1,24) = 5.81$, $p = 0.02$], between right central-parietal and right parieto-occipital regions [6 and 8, $F(1,24) = 7.75$, $p = 0.01$], with smaller coupling values in search condition (**Figure 5A**).

Due to the interaction between age and target visual field for these three connections [3 and 5, $F(1,24) = 4.29$, $p = 0.049$; 5 and 7, $F(1,24) = 7.54$, $p = 0.01$; 6 and 8, $F(1,24) = 4.38$, $p = 0.047$], we divided the test into two repeated measure ANOVA with condition and target field as the within-subject factors for both groups, respectively. There was only a main effect of target visual field [3 and 5, $F(1,12) = 6.73$, $p = 0.023$; 5 and 7, $F(1,12) = 9.69$, $p = 0.009$; 6 and 8, $F(1,12) = 8.93$, $p = 0.011$] for the younger group in these three connections, with bigger coupling values in left target than in right target, and no such effect was present for the older group. **Figures 5B–D** show the coupling values

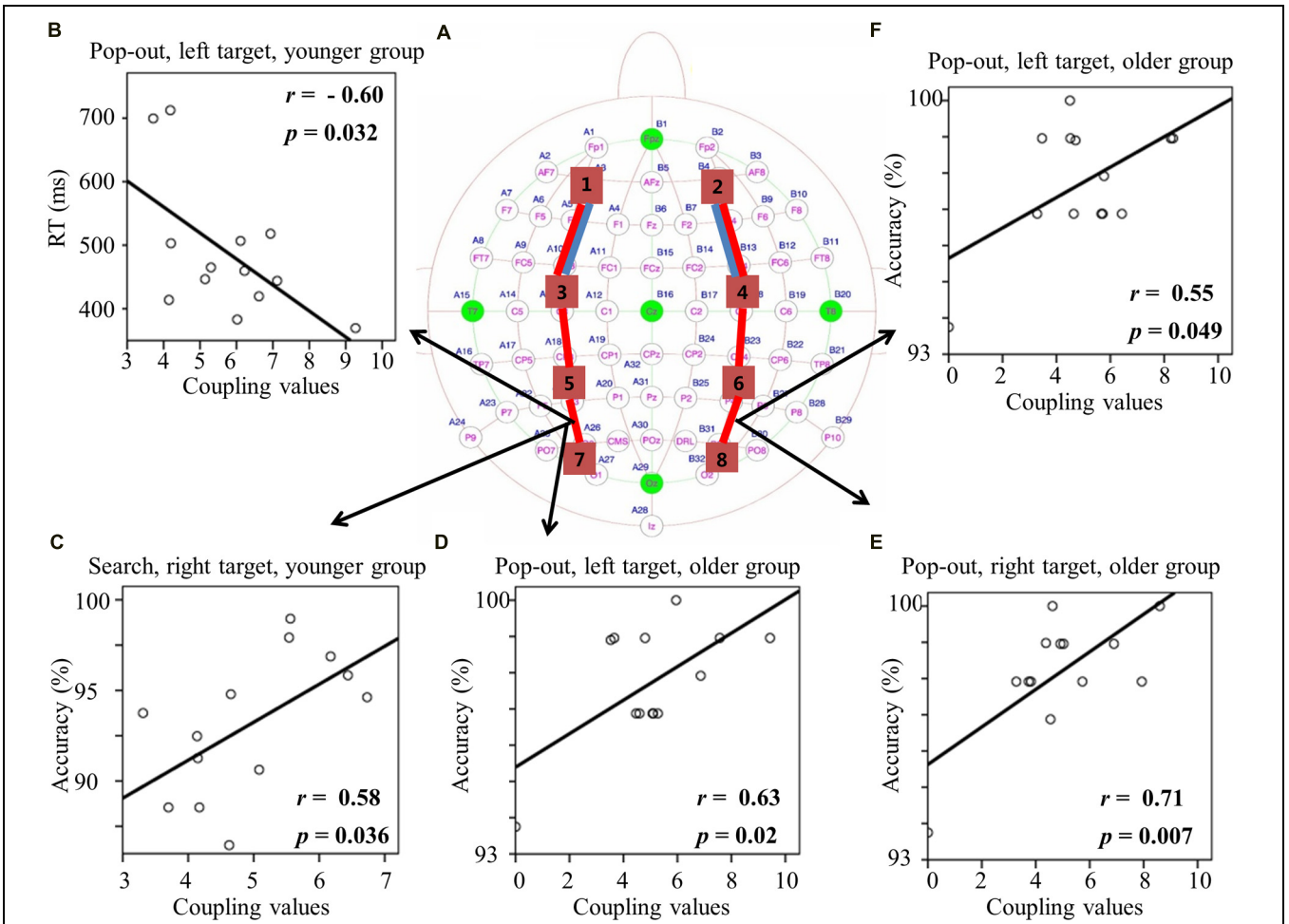


**FIGURE 6 | (A)** Inter-regions coupling in beta frequency band. Blue lines indicate main effect of age (younger > older) and red line indicates main effect of condition (pop-out > search). **(B)** Linear negative regression between mean RT and coupling value between left central-parietal and parietal-occipital regions for the pop-out condition with the left field target in the younger group. Linear positive regression between mean accuracy and coupling value between left central-parietal and parietal-occipital regions for the search condition with the right target in the younger group **(C)** and for the pop-out condition with the left target in the older group **(D)**. Linear positive regression between mean accuracy and coupling value between right central-parietal and parietal-occipital regions for the pop-out condition with the right target **(E)** and the left target **(F)** in the older group.

in both conditions and target fields for younger group at three connections.

For the coupling values between right prefrontal and central-frontal regions, there were significant positive linear relationships within the older subjects between values and RTs in all four conditions [pop-out and left: $r = 0.63$, $p = 0.02$; pop-out and right: $r = 0.61$, $p = 0.03$; search and left: $r = 0.58$, $p = 0.04$; search and left: $r = 0.58$, $p = 0.04$]. **Figures 6B,C** illustrate the significant positive linear relationships within the younger adults between coupling values of left central-parietal and parietal-occipital regions and performance in the pop-out condition with left target [RTs: $r = -0.60$, $p = 0.032$] and in the search condition with right visual field target [accuracy: $r = 0.58$, $p = 0.036$], respectively. **Figure 6D** illustrates the significant positive linear relationship within the older adults between coupling values of left central-parietal and parietal-occipital regions and accuracies in the pop-out condition with left target [$r = 0.63$, $p = 0.02$]. **Figures 6E,F** illustrate the significant positive linear relationships within the older adults between coupling values of right central-parietal and parietal-occipital regions and accuracies in the pop-out condition with left target [$r = 0.55$, $p = 0.049$] and right target [$r = 0.71$, $p = 0.007$], respectively. All other correlation between coupling values and RTs or accuracies was not significant ($p > 0.05$).

## DISCUSSION

### Aging Effects on Behavior and Inter-regions Coupling

Aging had prominent effects on both behavioral and EEG coupling strength under the control of top–down and bottom–up attention. Aging led to slowed RT and decreased accuracy (**Table 1**), indicating a slowing of

cognitive performance with advancing age (Salthouse, 1996). Specifically, greater age-related reductions in accuracy in the search condition than in the pop-out condition were shown, suggesting additional attentional demands for older subjects with increased task complexity (Greenwood et al., 1997; Hommel et al., 2004; Madden et al., 2004, 2007).

Aging was associated with a declined whole-brain coupling strength of theta and alpha frequency bands, with a greater age-related decline in the search than in the pop-out condition (**Table 2**), in accord with their accuracy. Specifically, older adults showed a decreased lateral prefronto-frontal coupling in theta, alpha and beta frequency bands in both conditions (**Figures 3A**, **4A**, and **5A**), which confirmed the well-established age-related decline in allocation of attentional resources efficiency or reduction in inhibitory control functions in attention (Colcombe et al., 2003; Madden et al., 2004; Andrés et al., 2006; Hasher et al., 2008; Lorenzo-López et al., 2008; Gola et al., 2012; Deiber et al., 2013; Gola et al., 2013; Kardos et al., 2014).

Greater prefronto-frontal coupling (left lateral theta coupling, **Figure 3B**; and bilateral alpha coupling, **Figures 4B,C**), greater fronto-parietal coupling (left beta coupling, **Figure 5B**), and greater parieto-occipital coupling (bilateral beta coupling, **Figures 5C,D**) in the left target than in the right target for younger group were presented, suggesting a left visual field advantage (Holländer et al., 2005; Verleger and Smigasiewicz, 2015). This advantage might be related to the right hemispheric dominance in the ventral attentional network, which seems to particularly activate regions largely lateralized to the right hemisphere and involves right temporo-parietal and ventral frontal cortices in healthy subjects (Corbetta and Shulman, 2002; Shulman and Corbetta, 2012; Hong et al., 2015). Left visual field advantage was reduced with aging, supporting the Hemispheric Asymmetry Reduction in Older Adults (HAROLD) theory (Cabeza, 2002). Furthermore, older adults showed a greater left prefronto-frontal theta coupling (right two bars in **Figure 3B**) in the right visual target than in the left visual target, in accord with their quicker RTs, supporting the idea that older adults use bilateral neural circuits as compensation to accomplish visual search tasks (Reuter-Lorenz and Lustig, 2005; Grady, 2008; Reuter-Lorenz and Cappell, 2008). Interestingly, there was a greater left fronto-parietal theta coupling (**Figure 3C**) in the right visual target than in the left visual target for older group, whereas there was no difference for younger group. For younger group, left visual field advantage and the greater activity in the contralateral hemisphere (right visual target) for directing of attention may be counteracting, resulting in no difference between the right and left visual targets. For older group, the contribution of left visual field advantage is reduced, so that the activity in the contralateral hemisphere (right visual target) is in dominance, which is advantageous for task performance. These findings support the idea that right hemispheric dominance in the ventral attentional network is reduced to compensate for the inhibitory dysfunction with aging (Cabeza, 2002).

## Attention Control Effects on Behavior and Inter-regions Coupling

The control of top–down and bottom–up attention had prominent effects on both behavioral and EEG coupling strength. Top–down control led to slowed RT and decreased accuracy for both groups (**Table 1**), indicating that the search task was sufficiently difficult to demand more cognitive effort (Treisman and Gelade, 1980). Top–down attentional control was associated with a declined whole-brain coupling strength of alpha and beta frequency bands, with a smaller coupling in the search than in the pop-out condition (**Table 2**). Specifically, search condition showed a decreased coupling of left fronto-parietal in theta and alpha frequency bands, of left prefronto-frontal in alpha-band, and of six inter-regions in beta-band compared to pop-out condition (**Figures 3A**, **4A**, and **5A**).

Pop-out target detection was mainly associated with greater parieto-occipital beta-coupling strength compared to search condition regardless of aging, in accord with their better performance, which confirmed previous findings that parietal power at beta-band (12–24 Hz) in human and parietal-extrastriate coherences at higher frequency band (35–55 Hz) in monkey were greater in the pop-out than in the search condition (Buschman and Miller, 2007; Li et al., 2010). This supports the idea that posterior parietal cortex is primarily responsible for the encoding of salient stimuli and automatic detection (Constantinidis and Steinmetz, 2005). Fronto-extrastriate coherences at intermediate frequency band (22–34 Hz) were greater in the search than in the pop-out condition (Buschman and Miller, 2007), but in the present study no significant difference in fronto-parietal theta-coupling strength between pop-out and search conditions for young subjects was observed (**Figure 3C**). This may be due to strict statistical method applied for significance in connections when constructing the network, as a result, weaker coupling may be ruled out. For example, if we use the normalized PLV values directly without threshold, a greater theta-coupling strength between left frontal and right occipital regions (regions 3 and 8) in the search than in the pop-out condition in left target for young subjects will be observed [3 and 8, paired $t$-test, $t_{(12)} = 3.59$, $p = 0.0037$]. We prefer to use strict statistical level to decrease the type I error. In summary, our results may indicate that the parieto-occipital coupling of beta-band could serve as a bottom-up function and be vulnerable to top–down attention control in both groups.

## Relationships between Behavior and Inter-regions Coupling

The greater prefronto-frontal coupling showed better performance in theta and alpha bands for younger subjects (**Figures 3D** and **4D**), but worse performance in alpha and beta bands for older subjects (**Figures 4E–G**). These results provided additional information regarding the age-related change in the prefronto-frontal coupling in attentional control during the visual search task, suggesting that prefronto-frontal coupling for both groups may be generated by distinct brain cortices. An fMRI study has reported that younger individuals with higher levels

of middle frontal gyrus activation exhibited better performance, and older individuals with higher levels of putamen activation showed worse performance during visual target detection (Madden et al., 2004). In present study, prefronto-frontal coupling results may most reflect connections within frontal gyrus for younger group, and most show connections within deep gray matter structures for older group in compensation for the age-related decline in visual search. Prefronto-frontal coupling was significant as a predictor of behavior for the younger and older groups, but in the opposite direction.

And the bigger parieto-occipital coupling in beta band led to better performance for both groups (**Figures 6B–F**), together with above results, indicating synchrony as a mechanism of attention (Miller and Buschman, 2013). Local synchrony between parieto-occipital cortices in beta-band and between prefronto-frontal cortices in theta, alpha and beta frequency bands may help the brain to improve its signal-to-noise ratio for better processing of bottom–up sensory input and top–down cognitive control, respectively. Parieto-occipital coupling in beta band was significant as a predictor of behavior for the younger and older groups in the same direction, and greater coupling may carry more bottom–up information.

In the current study, we found evidence for age-related changes in the differential roles of fronto-parieto-occipital connectivity at different oscillatory frequencies during the control of top–down and bottom–up attention. Together with evidence from past literature on the animal work on the networks contributing to top–down and bottom–up attention (Buschman and Miller, 2007; Miller and Buschman, 2013), these results suggest that bottom–up and top–down target lead to differential fronto-parieto-occipital connectivity at different oscillatory frequencies in younger and older adults. Greater prefronto-frontal coupling in theta and alpha-bands, fronto-parietal coupling in beta-band, and parieto-occipital coupling in beta-band in the left target than in the right target for younger group indicates a right hemispheric dominance in the ventral attentional network, which is reduced with aging to compensate for the inhibitory dysfunction. While pop-out target detection is mainly associated with greater parieto-occipital beta-coupling strength compared to search condition regardless of aging, in accord with their better performance. Prefronto-frontal coupling in theta, alpha, and beta bands and parieto-occipital coupling in beta band is a predictor of behavior for the both groups. Taken together these findings provide evidence that prefronto-frontal coupling of theta, alpha, and beta frequency bands may serve as a possible basis of aging during visual attention task, while parieto-occipital coupling in beta-band could serve for a bottom–up function and be vulnerable to top–down attention control for younger and older groups.

## AUTHOR CONTRIBUTIONS

LL: Conceived, designed and performed the experiments. LL and DZ: Analyzed the data. LL: Wrote the paper.

## ACKNOWLEDGMENTS

This research was supported by grants from the National Natural Science Foundation of China projects (NSFC, Nos. 61473062, 61203363, 91232725), 111 Project (B12027), and the Fundamental Research Funds for the Central Universities (ZYGX2014J077).

## SUPPLEMENTARY MATERIAL

The Supplementary Material for this article can be found online at: http://journal.frontiersin.org/article/10.3389/fnagi.2015.00223

**FIGURE S1 | Linear regression between mean reaction time (RT) and total coupling value for the pop-out condition with the left field target in the older group for theta frequency band.** Each subject is marked as a circle, with 13 circles in total. Pearson correlation coefficient ($r = 0.588$) was significant ($p = 0.035$), indicating a positive linear correlation between RT and total coupling value in this condition.

## REFERENCES

Anderson, N. D., Iidaka, T., Cabeza, R., Kapur, S., McIntosh, A. R., and Craik, F. I. M. (2000). The effects of divided attention on encoding- and retrieval-related brain activity: a PET study of younger and older adults. *J. Cogn. Neurosci.* 12, 775–792. doi: 10.1162/089892900562598

Andrés, P., Parmentier, F., and Escera, C. (2006). The effect of age on involuntary capture of attention by irrelevant sounds: a test of the frontal hypothesis of aging. *Neuropsychologia* 44, 2564–2568. doi: 10.1016/j.neuropsychologia.2006.05.005

Bledowski, C., Prvulovic, D., Goebel, R., Zanella, F. E., and Linden, D. E. (2004a). Attentional systems in target and distractor processing: a combined ERP and fMRI study. *Neuroimage* 22, 530–540. doi: 10.1016/j.neuroimage.2003.12.034

Bledowski, C., Prvulovic, D., Hoechstetter, K., Scherg, M., Wibral, M., Goebel, R., et al. (2004b). Localizing P300 generators in visual target and distractor processing: a combined event-related potential and functional magnetic resonance imaging study. *J. Neurosci.* 24, 9353–9360. doi: 10.1523/JNEUROSCI.1897-04.2004

Buschman, T. J., and Miller, E. K. (2007). Top-down versus bottom-up control of attention in the prefrontal and posterior parietal cortices. *Science* 315, 1860–1862. doi: 10.1126/science.1138071

Cabeza, R. (2002). Hemispheric asymmetry reduction in older adults: the HAROLD model. *Psychol. Aging* 17, 85–100. doi: 10.1037/0882-7974.17.1.85

Colcombe, A. M., Kramer, A. F., Irwin, D. E., Peterson, M. S., Colcombe, S., and Hahn, S. (2003). Age-related effects of attentional and oculomotor capture by onsets and color singletons as a function of experience. *Acta Psychol. (Amst.)* 113, 205–225. doi: 10.1016/S0001-6918(03)00019-2

Constantinidis, C., and Steinmetz, M. A. (2005). Posterior parietal cortex automatically encodes the location of salient stimuli. *J. Neurosci.* 25, 233–238. doi: 10.1523/JNEUROSCI.3379-04.2005

Corbetta, M., and Shulman, G. L. (2002). Control of goal-directed and stimulus-driven attention in the brain. *Nat. Rev. Neurosci.* 3, 201–215. doi: 10.1038/nrn755

Deiber, M. P., Ibanez, V., Missonnier, P., Rodriguez, C., and Giannakopoulos, P. (2013). Age-associated modulations of cerebral oscillatory patterns related to attention control. *Neuroimage* 82, 531–546. doi: 10.1016/j.neuroimage.2013.06.037

Delorme, A., and Makeig, S. (2004). EEGLAB: an open source toolbox for analysis of single-trial EEG dynamics including independent component analysis. *J. Neurosci. Meth.* 134, 9–21. doi: 10.1016/j.jneumeth.2003.10.009

Dennis, N. A., Hayes, S. M., Prince, S. E., Madden, D. J., Huettel, S. A., and Cabeza, R. (2008). Effects of aging on the neural correlates of successful item and source memory encoding. *J. Exp. Psychol. Learn. Mem. Cogn.* 34, 791–808. doi: 10.1037/0278-7393.34.4.791

Fotenos, A. F., Mintun, M. A., Snyder, A. Z., Morris, J. C., and Buckner, R. L. (2008). Brain volume decline in aging: evidence for a relation between socioeconomic status, preclinical Alzheimer disease, and reserve. *Arch. Neurol.* 65, 113–120. doi: 10.1001/archneurol.2007.27

Geerligs, L., Saliasi, E., Maurits, N. M., Renken, R. J., and Lorist, M. M. (2014). Brain mechanisms underlying the effects of aging on different aspects of selective attention. *Neuroimage* 91, 52–62. doi: 10.1016/j.neuroimage.2014.01.029

Giesbrecht, B., Woldorff, M. G., Song, A. W., and Mangun, G. R. (2003). Neural mechanisms of top-down control during spatial and feature attention. *Neuroimage* 19, 496–512. doi: 10.1016/S1053-8119(03)00162-9

Gola, M., Kaminski, J., Brzezicka, A., and Wrobel, A. (2012). Beta band oscillations as a correlate of alertness-changes in aging. *Int. J. Psychophysiol.* 85, 62–67. doi: 10.1016/j.ijpsycho.2011.09.001

Gola, M., Magnuski, M., Szumska, I., and Wrobel, A. (2013). EEG beta band activity is related to attention and attentional deficits in the visual performance of elderly subjects. *Int. J. Psychophysiol.* 89, 334–341. doi: 10.1016/j.ijpsycho.2013.05.007

Gordon, B. A., Rykhlevskaia, E. I., Brumback, C. R., Lee, Y., Elavsky, S., Konopack, J. F., et al. (2008). Neuroanatomical correlates of aging, cardiopulmonary fitness level, and education. *Psychophysiology* 45, 825–838. doi: 10.1111/j.1469-8986.2008.00676.x

Grady, C. L. (2008). Cognitive neuroscience of aging. *Year Cogn. Neurosci.* 1124, 127–144.

Grady, C. L., Bernstein, L. J., Beig, S., and Siegenthaler, A. L. (2002). The effects of encoding task on age-related differences in the functional neuroanatomy of face memory. *Psychol. Aging* 17, 7–23. doi: 10.1037/0882-7974.17.1.7

Greenwood, P. M., Parasuraman, R., and Alexander, G. E. (1997). Controlling the focus of spatial attention during visual search: effects of advanced aging and Alzheimer disease. *Neuropsychology* 11, 3–12. doi: 10.1037/0894-4105.11.1.3

Hasher, L., Lustig, C., and Zacks, R. (2008). "Inhibitory mechanisms and the control of attention," in *Variation in Working Memory*, eds A. R. A. Conway, C. Jarrold, M. J. Kane, A. Miyake, and J. N. Towse (New York, NY: Oxford University Press), 227–249.

Holländer, A., Corballis, M. C., and Hamm, J. P. (2005). Visual-field asymmetry in dual-stream RSVP. *Neuropsychologia* 43, 35–40. doi: 10.1016/j.neuropsychologia.2004.06.006

Hommel, B., Li, K. Z., and Li, S. C. (2004). Visual search across the life span. *Dev. Psychol.* 40, 545–558. doi: 10.1037/0012-1649.40.4.545

Hong, X., Sun, J., Bengson, J. J., Mangun, G. R., and Tong, S. (2015). Normal aging selectively diminishes alpha lateralization in visual spatial attention. *Neuroimage* 106, 353–363. doi: 10.1016/j.neuroimage.2014.11.019

Husain, M., and Nachev, P. (2007). Space and the parietal cortex. *Trends Cogn. Sci.* 11, 30–36. doi: 10.1016/j.tics.2006.10.011

Johnson, M. K., Mitchell, K. J., Raye, C. L., and Greene, E. J. (2004). An age-related deficit in prefrontal cortical function associated with refreshing information. *Psychol. Sci.* 15, 127–132. doi: 10.1111/j.0963-7214.2004.01502009.x

Kardos, Z., Toth, B., Boha, R., File, B., and Molnar, M. (2014). Age-related changes of frontal-midline theta is predictive of efficient memory maintenance. *Neuroscience* 273, 152–162. doi: 10.1016/j.neuroscience.2014.04.071

Kayser, J., and Tenke, C. E. (2006). Principal components analysis of Laplacian waveforms as a generic method for identifying ERP generator patterns: I. Evaluation with auditory oddball tasks. *Clin. Neurophysiol.* 117, 348–368. doi: 10.1016/j.clinph.2005.08.033

Knudsen, E. I. (2007). Fundamental components of attention. *Annu. Rev. Neurosci.* 30, 57–78. doi: 10.1146/annurev.neuro.30.051606.094256

Knyazev, G. G., Volf, N. V., and Belousova, L. V. (2015). Age-related differences in electroencephalogram connectivity and network topology. *Neurobiol. Aging* 36, 1849–1859. doi: 10.1016/j.neurobiolaging.2015.02.007

Kok, A. (2000). Age-related changes in involuntary and voluntary attention as reflected in components of the event-related potential (ERP). *Biol. Psychol.* 54, 107–143. doi: 10.1016/S0301-0511(00)00054-5

Lachaux, J. P., Rodriguez, E., Martinerie, J., and Varela, F. J. (1999). Measuring phase synchrony in brain signals. *Hum. Brain Mapp.* 8, 194–208.

Li, L., Gratton, C., Fabiani, M., and Knight, R. T. (2013). Age-related frontoparietal changes during the control of bottom-up and top-down attention: an ERP study. *Neurobiol. Aging* 34, 477–488. doi: 10.1016/j.neurobiolaging.2012.02.025

Li, L., Gratton, C., Yao, D., and Knight, R. T. (2010). Role of frontal and parietal cortices in the control of bottom-up and top-down attention in humans. *Brain Res.* 1344, 173–184. doi: 10.1016/j.brainres.2010.05.016

Lien, M. C., Gemperle, A., and Ruthruff, E. (2011). Aging and involuntary attention capture: electrophysiological evidence for preserved attentional control with advanced age. *Psychol. Aging* 26, 188–202. doi: 10.1037/a0021073

Lorenzo-López, L., Amenedo, E., Pascual-Marqui, R. D., and Cadaveira, F. (2008). Neural correlates of age-related visual search decline: a combined ERP and sLORETA study. *Neuroimage* 41, 511–524. doi: 10.1016/j.neuroimage.2008.02.041

Madden, D. J. (2007). Aging and visual attention. *Curr. Dir. Psychol. Sci.* 16, 70–74. doi: 10.1111/j.1467-8721.2007.00478.x

Madden, D. J., Costello, M. C., Dennis, N. A., Davis, S. W., Shepler, A. M., Spaniol, J., et al. (2010). Adult age differences in functional connectivity during executive control. *Neuroimage* 52, 643–657. doi: 10.1016/j.neuroimage.2010.04.249

Madden, D. J., Spaniol, J., Whiting, W. L., Bucur, B., Provenzale, J. M., Cabeza, R., et al. (2007). Adult age differences in the functional neuroanatomy of visual attention: a combined fMRI and DTI study. *Neurobiol. Aging* 28, 459–476. doi: 10.1016/j.neurobiolaging.2006.01.005

Madden, D. J., Whiting, W. L., and Huettel, S. A. (2005). "Age-related changes in neural activity during visual perception and attention," in *Cognitive Neuroscience of Aging: Linking Cognitive and Cerebral Aging*, eds R. Cabeza, L. Nyberg, and D. Park (New York, NY: Oxford University Press), 157–185.

Madden, D. J., Whiting, W. L., Provenzale, J. M., and Huettel, S. A. (2004). Age-related changes in neural activity during visual target detection measured by fMRI. *Cereb. Cortex* 14, 143–155. doi: 10.1093/cercor/bhg113

Milham, M. P., Erickson, K. I., Banich, M. T., Kramer, A. F., Webb, A., Wszalek, T., et al. (2002). Attentional control in the aging brain: insights from an fMRI study of the stroop task. *Brain Cogn.* 49, 277–296. doi: 10.1006/brcg.2001.1501

Miller, E. K., and Buschman, T. J. (2013). Cortical circuits for the control of attention. *Curr. Opin. Neurobiol.* 23, 216–222. doi: 10.1016/j.conb.2012.11.011

Mormann, F., Lehnertz, K., David, P., and Elger, C. E. (2000). Mean phase coherence as a measure for phase synchronization and its application to the EEG of epilepsy patients. *Physica D* 144, 358–369. doi: 10.1016/j.clinph.2013.09.047

Nunez, P. L., Srinivasan, R., Westdorp, A. F., Wijesinghe, R. S., Tucker, D. M., Silberstein, R. B., et al. (1997). EEG coherency. I: statistics, reference electrode, volume conduction, Laplacians, cortical imaging, and interpretation at multiple scales. *Electroencephalogr. Clin. Neurophysiol.* 103, 499–515. doi: 10.1016/S0013-4694(97)00066-7

Perrin, F., Pernier, J., Bertrand, O., and Echallier, J. F. (1989). Spherical splines for scalp potential and current density mapping. *Electroencephalogr. Clin. Neurophysiol.* 72, 184–187. doi: 10.1016/0013-4694(89)90180-6

Phillips, S., and Takeda, Y. (2009). Greater frontal-parietal synchrony at low gamma-band frequencies for inefficient than efficient visual search in human EEG. *Int. J. Psychophysiol.* 73, 350–354. doi: 10.1016/j.ijpsycho.2009.05.011

Plude, D. J., and Doussard-Roosevelt, J. A. (1989). Aging, selective attention, and feature integration. *Psychol. Aging* 4, 98–105. doi: 10.1037/0882-7974.4.1.98

Quian Quiroga, R., Kraskov, A., Kreuz, T., and Grassberger, P. (2002). Performance of different synchronization measures in real data: a case study on electroencephalographic signals. *Phys. Rev. E Stat. Nonlinear Soft Matter Phys.* 65:041903. doi: 10.1103/PhysRevE.65.041903

Raz, N., Lindenberger, U., Rodrigue, K. M., Kennedy, K. M., Head, D., Williamson, A., et al. (2005). Regional brain changes in aging healthy adults: general trends, individual differences and modifiers. *Cereb. Cortex* 15, 1676–1689. doi: 10.1093/cercor/bhi044

Reuter-Lorenz, P. A., and Cappell, K. A. (2008). Neurocognitive aging and the compensation hypothesis. *Curr. Dir. Psychol. Sci.* 17, 177–182. doi: 10.1111/j.1467-8721.2008.00570.x

Reuter-Lorenz, P. A., and Lustig, C. (2005). Brain aging: reorganizing discoveries about the aging mind. *Curr. Opin. Neurobiol.* 15, 245–251. doi: 10.1016/j.conb.2005.03.016

Reuter-Lorenz, P. A., and Park, D. C. (2010). Human neuroscience and the aging mind: a new look at old problems. *J. Gerontol. B Psychol. Sci. Soc. Sci.* 65, 405–415. doi: 10.1093/geronb/gbq035

Roski, C., Caspers, S., Langner, R., Laird, A. R., Fox, P. T., Zilles, K., et al. (2013). Adult age-dependent differences in resting-state connectivity within and between visual-attention and sensorimotor networks. *Front. Aging Neurosci.* 5:67. doi: 10.3389/fnagi.2013.00067

Salthouse, T. A. (1996). The processing-speed theory of adult age differences in cognition. *Psychol. Rev.* 103, 403–428. doi: 10.1037/0033-295X.103.3.403

Scahill, R. I., Frost, C., Jenkins, R., Whitwell, J. L., Rossor, M. N., and Fox, N. C. (2003). A longitudinal study of brain volume changes in normal aging using serial registered magnetic resonance imaging. *Arch. Neurol.* 60, 989–994. doi: 10.1001/archneur.60.7.989

Shulman, G. L., and Corbetta, M. (2012). "Two attentional networks. Identification and function within a larger cognitive architecture," in *Cognitive Neuroscience of Attention*, 2nd Edn, ed. M. I. Posner (New York, NY: Guilford Press), 113–128.

St Jacques, P. L., Dolcos, F., and Cabeza, R. (2009). Effects of aging on functional connectivity of the amygdala for subsequent memory of negative pictures: a network analysis of functional magnetic resonance imaging data. *Psychol. Sci.* 20, 74–84. doi: 10.1111/j.1467-9280.2008.02258.x

Treisman, A. M., and Gelade, G. (1980). A feature-integration theory of attention. *Cogn. Psychol.* 12, 97–136. doi: 10.1016/0010-0285(80)90005-5

Vallesi, A., Hasher, L., and Stuss, D. T. (2010). Age-related changes in transfer costs: evidence from go/nogo tasks. *Psychol. Aging* 25, 963–967. doi: 10.1037/a0020300

Verleger, R., and Smigasiewicz, K. (2015). Consciousness wanted, attention found: reasons for the advantage of the left visual field in identifying T2 among rapidly presented series. *Conscious. Cogn.* 35, 260–273. doi: 10.1016/j.concog.2015.02.013

**Conflict of Interest Statement:** The authors declare that the research was conducted in the absence of any commercial or financial relationships that could be construed as a potential conflict of interest.

frontiers in Aging Neuroscience

ORIGINAL RESEARCH
published: 23 March 2016
doi: 10.3389/fnagi.2016.00054

# Retrieval Deficiency in Brain Activity of Working Memory in Amnesic Mild Cognitive Impairment Patients: A Brain Event-Related Potentials Study

*Bin-Yin Li*[1], *Hui-Dong Tang*[1] *and Sheng-Di Chen*[1,2]*

[1] *Department of Neurology and Collaborative Innovation Center for Brain Science, Rui Jin Hospital Affiliated to Shanghai Jiao Tong University School of Medicine, Shanghai, China,* [2] *Laboratory of Neurodegenerative Diseases and Key Laboratory of Stem Cell Biology, Institute of Health Science, Shanghai Institutes for Biological Sciences, Chinese Academy of Science and Shanghai Jiao Tong University School of Medicine, Shanghai, China*

In the early stage of Alzheimer disease (AD) or mild cognitive impairment (MCI), working memory (WM) deficiency is prominent and could be attributed to failure in encoding, maintenance or retrieval of information. However, evidence for a retention or retrieval deficit remains equivocal. It is also unclear what cognitive mechanism in WM is impaired in MCI or early AD. We enrolled 46 subjects from our Memory Clinics and community, with 24 amnesic MCI patients and 22 normal subjects. After neurological and cognitive assessments, they performed a classic delayed match to sample (DMS) task with simultaneous event-related potential (ERP) recorded. The ERPs in encoding and retrieval epoch during WM were analyzed separately. The latency and amplitude of every ERP component were compared between two groups, and then analyzed to explore their relationship with neuropsychological performance. Finally, the locations of maximal difference in cortex were calculated by standard low-resolution tomographic analysis. A total of five components were found: P1, N1, P2, N2, and P300. The amplitude of P2 and P300 was larger in normal subjects than in MCI patients only during retrieval, not encoding epoch, while the latency did not show statistical difference. The latency and amplitude of P1 and N1 were similar in two groups. P2 amplitude in the retrieval epoch positively correlated with memory test (auditory verbal learning test) and visual spatial score of Chinese Addenbrooke's Cognitive Examination-Revised (ACE-R), while P300 amplitude correlated with ACE-R. The activation difference in P2 time range was maximal at medial frontal gyrus. However, the difference in cortex activation during P300 time range did not show significance. The amplitude of P2 indicated deficiency in memory retrieval process, potentially due to dysfunction of central executive in WM model. Regarding the location of P2 during WM task, medial frontal plays important role in memory retrieval. The findings in the present study suggested that MCI patients have retrieval deficit, probably due to central executive based on medial frontal gyrus. Thus, it may provide new biomarker for early detection and intervention for aMCI.

**Keywords: event-related potentials, amnesic mild cognitive impairment, working memory, retrieval, sLORETA**

OPEN ACCESS

***Edited by:***
*Chunbo Li,*
*Shanghai Jiao Tong University School of Medicine, China*

***Reviewed by:***
*Yury (Juri) Kropotov,*
*Institute of the Human Brain of the Russian Academy of Sciences, Russia*
*Jijun Wang,*
*Shanghai Mental Health Center, China*

***Correspondence:**
*Sheng-Di Chen*
*chen_sd@medmail.com.cn*

***Received:*** *30 December 2015*
***Accepted:*** *07 March 2016*
***Published:*** *23 March 2016*

***Citation:***
*Li B-Y, Tang H-D and Chen S-D (2016) Retrieval Deficiency in Brain Activity of Working Memory in Amnesic Mild Cognitive Impairment Patients: A Brain Event-Related Potentials Study. Front. Aging Neurosci. 8:54. doi: 10.3389/fnagi.2016.00054*

## INTRODUCTION

Cognitive decline is usually considered as an age-related phenomenon, which involves a continuous disease course from preclinical state, mild cognitive impairment (MCI) to Alzheimer's disease (AD). Prevalence of MCI in population-based epidemiological studies ranges from 3 to 20% in adults older than 60 or 65 years old (Gauthier et al., 2006; Ravaglia et al., 2008; Jia et al., 2014; Ding et al., 2015). Some MCI patients remain stable or even return to normal over time (Gauthier et al., 2006), while approximately half patients will progress to AD over 4–5 years.

Early detection and intervention for AD is remarkably important. Initially, most researchers agreed that the early and predominant cognitive deficit in AD is episodic memory impairment. However, cognitive processes under this kind of memory and their deficit in early AD were unclear in long period (Germano and Kinsella, 2005). Working memory (WM) provides a new insight into memory theory, which is defined as the capacity to hold information that is absent in mind for brief periods of time (Baddeley, 2012) and is closely related with daily activity performance.

In WM model, it involves at least three processes: information encoding, maintenance, and retrieval. All information-processing steps are regulated and controlled by the central executive. The central executive system is able to allocate attention to concurrent tasks, against potentially distracting irrelevant information. Long-term memory is formed when information is transferred from temporary or short-term storage to permanent episodic representation by rehearsal (Baddeley, 2001).

In early AD, memory complaint could be attributed to encoding, maintenance, and retrieval of information. The inability to encode and retrieve memory is present at the earliest stages of the disease and deteriorates during disease course (Aggarwal et al., 2005). Which part is the most problematic one? It is generally observed that a deficit in the acquisition of new information (encoding) is characteristic of early AD (Pasquier et al., 2001), while evidence for a retention or retrieval deficit in early AD remains equivocal (Grober and Kawas, 1997; Albert et al., 2001). However, all these observation is based on behavioral tests. As poor memory performance could be resulted from any deficit in the information processing, it is still unclear which cognitive mechanism is impaired in AD.

As WM works as a serial process at first a few seconds, event-related potentials (ERPs) provide a high temporal-resolution method to compare time-related cognitive process between different populations. Pinal et al. (2014) assessed the time course of brain activity during encoding and retrieval. Larger N2 amplitude and stronger activation of the left temporal lobe were found after long maintenance periods during information retrieval.

They also (Pinal et al., 2015a) used ERP recording and a delayed match to sample (DMS) task to assess age-related changes in young and old adults during successful information encoding in WM. The result revealed that smaller P2 and P300 amplitudes may signal the existence of an age dependent reduction in the processing resources available, and P2 and N2 latencies were longer in old than in young subjects.

In similar DMS, younger individuals have more posterior regions involved in WM processing, while adulthood has more anterior regions involved (Barriga-Paulino et al., 2015). Functional MRI (fMRI) study provided high spatial-resolution evidence. Galashan et al. (2015) combined EEG and fMRI with the same task, and they found a temporal pattern of source activities starting in occipital and temporal brain regions, followed by a simultaneous engagement of parietal and frontal brain regions and a later activity of a source in pre-supplementary motor area.

To our knowledge, no studies have compared the difference of cognitive process in WM between MCI and normal aging people. The encoding and retrieval deficit in WM also remains controversial in MCI patients. Amnesic MCI (aMCI) is one important type of pre-AD cognitive state with or without disability in other cognitive domains. WM studies in MCI patients revealed increased P200-N200 latencies, as well as an early dysfunction of neural generators within the parietal cortex in two-back paradigm (Missonnier et al., 2005, 2007). However, these studies did not uncover the deficit in information processing of WM. Therefore, we recruited aMCI patients from our memory clinics, and used ERP technique to precisely record time course of brain activity during encoding and retrieval in WM task.

## MATERIALS AND METHODS

### Subjects

We recruited normal elderly subjects from community and patients with memory complaint for more than 6 months from our Memory Clinics of the Department of Neurology, Rui Jin Hospital from December 2014 to July 2015. All participants were firstly evaluated by memory-disorders specialists and screened by the Mini Mental State Examination (MMSE, Chinese Version; Katzman et al., 1988), Zung Self-rating Anxiety Scale (SAS) and Zung Self-rating Depression scale (SDS). Each patient from memory clinics was subsequently performed blood test for possible causes of memory impairment including thyroid function, syphilis, HIV, folic acid, and vitamin B12, etc. Brain MRI scanning was also done for detecting vascular causes and hippocampus atrophy. Finally, the diagnosis of MCI was based on a detailed medical history, relevant physical and neurological examinations, negative laboratory findings, and neuroimaging studies. Exclusion criteria included evidence of stroke, Parkinson's disease, HIV/AIDS, mood problems, and reversible dementias, as well as treatment with benzodiazepines, antipsychotic, or antiepileptic medications. Patients with poor vision were also excluded.

A total of 46 subjects were finally enrolled. A patient was diagnosed as MCI patients if any of the following criteria were met as proposed by Petersen et al. (1999): memory has become worse gradually, as reported by the subject or his/her caregiver; objective evidence of impaired memory compared with normal controls matched for age, gender,

and education; Clinical Dementia Rating global score = 0.5; normal activities of daily living, and not demented. Finally, 24 patients were diagnosed as MCI and 22 subjects from community as normal control (CDR = 0 and normal activities of daily living) by two neurologists independently (Li and Chen; **Table 1**).

## Neuropsychological Assessment

A neuropsychological battery for multiple cognitive domains was performed in 35 subjects among 46 subjects by trained researcher who was blind to diagnosis (16 MCI patients and 19 normal subjects). These tests included the Chinese Addenbrooke's Cognitive Examination-Revised (ACE-R) (Fang et al., 2014), the Auditory Verbal Learning Test (AVLT)-Huashan version (Zhao et al., 2012), the Shape Trail Test (STT, including Part A and B), the Rey-Osterrieth Complex Figure Test (CFT), the Stroop Color-Word Test (SCWT), and the Symbol-Digit Modalities Test (SDMT).

Our study received ethical approval from the Research Ethics Committee, Rui Jin Hospital Affiliated to Shanghai Jiao Tong University School of Medicine, Shanghai, China. Written informed consent was obtained from all subjects or their guardians. All subjects were of unrelated Chinese Han descent with education level of secondary school or above, and knew English letter very well.

## The Delayed Match to Sample Task

Subjects first took a simple English letter test to make sure everyone knew all 26 letters. Then every subject was asked to complete a DMS task, which employed a visual task with WM. All visual stimuli were white presented on a dark background. In one trial, after a "+" in the middle of screen for 500 ms, one single letters (sample stimulus) randomly selected from 26 letters were displayed in the center of screen for 2000 ms. Subject was asked to keep it in mind. A blank followed the letter lasted for 3000 ms as an interruption. Probe stimulus (six letters randomly selected from 26 letters in a 2 * 3 matrix) was then presented in the middle of screen (**Figure 1**). Subject has to judge whether the letter seen before was among the six letters (press numeric keyboard "1" for "yes," "2," for "no"). The matrix was presented until the subject pressed key or for 2000 ms at maximum. After 5000 ms blank for a rest, a new trial started. Every individual underwent two sequential blocks. One contained 20 trials for practice, and the other contained 100 trials for test. In 50% of trials in each block, the correct answer was "yes," while the left was "no." "YES" and "No" trials were randomized in each block. Not until the subject had accuracy over 50% in practice block could she or he start the test block. The task was programmed and behavioral data (reaction time and accuracy) was recorded by E-Prime 2.0 software (Psychology Software Tools, Inc., Pittsburgh, PA, USA).

Memory storage of the first letters was required in order to compare it with the probe stimuli. The stimuli were large (height of 5.5° visual angle), bright (55 cd/m2), and presented in the middle of a computer monitor in order to make it easy for the subjects to see them. The whole test lasted for about 15–18 min.

**TABLE 1 | Demographic data and task performance (Mean ± Standard Deviation).**

| | MCI ($n = 24$) | Normal control ($n = 22$) | *P* |
|---|---|---|---|
| Age | 69.27 ± 7.55 | 69.17 ± 8.91 | 0.947 |
| Sex (female/all)* | 9/24 | 8/22 | 0.936 |
| Year of education# | 13.33 ± 2.80 | 14.18 ± 3.09 | 0.206 |
| MMSE# | 26.41 ± 2.12 | 28.95 ± 0.95 | <0.001 |
| Reaction time (ms)# | 1166.53 ± 160.33 | 1079.63 ± 141.08 | 0.068 |
| Accuracy (%)# | 68.58 ± 12.39 | 75.77 ± 11.37 | 0.090 |
| ACE-R## | 84.50 ± 7.33 | 93.26 ± 3.61 | <0.001 |
| AVLT-Immediate## | 5.04 ± 1.13 | 6.87 ± 1.33 | <0.001 |
| AVLT-20 min## | 2.81 ± 2.14 | 6.78 ± 2.68 | <0.001 |
| Digit-Symbol## | 35.12 ± 10.20 | 45.44 ± 8.55 | 0.003 |
| CFT-Copy## | 34.75 ± 1.48 | 35.38 ± 1.24 | 0.181 |
| CFT-recall## | 11.56 ± 8.62 | 19.53 ± 8.22 | 0.011 |
| SCWT C/A## | 3.38 ± 0.80 | 3.19 ± 1.10 | 0.566 |
| STT-A## | 68.36 ± 20.07 | 52.67 ± 17.76 | 0.020 |
| STT-B## | 168.73 ± 43.65 | 120.43 ± 38.57 | 0.001 |

**Chi-square test, #Mann-Whitney U-test, ##The total sample size is 35, with 16 subjects in MCI group and 19 subjects in control group. Independent t-test were performed. ACE-R, Addenbrooke's Cognitive Examination-Revised; AVLT, Auditory Verbal Learning Test-Huashan version; STT, Shape Trail Test (including Part A and B); CFT, the Rey-Osterrieth Complex Figure Test (CFT); SCWT, Stroop Color-Word Test.*

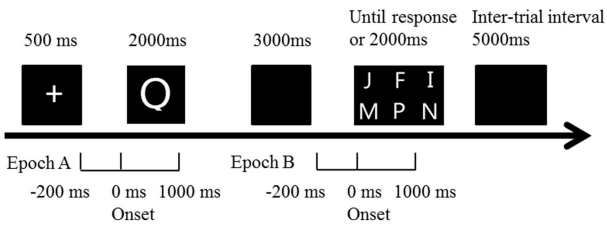


**FIGURE 1 | Illustration of the trial time course in the DMS paradigm.** Subjects were presented with one single letter (sample stimulus). They had to keep it in mind for a fixed delay (3 s) before judging as quickly and accurately as possible whether it was presented among the presenting six letters (probe stimulus). ERP epoch A (encoding period): extends from 200 ms prior to sample stimulus onset to 1000 ms after. ERP epoch B (retrieval period): extends from 200 ms prior to probe stimulus onset to 1000 ms after.

## EEG Recordings and Data Processing

EEG and electro-oculogram (EOG) were recorded with a 32-channel EEG amplifier (BrainAmp by Brain Products, Munich, Germany) using 32 Ag-AgCl electrodes. EEG electrodes were set in a standard EEG cap according to extended 10–20 system with inter-optode distances between 2 and 3 cm. Thirty-two scalp electrodes (Fp1, Fp2, F3, F4, C3, C4, P3, P4, O1, O2, F7, F8, T7, T8, P7, P8, Fz, FCz, Cz, Pz, FC1, FC2, CP1, CP2, FC5, FC6, CP5, CP6, FT9, FT10, TP9, TP10) with reference to bilateral linked ear lobes (TP9, TP10) recorded electrical brain activity while the subject performed the DMS task.

The sampling rate of every channel was 500 Hz, with frequency band-pass from 0.1 to 70 Hz. Artifact criteria were applied to all electrodes. Recorded data were passed through a digital filter with the high cut-off frequency set at 50 Hz and with

a low cut-off frequency set at 0.1 Hz. Notch-filter centered at 50 Hz was also applied to minimize electrical line noise. Ocular artifacts were corrected using the Infomax Restricted algorithm in an Independent Component Analysis as implemented in Brain Vision Analyzer 2.0 (Brain Products GmbH). Artifact rejection was followed by semi-automatic check (maximal allowed voltage step: 50 μV/ms; maximal allowed difference of values in intervals: 200 μV; lowest allowed activity in intervals: 0.5 μV). Mean artifact rejection rate for all MCI subjects was >1%. Then data was segmented in two epochs (**Figure 1**). Encoding epoch lasted from 200 ms before presentation of sample stimulus to 1000 ms after, while retrieval epoch lasted from 200 ms before probe stimulus to 1000 ms after. Baseline correction was done with the mean activity in the 200 ms prior to stimulus, and ERPs were based on correct trials.

## Statistical Analysis

### ERP Component Analysis

Based on the grand-averaged ERP waveforms, five ERP components were searched both in encoding and retrieval, according to the reports reviewed in the introduction section: N1, P1, N2, P2, and P300. We chose electrodes and then calculated peak latency and amplitude on the basis of studies with the same paradigm, as well as choosing the electrodes where amplitude was maximal. The N1 peak was measured as the voltage at the largest negative going peak in the latency window of 150–210 ms after stimulus onset at P7 and P8. The P1 was at the maximum peak in the latency window of 84–140 ms at O1, O2, P7 and P8. The N2 was considered at the most negative peak between 230 and 300 ms at F3, F4, C3, C4, CZ, FZ, FCz, while P2 was between 150 and 250 ms at FC1, FC1, CZ, FZ, FCz. P300 was identified as the maximum positive peak at O1, O1, and Pz between 250 and 450 ms after stimulus onset.

## Demographics, Psychometrics and ERPs

The difference of age, education level, MMSE score, reaction time, accuracy and sex between two groups was compared by the Mann-Whitney or Pearson's chi-square test. Reaction time (RT) was defined as the time between the onset of probe stimulus and subject's response, only in the correct trials. ERP components' parameters (latency and amplitude in each component) were compared by independent *t*-test between two groups in both encoding and retrieval epochs. Any statistically significant findings in the comparison lead to deep analysis for behavioral and electrophysiological association. The potential relationship between neuropsychological performance and brain activity was estimated by correlation analysis and linear regression. Pearson's correlation was calculated separately between each cognitive assessment score and ERP components parameters.

## Standard Low Resolution Tomography Analysis (s-LORETA)

The sLORETA is a functional imaging method for locating current source and widely used in EPR studies (Pandey et al., 2012). The LORETA algorithm has been identified as an efficient tool for functional mapping, also in encoding or retrieval period of WM studies (Pinal et al., 2015a). We employed sLORETA version that is identical with the one proved validated in previous studies (Pandey et al., 2012), available at: http://www.uzh.ch/keyinst/loreta.htm.

As described in sLORETA manual, a collection of volume elements in brain cortex has been modeled in the digitized Montreal Neurological Institute (MNI) coordinates corrected to the Talairach coordinates. In the study, the averaged waveforms (500 time samples, 1000 ms, post-stimulus) from 32 original recording montages for each subject were converted and saved into ASCII values. Transformation matrix was also constructed from these original data and electrode coordinates. The sLORETA values of each subject were computed for separately using ASCII values, electrode coordinates, and the transformation matrix. Regarding the sLORETA analysis, it compared differences between two groups in the time range of specific waveforms which showed difference in amplitude or latency, and constructed images to localize these differences in the three dimensional (3-D) space within the brain. For each comparison, one single test (Log of ratio of averages) was calculated for time-samples in significant ERP components (based on results from ERPs analysis above) with 5000 random permutations. The resultant values were then plotted in a 3-D brain model and evaluated for the level of significances. We also reported the maximum differences between groups at respective MNI coordinates and Brodmann areas (BA).

# RESULTS

## Demographics and Task Performance

The age, education years and sex proportion were similar in two groups. The independent Mann-Whitney *U*-test of task performance data (accuracy and RT) revealed marginally significant difference ($p = 0.090$ and 0.068), with a bit lower accuracy and longer reaction time in MCI patients. The MMSE score in MCI group was much lower than control group, consistent with their global cognitive ability and our clinical diagnosis. The matched age and education years in two groups helped to balance cognitive-related factors in the following analysis. Neuropsychological assessment also provided critical difference in cognitive tasks (AVLT, SDMT, CFT) where memory played a major role (**Table 1**).

## Brain Activity in Encoding and Retrieval

The number of valid trials used for averaging ERPs in both encoding and retrieval epoch did not differ between two groups (**Tables 2**, **3**). In the encoding epoch, no significant effect of group was found in parameters of all five ERPs components (**Figure 2**, **Table 2**). In the retrieval epoch (**Figure 3**), the independent *t*-test revealed significant effect of group in the amplitude of P2 and P300 components ($p = 0.025$ and 0.038). The P2 and P300 amplitude in aMCI group was smaller than in control group. However, latency of those two components was not significantly affected by the group effect. Regarding the N1, N2, and P1, neither difference in amplitude or latency reached statistically significant between two groups (**Table 3**).

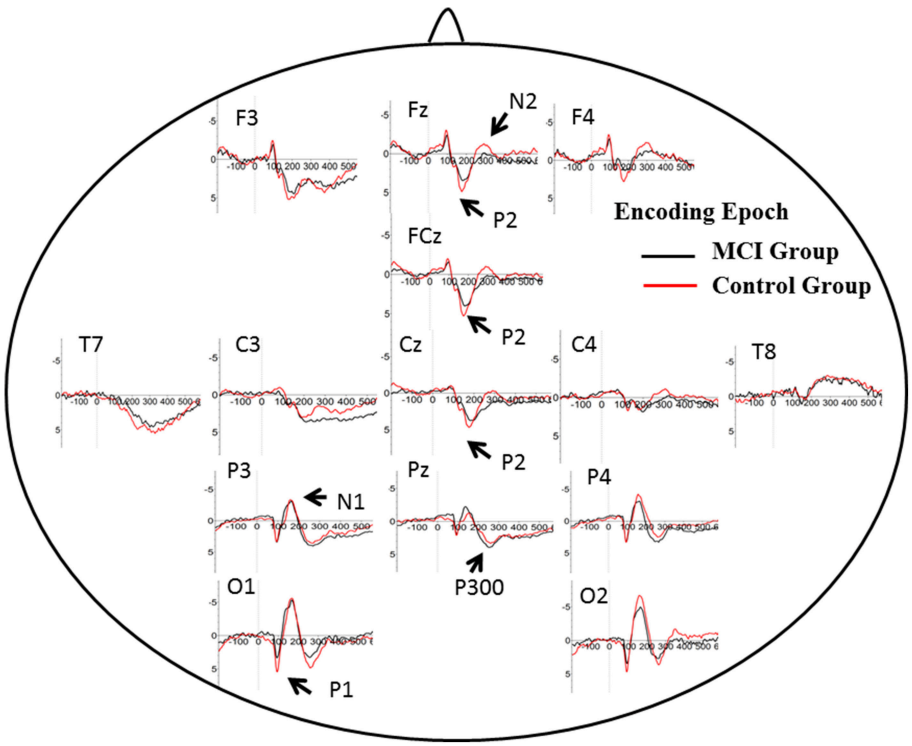


**FIGURE 2 | Grand average ERP waveform in aMCI (black line) and normal control group (red line) during retrieval period in WM task.** Time was shown in milliseconds where stimulus onset was at 0, and potentials were shown in micro-voltage.

**TABLE 2 | Parameters of ERP component in encoding epoch (Mean ± Standard deviation).**

| Encoding | | MCI ($n = 24$) | Normal control ($n = 22$) | $p$* |
|---|---|---|---|---|
| Number of valid trials | | 1643 | 1637 | 0.889 |
| P300 | Latency | 317.69 ± 46.51 | 312.64 ± 45.17 | 0.711 |
| | Amplitude | 4.37 ± 2.66 | 4.50 ± 2.88 | 0.803 |
| P2 | Latency | 191.65 ± 20.77 | 182.69 ± 16.59 | 0.115 |
| | Amplitude | 5.02 ± 2.04 | 5.77 ± 3.22 | 0.344 |
| N2 | Latency | 272.55 ± 18.12 | 269.58 ± 14.36 | 0.543 |
| | Amplitude | −0.29 ± 2.15 | −1.21 ± 2.27 | 0.164 |
| P1 | Latency | 79.72 ± 6.38 | 80.63 ± 8.40 | 0.676 |
| | Amplitude | 4.72 ± 2.65 | 5.06 ± 2.07 | 0.638 |
| N1 | Latency | 173.12 ± 12.08 | 173.45 ± 12.51 | 0.928 |
| | Amplitude | −6.27 ± 3.27 | −7.21 ± 3.24 | 0.335 |

*Latency and amplitude were measured in milliseconds (ms) and micro-voltage (μV). *Independent T-test.*

**TABLE 3 | Parameters of ERP component in retrieval epoch (Mean ± Standard deviation).**

| Retrieval | | MCI ($n = 24$) | Normal control ($n = 22$) | $p$* |
|---|---|---|---|---|
| Number of valid trials | | 1642 | 1604 | 0.634 |
| P300 | Latency | 296.67 ± 37.75 | 306.54 ± 34.80 | 0.363 |
| | Amplitude | 3.72 ± 2.31 | 5.45 ± 3.14 | ***0.038*** |
| P2 | Latency | 195.30 ± 28.33 | 183.87 ± 21.42 | 0.165 |
| | Amplitude | 4.83 ± 2.62 | 6.81 ± 3.14 | ***0.025*** |
| N2 | Latency | 267.25 ± 19.26 | 267.58 ± 16.92 | 0.951 |
| | Amplitude | 0.70 ± 2.62 | 1.21 ± 2.84 | 0.531 |
| P1 | Latency | 85.05 ± 7.28 | 82.91 ± 7.79 | 0.341 |
| | Amplitude | 4.44 ± 2.88 | 4.01 ± 2.47 | 0.597 |
| N1 | Latency | 167.08 ± 14.57 | 170.08 ± 10.96 | 0.396 |
| | Amplitude | −4.41 ± 3.52 | −5.96 ± 3.13 | 0.123 |

*Latency and amplitude were measured in milliseconds (ms) and micro-voltage (μV). *Independent T-test. Bold and italic values are indicated as statistical significance.*

## Brain Activity and Cognitive Ability

Among all subjects, a neuropsychological battery for multiple cognitive domains was performed in 35 subjects (16 MCI patients and 19 normal subjects). Based on the results of ERP components analysis, the Pearson's correlation was calculated in all subjects between cognitive assessment score and ERP components parameters (the amplitude of P2 and P300) separately. Regarding P2 amplitude, significant correlation was found in its relationship with AVLT-20 min recall ($r = 0.368$, $p = 0.030$) and scores of visual spatial ability in ACE-R. Scores in AVLT-5 min recall and recognition were marginally significant correlated with P2 amplitude ($r = 0.286$, $p = 0.096$; $r = 0.292$, $p = 0.089$). The amplitude of P300 was correlated with ACE-R ($r = 0.395$, $p = 0.019$), as well as scores of language fluency and visual spatial ability in ACE-R ($r = 0.374$, $p = 0.027$; $r = 0.363$, $p = 0.032$). A scatterplot was depicted to show the fit line and relationship between P2 amplitude and AVLT-20 min recall (**Figure 4**).

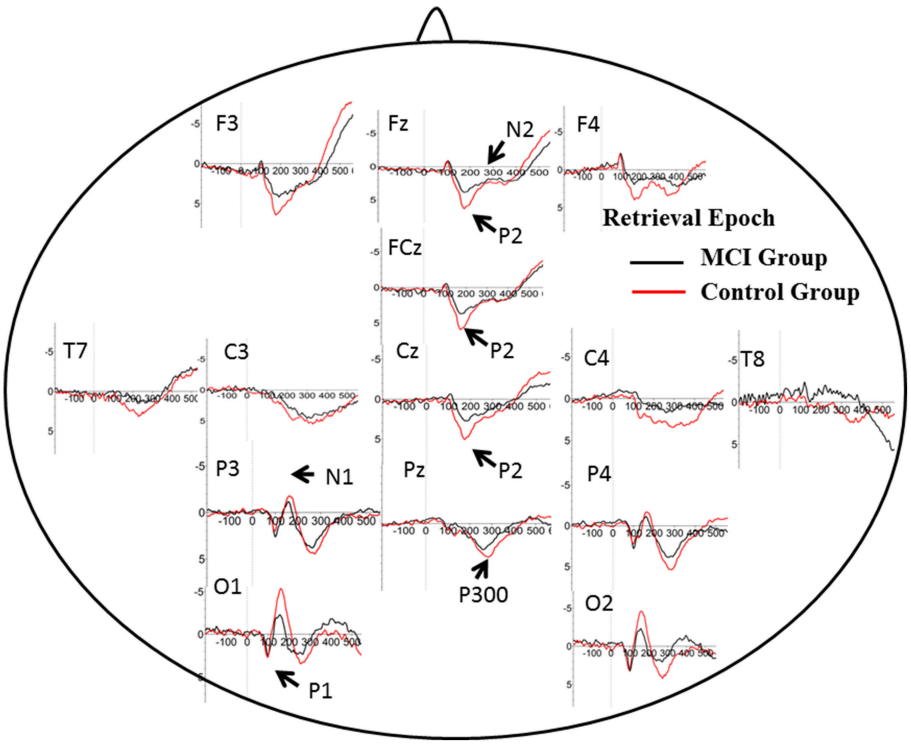


**FIGURE 3 | Grand average ERP waveform in aMCI (black line) and normal control group (red line) during encoding period in WM task.** Time was shown in milliseconds where stimulus onset was at 0, and potentials were shown in micro-voltage.

## Standardized Low Resolution Tomography Analysis (sLORETA)

Based on the results showed above, we performed statistical non-parametric mapping (SnPM) during P2 and P300 time range (in the retrieval epoch) to show different activation in these specific temporal intervals. The statistical difference between groups for current density at the source is shown in **Table 4**. The brain areas that show activation differences at <0.05 level are shown in **Figure 5** (positive in yellow color, while negative in blue color with reference of MCI group). As shown in **Table 4**, the difference in P2 time range was maximum at BA 11 (medial frontal gyrus) of the right frontal cortex (Log of ratio of averages = 0.846, $p < 0.01$). Besides, BA 10 (superior frontal gyrus) also showed markedly activated in control group during P2 time range. However, the difference in cortex activation during P300 time range did not reach significant level.

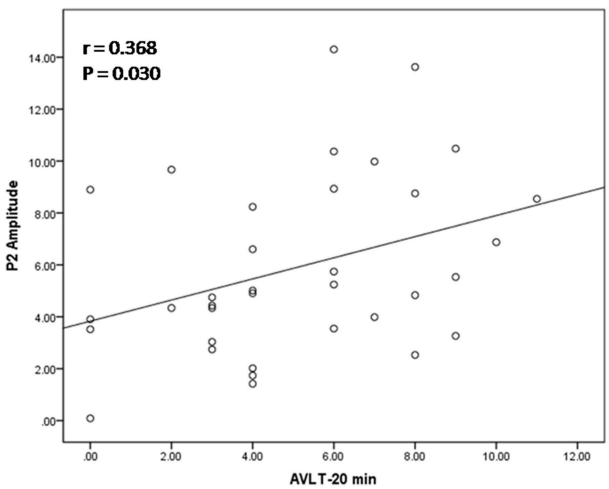


**FIGURE 4 | Relation between P2 amplitude and score of auditory verbal learning test (recall after 20 min).** The scatterplot and best fit line ($r = 0.368$ and $p = 0.030$) referred to Pearson's correlation analysis.

# DISCUSSION

## Working Memory Task Performance and ERPs

It is shown that in the MCI and AD patients, longer maintenance intervals hampered the task performance. Patients performed significantly worse than controls on the associative WM task (van Geldorp et al., 2015). In our study, the two groups had similar age, sex proportion and education level. Meanwhile, the interval between two stimuli was fixed and relatively short (Pinal et al., 2015b). Although aMCI patients did have poor cognitive ability in psychometric tests, the results showed similar WM task performance (reaction time and latency) in two groups. However, the brain activity measured as ERPs still uncovered difference

**TABLE 4 | Comparison of aMCI and normal control group in sLORETA (voxels showing maximal difference).**

| MNI coordinates | | | Brodmann area | Brain region | Log of ratio of average | *p*-Value |
|---|---|---|---|---|---|---|
| *X* | *y* | *Z* | | | | |
| **P2 TIME-RANGE DURING RETRIEVAL (150–250 ms)** | | | | | | |
| 25 | 45 | −10 | 11 | Frontal lobe, Medial Frontal Gyrus | 0.845 | <0.05 |
| 25 | 45 | −5 | 11 | Frontal lobe, Medial Frontal Gyrus | 0.845 | <0.05 |
| 20 | 45 | −5 | 10 | Frontal lobe, Superior Frontal Gyrus | 0.832 | <0.05 |
| **P300 TIME-RANGE DURING RETRIEVAL (250–450 ms)** | | | | | | |
| −5 | 55 | −25 | 11 | Frontal lobe, Rectal Gyrus | 0.512 | >0.1 |

*MNI, Montreal Neurological Institute.*

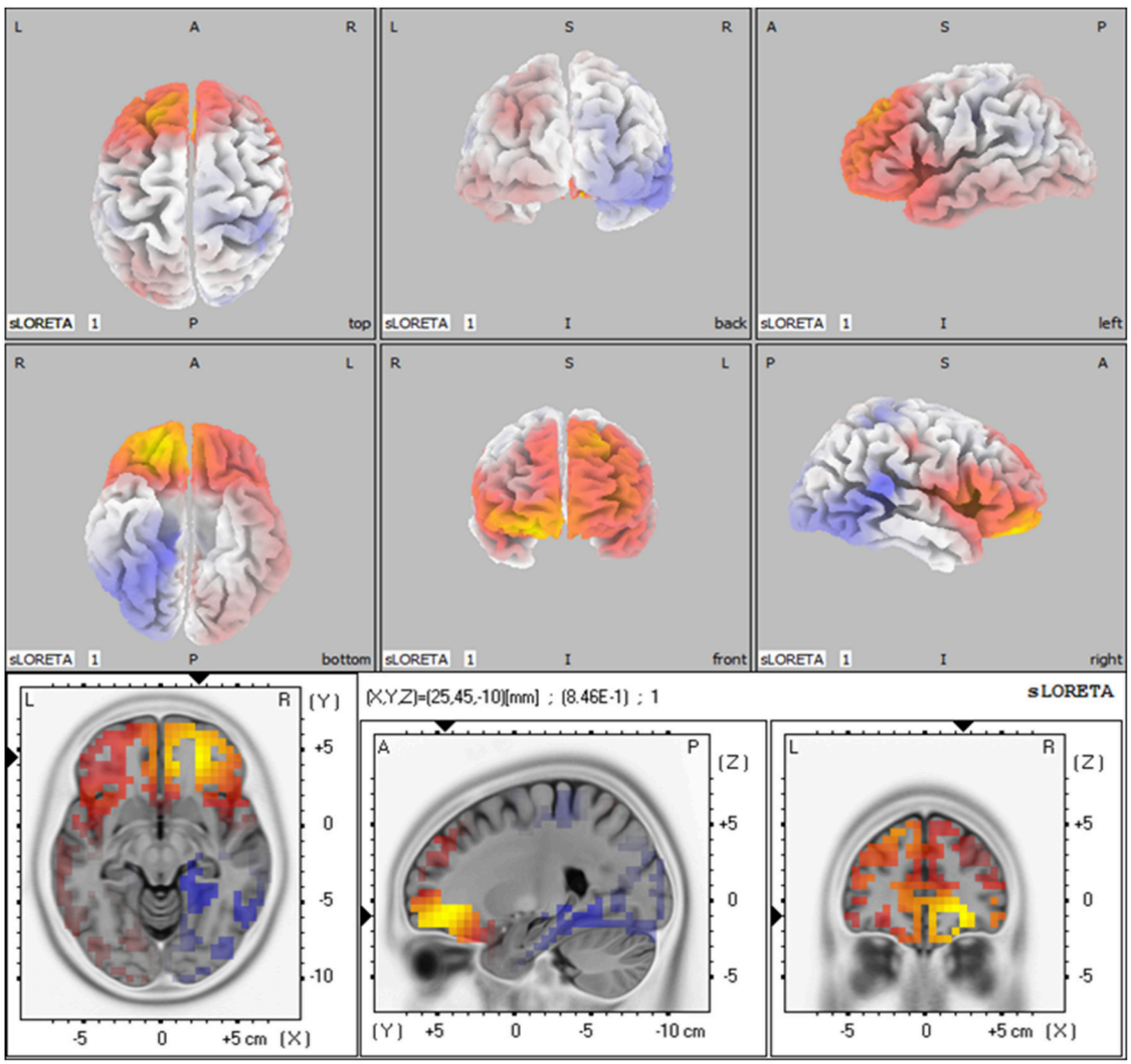


**FIGURE 5 | The sLORETA images showing statistical differences between aMCI and control group (3D-view and slice-view) in the P2 time-range.** The three slice-view images below located the maximal difference between aMCI group and control group (MNI coordinates *x*, *y*, *z* = 25, 45, −10). Positive difference was in yellow color with reference of MCI group.

under seemingly comparable WM performance. It suggested that brain activity deficit underlie behavioral change and the electrophysiological test provided opportunity of early detection and intervention.

## Brain Activity and Neuropsychological Function

It is still unclear whether encoding or retrieval is impaired in MCI patients. In this exploratory study, the ERPs in encoding and retrieval epoch were separately analyzed. Some ERP components proved sensitive to probe stimulus. It is noted that the findings in ERPs made no sense until it could be related with real cognitive ability. Every ERP should be analyzed with the consideration of behavioral and cognitive ability.

P2: P2 has been related to various cognitive process: a semantic effect (Peressotti et al., 2012), top–down mechanism for rapid evaluation of stimulus significance (Paynter et al., 2009) or subjectively relevant stimuli (Schapkin et al., 2000; Potts and Tucker, 2001). Larger amplitude for P2 was observed in the control group than in MCI group. In WM model, retrieval requires phonological loop and central executive, which is generally defined as attention allocation efficiency (Germano and Kinsella, 2005; Wang et al., 2010). Previous studies concerning aging effects on P2 amplitude showed larger P2 amplitude in younger adults, suggesting deficit in the allocation of processing resources for the evaluation of stimulus significance. Consistently, positive correlation was found between the degree of improvement in WM capacity and the post-pre difference in P2 amplitudes after WM training (Li et al., 2015). However, the latency of P2 in the present study did not differ in two groups. It suggested little slowing in stimulus judgment during information encoding and retrieval in WM.

In DMS task, subjects had to search probe stimulus (a 2∗3 letter matrix) for the sample, indicating involvement of attention allocation in the retrieval. Besides, the P2 amplitude found in retrieval epoch positively correlated with memory recall test (AVLT-20 min recall). These results supported the role of P2 in information retrieval, as well as regulation of attention allocation.

The P2 amplitude also showed correlation with visual-spatial score of ACE-R. The fact may give explanation that all subjects were not English native speakers and they largely recognize English letter via its appearance.

P300: P300 is widely studied in cognitive processes, and represented different psychological meaning under different tasks (Kirschner et al., 2015). Previous studies have found an age-related reduction in the amplitude of P300 component at parietal electrodes, suggesting lower amounts of processing resources available for allocation to stimulus categorization (McEvoy et al., 2001; Saliasi et al., 2013; Pinal et al., 2015a). However, the difference existed in encoding epoch, while our study showed difference of P300 amplitude in retrieval epoch when age was balanced between groups. Positive correlation was found between P300 amplitude and memory load, indicating its significance in modulating resources for stimulus classification and context updating (Pinal et al., 2014). As memory load was same in present two groups, difference in P300 suggested that aMCI patients could modulate fewer resources and thus evoked lower amplitude. Similar to P2, the latency of P300 in two groups did not differ from each other, suggesting relative spared processing speed in aMCI patients. The P300 amplitude also showed correlation with score of ACE-R, especially in language fluency and visual-spatial ability. It suggested that P300 might represent more general cognition ability, compared with P2.

N2: N2 (predominant in anterior part of brain) has been studied in correlation with visual information encoding (Nittono et al., 2007). Consistently, N2 waveform was obvious in anterior electrodes in the present study. Previous studies found positive association between N2 latency and task accuracy or N2 amplitude with memory load (Pinal et al., 2014, 2015a). Stimulus discrimination and classification may be reflected by N2 (Folstein and Van Petten, 2008), hence higher N2 amplitude happens when the stimulus includes more information load. There were no difference between aMCI and control group for N2 amplitude and latency. Low and fixed memory load (only one letter) in the present may give an explanation.

P1 and N1: It is generally accepted that these early ERP components usually represent perceptual processing of visual inputs (Vogel and Luck, 2000; Taylor, 2002). The present results indicate that the deficit in information retrieval does not affect perceptual processing of stimuli, which is also consist with DMS study in young and older subjects (Pinal et al., 2015a).

## Medial Frontal Lobe in Working Memory

In the present study, MCI patients had less activated brain area in medial frontal area than control subject during P2 time range in WM retrieval. As MRI has high spatial resolution than ERPs, fMRI provides more precise activated location.

At retrieval, "retrieval-success network" was found in brain areas which is thought to be content-independent (Wagner et al., 2005; Huijbers et al., 2010). These areas found in fMRI studies include the posterior midline region consisting of the precuneus, retrosplenial cortex, and posterior cingulate, the medial prefrontal cortex as well as the hippocampus.

In a fMRI study with DMS task, correct decision at WM probe was linked to activation in the anterior and posterior midline brain structures (Bergmann et al., 2015). The result was generally consisted with our findings in sLORETA. As ERP provided higher time-resolution, frontal midline structures in 150–250 ms were less activated in aMCI group. Animal experiment provided evidence that shifting of attention set in the rat impaired with lesions of prefrontal cortex, and medial frontal cortex associated with impairment in initial acquisition and reversal learning.

As discussed above, P2 correlated with attention allocation in the retrieval. Locations found in sLORETA further verified its neuro-anatomical basis and functional significance.

One limitation of the present study is a bit fewer channel data (32-channel data) in sLORETA analysis. Though our findings in sLORETA was generally consistent with fMRI study, 64 or 128-channel EEG cap in further studies could provide more detailed and accurate information.

# CONCLUSION

The aim of the present study was to explore brain activity changes in MCI patients during WM task. We tried to

find clinically significant electrophysiological waveform for WM and its location in the cortex. The results revealed that brain activity during retrieval process of WM was impaired in aMCI patients, while encoding process spared. In retrieval process, the amplitude of P2 indicated deficient function of central executive in the WM model. Besides, medial and superior frontal gyrus markedly activated during P2 time range in the control group. The findings in the present study suggested WM retrieval deficit in aMCI patients, probably due to dysfunction of central executive (attention allocation) based on medial and superior frontal gyrus. It may provide new biomarker for early detection and intervention for aMCI.

## AUTHOR CONTRIBUTIONS

All three authors cooperated and contributed to the design and plan of the present study. BL was in charge of ERP data acquisition, analysis and manuscript writing. HT was in charge of neuropsychological assessments and analysis. SC was in charge of clinical diagnosis and manuscript verifying.

## ACKNOWLEDGMENTS

This work was supported by grants from the National Natural Science Foundation of China [grant numbers 81400888, 91332107].

## REFERENCES

Aggarwal, N. T., Wilson, R. S., Beck, T. L., Bienias, J. L., and Bennett, D. A. (2005). Mild cognitive impairment in different functional domains and incident Alzheimer's disease. *J. Neurol. Neurosurg. Psychiatr.* 76, 1479–1484. doi: 10.1136/jnnp.2004.053561

Albert, M. S., Moss, M. B., Tanzi, R., and Jones, K. (2001). Preclinical prediction of AD using neuropsychological tests. *J. Int. Neuropsychol. Soc.* 7, 631–639. doi: 10.1017/S1355617701755105

Baddeley, A. (2012). Working memory: theories, models, and controversies. *Annu. Rev. Psychol.* 63, 1–29. doi: 10.1146/annurev-psych-120710-100422

Baddeley, A. D. (2001). Is working memory still working? *Am. Psychol.* 56, 851–864. doi: 10.1037/0003-066X.56.11.851

Barriga-Paulino, C. I., Rojas Benjumea, M. A., Rodriguez-Martinez, E. I., and Gomez Gonzalez, C. M. (2015). Fronto-temporo-occipital activity changes with age during a visual working memory developmental study in children, adolescents and adults. *Neurosci. Lett.* 599, 26–31. doi: 10.1016/j.neulet.2015.05.017

Bergmann, H. C., Daselaar, S. M., Beul, S. F., Rijpkema, M., Fernandez, G., and Kessels, R. P. (2015). Brain activation during associative short-term memory maintenance is not predictive for subsequent retrieval. *Front. Hum. Neurosci.* 9:479. doi: 10.3389/fnhum.2015.00479

Ding, D., Zhao, Q., Guo, Q., Meng, H., Wang, B., Luo, J., et al. (2015). Prevalence of mild cognitive impairment in an urban community in China: a cross-sectional analysis of the Shanghai aging study. *Alzheimers Dement.* 11, 300–309.e2. doi: 10.1016/j.jalz.2013.11.002

Fang, R., Wang, G., Huang, Y., Zhuang, J. P., Tang, H. D., Wang, Y., et al. (2014). Validation of the Chinese version of Addenbrooke's cognitive examination-revised for screening mild Alzheimer's disease and mild cognitive impairment. *Dement. Geriatr. Cogn. Disord.* 37, 223–231. doi: 10.1159/000353541

Folstein, J. R., and Van Petten, C. (2008). Influence of cognitive control and mismatch on the N2 component of the ERP: a review. *Psychophysiology* 45, 152–170. doi: 10.1111/j.1469-8986.2007.00602.x

Galashan, D., Fehr, T., and Herrmann, M. (2015). Differences between target and non-target probe processing-combined evidence from fMRI, EEG and fMRI-constrained source analysis. *Neuroimage* 111, 289–299. doi: 10.1016/j.neuroimage.2015.02.044

Gauthier, S., Reisberg, B., Zaudig, M., Petersen, R. C., Ritchie, K., Broich, K., et al. (2006). International psychogeriatric association expert conference on mild cognitive I. Mild cognitive impairment. *Lancet* 367, 1262–1270. doi: 10.1016/S0140-6736(06)68542-5

Germano, C., and Kinsella, G. J. (2005). Working memory and learning in early Alzheimer's disease. *Neuropsychol. Rev.* 15, 1–10. doi: 10.1007/s11065-005-3583-7

Grober, E., and Kawas, C. (1997). Learning and retention in preclinical and early Alzheimer's disease. *Psychol. Aging* 12, 183–188. doi: 10.1037/0882-7974.12.1.183

Huijbers, W., Pennartz, C. M., and Daselaar, S. M. (2010). Dissociating the "retrieval success" regions of the brain: effects of retrieval delay. *Neuropsychologia* 48, 491–497. doi: 10.1016/j.neuropsychologia.2009.10.006

Jia, J., Zhou, A., Wei, C., Jia, X., Wang, F., Li, F., et al. (2014). The prevalence of mild cognitive impairment and its etiological subtypes in elderly Chinese. *Alzheimers Dement.* 10, 439–447. doi: 10.1016/j.jalz.2013.09.008

Katzman, R., Zhang, M. Y., Ouang Ya, Q., Wang, Z. Y., Liu, W. T., Yu, E., et al. (1988). A Chinese version of the mini-mental state examination; impact of illiteracy in a Shanghai dementia survey. *J. Clin. Epidemiol.* 41, 971–978. doi: 10.1016/0895-4356(88)90034-0

Kirschner, A., Cruse, D., Chennu, S., Owen, A. M., and Hampshire, A. (2015). A P300-based cognitive assessment battery. *Brain Behav.* 5, e00336. doi: 10.1002/brb3.336

Li, W., Guo, Z., Jones, J. A., Huang, X., Chen, X., Liu, P., et al. (2015). Training of working memory impacts neural processing of vocal pitch regulation. *Sci. Rep.* 5:16562. doi: 10.1038/srep16562

McEvoy, L. K., Pellouchoud, E., Smith, M. E., and Gevins, A. (2001). Neurophysiological signals of working memory in normal aging. *Brain Res. Cogn. Brain Res.* 11, 363–376. doi: 10.1016/S0926-6410(01)00009-X

Missonnier, P., Deiber, M. P., Gold, G., Herrmann, F. R., Millet, P., Michon, A., et al. (2007). Working memory load-related electroencephalographic parameters can differentiate progressive from stable mild cognitive impairment. *Neuroscience* 150, 346–356. doi: 10.1016/j.neuroscience.2007.09.009

Missonnier, P., Gold, G., Fazio-Costa, L., Michel, J. P., Mulligan, R., Michon, A., et al. (2005). Early event-related potential changes during working memory activation predict rapid decline in mild cognitive impairment. *J. Gerontol. A Biol. Sci. Med. Sci.* 60, 660–666. doi: 10.1093/gerona/60.5.660

Nittono, H., Shibuya, Y., and Hori, T. (2007). Anterior N2 predicts subsequent viewing time and interest rating for novel drawings. *Psychophysiology* 44, 687–696. doi: 10.1111/j.1469-8986.2007.00539.x

Pandey, A. K., Kamarajan, C., Tang, Y., Chorlian, D. B., Roopesh, B. N., Manz, N., et al. (2012). Neurocognitive deficits in male alcoholics: an ERP/sLORETA analysis of the N2 component in an equal probability Go/NoGo task. *Biol. Psychol.* 89, 170–182. doi: 10.1016/j.biopsycho.2011.10.009

Pasquier, F., Grymonprez, L., Lebert, F., and Van der Linden, M. (2001). Memory impairment differs in frontotemporal dementia and Alzheimer's disease. *Neurocase* 7, 161–171. doi: 10.1093/neucas/7.2.161

Paynter, C. A., Reder, L. M., and Kieffaber, P. D. (2009). Knowing we know before we know: ERP correlates of initial feeling-of-knowing. *Neuropsychologia* 47, 796–803. doi: 10.1016/j.neuropsychologia.2008.12.009

Peressotti, F., Pesciarelli, F., Mulatti, C., and Dell'Acqua, R. (2012). Event-related potential evidence for two functionally dissociable sources of semantic effects in the attentional blink. *PLoS ONE* 7:e49099. doi: 10.1371/journal.pone.0049099

Petersen, R. C., Smith, G. E., Waring, S. C., Ivnik, R. J., Tangalos, E. G., and Kokmen, E. (1999). Mild cognitive impairment: clinical characterization and outcome. *Arch. Neurol.* 56, 303–308. doi: 10.1001/archneur.56.3.303

Pinal, D., Zurron, M., and Diaz, F. (2014). Effects of load and maintenance duration on the time course of information encoding and retrieval in working memory: from perceptual analysis to post-categorization processes. *Front. Hum. Neurosci.* 8:165. doi: 10.3389/fnhum.2014.00165

Pinal, D., Zurron, M., and Diaz, F. (2015a). Age-related changes in brain activity are specific for high order cognitive processes during successful encoding of information in working memory. *Front. Aging Neurosci.* 7:75. doi: 10.3389/fnagi.2015.00075

Pinal, D., Zurron, M., and Diaz, F. (2015b). An event related potentials study of the effects of age, load and maintenance duration on working memory recognition. *PLoS ONE* 10:e0143117. doi: 10.1371/journal.pone.0143117

Potts, G. F., and Tucker, D. M. (2001). Frontal evaluation and posterior representation in target detection. *Brain Res. Cogn. Brain Res.* 11, 147–156. doi: 10.1016/S0926-6410(00)00075-6

Ravaglia, G., Forti, P., Montesi, F., Lucicesare, A., Pisacane, N., Rietti, E., et al. (2008). Mild cognitive impairment: epidemiology and dementia risk in an elderly Italian population. *J. Am. Geriatr. Soc.* 56, 51–58. doi: 10.1111/j.1532-5415.2007.01503.x

Saliasi, E., Geerligs, L., Lorist, M. M., and Maurits, N. M. (2013). The relationship between P3 amplitude and working memory performance differs in young and older adults. *PLoS ONE* 8:e63701. doi: 10.1371/journal.pone.0063701

Schapkin, S. A., Gusev, A. N., and Kuhl, J. (2000). Categorization of unilaterally presented emotional words: an ERP analysis. *Acta Neurobiol. Exp. (Wars).* 60, 17–28.

Taylor, M. J. (2002). Non-spatial attentional effects on P1. *Clin. Neurophysiol.* 113, 1903–1908. doi: 10.1016/S1388-2457(02)00309-7

van Geldorp, B., Heringa, S. M., van den Berg, E., Olde Rikkert, M. G., Biessels, G. J., and Kessels, R. P. (2015). Working memory binding and episodic memory formation in aging, mild cognitive impairment, and Alzheimer's dementia. *J. Clin. Exp. Neuropsychol.* 37, 538–548. doi: 10.1080/13803395.2015.1037722

Vogel, E. K., and Luck, S. J. (2000). The visual N1 component as an index of a discrimination process. *Psychophysiology* 37, 190–203. doi: 10.1111/1469-8986.3720190

Wagner, A. D., Shannon, B. J., Kahn, I., and Buckner, R. L. (2005). Parietal lobe contributions to episodic memory retrieval. *Trends Cogn. Sci.* 9, 445–453. doi: 10.1016/j.tics.2005.07.001

Wang, Y., Song, Y., Qu, Z., and Ding, Y. (2010). Task difficulty modulates electrophysiological correlates of perceptual learning. *Int. J. Psychophysiol.* 75, 234–240. doi: 10.1016/j.ijpsycho.2009.11.006

Zhao, Q., Lv, Y., Zhou, Y., Hong, Z., and Guo, Q. (2012). Short-term delayed recall of auditory verbal learning test is equivalent to long-term delayed recall for identifying amnestic mild cognitive impairment. *PLoS ONE* 7:e51157. doi: 10.1371/journal.pone.0051157

**Conflict of Interest Statement:** The authors declare that the research was conducted in the absence of any commercial or financial relationships that could be construed as a potential conflict of interest.

frontiers in Aging Neuroscience

ORIGINAL RESEARCH
published: 24 December 2015
doi: 10.3389/fnagi.2015.00242

# Common Effects of Amnestic Mild Cognitive Impairment on Resting-State Connectivity Across Four Independent Studies

*Angela Tam[1,2,3]*, Christian Dansereau[3,4], AmanPreet Badhwar[3,4], Pierre Orban[2,3], Sylvie Belleville[3,4], Howard Chertkow[1], Alain Dagher[1], Alexandru Hanganu[3,5,6], Oury Monchi[3,4,5,6], Pedro Rosa-Neto[1,2], Amir Shmuel[1], Seqian Wang[1,2], John Breitner[1,2] and Pierre Bellec[3,4]* for the Alzheimer's Disease Neuroimaging Initiative[†]*

[1] McGill University, Montreal, QC, Canada, [2] Douglas Mental Health University Institute, Research Centre, Montreal, QC, Canada, [3] Centre de Recherche de L'institut Universitaire de Gériatrie de Montréal, Montreal, QC, Canada, [4] Université de Montréal, Montreal, QC, Canada, [5] University of Calgary, Calgary, AB, Canada, [6] Hotchkiss Brain Institute, Calgary, AB, Canada

Resting-state functional connectivity is a promising biomarker for Alzheimer's disease. However, previous resting-state functional magnetic resonance imaging studies in Alzheimer's disease and amnestic mild cognitive impairment (aMCI) have shown limited reproducibility as they have had small sample sizes and substantial variation in study protocol. We sought to identify functional brain networks and connections that could consistently discriminate normal aging from aMCI despite variations in scanner manufacturer, imaging protocol, and diagnostic procedure. We therefore combined four datasets collected independently, including 112 healthy controls and 143 patients with aMCI. We systematically tested multiple brain connections for associations with aMCI using a weighted average routinely used in meta-analyses. The largest effects involved the superior medial frontal cortex (including the anterior cingulate), dorsomedial prefrontal cortex, striatum, and middle temporal lobe. Compared with controls, patients with aMCI exhibited significantly decreased connectivity between default mode network nodes and between regions of the cortico-striatal-thalamic loop. Despite the heterogeneity of methods among the four datasets, we identified common aMCI-related connectivity changes with small to medium effect sizes and sample size estimates recommending a minimum of 140 to upwards of 600 total subjects to achieve adequate statistical power in the context of a multisite study with 5–10 scanning sites and about 10 subjects per group and per site. If our findings can be replicated and associated with other established biomarkers of Alzheimer's disease (e.g., amyloid and tau quantification), then these functional connections may be promising candidate biomarkers for Alzheimer's disease.

**Keywords: fMRI, mild cognitive impairment, connectome, resting-state, default mode network, meta-analysis**

OPEN ACCESS

***Edited by:***
*Junfeng Sun,*
*Shanghai Jiao Tong University, China*

***Reviewed by:***
*Donald G. McLaren,*
*University of Wisconsin-Madison, USA*
*Rui Li,*
*Chinese Academy of Sciences, China*

****Correspondence:***
*Angela Tam*
*angela.tam@mail.mcgill.ca;*
*Pierre Bellec*
*pierre.bellec@criugm.qc.ca*

[†] *Data used in preparing this article were obtained from the Alzheimer's Disease Neuroimaging Initiative (ADNI) database (adni.loni.usc.edu). As such, the investigators within the ADNI contributed to the design and implementation of ADNI and/or provided data but most of them did not participate in this analysis or writing this report. A complete list of ADNI investigators can be found at: http://adni.loni.usc.edu/wp-content/uploads/how_to_apply/ADNI_Acknowledgement_List.pdf.*

***Received:*** *28 August 2015*
***Accepted:*** *10 December 2015*
***Published:*** *24 December 2015*

***Citation:***
*Tam A, Dansereau C, Badhwar A, Orban P, Belleville S, Chertkow H, Dagher A, Hanganu A, Monchi O, Rosa-Neto P, Shmuel A, Wang S, Breitner J, Bellec P for the Alzheimer's Disease Neuroimaging Initiative (2015) Common Effects of Amnestic Mild Cognitive Impairment on Resting-State Connectivity Across Four Independent Studies. Front. Aging Neurosci. 7:242. doi: 10.3389/fnagi.2015.00242*

## INTRODUCTION

Resting-state connectivity in functional magnetic resonance imaging (fMRI) captures the spatial coherence of spontaneous fluctuations in blood oxygenation. Resting-state fMRI is a promising technique that may be useful as an early biomarker for Alzheimer's disease (AD), a neurodegenerative process that develops over decades before patients suffer from dementia. The possibility that disturbed resting-state connectivity may be an early marker for AD is supported by studies of mild cognitive impairment (MCI), a disorder characterized by objective cognitive deficits without dementia, i.e., without impairment in activities of daily living, and more specifically by studies of amnestic MCI (aMCI), the most common subtype of MCI characterized by memory deficits (Petersen et al., 2001). These studies showed altered functional connectivity in MCI compared with cognitively normal elderly (CN; Sorg et al., 2007; Bai et al., 2009; Liang et al., 2012; Wu et al., 2014), but they relied on small sample sizes ($n = \sim 40$) and differed in many aspects of their protocols, e.g., recruitment and image acquisition procedures. If resting-state fMRI is to serve as a useful biomarker of AD, or any pathology, for clinical practice or research, we must determine if changes in functional connectivity differences between groups of subjects are robust to such variation in study protocols. Therefore, we sought to identify brain connections that showed consistent MCI-related changes across multiple independent studies. If such connections exist, they may be used as targets to be examined alongside other established AD biomarkers (e.g., amyloid and tau measures) in order to validate resting-state fMRI's potential as a biomarker for AD.

Resting-state connectivity studies have consistently found decreased connectivity between nodes within the default mode network (DMN) in patients with AD or MCI compared with CN (Sorg et al., 2007; Bai et al., 2009; Zhang et al., 2010; Koch et al., 2012; Liang et al., 2012). Less consistent are reports of alterations in the executive attentional, frontoparietal, and anterior temporal networks (Sorg et al., 2007; Zhang et al., 2010; Gour et al., 2011; Agosta et al., 2012; Liang et al., 2012; Wu et al., 2014) due to the literature's bias toward investigating the DMN. Further inconsistencies can be found in some studies that have reported increased connectivity between the middle temporal lobe and other DMN areas in MCI (Qi et al., 2010), while others have reported decreased connectivity between these same regions (Bai et al., 2009) and others have reported no significant differences between MCI and CN (Koch et al., 2012).

One obvious explanation for such inconsistency may be these studies' small sample sizes resulting in low statistical power (Kelly et al., 2012). Beyond this, however, there are other methodological differences that may compromise the comparison of results across independent studies. For example, the criteria for recruiting subjects with MCI, e.g., Petersen (2004) vs. NIA-AA recommendations (Albert et al., 2011) may differ among studies. Different study samples may also reflect different socio-cultural characteristics of recruiting sites, e.g., ethnicity, language, diet, socioeconomic status. The fMRI measurements themselves can also be affected by differences in details of the image acquisition such as scanner make and model (Friedman et al., 2006), sequence parameters such as repetition time, flip angle, or acquisition volume (Friedman and Glover, 2006), experimental design such as eyes-open/eyes-closed (Yan et al., 2009) or experiment duration (van Dijk et al., 2010), and scanning environment such as sound attenuation measures (Elliott et al., 1999), room temperature (Vanhoutte et al., 2006), or head-motion restraint techniques (Edward et al., 2000).

To identify robust changes in resting-state connectivity between aMCI and CN, we implemented a meta-analysis of four independent resting-state fMRI datasets (ADNI2 and three small single-site studies) using a weighted average implemented by Willer et al. (2010). Rather than relying on a priori target regions or connections, we leveraged the large sample size to perform a systematic search of brain connections affected by aMCI, an approach termed a "connectome-wide association study" (Shehzad et al., 2014). In addition, we relied on functionally-defined brain parcellations using an automated clustering procedure and we explored the impact of the number of brain clusters (called resolution) on observed differences (Bellec et al., 2015).

## METHODS

### Participants

We combined data from four independent studies: the Alzheimer's Disease Neuroimaging Initiative 2 (ADNI2) sample, two samples from the Centre de recherche de l'institut universitaire de gériatrie de Montréal (CRIUGMa and CRIUGMb), and a sample from the Montreal Neurological Institute (MNI; Wu et al., 2014). All participants gave their written informed consent to engage in these studies, which were approved by the research ethics board of the respective institutions, and included consent for data sharing with collaborators as well as secondary analysis. Ethical approval was also obtained at the site of secondary analysis (CRIUGM).

The ADNI2 data used in the preparation of this article were obtained from the Alzheimer's Disease Neuroimaging Initiative (ADNI) database (adni.loni.usc.edu). ADNI was launched in 2003 by the National Institute on Aging, the National Institute of Biomedical Imaging and Bioengineering, the Food and Drug Administration, private pharmaceutical companies and non-profit organizations, as a $60 million, 5-year public-private partnership representing efforts of co-investigators from numerous academic institutions and private corporations. ADNI was followed by ADNI-GO and ADNI-2 that included newer techniques. Subjects included in this study were recruited by ADNI-2 from all 13 sites that acquired resting-state fMRI on Philips scanners across North America. For up-to-date information, see www.adni-info.org.

The combined sample included 112 CN and 143 aMCI prior to quality control. After quality control, 99 CN and 129 aMCI remained. In the CN group, the mean age was 72.0 ($s.d. = 7.0$) years, and 37% were men. Mean age of the aMCI subjects was 72.3 ($s.d. = 7.6$) years, and 50% were men. An independent samples $t$-test did not reveal any significant difference in age between the groups ($t = 0.759$, $p = 0.448$). A chi-squared test revealed a trend

toward a significant difference in gender distribution between the groups ($\chi^2 = 3.627$, $p = 0.057$). Note that both age and gender were entered as confounding variables in the statistical analysis below. See **Table 1** for sample size and demographic information from the individual studies after passing quality control (for information about the original cohorts before quality control, see Supplementary Table 1).

All subjects underwent cognitive testing (e.g., memory, language, and executive function; see **Table 2** for a list of specific tests used in each study). Exclusion criteria common to all studies included: Contraindications to MRI, presence or history of axis I psychiatric disorders (e.g., depression, bipolar disorder, schizophrenia), presence or history of neurologic disease with potential impact on cognition (e.g., Parkinson's disease), and presence or history of substance abuse. CN subjects could not meet criteria for MCI or dementia. Those with aMCI had memory complaints, objective cognitive loss (based on neuropsychological testing), but had intact functional abilities and did not meet criteria for dementia. In ADNI2, the diagnosis of aMCI was made based on an education adjusted abnormal score on the Logical Memory II subscale (Delayed Paragraph Recall, Paragraph A only) from the Wechsler Memory Scale and a Clinical Dementia Rating (CDR) of 0.5. In both CRIUGMa and CRIUGMb, the diagnosis of aMCI was made based on scores equal to or >1.5 standard deviations below the mean adjusted for age and education on memory tests. At the MNI, the diagnosis of aMCI relied on the Petersen criteria (2004). At both CRIUGMb and MNI, aMCI diagnoses were made with input from a neurologist. See the Supplementary Methods (Datasheet 1 in Supplementary Material) for greater details for each study.

## Imaging Data Acquisition

All resting-state fMRI and structural scans were acquired on 3T scanners. We performed analyses on the first usable scan (typically the baseline scan) from ADNI2 and applied clinical diagnoses from the same study time point as the first usable scan for each participant in that dataset. See **Table 3** for acquisition parameters for each sample.

## Computational Environment

All experiments were performed using the NeuroImaging Analysis Kit (NIAK[1]; Bellec et al., 2011) version 0.12.18, under CentOS version 6.3 with Octave[2] version 3.8.1 and the Minc toolkit[3] version 0.3.18. Analyses were executed in parallel on the "Guillimin" supercomputer[4], using the pipeline system for Octave and Matlab (Bellec et al., 2012), version 1.0.2. The scripts used for processing can be found on Github[5].

## Pre-processing

Each fMRI dataset was corrected for slice timing; a rigid-body motion was then estimated for each time frame, both within and between runs, as well as between one fMRI run and the T1 scan for each subject (Collins and Evans, 1997). The T1 scan was itself non-linearly co-registered to the Montreal Neurological Institute (MNI) ICBM152 stereotaxic symmetric template (Fonov et al., 2011), using the CIVET pipeline (Ad-Dab'bagh et al., 2006). The rigid-body, fMRI-to-T1 and T1-to-stereotaxic transformations were all combined to resample the fMRI in MNI space at a 3 mm isotropic resolution. To minimize artifacts due to excessive motion, all time frames showing a displacement >0.5 mm were removed (Power et al., 2012). A minimum of 50 unscrubbed volumes per run was required for further analysis (13 CN and 14 aMCI were rejected from the original cohort of 112 CN and 143 aMCI). Neither the rate of rejection nor the frame displacement values (before and after scrubbing) varied significantly among the

[1]http://simexp.github.io/niak/.
[2]https://www.gnu.org/software/octave/.
[3]http://www.bic.mni.mcgill.ca/ServicesSoftware/ServicesSoftwareMincToolKit.
[4]http://www.calculquebec.ca/en/resources/compute-servers/guillimin.
[5]https://github.com/SIMEXP/mcinet.

**TABLE 1 | Demographic information in all studies after quality control.**

| | | ADNI2 | CRIUGMa | CRIUGMb | MNI | Combined sample |
|---|---|---|---|---|---|---|
| **CN** | **N** | **49** | **18** | **17** | **15** | **99** |
| | Mean age (*s.d.*) | 74.4 (6.8) | 71.2 (8.0) | 70.4 (4.6) | 67.0 (5.7) | 72.0 (7.0) |
| | Number male (%) | 21 (43%) | 7 (39%) | 2 (12%) | 7 (47%) | 37 (37%) |
| | Mean years of education (*s.d.*)[a] | 16.9 (2.2) | 14.9 (2.3) | 15.1 (2.8) | 15.0 (3.1) | 16.0 (2.6) |
| | MMSE mean (range) | 28.7 (25–30) | 28.8 (27–30) | n/a | 29.0 (27–30) | n/a |
| | MoCA mean (range) | n/a | 27.8 (22–30) | 28.4 (26–30) | n/a | n/a |
| **aMCI** | **N** | **82** | **8** | **21** | **18** | **129** |
| | Mean age (*s.d.*) | 71.2 (7.3) | 79.9 (6.1) | 74.8 (7.0) | 71.2 (8.1) | 72.3 (7.6) |
| | Number male (%) | 43 (52%) | 3 (38%) | 12 (57%) | 7 (39%) | 65 (50%) |
| | Mean years of education (*s.d.*)[a] | 16.2 (2.6) | 13.7 (3.8) | 14.8 (4.2) | 13.1 (3.1) | 15.5 (3.2) |
| | MMSE mean (range) | 28.1 (24–30)* | 26.1 (22–29)* | n/a | 26.1 (22–30)* | n/a |
| | MoCA mean (range) | n/a | 23.3 (20–29)* | 24.6 (16–29)* | n/a | n/a |

*MMSE, Mini-mental state examination; MoCA, Montreal Cognitive Assessment.*
**Significant difference between aMCI and CN (within study) for independent samples t-test at $p \leq 0.05$.*
*[a]Missing values for education for subjects in ADNI2 (1 CN, 1 aMCI), CRIUGMb (2 aMCI), and MNI (3 CN, 6 aMCI).*

**TABLE 2 | Neuropsychological tests that were used in each study.**

| Test | ADNI2 | CRIUGMa | CRIUGMb | MNI |
|---|---|---|---|---|
| Mini-mental state examination (MMSE) | x | x | | x |
| Montreal Cognitive Assessment (MoCA) | x | x | x | |
| Clinical Dementia Rating (CDR) | x | | x | |
| ADAS-Cog | x | | | |
| Everyday Cognition (ECog) | x | | | |
| Trail making | x (Trails A and B) | x (Trails A and B) | x (Trails A and B) | x (DKEFS) |
| Boston naming test | x | x | x | x |
| Digit span | | x | x | x |
| Color-word interference (DKEFS) | | x | x | x |
| Rey auditory verbal learning test | x | x | | x |
| Verbal fluency | x | x | x (MEC) | x (DKEFS) |
| Clock drawing | x | x | | |
| Visual object and space perception battery | | x | | |
| Brixton spatial anticipation test | | | x | |
| Hooper visual organization test | | | x | |
| Rey complex figure | | x | x | x |
| Aggie figures learning test | | | | x |
| 16-Item free and cued recall (RL/RI-16) | | | x | |
| Pyramid and palm trees test | | x | | |
| Weschler memory scale—logical memory subtest | x | x | x | |

*MEC, Montréal évaluation de la communication; DKEFS, Delis–Kaplan Executive Function System.*

four samples or between CN and aMCI. The following nuisance covariates were regressed out from fMRI time series: slow time drifts (basis of discrete cosines with a 0.01 Hz high-pass cut-off), average signals in conservative masks of the white matter and the lateral ventricles as well as the first 3–10 principal components (median numbers for ADNI2, CRIUGMa, CRIUGMb, and MNI were 9, 6, 7, and 7, respectively, and accounting for 95% variance) of the six rigid-body motion parameters and their squares (Lund et al., 2006; Giove et al., 2009). The fMRI volumes were finally spatially smoothed with a 6 mm isotropic Gaussian blurring kernel. A more detailed description of the pipeline can be found on the NIAK website[6] and Github[7].

## Bootstrap Analysis of Stable Clusters (BASC)

We applied a BASC to identify clusters that consistently exhibited similar spontaneous BOLD fluctuations in individual subjects, and were spatially stable across subjects. We first applied a region-growing algorithm to reduce each fMRI dataset into a time × space array, with 957 regions (Bellec et al., 2006). BASC replicates a hierarchical Ward clustering 1000 times and computes the probability that a pair of regions fall in the same cluster, a measure called stability. The region × region stability matrix is fed into a clustering procedure to derive consensus clusters, which are composed of regions with a high average probability of being assigned to the same cluster across all replications. At the individual level, the clustering was applied to the similarity of regional time series, which was replicated using a circular block bootstrap. Consensus clustering was applied to the average individual stability matrix to identify group clusters. The group clustering was replicated via bootstrapping of subjects in the group. A consensus clustering was finally applied on the group stability matrix to generate group consensus clusters.

The cluster procedure was carried out at a specific number of clusters (called resolution). Using a "multiscale stepwise selection" (MSTEPS) method (Bellec, 2013), we determined a subset of resolutions that provided an accurate summary of the group stability matrices generated over a fine grid of resolutions: 4, 6, 12, 22, 33, 65, 111, and 208.

## Derivation of Functional Connectomes

For each resolution $K$, and each pair of distinct clusters, the between-clusters connectivity was measured by the Fisher transform of the Pearson's correlation between the average time series of the clusters. The within-cluster connectivity was the Fisher transform of the average correlation between time series inside the cluster. An individual connectome was thus a $K \times K$ matrix. See **Figures 1A,B** for an illustration of a parcellation and associated connectome.

## Statistical Testing

To test for differences between aMCI and CN at a given resolution, we used a general linear model (GLM) for each connection between two clusters. The GLM included an intercept, the age and sex of participants, and the average frame

[6]http://niak.simexp-lab.org/pipe_preprocessing.html.
[7]https://github.com/SIMEXP/mcinet/tree/master/preprocess.

**TABLE 3 | Structural and functional scan acquisition parameters.**

| | ADNI2[a] | CRIUGMa | CRIUGMb | MNI |
|---|---|---|---|---|
| **Scanner manufacturer** | **Philips** | **Siemens** | **Siemens** | **Siemens** |
| **STRUCTURAL** | | | | |
| No. channels | 8 | 32 | 32 | 32 |
| No. slices | 170 | 176 | 176 | 176 |
| Slice thickness (mm) | 1.2 | 1 | 1 | 1 |
| In-plane resolution (mm × mm) | 1 × 1 | 1 × 1 | 1 ×1 | 1 × 1 |
| Matrix size | 256 × 256 | 240 × 256 | 256 × 256 | 256 × 256 |
| FOV ($mm^2$) | 256 | 240/256 | 256 | 256 |
| TR (s) | 6.8 | 2.3 | 2.53 | 2.3 |
| TE (ms) | 3.09 | 2.91 | 1.64 | 2.98 |
| TI (s) | n/a | 0.9 | 1.2 | 0.9 |
| FA (°) | 9 | 9 | 7 | 9 |
| Slice gap | 0 | 0 | 0 | 0 |
| Imaging plane | Sagittal | Sagittal | Sagittal | Sagittal |
| NEX | 1 | 1 | 1 | 1 |
| **FUNCTIONAL** | | | | |
| No. runs | 1 | 1 | 3 | 3 |
| No. channels | 8 | 32 | 32 | 32 |
| No. volumes | 140 | 240 | 150 | 160 |
| No. slices | 48 | 33 | 42 | 38 |
| Slice thickness (mm) | 3.3 | 4 | 3.4 | 3.6 |
| In-plane resolution (mm × mm) | 3.3 × 3.3 | 3 × 3 | 3.4 × 3.4 | 3.6 × 3.6 |
| Matrix size | 64 × 64 | 64 × 64 | 64 × 64 | 64 × 64 |
| FOV ($mm^2$) | 212 | 192 | 218 | 230 |
| TR (s) | 3 | 2 | 2.6 | 2 |
| TE (ms) | 30 | 30 | 30 | 30 |
| FA (°) | 80 | 90 | 90 | 90 |
| Slice gap | 0 | 0 | 0 | 0 |
| Imaging plane | Axial | Axial | Axial | Axial |
| NEX | 1 | 1 | 1 | 1 |
| Total scan time (min:s) | 7:00 | 8:00 | 19:30 | 16:00 |

[a] *http://adni.loni.usc.edu/wp-content/uploads/2011/04/ADNI_3T_Philips_2.6.pdf.*

displacement of the runs involved in the analysis. The contrast of interest (aMCI–CN) was represented by a dummy covariate coding the difference in average connectivity between the two groups. All covariates except the intercept were corrected to a zero mean (**Figure 1C**). The GLM was estimated independently for each scanning protocol. In addition to distinguishing between CRIUGMa, CRIUGMb, MNI, and ADNI2, ADNI2 was subdivided into five sub-studies based on the use of different Philips scanner models (i.e., Achieva, Gemini, Ingenia, Ingenuity, and Intera). We dropped all subjects scanned with Ingenuity (2 CN, 1 aMCI) due to the elimination of all aMCI subjects within that site by the scrubbing procedure and its small sample size. We therefore estimated seven independent GLMs for each protocol (ADNI2-Achieva, ADNI2-Gemini, ADNI2-Ingenia, ADNI2-Intera, CRIUGMa, CRIUGMb, MNI). The estimated effects were combined across all protocols through inverse variance based weighted averaging (Willer et al., 2010; **Figure 1D**).

Resolutions containing fewer than 50 clusters have been suggested to have higher sensitivity based on prior independent work (Bellec et al., 2015). The GLM was first applied at an a priori resolution of $K = 33$, which was the lowest number of clusters for which the DMN could be clearly decomposed into subnetworks (Supplementary Figure 1, visit Figshare for 3D volumes of brain parcellations[8] and see Supplementary Table 2 for a list of the 33 clusters and their numerical IDs). The false-discovery rate (FDR) across connections was controlled at $q^{FDR} \leq 0.1$ (Benjamini and Hochberg, 1995). In addition to the analysis at resolution 33, we assessed the impact of that parameter by replicating the GLM analysis at the seven resolutions selected by MSTEPS (Supplementary Figure 2). We implemented an omnibus test (family-wise error rate $\alpha \leq 0.05$) to assess the overall presence of significant differences between groups, pooling FDR results across all resolutions (Bellec et al., 2015). If the omnibus test across resolutions was not significant, then no test would be deemed significant. Since this omnibus test was significant, we used the FDR threshold of $q \leq 0.1$ to explore single resolutions.

# RESULTS

## Functional Connectivity Differences Between aMCI and CN

The omnibus test pooling significant differences in connectivity between aMCI and CN across all resolutions was significant at $\alpha \leq 0.05$ ($p \leq 0.0056$). In line with prior observations on independent datasets (Bellec et al., 2015), resolutions containing fewer than 50 clusters were associated with a higher rate of discovery (**Figure 2**). At resolution 33, significant group differences between aMCI and CN were seen across the whole brain (**Figure 3A**). Four brain clusters were associated with 47% of all significant changes found across the connectome: the superior medial frontal cortex (including anterior cingulate), dorsomedial prefrontal cortex, striatum, and middle temporal lobe (**Figures 3B,C**, Supplementary Table 3). Supplementary Table 3 contains a list of parcels that account for all non-redundant significant connectivity differences between aMCI and CN. For example, the first-ranked seed (superior medial frontal cortex) was associated with 13.4% of connections that differ between the groups. The second-ranked seed (dorsomedial prefrontal cortex) was associated with an additional 12.7% of connectivity differences that did not overlap with or were not previously accounted for by the first seed. Note that if a given parcel was associated with a significant effect with another region that ranked in the table, then that parcel may not be listed in the table (i.e., this table is not a comprehensive list of parcels that show significant effects, as a given parcel may involve a region in the table at a higher rank which already accounted for its effects). Given that the top four clusters explained nearly half of the findings, they were further characterized in seed-based connectivity analyses, which revealed that aMCI showed decreased connectivity between DMN nodes and between areas of the cortico-striatal-thalamic loop (**Figure 4**). More specifically, in aMCI compared to CN, the superior medial frontal cortex displayed significantly reduced connectivity with

[8] http://dx.doi.org/10.6084/m9.figshare.1480461.

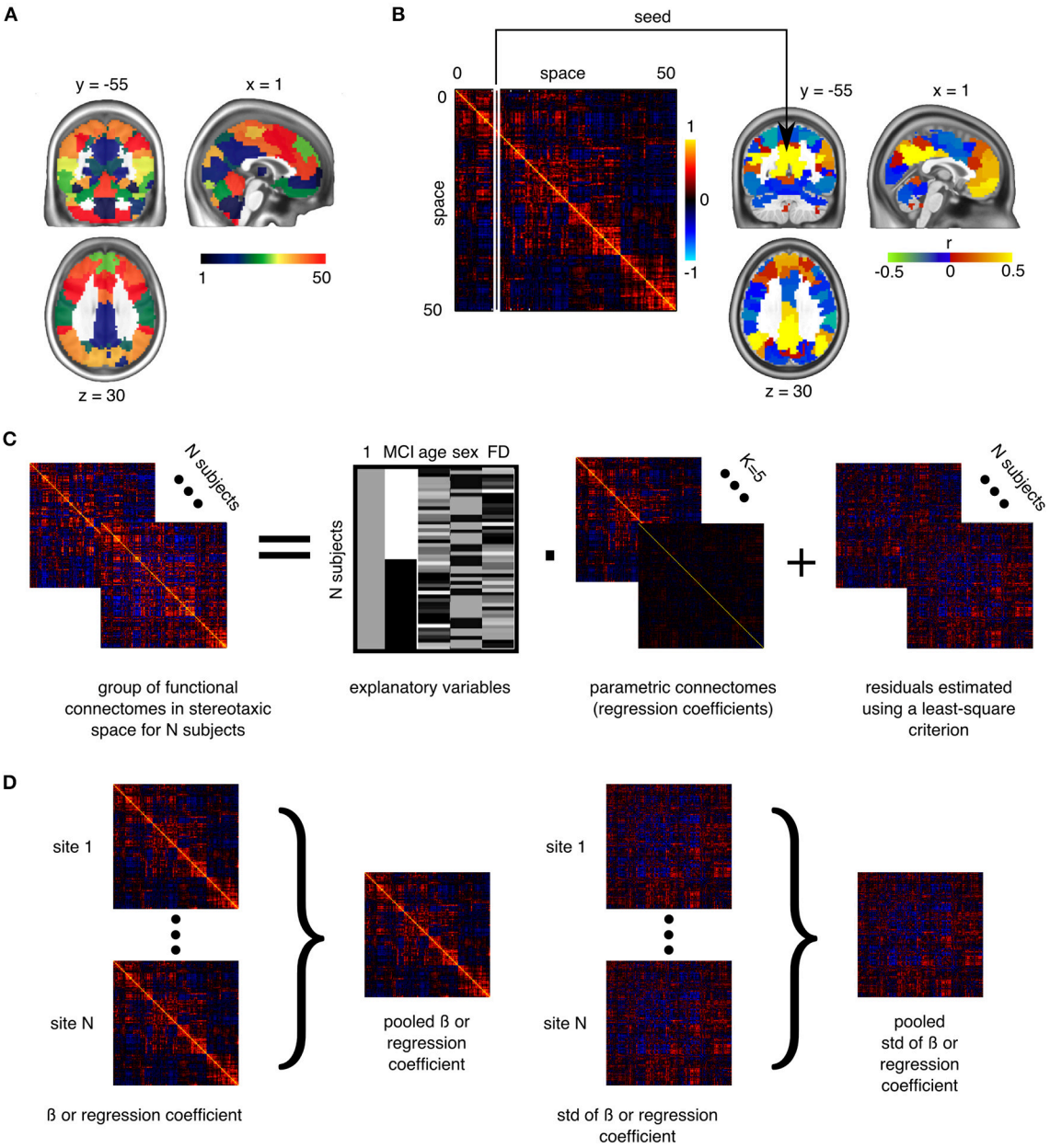


**FIGURE 1 | Application of general linear models to connectomes. (A)** The brain is functionally parcellated into *K* (e.g., 50) clusters generated through a clustering algorithm. **(B)** The connectome is a $K \times K$ matrix measuring functional connectivity between and within clusters. **(C)** A general linear model is used to test the association between phenotypes and connectomes, independently at each connection, at the group level. **(D)** In a multisite situation, independent site-specific effects are estimated and then pooled through weighted averaging (Willer et al., 2010).

the ventromedial prefrontal cortex, striatum, thalamus, temporal lobes, hippocampus, inferior parietal lobes, and precuneus (**Figure 4A**). aMCI showed reduced connectivity between the dorsomedial prefrontal cortex with temporal lobe regions, ventral frontal areas, thalamus, striatum, and the cuneus (**Figure 4B**). The striatum in aMCI also exhibited decreased connectivity with the sensorimotor cortex, thalamus, and frontal and parietal regions (**Figure 4C**). Lastly, in aMCI, the middle temporal lobe displayed significantly decreased connectivity with the posterior cingulate, precuneus, inferior parietal lobes, hippocampus, and frontal areas (**Figure 4D**).

## Sample-Specific Effects

The statistical model we used to combine GLM analyses across sites was based on a weighted average. The possibility thus existed that an effect would be significant in the pooled analysis because it was driven by a very strong effect in a single sample, instead of being consistent across all samples. When we examined

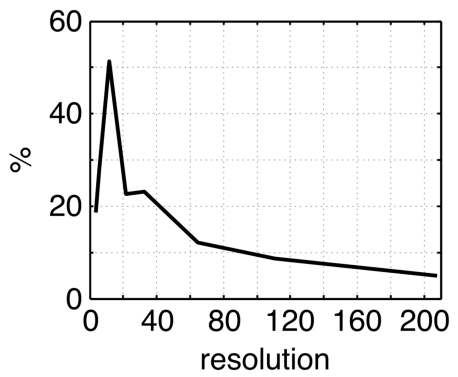


**FIGURE 2 | Plot of the percentage of connections identified as significant by the statistical comparison between aMCI and CN across the connectome ($q^{FDR} \leq 0.1$), as a function of the resolutions selected by MSTEPS.**

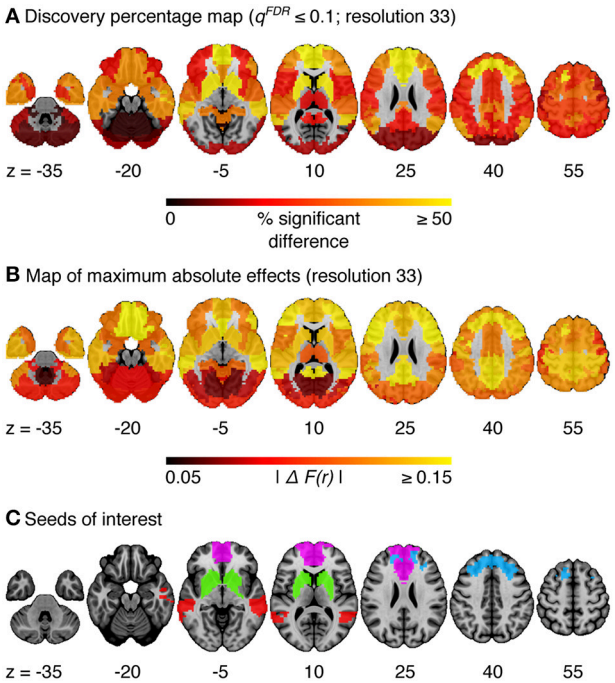


**FIGURE 3 | (A)** Map of the percentage of connections associated with a given cluster and identified as significant by the statistical comparison between aMCI and CN, at a resolution of 33 clusters ($q^{FDR} \leq 0.1$). **(B)** Maximum absolute difference in average connectivity between aMCI and CN, across all connections associated with a cluster, at resolution 33. ΔF(r) signifies the difference in Fisher-transformed correlation values between the groups. **(C)** Four clusters of interest (superior medial frontal cortex, dorsomedial prefrontal cortex, striatum, middle temporal lobe) were selected out of 33 for further characterization.

effects in each sample independently, we detected no findings or very few significant findings. We then explored the whole brain connectivity of the top four seed regions (superior medial frontal cortex, dorsomedial prefrontal cortex, striatum, and middle temporal lobe) within each sample. The majority of effects found at each sample did not appear to be consistent or reproducible across studies as the comparison between aMCI and CN varied substantially among the seven samples (**Figure 5**, Supplementary Figures 3–5). We assessed the extent at which findings among the seven samples were similar by calculating correlation coefficients across the spatial maps for the average connectivity values in CN, the average connectivity values in aMCI, and differences in connectivity values between aMCI and CN among the samples. We found that the difference maps, contrasting aMCI and CN, were weakly correlated on average across studies and protocols (mean $r = 0.06$, min $r = -0.64$, max $r = 0.69$). The average connectivity maps among studies in both CN and aMCI were generally highly correlated with each other (for CN, mean $r = 0.68$, min $r = -0.16$, max $r = 0.95$; for aMCI, mean $r = 0.67$, min $r = -0.10$, max $r = 0.97$). These results were expected given the small sample sizes of most independent samples (Kelly et al., 2012), but still sobering as the majority of the literature on aMCI and fMRI has used small sample sizes.

However, despite the large observed variations in the spatial distribution of aMCI vs. CN contrasts, there were still clear consistent trends across studies and protocols. We indeed found that aMCI-related connectivity changes that surpassed the FDR threshold in the pooled analysis showed similar trends in the vast majority of samples across seeds and connections, where the independent aMCI samples consistently exhibited decreased connectivity compared to the CN samples (**Figures 5**, **6**, Supplementary Figures 3–5). For example, the pooled analysis revealed that, compared to CN, aMCI exhibited significantly reduced connectivity between the superior medial frontal cortex cortex (the region in which connectivity was most affected by aMCI) and the middle temporal lobes. This change appeared to be common to the majority of the independent samples (**Figures 5**, **6A**). For this particular seed, the change in connectivity was mainly due to regions with positive correlations in CN having smaller correlation values closer to zero in aMCI in the individual samples (**Figures 5**, **6A**). For sample-specific effects in other seeds and connections, please see Supplementary Figures 3–9.

## Effect Sizes and Sample Size Estimates

We measured the effect sizes of the difference between groups at each significant connection by calculating Cohen's *d*, via a weighted average of the effect sizes per individual sample. We found small to medium effect sizes, ranging from $d = 0.10$–$0.48$, with an average effect size of $d = 0.32$. Note that these effect sizes are potentially inflated since we have focussed on significant results only. We also calculated the sample sizes required to achieve 80% power, based on the effect sizes estimated by Cohen's *d*, the assumption of balanced groups, Gaussian distributions, bilateral tests, and $\alpha = 0.05$, for each connection. We found that the estimated sample sizes ranged from 140 to upwards of 600 total subjects, which further suggests that findings from small samples, similar to the seven samples we included when assessed independently, are not expected to be reliable. As noted above, as we used the same sample to estimate the location of effects and

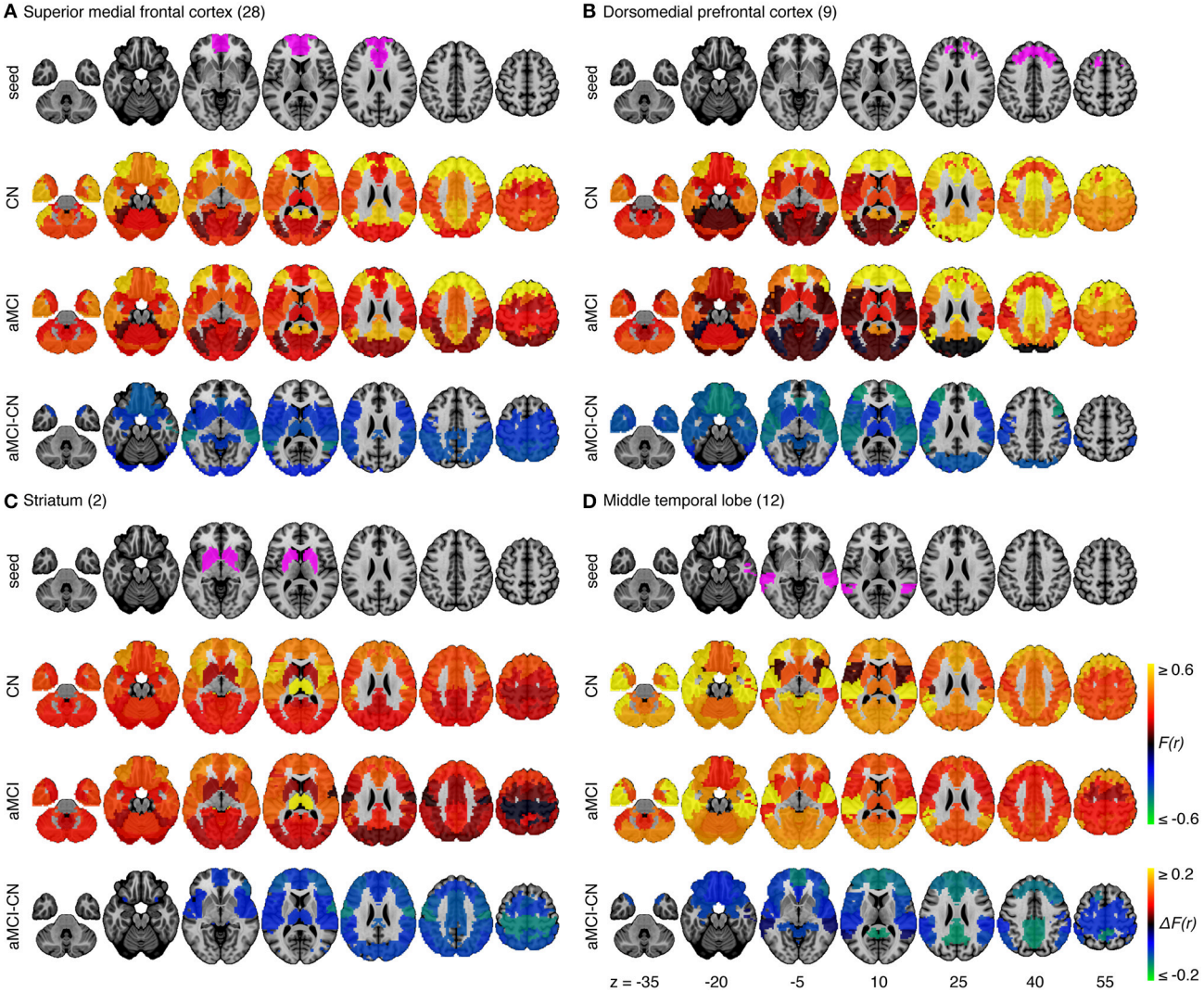


**FIGURE 4 | Effect maps for a selection of four seeds that show effects related to aMCI at resolution 33.** Effect maps reveal the spatial distribution of the changes in functional connectivity for **(A)** the superior medial frontal cortex, **(B)** the dorsomedial prefrontal cortex, **(C)** striatum, and **(D)** the middle temporal lobe. All connections shown in the maps of difference in average connectivity between aMCI and CN are significant at $q^{FDR} \leq 0.1$. For each panel, the top line maps the spatial location of the seed region in magenta, the second and third lines show the connectivity (Fisher-transformed correlation values, *F(r)*) between the designated seed region and the rest of the brain in CN and aMCI, respectively, and the fourth line shows a difference map between aMCI and CN [difference in Fisher-transformed correlation values, $\Delta F(r)$]. The numbers in parentheses refer to the numerical IDs of the clusters in the 3D parcellation volume, as listed in Supplementary Table 2.

their size, these sample size estimates are possibly optimistic, i.e., deflated compared to a replication on an independent sample. See **Figure 6** and Supplementary Figures 6–9 for Cohen's *d* and sample size estimates for each significant connection that was reported in **Figure 4**.

## Effect of Resolution on the GLM

The percentage of discoveries in significant differences between aMCI and CN across the connectomes varied markedly as a function of resolution, as selected by the MSTEPS procedure. Higher resolutions were associated with fewer discoveries, especially beyond resolution 65 (Supplementary Figure 10A). By contrast, the maximal amplitude of differences in average connectivity associated with a particular cluster did not decrease substantially, and sometimes increased, when the resolution increased (Supplementary Figure 10B). The decrease in percentage of discovery thus likely reflected a cost associated with an increased number of multiple comparisons in the FDR procedure, rather than a loss in signal quality. Regarding the clusters that were selected for our seed-based analyses (the superior medial frontal cortex, dorsomedial prefrontal cortex, striatum, and middle temporal lobe), the associated effect maps (without statistical threshold) were highly consistent across different resolutions (Supplementary Figures 11, 12), with the

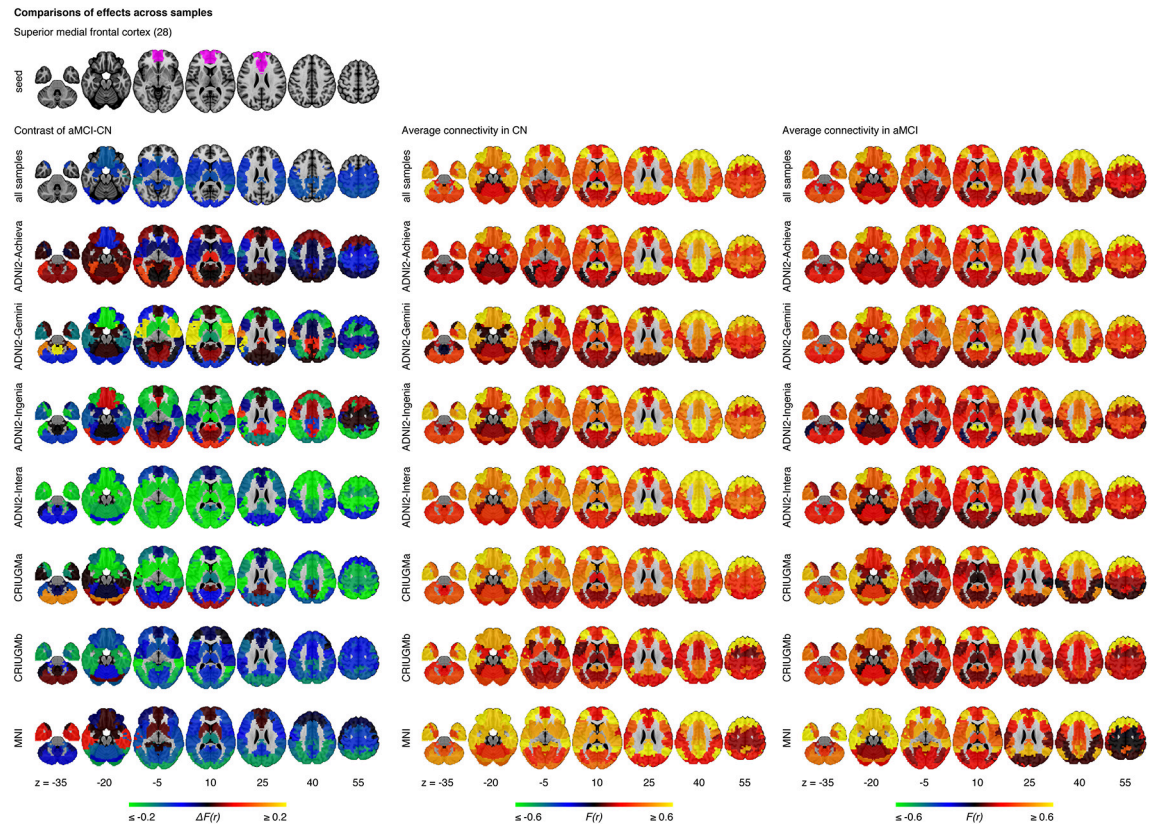


**FIGURE 5 | Comparisons of effects in the superior medial frontal cortex across samples.** This figure illustrates functional connectivity changes between aMCI and CN, average connectivity in CN, and average connectivity in aMCI in each site (ADNI2-Achieva, ADNI2-Gemini, ADNI2-Ingenia, ADNI2-Intera, CRIUGMa, CRIUGMb, MNI) independently of other sites and when samples are pooled together (all samples). The number in parentheses refers to the numerical ID of the seed in the 3D parcellation volume, as listed in Supplementary Table 2.

potential exception of very low resolutions where, for example, a relatively small cluster like the anterior cingulate got merged with a large distributed cortical network. This also replicated a prior study on the effect of multiresolution parcellations on GLM analysis (Bellec et al., 2015). Lastly, signal-to-noise ratio did not have a significant impact on the results (Supplementary Figure 13).

## DISCUSSION

We report resting-state functional connectivity differences in the superior medial frontal cortex, dorsomedial prefrontal cortex, striatum, and middle temporal lobe between aMCI and CN subjects when multiple studies were combined together. Despite protocol differences, we found that aMCI exhibited reduced connectivity within areas of the DMN and cortico-striatal-thalamic loop compared to CN. Previous studies suggested these altered patterns of functional connectivity in MCI may result from the coevolution of multiple AD-associated biological processes, namely structural degeneration (Pievani et al., 2010; Coupé et al., 2012), neurofibrillary and amyloid pathologies (Small et al., 2006), and cerebrovascular dysfunction (Villeneuve and Jagust, 2015).

The superior medial frontal cortex and middle temporal lobes, both of which are DMN nodes, were among the seed regions with the greatest amount of aMCI-related connectivity changes with other brain areas. Decreased connectivity in aMCI patients was found between these two nodes and other DMN regions, including the posterior cingulate, precuneus, inferior parietal lobes, ventromedial prefrontal cortex, and hippocampus. Our findings support previous studies that used small single-site samples and reported reduced DMN connectivity in MCI and AD patients (Sorg et al., 2007; Bai et al., 2009; Agosta et al., 2012; Koch et al., 2012). Alterations in the DMN may reflect increased amyloid burden in aMCI patients as it has been shown that amyloid plaques impair default mode connectivity (Hedden et al., 2009; Sheline et al., 2010b; Mormino et al., 2011).

We found reduced connectivity within the frontal lobes, notably between ventral and dorsal areas. Decreased functional connectivity between the ventral and dorsal frontal regions could reflect degeneration in gray matter and in white matter tracts connecting these areas. Longitudinal studies have shown greater prefrontal cortex atrophy in MCI over time, as well as in those transitioning to AD, compared to CN (McDonald et al., 2009; Carmichael et al., 2013). Cortico-cortical white matter bundles, e.g., superior longitudinal fasciculus, have also

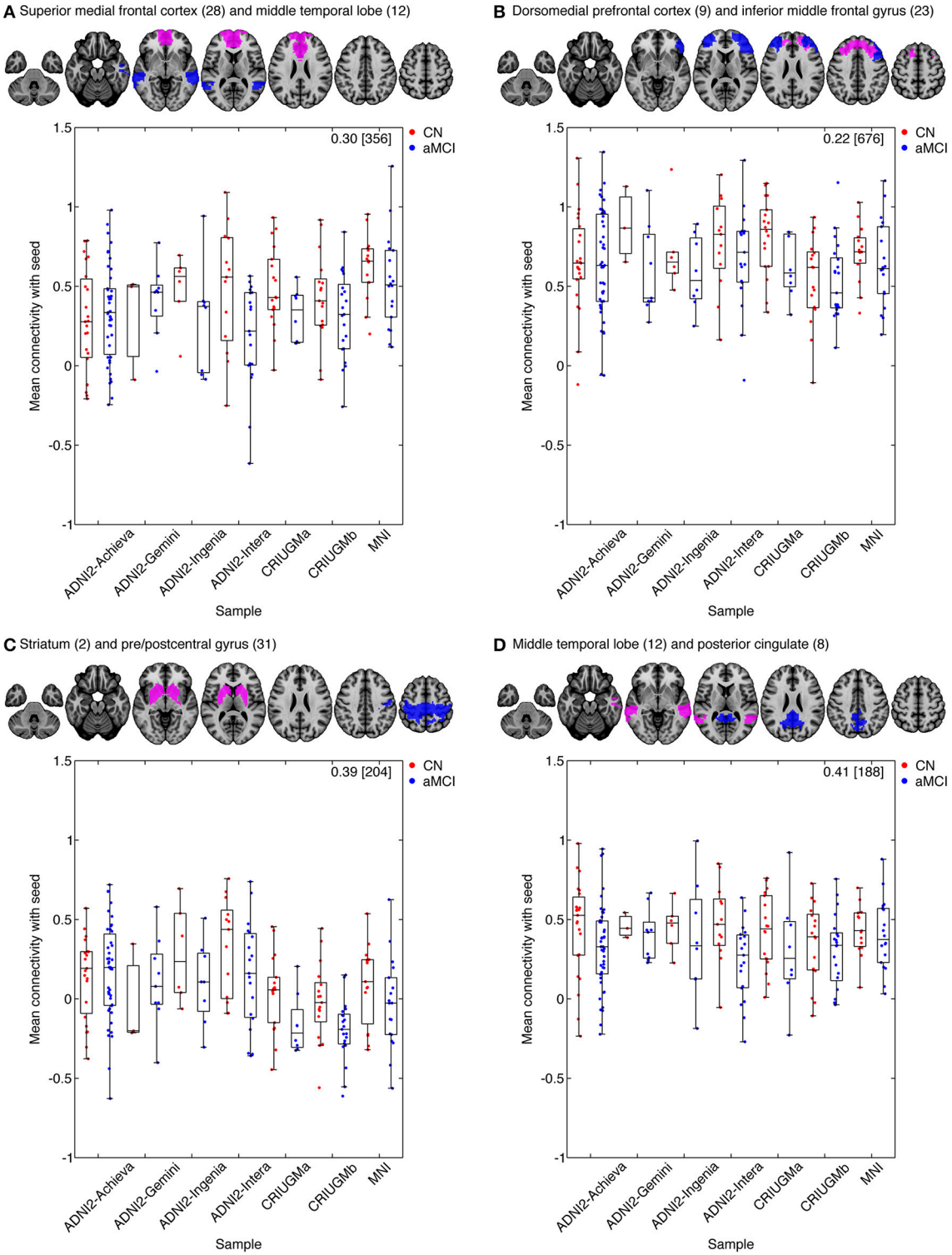


**FIGURE 6 | Mean connectivity between (A) the superior medial frontal cortex and middle temporal lobe, (B) the dorsomedial prefrontal cortex and middle frontal gyrus, (C) the striatum and pre/postcentral gyrus, and (D) middle temporal lobe and posterior cingulate in CN and aMCI in the independent samples.** Each map displays the seed (pink) and a selected cluster (blue) whose connectivity with the seed significantly differed between CN and aMCI in the pooled analysis. The box-whisker plots display the mean connectivity (Fisher-transformed correlation values) between the seed and the selected parcel, overlaid

*(Continued)*

**FIGURE 6 | Continued**
over individual data points, in the CN and MCI groups in the ADNI2-Achieva, ADNI2-Gemini, ADNI2-Ingenia, ADNI2-Intera, CRIUGMa, CRIUGMb, and MNI samples. We also report the Cohen's *d* (a weighted average of the effect sizes per sample) followed by a sample size estimate (for 80% power, balanced groups, bilateral tests, Gaussian distributions, and $\alpha = 0.05$) in square brackets in the top-right corner of each plot. The numbers in parentheses in the titles refer to the numerical IDs of the seeds in the 3D parcellation volume, as listed in Supplementary Table 2. For box-whisker plots for all significant clusters with each of these seeds, see Supplementary Figures 6–9.

been demonstrated to degenerate in patients with MCI and AD (Pievani et al., 2010). Additionally, functional connectivity changes may reflect the regional effect of increased amyloid burden (Sheline et al., 2010b), and PIB-PET work has shown the frontal lobe to be one of the first regions in which amyloid accumulates in autosomal dominant AD mutation carriers (Bateman et al., 2012). Our results may also be due to neurofibrillary pathology as it typically appears in the prefrontal cortex during MCI (Bossers et al., 2010). Lastly, cerebral hypoperfusion in the frontal lobe of MCI (Chao et al., 2009) may have contributed to our results.

We also observed functional disconnection between the temporal and frontal lobes in aMCI. Effects in the temporal lobes were expected given that the temporal lobe is a region known to suffer from significant AD pathology in preclinical phases (Guillozet et al., 2003). Structural connectivity may also explain the functional connectivity changes between the frontal and temporal regions, since degeneration of white matter tracts between these areas, e.g., the uncinate fasciculus, occurs with the progression from MCI to AD and correlates with episodic memory impairment in MCI (Pievani et al., 2010; Rémy et al., 2015). Furthermore, examining the integrity of the arcuate fasciculus, a major language tract that connects the frontal and temporal lobes (Dick and Tremblay, 2012), might reveal a biological basis for language impairments such as word-finding difficulties in MCI and AD, (Nutter-Upham et al., 2008). Brain areas that subserve language function could be important targets to investigate given recent evidence that multilingualism, like other forms of cognitive reserve, may help delay the onset of AD (Chertkow et al., 2010).

Unexpectedly, we also found significant effects in the striatum, which showed reduced connectivity in aMCI with the sensorimotor cortex, frontal and parietal regions, and thalamus. While not initially expected, these findings may reflect earlier observations that regions within the cortico-striatal-thalamic loops are vulnerable to AD pathology. For example, previous work demonstrated the presence of substantial amyloid burden in the striatum in both autosomal dominant and sporadic forms of AD (Braak and Braak, 1990; Villemagne et al., 2009), and the striatum may be the first region in which amyloid deposition occurs in autosomal dominant AD (Klunk et al., 2007; Bateman et al., 2012). Furthermore, significant neurodegeneration is known to occur with AD in the striatum and thalamus (de Jong et al., 2008; Madsen et al., 2010), so our results might reflect the brain's capacity for functional plasticity in response to amyloid or neurodegeneration in these regions. Motor cortex hyperexcitability has also been shown in AD, and this suggests that inhibitory circuits leading to the motor cortex may be affected in the disease (Ferreri et al., 2011). Patients with AD also demonstrate changes in swallowing which have been associated with altered cortical activity (Humbert et al., 2010). Our results may support these observations. Additionally, our findings may represent a biological basis for the cognitive and motor symptoms of MCI (Aggarwal et al., 2006) since the striatum and the rest of the basal ganglia have been implicated in stimulus-response associative learning and memory and motor skill acquisition and execution (Packard and Knowlton, 2002; Doyon et al., 2009). Future research should examine the potential relationship between connectivity in the cortico-striatal-thalamic loops and motor function in aMCI and AD.

Our findings contrasted with previous, smaller single-site studies that have variously reported decreased and increased connectivity. The reports of increased connectivity (Bai et al., 2009; Qi et al., 2010; Gour et al., 2011) may have reflected unique attributes of particular protocols or the choices made with respect to pre-processing steps, for example using global signal regression (Saad et al., 2012). Given that our sample size estimates suggest the use of hundreds of subjects to obtain adequate statistical power, it is not surprising that discrepancies between our results and previous findings generated from smaller, likely underpowered, studies exist. Even when we examined the samples in our study (ADNI2-Achieva, ADNI2-Gemini, ADNI2-Ingenia, ADNI2-Intera, CRIUGMa, CRIUGMb, MNI) independently of each other, we found inconsistent effects among the samples. It is only by combining the studies together in a meta-analysis that we were able to find some common differences in functional connectomes between patients with aMCI and CN. This finding underscores the need for multisite studies with large sample sizes in order to generate reproducible results, as previously suggested in the field of autism research (Haar et al., 2014).

Among our study's limitations is that it was not possible to model each of the 13 ADNI2 sites independently because the sites tended to be small and unbalanced in the numbers of patients and controls. We therefore chose to model each scanner model within ADNI2 separately based on the recommendation of a reviewer. A previous version of the analysis (published as a preprint[9]) had not modeled the different scanner models in ADNI2 and instead treated ADNI2 as a single site. This previous analysis yielded fewer significant findings, but the results were still mostly consistent with what is reported here. Our results suggest that modeling scanner models may have a positive impact on fMRI association studies, but further experiments would be required to confirm that this trend is reproducible. We must also note that the METAL averaging is only representative of the specific samples that were averaged, especially using only

[9]http://dx.doi.org/10.1101/019646.

Philips and Siemens scanners, and it is unclear how our findings may replicate in other studies that would employ a different combination of protocols, say using GE scanners. In particular, our sample size estimates have to be interpreted with caution. They may first be under-estimated, because they were not derived from pre-specified locations, but rather associated with the connections showing the largest effects in our particular sample. These sample sizes were also derived from a meta-analysis combining particular types of studies. We only had 3T scanners from two manufacturers, Siemens and Philips. For the Siemens studies, all were from the same model. For the Philips studies, the scanning protocol was identical at every site, and only the scanner model varied across scanners. Finally, a fairly large number of patients and controls (generally more than 10 subjects per group) was scanned for each variant of the scanning protocol. The sample size estimate may turn out quite differently for a single site study or on the contrary for a study with a very large number of sites and with only a few subjects per site.

Our study is also limited by its cross-sectional nature, which precludes inference that the functional changes we found would necessarily predict progression toward Alzheimer's dementia. Furthermore, aMCI has many underlying causes aside from AD. It is possible that some subjects in our cohort had cognitive impairments due to Lewy Body dementia, for example. However, all samples in the current study had inclusion criteria that enriched for subjects that had aMCI likely due to AD and excluded aMCI subjects with other co-morbidities, such as depression or Parkinson's disease. Also, we did not account for structural atrophy, despite a bias for increased detection in functional differences due to differences in underlying structure (Dukart and Bertolino, 2014). However, aMCI-related gray matter changes likely co-localize to some extent with functional changes, and the aim of our work was to map out functional changes rather than study their interaction with atrophy. We did not account for other variables, such as APOE genotype (Sheline et al., 2010a), amyloid deposition (Sheline et al., 2010b), presence of neurofibrillary tangles (Maruyama et al., 2013), and cerebrovascular mechanisms (Villeneuve and Jagust, 2015). At least some of these could potentially have explained the observed aMCI-related functional connectivity changes as part of an underlying disease mechanism. Large-scale multimodal studies, incorporating genomics, proteomics, and multimodal imaging will be needed to identify the interactions between these and other physiological facets of the pathology. Despite combining several samples together, we still only achieved relatively limited power, given that sample size estimates required at least 140 to over 600 total subjects to consistently identify effects between groups. Lastly, because of the explorative approach used in our study, the resulting estimates of effect sizes may have been inflated and discussion of possible pathological mechanisms for our findings was speculative. However, our discoveries may be used as follow-up targets in future work. Upcoming research should not only attempt to verify our findings by using these regions and their associated connections with hypothesis-driven approaches (e.g., seed-based correlation analyses), but also to extend them to cohorts that include Alzheimer's dementia and other clinical populations (e.g., CN with significant amyloid deposition) and to longitudinal studies that characterize individuals' progression to dementia. Finally, future studies should aim to determine whether our findings are associated with established biomarkers of AD (e.g., amyloid and tau quantification) in order to probe the potential of these functional connections as biomarkers.

Overall, our results supported previous findings of DMN connectivity changes in AD and MCI (Greicius et al., 2004; Sorg et al., 2007), given that three of the identified seeds (superior medial frontal cortex, dorsomedial prefrontal cortex, middle temporal lobe) are part of this network. It is noteworthy, however, that our strongest observed effects reported here were not in the same DMN regions typically described in earlier resting-state studies of MCI and AD, viz, posterior cingulate/precuneus (Sheline et al., 2010b; Zhang et al., 2010). Unexpected changes were also found in the striatum, and this may reflect the advantages of "mining" the whole-brain connectome to search for new biomarkers of mild cognitive impairment and possibly the early progression of the pathophysiologic substrate of Alzheimer's disease. If confirmed, our results could suggest the utility of these regions in resting-state fMRI as a biomarker endpoint in clinical trials.

## ACKNOWLEDGMENTS

We thank Sven Joubert, Isabelle Rouleau, and Sophie Benoit for their contribution in collection of the CRIUGMa dataset. We thank Tom Nichols for his comments and suggestions. Collection of the CRIUGMb dataset was supported by the Alzheimer's Society of Canada. Collection of the MNI dataset was supported by Industry Canada/Montreal Neurological Institute Centre of excellence in commercialization and research. This work was supported by CIHR (133359) and NSERC (436141-2013). Data collection and sharing for this project was funded by the Alzheimer's Disease Neuroimaging Initiative (ADNI; National Institutes of Health Grant U01 AG024904) and DOD ADNI (Department of Defense award number W81XWH-12-2-0012). ADNI is funded by the National Institute on Aging, the National Institute of Biomedical Imaging and Bioengineering, and through generous contributions from the following: Alzheimer's Association; Alzheimer's Drug Discovery Foundation; Araclon Biotech; BioClinica, Inc.; Biogen Idec Inc.; Bristol-Myers Squibb Company; Eisai Inc.; Elan Pharmaceuticals, Inc.; Eli Lilly and Company; EuroImmun; F. Hoffmann-La Roche Ltd., and its affiliated company Genentech, Inc.; Fujirebio; GE Healthcare; IXICO Ltd.; Janssen Alzheimer Immunotherapy Research & Development, LLC.; Johnson & Johnson Pharmaceutical Research & Development LLC.; Medpace, Inc.; Merck & Co., Inc.; Meso Scale Diagnostics, LLC.; NeuroRx Research; Neurotrack Technologies; Novartis Pharmaceuticals Corporation; Pfizer Inc.; Piramal Imaging; Servier; Synarc Inc.; and Takeda Pharmaceutical Company. The Canadian Institutes of Health Research is providing funds to support ADNI clinical sites in Canada. Private sector contributions are facilitated by the Foundation for the National Institutes of Health (www.fnih.org). The grantee organization is the Northern California Institute

for Research and Education, and the study is coordinated by the Alzheimer's Disease Cooperative Study at the University of California, San Diego. ADNI data are disseminated by the Laboratory for Neuro Imaging at the University of Southern California.

## SUPPLEMENTARY MATERIAL

The Supplementary Material for this article can be found online at: http://journal.frontiersin.org/article/10.3389/fnagi.2015.00242

## REFERENCES


Ad-Dab'bagh, Y., Einarson, D., Lyttelton, O., Muehlboeck, J. S., Mok, K., Ivanov, O., et al. (2006). "The CIVET image-processing environment: a fully automated comprehensive pipeline for anatomical neuroimaging research," in *Proceedings of the 12th Annual Meeting of the Organization for Human Brain Mapping* (Florence), 2266.

Aggarwal, N. T., Wilson, R. S., Beck, T. L., Bienias, J. L., and Bennett, D. A. (2006). Motor dysfunction in mild cognitive impairment and the risk of incident Alzheimer disease. *Arch. Neurol.* 63, 1763–1769. doi: 10.1001/archneur.63.12.1763

Agosta, F., Pievani, M., Geroldi, C., Copetti, M., Frisoni, G. B., and Filippi, M. (2012). Resting state fMRI in Alzheimer's disease: beyond the default mode network. *Neurobiol. Aging* 33, 1564–1578. doi: 10.1016/j.neurobiolaging.2011.06.007

Albert, M. S., DeKosky, S. T., Dickson, D., Dubois, B., Feldman, H. H., Fox, N. C., et al. (2011). The diagnosis of mild cognitive impairment due to Alzheimer's disease: recommendations from the National Institute on Aging-Alzheimer's Association workgroups on diagnostic guidelines for Alzheimer's disease. *Alzheimers. Dement.* 7, 270–279. doi: 10.1016/j.jalz.2011.03.008

Bai, F., Watson, D. R., Yu, H., Shi, Y., Yuan, Y., and Zhang, Z. (2009). Abnormal resting-state functional connectivity of posterior cingulate cortex in amnestic type mild cognitive impairment. *Brain Res.* 1302, 167–174. doi: 10.1016/j.brainres.2009.09.028

Bateman, R. J., Xiong, C., Benzinger, T. L. S., Fagan, A., Goate, A., Fox, N. C., et al. (2012). Clinical and biomarker changes in dominantly inherited Alzheimer's disease. *N. Engl. J. Med.* 367, 795–804. doi: 10.1056/NEJMoa1202753

Bellec, P. (2013). "Mining the hierarchy of resting-state brain networks: selection of representative clusters in a multiscale structure," in International Workshop on *Pattern Recognition in Neuroimaging* (Philadelphia, PA), 54–57. doi: 10.1109/prni.2013.23

Bellec, P., Benhajali, Y., Carbonell, F., Dansereau, C., Albouy, G., Pelland, M., et al. (2015). Impact of the resolution of brain parcels on connectome-wide association studies in fMRI. *NeuroImage* 123, 212–228. doi: 10.1016/j.neuroimage.2015.07.071

Bellec, P., Carbonell, F. M., Perlbarg, V., Lepage, C., Lyttelton, O., Fonov, V., et al. (2011). "A neuroimaging analysis kit for Matlab and Octave," in *Proceedings of the 17th International Conference on Functional Mapping of the Human Brain.* (Québec City, QC).

Bellec, P., Lavoie-Courchesne, S., Dickinson, P., Lerch, J. P., Zijdenbos, A. P., and Evans, A. (2012). The pipeline system for Octave and Matlab (PSOM): a lightweight scripting framework and execution engine for scientific workflows. *Front. Neuroinform.* 6:7. doi: 10.3389/fninf.2012.00007

Bellec, P., Perlbarg, V., Jbabdi, S., Pélégrini-Issac, M., Anton, J.-L., Doyon, J., et al. (2006). Identification of large-scale networks in the brain using fMRI. *Neuroimage* 29, 1231–1243. doi: 10.1016/j.neuroimage.2005.08.044

Benjamini, Y., and Hochberg, Y. (1995). Controlling the false discovery rate: a practical and powerful approach to multiple testing. *J. R. Stat. Soc. B* 57, 289–300. doi: 10.2307/2346101

Bossers, K., Wirz, K. T. S., Meerhoff, G. F., Essing, A. H. W., van Dongen, J. W., Houba, P., et al. (2010). Concerted changes in transcripts in the prefrontal cortex precede neuropathology in Alzheimer's disease. *Brain* 133, 3699–3723. doi: 10.1093/brain/awq258

Braak, H., and Braak, E. (1990). Alzheimer's disease: striatal amyloid deposits and neurofibrillary changes. *J. Neuropathol. Exp. Neurol.* 49, 215. doi: 10.1097/00005072-199005000-00003

Carmichael, O., McLaren, D. G., Tommet, D., Mungas, D., Jones, R. N., for the Alzheimer's Disease Neuroimaging Initiative (2013). Coevolution of brain structures in amnestic mild cognitive impairment. *NeuroImage* 66, 449–456. doi: 10.1016/j.neuroimage.2012.10.029

Chao, L. L., Pa, J., Duarte, A., Schuff, N., Weiner, M. W., Kramer, J. H., et al. (2009). Patterns of cerebral hypoperfusion in amnestic and dysexecutive MCI. Alzheimer Dis. Assoc. Disord. 23, 245–252. doi: 10.1097/WAD.0b013e318199ff46

Chertkow, H., Whitehead, V., Phillips, N., Wolfson, C., Atherton, J., and Bergman, H. (2010). Multilingualism (but not always bilingualism) delays the onset of alzheimer disease: evidence from a bilingual community. Alzheimer Dis. Assoc. Disord. 24, 118–125. doi: 10.1097/WAD.0b013e3181ca1221

Collins, D. L., and Evans, A. C. (1997). Animal: validation and applications of nonlinear registration-based segmentation. *Int. J. Patt. Recogn. Artif. Intell.* 11, 1271–1294. doi: 10.1142/S0218001497000597

Coupé, P., Eskildsen, S. F., Manjón, J. V., Fonov, V. S., Collins, D. L., for the Alzheimer's Disease Neuroimaging Initiative (2012). Simultaneous segmentation and grading of anatomical structures for patient"s classification: application to Alzheimer"s disease. *NeuroImage* 59, 3736–3747. doi: 10.1016/j.neuroimage.2011.10.080

de Jong, L. W., van der Hiele, K., Veer, I. M., Houwing, J. J., Westendorp, R. G. J., Bollen, E. L. E. M., et al. (2008). Strongly reduced volumes of putamen and thalamus in Alzheimer's disease: an MRI study. *Brain* 131, 3277–3285. doi: 10.1093/brain/awn278

Dick, A. S., and Tremblay, P. (2012). Beyond the arcuate fasciculus: consensus and controversy in the connectional anatomy of language. *Brain* 135, 3529–3550. doi: 10.1093/brain/aws222

Doyon, J., Bellec, P., Amsel, R., Penhune, V., Monchi, O., Carrier, J., et al. (2009). Contributions of the basal ganglia and functionally related brain structures to motor learning. *Behav. Brain Res.* 199, 61–75. doi: 10.1016/j.bbr.2008.11.012

Dukart, J., and Bertolino, A. (2014). When structure affects function – the need for partial volume effect correction in functional and resting state magnetic resonance imaging studies. *PLoS ONE* 9:e114227. doi: 10.1371/journal.pone.0114227

Edward, V., Windischberger, C., Cunnington, R., Erdler, M., Lanzenberger, R., Mayer, D., et al. (2000). Quantification of fMRI artifact reduction by a novel plaster cast head holder. *Hum. Brain Mapp.* 11, 207–213. doi: 10.1002/1097-0193(200011)11:3<207::AID-HBM60>3.0.CO;2-J

Elliott, M. R., Bowtell, R. W., and Morris, P. G. (1999). The effect of scanner sound in visual, motor, and auditory functional MRI. *Magn. Reson. Med.* 41, 1230–1235.

Ferreri, F., Pasqualetti, P., Määttä, S., Ponzo, D., Guerra, A., Bressi, F., et al. (2011). Motor cortex excitability in Alzheimer's disease: a transcranial magnetic stimulation follow-up study. *Neurosci. Lett.* 492, 94–98. doi: 10.1016/j.neulet.2011.01.064

Fonov, V., Evans, A., Botteron, K., Almli, C. R., McKinstry, R. C., and Collins, D. L. (2011). Unbiased average age-appropriate atlases for pediatric studies. *NeuroImage* 54, 313–327. doi: 10.1016/j.neuroimage.2010.07.033

Friedman, L., and Glover, G. H. (2006). Report on a multicenter fMRI quality assurance protocol. *J. Magn. Reson. Imaging* 23, 827–839. doi: 10.1002/jmri.20583

Friedman, L., Glover, G. H., and Fbirn Consortium (2006). Reducing interscanner variability of activation in a multicenter fMRI study: controlling for signal-to-fluctuation-noise-ratio (SFNR) differences. *NeuroImage* 33, 471–481. doi: 10.1016/j.neuroimage.2006.07.012

Giove, F., Gili, T., Iacovella, V., Macaluso, E., and Maraviglia, B. (2009). Images-based suppression of unwanted global signals in resting-state functional connectivity studies. *Magn. Reson. Imaging* 27, 1058–1064. doi: 10.1016/j.mri.2009.06.004

Gour, N., Ranjeva, J.-P., Ceccaldi, M., Confort-Gouny, S., Barbeau, E., Soulier, E., et al. (2011). Basal functional connectivity within the anterior temporal network is associated with performance on declarative memory tasks. *NeuroImage* 58, 687–697. doi: 10.1016/j.neuroimage.2011.05.090

Greicius, M. D., Srivastava, G., Reiss, A. L., and Menon, V. (2004). Default-mode network activity distinguishes Alzheimer's disease from healthy aging:

evidence from functional MRI. *Proc. Natl. Acad. Sci. U.S.A.* 101, 4637–4642. doi: 10.1073/pnas.0308627101

Guillozet, A. L., Weintraub, S., Mash, D. C., and Mesulam, M. M. (2003). Neurofibrillary tangles, amyloid, and memory in aging and mild cognitive impairment. *Arch. Neurol.* 60, 729–736. doi: 10.1001/archneur.60.5.729

Haar, S., Berman, S., Behrmann, M., and Dinstein, I. (2014). Anatomical Abnormalities in Autism? *Cereb. Cortex*. doi: 10.1093/cercor/bhu242. [Epub ahead of print].

Hedden, T., van Dijk, K. R. A., Becker, J. A., Sperling, R. A., Johnson, K. A., and Buckner, R. L. (2009). Disruption of functional connectivity in clinically normal older adults harboring amyloid burden. *J. Neurosci.* 29, 12686–12694. doi: 10.1523/JNEUROSCI.3189-09.2009

Humbert, I. A., McLaren, D. G., Kosmatka, K., Fitzgerald, M., Johnson, S., Porcaro, E., et al. (2010). Early deficits in cortical control of swallowing in Alzheimer's disease. *J. Alzheimers Dis.* 19, 1185–1197. doi: 10.3233/JAD-2010-1316

Kelly, C., Biswal, B. B., Craddock, R. C., Castellanos, F. X., and Milham, M. P. (2012). Characterizing variation in the functional connectome: promise and pitfalls. *Trends Cogn. Sci.* 16, 181–188. doi: 10.1016/j.tics.2012.02.001

Klunk, W. E., Price, J. C., Mathis, C. A., Tsopelas, N. D., Lopresti, B. J., Ziolko, S. K., et al. (2007). Amyloid deposition begins in the striatum of presenilin-1 mutation carriers from two unrelated pedigrees. *J. Neurosci.* 27, 6174–6184. doi: 10.1523/JNEUROSCI.0730-07.2007

Koch, W., Teipel, S., Mueller, S., Benninghoff, J., Wagner, M., Bokde, A. L. W., et al. (2012). Diagnostic power of default mode network resting state fMRI in the detection of Alzheimer's disease. *Neurobiol. Aging* 33, 466–478. doi: 10.1016/j.neurobiolaging.2010.04.013

Liang, P., Wang, Z., Yang, Y., and Li, K. (2012). Three subsystems of the inferior parietal cortex are differently affected in mild cognitive impairment. *J. Alzheimers Dis.* 30, 475–487. doi: 10.3233/JAD-2012-111721

Lund, T. E., Madsen, K. H., Sidaros, K., Luo, W.-L., and Nichols, T. E. (2006). Non-white noise in fMRI: does modelling have an impact? *Neuroimage* 29, 54–66. doi: 10.1016/j.neuroimage.2005.07.005

Madsen, S. K., Ho, A. J., Hua, X., Saharan, P. S., Toga, A. W., Jack, C. R., et al. (2010). 3D maps localize caudate nucleus atrophy in 400 Alzheimer's disease, mild cognitive impairment, and healthy elderly subjects. *Neurobiol. Aging* 31, 1312–1325. doi: 10.1016/j.neurobiolaging.2010.05.002

Maruyama, M., Shimada, H., Suhara, T., Shinotoh, H., Ji, B., Maeda, J., et al. (2013). Imaging of tau pathology in a tauopathy mouse model and in alzheimer patients compared to normal controls. *Neuron* 79, 1094–1108. doi: 10.1016/j.neuron.2013.07.037

McDonald, C. R., McEvoy, L. K., Gharapetian, L., Fennema-Notestine, C., Hagler, D. J., Holland, D., et al. (2009). Regional rates of neocortical atrophy from normal aging to early Alzheimer disease. *Neurology* 73, 457–465. doi: 10.1212/WNL.0b013e3181b16431

Mormino, E. C., Smiljic, A., Hayenga, A. O., Onami, S. H., Greicius, M. D., Rabinovici, G. D., et al. (2011). Relationships between β-amyloid and functional connectivity in different components of the default mode network in aging. *Cereb. Cortex* 21, 2399–2407. doi: 10.1093/cercor/bhr025

Nutter-Upham, K. E., Saykin, A. J., Rabin, L. A., Roth, R. M., Wishart, H. A., Pare, N., et al. (2008). Verbal fluency performance in amnestic MCI and older adults with cognitive complaints. *Arch. Clin. Neuropsychol.* 23, 229–241. doi: 10.1016/j.acn.2008.01.005

Packard, M. G., and Knowlton, B. J. (2002). Learning and memory functions of the Basal Ganglia. *Annu. Rev. Neurosci.* 25, 563–593. doi: 10.1146/annurev.neuro.25.112701.142937

Petersen, R. C. (2004). Mild cognitive impairment as a diagnostic entity. *J. Intern. Med.* 256, 183–194. doi: 10.1111/j.1365-2796.2004.01388.x

Petersen, R. C., Doody, R., Kurz, A., Mohs, R. C., Morris, J. C., Rabins, P. V., et al. (2001). Current concepts in mild cognitive impairment. *Arch. Neurol.* 58, 1985–1992. doi: 10.1001/archneur.58.12.1985

Pievani, M., Agosta, F., Pagani, E., Canu, E., Sala, S., Absinta, M., et al. (2010). Assessment of white matter tract damage in mild cognitive impairment and Alzheimer's disease. *Hum. Brain Mapp.* 31, 1862–1875. doi: 10.1002/hbm.20978

Power, J. D., Barnes, K. A., Snyder, A. Z., Schlaggar, B. L., and Petersen, S. E. (2012). Spurious but systematic correlations in functional connectivity MRI networks arise from subject motion. *Neuroimage* 59, 2142–2154. doi: 10.1016/j.neuroimage.2011.10.018

Qi, Z., Wu, X., Wang, Z., Zhang, N., Dong, H., Yao, L., et al. (2010). Impairment and compensation coexist in amnestic MCI default mode network. *Neuroimage* 50, 48–55. doi: 10.1016/j.neuroimage.2009.12.025

Rémy, F., Vayssière, N., Saint-Aubert, L., Barbeau, E., and Pariente, J. (2015). White matter disruption at the prodromal stage of Alzheimer's disease: relationships with hippocampal atrophy and episodic memory performance. *Neuroimage Clin.* 7, 482–492. doi: 10.1016/j.nicl.2015.01.014

Saad, Z. S., Gotts, S. J., Murphy, K., Chen, G., Jo, H. J., Martin, A., et al. (2012). Trouble at rest: how correlation patterns and group differences become distorted after global signal regression. *Brain Connect.* 2, 25–32. doi: 10.1089/brain.2012.0080

Shehzad, Z., Kelly, C., Reiss, P. T., Cameron Craddock, R., Emerson, J. W., McMahon, K., et al. (2014). A multivariate distance-based analytic framework for connectome-wide association studies. *NeuroImage* 93(Pt 1), 74–94. doi: 10.1016/j.neuroimage.2014.02.024

Sheline, Y. I., Morris, J. C., Snyder, A. Z., Price, J. L., Yan, Z., D'Angelo, G., et al. (2010a). APOE4 allele disrupts resting state fMRI connectivity in the absence of amyloid plaques or decreased CSF A 42. *J. Neurosci.* 30, 17035–17040. doi: 10.1523/JNEUROSCI.3987-10.2010

Sheline, Y. I., Raichle, M. E., Snyder, A. Z., Morris, J. C., Head, D., Wang, S., et al. (2010b). Amyloid plaques disrupt resting state default mode network connectivity in cognitively normal elderly. *Biol. Psychiatry* 67, 584–587. doi: 10.1016/j.biopsych.2009.08.024

Small, G. W., Kepe, V., Ercoli, L. M., Siddarth, P., Bookheimer, S. Y., Miller, K. J., et al. (2006). PET of brain amyloid and tau in mild cognitive impairment. *N. Engl. J. Med.* 355, 2652–2663. doi: 10.1056/NEJMoa054625

Sorg, C., Riedl, V., Mühlau, M., Calhoun, V. D., Eichele, T., Läer, L., et al. (2007). Selective changes of resting-state networks in individuals at risk for Alzheimer's disease. *Proc. Natl. Acad. Sci. U.S.A.* 104, 18760–18765. doi: 10.1073/pnas.0708803104

van Dijk, K. R. A., Hedden, T., Venkataraman, A., Evans, K. C., Lazar, S. W., and Buckner, R. L. (2010). Intrinsic functional connectivity as a tool for human connectomics: theory, properties, and optimization. *J. Neurophysiol.* 103, 297–321. doi: 10.1152/jn.00783.2009

Vanhoutte, G., Verhoye, M., and van der Linden, A. (2006). Changing body temperature affects the T2* signal in the rat brain and reveals hypothalamic activity. *Magn. Reson. Med.* 55, 1006–1012. doi: 10.1002/mrm.20861

Villemagne, V. L., Ataka, S., Mizuno, T., Brooks, W. S., Wada, Y., Kondo, M., et al. (2009). High striatal amyloid beta-peptide deposition across different autosomal Alzheimer disease mutation types. *Arch. Neurol.* 66, 1537–1544. doi: 10.1001/archneurol.2009.285

Villeneuve, S., and Jagust, W. J. (2015). Imaging vascular disease and amyloid in the aging brain: implications for treatment. *J. Prev. Alzheimers Dis.* 2, 64–70. doi: 10.14283/jpad.2015.47

Willer, C. J., Li, Y., and Abecasis, G. R. (2010). METAL: fast and efficient meta-analysis of genomewide association scans. *Bioinformatics* 26, 2190–2191. doi: 10.1093/bioinformatics/btq340

Wu, L., Soder, R. B., Schoemaker, D., Carbonnell, F., Sziklas, V., Rowley, J., et al. (2014). Resting state executive control network adaptations in amnestic mild cognitive impairment. *J. Alzheimers Dis.* 40, 993–1004. doi: 10.3233/JAD-131574

Yan, C.-G., Liu, D., He, Y., Zou, Q., Zhu, C., Zuo, X., et al. (2009). Spontaneous Brain activity in the default mode network is sensitive to different resting-state conditions with limited cognitive load. *PLoS ONE* 4:e5743. doi: 10.1371/journal.pone.0005743

Zhang, H.-Y., Wang, S.-J., Liu, B., Ma, Z.-L., Yang, M., Zhang, Z., et al. (2010). Resting brain connectivity: changes during the progress of Alzheimer disease. *Radiology* 256, 598–606. doi: 10.1148/radiol.10091701

**Conflict of Interest Statement:** The authors declare that the research was conducted in the absence of any commercial or financial relationships that could be construed as a potential conflict of interest.

frontiers in Aging Neuroscience

ORIGINAL RESEARCH
published: 09 June 2015
doi: 10.3389/fnagi.2015.00111

# Non-monotonic reorganization of brain networks with Alzheimer's disease progression

*HyoungKyu Kim*[1†], *Kwangsun Yoo*[1†], *Duk L. Na*[2,3], *Sang Won Seo*[2,3], *Jaeseung Jeong*[1*] *and Yong Jeong*[1*]

[1] *Department of Bio and Brain Engineering, Korea Advanced Institute of Science and Technology, Daejeon, South Korea,*
[2] *Department of Neurology, Samsung Medical Center, Sungkyunkwan University School of Medicine, Seoul, South Korea,*
[3] *Neuroscience Center, Samsung Medical Center, Seoul, South Korea*

OPEN ACCESS

***Edited by:***
*Junfeng Sun,*
*Shanghai Jiao Tong University, China*

***Reviewed by:***
*Franziska Matthäus,*
*University of Heidelberg, Germany*
*Rong Fang,*
*Rui Jin Hospital North Affiliated to Shanghai Jiao Tong University School of Medicine, China*

****Correspondence:***
*Jaeseung Jeong,*
*Department of Bio and Brain Engineering, Korea Advanced Institute of Science and Technology, 291 Daehak-ro, Yuseong-gu, Daejeon 305-701, South Korea*
*jsjeong@kaist.ac.kr;*
*Yong Jeong,*
*Laboratory for Cognitive Neuroscience and NeuroImaging, Department of Bio and Brain Engineering, Korea Advanced Institute of Science and Technology, 291 Daehak-ro, Yuseong-gu, Daejeon 305-701, South Korea*
*yong@kaist.ac.kr*

*†These authors have contributed equally to this work.*

***Received:*** *23 October 2014*
***Accepted:*** *27 May 2015*
***Published:*** *09 June 2015*

***Citation:***
*Kim H, Yoo K, Na DL, Seo SW, Jeong J and Jeong Y (2015) Non-monotonic reorganization of brain networks with Alzheimer's disease progression. Front. Aging Neurosci. 7:111. doi: 10.3389/fnagi.2015.00111*

**Background:** Identification of stage-specific changes in brain network of patients with Alzheimer's disease (AD) is critical for rationally designed therapeutics that delays the progression of the disease. However, pathological neural processes and their resulting changes in brain network topology with disease progression are not clearly known.

**Methods:** The current study was designed to investigate the alterations in network topology of resting state fMRI among patients in three different clinical dementia rating (CDR) groups (i.e., CDR = 0.5, 1, 2) and amnestic mild cognitive impairment (aMCI) and age-matched healthy subject groups. We constructed density networks from these 5 groups and analyzed their network properties using graph theoretical measures.

**Results:** The topological properties of AD brain networks differed in a non-monotonic, stage-specific manner. Interestingly, local and global efficiency and betweenness of the network were rather higher in the aMCI and AD (CDR 1) groups than those of prior stage groups. The number, location, and structure of rich-clubs changed dynamically as the disease progressed.

**Conclusions:** The alterations in network topology of the brain are quite dynamic with AD progression, and these dynamic changes in network patterns should be considered meticulously for efficient therapeutic interventions of AD.

**Keywords: Alzheimer's disease, complex network, resting state fMRI, functional connectivity, graph theory**

## Introduction

Alzheimer's disease (AD) is the most common type of dementia, affecting about 5–10% of the population above the age of 65 (Sunderland et al., 2006). Clinical symptoms of AD are characterized by progressive amnesia, followed by a gradual decline in all cognitive functions, resulting in dementia (Sunderland et al., 2006). AD usually exhibits a typical clinical course reflecting the underlying progressing neuropathology (Bianchetti and Trabucchi, 2001; Storey et al., 2002). In the early stage, memory impairment is the prominent feature because the pathology initiates near the medial temporal cortex. In the moderate stage, language problems or visuospatial dysfunctions become conspicuous as the pathology propagates to the other temporal and parietal cortices (Förstl and Kurz, 1999; Bianchetti and Trabucchi, 2001). In the late stage of the illness, most cognitive functions are severely impaired, including frontal executive functions such as judgment, abstract, or logical reasoning, and planning (Braak and Braak, 1991; Fox et al., 2001). The mild cognitive

impairment (MCI) is accompanied by mild memory deterioration but does not disrupt the activities of daily living. Although MCI is very heterogeneous and has multiple subtypes, it is considered to represent an intermediate stage between normal and dementia. MCI has been shown to be more likely to develop AD than cognitively normal (Boyle et al., 2006). Among MCI subtypes, Anmestic MCI (aMCI) is considered as a prodromal stage of AD, having a high-risk for progression to AD (Fischer et al., 2007). In addition, aMCI has been intensitvely investigated for early diagnosis of AD (Petersen, 2004).

Identification of clinical stages in Alzheimer's patients is crucial for the development of appropriate therapeutics that may delay the progression of the disease (Trojanowski et al., 2010). Several studies have attempted to determine the characteristics of each clinical stage of AD based on the distributions and patterns of the neuropathology (Braak and Braak, 1991), cognitive and behavioral performance (Folstein et al., 1975) and severity of clinical features such as the clinical dementia rating (CDR) (Hughes et al., 1982). For example, studies using structural MR imaging have shown that the regional patterns and rate of atrophy differ across AD stages (Scahill et al., 2002; Thompson et al., 2003). Atrophy in the medial temporal lobe commences prior to symptom onset, and is then followed by a reduction in gray matter in the limbic and other neocortices with relative sparing of primary sensory areas. These results are generally consistent with the tau accumulation and the corresponding clinical features (Scahill et al., 2002; Thompson et al., 2003).

In another aspect, there have been several studies supporting the hypothesis that AD is a "disconnection syndrome" (Delbeuck et al., 2003). According to this hypothesis, AD results from the disruption of neuronal connections due to synaptic loss and eventually neuronal death. This feature can be approached by adopting the concept of functional or structural connectivity. As the severity of the disease increases, the functional connectivity among brain regions is assumed to be gradually reduced. Indeed, prior neuroimaging studies have shown that AD patients show disrupted white matter integrity and functional connectivity among distant brain regions (Celone et al., 2006; Zhang et al., 2007). However, how different degrees of disruptions of connectivity in AD across clinical stages influence global information processing of the brain is not clearly understood yet (Wang et al., 2006; Zhou et al., 2008; Bai et al., 2011).

To address this question, the current study employed complex network analysis methods and investigated brain network properties from resting state fMRI in AD, aMCI, and healthy subjects (HS) (Strogatz, 2001; Bullmore and Sporns, 2009). Complex network analysis has shown that the brain has non-random network properties including small world and scale free features and exhibits hierarchical organization with modularity (Achard et al., 2006; Hagmann et al., 2008). Several fMRI and MEG studies have reported that AD and aMCI patients have reduced small-worldness characterized by a longer characteristic path length than that of HS (Stam et al., 2007, 2009; Kendi et al., 2008; Lo et al., 2010). However, we should note that some network properties in AD are not consistent across studies (for reviews, Xie and He, 2011; Tijms et al., 2013), for example, different studies have found increases (Kendi et al., 2008), decreases (Stam et al., 2009), or no significant changes in the clustering coefficient of the brain network in AD patients (Stam et al., 2007; Lo et al., 2010; Sanz-Arigita et al., 2010). Moreover, some studies have reported conflicting results regarding the characteristic path length; one study showed a decrease in the characteristic path length in AD brains (Sanz-Arigita et al., 2010), whereas another study reported no change (Supekar et al., 2008). This discrepancy regarding the change in the network topology of the AD brain might result from the heterogeneity of patient populations at different clinical stages of AD or the different strategy of generating network in the previous studies. To overcome this, we attempted to use the uniformly measured data sets and to raise the stability of network topology during the constructing networks. The parameters of realignment and segmentation of MR images were chosen based on the previous neuroimaging studies using SPM (Della-Maggiore et al., 2002; Maldjian et al., 2003). The density threshold values were also determined as to show the clear features of the brain network as the density value changes in a wide range. The threshold values for the same density network are in Supplementary Table 1.

To the best of our knowledge, there have been no previous studies using graph theoretical measures to investigate the consecutive changes in brain network topology with AD progression. Therefore, the current study investigated and compared topological properties of the brain networks in AD patients in three different CDR stages, patients with aMCI, and age-matched HS.

## Materials and Methods

### Participants

A total of 278 subjects (112 AD, 87 aMCI, and 79 HS) were recruited consecutively at the memory disorder clinic in the Department of Neurology at Samsung Medical Center in Seoul, South Korea between March 2008 and February 2009. Each participant underwent MR scans, clinical interviews, neurological examinations, and comprehensive neuropsychological assessments. Patients with aMCI met the criteria proposed by Petersen et al. (1999). We diagnosed aMCI based on criteria of −1.5 to −1 SD of SVLT score. Patients with AD fulfilled the criteria for probable AD proposed by the National Institute of Neurological and Communicative Disorders and Stroke and the AD and Related Disorders Associations (NINCDS-ADRDA) (McKhann et al., 1984). AD patients were subdivided into three groups according to their CDR (Morris, 1993), 36 with a CDR of 0.5, 55 with a CDR of 1, and 22 with a CDR of 2. The HS group was comprised of 79 subjects with no history of cognitive impairment or neurological or psychiatric illness, and the subjects exhibited normal performance during neuropsychological testing. During various phases, 126 subjects were excluded from the study, and data from 152 subjects was included in the analysis.

While reviewing their neuropsychological tests, we excluded 31 subjects (5 NL, 6 aMCI, 3 AD patients with a CDR score of 0.5, 10 AD patients with a CDR score of 1, and 7 AD patients with a CDR score of 2 whose clinical information was incomplete on at least one neuropsychological item. We then constructed an

individual brain network according to the method described in the following Section Construction of a Brain Network Using Resting State fMRI, but with a threshold of 0.8. We excluded outliers with network degrees below [the first quartile −1.5 times the interquartile range] or above [the third quartile +1.5 times the interquartile range]. The networks with small degrees during the measurement were considered to be noisy data, and the networks with large degrees could be affected by artifacts. The number of outliers excluded in this step was 82. We then again checked group-wise average ages. To match the average age among groups, we additionally excluded 13 subjects in the HS group. Every participant or their caregivers in this study provided written informed consent. This study was approved by the Institutional Review Board of Samsung Medical Center, Seoul, South Korea.

## Neuropsychological Assessments

Each participant underwent neuropsychological testing using the Seoul Neuropsychological Screening Battery (SNSB), a standardized neuropsychological battery that includes validated tests for a variety of cognitive functions such as attention, language, visuospatial function, verbal, and visual memory, frontal executive function, and CDR (Kang and Na, 2003). Among these evaluations, scorable tests included the Digit Span Backward, the Korean version of the Boston Naming Test (K-BNT) (Kim and Na, 1999), the Rey-Osterrieth Complex Figure Test (RCFT) (Lezak, 1983), the Seoul Verbal Learning Test (SVLT; three learning-free recall trials of 12 words, a 20 min delayed recall trial for these 12 items, and a recognition test), motor tests (Contrasting program, a Go/NoGo test), the phonemic and semantic Controlled Oral Word Association Test (COWAT), and the Stroop Test (Color reading of 112 items during 2 min).

## Acquisition and Preprocessing of MRI

MR images were acquired using a 3 Tesla MR scanner (Philips Intera Achieva, Philips Healthcare, The Netherlands). T1-weighted anatomical MR images (TR = 9.9 ms; TE = 4.6 ms; flip angle = 8°; FOV [FH, AP, RL] = 240 × 240 × 180 $mm^2$; matrix = 480 × 480; 360 slices [sagittal]; voxel size = 0.5 × 0.5 × 0.5 $mm^3$) and T2*-weighted MR images (resting state fMRI) were obtained using a gradient echo planar imaging pulse sequence (TR = 3000 ms; TE = 35 ms; flip angle = 90°; FOV [RL, AP, FH] = 220 × 220 × 140 $mm^2$; matrix = 128 × 128; 35 slices [transverse]; voxel size [RL, AP, FH] = 1.72 × 1.72 × 4 $mm^3$).

Pre-processing steps for resting state fMRI included slice-timing correction, motion correction, co-registration, segmentation, spatial normalization into Montreal Neurological Institute (MNI) space, and smoothing as described previously (Yoo et al., 2013). Pre-processing was performed using Statistical Parametric Mapping software 8.0 (SPM, http://www.fil.ion.ucl.ac.uk/spm/) in MATLAB R2011a (7.12).

## Construction of a Brain Network Using Resting State fMRI

We selected 90 brain regions as nodes to construct a brain network using an Automated Anatomical Labeling (AAL) parcellation scheme (Tzourio-Mazoyer et al., 2002). To determine the functional connectivity (i.e., the edges) between the nodes, we calculated mutual information for each pair of 90 fMRI time series extracted from each node. We then constructed a network with the same density for each individual and containing the same number of edges in every individual graph to facilitate comparison of network properties. This allows the comparison between groups with a controlled number of nodes and edges, because network properties with the same threshold change dramatically with their number of degrees.

$$\text{Mutual information} = \sum_{y}\sum_{x} p(x,y) log\left(\frac{p(x,y)}{p\,(x)\,p\,(y)}\right)$$

where $p(x,y)$ is the joint probability distribution function of X and Y, $p(x)$ and $p(y)$ are the marginal probability distribution functions of X and Y, and X, Y are the serial values of fMRI from selected two regions in this study.

The various density values were tested to construct brain networks. Among them, we finally selected the lowest fixed density that provided a sufficiently sparse network with a lower bound of density, minimizing the number of isolated nodes. The threshold of each network was applied separately for fixed density, 7%. The density equals the number of edges divided by possible connections in the network,

$$\text{Density} = \frac{2E}{N(N-1)}$$

wherein the number of nodes $N$ and edges $E$. This allows the controlled comparison of network structure and properties among different groups.

## Graph Theoretical Analysis of the Brain Network

After constructing an individual brain network for each subject, graph theoretical analysis was performed to obtain the topological information of the network. We then compared the whole brain network properties among the five groups (HS, aMCI, CDR 0.5, CDR 1, and CDR 2, ANOVA, and *post-hoc*). We compared seven network parameters, including the characteristic path length, clustering coefficient, global efficiency, local efficiency, betweenness centrality, assortativity, and modularity. The characteristic path length is the average of the minimum number of edges that have to be passed through between nodes. The clustering coefficient of a node is the rate of existing edges between the nearest neighbors vs. possible connections. Global and local efficiency indicate the information transfer between nodes. Global efficiency is the average of the inverse of the shortest path lengths of individual nodes. The local efficiency of an individual node is the inverse of the shortest path length connecting all neighbors of that node. The betweenness centrality of a single node is the number of shortest paths between nodes that must pass through the selected node dividing by the number of all paths to normalize. Assortativity is the correlation between the degrees of connected nodes. A positive assortativity indicates that high-degree nodes tend to connect to each other. The modularity is the fraction of the edges that fall

within the given groups minus the expected fraction if edges were distributed at random. This analysis was performed using the Brain connectivity toolbox (Rubinov and Sporns, 2010). We also investigated the network properties of each brain lobe (frontal, parietal, occipital, and temporal lobes and the subcortical area). To do this, we first calculated nodal values for each of the 90 AAL ROIs and then took the average of these values within each lobe or area. We compared these lobar or areal properties across the five groups with AD progression (ANOVA and *post-hoc*). In this lobar analysis, we supposed that tests for each lobe are independent, hence no correction was applied.

### Correlation Analysis between Network Topology and Clinical Information

We tested whether network properties were correlated with clinical measures by two methods. First, we examined whether a significant correlation existed between network properties and clinical information within each of the five groups. Second, we performed the same correlation analysis including all subjects regardless of groups. We calculated the Pearson's correlation coefficient between the network properties and clinical measures and determined the significance of correlation based on the $p$-value ($p < 0.05$). For the correlation analysis, uncorrected $p$-value was used.

### Rich-club organization

The rich-club in a complex network is a group of hubs having dense connections among themselves. The rich-club organization provides important information on the higher-order hierarchical backbone structure of networks (Colizza et al., 2006; McAuley et al., 2007). The rich-club phenomenon in networks is designed to measure when the hubs of a network tend to be more densely connected among themselves than nodes of a lower degree (Colizza et al., 2006). Networks having a relatively high rich-club coefficient show the rich-club effect and have many links between high degree nodes. The rich-club coefficient of a network is can be a measurement of the robustness. The networks are usually resilient with high rich-club coefficient, because the densely connected hubs can maintain the network structure easily. The rich-club coefficients of networks were also calculated in each group. We computed the rich-club coefficients $\Phi(k)$ of the networks over a range of degrees ($k$). For a degree ($k$), the edges and nodes with a smaller degree than $k$ were removed from the network. In the remaining network, the rich-club coefficient $\Phi(k)$ is the ratio of the current edges and possible number of edges among remaining nodes,

$$\Phi\left(k\right) = \frac{2E_{>k}}{N_{>k}\left(N_{>k}-1\right)}$$

where $N$ is the number of remaining nodes and $E$ is the number of current edges. The rich-club coefficient $\Phi(k)$ can be normalized with a set of random networks of the same size and similar degree distribution. A normalized rich-club coefficient $\Phi_{norm}$ of >1 can be described as a rich-club organization in a network (Colizza et al., 2006). We calculated the rich-club curve comparing the rich-club coefficient between subject groups and 1000 random networks by rewiring edges with a similar degree distribution for each level of $k$,

$$\Phi_{norm}\left(k\right) = \frac{\Phi\left(k\right)}{\Phi_{random}\left(k\right)}$$

We also determined whether the permutation test from the 1000 random networks was statistically significant. We showed that $\Phi\left(k\right)$ was significantly greater than the distribution of $\Phi_{random}\left(k\right)$, with a $p < 0.05$.

### Statistical Test

For the statistical tests, we used One-Way ANOVA for group difference of each property, and the Tukey's honest significant difference (HSD) test for *post-hoc* test in every comparison. The Tukey's HSD was optimal for One-Way ANOVA and similar procedures with equal sizes originally. As you already know, it has been confirmed to be conservative for One-Way ANOVA with the different sample sizes as well.

## Results

The demographics and neuropsychological results of subjects in the current study are listed in **Table 1**. There were significant differences among groups, with the higher CDR group showing poorer performance in every cognitive domain.

We investigated changes in the topology of brain networks spanning from HS, to subjects with aMCI, to subjects in the AD spectrum. **Figure 1** shows the reorganization of the network from the HS to AD patients with a CDR of 2 (ANOVA and *post-hoc*) with respect to three parameters: global efficiency, local efficiency, and betweenness centrality. We found a non-monotonic change in the brain network as AD progressed; these 3 network properties are higher in aMCI and CDR 1 groups than other three groups. In common, these three network properties were significantly lower in the CDR 0.5 group compared with the aMCI group or the CDR 1 group ($p < 0.05$, uncorrected).In addition, we estimated the characteristic path length, clustering coefficient, modularity, and assortativity and found similar fluctuating patterns with AD progression (see Supplementary Figure 1).

We then determined whether the topology of the brain network correlated with the performance of particular cognitive functions. We performed a correlation analysis between network measures and neuropsychological test scores for each group separately (**Table 2** and Supplementary Table 2). We found significant correlations between network properties and neuropsychological test scores primarily in the aMCI group ($p < 0.05$, uncorrected). The aMCI group showed a negative correlation between the scores of the Digit Span Backward, Naming K-BNT, RCFT copy, Go/NoGo, and COWAT Semantic tests and network properties. The HS showed significant correlations between the Stroop Test scores and network measures (global efficiency, betweenness centrality, and characteristic path length). In addition, the CDR 0.5 group showed significant positive correlations between the COWAT Phonemic score and betweenness centrality and characteristic

**TABLE 1 | Demographics and clinical information.**

| | HC | aMCI | AD CDR 0.5 | AD CDR 1 | AD CDR 2 |
|---|---|---|---|---|---|
| Subjects | 31 (26F) | 50 (28F) | 25 (15F) | 36 (20F) | 10 (6F) |
| Age | 67.6 (±6.3) | 70.4 (±7.6) | 70.0 (±8.4) | 72.6 (±7.7) | 70.9 (±6.9) |
| Digit span backward | 4.3 (±1.5) | 3.5 (±1.0) | 2.9 (±1.3)$^{aaa}$ | 2.8 (±1.3)$^{aaa}$ | 2.9 (±1.1)$^{a}$ |
| K-BNT | 48.5 (±7.5) | 40.6 (±9.3)$^{aa}$ | 35.0 (±12.5)$^{aaa}$ | 36.5 (±10.1)$^{aaa}$ | 30.6 (±11.7)$^{aaab}$ |
| RCFT copy | 32.2 (±5.0) | 29.9 (±5.2) | 23.8 (±11.4)$^{aab}$ | 23.4 (±9.9)$^{aaabb}$ | 21.4 (±10.9)$^{aab}$ |
| SVLT delayed | 7.4 (±2.0) | 2.5 (±2.4)$^{aaa}$ | 1.0 (±1.9)$^{aaab}$ | 0.6 (±1.1)$^{aaabbb}$ | 0.4 (±1.3)$^{aaab}$ |
| RCFT delayed | 15.0 (±3.9) | 7.9 (±5.2)$^{aaa}$ | 2.6 (±2.8)$^{aaabbb}$ | 1.7 (±3.0)$^{aaabbb}$ | 1.1 (±1.9)$^{aaabbb}$ |
| Contrasting program | 19.9 (±0.2) | 19.7 (±1.4) | 18.4 (±4.5) | 15.4 (±7.2)$^{aaabbb}$ | 11.4 (±8.6)$^{aaabbbccc}$ |
| Go/NoGo test | 19.6 (±1.1) | 18.7 (±3.1) | 16.1 (±5.3) | 12.0 (±6.7)$^{aaabbbcc}$ | 8.2 (±6.7)$^{aaabbbccc}$ |
| Stroop test color reading | 87.7 (±23.3) | 73.8 (±23.9) | 48.8 (±29.5)$^{aaabbb}$ | 39.5 (±25.1)$^{aaabbb}$ | 20.6 (±16.0)$^{aaabbbc}$ |
| MMSE | 28.6 (±1.9) | 26.5 (±2.2)$^{a}$ | 22.4 (±3.9)$^{aaabbb}$ | 19.6 (±4.0)$^{aaabbbcc}$ | 17.0 (±3.4)$^{aaabbbccc}$ |
| CDR sum of boxes (SNSB) | 0.7 (±0.5) | 1.3 (±0.8) | 3.1 (±1.3)$^{aaabbb}$ | 5.2 (±1.4)$^{aaabbbccc}$ | 10.8 (±1.9)$^{aaabbbcccddd}$ |
| COWAT semantic | 32.4 (±7.5) | 24.4 (±7.5)$^{aaa}$ | 21.4 (±6.9)$^{aaa}$ | 18.2 (±6.9)$^{aaabbb}$ | 12.9 (±5.3)$^{aaabbbc}$ |
| COWAT phonemic | 28.1 (±10.8) | 18.4 (±9.7)$^{aaa}$ | 17.6 (±11.1)$^{aaa}$ | 13.5 (±8.3)$^{aaa}$ | 11.8 (±8.8)$^{aaa}$ |

*ANOVA and post-hoc analysis was performed.*
*Significantly different when compared to normal (a: $p < 0.05$, aa: $p < 0.01$, aaa: $p < 0.001$).*
*Compared to aMCI (b: $p < 0.05$, bb: $p < 0.01$, bbb: $p < 0.001$).*
*Compared to AD CDR 0.5 (c: $p < 0.05$, cc: $p < 0.01$, ccc: $p < 0.001$).*
*Compared to AD CDR 1 (ddd: $p < 0.001$).*

path length. In contrast, no significant correlations were found between neuropsychological test performances and network measures in the CDR 1 and CDR 2 groups. All significant results were negative correlations (except those found in the CDR 0.5 group) and are shown in **Table 2** and Supplementary Table 2. In addition, we performed the same analysis for all subjects and found a significant negative correlation of the COWAT semantic score with network topologies (betweenness centrality, characteristic path length, and clustering coefficient, $p < 0.05$, uncorrected, Supplementary Table 3).

Next, we examined whether the changes in the network properties of each lobe were reflected in whole-brain topology as AD progresses. For each of the three network measures, global, and local efficiency and betweenness centrality, the bilateral temporal lobe and right subcortex showed a non-monotonic reorganization with AD progression (**Figure 2**). Particularly, the left frontal lobe exhibited this reorganization pattern for global efficiency and betweenness centrality, whereas the left subcortex exhibited this reorganization with respect to local efficiency and betweenness (**Figure 2**). In addition, the right frontal and parietal lobes displayed similar non-monotonic reorganization only for betweenness centrality.

We determined if there were significant changes in lobar network properties among AD groups. For global efficiency, the right parietal lobe showed significantly lower efficiency in the CDR 0.5 and CDR 2 groups compared to the HS group ($p < 0.05$), and the right temporal lobe showed an higher in the CDR 1 group compared with the CDR 0.5 group ($p < 0.05$). For local efficiency, the right parietal lobe showed lower efficiency in the aMCI compared to the HS group ($p < 0.05$), and the right temporal lobe was higher in the CDR 1 group compared to its preceding group, CDR 0.5 ($p < 0.05$). In left hemisphere, the temporal lobe was higher in the aMCI and CDR 1 groups compared to the HS and CDR 0.5 groups, respectively ($p < 0.05$). All significant results are shown in **Figure 2**. Other network properties, i.e., the characteristic path length, clustering coefficient, modularity, and assortativity, also exhibited a similar pattern of change with AD progression (see Supplementary Figure 2).

Lastly, we examined the rich-club organization of the brain networks with AD progression. **Figures 3A–D**) shows the rich-club coefficient, normalized rich-club coefficient, number of nodes, and number of edges as a function of degree threshold k from 1 to 15 for AD patients in different CDR stages and HS. For $k$-values larger than 9, the largest normalized rich-club coefficient was observed in the HS group, followed by the CDR 1 group. The remaining groups showed similar normalized rich-club coefficients within a range of 1–1.5. For $k$-values equal to 9, the aMCI and CDR 1 groups exhibited higher original and normalized rich-club coefficients and a greater number of links within the rich-club organization relative to the other AD stages.

We observed varying distribution patterns of rich-club nodes for the degree threshold $k = 9$ across AD stages (**Figure 3E**). For a $k$ of 9, the numbers of nodes of the rich-clubs were 21, 28, 25, 22, and 25, and the numbers of edges were 68, 124, 70, 93, and 88 from the HS to the CDR 2 group. The original rich-club coefficients for $k = 9$ were 0.32, 0.33, 0.23, 0.4, and 0.29, and the normalized rich-club coefficients were 1.41, 1.42, 1.05, 1.76, and 1.30 from the HS to the CDR 2 group. The rich-club coefficients of the original and normalized values and the number of edges within the rich-club varied non-monotonically, similar to the change of the whole brain network properties as AD progresses. Within the rich-club core of the brain, frontal regions were not connected with posterior regions in the HS group. In contrast, in the aMCI group, the rich-club consisted of an increased number of frontal regions, and those were well-connected with the other

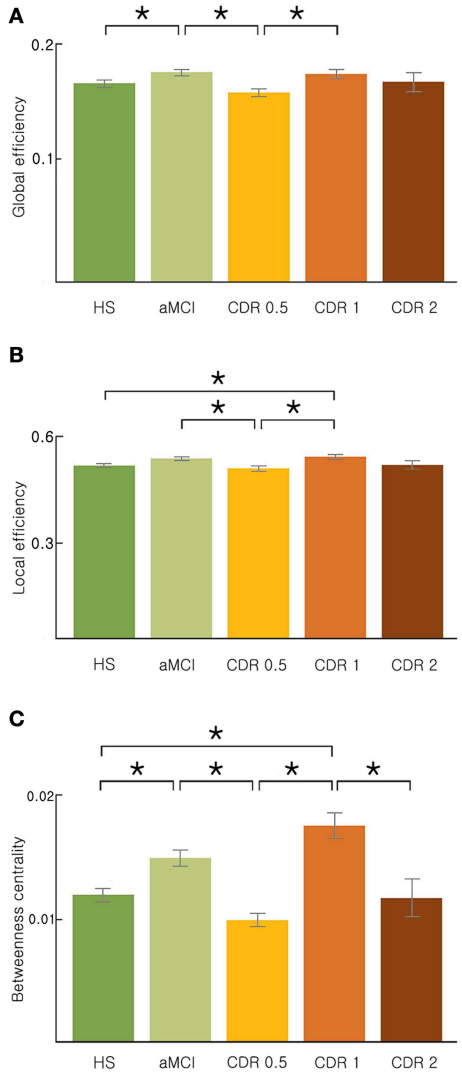


**FIGURE 1 | Topological properties of the AD brain networks with the disease progression. (A)** Global efficiency, **(B)** local efficiency, and **(C)** betweenness centrality changed stage-specifically in a non-monotonic manner. Significance is represented by an asterisk ($p < 0.05$, ANOVA and *post-hoc*).

posterior (parietal and occipital) regions. Interestingly, these frontal regions and their connectivity gradually decreased and disappeared in the CDR 1 group before increasing again in the CDR 2 group.

## Discussion

We investigated changes in network properties from HS to subjects with prodromal and intermediate stages of AD by comparing topological measures of the brain network and determining their relationship with behavioral and clinical test scores. The current study first examined the whole process of alterations in brain networks from the time before AD onset to a severe AD stage. To properly examine and compare the topological reorganization of the brain network, it was necessary to construct networks with similar size. In the current study, we constructed a brain network with the same density (sparsity), avoiding the use of a specific threshold value. Because the density network contains the same number of edges, we were able to compare brain networks of the same size among groups.

We demonstrated the ongoing reorganization process of the brain network with AD progression. However, we did not observe a correlation between any network measure and clinical deterioration, e.g., CDR. Unexpectedly, this reorganization occurred stage-specifically in a non-monotonic manner (**Figure 1** and Supplementary Figure 1). It has been proposed that the progression of AD follows a sigmoidal curve (Jack and Holtzman, 2013). However, the smooth progressive change in each parameter is rather presumptive and mainly based on interpolation or extrapolation of limited evidence. Given the five stages of AD progression, we revealed that network topological properties, including network efficiency and betweenness centrality, were higher in the aMCI and CDR 1 groups compared to other AD groups or HS. First, the brain network in the aMCI group exhibited significantly higher efficiency compared to that of the previous stage, the HS group. Higher network efficiency and betweenness centrality would result from the presence of additional hub regions. In addition, the results from the correlation analysis between neuropsychological test scores and network properties support a stage-specific non-monotonicity. We found that correlations between neuropsychological scores

**TABLE 2 | Correlation between network properties and clinical information within each group ($p < 0.05$, uncorrected, $p/R^2/r$).**

| | | Global efficiency | Local efficiency | Betweenness centrality |
|---|---|---|---|---|
| HS | Stroop test color-reading correct | 0.035/0.145/−0.381 | – | 0.025/0.162/−0.402 |
| aMCI | Digit span backward | – | – | 0.028/0.096/−0.310 |
| | Naming K-BNT | – | 0.021/0.106/−0.325 | 0.022/0.104/−0.323 |
| | RCFT copy | – | 0.028/0.096/−0.310 | – |
| | Go/NoGo | – | 0.010/0.131/−0.361 | 0.025/0.100/−0.317 |
| | COWAT semantic | 0.029/0.096/−0.310 | 0.010/0.131/−0.361 | 0.010/0.132/−0.363 |
| AD CDR 0.5 | COWAT phonemic | – | – | 0.031/0.187/0.433 |

*HS, healthy subject; aMCI, amnestic mild cognitive impairment; AD, Alzheimer's disease; CDR, clinical dementia rating.*
*$R^2$: goodness of fit by coefficient of determination; r: Person's correlation coefficient.*

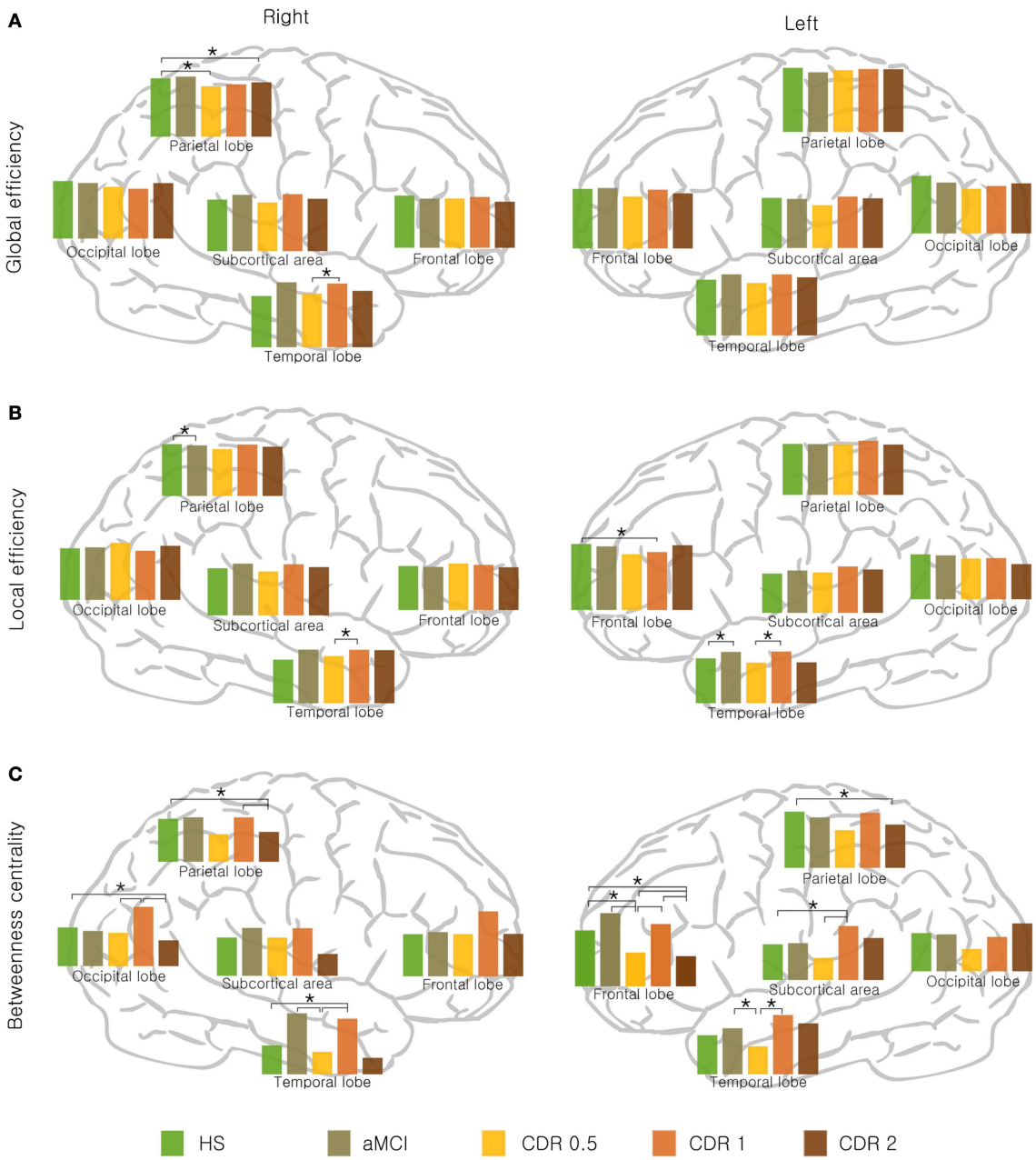


**FIGURE 2 | Lobar network properties with AD progression. (A)** Global efficiency, **(B)** local efficiency, and **(C)** betweenness centrality changed stage-specifically in a non-monotonic manner. Significance is represented by an asterisk ($p < 0.05$, ANOVA and *post-hoc*).

and network properties were distinguishable among each group of AD progression (**Table 2**, and Supplementary Tables 2, 3). The speculation for this finding is described in Supplementary Material.

It is interesting and unusual that an advanced disease stage has higher network efficiency than a previous stage. We speculate that this finding is in line with previous studies reporting hyperactivation in the hippocampus and other memory-related areas during cognitive and memory-related tasks in MCI patients (Dickerson et al., 2005; Hämäläinen et al., 2007) compared to HS and AD patients. In addition to the task-induced activation, increased resting state connectivity in aMCI patients compared to HS has also been reported (Sohn et al., 2014). Another study demonstrated that MCI patients exhibiting faster cognitive decline have greater hippocampal activation (Miller et al., 2008). Given that the resting state connectivity and the brain activation show a positive correlation with each other (Mennes et al., 2011), our result of increased brain network efficiency in aMCI patients is consistent with the aforementioned studies. The reorganization process of the rich-club core with AD progression is speculated

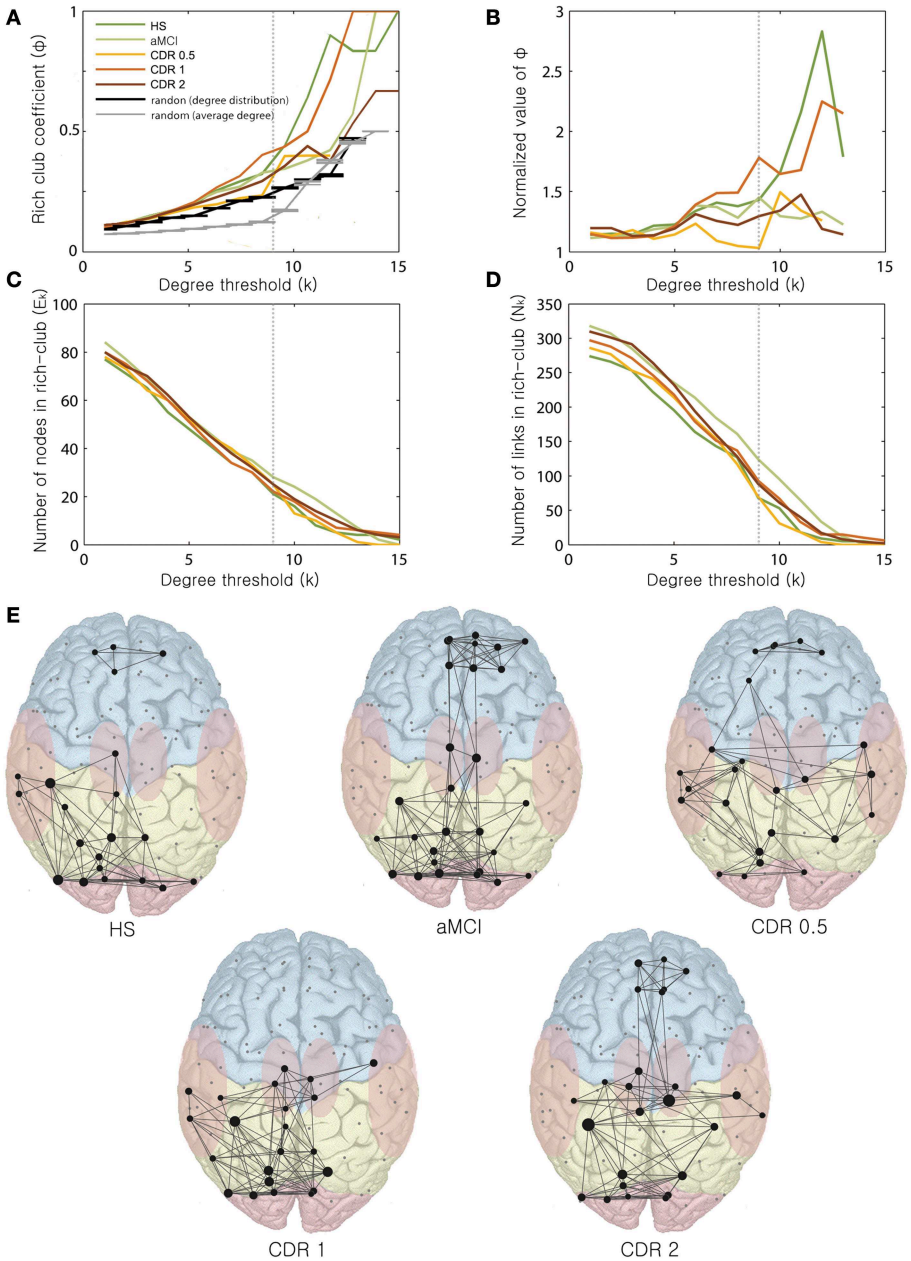


**FIGURE 3 | Changes in rich-club organization as a function of k.** Changes of the **(A)** rich-club coefficient, **(B)** normalized rich-club coefficient, **(C)** number of nodes within the rich-club, and **(D)** number of links within the rich-club are displayed with varying *k*-values ranging from 0 to 15. **(E)** Rich-club organization with AD progression. Representative networks for each stage are shown for $k = 9$.

in detail with other possibilities and scenarios of non-monotonic changes in AD brain networks in Supplementary Material.

We should be cautious in interpreting the results, because there are several limitations and ambiguous outcomes from these analyses. Moreover, we should note that these results appear to contrast with those of other previous studies. Based on this discrepancy, it is likely uncertain whether the non-monotonic changes in network parameters are generated by disease progression or not. We also mention that the mechanisms underlying the connections between network parameters and disease progression are not clear, because the parameters tended to be non-monotonic. Another recent study showed increasing path length and decreasing small-worldness of the density network with AD progression (Sun et al., 2014). This can be seen as opposite contrasting result with our study, although that study used different group stratification and different measurements of network construction compared with this study. We chose mutual information as a measure of functional connectivity, whereas the most common measure is the Pearson's correlation coefficient. The Pearson's correlation

provides information about the linear relationship between regions but does not detect non-linear interactions among regions. Therefore, as an alternative approach that accounts for non-linear interactions, we used mutual information to construct the information transmission network of the brain. However, the path length used in the current study showed a mildly significant increase with the disease progression, whereas Sun et al. showed some regional betweenness centrality changes in non-monotonic values with disease progression. This discrepancy in the results between the studies using similar data and methods suggest that other elements may influence these network properties and indicate our limited understanding of the innate causal relationship between network parameters and AD. Based on these potential explanations for the observed non-monotonic network parameter changes in the current study, the possibility that our conclusions are incorrect or produced from other influences may not be excluded.

Rich-club organization also plays an unclear role in these results. Differences in rich-club network structure were observed not only between the groups exhibiting significantly different network parameters but also between groups exhibiting similar values. This makes our results difficult to interpret because the innate cause of rich-club structure changes remains still unclear. We should admit that the *post-hoc* analysis did not produce significant results in the analysis of lobar parameters. Because of the insufficient number of subjects in some groups, it is likely assumed that the lobar parameters are independent of each other. The *post-hoc* tests were calculated only for group dependency. This limitation suggests that we should interpret our major finding of the non-monotonic changes in the lobar parameters with extreme caution. In addition, we noted that HS, aMCI and AD severity in each CDR category were continuous variables in this analysis; however, since this study was a cross-sectional study, a longitudinal analysis is required to investigate the changes in each patient over time. The diagnoses of AD and aMCI were based on clinical criteria without any pathological or amyloid imaging data. Thus, dementia of other origins may have been included in these diagnoses, particularly aMCI. The large number of excluded subjects due to age-matching and abnormal correlation values between regions is another limitation of this study.

The change of brain network by AD progression and the innate principles are not fully uncovered. The diverse and even opposed results are reported through attempting various methods and measurements. This can be a good time to investigate this issue more seriously to find the causal relationship between brain network and disease progress of AD.

## Acknowledgments

This research was supported by Basic Science Research Program through the National Research Foundation of Korea (NRF) funded by the Ministry of Education (NRF-2012R1A1A2044776), the Brain Research Program through the National Research Foundation of Korea (NRF) funded by the Ministry of Science, ICT and Future Planning (NRF-2010-0018843), the Basic Science Program through the National Research Foundation of Korea (NRF) funded by the Ministry of Education (NRF-2006-2005399), and the Brain Research Program through the National Research Foundation of Korea (NRF) funded by the Ministry of Science, ICT and Future Planning (NRF-2013R1A1A2011570).

## Supplementary Material

The Supplementary Material for this article can be found online at: http://journal.frontiersin.org/article/10.3389/fnagi.2015.00111/abstract

## References

Achard, S., Salvador, R., Whitcher, B., Suckling, J., and Bullmore, E. (2006). A resilient, low-frequency, small-world human brain functional network with highly connected association cortical hubs. *J. Neurosci.* 26, 63–72. doi: 10.1523/JNEUROSCI.3874-05.2006

Bai, F., Xie, C., Watson, D. R., Shi, Y., Yuan, Y., Wang, Y., et al. (2011). Aberrant hippocampal subregion networks associated with the classifications of aMCI subjects: a longitudinal resting-state study. *PLoS ONE* 6:e29288. doi: 10.1371/journal.pone.0029288

Bianchetti, A., and Trabucchi, M. (2001). Clinical aspects of Alzheimer's disease. *Aging Clin. Exp. Res.* 13, 221–230. doi: 10.1007/BF03351480

Boyle, P. A., Wilson, R. S., Aggarwal, N. T., Tang, Y., and Bennett, D. A. (2006). Mild cognitive impairment: risk of Alzheimer disease and rate of cognitive decline. *Neurology* 67, 441–445. doi: 10.1212/01.wnl.0000228244.10416.20

Braak, H., and Braak, E. (1991). Neuropathological stageing of Alzheimer-related changes. *Acta Neuropathol.* 82, 239–259. doi: 10.1007/BF00308809

Bullmore, E., and Sporns, O. (2009). Complex brain networks: graph theoretical analysis of structural and functional systems. *Nat. Rev. Neurosci.* 10, 186–198. doi: 10.1038/nrn2575

Celone, K. A., Calhoun, V. D., Dickerson, B. C., Atri, A., Chua, E. F., Miller, S. L., et al. (2006). Alterations in memory networks in mild cognitive impairment and Alzheimer's disease: an independent component analysis. *J. Neurosci.* 26, 10222–10231. doi: 10.1523/JNEUROSCI.2250-06.2006

Colizza, V., Flammini, A., Serrano, M. A., and Vespignani, A. (2006). Detecting rich-club ordering in complex networks. *Nat. Phys.* 2, 110–115. doi: 10.1038/nphys209

Delbeuck, X., van der Linden, M., and Collette, F. (2003). Alzheimer' Disease as a Disconnection Syndrome? *Neuropsychol. Rev.* 13, 79–92. doi: 10.1023/A:1023832305702

Della-Maggiore, V., Chau, W., Peres-Neto, P. R., and McIntosh, A. R. (2002). An empirical comparison of SPM preprocessing parameters to the analysis of fMRI data. *Neuroimage* 17, 19–28. doi: 10.1006/nimg.2002.1113

Dickerson, B., Salat, D., Greve, D., Chua, E., Rand-Giovannetti, E., Rentz, D., et al. (2005). Increased hippocampal activation in mild cognitive impairment compared to normal aging and AD. *Neurology* 65, 404–411. doi: 10.1212/01.wnl.0000171450.97464.49

Fischer, P., Jungwirth, S., Zehetmayer, S., Weissgram, S., Hoenigschnabl, S., Gelpi, E., et al. (2007). Conversion from subtypes of mild cognitive impairment to Alzheimer dementia. *Neurology* 68, 288–291. doi: 10.1212/01.wnl.0000252358.03285.9d

Folstein, M. F., Folstein, S. E., and McHugh, P. R. (1975). "Mini-mental state": a practical method for grading the cognitive state of patients for the clinician. *J. Psychiatr. Res.* 12, 189–198. doi: 10.1016/0022-3956(75)90026-6

Förstl, H., and Kurz, A. (1999). Clinical features of Alzheimer's disease. *Eur. Arch. Psychiatry Clin. Neurosci.* 249, 288–290. doi: 10.1007/s004060050101

Fox, N. C., Crum, W. R., Scahill, R. I., Stevens, J. M., Janssen, J. C., and Rossor, M. N. (2001). Imaging of onset and progression of Alzheimer's disease with

voxel-compression mapping of serial magnetic resonance images. *Lancet* 358, 201–205. doi: 10.1016/S0140-6736(01)05408-3

Hagmann, P., Cammoun, L., Gigandet, X., Meuli, R., Honey, C. J., Wedeen, V. J., et al. (2008). Mapping the structural core of human cerebral cortex. *PLoS Biol.* 6:e159. doi: 10.1371/journal.pbio.0060159

Hämäläinen, A., Pihlajamäki, M., Tanila, H., Hänninen, T., Niskanen, E., Tervo, S., et al. (2007). Increased fMRI responses during encoding in mild cognitive impairment. *Neurobiol. Aging* 28, 1889–1903. doi: 10.1016/j.neurobiolaging.2006.08.008

Hughes, C. P., Berg, L., Danziger, W. L., Coben, L. A., and Martin, R. L. (1982). A new clinical scale for the staging of dementia. *Br. J. Psychiatry* 140, 566–572. doi: 10.1192/bjp.140.6.566

Jack, C. R. Jr., and Holtzman, D. M. (2013). Biomarker modeling of Alzheimer's disease. *Neuron* 80, 1347–1358. doi: 10.1016/j.neuron.2013.12.003

Kang, Y., and Na, D. (2003). *Seoul Neuropsychological Screening Battery*. Incheon: Human Brain Research & Consulting Co.

Kendi, A. K., Lehericy, S., Luciana, M., Ugurbil, K., and Tuite, P. (2008). Altered diffusion in the frontal lobe in Parkinson disease. *Am. J. Neuroradiol.* 29, 501–505. doi: 10.3174/ajnr.A0850

Kim, H., and Na, D. L. (1999). BRIEF REPORT normative data on the Korean version of the Boston naming test. *J. Clin. Exp. Neuropsychol.* 21, 127–133. doi: 10.1076/jcen.21.1.127.942

Lezak, M. (1983). *Neuropsychological Assessment*. New York, NY: Oxford University Press.

Lo, C.-Y., Wang, P.-N., Chou, K.-H., Wang, J., He, Y., and Lin, C.-P. (2010). Diffusion tensor tractography reveals abnormal topological organization in structural cortical networks in Alzheimer's disease. *J. Neurosci.* 30, 16876–16885. doi: 10.1523/JNEUROSCI.4136-10.2010

Maldjian, J. A., Laurienti, P. J., Kraft, R. A., and Burdette, J. H. (2003). An automated method for neuroanatomic and cytoarchitectonic atlas-based interrogatino of fMRi data sets. *Neuroimage* 19, 1233–1239. doi: 10.1016/S1053-8119(03)00169-1

McAuley, J. J., da Fontoura Costa, L., and Caetano, T. S. (2007). Rich-club phenomenon across complex network hierarchies. *Appl. Phys. Lett.* 91, 084103. doi: 10.1063/1.2773951

McKhann, G., Drachman, D., Folstein, M., Katzman, R., Price, D., and Stadlan, E. M. (1984). Clinical diagnosis of Alzheimer's disease Report of the NINCDS—ADRDA Work Group* under the auspices of department of health and human services task force on Alzheimer's disease. *Neurology* 34, 939–939. doi: 10.1212/WNL.34.7.939

Mennes, M., Zuo, X.-N., Kelly, C., Di Martino, A., Zang, Y.-F., Biswal, B., et al. (2011). Linking inter-individual differences in neural activation and behavior to intrinsic brain dynamics. *Neuroimage* 54, 2950–2959. doi: 10.1016/j.neuroimage.2010.10.046

Miller, S. L., Fenstermacher, E., Bates, J., Blacker, D., Sperling, R. A., and Dickerson, B. C. (2008). Hippocampal activation in adults with mild cognitive impairment predicts subsequent cognitive decline. *J. Neurol. Neurosurg. Psychiatry* 79, 630–635. doi: 10.1136/jnnp.2007.124149

Morris, J. C. (1993). The clinical dementia rating (CDR): current version and scoring rules. *Neurology* 43, 2412–2414. doi: 10.1212/WNL.43.11.2412-a

Petersen, R. C. (2004). Mild cognitive impairment as a diagnostic entity. *J. Intern. Med.* 256, 183–194. doi: 10.1111/j.1365-2796.2004.01388.x

Petersen, R. C., Smith, G. E., Waring, S. C., Ivnik, R. J., Tangalos, E. G., and Kokmen, E. (1999). Mild cognitive impairment: clinical characterization and outcome. *Arch. Neurol.* 56, 303–308. doi: 10.1001/archneur.56.3.303

Rubinov, M., and Sporns, O. (2010). Complex network measures of brain connectivity: uses and interpretations. *Neuroimage* 52, 1059–1069. doi: 10.1016/j.neuroimage.2009.10.003

Sanz-Arigita, E. J., Schoonheim, M. M., Damoiseaux, J. S., Rombouts, S. A., Maris, E., Barkhof, F., et al. (2010). Loss of 'small-world' networks in Alzheimer's disease: graph analysis of FMRI resting-state functional connectivity. *PLoS ONE* 5:e13788. doi: 10.1371/journal.pone.0013788

Scahill, R. I., Schott, J. M., Stevens, J. M., Rossor, M. N., and Fox, N. C. (2002). Mapping the evolution of regional atrophy in Alzheimer's disease: unbiased analysis of fluid-registered serial MRI. *Proc. Natl. Acad. Sci. U.S.A.* 99, 4703–4707. doi: 10.1073/pnas.052587399

Sohn, W. S., Yoo, K., Na, D. L., and Jeong, Y. (2014). Progressive changes in hippocampal resting-state connectivity across cognitive impairment: a cross-sectional study from normal to alzheimer disease. *Alzheimer Dis. Ass. Disord.* 28, 239–246. doi: 10.1097/WAD.0000000000000027

Stam, C., de Haan, W., Daffertshofer, A., Jones, B., Manshanden, I., van Walsum, A. V. C., et al. (2009). Graph theoretical analysis of magnetoencephalographic functional connectivity in Alzheimer's disease. *Brain* 132, 213–224. doi: 10.1093/brain/awn262

Stam, C., Jones, B., Nolte, G., Breakspear, M., and Scheltens, P. (2007). Small-world networks and functional connectivity in Alzheimer's disease. *Cereb. Cortex* 17, 92–99. doi: 10.1093/cercor/bhj127

Storey, E., Slavin, M. J., and Kinsella, G. J. (2002). Patterns of cognitive impairment in Alzheimer's disease: assessment and differential diagnosis. *Front. Biosci.* 7, e155–184. doi: 10.2741/storey

Strogatz, S. H. (2001). Exploring complex networks. *Nature* 410, 268–276. doi: 10.1038/35065725

Sun, Y., Yin, Q., Fang, R., Yan, X., Wang, Y., Bezerianos, A., et al. (2014). Disrupted functional brain connectivity and its association to structural connectivity in amnestic mild cognitive impairment and Alzheimer's disease. *PLoS ONE* 9:e96505. doi: 10.1371/journal.pone.0096505

Sunderland, T., Hampel, H., Takeda, M., Putnam, K. T., and Cohen, R. M. (2006). Biomarkers in the diagnosis of Alzheimer's disease: are we ready? *J. Geriatr. Psychiatry Neurol.* 19, 172–179. doi: 10.1177/0891988706291088

Supekar, K., Menon, V., Rubin, D., Musen, M., and Greicius, M. D. (2008). Network analysis of intrinsic functional brain connectivity in Alzheimer's disease. *PLoS Comput. Biol.* 4:e1000100. doi: 10.1371/journal.pcbi.1000100

Thompson, P. M., Hayashi, K. M., de Zubicaray, G., Janke, A. L., Rose, S. E., Semple, J., et al. (2003). Dynamics of gray matter loss in Alzheimer's disease. *J. Neurosci.* 23, 994–1005.

Tijms, B. M., Wink, A. M., de Haan, W., van der Flier, W. M., Stam, C. J., Scheltens, P., et al. (2013). Alzheimer's disease: connecting findings from graph theoretical studies of brain networks. *Neurobiol. Aging* 34, 2023–2036. doi: 10.1016/j.neurobiolaging.2013.02.020

Trojanowski, J. Q., Vandeerstichele, H., Korecka, M., Clark, C. M., Aisen, P. S., Petersen, R. C., et al. (2010). Update on the biomarker core of the Alzheimer's Disease Neuroimaging Initiative subjects. *Alzheimer Dement.* 6, 230–238. doi: 10.1016/j.jalz.2010.03.008

Tzourio-Mazoyer, N., Landeau, B., Papathanassiou, D., Crivello, F., Etard, O., Delcroix, N., et al. (2002). Automated anatomical labeling of activations in SPM using a macroscopic anatomical parcellation of the MNI MRI single-subject brain. *Neuroimage* 15, 273–289. doi: 10.1006/nimg.2001.0978

Wang, L., Zang, Y., He, Y., Liang, M., Zhang, X., Tian, L., et al. (2006). Changes in hippocampal connectivity in the early stages of Alzheimer's disease: evidence from resting state fMRI. *Neuroimage* 31, 496–504. doi: 10.1016/j.neuroimage.2005.12.033

Xie, T., and He, Y. (2011). Mapping the Alzheimer's brain with connectomics. *Front. Psychiatry* 2:77. doi: 10.3389/fpsyt.2011.00077

Yoo, K., Sohn, W. S., and Jeong, Y. (2013). Tool-use practice induces changes in intrinsic functional connectivity of parietal areas. *Front. Hum. Neurosci.* 7:49. doi: 10.3389/fnhum.2013.00049

Zhang, Y., Schuff, N., Jahng, G.-H., Bayne, W., Mori, S., Schad, L., et al. (2007). Diffusion tensor imaging of cingulum fibers in mild cognitive impairment and Alzheimer disease. *Neurology* 68, 13–19. doi: 10.1212/01.wnl.0000250326.77323.01

Zhou, Y., Dougherty J. H. Jr., Hubner, K. F., Bai, B., Cannon, R. L., and Hutson, R. K. (2008). Abnormal connectivity in the posterior cingulate and hippocampus in early Alzheimer's disease and mild cognitive impairment. *Alzheimer Dement.* 4, 265–270. doi: 10.1016/j.jalz.2008.04.006

**Conflict of Interest Statement:** The authors declare that the research was conducted in the absence of any commercial or financial relationships that could be construed as a potential conflict of interest.

frontiers in Aging Neuroscience

ORIGINAL RESEARCH
published: 19 April 2016
doi: 10.3389/fnagi.2016.00076

# Prediction of Conversion from Mild Cognitive Impairment to Alzheimer's Disease Using MRI and Structural Network Features

*Rizhen Wei*[1], *Chuhan Li*[1,2], *Noa Fogelson*[3], *Ling Li*[1]* *for the Alzheimer's Disease Neuroimaging Initiative*[†]

[1] Key Laboratory for NeuroInformation of Ministry of Education, High-Field Magnetic Resonance Brain Imaging Key Laboratory of Sichuan Province, Center for Information in Medicine, School of Life Science and Technology, University of Electronic Science and Technology of China, Chengdu, China, [2] School of Computer Science and Engineering, University of Electronic Science and Technology of China, Chengdu, China, [3] EEG and Cognition Laboratory, University of A Coruña, A Coruña, Spain

OPEN ACCESS

**Edited by:**
Junfeng Sun,
Shanghai Jiao Tong University, China

**Reviewed by:**
Ramesh Kandimalla,
Emory University, USA
Yingying Tang,
Shanghai Mental Health Center, China

***Correspondence:**
Ling Li
liling@uestc.edu.cn

[†] Data used in preparation of this article were obtained from the Alzheimer's Disease Neuroimaging Initiative (ADNI) database (http://adni.loni.usc.edu). As such, the investigators within the ADNI contributed to the design and implementation of ADNI and/or provided data but did not participate in analysis or writing of this report. A complete listing of ADNI investigators can be found at: http://adni.loni.usc.edu/wp-content/uploads/how_to_apply/ADNI_Acknowledgement_List.pdf

**Received:** 11 January 2016
**Accepted:** 29 March 2016
**Published:** 19 April 2016

**Citation:**
Wei R, Li C, Fogelson N, Li L for the Alzheimer's Disease Neuroimaging Initiative (2016) Prediction of Conversion from Mild Cognitive Impairment to Alzheimer's Disease Using MRI and Structural Network Features. Front. Aging Neurosci. 8:76. doi: 10.3389/fnagi.2016.00076

Optimized magnetic resonance imaging (MRI) features and abnormalities of brain network architectures may allow earlier detection and accurate prediction of the progression from mild cognitive impairment (MCI) to Alzheimer's disease (AD). In this study, we proposed a classification framework to distinguish MCI converters (MCIc) from MCI non-converters (MCInc) by using a combination of FreeSurfer-derived MRI features and nodal features derived from the thickness network. At the feature selection step, we first employed sparse linear regression with stability selection, for the selection of discriminative features in the iterative combinations of MRI and network measures. Subsequently the top $K$ features of available combinations were selected as optimal features for classification. To obtain unbiased results, support vector machine (SVM) classifiers with nested cross validation were used for classification. The combination of 10 features including those from MRI and network measures attained accuracies of 66.04, 76.39, 74.66, and 73.91% for mixed conversion time, 6, 12, and 18 months before diagnosis of probable AD, respectively. Analysis of the diagnostic power of different time periods before diagnosis of probable AD showed that short-term prediction (6 and 12 months) achieved more stable and higher AUC scores compared with long-term prediction (18 months), with $K$-values from 1 to 30. The present results suggest that meaningful predictors composed of MRI and network measures may offer the possibility for early detection of progression from MCI to AD.

**Keywords: mild cognitive impairment, MRI, structural network, prediction, early detection**

## INTRODUCTION

Mild cognitive impairment (MCI), commonly characterized by slight cognitive deficits but largely intact activities of daily living (Petersen, 2004), is a transitional stage between the healthy aging and dementia. Several studies have suggested that individuals with MCI tend to progress to Alzheimer's disease (AD) at a rate of approximately 10–15% per year (Hänninen et al., 2002; Grundman et al., 2004), while normal controls (NC) develop dementia at a lower rate of 1–2% per year (Bischkopf et al., 2002). In these studies, conversion was considered over the course of 6 months up to a 4-year

follow-up period. MCI remains challenging for diagnosis due to the mild symptoms of cognitive impairment, various etiologies and pathologies, and high rates of reversion back to normal. Thus, early detection of MCI individuals who are suffering from a high risk of conversion from MCI to AD is of increasing clinical importance in potentially delaying or preventing the transition from MCI to AD.

Magnetic resonance imaging (MRI) techniques have provided an efficient and non-invasive way to delineate brain atrophy. Recently, several studies have demonstrated that cortical thickness and subcortical volumetry/shape derived from baselines MRI scans can detect patterns of cerebral atrophy in AD (Fan et al., 2008; Lerch et al., 2008; Vemuri et al., 2008; Frisoni et al., 2010; Julkunen et al., 2010), but with that these have limited prediction accuracy of the conversion to AD in MCI patients (Risacher et al., 2009; Cuingnet et al., 2011). The limited sensitivity of MRI biomarkers in predicting the conversion of MCI subjects has prompted researchers to evaluate the combined prognostic value of different biomarkers. Recent findings (Cui et al., 2011; Gomar et al., 2011; Ewers et al., 2012; Westman et al., 2012; Liu et al., 2014) show that the combination of a range of different biomarkers have better predictive power compared with a single biomarker. However, collecting multi-modality data at the same time may not be applicable in practice.

In addition to the raw features obtained from MRI, structural brain network measures, referred to as the anatomical connection pattern between different neuronal elements (He et al., 2009; Jie et al., 2014; Li and Zhao, 2015), provide new insights into the network organization, topology, and complex dynamics of the brain, as well as further understanding of the pathogenesis of neurological disorders (Bullmore and Sporns, 2009; Zalesky et al., 2010). Abnormalities of structural networks have been observed in AD and MCI patients (Stam et al., 2007; He et al., 2008; Yao et al., 2010; Tijms et al., 2013; Zhou and Lui, 2013). Yao and colleagues used thickness cortical networks to study the aberrant brain structures in MCI and report that the nodal centrality in MCI, compared with a NC group, showed decreases in the left lingual gyrus, middle temporal gyrus (MTG), and increases in the precuneus cortex (Yao et al., 2010). Zhou and Lui (2013) also used cortical thickness to detect small-world properties alteration in MCI and reported that MCI converters (MCIc) showed the lowest local efficiency during the conversion period to AD; while the MCI non-converters (MCInc) showed the highest local and global efficiency.

These approaches which used optimized MRI features achieve encouraging accuracies (over 60%). However, few studies analyzed the co-variation of abnormalities in different regions of interest (ROIs), which can be characterized by network patterns and could contribute to reliable and sensitive classification (Dai et al., 2013). Indeed, the pattern of AD pathology is complex and evolves as disease progresses (Fan et al., 2008) and many regions share similar patterns of abnormal brain morphometric. Thus, informative network topology may be potentially useful for classification. In addition, many factors such as the heterogeneity of the MRI images (Eskildsen et al., 2013) and the imbalanced data between groups (Johnstone et al., 2012; Dubey et al., 2014) can also lead to overestimations.

The main objective of the current study was to determine whether the combined use of structural brain measures and thickness network alterations, may improve the accuracy and the sensitivity in identifying prodromal AD. To this end, we proposed a classification framework to distinguish MCIc from MCInc by using a combination of features from FreeSurfer-derived MRI features and nodal parameters derived from thickness network. To obtain predictive nodal information for each individual, we first established a weight network by using a kernel function and then thresholded it to a binary network. Finally, nodal properties were measured at a high discriminative connection cost. At the feature selection step, we first employed sparse linear regression with stability selection for robust feature selection in the iterative combination of MRI and network measures, and then top $K$ features of available combinations were selected as optimal features for classification. To obtain unbiased results, support vector machine (SVM) classifiers with nested cross validation were used for classification. The secondary goal of this study was to measure the impact of different conversion time periods before diagnosis of probable AD, and to evaluate different predictive values between two groups. To that purpose, we homogenized the MCIc images with respect to "time to conversion." Thus, MCIc patients were subdivided into four groups: mixed for baseline, 6, 12, and 18 months before diagnosis of probable AD. Our hypothesis was that network topological measures might be potentially useful for classification of imminent conversion, and the effective combination of brain morphometric and thickness network measures may improve the prediction of conversion from MCI to AD. Besides, more stable and higher classification accuracy could be obtained for the short-term prediction (6 and 12 months) compared with the long-term prediction (18 months).

# MATERIALS AND METHODS

## Participants

Data used in this article were obtained from the Alzheimer's Disease Neuroimaging Initiative (ADNI) database (adni.loni.usc.edu). The ADNI was launched in 2003 as a public-private partnership, led by Principal Investigator Michael W. Weiner, MD. The primary goal of ADNI has been to test whether serial MRI, positron emission tomography (PET), other biological markers, and clinical and neuropsychological assessment can be combined to measure the progression of MCI and early Alzheimer's disease (AD).

The eligibility criteria for inclusion of subjects are described at: http://adni.loni.usc.edu/wp-content/uploads/2010/09/ADNI_GeneralProceduresManual.pdf. General criteria for MCI were as follows: (1) Mini-Mental-State-Examination (MMSE) scores between 24 and 30 (inclusive), (2) a memory complaint, objective memory loss measured by education adjusted scores on the Wechsler Memory Scale Logical Memory II, (3) a Clinical Dementia Rating (CDR) of 0.5, and (4) absence of significant levels of impairment in other cognitive domains, essentially preserved activities of daily living, and an absence of dementia.

Several studies, which rendered the MCI converters with respect to "time to conversion," have used baseline MRI scans

**TABLE 1 | Subject characteristics.**

| | MCIc_mixed | MCIc_m6 | MCIc_m12 | MCIc_m18 | MCInc | *P*-value |
|---|---|---|---|---|---|---|
| Gender(F/M) | 30/46 | 25/36 | 26/37 | 16/26 | 29/54 | NS |
| Age | 73.6 ± 7.8 | 74.5 ± 7.5 | 74.0 ± 7.8 | 74.3 ± 7.6 | 74.1 ± 7.3 | NS |
| Education | 15.8 ± 3.1 | 15.6 ± 3.1 | 15.9 ± 2.8 | 15.8 ± 2.9 | 15.8 ± 3.0 | NS |
| CDR-SB | 1.7 ± 1.1[a] | 2.5 ± 1.2[a] | 2.1 ± 1.1[a] | 1.8 ± 1.0[a] | 1.3 ± 0.6 | $p < 0.001$ |
| MMSE | 26.5 ± 1.6 | 25.2 ± 2.5[a] | 26.1 ± 2.1 | 25.9 ± 2.2 | 27.5 ± 1.7 | $p = 0.015$ |

*Values represent mean ± SD. CDR-SB, Clinical Dementia Rating Sum of Boxes; MMSE, Mini Mental State Examination. Chi-square was used for gender comparison. A two-way student t-test was used for age, education, and neuropsychological test comparisons. NS, not significant.*
*[a]Indicates significance compared to the MCInc group.*

**TABLE 2 | Anatomical regions.**

| Anatomical region | Abbreviation | Anatomical region | Abbreviation |
|---|---|---|---|
| Banks superior temporal sulcus | BSTS | Pars Orbitalis | PORB |
| Caudal anterior cingulate cortex | cACC | Pars Triangularis | PTri |
| Caudal middle frontal gyrus | cMFG | Pericalcarine cortex | PCAL |
| Cuneus cortex | CUN | Postcentral gyrus | PoCG |
| Entorhinal cortex | ENT | Posterior cingulate cortex | PCC |
| Fusiform gyrus | FG | Precentral gyrus | PreCG |
| Inferior parietal cortex | IPC | Precuneus cortex | PCUN |
| Inferior temporal gyrus | ITG | Rostral anterior cingulate cortex | rACC |
| Isthmus of cingulate cortex | IstCC | Rostral middle frontal gyrus | rMFG |
| Lateral occipital cortex | LOC | Superior frontal gyrus | SFG |
| Lateral orbital frontal cortex | ORBlat | Superior parietal cortex | SPC |
| Lingual gyrus | LING | Superior temporal gyrus | STG |
| Medial orbital frontal cortex | ORBmid | Supramarginal gyrus | SMG |
| Middle temporal gyrus | MTG | Frontal pole | FP |
| Parahippocampal gyrus | PHG | Temporal pole | TP |
| Paracentral lobule | PCL | Transverse temporal cortex | TTC |
| Pars Opercularis | POperc | Insula | INS |

to predict the conversion, since the MCI patients could convert anytime over the course of 6 months to 4 years. We categorized the MCI patients into converters and non-converters as in Wolz et al. (2011), where non-converters were defined as those that did not have a change of diagnosis within 36 months and the complementary MCI patients constituted the MCIc group. To assess the diagnostic power of different time periods before diagnosis of probable AD, we selected scans at various intervals prior to diagnosis. We selected MCIc scans at 6 (MCIc_m6), 12 (MCIc_m12), and 18 months (MCIc_m18) prior to AD diagnosis. MCIc scans at 24 and 36 months prior to AD diagnosis were excluded from the analysis due to the small samples and large imbalances between the two groups. To evaluate our method in comparison with the method using baseline scans for prediction, we also selected MCIc baseline data (MCIc_mixed) for prediction. **Table 1** summarizes the selected MCI patients in our study.

## MRI Imaging Acquisition

All scans used in the study were T1-weighted MPRAGE images acquired in 1.5-Tesla MR imaging instruments using a standardized protocol (Jack et al., 2008). Pre-processing images were downloaded from the public ADNI site (adni.loni.usc.edu). The images were preprocessed according to a number of steps detailed in the ADNI website, which contained (1) grad warp correction of image geometry distortion due to gradient non-linearity, (2) B1 non-uniformity processing to correct the image intensity non-uniformity, and (3) N3 processing to reduce residual intensity non-uniformity.

## Feature Extraction

### MRI Features

The FreeSurfer 5.30 software package was utilized for cortical reconstruction and volumetric segmentation (FreeSurfer v5.30, http://surfer.nmr.mgh.harvard.edu/fswiki). In brief, the processing contains automated Talairach spaces transformation, intensity inhomogeneity correction, removal of non-brain tissue, intensity normalization, tissue segmentation (Fischl et al., 2002), automated topology correction, surface deformation to generate the gray/white matter boundary and gray matter/Cerebrospinal Fluid (CSF) boundary, and parcellation of the cerebral cortex (Desikan et al., 2006). The quality of the raw MRI images, Talairach registration, intensity normalization, brain segmentation, and surface demarcation were assessed using a manual inspection protocol. The images that failed the stages of quality assurance were removed from subsequent analysis. The atlas used in FreeSurfer included 34 cortical ROIs per hemisphere (**Table 2**). For each cortical ROI, cortical thickness (CT), cortical volume (CV), and cortical surface area (CS) were calculated as three subtypes of MRI features. CT at each vertex of the cortex was calculated as the average shortest distance between white and pail surfaces. CS was calculated by computing the area of every triangle in a standardized spherical surface tessellation. CV at each vertex was computed by the product of the CS and CT at each surface vertex. This yielded a total of 204 cortical features for each subject (**Figure 1A**).

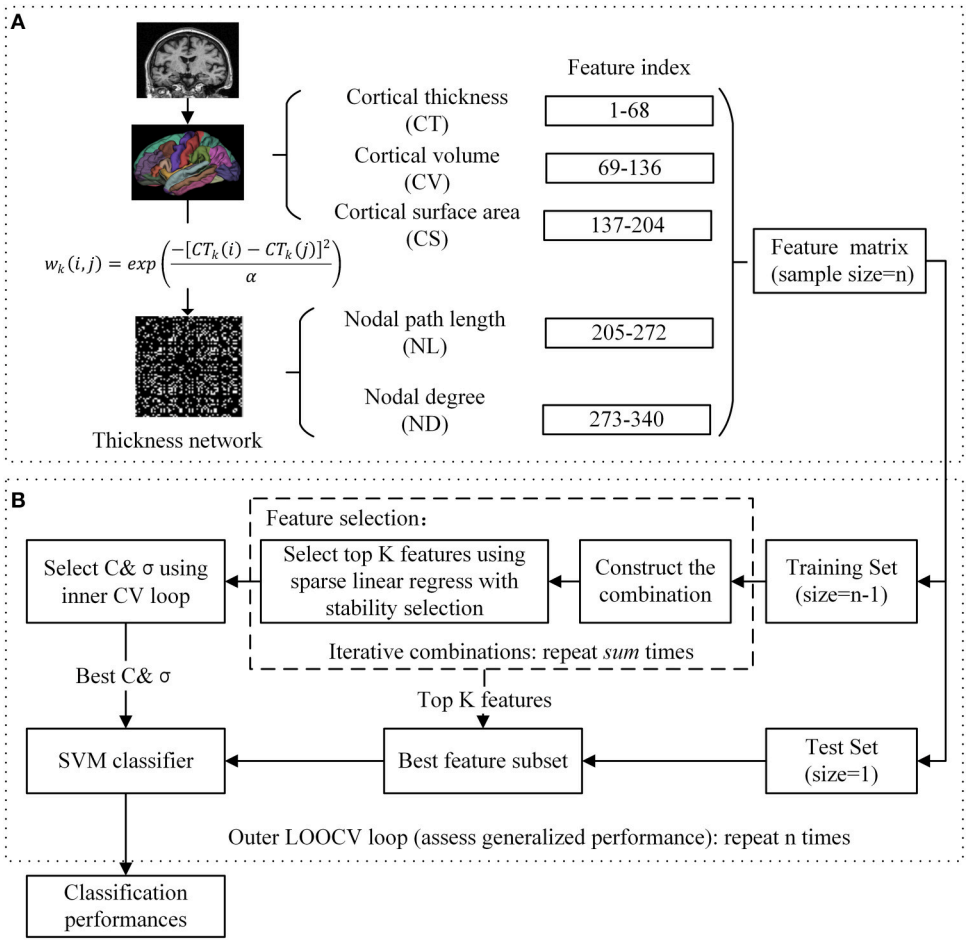


**FIGURE 1 | Proposed prediction framework. (A)** Feature extraction: T1-weigthed images are processed and individual thickness network is constructed based on the difference in cortical thickness of a pair of ROIs. **(B)** Classification: SVM classifier with nested cross validation is implemented for classification.

## Thickness Network Features

Similar to a prior study (Dai et al., 2013), the thickness network matrix $W_{ij}\left(i, j = 1, 2, \ldots, N, here\ N = 68\right)$ for each individual was obtained by calculating the difference in cortical thickness between each pair of regions, and measured using the following kernel, with the weight defined as:

$$w_k\left(i,j\right) = exp\left(\frac{-\left[CT_k\left(i\right) - CT_k\left(j\right)\right]^2}{\alpha}\right) \quad (1)$$

where $CT_k\left(i\right)$ represents the cortical thickness of $i$ ROI of $k$ subjects, and the kernel width $\alpha$ is 0.01. To simplify the statistical calculation, the thickness network matrix of each individual was thresholded into a binary matrix $B_{ij} = \left[b_{ij}\right]$, where the $b_{ij}$ was 1 if the weight of the two ROIs was larger than the given threshold, and 0 otherwise. The threshold represents the network connection cost, defined as the ratio of the supra-threshold connections relative to the total possible number of connections in the network (Fornito et al., 2010). After applying each threshold, these binary matrices were then used as a basis for the network construction and graph analysis. We analyzed the full range of costs from 8 to 40%, at 1% intervals. The nodal properties were then extracted at a connection cost of 18%, at which the clustering coefficient showed the largest difference between the MCIc_mixed and MCInc groups. Finally, 136 nodal features including nodal path length (NL) and nodal degree (ND) were employed for subsequent analysis (**Figure 1A**). In brief, for a given node $i$, nodal path length and nodal degree were defined as follows:

$$L_i = \frac{\sum_{j \neq i \in V} L_{ij}}{(V-1)} \quad (2)$$

$$k_i = \sum_{j \in V} b_{ij} \quad (3)$$

where $L_{ij}$ refers to the minimum number of edges between node pairs $i$ and $j$, $V$ is the size of a graph, and $b_{ij}$ is the connection status between the node pairs $i$ and $j$. Intuitively, path length $L_i$ measures the speed of the message that passes through a given node, and the degree of an individual node $k_i$ is equal to the

number of links connected to that node, thus reflecting the level of interaction in the network.

## Feature Selection

In the current study, as shown in **Figure 1**, we evaluated 340 features from five different categories (three types of MRI features and two types of network features) for each subject. We implemented the combination in an iterative manner to avoid making an arbitrary choice of the combination. Features were combined in every possible combination. The iteration pattern was described as follows:

$$sum = \sum_{i=1}^{i=5} C_5^i \tag{4}$$

where $i$ refers to the type of features, *sum* refers to the number of total iterative models. A total of 31 combinations were obtained for each diagnostic pair.

In each combination, we applied sparse linear regression for features selection using the $L_1$-norm regularization (Tibshirani, 1996). Let $\boldsymbol{X} = [x_1, x_2, \ldots, x_n]^T \in \mathbb{R}^{n\times m}$be a $n \times m$ matrix that represents $m$ features of $n$ samples, $\boldsymbol{y} = [y_1, y_2, \ldots, y_n]^T \in \mathbb{R}^{n\times 1}$ be a $n$ dimensional corresponding classification labels ($y_i = 1$ for MCIc and $y_i = -1$ for MCInc). The linear regression model was defined as follows:

$$\widehat{\mathbf{y}} = \boldsymbol{Xw} \tag{5}$$

where $\boldsymbol{w} = [w_1, w_2, \ldots, w_m]^T \in \mathbb{R}^{m\times 1}$ and $\widehat{\boldsymbol{y}}$ denotes the regression coefficient vector and the predicted label vector. One approach is to estimate the $\boldsymbol{w}$ by minimizing the following objective function:

$$\min_{w} \frac{1}{2}\left\|\boldsymbol{Xw}-\boldsymbol{y}\right\|_2^2+\lambda\|\boldsymbol{w}\|_1 \tag{6}$$

where $\lambda > 0$ is a regularization parameter which controls the sparsity of the model, i.e., many of the entries of $\boldsymbol{w}$ are zero, and $\|\boldsymbol{w}\|_1$is the $L_1$-norm of $\boldsymbol{w}$, which is defined as $\sum_{i=1}^{m}|w_i|$. In this study, the SLEP package (Liu et al., 2009) was used for solving sparse linear regression. To address the problem of proper regularization we applied the stability selection using subsampling or bootstrapping (Meinshausen and Bühlmann, 2010) for robust feature selection. For each combination, we selected the top $K$ ($K = 10$) features for subsequent analysis. After feature selection of each combination, the likelihood $\mathcal{L}$ for a feature index being selected in the combinations was calculated as follows:

$$\mathcal{L}\left(l\right) = \frac{1}{sum}\sum_{i=1}^{sum} sf_i\left(l\right), \; where \; sf\left(l\right) = \begin{cases} 1, if \; selected \\ 0, otherwise \end{cases} \tag{7}$$

where *sum* is the number of combinations, $l$ is the features index and *sf* is a binary function determining if $l$ is selected in a combination. $\mathcal{L}$ is an expression of how often a feature is included among all combinations. Finally, the top K features were selected for classification.

## Classification

For the selected features, the SVM classifier was implemented using the LIBSVM toolbox (Chang and Lin, 2011), with radial basis function (RBF) and an optimal value for the penalized coefficient $C$ (a constant determining the tradeoff between training error and model flatness). The RBF kernel was defined as follows:

$$K\left(x_1, x_2\right) = exp\left(-\frac{\|x_1 - x_2\|}{2\sigma^2}\right) \tag{8}$$

where $x_1, x_2$ are the two feature vectors and σ controls the width of the RBF kernel. In order to obtain an unbiased estimation and select the optimal SVM model, a nested cross validation (CV) was employed. For a training set, we selected the optimal hyperparameters ($C$ and σ) through a grid-search and a 10-fold CV (inner CV). The outer CV that we used was the leave-one-out cross validation (LOOCV). In each fold of the outer CV, one sample was kept out for validation and the remaining were used for feature selection and training the classifier; then the performance of the training classifier was evaluated using the held-out sample. This run was repeated until all the subjects were excluded. The pipeline of our classification framework is presented in **Figure 1**. To evaluate the quality of the classification, we report four established measures: accuracy, sensitivity, specificity, and area under the curve (AUC). These measures were defined as follows:

$$Accuracy = \frac{TP + TN}{TP + TN + FP + FN}, \; Sensitivity = \frac{TP}{TP + FN}, \; Specificity = \frac{TN}{TN + FP} \tag{9}$$

where TP, TN, FP, FN denote true positive, true negative, false positive, and false negative, respectively. Following a common convention, we considered a correctly predicted MCIc as a true positive.

# RESULTS

The LOOCV results of classification and receiver operating characteristic curves (ROCs) are depicted in **Table 3** and **Figure 2A**. For the MCInc vs. MCIc_mixed model, the proposed method achieved a classification accuracy of 66.04% (sensitivity = 55.26%, specificity = 75.90%, AUC = 0.7346). For classifying MCIc_m6 from MCInc, combining the MRI with network measures, resulted in a higher accuracy of 76.39% (sensitivity = 65.57%, specificity = 84.34%, AUC = 0.8130). Specifically, we obtained slightly lower levels of accuracies for 12 and 18 months (74.66 and 73.91%, respectively) compared to the classification of MCInc vs. MCIc_m6.

By using the top 10 combined features, the features most often selected by the sparse linear regression with the stability selection, we achieved AUC scores in a range between 0.7346 and 0.8130. The features selected (listed in **Table 4**) show roughly similar features among four diagnostic pairs and include the left inferior parietal cortex (IPC), left frontal pole, left precuneus cortex, left postcentral gyrus, left entorhinal cortex, left MTG,

left banks superior temporal sulcus, right caudal middle frontal gyrus, right supramarginal gyrus, right posterior cingulate cortex, right isthmus of the cingulate cortex, and right lingual gyrus. These selected regions have been shown to be related with MCI conversion (Chételat et al., 2005; Fan et al., 2008; Misra et al., 2009; Risacher et al., 2009; Yao et al., 2010; Cai et al., 2015; Kandiah et al., 2015). Moreover, note that nearly all involved network features included the nodal degree (ND).

To demonstrate the impact of the number of selected features, we conducted the classification using the top $K$ combined features for $K = 1, 2, \ldots, 30$. The classification performances and AUC scores are depicted in Supplementary Table 1 and **Figure 3**, respectively. As shown in **Figure 3**, the AUC stabilizes after the top 12–15 features are included and the best classification results are observed in the classification of MCInc vs. MCIc_m6 and MCInc vs. MCIc_m12.

To examine the added benefit of the network measures, we applied the sparse linear regression with the stability selection to either the MRI or the network measures. The classifier model performances and ROCs are depicted in **Table 5** and **Figure 2**. As shown in **Table 5**, MRI achieved the best AUC scores (0.8002 for MCInc vs. MCIc_m6), while the network biomarkers performed slightly worse (AUC = 0.6974, 0.6006, 0.7481, 0.6140, for mixed, 6, 12, and 18 months before diagnosis of probable AD, respectively). The top 10 MRI and network features are listed in Supplementary Tables 2, 3. Note that most items in **Table 4** and Supplementary Tables 2, 3 match, and that several cortical surface area (CS) features were included in the classifier, only when the signal MRI was used for prediction.

**TABLE 3 | The LOOCV results using the top 10 combined features.**

| Diagnostic pair | ACC (%) | SEN (%) | SPE (%) | AUC |
|---|---|---|---|---|
| MCInc vs. MCIc_mixed | 66.04 | 55.26 | 75.90 | 0.7346 |
| MCInc vs. MCIc_m6 | 76.39 | 65.57 | 84.34 | 0.8130 |
| MCInc vs. MCIc_m12 | 74.66 | 65.08 | 81.93 | 0.7850 |
| MCInc vs. MCIc_m18 | 73.91 | 70.51 | 77.11 | 0.7729 |

*ACC, accuracy; SEN, sensitivity; SPE, specificity; AUC, area under the curve.*

## DISCUSSION

In this study, we established an efficient MCI conversion classification framework using a combination of MRI and network measures. The increased prediction accuracies that we observed suggest that it may be possible to identify conversion from MCI to AD using the combination of MRI and network measures. Moreover, the homogenization of the MCIc sub-groups showed improved classification of the short-term prediction, yielding a more consistent pattern of cortical neurodegeneration.

Our findings show (**Tables 3, 5**) that the combination of MRI and thickness network measures outperforms either MRI or network measures alone, in the prediction of conversion from MCI to AD. In addition, the results showed that brain morphometric was a better predictor compared with thickness network measures, suggesting abnormalities may exist across different ROIs during the conversion period to AD. Moreover, the increased predictive power of the combined classification methodology suggests that a co-variation of the abnormalities across different regions is necessary for the detection of the early transition from MCI to AD. Without requiring new sources of information, our prediction AUCs are in line with previous studies (Cui et al., 2011; Ye et al., 2012; Eskildsen et al., 2013; Raamana et al., 2015), which used multivariate biomarkers including thickness, thickness network, CSF, and cognitive measures. Cui et al. (2011) showed that with a combination of MRI, CSF, neuropsychological and functional measures (NMs), MCInc vs. MCIc were classified with an AUC of 0.796 at baseline. However, the specificity that was achieved was under 50% (48.28%), despite adding CSF and five NMs measures that have been thought to be useful in conversion prediction. On the other hand, Ye et al. (2012) who used a spare logistic regression with stability selection and a combination of 15 features including

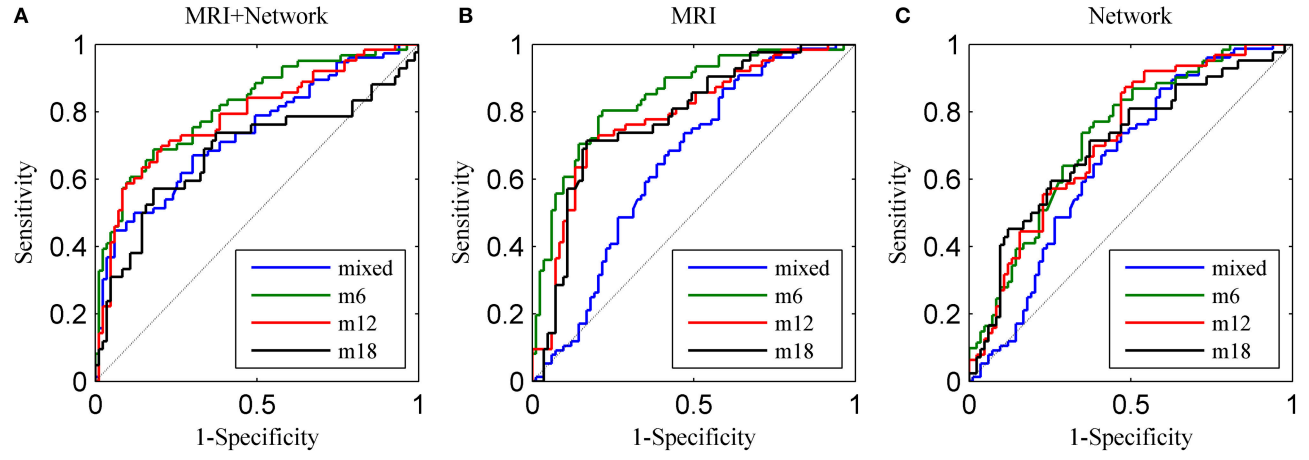


**FIGURE 2 | ROC curves for the four diagnostic pairs using (A) top 10 combined features, (B) top 10 MRI features, and (C) top 10 network features.**

**TABLE 4 | Top 10 combined features selected by the sparse linear regression with stability selection in the LOOCV experiments.**

| Feature | Frequency (%) | Feature | Frequency (%) |
|---|---|---|---|
| MCInc vs. MCIc_mixed | | MCInc vs. MCIc_m12 | |
| CT: IPC_L | 100 | CT: IPC_L | 100 |
| CV: IPC_L | 100 | CT: cMFG_R | 100 |
| ND: MTG_L | 100 | CV: IPC_L | 100 |
| ND: PoCG_L | 100 | CV: MTG_L | 100 |
| ND: LING_R | 100 | ND: FP_L | 100 |
| NL: IPC_L | 100 | ND: MTG_L | 100 |
| CV: SMG_R | 99 | ND: PoCG_L | 100 |
| ND: PCC_R | 97 | ND: LING_R | 100 |
| CV: MTG_L | 96 | CV: SMG_R | 87 |
| ND: IPC_L | 47 | CT: BSTS_L | 63 |
| MCInc vs. MCIc_m6 | | MCInc vs. MCIc_m18 | |
| CT: IPC_L | 100 | CT: IPC_L | 100 |
| CT: MTG_L | 100 | CT: MTG_L | 100 |
| CV: IPC_L | 100 | CT: cMFG_R | 100 |
| ND: MTG_L | 100 | CT: PCUN_L | 99 |
| ND: LING_R | 100 | ND: PCC_R | 99 |
| CV: MTG_L | 99 | CT: lstCC_R | 98 |
| ND: PoCG_L | 99 | CT: BSTS_L | 90 |
| NL: ENT_L | 88 | CV: IPC_L | 90 |
| CV: SMG_R | 85 | ND: MTG_L | 70 |
| NL: IPC_L | 74 | CV: MTG_L | 53 |

*CT, cortical thickness; CV, cortical volume; CS, cortical surface area; NL, nodal length path; ND, nodal degree, L, left hemisphere; R, right hemisphere.*

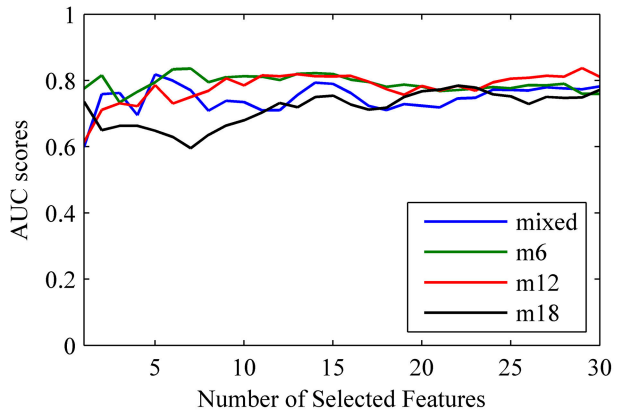


**FIGURE 3 | The change of AUC scores as a function of the number of combined features.**

MRI, APOE gene, and cognitive measures, achieved the best reported classification results to date with an AUC of 0.8587 (Ye et al., 2012). Our results demonstrate slightly lower accuracy levels, but we only used one source of information and a smaller number of selected features. In addition, obtaining CSF and APOE gene measures may not be applicable for some subjects, and thus make be difficult to obtain during data integration. Eskildsen et al. (2013) have also distinguished MCIc from MCInc at various intervals prior to diagnosis, with AUC scores of 0.809 and 0.762 for MCIc_m6 and MCIc_m12, respectively. Raamana et al. (2015) achieved an AUC of 0.680 using a novel approach that utilizes thickness network fusion measures for the prediction of MCI conversion. Classification results are summarized in **Table 6**.

Importantly, the stability selection provides a small subset of discriminative patterns (see **Table 4** and Supplementary Tables 2, 3) for effective and efficient screens. Our findings showed that most of the MRI features in the top 10 combined features were cortical thickness and volume. The consistent features that were included in most pairs with a high frequency were the cortical thickness and volume of the left IPC; and the cortical volume of the left MTG and of the right supramarginal gyrus (SMG), suggesting that abnormities in these regions may be important predictors of conversion (Chételat et al., 2005; Pennanen et al., 2005; Fan et al., 2008; Karas et al., 2008; Whitwell et al., 2008; Desikan et al., 2009; Schroeter et al., 2009; Li et al., 2011; Wang et al., 2016). Additionally, we found that the features selected were predominately in the left hemisphere (**Table 4**). The potential asymmetry is possible related to the disease progression, since the pattern of atrophy in AD was fairly symmetric (Fan et al., 2008). Besides, the selected ROIs were functionally associated with episodic memory (MTG, IPC) and attention (posterior cingulate cortex). Other features that were included were the nodal degree of the left MTG, the right lingual gyrus (LING) and the left postcentral gyrus (PoCG). Previous studies have found that subjects with MCI have abnormal network patterns in the LING and MTG (Yao et al., 2010). In addition, He and colleagues demonstrated an abnormal correlation between bilateral PoCG in AD (He et al., 2008). Moreover, the ROIs selected showed a small overlap between MRI and thickness network, suggesting that informative co-variation of the abnormalities may provide complementary information for classification. Together, our results suggest that changes in the cortical regions may be associated with mechanisms underlying the conversion of MCI to AD, and structural network architecture can be a potential predictor for the classification of imminent conversion.

The classification performances obtained for the MCIc subgroups showed an improvement when time-homogenization was utilized, which was in line with a previous study (Eskildsen et al., 2013). We found that short-term prediction (6 and 12 months follow up) showed slightly better performances compared with long-term prediction of 18 months (**Figure 3**). The likelihood for MCIc subjects to be accurately predicted increased with the reduction of conversion prior diagnosis. The small overlap in brain atrophy and network topology, we believe, is the primary reason for improving short-term predictions. Additionally, the relatively low sensitivity for MCInc vs. MCInc_m18 possibly due to the small sample size available to construct the long-term (18 months) classifier model.

On the other hand, we investigates whether the number of features selected influences the classification results. Overall, we found that the AUC scores stabilized after the top nine features were added to the classifier model for the 6 and 12 months follow up. In contrast, for the 18 months follow up, the AUC values

**TABLE 5 | The LOOCV results using top 10 MRI features and top 10 network features.**

| Diagnostic pair | Top 10 MRI features | | | | Top 10 network features | | | |
|---|---|---|---|---|---|---|---|---|
| | ACC (%) | SEN (%) | SPE (%) | AUC | ACC (%) | SEN (%) | SPE (%) | AUC |
| MCInc vs. MCIc_mixed | 72.33 | 68.42 | 75.90 | 0.7865 | 64.78 | 61.84 | 67.47 | 0.6974 |
| MCInc vs. MCIc_m6 | 75.00 | 63.93 | 83.13 | 0.8002 | 61.81 | 49.18 | 71.08 | 0.6006 |
| MCInc vs. MCIc_m12 | 73.29 | 63.49 | 80.72 | 0.7885 | 70.55 | 61.90 | 77.11 | 0.7481 |
| MCInc vs. MCIc_m18 | 78.40 | 45.24 | 95.18 | 0.7321 | 66.40 | 33.33 | 83.13 | 0.6410 |

*ACC, accuracy; SEN, sensitivity; SPE, specificity; AUC, area under the curve.*

**TABLE 6 | Comparison of classification performance of different methods.**

| Article | Method | MCInc/MCIc | Scans | ACC (%) | SEN (%) | SPE (%) | AUC |
|---|---|---|---|---|---|---|---|
| Cui et al., 2011 | Multivariate predictors (MRI, CSF, and NM scores) | 87/56 | baseline | 67.1 | 96.4 | 48.3 | 0.796 |
| Ye et al., 2012 | SLR+SS (MRI, genetic, and cognitive measures) | 177/142 | baseline | – | – | – | 0.859 |
| Eskildsen et al., 2013 | Patterns of cortical thinning | 134/122 | 6 months | 75.8 | 75.4 | 76.1 | 0.809 |
| | | 134/123 | 12 months | 72.9 | 75.8 | 70.2 | 0.762 |
| Raamana et al., 2015 | Thickness network fusion | 130/56 | baseline | 64.0 | 65.0 | 64.0 | 0.680 |
| Proposed | Combination of MRI and thickness network | 83/76 | baseline | 66.0 | 55.3 | 75.9 | 0.735 |
| | | 83/61 | 6 months | 76.4 | 65.6 | 84.3 | 0.813 |
| | | 83/63 | 12 months | 74.7 | 65.1 | 81.9 | 0.785 |
| | | 83/42 | 18 months | 73.9 | 70.5 | 77.1 | 0.773 |

*The best multivariate predictors of MCI conversion are shown for each study.*
*ACC, accuracy; SEN, sensitivity; SPE, specificity; AUC, area under the curve; CSF, Cerebrospinal Fluid; NMs, neuropsychological and functional measures; SLR+SS, sparse logistic regression with stability selection.*

increased when the number of selected features was increased, and a strong relationship was observed in the classification of MCInc vs. MCIc_mixed. The stable performances that were observed for the short-term predictions may be attributed to mechanisms associated with the conversion to AD, suggesting more consistent patterns of abnormalities in brain atrophy and network features. The effect of the homogenization of the MCIc patients reveals that predictions are superior when subjects display variable time periods to conversion. Specifically, compared to combined MRI and network features, the top 10 MRI features showed similar performances for short-term predictions, suggesting that the abnormal brain atrophy patterns are strong predictors for short-term prediction. For MCIC_m18 prediction, the sensitivity increased by 25% and the AUC increased by 4%, when we used combined feature sets compared with MRI measures alone, which may indicate that these classes of measures provide complementary information for diagnostic classification. Therefore, informative structural network measures could be potentially useful for classification, especially at the early stage of impairment.

This study has several limitations. One limitation is that there is no consensus regarding the time boundary for MCI converters and MCI non-converters. Another limitation related to network features, is whether the extracted network features reflect characteristics related to AD in an integral and accurate manner. Although several studies (Stam et al., 2007, 2009; He et al., 2008; Yao et al., 2010; Shu et al., 2012; Zhao et al., 2012; Tijms et al., 2014) show that AD and MCI are associated with changes in network properties, there is little agreement about the nature of these changes. Another drawback is that the accuracy of some discriminant classifiers should be interpreted with caution. Future studies are warranted where larger samples and more advanced fusion methods, using more than just node quantitative measurements, may limit overestimation and may overcome direct comparison. Moreover, further studies are needed in order to examine the diagnostic power of the relationship between structural and functional connectivity abnormalities in MCI sub-groups.

## CONCLUSION

This study investigated the diagnostic power of the combination of MRI and thickness network measures derived from structural MRI to distinguish individuals with MCIc from MCInc. Without requiring new sources of information, our approach shows that the effective combination of MRI and thickness network measures improves the discrimination between MCIc and MCInc, compared with the use of either MRI or network measures separately. Moreover, the selected features are interpretable and are in line with previous findings, and the similar spatial patterns of brain morphometric and structural network alterations are shared among the four groups that we examined. By using longitudinal measures, we also found that short-term prediction shows more stable and better performances compared with long-term prediction. Together,

our study provides a new insight into the prediction of MCI to AD conversion, and revealed that structural connectivity is a potential predictor for classification of imminent conversion.

## AUTHOR CONTRIBUTIONS

RW was in charge of the data analysis and manuscript writing. CL helped in speeding up the data analysis. LL helped in calculation and manuscript writing. NF helped was in charge of manuscript verifying. All authors reviewed the manuscript.

## FUNDING

This research was supported by grants from NSFC (Nos. 61203363 and 61473062), Spanish Ministry of Science and Innovation (PSI2012-34212), the Ramón y Cajal national fellowship program, the 111 project (B12027), and the Fundamental Research Funds for the Central Universities.

## ACKNOWLEDGMENTS

Data collection and sharing for this project was funded by the Alzheimer's Disease Neuroimaging Initiative (ADNI) (National Institutes of Health Grant U01 AG024904) and DOD ADNI (Department of Defense award number W81XWH-12-2-0012). ADNI is funded by the National Institute on Aging, the National Institute of Biomedical Imaging and Bioengineering, and through generous contributions from the following: AbbVie, Alzheimer's Association; Alzheimer's Drug Discovery Foundation; Araclon Biotech; BioClinica, Inc.; Biogen; Bristol-Myers Squibb Company; CereSpir, Inc.; Eisai Inc.; Elan Pharmaceuticals, Inc.; Eli Lilly and Company; EuroImmun; F. Hoffmann-La Roche Ltd and its affiliated company Genentech, Inc.; Fujirebio; GE Healthcare; IXICO Ltd.; Janssen Alzheimer Immunotherapy Research & Development, LLC.; Johnson & Johnson Pharmaceutical Research & Development LLC.; Lumosity; Lundbeck; Merck & Co., Inc.; Meso Scale Diagnostics, LLC.; NeuroRx Research; Neurotrack Technologies; Novartis Pharmaceuticals Corporation; Pfizer Inc.; Piramal Imaging; Servier; Takeda Pharmaceutical Company; and Transition Therapeutics. The Canadian Institutes of Health Research is providing funds to support ADNI clinical sites in Canada. Private sector contributions are facilitated by the Foundation for the National Institutes of Health (www.fnih.org). The grantee organization is the Northern California Institute for Research and Education, and the study is coordinated by the Alzheimer's Disease Cooperative Study at the University of California, San Diego. ADNI data are disseminated by the Laboratory for Neuro Imaging at the University of Southern California.

## SUPPLEMENTARY MATERIAL

The Supplementary Material for this article can be found online at: http://journal.frontiersin.org/article/10.3389/fnagi.2016.00076

## REFERENCES

Bischkopf, J., Busse, A., and Angermeyer, M. C. (2002). Mild cognitive impairment–a review of prevalence, incidence and outcome according to current approaches. *Acta Psychiatr. Scand.* 106, 403–414. doi: 10.1034/j.1600-0447.2002.01417.x

Bullmore, E., and Sporns, O. (2009). Complex brain networks: graph theoretical analysis of structural and functional systems. *Nat. Rev. Neurosci.* 10, 186–198. doi: 10.1038/nrn2575

Cai, S., Huang, L., Zou, J., Jing, L., Zhai, B., Ji, G., et al. (2015). Changes in thalamic connectivity in the early and late stages of amnestic mild cognitive impairment: a resting-state functional magnetic resonance study from ADNI. *PLoS ONE* 10:e0115573. doi: 10.1371/journal.pone.0115573

Chang, C. C., and Lin, C. J. (2011). LIBSVM: a library for support vector machines. *Acm Trans. Intell. Syst. Technol.* 2, 2–27. doi: 10.1145/1961189.1961199

Chételat, G., Landeau, B., Eustache, F., Mézenge, F., Viader, F., De La Sayette, V., et al. (2005). Using voxel-based morphometry to map the structural changes associated with rapid conversion in MCI: a longitudinal MRI study. *Neuroimage* 27, 934–946. doi: 10.1016/j.neuroimage.2005.05.015

Cui, Y., Liu, B., Luo, S., Zhen, X., Fan, M., Liu, T., et al. (2011). Identification of conversion from mild cognitive impairment to Alzheimer's disease using multivariate predictors. *PLoS ONE* 6:e21896. doi: 10.1371/journal.pone.0021896

Cuingnet, R., Gerardin, E., Tessieras, J., Auzias, G., Lehéricy, S., Habert, M. O., et al. (2011). Automatic classification of patients with Alzheimer's disease from structural MRI: a comparison of ten methods using the ADNI database. *Neuroimage* 56, 766–781. doi: 10.1016/j.neuroimage.2010.06.013

Dai, D., He, H. G., Vogelstein, J. T., and Hou, Z. G. (2013). Accurate prediction of AD patients using cortical thickness networks. *Mach. Vision Appl.* 24, 1445–1457. doi: 10.1007/s00138-012-0462-0

Desikan, R. S., Cabral, H. J., Fischl, B., Guttmann, C. R., Blacker, D., Hyman, B. T., et al. (2009). Temporoparietal MR imaging measures of atrophy in subjects with mild cognitive impairment that predict subsequent diagnosis of Alzheimer disease. *AJNR Am. J. Neuroradiol.* 30, 532–538. doi: 10.3174/ajnr.A1397

Desikan, R. S., Segonne, F., Fischl, B., Quinn, B. T., Dickerson, B. C., Blacker, D., et al. (2006). An automated labeling system for subdividing the human cerebral cortex on MRI scans into gyral based regions of interest. *Neuroimage* 31, 968–980. doi: 10.1016/j.neuroimage.2006.01.021

Dubey, R., Zhou, J., Wang, Y., Thompson, P. M., and Ye, J. (2014). Analysis of sampling techniques for imbalanced data: an n = 648 ADNI study. *Neuroimage* 87, 220–241. doi: 10.1016/j.neuroimage.2013.10.005

Eskildsen, S. F., Coupé, P., García-Lorenzo, D., Fonov, V., Pruessner, J. C., Collins, D. L., et al. (2013). Prediction of Alzheimer's disease in subjects with mild cognitive impairment from the ADNI cohort using patterns of cortical thinning. *Neuroimage* 65, 511–521. doi: 10.1016/j.neuroimage.2012.09.058

Ewers, M., Walsh, C., Trojanowski, J. Q., Shaw, L. M., Petersen, R. C., Jack, C. R. Jr., et al. (2012). Prediction of conversion from mild cognitive impairment to Alzheimer's disease dementia based upon biomarkers and neuropsychological test performance. *Neurobiol. Aging* 33, 1203–1214. doi: 10.1016/j.neurobiolaging.2010.10.019

Fan, Y., Batmanghelich, N., Clark, C. M., and Davatzikos, C. (2008). Spatial patterns of brain atrophy in MCI patients, identified via high-dimensional pattern classification, predict subsequent cognitive decline. *Neuroimage* 39, 1731–1743. doi: 10.1016/j.neuroimage.2007.10.031

Fischl, B., Salat, D. H., Busa, E., Albert, M., Dieterich, M., Haselgrove, C., et al. (2002). Whole brain segmentation: automated labeling of neuroanatomical structures in the human brain. *Neuron* 33, 341–355. doi: 10.1016/S0896-6273(02)00569-X

Fornito, A., Zalesky, A., and Bullmore, E. T. (2010). Network scaling effects in graph analytic studies of human resting-state FMRI data. *Front. Syst. Neurosci.* 4:22. doi: 10.3389/fnsys.2010.00022

Frisoni, G. B., Fox, N. C., Jack, C. R. Jr., Scheltens, P., and Thompson, P. M. (2010). The clinical use of structural MRI in Alzheimer disease. *Nat. Rev. Neurol.* 6, 67–77. doi: 10.1038/nrneurol.2009.215

Gomar, J. J., Bobes-Bascaran, M. T., Conejero-Goldberg, C., Davies, P., and Goldberg, T. E. (2011). Utility of combinations of biomarkers, cognitive markers, and risk factors to predict conversion from mild cognitive impairment to Alzheimer disease in patients in the Alzheimer's disease neuroimaging initiative. *Arch. Gen. Psychiatry* 68, 961–969. doi: 10.1001/archgenpsychiatry.2011.96

Grundman, M., Petersen, R. C., Ferris, S. H., Thomas, R. G., Aisen, P. S., Bennett, D. A., et al. (2004). Mild cognitive impairment can be distinguished from Alzheimer disease and normal aging for clinical trials. *Arch. Neurol.* 61, 59–66. doi: 10.1001/archneur.61.1.59

Hänninen, T., Hallikainen, M., Tuomainen, S., Vanhanen, M., and Soininen, H. (2002). Prevalence of mild cognitive impairment: a population-based study in elderly subjects. *Acta Neurol. Scand.* 106, 148–154. doi: 10.1034/j.1600-0404.2002.01225.x

He, Y., Chen, Z., and Evans, A. (2008). Structural insights into aberrant topological patterns of large-scale cortical networks in Alzheimer's disease. *J. Neurosci.* 28, 4756–4766. doi: 10.1523/JNEUROSCI.0141-08.2008

He, Y., Chen, Z., Gong, G., and Evans, A. (2009). Neuronal networks in Alzheimer's disease. *Neuroscientist* 15, 333–350. doi: 10.1177/1073858409334423

Jack, C. R. Jr., Bernstein, M. A., Fox, N. C., Thompson, P., Alexander, G., Harvey, D., et al. (2008). The Alzheimer's Disease Neuroimaging Initiative (ADNI): MRI methods. *J. Magn. Reson. Imaging* 27, 685–691. doi: 10.1002/jmri.21049

Jie, B., Zhang, D., Wee, C. Y., and Shen, D. (2014). Topological graph kernel on multiple thresholded functional connectivity networks for mild cognitive impairment classification. *Hum. Brain Mapp.* 35, 2876–2897. doi: 10.1002/hbm.22353

Johnstone, D., Milward, E. A., Berretta, R., and Moscato, P. (2012). Multivariate protein signatures of pre-clinical Alzheimer's disease in the Alzheimer's disease neuroimaging initiative (ADNI) plasma proteome dataset. *PLoS ONE* 7:e34341. doi: 10.1371/journal.pone.0034341

Julkunen, V., Niskanen, E., Koikkalainen, J., Herukka, S. K., Pihlajamäki, M., Hallikainen, M., et al. (2010). Differences in cortical thickness in healthy controls, subjects with mild cognitive impairment, and Alzheimer's disease patients: a longitudinal study. *J. Alzheimers Dis.* 21, 1141–1151. doi: 10.3233/JAD-2010-100114

Kandiah, N., Chander, R. J., Ng, A., Wen, M. C., Cenina, A. R., and Assam, P. N. (2015). Association between white matter hyperintensity and medial temporal atrophy at various stages of Alzheimer's disease. *Eur. J. Neurol.* 22, 150–155. doi: 10.1111/ene.12546

Karas, G., Sluimer, J., Goekoop, R., Van Der Flier, W., Rombouts, S. A., Vrenken, H., et al. (2008). Amnestic mild cognitive impairment: structural MR imaging findings predictive of conversion to Alzheimer disease. *AJNR Am. J. Neuroradiol.* 29, 944–949. doi: 10.3174/ajnr.A0949

Lerch, J. P., Pruessner, J., Zijdenbos, A. P., Collins, D. L., Teipel, S. J., Hampel, H., et al. (2008). Automated cortical thickness measurements from MRI can accurately separate Alzheimer's patients from normal elderly controls. *Neurobiol. Aging* 29, 23–30. doi: 10.1016/j.neurobiolaging.2006.09.013

Li, C., Wang, J., Gui, L., Zheng, J., Liu, C., and Du, H. (2011). Alterations of whole-brain cortical area and thickness in mild cognitive impairment and Alzheimer's disease. *J. Alzheimers Dis.* 27, 281–290. doi: 10.3233/JAD-2011-110497

Li, L., and Zhao, D. (2015). Age-related inter-region EEG coupling changes during the control of bottom-up and top-down attention. *Front. Aging Neurosci.* 7:223. doi: 10.3389/fnagi.2015.00223

Liu, F., Wee, C. Y., Chen, H., and Shen, D. (2014). Inter-modality relationship constrained multi-modality multi-task feature selection for Alzheimer's Disease and mild cognitive impairment identification. *Neuroimage* 84, 466–475. doi: 10.1016/j.neuroimage.2013.09.015

Liu, J., Ji, S. W., and Ye, J. P. (2009). *SLEP: Sparse Learning with Efficient Projections: Arizona State University* [Online]. Available online at: http://www.public.asu.edu/~jye02/Software/SLEP

Meinshausen, N., and Bühlmann, P. (2010). Stability selection. *J. R. Stat. Soc. Ser. B Stat. Methodol.* 72, 417–473. doi: 10.1111/j.1467-9868.2010.00740.x

Misra, C., Fan, Y., and Davatzikos, C. (2009). Baseline and longitudinal patterns of brain atrophy in MCI patients, and their use in prediction of short-term conversion to AD: results from ADNI. *Neuroimage* 44, 1415–1422. doi: 10.1016/j.neuroimage.2008.10.031

Pennanen, C., Testa, C., Laakso, M. P., Hallikainen, M., Helkala, E. L., Hänninen, T., et al. (2005). A voxel based morphometry study on mild cognitive impairment. *J. Neurol. Neurosurg. Psychiatry* 76, 11–14. doi: 10.1136/jnnp.2004.035600

Petersen, R. C. (2004). Mild cognitive impairment as a diagnostic entity. *J. Intern. Med.* 256, 183–194. doi: 10.1111/j.1365-2796.2004.01388.x

Raamana, P. R., Weiner, M. W., Wang, L., and Beg, M. F. (2015). Thickness network features for prognostic applications in dementia. *Neurobiol. Aging* 36(Suppl. 1), S91–S102. doi: 10.1016/j.neurobiolaging.2014.05.040

Risacher, S. L., Saykin, A. J., West, J. D., Shen, L., Firpi, H. A., and McDonald, B. C. (2009). Baseline MRI predictors of conversion from MCI to probable AD in the ADNI cohort. *Curr. Alzheimer Res.* 6, 347–361. doi: 10.2174/156720509788929273

Schroeter, M. L., Stein, T., Maslowski, N., and Neumann, J. (2009). Neural correlates of Alzheimer's disease and mild cognitive impairment: a systematic and quantitative meta-analysis involving 1351 patients. *Neuroimage* 47, 1196–1206. doi: 10.1016/j.neuroimage.2009.05.037

Shu, N., Liang, Y., Li, H., Zhang, J., Li, X., Wang, L., et al. (2012). Disrupted topological organization in white matter structural networks in amnestic mild cognitive impairment: relationship to subtype. *Radiology* 265, 518–527. doi: 10.1148/radiol.12112361

Stam, C. J., De Haan, W., Daffertshofer, A., Jones, B. F., Manshanden, I., Van Cappellen Van Walsum, A. M., et al. (2009). Graph theoretical analysis of magnetoencephalographic functional connectivity in Alzheimer's disease. *Brain* 132, 213–224. doi: 10.1093/brain/awn262

Stam, C. J., Jones, B. F., Nolte, G., Breakspear, M., and Scheltens, P. (2007). Small-world networks and functional connectivity in Alzheimer's disease. *Cereb. Cortex* 17, 92–99. doi: 10.1093/cercor/bhj127

Tibshirani, R. (1996). Regression shrinkage and selection via the Lasso. *J. R. Stat. Soc. Ser. B Methodol.* 58, 267–288.

Tijms, B. M., Wink, A. M., De Haan, W., Van Der Flier, W. M., Stam, C. J., Scheltens, P., et al. (2013). Alzheimer's disease: connecting findings from graph theoretical studies of brain networks. *Neurobiol. Aging* 34, 2023–2036. doi: 10.1016/j.neurobiolaging.2013.02.020

Tijms, B. M., Yeung, H. M., Sikkes, S. A., Möller, C., Smits, L. L., Stam, C. J., et al. (2014). Single-subject gray matter graph properties and their relationship with cognitive impairment in early- and late-onset Alzheimer's disease. *Brain Connect.* 4, 337–346. doi: 10.1089/brain.2013.0209

Vemuri, P., Gunter, J. L., Senjem, M. L., Whitwell, J. L., Kantarci, K., Knopman, D. S., et al. (2008). Alzheimer's disease diagnosis in individual subjects using structural MR images: validation studies. *Neuroimage* 39, 1186–1197. doi: 10.1016/j.neuroimage.2007.09.073

Wang, M., Yang, P., Zhao, Q. J., Wang, M., Jin, Z., and Li, L. (2016). Differential preparation intervals modulate repetition processes in task switching: an ERP study. *Front. Hum. Neurosci.* 10:57. doi: 10.3389/fnhum.2016.00057

Westman, E., Muehlboeck, J. S., and Simmons, A. (2012). Combining MRI and CSF measures for classification of Alzheimer's disease and prediction of mild cognitive impairment conversion. *Neuroimage* 62, 229–238. doi: 10.1016/j.neuroimage.2012.04.056

Whitwell, J. L., Shiung, M. M., Przybelski, S. A., Weigand, S. D., Knopman, D. S., Boeve, B. F., et al. (2008). MRI patterns of atrophy associated with progression to AD in amnestic mild cognitive impairment. *Neurology* 70, 512–520. doi: 10.1212/01.wnl.0000280575.77437.a2

Wolz, R., Julkunen, V., Koikkalainen, J., Niskanen, E., Zhang, D. P., Rueckert, D., et al. (2011). Multi-method analysis of MRI images in early diagnostics

of Alzheimer's disease. *PLoS ONE* 6:e25446. doi: 10.1371/journal.pone.0025446

Yao, Z., Zhang, Y., Lin, L., Zhou, Y., Xu, C., Jiang, T., et al. (2010). Abnormal cortical networks in mild cognitive impairment and Alzheimer's disease. *PLoS Comput. Biol.* 6:e1001006. doi: 10.1371/journal.pcbi.1001006

Ye, J., Farnum, M., Yang, E., Verbeeck, R., Lobanov, V., Raghavan, N., et al. (2012). Sparse learning and stability selection for predicting MCI to AD conversion using baseline ADNI data. *BMC Neurol.* 12:46. doi: 10.1186/1471-2377-12-46

Zalesky, A., Fornito, A., and Bullmore, E. T. (2010). Network-based statistic: identifying differences in brain networks. *Neuroimage* 53, 1197–1207. doi: 10.1016/j.neuroimage.2010.06.041

Zhao, X., Liu, Y., Wang, X., Liu, B., Xi, Q., Guo, Q., et al. (2012). Disrupted small-world brain networks in moderate Alzheimer's disease: a resting-state FMRI study. *PLoS ONE* 7:e33540. doi: 10.1371/journal.pone.0033540

Zhou, Y., and Lui, Y. W. (2013). Small-world properties in mild cognitive impairment and early Alzheimer's disease: a cortical thickness MRI study. *ISRN geriatr.* 2013:542080. doi: 10.1155/2013/542080

**Conflict of Interest Statement:** The authors declare that the research was conducted in the absence of any commercial or financial relationships that could be construed as a potential conflict of interest.

frontiers in Aging Neuroscience

ORIGINAL RESEARCH
published: 24 May 2016
doi: 10.3389/fnagi.2016.00118

# Cortical Thickness Changes Correlate with Cognition Changes after Cognitive Training: Evidence from a Chinese Community Study

*Lijuan Jiang[1,2,3], Xinyi Cao[1,2,3], Ting Li[4], Yingying Tang[1,2,3], Wei Li[1,2,3], Jijun Wang[1,2,3]*, Raymond C. Chan[5] and Chunbo Li[1,2,3]**

[1] *Shanghai Key Laboratory of Psychotic Disorders, Shanghai Mental Health Center, Shanghai Jiao Tong University School of Medicine, Shanghai, China,* [2] *Bio-X Institutes, Key Laboratory for the Genetics of Developmental and Neuropsychiatric Disorders, Ministry of Education, Shanghai Jiao Tong University, Shanghai, China,* [3] *Brain Science and Technology Research Center, Shanghai Jiao Tong University, Shanghai, China,* [4] *Shanghai Chang Ning Mental Health Center, Shanghai, China,* [5] *Neuropsychology and Applied Cognitive Neuroscience Laboratory, Key Laboratory of Mental Health, Institute of Psychology, Chinese Academy of Sciences, Beijing, China*

The aim of this study was to investigate whether changes in cortical thickness correlated with cognitive function changes in healthy older adults after receiving cognitive training interventions. Moreover, it also aimed to examine the differential impacts of a multi-domain and a single-domain cognitive training interventions. Longitudinal magnetic resonance imaging (MRI) scanning was performed on participants 65–75 years of age using the Siemens 3.0 T Trio Tim with the Magnetization Prepared Rapid Gradient Echo (MPRAGE) sequence. The cortical thickness was determined using FreeSurfer Software. Cognitive functioning was evaluated using the Repeatable Battery for the Assessment of Neuropsychological Status (RBANS). There were significant group × time interaction effects on the left supramarginal, the left frontal pole cortical regions; and a marginal significant group × time interaction effects on visuospatial/constructional and delayed memory scores. In a multi-domain cognitive training group, a number of cortical region changes were significantly positively correlated with changes in attention, delayed memory, and the total score, but significantly negatively correlated with changes in immediate memory and language scores. In the single-domain cognitive training group, some cortical region changes were significantly positively associated with changes in immediate memory, delayed memory, and the total score, while they were significantly negatively associated with changes in visuospatial/constructional, language, and attention scores. Overall, multi-domain cognitive training offered more advantages in visuospatial/constructional, attention, and delayed memory abilities, while single-domain cognitive training benefited immediate memory ability more effectively. These findings suggest that healthy older adults benefit more from the multi-domain cognitive training than single-domain cognitive training. Cognitive training has impacted on cortical thickness changes in healthy elderly.

**Keywords: aging, cognitive function, cortical thickness, multi-domain, single-domain**

OPEN ACCESS

***Edited by:***
*Junming Wang, University of Mississippi Medical Center, USA*

***Reviewed by:***
*Rubem C. A. Guedes, Universidade Federal de Pernambuco, Brazil*
*Minghao Dong, Xidian University, China*
*Kenneth Ray Butler, University of Mississippi Medical Center, USA*

****Correspondence:***
*Jijun Wang*
*jijunwang27@163.com;*
*Chunbo Li*
*chunbo_li@163.com*

***Received:*** *24 December 2015*
***Accepted:*** *09 May 2016*
***Published:*** *24 May 2016*

***Citation:***
*Jiang L, Cao X, Li T, Tang Y, Li W, Wang J, Chan RC and Li C (2016) Cortical Thickness Changes Correlate with Cognition Changes after Cognitive Training: Evidence from a Chinese Community Study. Front. Aging Neurosci. 8:118. doi: 10.3389/fnagi.2016.00118*

## INTRODUCTION

As the average human lifespan increases and the world's aging population grows, issues surrounding the health and care of the aging are gaining increasing attention (Hu et al., 2014). Cognitive decline associated with aging, especially in episodic memory, attention, and executive functions, has been reported in both longitudinal (Meijer et al., 2009) and cross-sectional studies (Coubard et al., 2011; Kobayashi et al., 2015). As a means of prevention and treatment, cognitive training is designed to restore, increase, or optimize capacities in persons with cognitive decline or normal aging (Thompson and Foth, 2005; Belleville and Bherer, 2012; Rebok et al., 2014). Single-domain cognitive training focuses either on memory (Ball et al., 2002; Sisco et al., 2013), reasoning (Payne et al., 2012), strategy training (Kirchhoff et al., 2012) or processing speed (Cody et al., 2015). While multi-domain cognitive training combines several cognitive functions and demands their interplay (Corbett et al., 2015; Rahe et al., 2015). Beneficial changes at the behavioral level in cognitive function, as well as the structural level in the aging brain, have been proven possible as the result of cognitive training (Lustig et al., 2009; Reijnders et al., 2013; Rahe et al., 2015).

A number of randomized controlled trials (RCTs) have shown that cognitive training can improve cognitive performance in healthy older adults (Engvig et al., 2010; Mozolic et al., 2011; Kwok et al., 2013; Sisco et al., 2013; Corbett et al., 2015). For instance, Kwok et al. (2013) reported that the Active Mind cognitive-training program was effective in improving the cognitive function and quality of life for community-dwelling Chinese older adults in Hong Kong. Sisco et al. (2013) demonstrated that multifactorial memory training can improve the verbatim recall of prose in healthy older adults aged 65–91. Online cognitive training package (including memory, reasoning, attention training) in older adults has shown benefited to reasoning and verbal learning (Corbett et al., 2015).

Many studies have relied on structural brain imaging, such as whole-brain volume, regional gray matter volumes, and cortical thickness, to assess the effect of cognitive training in aging patients. The cortex, which is a tightly folded sheet of neurons, ranges in thickness between 1.5 and 4.5 mm (Parent and Carpenter, 1995). Measurements of cortical thickness can reflect the size, density, and arrangement of cells, which may be more closely linked with cognition ability than volumetric or intensity-based gray matter (GM) concentration measures, although these have also been shown to relate to other local measures of GM (Narr et al., 2007). Therefore, measurements of cortical thickness could provide important information about the regional integrity of the cerebral cortex and supply new insights into cognitive training (Liu et al., 2014).

The relationship between brain volumes and cognitive functions has been long-standing research interest. For example, some researchers have found positive correlations between GM volume and executive functions (Newman et al., 2007; Ruscheweyh et al., 2013) in cognitively healthy adults, and memory impairment is often associated with the atrophy of limbic structures (including the hippocampus and parahippocampal gyrus; Jack et al., 1992). However, fewer have shown the cortical thickness is correlated with cognitive functions (Ehrlich et al., 2012; Velayudhan et al., 2013; Kim et al., 2015b). For instance, Velayudhan et al. (2013) found that reduced thickness of the entorhinal cortex was related to reduced scores on perceptual and executive function tests, including perceptual speed and aspects of working memory in Alzheimer's disease. In another study, right parahippocampal gyrus atrophy showed a significant correlation with the executive and visuospatial functions impairment in Parkinson's disease (Kim et al., 2015b).

Taken together, we hypothesized that cortical thickness changes would significantly associated with changes in cognition, thereby revealing more brain mechanism of the cognitive training effect on healthy older adults. However, to our knowledge, no randomized, controlled study comparing multi-domain and single-domain cognitive training interventions in healthy older adults has been performed prior to our study. We also evaluated the effects of multi-domain and single-domain cognitive training interventions in healthy older adults.

## MATERIALS AND METHODS

### Subjects

Participants were community-dwelling elders living in a neighborhood located in the Putuo District of Shanghai from March 2008 to April 2008. Inclusion criteria mandated that participants: (a) were 65–75 years of age; (b) had no severe physical or mental illnesses (such as brain tumor, cerebral infarction, cerebral hemorrhage, malnutrition, major depressive disorder and schizophrenia); (c) were able to live independently; (d) had no disability, and no difficulties in hearing, vision or communication; (e) had at least 1 year of formal education; and (f) had an education-adjusted normal score on the Chinese version of the Mini-Mental State Examination (MMSE; Li et al., 2006; $>14$ for those who had not finished primary school; $>19$ for those who completed primary school; or $>24$ for those who had graduated from middle school). Any participants exhibiting obvious cognitive decline, or who had received a diagnosis of Alzheimer's disease or other major medical conditions, were excluded.

All participants underwent magnetic resonance imaging (MRI) scanning and cognitive assessments at baseline (Time 1) and a 12-month follow-up after the intervention (Time 2). Participants who were absent for one MRI scanning or one cognitive assessment were excluded from data analysis. All participants in this study provided a written informed consent form (LL(H)-09-04). This study was approved by the Human Research Ethics Committee of Tongji Hospital in Shanghai, China.

### Cognitive Training Program

The cognitive training intervention was delivered by a trained expert in small groups ($n \leq 15$). Each participant from the

groups attended a total of 24 sessions, with each session being 60 min long, 2 days a week, for 12 weeks. The multi-domain cognitive training consisted of activities geared towards memory, reasoning, problem solving strategies, visuospatial map reading skills development, handcraft making, and health and physical exercise; the single-domain cognitive training specifically targeted reasoning training, including the Tower of Hanoi, numerical reasoning, Raven Progressive Matrices, and verbal reasoning. Booster training was provided to each group, which included one additional 60-min training session every month, from the 6-month follow-up to the 9-month follow-up after the intervention. A detailed description of the program was provided in the previous publication (Cheng et al., 2012).

## Cognitive Assessment

The Repeatable Battery for the Assessment of Neuropsychological Status (RBANS, Form A; Randolph et al., 1998) was administered to participants in order to assess cognitive functioning. It consists of 12 tasks that measure five domains of cognitive functioning: (a) immediate memory was measured using a list learning task (40 points) and a story memory task (24 points); (b) visuospatial/constructional ability was measured using a figure copy task (20 points) and a line orientation task (20 points); (c) language was measured using a picture naming task (10 points) and a semantic fluency task (40 points); (d) attention was measured using a digit span task (16 points) and a coding task (89 points); and (e) delayed memory was measured using a list recall task (10 points), a list recognition task (20 points), a story recall task (12 points), and a figure recall task (20 points). The RBANS includes six scores: total scale score and five index scores. Administration and scoring of the RBANS in this study were conducted by trained personnel according to standardized instructions (Randolph et al., 1998). RBANS (Form A) had good validity and reliability in a Chinese community-living elderly sample (Lim et al., 2010; Cheng et al., 2011).

## Image Acquisition

Structural MRI scans were performed using a Siemens Tim Trio 3T scanner (Siemens Medical Solutions, Erlangen, Germany) with a 12 channel head coil. The pulse sequence used for morphometric analyses was three-dimensional T1-weighted Magnetization Prepared Rapid Gradient Echo (MPRAGE), with the following parameters: repetition time (TR) = 1900 ms, echo time (TE) = 3.43 ms, flip angle = 9°, image matrix = 256 × 256 mm, field of view (FOV) = 24 cm. Each scan took 5 min. Each volume consisted of 160 sagittal slices with a 1.0 mm slice thickness, voxel size = 0.9 × 0.9 × 1.0 $mm^3$. Images were reconstructed and visually checked for major artifacts (e.g., motion, ringing, wrap around and neurological abnormalities) before further processing.

## Cortical Thickness Analysis

For the image analysis, we used the FreeSurfer software package 5.3.0[1] for Mac OS. To estimate cortical thickness, images were automatically processed with the longitudinal stream in FreeSurfer (Reuter et al., 2012). All scans from two time points (Time 1 and Time 2) were first preprocessed independently with the cross-sectional stream. Then, each subject's base template was created from the scans of his or her two time points, which operates as an initial estimate for the segmentation and surface reconstruction. The two measurement time points were then registered to the base template in order to ensure non-biased analysis with regard to the two time points (Wenger et al., 2012). All reconstructed data were visually checked for segmentation accuracy at each time point. This work flow has been shown to significantly increase reliability and statistical power (Han et al., 2006). Based on gyral and sulcal anatomy, 34 distinct cortical regions were then segmented for each hemisphere, using the Desikan–Killiany Atlas (Desikan et al., 2006). Finally, the cortical thickness was measured as the shortest distance (in mm) between the white matter surface and the pial surface (Fischl and Dale, 2000).

[1]http://surfer.nmr.mgh.harvard.edu

## Statistical Analysis

All statistical analyses were performed using the Statistical Package for the Social Sciences (SPSS; SPSSInc., Chicago, IL, USA) version 17.0 for Windows. The statistical significance threshold was set at $p < 0.05$. A repeated-measures analysis of variance (ANOVA) was performed to evaluate the training effect on RBANS scores and cortical thickness. Correlation between the RBANS change scores and cortical thickness changes in the participants using partial correlation after correcting for age, gender, years of education, and estimated total intracranial volume (eTIV). We computed RBANS change scores (Time 2 minus Time 1), as well as cortical thickness changes (Time 2 minus Time 1). We analyzed the multi-domain and single-domain cognitive training groups separately.

# RESULTS

## Characteristics of Study Participants

The demographic and cognitive outcomes of healthy older adults at baseline and 12-month follow-up are shown in **Table 1**. At baseline, 24 subjects from the multi-domain training group and 24 subjects from the single-domain training group underwent cognitive assessment and the MRI scanning. Eighteen of the multi-domain training group and 18 of the single-domain training group finished the cognitive assessment and MRI scanning at 12-month follow-up after the intervention. A total of 12 participants withdrew, two due to left-handedness, one due to death, two due to intestinal cancer, one due to her husband's death, two due to operation and four due to rejecting the scanning. There were no significant differences between groups in terms of age, gender, or any cognitive outcome measurements, except for the years of education ($t = 2.63$, $p = 0.013$) at the 12-month follow-up. Due to some participants missing one MRI scanning or one cognitive assessment at the 12-month follow-up, these results were excluded from data analysis, thus leading to the single-domain training group demonstrating a lower figure

**TABLE 1 | Characteristics of demographic information and cognitive outcomes.**

| | | Multi-domain training group | Single-domain training group | $t/\chi^2$ | $p$ |
|---|---|---|---|---|---|
| Age | Baseline | 70.54 ± 3.23 | 70.00 ± 3.90 | 0.52 | 0.603 |
| | 12-month follow-up | 71.33 ± 3.31 | 71.17 ± 3.87 | 0.14 | 0.890 |
| Years of education | Baseline | 10.83 ± 3.60 | 9.08 ± 4.06 | 1.58 | 0.121 |
| | 12-month follow-up | 11.67 ± 3.20 | 8.39 ± 4.22 | 2.63 | **0.013*** |
| Gender (male:female) | Baseline | 17:7 | 12:12 | 2.18 | 0.140 |
| | 12-month follow-up | 13:5 | 8:10 | 2.86 | 0.091 |
| RBANS total score | Baseline | 90.13 ± 16.01 | 92.13 ± 14.12 | −0.46 | 0.648 |
| | 12-month follow-up | 106.94 ± 12.90 | 102.50 ± 16.30 | 0.91 | 0.371 |
| Immediate memory | Baseline | 84.17 ± 15.38 | 85.88 ± 15.47 | −0.38 | 0.703 |
| | 12-month follow-up | 103.17 ± 23.35 | 101.61 ± 18.67 | 0.22 | 0.827 |
| Visuospatial/Constructional | Baseline | 103.88 ± 15.59 | 101.79 ± 11.28 | 0.53 | 0.598 |
| | 12-month follow-up | 103.94 ± 11.56 | 103.50 ± 17.24 | 0.09 | 0.928 |
| Language | Baseline | 92.46 ± 13.47 | 93.83 ± 11.01 | −0.39 | 0.700 |
| | 12-month follow-up | 101.00 ± 8.39 | 99.11 ± 8.47 | 0.67 | 0.506 |
| Attention | Baseline | 86.08 ± 20.02 | 90.63 ± 15.81 | −0.87 | 0.388 |
| | 12-month follow-up | 94.94 ± 15.17 | 94.94 ± 18.57 | 0.00 | 1.000 |
| Delayed memory | Baseline | 96.54 ± 16.87 | 99.21 ± 20.11 | −0.50 | 0.621 |
| | 12-month follow-up | 118.50 ± 12.41 | 109.56 ± 19.79 | 1.63 | 0.113 |

*$p < 0.05$ significant two-sided testing.

for years of education than the multi-domain training group at the 12-month follow-up.

## The Effect of Training on Cortical Thickness and Cognition

To investigate the impact of the cognitive training on the cortical thickness, the repeated-measures ANOVA showed a significant group × time interaction effects on the left supramarginal region ($p$ = 0.025) and the left frontal pole region ($p$ = 0.040; **Figure 1**). Tests of simple main effects revealed that the left supramarginal region ($p$ = 0.020) cortical thickness was significantly reduced comparing to baseline in the single-domain training group, but not in the multi-domain training group. When the analyses were to investigate the impact of training on cognitive scores, a repeated-measures ANOVA revealed a marginal significant group × time interaction effects on visuospatial/constructional scores ($p$ = 0.081) and delayed memory scores ($p$ = 0.060). However, there were no group × time interaction effects on the other cortical regions and cognitive scores.

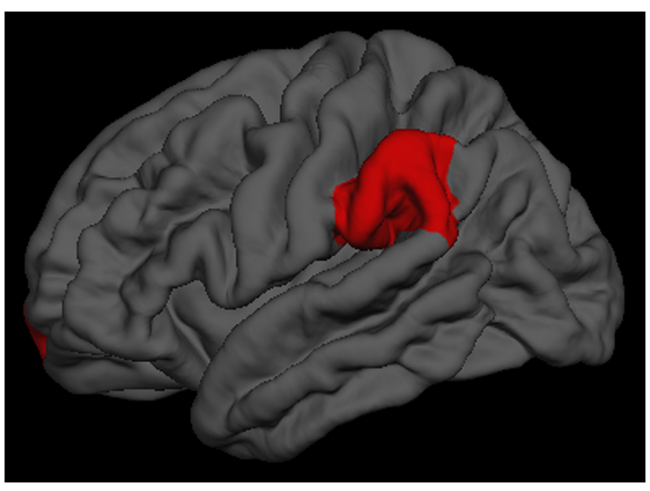

**FIGURE 1 | The left supramarginal and left frontal pole regions had significantly group × time interaction effects.**

## Associations of Cortical Thickness and Cognition

As shown in **Tables 2**, **3**, the cortical thickness changes associated with specific cognitive functions change scores are somewhat different in the multi-domain and single-domain training groups. **Table 2** presents the correlations between cognitive function change scores and cortical thickness changes in the multi-domain training group, after controlling for age, gender, education, and eTIV. It shows that the immediate memory change scores were significantly negatively associated with the changes in the left parahippocampal and right transverse temporal regions. In this group, visuospatial/constructional change scores were not significantly associated with any of the cortical thickness changes. However, significant negative correlations between language change scores and cortical thickness changes were observed in the change of the left parahippocampal region, and significant positive correlations between the attention change scores and cortical thickness changes were indicated in the change of the right frontal pole region. Furthermore, significant positive correlations between delayed memory change scores and cortical thickness changes were presented in the changes of the left inferior parietal, lateral occipital, lingual, superior parietal, and supramarginal, as well as the right cuneus, inferior parietal, lateral occipital, lateral orbitofrontal, pars orbitalis, posterior cingulate, rostral anterior cingulate, and insula regions. Finally, significant positive correlations between total change scores and cortical thickness changes were observed in changes to the left superior parietal and the right lateral occipital, temporal pole regions.

**TABLE 2 | Partial correlations between repeatable battery for the assessment of neuropsychological status (RBANS) change scores and cortical thickness changes in the multi-domain training group, by controlling for age, gender, education, and estimated total intracranial volume (eTIV)**.

| | Immediate memory | | Language | | Attention | | Delayed memory | | Total score | |
|---|---|---|---|---|---|---|---|---|---|---|
| **Cortical regions** | *r* | *p* | *r* | *p* | *r* | *p* | *r* | *p* | *r* | *p* |
| **Left hemisphere** | | | | | | | | | | |
| Inferior parietal | | | | | | | 0.552 | **0.040*** | | |
| Lateral occipital | | | | | | | 0.546 | **0.044*** | | |
| Lingual | | | | | | | 0.570 | **0.033*** | | |
| Parahippocampal | −0.582 | **0.029*** | −0.616 | **0.019*** | | | | | | |
| Superior parietal | | | | | | | 0.776 | **0.001*** | 0.608 | **0.021*** |
| Supramarginal | | | | | | | 0.578 | **0.030*** | | |
| **Right hemisphere** | | | | | | | | | | |
| Cuneus | | | | | | | 0.609 | **0.021*** | | |
| Inferior parietal | | | | | | | 0.565 | **0.035*** | | |
| Lateral occipital | | | | | | | 0.732 | **0.003*** | 0.554 | **0.040*** |
| Lateral orbitofrontal | | | | | | | 0.609 | **0.021*** | | |
| Pars orbitalis | | | | | | | 0.650 | **0.012*** | | |
| Posterior cingulate | | | | | | | 0.652 | **0.012*** | | |
| Rostral anterior cingulate | | | | | | | 0.561 | **0.037*** | | |
| Frontal pole | | | | | 0.636 | **0.015*** | | | | |
| Temporal pole | | | | | | | | | 0.605 | **0.022*** |
| Transverse temporal | −0.606 | **0.022*** | | | | | | | | |
| Insula | | | | | | | 0.550 | **0.042*** | | |

*RBANS, Repeatable Battery for the Assessment of Neuropsychological Status; eTIV, estimated total intracranial volume; *p < 0.05 significant two-sided testing.*

**TABLE 3 | Partial correlations between RBANS change scores and cortical thickness changes in the single-domain training group, by controlling for age, gender, education, and eTIV**.

| | Immediate memory | | Visuospatial/Constructional | | Language | | Attention | | Delayed memory | | Total score | |
|---|---|---|---|---|---|---|---|---|---|---|---|---|
| **Cortical regions** | *r* | *p* | *r* | *p* | *r* | *p* | *r* | *p* | *r* | *p* | *r* | *p* |
| **Left hemisphere:** | | | | | | | | | | | | |
| Entorhinal | | | | | | | | | 0.608 | **0.021*** | | |
| Paracentral | | | −0.697 | **0.006*** | | | | | | | | |
| Pars orbitalis | | | | | | | | | 0.710 | **0.004*** | | |
| Posterior cingulate | | | | | | | | | 0.646 | **0.013*** | | |
| Precuneus | | | | | | | | | 0.645 | **0.013*** | | |
| Rostral anterior cingulate | | | | | | | | | 0.543 | **0.045*** | | |
| Supramarginal | 0.557 | **0.039*** | | | | | | | 0.722 | **0.004*** | | |
| **Right hemisphere:** | | | | | | | | | | | | |
| Entorhinal | 0.595 | **0.025*** | | | | | | | | | | |
| Lateral occipital | | | | | | | −0.601 | **0.023*** | | | | |
| Lingual | | | | | | | −0.605 | **0.022*** | | | | |
| Paracentral | | | −0.542 | **0.045*** | | | | | | | | |
| Pericalcarine | | | | | | | −0.584 | **0.028*** | | | | |
| Posterior cingulate | | | | | | | | | 0.556 | **0.039*** | | |
| Precentral | | | | | | | −0.598 | **0.024*** | | | | |
| Precuneus | | | | | | | | | 0.589 | **0.027*** | | |
| Rostral anterior cingulate | | | | | −0.647 | **0.012*** | | | | | | |
| Superior parietal | | | | | | | | | 0.662 | **0.010*** | | |
| Frontal pole | | | | | | | | | | | 0.585 | **0.028*** |

*RBANS, Repeatable Battery for the Assessment of Neuropsychological Status; eTIV, estimated total intracranial volume; *p < 0.05 significant two-sided testing.*

**Table 3** presents the correlations between cognitive function change scores and cortical thickness changes in the single-domain training group, after controlling for age, gender, education, and eTIV. These results revealed that immediate memory change scores were significantly positively associated with the changes of the left supramarginal and the right entorhinal regions. Visuospatial/constructional change scores were significantly negatively associated with the changes of the left paracentral and the right paracentral regions and significant negative correlations between language change scores and cortical thickness changes were observed in the change of the right rostral anterior cingulate region. Attention change scores were significantly negatively correlated with the changes of the right lateral occipital, lingual, pericalcarine, and precentral regions. Significant positive correlations between delayed memory change scores and cortical thickness changes

were presented in the changes of the left entorhinal, pars orbitalis, posterior cingulate, precuneus, rostral anterior cingulate, and supramarginal, as well as the right posterior cingulate, precuneus, and superior parietal regions. Lastly, significant positive correlations between total change scores and cortical thickness changes were observed in the change of the right frontal pole region.

## DISCUSSION

The main finding of this study was that the cortical thickness changes were significantly associated with cognitive function changes in healthy elderly after receiving cognitive training interventions, and healthy older adults benefited more from the multi-domain cognitive training than single-domain cognitive training. Single-domain training targets highly specific cognitive abilities, it may allow researchers to evaluate direct training-related effects (Cheng et al., 2012). However, multi-domain training may have more practical advantages for older adults because that will increase engagement and transfer (Binder et al., 2015; Kim et al., 2015a).

There were significantly group × time interaction effects on the left supramarginal and the left frontal pole cortical regions, which two regions were parts of attention network (Fan et al., 2005; Grant et al., 2013). These findings implicated that the multi-domain cognitive training would offer more advantages in attention in the healthy older adults. Due to the relative small sample size, the results from the repeated-measures ANOVA may lead to an underestimation of interaction effects, the visuospatial/constructional scores and delayed memory scores showed a marginal significant group × time interaction effects. As such, cognitive training could delay age-associated cortical change and cognitive decline, it was an efficacious behavioral strategy for improving or maintaining cognitive health in the healthy elderly (Kim et al., 2015a; Smith-Ray et al., 2015).

In our study, both the multi-domain and single-domain training groups demonstrated delayed memory change scores that were significantly positively correlated with many distinct cortical region changes. These distinct cortical regions exhibited normal functions that were directly involved in improving delayed memory. This result showed that cognitive training can improve delayed memory in older persons living in a community.

As indicated previously, changes in brain structure, as well as cognitive functions, are commonly seen in the aging population. The human brain is a complex network of functionally and structurally interconnected regions. For example, the attention network contains the integrated regions of the frontal lobe, superior parietal lobe, fusiform gyrus, anterior cingulated, thalamus, and left precentral gyrus (Fan et al., 2005). Similar to previous studies (Fan et al., 2005), we observed significantly positive correlations between changes in attention scores and right frontal poles in the multi-domain training group. However, in the single-domain training group, attention change scores were significantly negatively correlated with change in the right lateral occipital, lingual, pericalcarine, and precentral. Cognitive function in aging does not have a single etiology, as there is not one exclusive brain region or system that is affected. According to a compensation view (Grady, 2012; Walhovd et al., 2014; Morcom and Johnson, 2015), it may be that the right lateral occipital, lingual, pericalcarine, and precentral regions are indirectly involved in improving attention, and require other brain regions to be involved in the process. Our analysis suggests that multi-domain training was more beneficial to attention improvement than single-domain training in healthy older adult participants. In accordance with a compensation view, we also concluded that multi-domain cognitive training was more effective in improving visuospatial/constructional skills, and single-domain cognitive training was more effective in improving immediate memory.

There are several limitations to this study that should be kept in mind when interpreting our results. The first major limitation involves the relatively conservative number of subjects, as we only included a small proportion of all identified community members who met the criteria for the study. Larger sample size is needed to evaluate the effect of cognitive training on the aging brain. Second, the multi-domain training group had a slightly higher education level than the single-domain training group at the 12-month follow-up (as explained in "Results" Section). However, years of education was used as covariate in our analysis. Finally, our study only has two time points: MRI data at baseline and the 12-month follow-up. In other words, we did not collect data immediately following the completion of the intervention. These limitations may affect the external validity of the study, and deserve to be examined further.

## CONCLUSION

In summary, our findings may contribute to an understanding of the mechanism of normal aging in the human brain and help to distinguish the different effects of multi-domain and single-domain cognitive training interventions in healthy older adults. Specifically, multi-domain cognitive training demonstrated more advantages in visuospatial/constructional, attention, and delayed memory abilities, while single-domain cognitive training primarily benefited immediate memory ability. In the end, multi-domain cognitive training may represent the best opportunity to improve the cognitive function of healthy older adults.

## AUTHOR CONTRIBUTIONS

Conceived the study: CL, JW. Designed the experiment: CL, JW, LJ, XC, TL. Performed the experiment: LJ, XC, TL, WL. Analyzed the data: LJ, YT, WL, RCC. Wrote the manuscript: LJ, XC, TL, RCC, CL, JW. All authors provided critical revisions to the manuscript and approved the final version of the article.

## ACKNOWLEDGMENTS

We thank other members of the research group: Yan Cheng, Wei Feng, Yikang Zhu, Huiru Cui, Hongmei Liu and Lanlan Zhang contributed to data collection. We thank Dr. Yi Jin

from the Chinese Academy of Sciences for assistance in the data analysis. This work was supported by National Nature Science Foundation of China (81371505, 30770769), the Science and Technology Commission of Shanghai Municipality (134119a2501, 13dz2260500) and the Shanghai Mental Health Center (2013-YJ-09, 2014-YJ-05).

## REFERENCES

Ball, K., Berch, D. B., Helmers, K. F., Jobe, J. B., Leveck, M. D., Marsiske, M., et al. (2002). Effects of cognitive training interventions with older adults: a randomized controlled trial. *JAMA* 288, 2271–2281. doi: 10.1001/jama.288.18.2271

Belleville, S., and Bherer, L. (2012). Biomarkers of cognitive training effects in aging. *Curr. Transl. Geriatr. Exp. Gerontol. Rep.* 1, 104–110. doi: 10.1007/s13670-012-0014-5

Binder, J. C., Zöllig, J., Eschen, A., Mérillat, S., Röcke, C., Schoch, S. F., et al. (2015). Multi-domain training in healthy old age: hotel plastisse as an ipad-based serious game to systematically compare multi-domain and single-domain training. *Front. Aging Neurosci.* 7:137. doi: 10.3389/fnagi.2015.00137

Cheng, Y., Wu, W., Feng, W., Wang, J., Chen, Y., Shen, Y., et al. (2012). The effects of multi-domain versus single-domain cognitive training in non-demented older people: a randomized controlled trial. *BMC Med.* 10:30. doi: 10.1186/1741-7015-10-30

Cheng, Y., Wu, W., Wang, J., Feng, W., Wu, X., and Li, C. (2011). Reliability and validity of the repeatable battery for the assessment of neuropsychological status in community-dwelling elderly. *Arch. Med. Sci.* 7, 850–857. doi: 10.5114/aoms.2011.25561

Cody, S. L., Fazeli, P., and Vance, D. E. (2015). Feasibility of a home-based speed of processing training program in middle-aged and older adults with HIV. *J. Neurosci. Nurs.* 47, 247–254. doi: 10.1097/JNN.0000000000000147

Corbett, A., Owen, A., Hampshire, A., Grahn, J., Stenton, R., Dajani, S., et al. (2015). The effect of an online cognitive training package in healthy older adults: an online randomized controlled trial. *J. Am. Med. Dir. Assoc.* 16, 990–997. doi: 10.1016/j.jamda.2015.06.014

Coubard, O. A., Ferrufino, L., Boura, M., Gripon, A., Renaud, M., and Bherer, L. (2011). Attentional control in normal aging and Alzheimer's disease. *Neuropsychology* 25, 353–367. doi: 10.1037/a002205

Desikan, R. S., Ségonne, F., Fischl, B., Quinn, B. T., Dickerson, B. C., Blacker, D., et al. (2006). An automated labeling system for subdividing the human cerebral cortex on MRI scans into gyral based regions of interest. *Neuroimage* 31, 968–980. doi: 10.1016/j.neuroimage.2006.01.021

Ehrlich, S., Brauns, S., Yendiki, A., Ho, B. C., Calhoun, V., Schulz, S. C., et al. (2012). Associations of cortical thickness and cognition in patients with schizophrenia and healthy controls. *Schizophr. Bull.* 38, 1050–1062. doi: 10.1093/schbul/sbr018

Engvig, A., Fjell, A. M., Westlye, L. T., Moberget, T., Sundseth, Ø., Larsen, V. A., et al. (2010). Effects of memory training on cortical thickness in the elderly. *Neuroimage* 52, 1667–1676. doi: 10.1016/j.neuroimage.2010.05.041

Fan, J., McCandliss, B. D., Fossella, J., Flombaum, J. I., and Posner, M. I. (2005). The activation of attentional networks. *Neuroimage* 26, 471–479. doi: 10.1016/j.neuroimage.2005.02.004

Fischl, B., and Dale, A. M. (2000). Measuring the thickness of the human cerebral cortex from magnetic resonance images. *Proc. Natl. Acad. Sci. U S A* 97, 11050–11055. doi: 10.1073/pnas.200033797

Grady, C. (2012). The cognitive neuroscience of aging. *Nat. Rev. Neurosci.* 13, 491–505. doi: 10.1038/nrn3256

Grant, J. A., Duerden, E. G., Courtemanche, J., Cherkasova, M., Duncan, G. H., and Rainville, P. (2013). Cortical thickness, mental absorption and meditative practice: possible implications for disorders of attention. *Biol. Psychol.* 92, 275–281. doi: 10.1016/j.biopsycho.2012.09.007

Han, X., Jovicich, J., Salat, D., van der Kouwe, A., Quinn, B., Czanner, S., et al. (2006). Reliability of MRI-derived measurements of human cerebral cortical thickness: the effects of field strength, scanner upgrade and manufacturer. *Neuroimage* 32, 180–194. doi: 10.1016/j.neuroimage.2006.02.051

Hu, J. P., Guo, Y. H., Wang, F., Zhao, X. P., Zhang, Q. H., and Song, Q. H. (2014). Exercise improves cognitive function in aging patients. *Int. J. Clin. Exp. Med.* 7, 3144–3149.

Jack, C. R., Petersen, R. C., O'Brien, P. C., and Tangalos, E. G. (1992). MR-based hippocampal volumetry in the diagnosis of Alzheimer' disease. *Neurology* 42, 183–188. doi: 10.1212/wnl.42.1.183

Kim, G. H., Jeon, S., Im, K., Kwon, H., Lee, B. H., Kim, G. Y., et al. (2015a). Structural brain changes after traditional and robot-assisted multi-domain cognitive training in community-dwelling healthy elderly. *PLoS One* 10:e0123251. doi: 10.1371/journal.pone.0123251

Kim, J. S., Yang, J. J., Lee, D. K., Lee, J. M., Youn, J., and Cho, J. W. (2015b). Cognitive impairment and its structural correlates in the parkinsonian subtype of multiple system atrophy. *Neurodegener. Dis.* 15, 294–300. doi: 10.1159/000430953

Kirchhoff, B. A., Anderson, B. A., Barch, D. M., and Jacoby, L. L. (2012). Cognitive and neural effects of semantic encoding strategy training in older adults. *Cereb. Cortex* 22, 788–799. doi: 10.1093/cercor/bhr129

Kobayashi, L. C., Smith, S. G., O'Conor, R., Curtis, L. M., Park, D., von Wagner, C., et al. (2015). The role of cognitive function in the relationship between age and health literacy: a cross-sectional analysis of older adults in Chicago, USA. *BMJ Open* 5:e007222. doi: 10.1136/bmjopen-2014-007222

Kwok, T., Wong, A., Chan, G., Shiu, Y. Y., Lam, K. C., Young, D., et al. (2013). Effectiveness of cognitive training for Chinese elderly in Hong Kong. *Clin. Interv. Aging* 8, 213–219. doi: 10.2147/CIA.s38070

Li, C., Wu, W., Jin, H., Zhang, X., Xue, H., He, Y., et al. (2006). Successful aging in Shanghai, China: definition, distribution and related factors. *Int. Psychogeriatr.* 18, 551–563. doi: 10.1017/s1041610205002966

Lim, M. L., Collinson, S. L., Feng, L., and Ng, T. P. (2010). Cross-cultural application of the repeatable battery for the assessment of neuropsychological status (RBANS): performances of elderly Chinese Singaporeans. *Clin. Neuropsychol.* 24, 811–826. doi: 10.1080/13854046.2010.490789

Liu, Y., Xie, T., He, Y., Duan, Y., Huang, J., Ren, Z., et al. (2014). Cortical thinning correlates with cognitive change in multiple sclerosis but not in neuromyelitis optica. *Eur. Radiol.* 24, 2334–2343. doi: 10.1007/s00330-014-3239-1

Lustig, C., Shah, P., Seidler, R., and Reuter-Lorenz, P. A. (2009). Aging, training and the brain: a review and future directions. *Neuropsychol. Rev.* 19, 504–522. doi: 10.1007/s11065-009-9119-9

Meijer, W. A., van Boxtel, M. P., Van Gerven, P. W., van Hooren, S. A., and Jolles, J. (2009). Interaction effects of education and health status on cognitive change: a 6-year follow-up of the Maastricht aging study. *Aging Ment. Health* 13, 521–529. doi: 10.1080/13607860902860821

Morcom, A. M., and Johnson, W. (2015). Neural reorganization and compensation in aging. *J. Cogn. Neurosci.* 27, 1275–1285. doi: 10.1162/jocn_a_00783

Mozolic, J. L., Long, A. B., Morgan, A. R., Rawley-Payne, M., and Laurienti, P. J. (2011). A cognitive training intervention improves modality-specific attention in a randomized controlled trial of healthy older adults. *Neurobiol. Aging* 32, 655–668. doi: 10.1016/j.neurobiolaging.2009.04.013

Narr, K. L., Woods, R. P., Thompson, P. M., Szeszko, P., Robinson, D., Dimtcheva, T., et al. (2007). Relationships between IQ and regional cortical gray matter thickness in healthy adults. *Cereb. Cortex* 17, 2163–2171. doi: 10.1093/cercor/bhl125

Newman, L. M., Trivedi, M. A., Bendlin, B. B., Ries, M. L., and Johnson, S. C. (2007). The relationship between gray matter morphometry and neuropsychological performance in a large sample of cognitively healthy adults. *Brain Imaging Behav.* 1, 3–10. doi: 10.1007/s11682-007-9000-5

Parent, A., and Carpenter, M. B. (1995). *Human Neuroanatomy.* Baltimore, MD: Williams and Wilkins.

Payne, B. R., Jackson, J. J., Hill, P. L., Gao, X. F., Roberts, B. W., and Stine-Morrow, E. A. L. (2012). Memory self-efficacy predicts responsiveness to inductive reasoning training in older adults. *J. Gerontol. B Psychol. Sci. Soc. Sci.* 67, 27–35. doi: 10.1093/geronb/gbr073

Rahe, J., Petrelli, A., Kaesberg, S., Fink, G. R., Kessler, J., and Kalbe, E. (2015). Effects of cognitive training with additional physical activity compared to pure

cognitive training in healthy older adults. *Clin. Interv. Aging* 10, 297–310. doi: 10.2147/CIA.S74071

Randolph, C., Tierney, M. C., Mohr, E., and Chase, T. N. (1998). The repeatable battery for the assessment of neuropsychological status (RBANS): preliminary clinical validity. *J. Clin. Exp. Neuropsychol.* 20, 310–319. doi: 10.1076/jcen.20.3.310.823

Rebok, G. W., Ball, K., Guey, L. T., Jones, R. N., Kim, H. Y., King, J. W., et al. (2014). Ten-year effects of the advanced cognitive training for independent and vital elderly cognitive training trial on cognition and everyday functioning in older adults. *J. Am. Geriatr. Soc.* 62, 16–24. doi: 10.1111/jgs.12607

Reijnders, J., van Heugten, C., and van Boxtel, M. (2013). Cognitive interventions in healthy older adults and people with mild cognitive impairment: a systematic review. *Aging Res. Rev.* 12, 263–275. doi: 10.1016/j.arr.2012.07.003

Reuter, M., Schmansky, N. J., Rosas, H. D., and Fischl, B. (2012). Within-subject template estimation for unbiased longitudinal image analysis. *Neuroimage* 61, 1402–1418. doi: 10.1016/j.neuroimage.2012.02.084

Ruscheweyh, R., Deppe, M., Lohmann, H., Wersching, H., Korsukewitz, C., Duning, T., et al. (2013). Executive performance is related to regional gray matter volume in healthy older individuals. *Hum. Brain Mapp.* 34, 3333–3346. doi: 10.1002/hbm.22146

Sisco, S. M., Marsiske, M., Gross, A. L., and Rebok, G. W. (2013). The influence of cognitive training on older adults' recall for short stories. *J. Aging Health* 25, 230S–248S. doi: 10.1177/0898264313501386

Smith-Ray, R. L., Hughes, S. L., Prohaska, T. R., Little, D. M., Jurivich, D. A., and Hedeker, D. (2015). Impact of cognitive training on balance and gait in older adults. *J. Gerontol. B Psychol. Sci. Soc. Sci.* 70, 357–366. doi: 10.1093/geronb/gbt097

Thompson, G., and Foth, D. (2005). Cognitive-training programs for older adults: what are they and can they enhance mental fitness? *Educ. Gerontol.* 31, 603–626. doi: 10.1080/03601270591003364

Velayudhan, L., Proitsi, P., Westman, E., Muehlboeck, J. S., Mecocci, P., Vellas, B., et al. (2013). Entorhinal cortex thickness predicts cognitive decline in Alzheimer's disease. *J. Alzheimers Dis.* 33, 755–766. doi: 10.3233/JAD-2012-121408

Walhovd, K. B., Fjell, A. M., and Espeseth, T. (2014). Cognitive decline and brain pathology in aging—need for a dimensional, lifespan and systems vulnerability view. *Scand. J. Psychol.* 55, 244–254. doi: 10.1111/sjop.12120

Wenger, E., Schaefer, S., Noack, H., Kühn, S., Mårtensson, J., Heinze, H. J., et al. (2012). Cortical thickness changes following spatial navigation training in adulthood and aging. *Neuroimage* 59, 3389–3397. doi: 10.1016/j.neuroimage.2011.11.015

**Conflict of Interest Statement**: The authors declare that the research was conducted in the absence of any commercial or financial relationships that could be construed as a potential conflict of interest.

The reviewer KRB and handling Editor declared their shared affiliation, and the handling Editor states that the process nevertheless met the standards of a fair and objective review.

frontiers in Aging Neuroscience

ORIGINAL RESEARCH
published: 12 April 2016
doi: 10.3389/fnagi.2016.00070

# Effects of Cognitive Training on Resting-State Functional Connectivity of Default Mode, Salience, and Central Executive Networks

*Weifang Cao[1†], Xinyi Cao[2†], Changyue Hou[1], Ting Li[3], Yan Cheng[2], Lijuan Jiang[2], Cheng Luo[1]*, Chunbo Li[2,4,5]* and Dezhong Yao[1]*

[1] Key Laboratory for NeuroInformation of Ministry of Education, Center for Information in Medicine, High-Field Magnetic Resonance Brain Imaging Key Laboratory of Sichuan Province, School of Life Science and Technology, University of Electronic Science and Technology of China, Chengdu, China, [2] Shanghai Key Laboratory of Psychotic Disorders, Shanghai Mental Health Center, Shanghai Jiao Tong University School of Medicine, Shanghai, China, [3] Shanghai Changning Mental Health Center, Shanghai, China, [4] Bio-X Institutes, Key Laboratory for the Genetics of Developmental and Neuropsychiatric Disorders, Ministry of Education, Shanghai Jiao Tong University, Shanghai, China, [5] Brain Science and Technology Research Center, Shanghai Jiao Tong University, Shanghai, China

Neuroimaging studies have documented that aging can disrupt certain higher cognitive systems such as the default mode network (DMN), the salience network and the central executive network (CEN). The effect of cognitive training on higher cognitive systems remains unclear. This study used a 1-year longitudinal design to explore the cognitive training effect on three higher cognitive networks in healthy older adults. The community-living healthy older adults were divided into two groups: the multi-domain cognitive training group (24 sessions of cognitive training over a 3-months period) and the wait-list control group. All subjects underwent cognitive measurements and resting-state functional magnetic resonance imaging scanning at baseline and at 1 year after the training ended. We examined training-related changes in functional connectivity (FC) within and between three networks. Compared with the baseline, we observed maintained or increased FC within all three networks after training. The scans after training also showed maintained anti-correlation of FC between the DMN and CEN compared to the baseline. These findings demonstrated that cognitive training maintained or improved the functional integration within networks and the coupling between the DMN and CEN in older adults. Our findings suggested that multi-domain cognitive training can mitigate the aging-related dysfunction of higher cognitive networks.

**Keywords: aging, cognitive training, resting-state fMRI, functional connectivity, brain network**

OPEN ACCESS

***Edited by:***
*Alessio Avenanti,*
*Alma Mater Studiorum – University of Bologna, Italy*

***Reviewed by:***
*Antonio Gallo,*
*Second University of Naples, Italy*
*Jason S. Nomi,*
*University of Miami, USA*

****Correspondence:***
*Cheng Luo*
*chengluo@uestc.edu.cn;*
*Chunbo Li*
*chunbo_li@163.com*

*† These authors have contributed equally to this work.*

***Received:*** *08 December 2015*
***Accepted:*** *24 March 2016*
***Published:*** *12 April 2016*

***Citation:***
*Cao W, Cao X, Hou C, Li T, Cheng Y, Jiang L, Luo C, Li C and Yao D (2016) Effects of Cognitive Training on Resting-State Functional Connectivity of Default Mode, Salience, and Central Executive Networks. Front. Aging Neurosci. 8:70. doi: 10.3389/fnagi.2016.00070*

## INTRODUCTION

As people age, they experience cognitive decline, which involves working memory, executive function and attention, among other functions, and this occurs with particular frequency in late life, resulting in an increasingly poor quality of life (Hedden and Gabrieli, 2004; Grady, 2012). To postpone the cognitive decline associated with aging, increasing numbers of studies have conducted

interventions with older adults, focusing on cognitive training and physical exercise (Park and Bischof, 2013; Tanigawa et al., 2014). Results of neuropsychological studies have demonstrated benefits of cognitive functions after interventions in old adults, including improvements in working memory capacity, reasoning, and processing speed (Neely and Backman, 1995; Oswald et al., 2006; Bamidis et al., 2015; Leung et al., 2015). Our previous study has also demonstrated that the effects of interventions on cognition are maintained at 1 year after the training ended (Cheng et al., 2012). On the other hand, neuroimaging studies have proved that multi-domain training affects the spontaneous brain activity in healthy older adults, for example, altered regional homogeneity of spontaneous fluctuations in temporal gyrus and cerebellum, enhanced amplitude of low frequency fluctuations in frontal gyrus and cerebellum (Yin et al., 2014; Zheng et al., 2015). In another study, improved memory performance during memory task after training has been shown to associate with increased brain activation in the prefrontal, temporal, and parietal area in older adults (Kirchhoff et al., 2012). Also, the reduction in functional connection (FC) between the superior parietal cortex and inferior temporal lobe is observed after training in older adults, which is associated with training success (Strenziok et al., 2014). These findings suggest that the interventions bring about not only enhanced behavioral outcomes but improvement of the brain function in older adults (Kraft, 2012; Bamidis et al., 2014).

Recent studies suggest that functional brain networks, a higher level of organization of brain regions, are needed to better understand improved cognitive function after intervention (Langer et al., 2013; Bamidis et al., 2014). Using functional magnetic resonance imaging (fMRI), more than ten functional brain networks constituted of spatially distinct brain regions have been identified either at specific tasks (Calhoun et al., 2009) or at rest, including the default mode network (DMN), the salience network (SN) and the central executive network (CEN; Smith et al., 2009; Luo et al., 2012). Three (DMN, SN, and CEN) of these stable networks have been considered the 'core' neurocognitive networks for understanding higher cognitive functions and have received the most attention in cognitive studies (Sridharan et al., 2008; Bressler and Menon, 2010; Luo et al., 2011, 2014b). The DMN, which includes mainly the posterior cingulate cortex (PCC), medial prefrontal cortex (MPFC) and inferior parietal lobe (IPL), is involved in self-referential and autobiographical memory functions (Raichle et al., 2001; Buckner et al., 2008). The SN includes the bilateral anterior insula (AI) and dorsal anterior cingulate cortex, and it is associated with detecting internal and external events salient to homeostasis. In contrast, the CEN, composed of the dorsolateral frontal and parietal neocortices, is engaged in cognitively demanding tasks, such as decision making and working memory (Seeley et al., 2007). Many studies have indicated that these three networks, along with the disruption of FC within network and the anti-correlation between the DMN and CEN, are strongly affected by normal aging and Alzheimer's disease, which is associated with cognitive impairments (Meunier et al., 2009; Wu et al., 2011; Onoda et al., 2012; Tomasi and Volkow, 2012; Cao et al., 2014).

Previous studies have shown that brain networks are affected by interventions, such as the DMN and CEN, associated with improved behavioral outcomes and cognitive performances (Patel et al., 2013; Bamidis et al., 2014; Luo et al., 2014a; Tang and Posner, 2014). For instance, intervention studies, including either cognitive or physical training, reveal changes in the resting-state FC within the DMN and CEN in healthy adults (Voss et al., 2010, 2013; Taylor et al., 2013). Interventions have also been conducted on older adults to investigate the changes in brain networks that subserve cognitive function (Voss et al., 2010; Bamidis et al., 2014; Luo et al., 2016). A study of multimodal intervention in older adults has shown improved resting-state FC between the MPFC and medial temporal lobe in the DMN after training, suggesting an association with better cognitive performance (Li et al., 2014). Increases in cerebral blood flow and resting-state FC within the DMN and CEN are also observed after complex cognitive training in healthy seniors (Chapman et al., 2015). In addition, a study also demonstrated the decreased FC between the DMN and CEN after working memory training in health adults (Takeuchi et al., 2013). These findings suggest that training can affect FC of certain brain networks, such as DMN, CEN. However, no study has investigated the effects of multi-domain cognitive training on resting-state FC within and among the three networks (DMN, SN, and CEN) in older adults.

The purpose of this study is to explore the effects of cognitive training on resting-state FCs within and between the three networks in old adults. We hypothesized that multi-domain cognitive training would result in changes of resting-state FC within and among the three networks in healthy older adults, which might be beneficial for counteracting decreased integration within network and impaired coupling between networks with aging. In our work, we investigated the resting-state FC of three networks using seed-based FC analysis at baseline and at 1 year after training ended. The relationship between cognitive improvements and the changes of FC was also analyzed.

## MATERIALS AND METHODS

### Participants

The current work included 40 healthy older adults from two randomized groups [the multi-domain training group ($n = 23$) and the control group ($n = 17$)], who were recruited through a dispatched notice/broadcasting by the local institute of community service in three community centers around Tongji Hospital in Shanghai from March 2008 to April 2008. After a personal interview with professional interviewers, all participants then underwent cognitive measurements and fMRI scanning. The inclusion criteria included the following: age (65–75 years); educational year (more than 1 year); normal hearing, vision, or communication status; normal functional capacity; living independently in the community; score on the Chinese version of the Mini-Mental State Examination (MMSE) of 19 or above [the lower cut-off point of the MMSE score is due to the lower educational level in China (Li et al., 2006)]; and being free of neurological or psychiatric disorders and of brain injury. Exclusion criteria included the following: obvious

cognitive decline, a diagnosis of AD; serious neurological or psychiatric disorders such as major depressive disorder, brain cancer, and schizophrenia. One left-handed subject in the multi-domain training group was included due to the absence of a relationship between the training-related changes and handedness (Mackey et al., 2013). This study was approved by the Ethical Committee of the East China Normal University. All participants gave written informed consent, and they were not provided monetary compensation for their participation in this study.

## Neuropsychological Measurements

### Interventions

Cognitive training employed a randomized, controlled design. The multi-domain training group was divided into a small group, and the training procedure took place in a classroom in Tongji Hospital. All participants received 24 sessions of cognitive training over a 3-months period at a frequency of twice a week. The multi-domain cognitive training targeted memory, reasoning, and problem-solving strategies using approaches such as visual-spatial map reading, handcraft making, healthy living, and physical exercise. Each session lasted 60 min. A lecture about a common disease in aging people was presented during the first 15 min of each session. Then, the trainer taught the participants about a special cognitive strategy or technique via slide lecture during the second 30 min. The newly practiced skills were consolidated by dealing with some real-life problems during the last 15 min. The wait-list control group served as a match for the social contact associated with cognitive training. The multi-domain training group and the control group attended a lecture about healthy living every 2 months. More details about the training are provided in our previous study (Cheng et al., 2012).

### Cognitive Measurements

To evaluate the effects of intervention on cognitive function, composite outcome measurements were created, including the Repeatable Battery for the Assessment of Neuropsychological Status (RBANS, Form A), which shows good validity and reliability in a Chinese community-living elderly sample (Lim et al., 2010; Cheng et al., 2011), the trail-making test (TMT; Ashendorf et al., 2008), the visual reasoning test (Xiao et al., 2002) and the Color Word Stroop test (CWST; van Boxtel et al., 2001). All measurements were conducted at baseline and at 1 year after training.

To examine the effect of cognitive training on cognition, we compared the pre- and post-training changes between the multi-domain cognitive group and the control group using one-way analyses of covariance (ANCOVAs) with the differences between the 1-year post-test and baseline measurements as dependent variables and scores at baseline as covariates to exclude the possibility that any pre-existing difference in the measures between the groups affected the results of each measure ($p < 0.05$). In addition, two-sample $t$-tests were applied to investigate the differences in cognition measurements at baseline between the two groups. The confounding covariates, including age, gender and education years, were regressed in all statistical analyses.

## Data Acquisition

All functional and structural imaging data were acquired using a Siemens 3T MRI scanner (Erlangen, Germany) at East China Normal University, Shanghai, China. All participants underwent scanning twice, at baseline and at 1 year after training. To minimize head motion, we fixed the subjects' heads using foam pads. Resting-state functional images were collected using a single-shot, gradient-recalled echo planar imaging sequence [repetition time (TR) = 2000 ms, echo time (TE) = 25 ms and flip angle (FA) = 90°, field of view (FOV) = 240 mm × 240 mm, in-plane matrix = 64 × 64, slice thickness = 5 mm, voxel size = 3.75 mm × 3.75 mm × 5 mm], generating 32 slices. The functional scanning lasted for 310 s, yielding a total of 155 volumes. To ensure magnetic field stabilization, the first five volumes were discarded. During the resting-state scanning, the subjects were asked to lie with their eyes closed, not to fall asleep, and not to think of anything in particular. Axial T1-weighted anatomical images were acquired using a magnetisation-prepared rapid gradient-echo sequence, generating 160 slices (TR = 1900 ms, TE = 3.43 ms, FA = 90°, matrix size = 256 × 256, FOV = 240 mm × 240 mm, slice thickness = 1 mm, voxel size = 0.9375 mm × 0.9375 mm × 1 mm).

## Data Preprocessing

### Resting-State fMRI Data

Imaging data preprocessing was performed using the SPM8 software package[1]. First, all imaging data were corrected for the slice-timing and realigned for head movement correction. Accounting for the effect of head motion on the FC analysis, we excluded all the participants whose head movement exceeded 1 mm or 1°. Furthermore, we also calculated the framewise displacement (FD) given by

$$FD_i = |\Delta d_{ix}| + |\Delta d_{iy}| + |\Delta d_{iz}| + |\Delta \alpha_i| + |\Delta \beta_i| + |\Delta \gamma_i|, \quad (1)$$

where $i$ is the $i$-th time point and

$$\Delta d_{ix} = d_{(i-1)x} - d_{ix}(similarly for d_{iy}, d_{iz}, \alpha_i, \beta_i, \gamma_i). \quad (2)$$

The $FD_0$ was set to zero and rotational displacements were converted from degrees to millimeters (Power et al., 2012). Then, the resulting functional data were normalized to the Montreal Neurological Institute (MNI) template using a 12-parameter affine transformation (resampled to 3 mm × 3 mm × 3 mm). Finally, the imaging data were spatially smoothed with a 6-mm full-width at half maximum (FWHM) Gaussian kernel. We applied a temporal band-pass filter (the frequency range of 0.01 and 0.08 Hz) to reduce the low frequency drift and high frequency physiological noise (Fox et al., 2005; Jiang et al., 2015; Luo et al., 2015). Several nuisance covariates including white matter (WM) signal, cerebrospinal fluid (CSF) signal, global signal, and six head motion parameters were also removed from the time course of all brain voxels using a multiple linear regression analysis.

[1] http://www.fil.ion.ucl.ac.uk/spm/

### Preprocessing of T1-Weighted Images

Previous studies provided the evidence of the loss of gray matter volume (GMV) with aging and of the potential effects on the functional results (Damoiseaux et al., 2008). In the present study, we increased the reliability of resting-state fMRI analysis by controlling for the GMV. The T1-weighted images were preprocessed using the voxel-based morphometry (VBM8[2]) toolbox in SPM8. The native T1-weighted image was normalized to MNI space using an exponentiated lie algebra (DARTEL) approach. The resulting images were then segmented into gray matter (GM), WM and CSF. For each subject, the GMV of the whole brain was calculated.

### Functional Connectivity Analysis

To evaluate our hypothesis, a seed-based FC analysis was performed to examine the training effect on FC within and between the DMN, SN, and CEN. Three seeds were selected based on previous studies: the PCC (0, −52, 20), the right AI (38, 26, −10) and the right dorsolateral prefrontal cortex [right DLPFC (44, 36, 20)] to constitute the DMN, SN, and CEN, respectively (Fransson, 2006; Seeley et al., 2007; Luo et al., 2011). The average signal of spherical regions with nine-millimeter diameter centered at the three seeds was extracted. The FC map for each network was obtained by calculating Pearson correlation coefficient between the average time course of seed and each voxel in the whole brain for each subject. A Fisher z-transformation was used to convert the correlation coefficient of each voxel to a normal distribution (Shao et al., 2012; Chen et al., 2015). Thus, the individual z-score maps were obtained for each seed and subject. A one-sample *t*-test was used to identify the within-group FC map for each network. The significance level was set at $p < 0.05$ (FDR-corrected, cluster size $> 621$ mm$^3$).

### Statistical Analysis

To evaluate the training effect on FC within and between the three networks, a whole-brain voxel-wise 2 (between-subject factor: training and control groups) × 2 (within-subject factor: baseline and 1-year after training ending) repeated analysis of variance (ANOVA) was performed using the explicit mask from the union set of the one-sample *t*-test results of three networks, by controlling for the whole brain GMV, as well as age, gender, education years and FD as confounding covariates. This analysis was performed using SPM8, and the significance level was set at $p < 0.05$ (cluster size $> 621$ mm$^3$). *Post hoc* comparisons (paired *t*-tests) were carried out for each significant interaction effect to clarify the effect of training on FC for each group.

### Neural Correlate Analysis

To explore the relationship between FC and cognitive measurements, z-transformed connectivity values were extracted from regions that showed significant training-related effect, and the difference between the baseline and post-test was computed. Partial correlations were performed between the changes of resting-state FC and the pre- and post-training differences in the scores on the cognitive measures, while controlling for age, gender, and education years.

[2]http://dbm.neuro.uni-jena.de/

## RESULTS

### Demographic and Neuropsychological Tests

At baseline, 23 subjects (one left-handed) from the multi-domain training group and 17 subjects from the control group underwent cognitive measurements and the fMRI scanning. Eighteen subjects in the multi-domain training group and 14 in the control group finished both the cognitive measurements and the fMRI scanning at 1 year after the intervention, and they were involved in the final analysis. A total of eight participants withdrew (one death, two cancers, one operation, and four rejecting scanning). No significant differences in age, gender, education years, FD and MMSE score were found between the multi-domain training group and the control group ($p > 0.05$; **Table 1**).

No significant differences in all cognitive measurements were found at baseline between the two groups ($p > 0.05$; **Table 2**). However, the multi-domain training group showed significant improvements in performance on language ($p = 0.036$) and delayed memory ($p = 0.027$) and marginally significant improvement on the RBANS total score ($p = 0.058$) at 1-year after training compared to the baseline (**Table 2**).

### The Effect of Cognitive Training on Networks

Three networks were constituted by seed-based FC analysis, seeding at the PCC for the DMN, at the right AI for the SN and at the right DLPFC for the CEN. The DMN mainly involved the PCC/precuneus, VMPFC, DMPFC, bilateral IPL, bilateral temporal lobe, cerebellar lobule IX and crus II (Supplementary Figure S1). The SN mainly included the bilateral AI, DMPFC, dACC, and bilateral TPJ (Supplementary Figure S2), and the CEN was composed of the DLPFC, DMPFC, and IPL, all bilaterally (Supplementary Figure S3).

**TABLE 1 | Demographic information about the subjects at different timepoints.**

| | | Multi-domain training group | Control group | *p* |
|---|---|---|---|---|
| Age (year) | Baseline | 70.61 ± 3.29 | 68.59 ± 3.24 | 0.838 |
| (mean ± SD) | One-year post-test | 72.39 ± 3.43 | 70.85 ± 4.05 | 0.782 |
| Gender (male) | Baseline | 23 (16) | 17 (9) | 0.283 |
| | One-year post-test | 18 (13) | 14 (9) | 0.631 |
| Education (year) | Baseline | 10.91 ± 3.65 | 10.64 ± 3.06 | 0.452 |
| (mean ± SD) | One-year post-test | 11.11 ± 4.25 | 10.09 ± 3.34 | 0.383 |
| MMSE | Baseline | 27.57 ± 2.57 | 28.17 ± 1.94 | 0.505 |
| (mean ± SD) | One-year post-test | 27.72 ± 2.16 | 27.85 ± 2.31 | 0.900 |
| FD | Baseline | 0.12 ± 0.04 | 0.14 ± 0.05 | 0.448 |
| (mean ± SD) | One-year post-test | 0.12 ± 0.04 | 0.16 ± 0.07 | 0.068 |

*FD, Framewise displacement; MMSE, the Mini-Mental State Examination; SD, standard deviation.*

**TABLE 2 | Baseline and 1-year post-test scores for psychological measures (mean ± SD).**

| | Multi-domain training | | Contorl | | | |
|---|---|---|---|---|---|---|
| | Baseline | One-year Post-test | Baseline | One-year Post-test | $P^a$ | $P^b$ |
| RBANS total score | 93.17 ± 16.10 | 106.94 ± 12.90 | 93.07 ± 15.00 | 99.57 ± 13.75 | 0.058 | 0.971 |
| Immediate memory | 86.22 ± 16.45 | 103.17 ± 23.35 | 84.00 ± 14.34 | 100.5 ± 14.33 | 0.695 | 0.694 |
| Visuospatial | 106.78 ± 12.86 | 103.9 ± 11.56 | 106.86 ± 19.05 | 103.00 ± 16.81 | 0.981 | 0.922 |
| Language | 92.44 ± 12.92 | 101.00 ± 8.39 | 93.29 ± 7.12 | 95.86 ± 5.86 | **0.036*** | 0.861 |
| Attention | 90.67 ± 19.39 | 94.94 ± 15.17 | 91.5 ± 15.25 | 88.93 ± 15.24 | 0.22 | 0.776 |
| Delayed memory | 98.28 ± 18.86 | 118.50 ± 12.41 | 99.00 ± 13.13 | 110.21 ± 14.80 | **0.027*** | 0.999 |
| The CWST | | | | | | |
| Color interfere | 20.16 ± 13.95 | 27.33 ± 17.01 | 14.57 ± 7.62 | 23.85 ± 14.33 | 0.884 | 0.125 |
| Word interfere | 38.61 ± 15.56 | 39.89 ± 17.35 | 39.71 ± 14.10 | 42.00 ± 19.00 | 0.669 | 0.642 |
| The Visual Reasoning Test | 5.78 ± 1.35 | 6.56 ± 1.89 | 5.86 ± 2.74 | 5.93 ± 2.46 | 0.169 | 0.894 |
| The TMT | | | | | | |
| Trail A complete time | 79.50 ± 23.60 | 73.72 ± 33.93 | 87.21 ± 37.37 | 77.07 ± 29.22 | 0.739 | 0.381 |
| Trail B complete time | 157.89 ± 55.41 | 138.5 ± 48.27 | 153.5 ± 68.11 | 142.57 ± 49.6 | 0.634 | 0.830 |

*$p<0.05$. *CWST, Color Word Stroop test; RBANS, Repeatable Battery for the Assessment of Neuropsychological Status; TMT, Trail Making test.* [a]*One-way ANCOVAs with differences between 1-year post-test and baseline in psychological measures as dependent variables, by controlling for scores of the psychological measures at baseline, age, gender and education years as covariates.* [b]*Two sample t-test with scores of the psychological measures at baseline as dependent variables, by controlling for age, gender, and education years as covariates.*

The 2 × 2 repeated measure ANOVA revealed significant interactions ($p < 0.05$) for FC within and between networks. In this study, this analysis was performed for the FCs that showed no significant difference between the training and control groups at baseline, because a training-related effect was the only possibility.

The ANOVA revealed the significant interactions for the FC within the DMN [PCC – left superior frontal gyrus (SFG) and PCC – cerebellar lobule IX]; within the SN (right AI – right middle/posterior insula, and right AI – left frontoinsula) and within the CEN (right DLPFC – bilateral DLPFC and right DLPFC – right SFG). *Post hoc* comparison demonstrated that some connections showed increased or maintained FC in the training group but decreased FC in the control group, including those between the PCC and the left SFG and between the PCC and cerebellar lobule IX within the DMN, between the right AI and left frontoinsula within the SN, and between the right DLPFC and the bilateral DLPFC and between the right DLPFC and the right SFG within the CEN (**Figure 1**; **Table 3**). In addition, we observed increased FC between the right AI and right middle/posterior insula in the control group but maintained FC after training in the training group (**Figure 1**; **Table 3**).

Our results also revealed significant interactions in the FCs between networks, including between DMN and CEN and between DMN and SN. *Post hoc* comparisons showed that the anti-correlations between the DMN and CEN were maintained or increased after training, including an increase in the anti-correlation between the PCC and the left DLPFC in the training group, while this correlation was maintained in control group; meanwhile, the anti-correlation between the PCC and the right DLPFC was maintained in training group and decreased in the control group. For the seed at the right DLPFC, the anti-correlation between the right DLPFC and left IPL was maintained in the training group and increased in the control group. For the connection between the DMN and SN, the connectivity between the PCC and the right putamen was maintained in the training group and decreased in the control group (**Figure 2**; **Table 3**).

## The Correlation between Cognitive Measures and Resting-State fMRI

We found a significant relationship between the changes in FC (between the two fMRI sessions) and the improvements in cognitive performances ($p < 0.05$, uncorrected). As shown in **Figure 3**, the increased FC between the right DLPFC and the right SFG had a slim positive correlation with the RBANS test scores in the multi-domain training group (**Figure 3A**). The increased FC between the right AI and the right middle/posterior insula predicted poorer delayed memory and RBANS scores in the control group (**Figures 3B,C**).

# DISCUSSION

In the present study, we used resting-state fMRI analysis to examine the effects of multi-domain cognitive training on FC within and among three networks (DMN, SN, and CEN). Consistent with our *a priori hypothesis*, changes in resting-state FC within and among the three networks were found at the 1-year after multi-domain cognitive training ended in training group compared to the wait-list control group. After training, the maintained or increased anterior–posterior and interhemispheric FCs within network, including PCC – left SFG (DMN), PCC – cerebellar lobule IX (DMN), right AI – left AI (SN), and right DLPFC – left DLPFC (CEN), were observed in the training group, while these FCs decreased in the control group. Compared to the control group, the training group showed increased or maintained anti-correlated FC between DMN and CEN (PCC – DLPFC

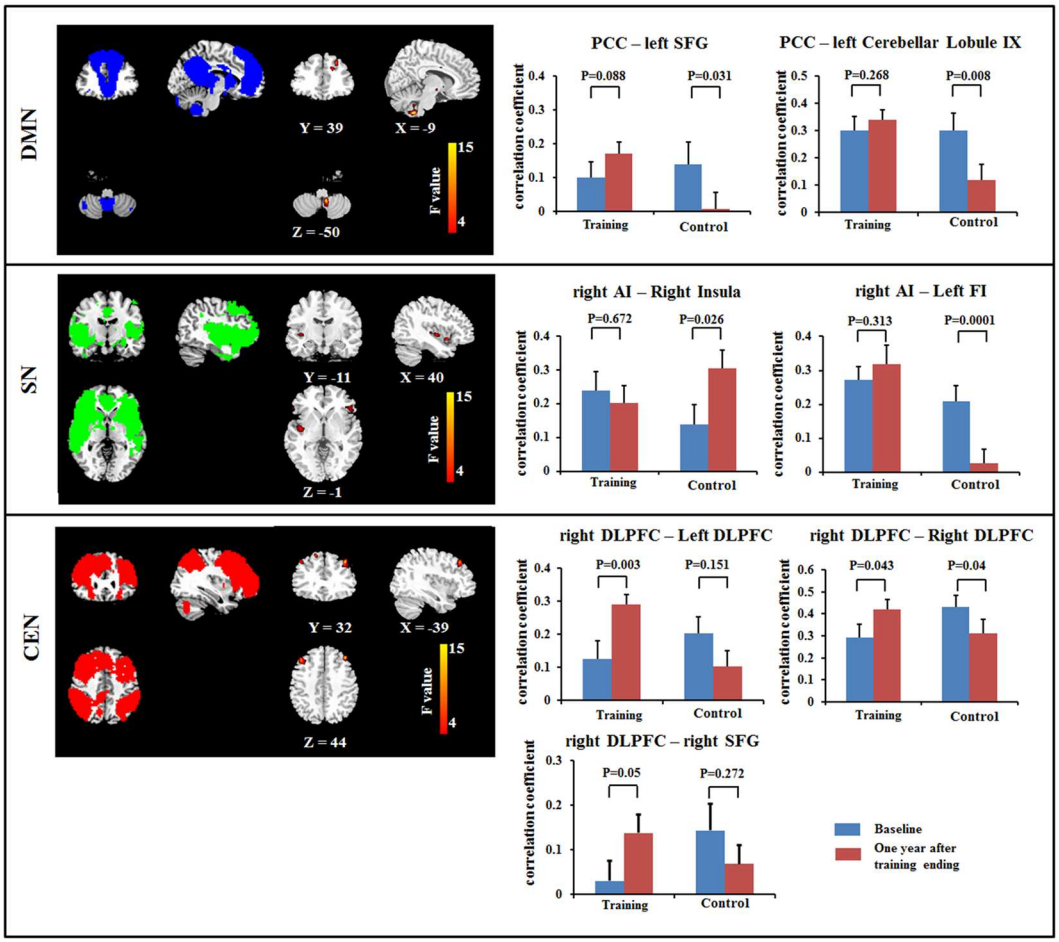


**FIGURE 1 | Results of Resting-state functional connectivity (FC) within the DMN (top), within the SN (middle) and within the CEN (bottom) using a voxel-based 2 × 2 repeated ANOVA analysis ($p < 0.05$, cluster size > 621 mm$^3$).** Bars at the right show the mean correlation coefficient of significantly altered FC within networks in training and control groups at the baseline (blue) and 1-year after training ended (red). CEN, Central executive network; DMN, default mode network; DLPFC, dorsolateral prefrontal cortex; FI, frontoinsula; PCC, posterior cingulate cortex; SFG, superior frontal gyrus; SN, salience network. The left side of the image corresponds to the right side of the subject.

**TABLE 3 | Brain areas showing significant interactions for resting-state functional connectivity using a 2 (between-subject factor: training and control groups) × 2 (within-subject factor: baseline and 1-year after training ended) repeated ANOVA.**

| Seed | Brain region | BA | MNI coordinate | | | *F*-score | Cluster size (mm$^3$) |
|---|---|---|---|---|---|---|---|
| | | | *X* | *Y* | *Z* | | |
| PCC | Left dorsolateral prefrontal lobe | 20 | −33 | 15 | 24 | 18.64 | 2187 |
| | Left cerebellar lobule IX | | −6 | −51 | −54 | 16.2 | 2241 |
| | Right putamen | 9 | 18 | 15 | −9 | 13.17 | 1377 |
| | Right dorsolateral prefrontal lobe | | 51 | 0 | 30 | 12.86 | 1782 |
| | Left superior frontal gyrus | 20 | −24 | 36 | 39 | 11.66 | 1323 |
| Right AI | Right insula | 45 | 30 | −9 | −18 | 15.82 | 4644 |
| | Left frontoinsula | 45 | −51 | 33 | −12 | 11.67 | 2538 |
| Right DLPFC | Right superior frontal cortex | 11 | 15 | 27 | 54 | 13.30 | 3186 |
| | Left dorsolateral prefrontal cortex | 9 | −39 | 30 | 42 | 12.78 | 1647 |
| | Left inferior parietal lobe | | −30 | −63 | 30 | 13 | 1431 |
| | Right superior frontal gyrus | | 42 | 27 | 42 | 12.12 | 2970 |

*BA, Broadmann area; CEN, central executive network; DMN, default mode network; SN, salience network; DLPFC, dorsolateral prefrontal cortex; AI, anterior insula; PCC, posterior cingulate cortex.*

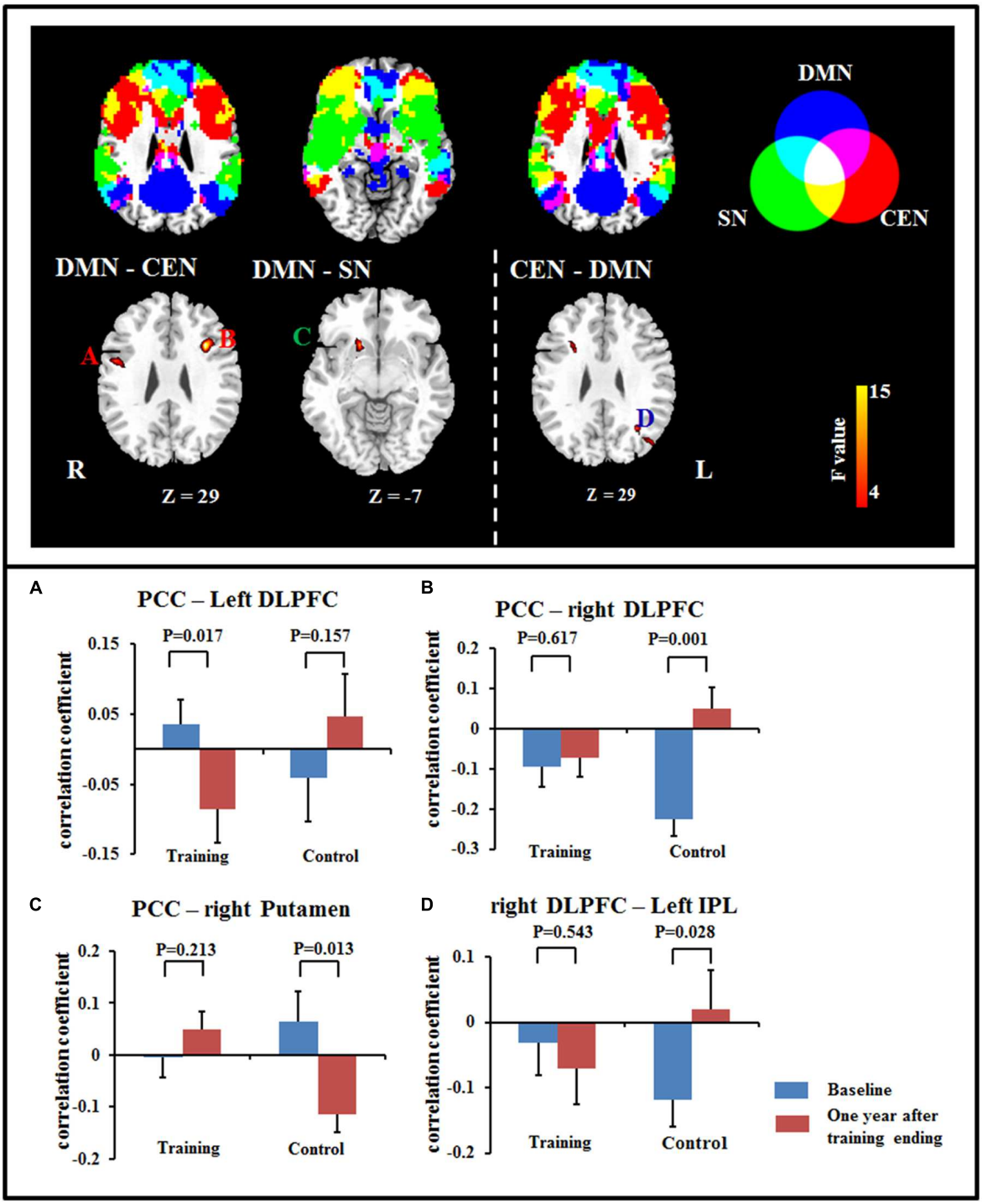


**FIGURE 2 | Significant differences in FC were observed between DMN and CEN (A,B), between DMN and SN (C), and between CEN and DMN (D) using a voxel-based 2 × 2 repeated measure ANOVA ($p < 0.05$, cluster size > 621 mm$^3$).** Bars at the bottom show the mean correlation coefficient of significant altered FC between networks in training and control groups at the baseline (blue) and 1-year after training ended (red). CEN, Central executive network; DMN, default mode network; DLPFC, dorsolateral prefrontal cortex; IPL, inferior parietal lobe; PCC, posterior cingulate cortex; SN, salience network.

and DLPFC – IPL). The coupling between DMN and SN (PCC – putamen) was also maintained in training group, but decreased in the control group. These findings suggested that multi-domain cognitive training might counteract decreased integration within network and impaired coupling between networks with aging.

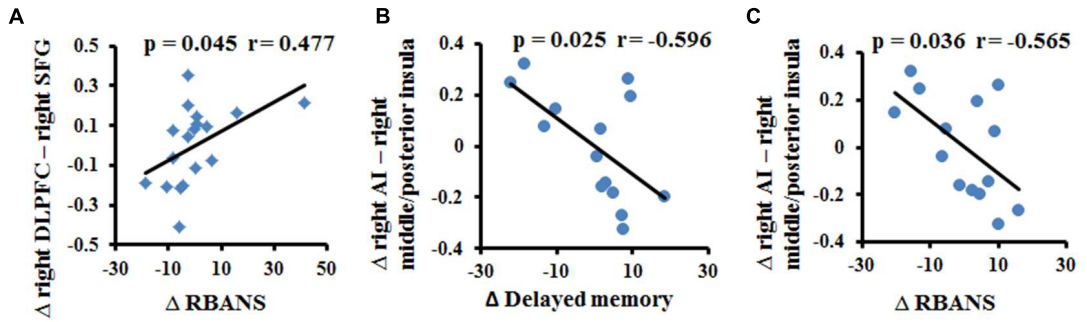


**FIGURE 3 | Correlation between the change in resting-state FC and the change in cognitive performance in the multi-domain training group (A) and in the control group (B,C).**

## Training Effects on FC within Networks

This study found training-related enhanced integration of FC within the DMN, SN, and CEN. In particular, we observed that FCs between PCC and SFG and between PCC and cerebellar lobule IX were maintained in the multi-domain training group, but decreased in the control group. Previous studies have provided consistent evidence that healthy aging is accompanied by decreased FC within the DMN, particularly an anterior–posterior disruption of FC (Andrews-Hanna et al., 2007; Mevel et al., 2013). The decreased FC between the PCC and the SFG in the control group was consistent with previous findings, highlighting age-related disruption of connectivity at rest along the anterior–posterior axis of the DMN (Andrews-Hanna et al., 2007). The role of the cerebellum in cognitive function has been accepted. For example, lobule IX has been mentioned in association with DMN (Habas et al., 2009), and the FC between DMN nodes (PCC and MPFC) and cerebellar regions has been described as modified by aging and by diseases such as dementia (Bernard et al., 2013; Guo et al., 2015). Unlike the decreased FC with normal aging in the control group, multi-domain cognitive training maintained these FCs from the PCC to the SFG and to lobule IX of the cerebellum, suggesting that cognitive training might resist or postpone age-related disruption of FC within the DMN. In the CEN, we also observed increased FC between the right DLPFC and the frontal lobe (bilateral DLPFC and right SFG) at 1 year after training compared with baseline in the multi-domain training group, while these FCs decreased in the control group. These frontal regions have been found to be involved in executive and cognitive function (Ridderinkhof et al., 2004; Grady, 2012), such as working memory, and to be activated by tasks related to these function when the age-related effects were investigated (Grady, 2012). The frontal lobe is known to be affected by training (Park and Bischof, 2013). In addition, the change of FC between the right DLPFC and the right SFG was slight positively correlated with the improvement on the RBANS test in the training group. Thus, we presumed that the multi-domain training might have positive effects on improvement of behavior via enhancing the FC. However, a larger sample size should be considered to verify the relationship between the FC and cognitive function. A recent study of complex cognitive training in healthy seniors also found increased resting-state FC of the DMN and CEN, as well as increased cerebral blood flow (Chapman et al., 2015). Consistent with those reports, our results showed changes in intranetwork FC in the DMN and CEN after cognitive training. These findings might suggest that the cognitive training enhanced integration of FC within networks, resulting in the improvement of cognitive function.

Recent studies demonstrated that the decreased FC within the SN is an important feature of normal aging and is associated with the cognitive impairments (Onoda et al., 2012; He et al., 2013). Consistent with previous studies, we found decreased FC between the right AI and the left frontoinsula in the control group between the two timepoints scanned. However, the FC was maintained in the training group, as indicated by the absence of a difference between the FC values from before and after multi-domain cognitive training. In addition, we observed the FC between the right AI and right middle/posterior insula was maintained in the training group, but increase in the control group. The right AI, as a key node of the SN, is involved in cognitive function; by contrast, the middle/posterior insula serves in sensorimotor functions (Kurth et al., 2010). The increased FC between the right AI and right middle/posterior insula might indicate the disrupted function of the insula, likely reflecting an association with the cognitive decline in old adults. Here, we observed the negative correlation between the increase in the FC between the right anterior and right middle/posterior insula and the improvement of delayed memory and RBANS scores in the control group, probably implicating the relationship between the FC within the SN and the cognition. Thus, we speculated that cognitive training enhanced integration of the SN to retain at least some of the cognitive performance.

## Training-Related Changes of FC between Networks

The triple network model of the DMN, SN, and CEN has been used to understand cognitive dysfunction in neurological and psychiatric disorders (Menon, 2011). A previous study provided evidence for a decrease in the anti-correlation between DMN and CEN in normal aging (Wu et al., 2011).

Here, we found that the aging-sensitive anti-correlation between DMN and CEN was maintained after training. A higher anti-correlation between DMN and CEN was also found after working memory training in healthy adults (Takeuchi et al., 2013). In addition, the disruption of SN and DMN connectivity has been observed in dementia (Zhou et al., 2010). Here, the connection between the DMN and SN was maintained in the training group, but decreased in the control group. Our results might also suggest that the anti-correlation of DMN and CEN is relatively sensitive to cognitive training.

### Limitations

Interpreting the present findings requires the consideration of a few key limitations. First, our demographic characteristics, such as sample size and educational level, might affect the generalisability of the results. A larger sample size and a more consistent educational level among the subjects are necessary to verify the effect of cognitive training on the resting-state FC of three networks. Second, because the imaging data were not acquired at intermediate stages and or immediately after the completion of training completion, the effects of training on FCs within and between networks at additional intermediate timepoints and immediately after the completion of training are not studied. Third, we considered the effects of brain atrophy on FC in this work. However, the other focal damage (i.e., vascular lesions) is prevalent in the population and may have contributed to our findings. Fourth, the effects of cognitive training on resting-state FCs of three networks were observed in our study. This result suggested that the training was valid in the current population; however, further work should be performed to verify these conclusions in other populations. Finally, another control group of younger subjects should be considered in future work to determine whether the effects of cognitive training are specific to older adults.

## CONCLUSION

We found changes in resting-state FC within networks and between the three networks at 1 year post-training, perhaps reflecting that cognitive training enhanced integration within network and maintenance of segregation between DMN and CEN. Our findings provide evidence that multi-domain cognitive training could mitigate the age-related functional alterations involving DMN, SN and CEN, thereby helping older adults maintain brain health.

## AUTHOR CONTRIBUTIONS

Conceived and designed the work: WC, Cheng Luo, Chunbo Li, DY. Acquired the data: YC, XC, TL, LJ. Analyzed the data: WC, CH, XC, YC. Wrote the paper: WC, Cheng Luo. All authors revised the work for important intellectual content. All of the authors have read and approved the manuscript.

## ACKNOWLEDGMENTS

This project was funded by the National Nature Science Foundation of China (81330032, 81371505, 91232725, 81271547, and 30770769), the Science and Technology Commission of Shanghai Municipality (134119a2501, 13dz2260500) and SHSMU-ION Research Center for Brain Disorders. This study was also sponsored by the '111' project of China (No. B12027).

## SUPPLEMENTARY MATERIAL

The Supplementary Material for this article can be found online at: http://journal.frontiersin.org/article/10.3389/fnagi.2016.00070

## REFERENCES

Andrews-Hanna, J. R., Snyder, A. Z., Vincent, J. L., Lustig, C., Head, D., Raichle, M. E., et al. (2007). Disruption of large-scale brain systems in advanced aging. *Neuron* 56, 924–935. doi: 10.1016/j.neuron.2007.10.038

Ashendorf, L., Jefferson, A. L., O'Connor, M. K., Chaisson, C., Green, R. C., and Stern, R. A. (2008). Trail Making Test errors in normal aging, mild cognitive impairment, and dementia. *Arch. Clin. Neuropsychol.* 23, 129–137. doi: 10.1016/j.acn.2007.11.005

Bamidis, P. D., Fissler, P., Papageorgiou, S. G., Zilidou, V., Konstantinidis, E. I., Billis, A. S., et al. (2015). Gains in cognition through combined cognitive and physical training: the role of training dosage and severity of neurocognitive disorder. *Front. Aging Neurosci.* 7:152. doi: 10.3389/fnagi.2015.00152

Bamidis, P. D., Vivas, A. B., Styliadis, C., Frantzidis, C., Klados, M., Schlee, W., et al. (2014). A review of physical and cognitive interventions in aging. *Neurosci. Biobehav. Rev.* 44, 206–220. doi: 10.1016/j.neubiorev.2014.03.019

Bernard, J. A., Peltier, S. J., Wiggins, J. L., Jaeggi, S. M., Buschkuehl, M., Fling, B. W., et al. (2013). Disrupted cortico-cerebellar connectivity in older adults. *Neuroimage* 83C, 103–119. doi: 10.1016/j.neuroimage.2013.06.042

Bressler, S. L., and Menon, V. (2010). Large-scale brain networks in cognition: emerging methods and principles. *Trends Cogn Sci.* 14, 277–290. doi: 10.1016/j.tics.2010.04.004

Buckner, R. L., Andrews-Hanna, J. R., and Schacter, D. L. (2008). The brain's default network: anatomy, function, and relevance to disease. *Ann. N. Y. Acad. Sci.* 1124, 1–38. doi: 10.1196/annals.1440.011

Calhoun, V. D., Eichele, T., and Pearlson, G. (2009). Functional brain networks in schizophrenia: a review. *Front. Hum. Neurosci.* 3:17. doi: 10.3389/neuro.09.017.2009

Cao, W., Luo, C., Zhu, B., Zhang, D., Dong, L., Gong, J., et al. (2014). Resting-state functional connectivity in anterior cingulate cortex in normal aging. *Front. Aging Neurosci.* 6:280. doi: 10.3389/fnagi.2014.00280

Chapman, S. B., Aslan, S., Spence, J. S., Hart, J. J. Jr., Bartz, E. K., Didehbani, N., et al. (2015). Neural mechanisms of brain plasticity with complex cognitive training in healthy seniors. *Cereb. Cortex* 25, 396–405. doi: 10.1093/cercor/bht234

Chen, X., Duan, M., Xie, Q., Lai, Y., Dong, L., Cao, W., et al. (2015). Functional disconnection between the visual cortex and the sensorimotor cortex suggests a potential mechanism for self-disorder in schizophrenia. *Schizophr. Res.* 166, 151–157. doi: 10.1016/j.schres.2015.06.014

Cheng, Y., Wu, W., Feng, W., Wang, J., Chen, Y., Shen, Y., et al. (2012). The effects of multi-domain versus single-domain cognitive training in non-demented older people: a randomized controlled trial. *BMC Med.* 10:30. doi: 10.1186/1741-7015-10–30

Cheng, Y., Wu, W., Wang, J., Feng, W., Wu, X., and Li, C. (2011). Reliability and validity of the repeatable battery for the assessment of neuropsychological

status in community-dwelling elderly. *Arch. Med. Sci.* 7, 850–857. doi: 10.5114/aoms.2011.25561

Damoiseaux, J. S., Beckmann, C. F., Arigita, E. J., Barkhof, F., Scheltens, P., Stam, C. J., et al. (2008). Reduced resting-state brain activity in the "default network" in normal aging. *Cereb. Cortex* 18, 1856–1864. doi: 10.1093/cercor/bhm207

Fox, M. D., Snyder, A. Z., Vincent, J. L., Corbetta, M., Van Essen, D. C., and Raichle, M. E. (2005). The human brain is intrinsically organized into dynamic, anticorrelated functional networks. *Proc. Natl. Acad. Sci. U.S.A.* 102, 9673–9678. doi: 10.1073/pnas.0504136102

Fransson, P. (2006). How default is the default mode of brain function? Further evidence from intrinsic BOLD signal fluctuations. *Neuropsychologia* 44, 2836–2845. doi: 10.1016/j.neuropsychologia.2006.06.017

Grady, C. (2012). The cognitive neuroscience of ageing. *Nat. Rev. Neurosci.* 13, 491–505. doi: 10.1038/nrn3256

Guo, W., Liu, F., Zhang, Z., Liu, G., Liu, J., Yu, L., et al. (2015). Increased cerebellar functional connectivity with the default-mode network in unaffected siblings of schizophrenia patients at rest. *Schizophr. Bull.* 41, 1317–1325. doi: 10.1093/schbul/sbv062

Habas, C., Kamdar, N., Nguyen, D., Prater, K., Beckmann, C. F., Menon, V., et al. (2009). Distinct cerebellar contributions to intrinsic connectivity networks. *J. Neurosci.* 29, 8586–8594. doi: 10.1523/JNEUROSCI.1868-09.2009

He, X., Qin, W., Liu, Y., Zhang, X., Duan, Y., Song, J., et al. (2013). Abnormal salience network in normal aging and in amnestic mild cognitive impairment and Alzheimer's disease. *Hum. Brain Mapp.* 35, 3446–3464. doi: 10.1002/hbm.22414

Hedden, T., and Gabrieli, J. D. (2004). Insights into the ageing mind: a view from cognitive neuroscience. *Nat. Rev. Neurosci.* 5, 87–96. doi: 10.1038/nrn1323

Jiang, S., Luo, C., Liu, Z., Hou, C., Wang, P., Dong, L., et al. (2015). Altered local spontaneous brain activity in juvenile myoclonic epilepsy: a preliminary resting-state fMRI study. *Neural Plast.* 2015:635196. doi: 10.1155/2016/3547203

Kirchhoff, B. A., Anderson, B. A., Barch, D. M., and Jacoby, L. L. (2012). Cognitive and neural effects of semantic encoding strategy training in older adults. *Cereb. Cortex* 22, 788–799. doi: 10.1093/cercor/bhr129

Kraft, E. (2012). Cognitive function, physical activity, and aging: possible biological links and implications for multimodal interventions. *Neuropsychol. Dev. Cogn. B Aging Neuropsychol. Cogn.* 19, 248–263. doi: 10.1080/13825585.2011.645010

Kurth, F., Zilles, K., Fox, P. T., Laird, A. R., and Eickhoff, S. B. (2010). A link between the systems: functional differentiation and integration within the human insula revealed by meta-analysis. *Brain Struct. Funct.* 214, 519–534. doi: 10.1007/s00429-010-0255-z

Langer, N., von Bastian, C. C., Wirz, H., Oberauer, K., and Jancke, L. (2013). The effects of working memory training on functional brain network efficiency. *Cortex* 49, 2424–2438. doi: 10.1016/j.cortex.2013.01.008

Leung, N. T., Tam, H. M., Chu, L. W., Kwok, T. C., Chan, F., Lam, L. C., et al. (2015). Neural plastic effects of cognitive training on aging brain. *Neural Plast.* 2015:535618. doi: 10.1155/2015/535618

Li, C., Wu, W., Jin, H., Zhang, X., Xue, H., He, Y., et al. (2006). Successful aging in Shanghai, China: definition, distribution and related factors. *Int. Psychogeriatr.* 18, 551–563. doi: 10.1017/S1041610205002966

Li, R., Zhu, X., Yin, S., Niu, Y., Zheng, Z., Huang, X., et al. (2014). Multimodal intervention in older adults improves resting-state functional connectivity between the medial prefrontal cortex and medial temporal lobe. *Front. Aging Neurosci.* 6:39. doi: 10.3389/fnagi.2014.00039

Lim, M. L., Collinson, S. L., Feng, L., and Ng, T. P. (2010). Cross-cultural application of the repeatable battery for the assessment of neuropsychological status (rbans): performances of elderly Chinese Singaporeans. *Clin. Neuropsychol.* 24, 811–826. doi: 10.1080/13854046.2010.490789

Luo, C., Li, Q., Lai, Y., Xia, Y., Qin, Y., Liao, W., et al. (2011). Altered functional connectivity in default mode network in absence epilepsy: a resting-state fMRI study. *Hum. Brain Mapp.* 32, 438–449. doi: 10.1002/hbm.21034

Luo, C., Qiu, C., Guo, Z., Fang, J., Li, Q., Lei, X., et al. (2012). Disrupted functional brain connectivity in partial epilepsy: a resting-state fMRI study. *PLoS ONE* 7:e28196. doi: 10.1371/journal.pone.0028196

Luo, C., Tu, S., Peng, Y., Gao, S., Li, J., Dong, L., et al. (2014a). Long-term effects of musical training and functional plasticity in salience system. *Neural Plast.* 2014:180138. doi: 10.1155/2014/180138

Luo, C., Yang, T., Tu, S., Deng, J., Liu, D., Li, Q., et al. (2014b). Altered intrinsic functional connectivity of the salience network in childhood absence epilepsy. *J. Neurol. Sci.* 339, 189–195. doi: 10.1016/j.jns.2014.02.016

Luo, C., Zhang, X., Cao, X., Gan, Y., Li, T., Cheng, Y., et al. (2016). The lateralization of intrinsic networks in the aging brain implicates the effects of cognitive training. *Front. Aging Neurosci.* 8:32. doi: 10.3389/fnagi.2016.00032

Luo, C., Zhang, Y., Cao, W., Huang, Y., Yang, F., Wang, J., et al. (2015). Altered structural and functional feature of striato-cortical circuit in benign epilepsy with centrotemporal spikes. *Int. J. Neural. Syst.* 25:1550027. doi: 10.1142/S0129065715500276

Mackey, A. P., Miller Singley, A. T., and Bunge, S. A. (2013). Intensive reasoning training alters patterns of brain connectivity at rest. *J. Neurosci.* 33, 4796–4803. doi: 10.1523/JNEUROSCI.4141-12.2013

Menon, V. (2011). Large-scale brain networks and psychopathology: a unifying triple network model. *Trends Cogn. Sci.* 15, 483–506. doi: 10.1016/j.tics.2011.08.003

Meunier, D., Achard, S., Morcom, A., and Bullmore, E. (2009). Age-related changes in modular organization of human brain functional networks. *Neuroimage* 44, 715–723. doi: 10.1016/j.neuroimage.2008.09.062

Mevel, K., Landeau, B., Fouquet, M., La Joie, R., Villain, N., Mezenge, F., et al. (2013). Age effect on the default mode network, inner thoughts, and cognitive abilities. *Neurobiol. Aging* 34, 1292–1301. doi: 10.1016/j.neurobiolaging.2012.08.018

Neely, A. S., and Backman, L. (1995). Effects of multifactorial memory training in old age: generalizability across tasks and individuals. *J. Gerontol. B Psychol. Sci. Soc. Sci.* 50, 134–140. doi: 10.1093/geronb/50B.3.P134

Onoda, K., Ishihara, M., and Yamaguchi, S. (2012). Decreased functional connectivity by aging is associated with cognitive decline. *J. Cogn. Neurosci.* 24, 2186–2198. doi: 10.1162/jocn_a_00269

Oswald, W. D., Gunzelmann, T., Rupprecht, R., and Hagen, B. (2006). Differential effects of single versus combined cognitive and physical training with older adults: the SimA study in a 5-year perspective. *Eur. J. Ageing* 3, 179–192. doi: 10.1007/s10433-006-0035-z

Park, D. C., and Bischof, G. N. (2013). The aging mind: neuroplasticity in response to cognitive training. *Dialogues Clin. Neurosci.* 15, 109–119.

Patel, R., Spreng, R. N., and Turner, G. R. (2013). Functional brain changes following cognitive and motor skills training: a quantitative meta-analysis. *Neurorehabil. Neural Repair* 27, 187–199. doi: 10.1177/1545968312461718

Power, J. D., Barnes, K. A., Snyder, A. Z., Schlaggar, B. L., and Petersen, S. E. (2012). Spurious but systematic correlations in functional connectivity MRI networks arise from subject motion. *Neuroimage* 59, 2142–2154. doi: 10.1016/j.neuroimage.2011.10.018

Raichle, M. E., MacLeod, A. M., Snyder, A. Z., Powers, W. J., Gusnard, D. A., and Shulman, G. L. (2001). A default mode of brain function. *Proc. Natl. Acad. Sci. U.S.A.* 98, 676–682. doi: 10.1073/pnas.98.2.676

Ridderinkhof, K. R., van den Wildenberg, W. P., Segalowitz, S. J., and Carter, C. S. (2004). Neurocognitive mechanisms of cognitive control: the role of prefrontal cortex in action selection, response inhibition, performance monitoring, and reward-based learning. *Brain Cogn.* 56, 129–140. doi: 10.1016/j.bandc.2004.09.016

Seeley, W. W., Menon, V., Schatzberg, A. F., Keller, J., Glover, G. H., Kenna, H., et al. (2007). Dissociable intrinsic connectivity networks for salience processing and executive control. *J. Neurosci.* 27, 2349–2356. doi: 10.1523/JNEUROSCI.5587-06.2007

Shao, J., Myers, N., Yang, Q., Feng, J., Plant, C., Bohm, C., et al. (2012). Prediction of Alzheimer's disease using individual structural connectivity networks. *Neurobiol. Aging* 33, 2756–2765. doi: 10.1016/j.neurobiolaging.2012.01.017

Smith, S. M., Fox, P. T., Miller, K. L., Glahn, D. C., Fox, P. M., Mackay, C. E., et al. (2009). Correspondence of the brain's functional architecture during activation and rest. *Proc. Natl. Acad. Sci. U.S.A.* 106, 13040–13045. doi: 10.1073/pnas.0905267106

Sridharan, D., Levitin, D. J., and Menon, V. (2008). A critical role for the right fronto-insular cortex in switching between central-executive and default-mode networks. *Proc. Natl. Acad. Sci. U.S.A.* 105, 12569–12574. doi: 10.1073/pnas.0800005105

Strenziok, M., Parasuraman, R., Clarke, E., Cisler, D. S., Thompson, J. C., and Greenwood, P. M. (2014). Neurocognitive enhancement in older adults: comparison of three cognitive training tasks to test a hypothesis of

training transfer in brain connectivity. *Neuroimage* 85(Pt 3), 1027–1039. doi: 10.1016/j.neuroimage.2013.07.069

Takeuchi, H., Taki, Y., Nouchi, R., Hashizume, H., Sekiguchi, A., Kotozaki, Y., et al. (2013). Effects of working memory training on functional connectivity and cerebral blood flow during rest. *Cortex* 49, 2106–2125. doi: 10.1016/j.cortex.2012.09.007

Tang, Y. Y., and Posner, M. I. (2014). Training brain networks and states. *Trends Cogn. Sci.* 18, 345–350. doi: 10.1016/j.tics.2014.04.002

Tanigawa, T., Takechi, H., Arai, H., Yamada, M., Nishiguchi, S., and Aoyama, T. (2014). Effect of physical activity on memory function in older adults with mild Alzheimer's disease and mild cognitive impairment. *Geriatr. Gerontol. Int.* 14, 758–762. doi: 10.1111/ggi.12159

Taylor, V. A., Daneault, V., Grant, J., Scavone, G., Breton, E., Roffe-Vidal, S., et al. (2013). Impact of meditation training on the default mode network during a restful state. *Soc. Cogn. Affect. Neurosci.* 8, 4–14. doi: 10.1093/scan/nsr087

Tomasi, D., and Volkow, N. D. (2012). Aging and functional brain networks. *Mol. Psychiatry* 17, 549–458. doi: 10.1038/mp.2011.81

van Boxtel, M. P., ten Tusscher, M. P., Metsemakers, J. F., Willems, B., and Jolles, J. (2001). Visual determinants of reduced performance on the Stroop color-word test in normal aging individuals. *J. Clin. Exp. Neuropsychol.* 23, 620–627. doi: 10.1076/jcen.23.5.620.1245

Voss, M. W., Erickson, K. I., Prakash, R. S., Chaddock, L., Kim, J. S., Alves, H., et al. (2013). Neurobiological markers of exercise-related brain plasticity in older adults. *Brain Behav. Immun.* 28, 90–99. doi: 10.1016/j.bbi.2012.10.021

Voss, M. W., Prakash, R. S., Erickson, K. I., Basak, C., Chaddock, L., Kim, J. S., et al. (2010). Plasticity of brain networks in a randomized intervention trial of exercise training in older adults. *Front. Aging Neurosci.* 2:32. doi: 10.3389/fnagi.2010.00032

Wu, J. T., Wu, H. Z., Yan, C. G., Chen, W. X., Zhang, H. Y., He, Y., et al. (2011). Aging-related changes in the default mode network and its anti-correlated networks: a resting-state fMRI study. *Neurosci. Lett.* 504, 62–67. doi: 10.1016/j.neulet.2011.08.059

Xiao, S., Yao, P., Li, X., and Zhang, M. (2002). Neuropsychological testing profiles of patients with Alzheimer's Disease and mild cognitive impairment: a case-control study. *Hong Kong J. Psychiatry* 12, 2–5.

Yin, S., Zhu, X., Li, R., Niu, Y., Wang, B., Zheng, Z., et al. (2014). Intervention-induced enhancement in intrinsic brain activity in healthy older adults. *Sci. Rep.* 4:7309. doi: 10.1038/srep07309

Zheng, Z., Zhu, X., Yin, S., Wang, B., Niu, Y., Huang, X., et al. (2015). Combined cognitive-psychological-physical intervention induces reorganization of intrinsic functional brain architecture in older adults. *Neural Plast* 2015:713104. doi: 10.1155/2015/713104

Zhou, J., Greicius, M. D., Gennatas, E. D., Growdon, M. E., Jang, J. Y., Rabinovici, G. D., et al. (2010). Divergent network connectivity changes in behavioural variant frontotemporal dementia and Alzheimer's disease. *Brain* 133, 1352–1367. doi: 10.1093/brain/awq075

**Conflict of Interest Statement:** The authors declare that the research was conducted in the absence of any commercial or financial relationships that could be construed as a potential conflict of interest.

frontiers in Aging Neuroscience

ORIGINAL RESEARCH
published: 03 March 2016
doi: 10.3389/fnagi.2016.00032

# The Lateralization of Intrinsic Networks in the Aging Brain Implicates the Effects of Cognitive Training

*Cheng Luo[1], Xingxing Zhang[1], Xinyi Cao[2], Yulong Gan[1], Ting Li[3], Yan Cheng[2], Weifang Cao[1], Lijuan Jiang[2], Dezhong Yao[1]* and Chunbo Li[2,4]**

[1] Key Laboratory for NeuroInformation of Ministry of Education, High-Field Magnetic Resonance Brain Imaging Key Laboratory of Sichuan Province, Center for Information in Medicine, School of Life Science and Technology, University of Electronic Science and Technology of China, Chengdu, China, [2] Shanghai Key Laboratory of Psychotic Disorders, Shanghai Mental Health Center, Shanghai Jiao Tong University School of Medicine, Shanghai, China, [3] Changning Mental Health Center, Shanghai, China, [4] Bio-X Institutes, Key Laboratory for the Genetics of Developmental and Neuropsychiatric Disorders, Ministry of Education, Shanghai Jiao Tong University, Shanghai, China

Lateralization of function is an important organization of the human brain. The distribution of intrinsic networks in the resting brain is strongly related to cognitive function, gender and age. In this study, a longitudinal design with 1 year's duration was used to evaluate the cognitive training effects on the lateralization of intrinsic networks among healthy older adults. The subjects were divided into two groups randomly: one with multi-domain cognitive training over 3 months and the other as a wait-list control group. Resting state fMRI data were acquired before training and 1 year after training. We analyzed the functional lateralization in 10 common resting state fMRI networks. We observed statically significant training effects on the lateralization of two important RSNs related to high-level cognition: right- and left- frontoparietal networks (FPNs). The lateralization of the left-FPN was retained especially well in the training group but decreased in the control group. The increased lateralization with aging was observed in the cerebellum network (CereN), in which the lateralization was significantly increased in the control group, although the same change tendency was observed in the training group. These findings indicate that the lateralization of the high-level cognitive intrinsic networks is sensitive to multi-domain cognitive training. This study provides neuroimaging evidence to support the hypothesis that cognitive training should have an advantage in preventing cognitive decline in healthy older adults.

**Keywords: aging, fMRI, lateralization, functional network, cognitive training**

OPEN ACCESS

***Edited by:***
*Michael Hornberger, University of East Anglia, UK*

***Reviewed by:***
*Qing Jiao, Taishan Medical University, China*
*Yuan Zhong, Nanjing Normal University, China*

****Correspondence:***
*Dezhong Yao*
*dyao@uestc.edu.cn;*
*Chunbo Li*
*chunbo_li@163.com*

***Received:*** *01 December 2015*
***Accepted:*** *08 February 2016*
***Published:*** *03 March 2016*

***Citation:***
*Luo C, Zhang X, Cao X, Gan Y, Li T, Cheng Y, Cao W, Jiang L, Yao D and Li C (2016) The Lateralization of Intrinsic Networks in the Aging Brain Implicates the Effects of Cognitive Training. Front. Aging Neurosci. 8:32. doi: 10.3389/fnagi.2016.00032*

## INTRODUCTION

The human brain is the most complex system in nature. The interhemispheric interaction is crucial to brain functions such as motor and cognitive processes. However, hemispheric specialization is also an obvious organizing principle for efficient information processing, such as leftward lateralization for speech and rightward lateralization for visuospatial attention (Corballis, 2014).

Postmortem and neuroimaging studies have displayed the asymmetries of the human brain (Goldberg et al., 2013). Recently, resting state functional magnetic resonance imaging (fMRI) has been widely used in the studies of the human brain in which it was organized into several intrinsic resting state networks (RSNs). More and more studies have provided the evidence to support the importance of these RSNs on the brain function, such as default mode and attention. In general, the spatial pattern of these RSNs is relatively stable across subjects. These RSNs demonstrate either spatial hemispheric symmetry, such as the default mode network (DMN) and sensorimotor network (SMN), or hemispheric asymmetry, such as the frontoparietal network (FPN) and attention network (Fox et al., 2006). Hemispheric symmetry, which is represented by the spatial lateralization of RSNs, may reflect the slight changes of RSNs in different states of the brain. For example, the lateralization is influenced by development (Kelly et al., 2009), gender (Agcaoglu et al., 2015) and diseases (Luo et al., 2014b). The lateralization of RSNs is also observed to be significantly altered in healthy older adults compared with younger adults (Agcaoglu et al., 2015; Seidler et al., 2015).

Neurodegeneration is associated with increasing age (Seidler et al., 2010), i.e., declining cognition and decreases in motor performance (Cheng et al., 2012; Brown et al., 2013). Physical activity and exercise have positive influences on neurodegeneration (Brown et al., 2013). It has been observed that directed cognitive training interventions will increase mental activity in older adults, helping them to resist age-related cognitive decline and even potentially reducing the risk of dementia (Gates and Valenzuela, 2010). In a previous behavioral study, we observed that cognitive training can improve multi-cognition in community-living older adults, including memory, attention and neuropsychological status (Cheng et al., 2012). However, the underlying brain mechanism allowing the training to enhance function has been unclear till now. Noninvasive neuroimaging techniques, especially fMRI, are used to investigate the association between the intervention and brain function. For example, musical training would enhance the functional connectivity in perceptual and motor systems (Luo et al., 2012a) and salience network (Luo et al., 2014a). Additionally, the motor-related exercise increased the integration of motor performance and imaging systems (Gong et al., 2015, 2016; Li et al., 2015a). MRI studies of aging adults have shown enlarged local cortex thickness and enhanced functional integration related to the expertise in cognitive and sensorimotor interventions (Boyke et al., 2008; Lustig et al., 2009; Cao et al., 2014; Li et al., 2014). Therefore, we hypothesized that the lateralization of RSNs found in resting state fMRI scanning might provide an approach to reflect the influence of cognitive training on healthy older adults.

In this study, to test our hypothesis, a longitudinal design with 1 year's duration was used to evaluate the cognitive training effects on the lateralization of intrinsic networks among healthy older adults. Healthy older adults with community-living were recruited and divided into two groups randomly: one received a multi-domain cognitive training over 3 months; the other was included in a wait-list control group. Resting state fMRI data were acquired before training and 1 year after training. The functional lateralization of 10 common resting state fMRI networks was evaluated between two groups using repeated measures analysis of variance (ANOVA).

# MATERIALS AND METHODS

## Participants

Forty healthy older adults were recruited from three community centers around Tongji Hospital in Shanghai via a dispatched notice/broadcasting by the local institute of community service from March 2008 to April 2008. All participants were admitted to the study after a personal interview according to the inclusion criteria as follows: normal functional capacity; independent living in the community; age (range: 65–75 years); educational level (more than 1 year); no abnormality in hearing, vision, or communication status; a score of 19 or above (the lower normal cut-off point of the MMSE score is due to the lower educational level in China than in the US; Li et al., 2006) using the Chinese version of the Mini-Mental State Examination (MMSE); and no physical disease or psychotic disorder. The subjects with obvious cognitive decline, a diagnosis of AD, a brain tumor, or serious neurological and/or psychiatric disorders such as major depressive disorder and schizophrenia were excluded in this study. All of participants underwent cognitive measurements and fMRI scanning at baseline and at 1 year after training. They were divided randomly into two groups, including the multi-domain training group ($n$ = 23) and the control group ($n$ = 17). One participant out of 23 in the multi-domain training group and one in the single-domain training group were excluded because of left-handedness, which would interrupt the study of the lateralization of brain (Mackey et al., 2013). This study was reviewed and approved by the Ethical Committee of the East China Normal University. This study was performed according to the recommendation of the Ethical Committee of the East China Normal University with written informed consent from all subjects. All subjects gave written informed consent in accordance with the Declaration of Helsinki.

## Cognitive Interventions and Neuropsychological Tests

We conducted a randomized, controlled design to determine the effect of cognitive training on brain function and cognitive function (Cheng et al., 2012). The neuroimaging data and cognitive measurement were collected at baseline and at 1 year after training.

The multi-domain training group received 24 sessions (each session was 60 min) of cognitive training at a frequency of twice a week over a 12-week period, and the training procedure took place in a classroom in Tongji Hospital. The multi-domain cognitive training targeted memory, reasoning, problem-solving strategies, visual-spatial map reading skill developments, handcraft making, and health and physical exercise. A lecture about a common disease in aging people was presented during the first 15 min of each session. Then, the

trainer taught the participants about a special cognitive strategy or technique via slide lecture during the second 30 min. The newly practiced skills were consolidated by dealing with some real-life problems during the last 15 min.

The wait-list control group served as a match for the social contact associated with cognitive training. The multi-domain training group and the control group attended a lecture about healthy living every 2 months (the training details are found in our previous study; Cheng et al., 2012).

To evaluate the effects of intervention on cognitive function, all measurements were administered at baseline and at 1 year after intervention, including the Repeatable Battery for the Assessment of Neuropsychological Status (RBANS, Form A), which has good validity and reliability in a Chinese community-living elderly sample (Lim et al., 2010; Cheng et al., 2011), the trail making test (TMT; Ashendorf et al., 2008), the visual reasoning test (Xiao et al., 2002) and the Color Word Stroop test (CWST; van Boxtel et al., 2001).

## Data Acquisition

All participants were scanned using a Siemens 3T MRI Scanner (Erlangen, Germany) at baseline and at 1 year after training ending at East China Normal University, Shanghai, China. To minimize head motion, foam pads were used to fix the subjects' heads. High-resolution T1-weighted images were acquired using a magnetization-prepared rapid gradient-echo sequence, generating 160 slices (repetition time (TR) = 1900 ms, echo time (TE) = 3.43 ms, flip angle (FA) = 90 degrees, matrix size = 256 × 256, field of view (FOV) = 240 × 240 $mm^2$, slice thickness = 1 mm; no gap). Resting state functional images were acquired using a single-shot, gradient-recalled echo planar imaging sequence (TR = 2000 ms, TE = 25 ms and FA = 90 degrees, FOV = 240 × 240 $mm^2$, matrix = 64 × 64, slice thickness = 5 mm (no gap), 32 slices per volume). All subjects underwent a 310 s scanning to yield a total of 155 volumes. The subjects were instructed to rest with their eyes closed, not to think of anything in particular, and not to fall asleep.

## Data Pre-process Analysis

Pre-processing of fMRI data were conducted using the SPM8 Software Package [statistical parametric mapping[1]]. The slice time correction, 3D motion detection and correction, spatial normalization and resample (3 mm × 3 mm × 3 mm), and spatial smoothing using an isotropic Gaussian kernel (6 mm full width at half maximum) were applied. The processing is identical to that used in prior studies (Chen et al., 2015; Jiang et al., 2016). Only the subjects with head motion less than 1.5 mm and 1.5° during fMRI acquisition were included in the following preprocessing. In addition, the translation and rotation of the subjects were assessed by frame wise displacement (FD),

$$FD_i = \left|\Delta d_{ix}\right| + \left|\Delta d_{iy}\right| + \left|\Delta d_{iz}\right| + \left|\Delta \alpha_i\right| + \left|\Delta \beta_i\right| + \left|\Delta \gamma_i\right|,$$

where $i$ is the $i$-th time point, and $\Delta d_{ix} = d_{(i-1)x} - d_{ix}$ (similarly for the other head motion/rotation parameters; Power et al., 2012). No significant differences were found between groups in FD. Additional preprocessing in preparation included voxelwise nuisance correction by regressing out six motion signals.

## ICA Decomposition

Similar to the approaches in our previous studies (Luo et al., 2012c; Li et al., 2015b), we first conducted spatial group ICA in which two times of data of all subjects were included in one group, using the GIFT Software, version 2.0a[2]. The time courses were temporally concatenated across subjects and reduced by means of principal component analysis in temporal domain, followed by an IC estimation using the FastICA algorithm. This algorithm was repeated 20 times in ICASSO[3], and the resulting components were clustered to estimate the reliability of the decomposition (Himberg et al., 2004). Dimension estimation on all subjects was performed using the minimum description length (MDL) criterion to determine the number of independent components (ICs). The ICs were back-constructed for each scans and each subject using the dual-regression approach (Zhang et al., 2010). Finally, we interrogated all components to identify RSNs. Ten RSNs were chosen based on the average power spectra and spatial map of the components such as in the previous studies (Luo et al., 2012c; Li et al., 2015b). Here, the power spectra of time course of ICs was analyzed, and the power spectra of the selected IC should show the frequency content was mainly concentrated below 0.1 Hz (Beckmann et al., 2005; Luo et al., 2012b).

## Spatial Normalization to Symmetric Templates

To acquire the hemispheric symmetries' RSNs, the warping step was performed from the resulted RSNs to the symmetries' templates. First, the MNI template was warped to a symmetrized version of the MNI template because all subjects' functional images were normalized into the MNI template. Then, the MNI template was normalized to the symmetrized template. Finally, the warping parameters were applied to all components for the symmetrizing RSNs in all subjects.

## Calculation of Voxelwise Homotopic Maps

The component values were initially normalized across voxels using $z$-score. The differences ($B_v$) between component values of both homotopic voxels on both sides of cerebral cortex were calculated using the following formula 1. As with our previous study (Agcaoglu et al., 2015), the difference was shown in a map with a positive difference ($R > L$) on the right side of the brain and negative difference ($L > R$) on the left side of the brain.

$$B_v = \begin{cases} (R_v - L_v)\ if\ R_v > L_v \\ (L_v - R_v)\ if\ L_v > R_v \\ 0 \quad otherwise \end{cases} \tag{1}$$

where $R$ and $L$ represents the right hemisphere and left hemisphere for each pairs of homotopic voxels $v$.

[1]http://www.fil.ion.ucl.ac.uk/spm

[2]http://icatb.sourceforge.net/

[3]http://research.ics.tkk.fi/ica/icasso

Hence, the voxelwise homotopic map was produced for each subject each RSN.

## Laterality Cofactor

The laterality cofactor (LCF) was defined based on a voxelwise homotopic map, as in the previous study (Agcaoglu et al., 2015). The amount of laterality for a given RSN was calculated in the global laterality metric. The LCF was acquired by taking the differences between the sum of all intensities of laterality on the right and left hemispheres with respect to the sum of all intensities across the brain (Formula 2). The LCF was computed for the average models for each group. In addition, individual LCF was calculated to evaluate the alteration of LCFs related with training.

$$\mathrm{LCF} = \frac{S_l - S_r}{S_l + S_r} \tag{2}$$

Where $S_l$ and $S_r$ represents the sum of all intensities of laterality on the left and right hemispheres.

## Statistical Test

For each of the components, one sample *t*-test was performed in voxelwise homotopic maps in three groups. Here, the pretraining fMRI data from all the subjects were included in one group; the second data were divided into training and control groups on the basis of receiving the training or not. For the three *t*-value maps, we then applied a mask to retain those voxels whose *t*-values exceed one standard deviation of the *t*-value across voxels. The thresholded *t*-maps were used to compute the LCFs of group level (Global LCF) according to the same formula to calculate the LCF (Formula 2).

According to the formula 2, the LCF value range was between −1 and 1. The Fisher-*z*-translation of individual LCF was performed for the distribution normality for each RSN. The individual LCF of each RSN was also evaluated used the ANOVA for repeated measurement data with *post hoc*, pair-wise Scheffe test in SPSS v20 (IBM Corp., Somer, NY, USA).

# RESULTS

## Demographic Information

At baseline, 23 subjects from the multi-domain training group and 17 subjects from the control group underwent cognitive measurements and fMRI scanning. Eighteen of the multi-domain training group and 14 of the control group finished the cognitive measurements and fMRI scanning at 1 year after the intervention. A total of eight participants withdrew, one due to death, two due to intestinal cancer, one due to her husband's death, one due to operation and three due to rejecting the scanning. No significant differences with regard to age, gender, education and MMSE score were found between the multi-domain training group and the control group (**Table 1**).

**TABLE 1 | Demographic information of the subjects.**

| | | Multi-domain training group | Control group | *p* |
|---|---|---|---|---|
| Age (year) | Baseline | 70.61 ± 3.29 | 68.59 ± 3.24 | 0.838 |
| | One-year Posttest | 72.39 ± 3.43 | 70.85 ± 4.05 | 0.782 |
| Gender (male) | Baseline | 23 (16) | 17 (9) | 0.283 |
| | One-year Posttest | 18 (13) | 14 (9) | 0.631 |
| Education (year) | Baseline | 10.91 ± 3.65 | 10.64 ± 3.06 | 0.452 |
| MMSE | Baseline | 27.57 ± 2.57 | 28.17 ± 1.94 | 0.505 |
| | One-year Posttest | 27.72 ± 2.16 | 27.85 ± 2.31 | 0.900 |

## Identification of RSN and Voxelwise Homotopic Maps

There were 45 components resulting from the group ICA. Ten components were selected as nonartifactual, relevant networks by visual inspection in accordance with published results (Luo et al., 2012c; Li et al., 2015b). The spatial maps of these RSNs were highly stable (reliability index >0.83) as determined by ICASSO. The 10 RSNs were shown in **Figure 1** and labeled as follows:

V1N: primary visual network. The visual cortex is often apparent in two separate components. This network showed spatial patterns consisting of primary visual area (Damoiseaux et al., 2006; Luo et al., 2012c).

V2N: the second visual network illustrated spatial patterns consisting of more lateral visual arear in the occipital lobe

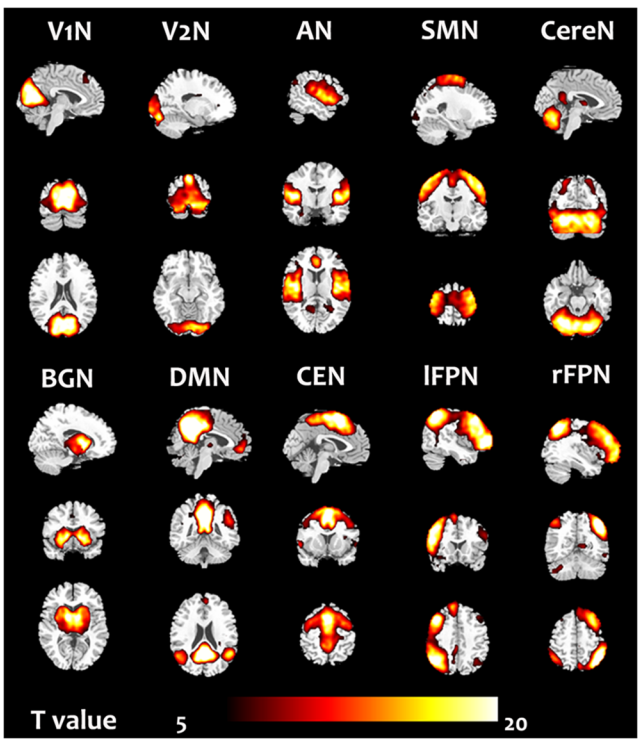


**FIGURE 1 | Ten resting state networks (RSN) were chosen.** The one sample *t*-test in the group included all subjects in the pre-training scans was performed.

which were previously known to be involved in visual processing (Damoiseaux et al., 2006; Luo et al., 2012c).

AN: auditory network (AN) primarily encompassed bilateral middle, superior temporal gyrus, temporal pole and insular, corresponded to the auditory system (Damoiseaux et al., 2006; Luo et al., 2012c).

SMN: sensorimotor network (SMN) was a network corresponding to sensory-motor function. This network includes pre- and postcentral gyrus, the primary sensorimotor cortices, and the supplementary motor area (Damoiseaux et al., 2006; Luo et al., 2012c).

CereN: cerebellum network included bilateral cerebellum hemispheres.

DMN: default mode network (DMN) mainly encompasses posterior cingulate cortex, medial prefrontal gyrus, bilateral superior frontal gyrus, and bilateral angular gyri (Raichle et al., 2001; Damoiseaux et al., 2006; Luo et al., 2012c).

lFPN: left lateral FPN (lFPN) along with right lateral FPN showed the similar spatial patterns with DAN consisting of regions previously known to be involved in goal-directed top-down processing (Damoiseaux et al., 2006; Luo et al., 2012c). This network primarily involved precuneus, inferior parietal lobule, middle frontal gyrus, superior parietal lobule.

rFPN: right lateral FPN (rFPN) including clusters lateralized to the right hemisphere putatively associated with DAN. lFPN and rFPN were the only maps to be strongly lateralized and were largely left–right mirrors of each other (Damoiseaux et al., 2006; Luo et al., 2012c).

CEN: central executive network showed spatial patterns consisting of the superior and middle prefrontal cortices, anterior cingulate and paracingulate gyri, and ventrolateral prefrontal cortex (Beckmann et al., 2005).

BGN: basal ganglia network, encompassed middle temporal gyrus, superior temporal gyrus, insular and temporal pole and corresponded to the auditory system (Luo et al., 2012b).

For 10 RSNs, their voxelwise homotopic maps were calculated for each group. Because the homotopic maps were similar to each other among groups, the group level maps resulted from the pre-training scans were illustrated in the **Figure 2**.

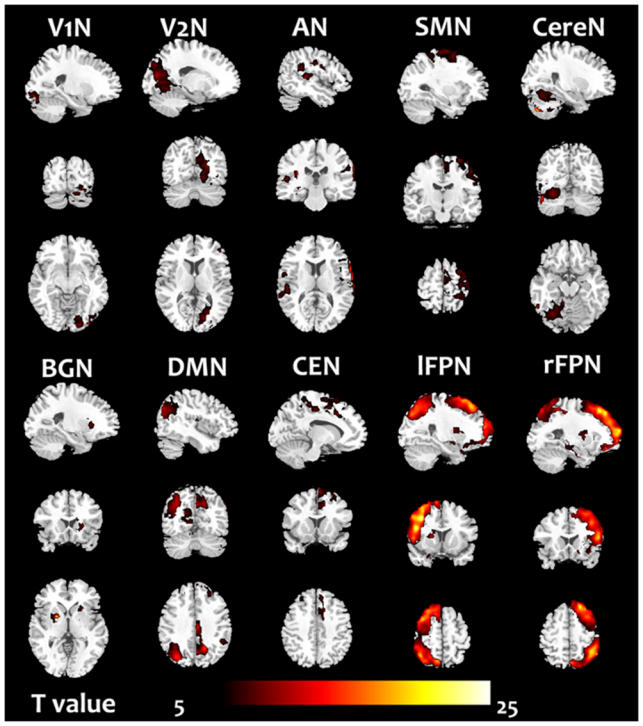


**FIGURE 2 | The homotopic maps of the 10 RSN.** The group level maps resulted from one sample *t*-test in the groups including the pre-training scans (before cognitive training) of all subjects.

## Laterality Cofactors

In the three groups, the global LCF of each RSN were illustrated in **Figure 3**. According to the previous criteria (Agcaoglu et al., 2015), the LCFs are called highly lateralized when it has absolute value above 0.75 or has lateralized with absolute value above 0.2; the LCFs in rFPN and lFPN were highly lateralized in three groups. The remaining eight RSNs did not have marked lateralization, in which the LCFs have absolute value less than 0.2.

To investigate the influence of the multiple cognitive training on the laterality of RSN, the LCFs of each RSN and each subject were also evaluated (**Table 2**, **Figure 4**). After the Fisher *r*-to-*z* translation, a repeated measure ANOVA revealed that both groups improved their LCFs in CereN as indicated by a significant main effect of time ($F$ = 6.903, $p$ = 0.015). In addition, a significant training main effect on the LCF in rFPN ($F$ = 5.897, $p$ = 0.021) and lFPN ($F$ = 7.641, $p$ = 0.01), as well as interactions of LCF of lFPN ($F$ = 8.908, $p$ = 0.006), were observed. *Post hoc* analysis showed significantly increased LCF of lFPN in the training group compared with the control group at the second scan ($T$ = 3.48, $p$ = 0.001). Paired-sample *t*-tests revealed that the global LCF of CereN ($T$ = 2.30, $p$ = 0.03) was significantly increased after the training scan compared with the before-training scan in the control group but not in the training group. Similarly, compared with the before-training scan, the after-training scan showed the decreased LCF of lFPN ($T$ = 2.21, $p$ = 0.04) in the control group, whereas a marginal significant increase ($T$ = 2.02, $p$ = 0.06) was observed in the training group.

## DISCUSSION

The lateralization of human brain function is an obvious sign reflecting functional specialization. Neurodegeneration would alter the functional specialization in aging. In this study, we used the LCF (Agcaoglu et al., 2015) of intrinsic networks resulting from the resting fMRI to investigate the effects of multi-domain cognitive training on healthy older adults. We observed statistically significant training effects on the lateralization of two important RSNs related to high-level cognition: right- and left- FPNs. In particular, the lateralization of lFPN were retained well in the training group but decreased in the control group. The increased lateralization with aging

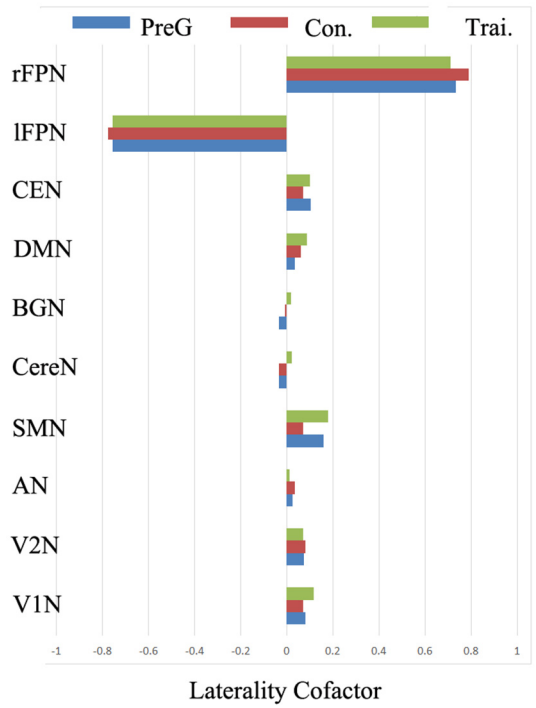


**FIGURE 3 | The group level laterality cofactor (LCF) resulted from the three group *Bv* homotopic maps for each RSN**. Three groups included the pre-training group including all subjects, the post-training group and the control group of the second scans.

was observed in the CereN, in which the lateralization was significantly increased in the control group, although the same change tendency was observed in the training group. These findings indicate that the lateralization of the high-level cognitive intrinsic networks is sensitive to multi-domain cognitive training. This study provides neuroimaging evidence to support the idea that cognitive training should have advantages in preventing the cognitive decline in healthy older adults.

Both human and animal studies indicates neural plasticity across the lifespan (Ball et al., 2002; Papp et al., 2009). A number of studies support the protective effects of late-life cognitive training on dementia (Ball et al., 2002; Wilson et al., 2002; Snowball et al., 2013). Our previous study has illustrated positive effects of multi-domain cognitive training interventions in healthy older adults. Here, the findings from neuroimaging were provided to uncover the potential brain changes to response the effects of interventions. The functional neuroimaging biomarkers can play an important role in detecting, assessing and diagnosing neurodegeneration (Horwitz and Rowe, 2011). In addition, there was altered intrinsic connectivity in the special targeted networks such as DMN and salience network to different neurodegenerative disorders (Seeley et al., 2009). Recently, the lateralization of RSNs was observed as an alteration accompanied by increased aging (Wilson et al., 2002). The hemispheric lateralization was also associated with enhanced cognitive ability (Gotts et al., 2013). Thus, the spatial pattern of intrinsic networks would be a candidate feature for the cognitive training intervention in older adults. Enhancement and maintenance of memory, visuospatial/construction and attention endured in healthy older adults with multi-domain cognitive interventions (Cheng et al., 2012). The changed lateralization of FPN and CereN which was observed in the cohort might be related to the brain mechanism of these behavior improvements.

The FPNs are associated with attention, cognitive performance and control processes. In the studies of resting state fMRI, the FPN is often identified using ICA. FPNs have marked asymmetry, which is involved in a multitude of cognitions; the right is more involved in monitoring processes whereas the left is putatively more involved in production processes (Cabeza et al., 2003). Combining lFPN and rFPN showed a similar spatial pattern, with a dorsal attention network consisting of regions previously known to be involved in goal-directed top-down processing (Damoiseaux et al., 2006; Luo et al., 2012c). Significant interactions of global LCF of lFPN were observed in this study. Global LCF of lFPN was significantly decreased in healthy controls whereas a marginal significant increase was observed in the training group. We presumed that the lateralization of lFPN would be an important predictor for maintenance of attention functioning and production processes. These findings implicated that the multi-domain cognitive training would contribute to the top-down attention function in the healthy older adults. Although the training main effects were also observed in the rFPN using repeated measure ANOVA, as indicated by the difference between the training group and control group, the training main effects might be stained by the initial distinction between groups (**Figure 4**). Thus the influence of training on the rFPN would not be evaluated directly in this study. In general, the FPN would be a target to multi-domain cognitive training.

Motor-related function decline is another physiological sign in old adults compared with younger adults. Accumulating evidence demonstrates decreased functional connectivity in the motor-related networks in aging, including the CereN and sensory-motor network (Tomasi and Volkow, 2012). Consistent with the previous studies, we found that the CereN is symmetrical at baseline (first scanning). However, improved lateralization of the CereN was observed in both group as indicated by a significant main effect of time in repeated measure ANOVA. The laterality significantly increased between two times of scans with interval of 1 year in healthy control groups whereas it did not in the training group. This finding reflected that the symmetry of the CereN was maintained in healthy older adults with multi-domain cognitive training. Recently, the functional connectivity studies indicate that the cerebellum participates in functional networks with motor control and cognitive processes (Habas et al., 2009; Krienen and Buckner, 2009). Thus, our findings might implicate that the multi-domain cognitive intervention contributed to the improvement of motor control in older adults. Actually, SMN would be directly related with motor performance (Zhang et al., 2015). Seidler et al. (2015) found greater network interactivity of SMN in older adults and suggested the protection

**TABLE 2 | The results of the repeated measure ANOVA for the laterality cofactors of individual *Bv* maps in 10 RSNs.**

| | | V1N | V2N | AN | SMN | CereN | BGN | DMN | CEN | lFPN | rFPN |
|---|---|---|---|---|---|---|---|---|---|---|---|
| Time main effects | *F* value | 3.498 | 0.279 | 0.111 | 3.888 | 6.903 | 1.044 | 0.677 | 0.901 | 0.006 | 1.183 |
| | *P* value | 0.071 | 0.601 | 0.741 | 0.058 | 0.015* | 0.315 | 0.417 | 0.35 | 0.939 | 0.285 |
| Training main effects | *F* value | 0.192 | 0.264 | 0.048 | 0.699 | 0.499 | 3.808 | 1.088 | 0.026 | 7.641 | 5.897 |
| | *P* value | 0.664 | 0.611 | 0.828 | 0.41 | 0.485 | 0.06 | 0.305 | 0.872 | 0.01* | 0.021* |
| Interaction effects | *F* value | 0.229 | 0.012 | 0.821 | 1.858 | 0.945 | 0.27 | 1.057 | 0.102 | 8.908 | 0.649 |
| | *P* value | 0.636 | 0.915 | 0.372 | 0.183 | 0.339 | 0.607 | 0.312 | 0.752 | 0.006* | 0.427 |

*Note: *Represented the statistical significance $p < 0.05$.*

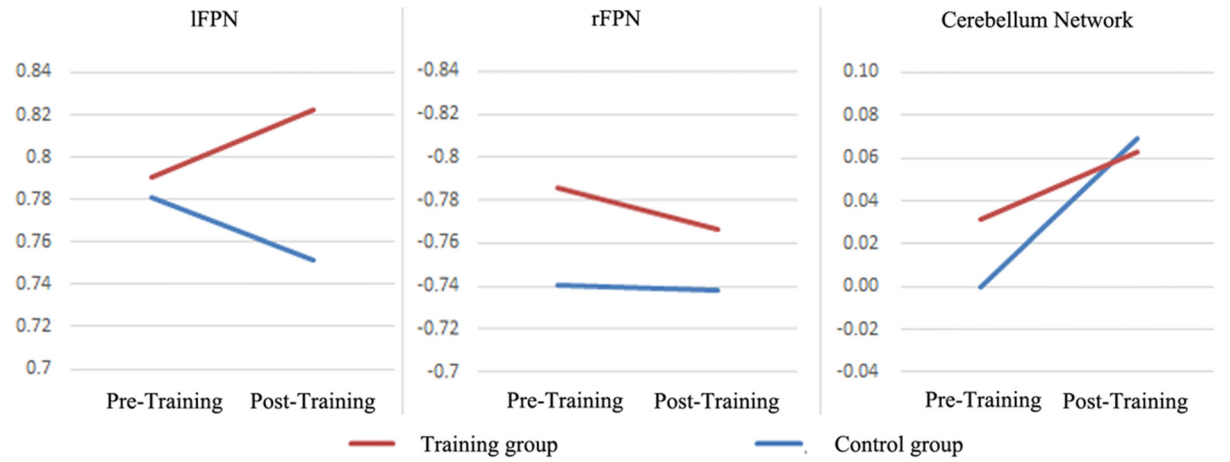


**FIGURE 4 | The LCFs of individual *Bv* maps in the lFPN, rFPN and CereN.** The repeated measure ANOVA were performed. The significance of statistical test was demonstrated in the **Table 2**.

against age declines in motor performance. However, no difference of the lateralization was found in the SMN in this study. It did not mean that the negative effects of cognitive training on the motor performance and motor prediction which are related with SMN are responsible. Future studies should focus on the various aspects of motor function associated with the cognitive intervention.

There are several limitations which should be mentioned here. First, the longitudinal design with 1-year duration was adopted in this study. The subjects were randomly grouped, and the behavior scores and genders were matched between groups. However, some connectivity features from the resting state fMRI might not match because their features could be calculated according to different methods. Thus, some features whose difference illustrated by repeated measure ANOVA might be stained by the mismatch in baseline (the first time) measures. Second, the relative small sample size would be another shortage of our study. In the future, more subjects should be recruited into the longitudinal study. Finally, the Group ICA was used to investigate the symmetry of the spatial pattern of RSNs. However, the number of ICs might be an underlying confounding factor. Till now, there has been no validated way to identify the number of ICs in ICA analysis. In this work, the MDL criteria implanted in GIFT software was used to determine the number of ICs.

In conclusion, lateralization of function is an important organization of the human brain. The distribution of intrinsic networks in the resting brain and their association with the multi-domain cognitive training is analyzed in this study. The lateralization of bilateral FPN and CereN was related to both aging and the multi-domain cognitive training in healthy older adults. These findings provide a neuroimaging evidence to support the positive effects of the cognitive training on enhancement and maintenance cognitive and motor function in healthy older adults.

## AUTHOR CONTRIBUTIONS

Conceived and designed the work: CLi, CLuo and DY; Acquired the data: XC, TL, YC and LJ; Analyzed the data: WC, XZ, CLuo, YG, XC and YC; Wrote the article: CLuo, CLi and DY. All authors revised the work for important intellectual content. All of the authors have read and approved the manuscript.

## ACKNOWLEDGMENTS

This study was funded by grants from the National Nature Science Foundation of China (81330032, 81371505, 81271547, 81471638), the Science and Technology Commission of Shanghai Municipality (134119a2501, 13dz2260500), the "111" project (B12027), SHSMU-ION Research Center for Brain Disorders.

## REFERENCES


Agcaoglu, O., Miller, R., Mayer, A. R., Hugdahl, K., and Calhoun, V. D. (2015). Lateralization of resting state networks and relationship to age and gender. *Neuroimage* 104, 310–325. doi: 10.1016/j.neuroimage.2014.09.001

Ashendorf, L., Jefferson, A. L., O'Conno, M. K., Chaisson, C., Green, R. C., and Stern, R. A. (2008). Trail making test errors in normal aging, mild cognitive impairment and dementia. *Arch. Clin. Neuropsychol.* 23, 129–137. doi: 10.1016/j.acn.2007.11.005

Ball, K., Berch, D. B., Helmers, K. F., Jobe, J. B., Leveck, M. D., Marsiske, M., et al. (2002). Effects of cognitive training interventions with older adults: a randomized controlled trial. *JAMA* 288, 2271–2281. doi: 10.1001/jama.288.18.2271

Beckmann, C. F., Deluca, M., Devlin, J. T., and Smith, S. M. (2005). Investigations into resting-state connectivity using independent component analysis. *Philos. Trans. R. Soc. Lond. B Biol. Sci.* 360, 1001–1013. doi: 10.1098/rstb.2005.1634

Boyke, J., Driemeyer, J., Gaser, C., Buchel, C., and May, A. (2008). Training-induced brain structure changes in the elderly. *J. Neurosci.* 28, 7031–7035. doi: 10.1523/JNEUROSCI.0742-08.2008

Brown, B. M., Peiffer, J. J., and Martins, R. N. (2013). Multiple effects of physical activity on molecular and cognitive signs of brain aging: can exercise slow neurodegeneration and delay Alzheimer's disease? *Mol. Psychiatry* 18, 864–874. doi: 10.1038/mp.2012.162

Cabeza, R., Locantore, J. K., and Anderson, N. D. (2003). Lateralization of prefrontal activity during episodic memory retrieval: evidence for the production-monitoring hypothesis. *J. Cogn. Neurosci.* 15, 249–259. doi: 10.1162/089892903321208187

Cao, W., Luo, C., Zhu, B., Zhang, D., Dong, L., Gong, J., et al. (2014). Resting-state functional connectivity in anterior cingulate cortex in normal aging. *Front. Aging Neurosci.* 6:280. doi: 10.3389/fnagi.2014.00280

Chen, X., Duan, M., Xie, Q., Lai, Y., Dong, L., Cao, W., et al. (2015). Functional disconnection between the visual cortex and the sensorimotor cortex suggests a potential mechanism for self-disorder in schizophrenia. *Schizophr. Res.* 166, 151–157. doi: 10.1016/j.schres.2015.06.014

Cheng, Y., Wu, W., Feng, W., Wang, J., Chen, Y., Shen, Y., et al. (2012). The effects of multi-domain versus single-domain cognitive training in non-demented older people: a randomized controlled trial. *BMC Med.* 10:30. doi: 10.1186/1741-7015-10-30

Cheng, Y., Wu, W., Wang, J., Feng, W., Wu, X., and Li, C. (2011). Reliability and validity of the repeatable battery for the assessment of neuropsychological status in community-dwelling elderly. *Arch. Med. Sci.* 7, 850–857. doi: 10.5114/aoms.2011.25561

Corballis, M. C. (2014). Left brain, right brain: facts and fantasies. *PLoS Biol.* 12:e1001767. doi: 10.1371/journal.pbio.1001767

Damoiseaux, J. S., Rombouts, S. A., Barkhof, F., Scheltens, P., Stam, C. J., Smith, S. M., et al. (2006). Consistent resting-state networks across healthy subjects. *Proc. Natl. Acad. Sci. U S A* 103, 13848–13853. doi: 10.1073/pnas.0601417103

Fox, M. D., Corbetta, M., Snyder, A. Z., Vincent, J. L., and Raichle, M. E. (2006). Spontaneous neuronal activity distinguishes human dorsal and ventral attention systems. *Proc. Natl. Acad. Sci. U S A* 103, 10046–10051. doi: 10.1073/pnas.0604187103

Gates, N., and Valenzuela, M. (2010). Cognitive exercise and its role in cognitive function in older adults. *Curr. Psychiatry Rep.* 12, 20–27. doi: 10.1007/s11920-009-0085-y

Goldberg, E., Roediger, D., Kucukboyaci, N. E., Carlson, C., Devinsky, O., Kuzniecky, R., et al. (2013). Hemispheric asymmetries of cortical volume in the human brain. *Cortex* 49, 200–210. doi: 10.1016/j.cortex.2011.11.002

Gong, D., He, H., Liu, D., Ma, W., Dong, L., Luo, C., et al. (2015). Enhanced functional connectivity and increased gray matter volume of insula related to action video game playing. *Sci. Rep.* 5:9763. doi: 10.1038/srep09763

Gong, D., He, H., Ma, W., Liu, D., Huang, M., Dong, L., et al. (2016). Functional integration between salience and central executive networks: a role for action video game experience. *Neural Plast.* 2015, 2016:9803165. doi: 10.1155/2016/9803165

Gotts, S. J., Jo, H. J., Wallace, G. L., Saad, Z. S., Cox, R. W., and Martin, A. (2013). Two distinct forms of functional lateralization in the human brain. *Proc. Natl. Acad. Sci. U S A* 110, E3435–E3444. doi: 10.1073/pnas.1302581110

Habas, C., Kamdar, N., Nguyen, D., Prater, K., Beckmann, C. F., Menon, V., et al. (2009). Distinct cerebellar contributions to intrinsic connectivity networks. *J. Neurosci.* 29, 8586–8594. doi: 10.1523/JNEUROSCI.1868-09.2009

Himberg, J., Hyvärinen, A., and Esposito, F. (2004). Validating the independent components of neuroimaging time series via clustering and visualization. *Neuroimage* 22, 1214–1222. doi: 10.1016/j.neuroimage.2004.03.027

Horwitz, B., and Rowe, J. B. (2011). Functional biomarkers for neurodegenerative disorders based on the network paradigm. *Prog. Neurobiol.* 95, 505–509. doi: 10.1016/j.pneurobio.2011.07.005

Jiang, S., Luo, C., Liu, Z., Hou, C., Wang, P., Dong, L., et al. (2016). Altered local spontaneous brain activity in juvenile myoclonic epilepsy: a preliminary resting-state fMRI study. *Neural Plast.* 2016:3547203. doi: 10.1155/2016/3547203

Kelly, A. M., Di Martino, A., Uddin, L. Q., Shehzad, Z., Gee, D. G., Reiss, P. T., et al. (2009). Development of anterior cingulate functional connectivity from late childhood to early adulthood. *Cereb. Cortex* 19, 640–657. doi: 10.1093/cercor/bhn117

Krienen, F. M., and Buckner, R. L. (2009). Segregated fronto-cerebellar circuits revealed by intrinsic functional connectivity. *Cereb. Cortex* 19, 2485–2497. doi: 10.1093/cercor/bhp135

Li, G., He, H., Huang, M., Zhang, X., Lu, J., Lai, Y., et al. (2015a). Identifying enhanced cortico-basal ganglia loops associated with prolonged dance training. *Sci. Rep.* 5:10271. doi: 10.1038/srep10271

Li, Q., Cao, W., Liao, X., Chen, Z., Yang, T., Gong, Q., et al. (2015b). Altered resting state functional network connectivity in children absence epilepsy. *J. Neurol. Sci.* 354, 79–85. doi: 10.1016/j.jns.2015.04.054

Li, J., Luo, C., Peng, Y., Xie, Q., Gong, J., Dong, L., et al. (2014). Probabilistic diffusion tractography reveals improvement of structural network in musicians. *PLoS One* 9:e105508. doi: 10.1371/journal.pone.0105508

Li, C., Wu, W., Jin, H., Zhang, X., Xue, H., He, Y., et al. (2006). Successful aging in Shanghai, China: definition, distribution and related factors. *Int. Psychogeriatr.* 18, 551–563. doi: 10.1017/s1041610205002966

Lim, M. L., Collinson, S. L., Feng, L., and Ng, T. P. (2010). Cross-cultural application of the Repeatable Battery for the Assessment of Neuropsychological Status (RBANS): performances of elderly Chinese Singaporeans. *Clin. Neuropsychol.* 24, 811–826. doi: 10.1080/13854046.2010.490789

Luo, C., Guo, Z. W., Lai, Y. X., Liao, W., Liu, Q., Kendrick, K. M., et al. (2012a). Musical training induces functional plasticity in perceptual and motor networks: insights from resting-state FMRI. *PLoS One* 7:e36568. doi: 10.1371/journal.pone.0036568

Luo, C., Li, Q., Xia, Y., Lei, X., Xue, K., Yao, Z., et al. (2012b). Resting state basal ganglia network in idiopathic generalized epilepsy. *Hum. Brain Mapp.* 33, 1279–1294. doi: 10.1002/hbm.21286

Luo, C., Qiu, C., Guo, Z., Fang, J., Li, Q., Lei, X., et al. (2012c). Disrupted functional brain connectivity in partial epilepsy: a resting-state fMRI study. *PLoS One* 7:e28196. doi: 10.1371/journal.pone.0028196

Luo, C., Tu, S., Peng, Y., Gao, S., Li, J., Dong, L., et al. (2014a). Long-term effects of musical training and functional plasticity in salience system. *Neural Plast.* 2014:180138. doi: 10.1155/2014/180138

Luo, C., Yang, T., Tu, S., Deng, J., Liu, D., Li, Q., et al. (2014b). Altered intrinsic functional connectivity of the salience network in childhood absence epilepsy. *J. Neurol. Sci.* 339, 189–195. doi: 10.1016/j.jns.2014.02.016

Lustig, C., Shah, P., Seidler, R., and Reuter-Lorenz, P. A. (2009). Aging, training and the brain: a review and future directions. *Neuropsychol. Rev.* 19, 504–522. doi: 10.1007/s11065-009-9119-9

Mackey, A. P., Miller Singley, A. T., and Bunge, S. A. (2013). Intensive reasoning training alters patterns of brain connectivity at rest. *J. Neurosci.* 33, 4796–4803. doi: 10.1523/JNEUROSCI.4141-12.2013

Papp, K. V., Walsh, S. J., and Snyder, P. J. (2009). Immediate and delayed effects of cognitive interventions in healthy elderly: a review of current literature and future directions. *Alzheimers Dement.* 5, 50–60. doi: 10.1016/j.jalz.2008.10.008

Power, J. D., Barnes, K. A., Snyder, A. Z., Schlaggar, B. L., and Petersen, S. E. (2012). Spurious but systematic correlations in functional connectivity MRI networks arise from subject motion. *Neuroimage* 59, 2142–2154. doi: 10.1016/j.neuroimage.2011.10.018

Raichle, M. E., MacLeod, A. M., Snyder, A. Z., Powers, W. J., Gusnard, D. A., and Shulman, G. L. (2001). A default mode of brain function. *Proc. Natl. Acad. Sci. U S A* 98, 676–682. doi: 10.1073/pnas.98.2.676

Seeley, W. W., Crawford, R. K., Zhou, J., Miller, B. L., and Greicius, M. D. (2009). Neurodegenerative diseases target large-scale human brain networks. *Neuron* 62, 42–52. doi: 10.1016/j.neuron.2009.03.024

Seidler, R. D., Bernard, J. A., Burutolu, T. B., Fling, B. W., Gordon, M. T., Gwin, J. T., et al. (2010). Motor control and aging: links to age-related brain structural, functional and biochemical effects. *Neurosci. Biobehav. Rev.* 34, 721–733. doi: 10.1016/j.neubiorev.2009.10.005

Seidler, R., Erdeniz, B., Koppelmans, V., Hirsiger, S., Mérillat, S., and Jäncke, L. (2015). Associations between age, motor function and resting state sensorimotor network connectivity in healthy older adults. *Neuroimage* 108, 47–59. doi: 10.1016/j.neuroimage.2014.12.023

Snowball, A., Tachtsidis, I., Popescu, T., Thompson, J., Delazer, M., Zamarian, L., et al. (2013). Long-term enhancement of brain function and cognition using cognitive training and brain stimulation. *Curr. Biol.* 23, 987–992. doi: 10.1016/j.cub.2013.04.045

Tomasi, D., and Volkow, N. D. (2012). Aging and functional brain networks. *Mol. Psychiatry* 17, 471, 549–458. doi: 10.1038/mp.2011.81

van Boxtel, M. P., ten Tusscher, M. P., Metsemakers, J. F., Willems, B., and Jolles, J. (2001). Visual determinants of reduced performance on the stroop color-word test in normal aging individuals. *J. Clin. Exp. Neuropsychol.* 23, 620–627. doi: 10.1076/jcen.23.5.620.1245

Wilson, R. S., Mendes De Leon, C. F., Barnes, L. L., Schneider, J. A., Bienias, J. L., Evans, D. A., et al. (2002). Participation in cognitively stimulating activities and risk of incident Alzheimer disease. *JAMA* 287, 742–748. doi: 10.1001/jama.287.6.742

Xiao, S., Yao, P., Li, X., and Zhang, M. (2002). Neuropsychological testing profiles of patients with Alzheimer's disease and mild cognitive impairment: a case-control study. *Hong Kong J. Psychiatry* 12, 2–5.

Zhang, R., Yao, D., Valdés-Sosa, P. A., Li, F., Li, P., Zhang, T., et al. (2015). Efficient resting-state EEG network facilitates motor imagery performance. *J. Neural Eng.* 12:066024. doi: 10.1088/1741-2560/12/6/066024 [Epub ahead of print].

Zhang, H., Zuo, X. N., Ma, S. Y., Zang, Y. F., Milham, M. P., and Zhu, C. Z. (2010). Subject order-independent group ICA (SOI-GICA) for functional MRI data analysis. *Neuroimage* 51, 1414–1424. doi: 10.1016/j.neuroimage.2010.03.039

**Conflict of Interest Statement**: The authors declare that the research was conducted in the absence of any commercial or financial relationships that could be construed as a potential conflict of interest.

frontiers in Aging Neuroscience

GENERAL COMMENTARY
published: 23 September 2015
doi: 10.3389/fnagi.2015.00183

# Commentary: Duration-dependent effects of the BDNF Val66Met polymorphism on anodal tDCS induced motor cortex plasticity in older adults: a group and individual perspective

*Anna Shpektor*[1], *David Bartrés-Faz*[2] *and Matteo Feurra*[1,3]*

[1] School of Psychology, Centre for Cognition and Decision Making, National Research University Higher School of Economics, Moscow, Russia, [2] Department of Psychiatry and Clinical Psychobiology, University of Barcelona, Barcelona, Spain, [3] Unit of Neurology and Clinical Neurophysiology, Brain Investigation and Neuromodulation laboratory (Si-BIN Lab), Department of Medicine, Surgery and Neuroscience, Azienda Ospedaliera Universitaria of Siena, Siena, Italy

**Keywords: BDNF, tDCS, synaptic plasticity, primary motor cortex, aging**

**A commentary on**

**Duration-dependent effects of the BDNF Val66Met polymorphism on anodal tDCS induced motor cortex plasticity in older adults: a group and individual perspective**
*by Puri R., Hinder M. R., Fujiyama H., Gomez R., Carson R. G., and Summers, J. J. (2015). Front. Aging Neurosci. 7:107. doi: 10.3389/fnagi.2015.00107*

OPEN ACCESS

***Edited by:***
*Junfeng Sun,*
*Shanghai Jiao Tong University, China*

***Reviewed by:***
*José M. Delgado-García,*
*University Pablo de Olavide, Spain*
*Vincenzo Di Lazzaro,*
*Università Campus Biomedico di Roma, Italy*

***Correspondence:**
*Matteo Feurra,*
*mfeurra@hse.ru*

***Received:*** *03 August 2015*
***Accepted:*** *07 September 2015*
***Published:*** *23 September 2015*

***Citation:***
*Shpektor A, Bartrés-Faz D and Feurra M (2015) Commentary: Duration-dependent effects of the BDNF Val66Met polymorphism on anodal tDCS induced motor cortex plasticity in older adults: a group and individual perspective. Front. Aging Neurosci. 7:183. doi: 10.3389/fnagi.2015.00183*

The Brain Derived Neurotrophic Factor (BDNF) is a neurotrophic protein that is strongly expressed in the Central Nervous System (CNS) and supports neuronal growth and survival (Conner et al., 1997). BDNF activates two neurotrophin receptors: Tropomyosin receptor kinase B (TrkB), that is necessary for hippocampal long-term potentiation (LTP) and associative learning, and Low-Affinity Nerve Growth Factor Receptor ($P75^{NTR}$), that is required for hippocampal long-term depression (LTD; Patterson et al., 1996; Gruart et al., 2007; Chapleau and Pozzo-Miller, 2012). Val66Met is a common single nucleotide polymorphism (SNP) placed in the human BDNF gene that leads to an amino-acid substitution of valine to methionine at codon 66 and cause a 18–30% decrease of BDNF neurotrophin secretion (Egan et al., 2003; Chen et al., 2006). In Met-carriers, the reduction of BDNF secretion results in variation of cortical morphology (Pezawas et al., 2004). This affects performance of memory and learning tasks (Egan et al., 2003; Hariri et al., 2003) and it may cause neuropsychological disorders (Lu et al., 2013; Moreira et al., 2015; van der Kolk et al., 2015). On this vein, it has been shown that Val66Met polymorphism play a complex role both for plasticity changes and recovery processes in after-stroke patients (Di Lazzaro et al., 2015; Di Pino et al., 2015).

The Val66Met polymorphism also alters sensorimotor system processes. McHughen et al. (2010) showed that during a simple right index finger movement task, Val/Met carriers exhibited reduced activation volumes on different brain regions (including motor cortex, premotor cortex, supplementary motor area) with respect to Val/Val carriers. Interestingly, after training, Val/Val showed a greater activation volume expansion whereas Val/Met carriers a greater activation volume reduction. Moreover, inside a driving-based motor learning task, subjects with polymorphism benefitted less from training. All together, these findings highlight that differences in volume

activation, accordingly to the polymorphism, increase with presence of training.

Recently, it has been shown that Transcranial Direct Current Stimulation (tDCS), might be an optimal tool to investigate the role of BDNF polymorphism in activity-dependent plasticity (Fritsch et al., 2010). In the human motor system, tDCS induces long-lasting and polarity-specific changes in the excitability of the motor cortex (Nitsche and Paulus, 2000). Anodal tDCS induces facilitatory effect by a membrane depolarization and by an increase in the excitability of corticospinal axons (Di Lazzaro et al., 2013), while cathodal tDCS induces inhibitory effects by a membrane hyperpolarization (Wagner et al., 2007). Animal models showed that tDCS modify thalamocortical synapses at presynaptic sites by changes in the membrane potential of cortical neurons (Márquez-Ruiz et al., 2012).

As discussed above, BDNF protein partly modulates LTP and LTD; interestingly it also modulates the effect of tDCS in both humans and animals. In mice, Fritsch and collaborators (Fritsch et al., 2010) showed that anodal tDCS coupled with repetitive low-frequency synaptic activation (LFS) induced a long-lasting synaptic potentiation (DCS-LTP). BDNF was a key modulator of this process: its secretion was enhanced by coupled tDCS-LFS and tDCS did not induce LTP in the absence of BDNF secretion (BDNF and TrkB mutant mice). At the same time, anodal tDCS over the primary motor cortex (M1) induced minor effects on the group with a reduced BDNF expression (Val/Met carriers) during a pinch-force task. Taken together, these results showed that tDCS might improve motor skills by inducing synaptic plasticity, which requires BDNF secretion in both humans and mice (Fritsch et al., 2010).

In a recent paper in *Frontiers in Aging Neuroscience*, Puri and collaborators (Puri et al., 2015), addressed the question about BDNF influence on tDCS effects in aging. They applied anodal tDCS for 10 and 20 min by stimulating left M1 on Val/Val and Val/Met subjects at rest. By using single pulse TMS, corticospinal excitability was measured before and each 5 min after tDCS offset. Results showed group- and time-dependent effects: Met carriers showed higher increase of M1 cortical excitability compared to Val/Val carriers. This effect was present only after 20 min of stimulation. Despite a previous tDCS study highlighted brain stimulation effects to be more pronounced on a Val/Met group (Antal et al., 2010), here authors showed the first evidence of the Val66Met SNP influence on M1 cortical excitability when tDCS was delivered at rest, as reflected by a significant between-groups interaction. These findings may be controversial: based on the previous literature, tDCS effects at rest did not differ between Val/Val and Val/Met carriers (Cheeran et al., 2008; Di Lazzaro et al., 2012; Fujiyama et al., 2014). Instead, influence of Val66Met polymorphism becomes more pronounced during task performance (Fritsch et al., 2010; McHughen et al., 2010). This might be due to the activity-dependence of BDNF secretion (Egan et al., 2003). The study by Puri et al. (2015) is also the first one that pointed out the crucial role of interaction between Val66Met SNP and duration of tDCS-M1 at rest: differences in cortical excitability occurred after 20 min of stimulation, but not after 10 min. However, these results do not fit with previous studies which showed no differences by tDCS at rest, when stimulation was applied for 10, 20, and 30 min (Cheeran et al., 2008; Di Lazzaro et al., 2012; Fujiyama et al., 2014). Results by Puri et al. (2015), may have different interpretations.

One possibility is that the two groups were unbalanced in terms of number of subjects: the sample size of Val/Val carriers was three times higher than Val/Met carriers. On one hand, this allowed authors to be blinded to the genotype during the experiment. On the other hand, since tDCS affected only the smaller group (Met-carriers), unbalanced analysis might have affected statistical sensitivity (Hector et al., 2010). Another possibility is that BDNF protein could have affected differently motor control processes in elder population, as was shown that its influence on memory functions changes during the lifespan (Kennedy et al., 2015; Papenberg et al., 2015). In summary the study by Puri and collaborators showed an interesting effect of Val66Met SNP in aging. Results were also stable as shown by less inter-individual variability inside the Met group which showed a more robust tDCS after-effect. The fact that 77% of Met carriers but only 35% of Val carriers showed the expected facilitation in both sessions could be used to stratify sample selection in aging studies where more homogeneous responses to Non Invasive Brain Stimulation are required. Finally, a further study with larger and balanced group of participants is needed. It will be interesting to have a control group of younger adults to understand the role of aging in the BDNF influence on motor plasticity at rest.

## Acknowledgments

The article was prepared within the framework of a subsidy granted to the HSE by the Government of the Russian Federation for the implementation of the Global Competitiveness Program.

## References

Antal, A., Chaieb, L., Moliadze, V., Monte-Silva, K., Poreisz, C., Thirugnanasambandam, N., et al. (2010). Brain-derived neurotrophic factor (BDNF) gene polymorphisms shape cortical plasticity in humans. *Brain Stimul.* 3, 230–237. doi: 10.1016/j.brs.2009.12.003

Chapleau, C. A., and Pozzo-Miller, L. (2012). Divergent roles of p75NTR and Trk receptors in BDNF's effects on dendritic spine density and morphology. *Neural Plast.* 2012:578057. doi: 10.1155/2012/578057

Cheeran, B., Talelli, P., Mori, F., Koch, G., Suppa, A., Edwards, M., et al. (2008). A common polymorphism in the brain-derived neurotrophic factor gene (BDNF) modulates human cortical plasticity and the response to rTMS. *J. Physiol.* 586, 5717–5725. doi: 10.1113/jphysiol.2008.159905

Chen, Z. Y., Jing, D., Bath, K. G., Ieraci, A., Khan, T., Siao, C. J., et al. (2006). Genetic variant BDNF (Val66Met) polymorphism alters anxiety-related behavior. *Science* 314, 140–143. doi: 10.1126/science.1129663

Conner, J. M., Lauterborn, J. C., Yan, Q., Gall, C. M., and Varon, S. (1997). Distribution of brain-derived neurotrophic factor (BDNF) protein and mRNA in the normal adult rat CNS: evidence for anterograde axonal transport. *J. Neurosci.* 17, 2295–2313.

Di Lazzaro, V., Manganelli, F., Dileone, M., Notturno, F., Esposito, M., Capasso, M., et al. (2012). The effects of prolonged cathodal direct current stimulation on

the excitatory and inhibitory circuits of the ipsilateral and contralateral motor cortex. *J. Neural Transm*. 119, 1499–1506. doi: 10.1007/s00702-012-0845-4

Di Lazzaro, V., Pellegrino, G., Di, P. G., Corbetto, M., Ranieri, F., Brunelli, N., et al. (2015). Val66Met BDNF gene polymorphism influences human motor cortex plasticity in acute stroke. *Brain Stimul*. 8, 92–96. doi: 10.1016/j.brs.2014.08.006

Di Lazzaro, V., Ranieri, F., Profice, P., Pilato, F., Mazzone, P., Capone, F., et al. (2013). Transcranial direct current stimulation effects on the excitability of corticospinal axons of the human cerebral cortex. *Brain Stimul*. 6, 641–643. doi: 10.1016/j.brs.2012.09.006

Di Pino, G., Pellegrino, G., Capone, F., Assenza, G., Florio, L., Falato, E., et al. (2015). Val66Met BDNF polymorphism implies a different way to recover from stroke rather than a worse overall recoverability. *Neurorehabil. Neural Repair*. doi: 10.1177/1545968315583721. [Epub ahead of print].

Egan, M. F., Kojima, M., Callicott, J. H., Goldberg, T. E., Kolachana, B. S., Bertolino, A., et al. (2003). The BDNF val66met polymorphism affects activity-dependent secretion of BDNF and human memory and hippocampal function. *Cell* 112, 257–269. doi: 10.1016/S0092-8674(03)00035-7

Fritsch, B., Reis, J., Martinowich, K., Schambra, H. M., Ji, Y., Cohen, L. G., et al. (2010). Direct current stimulation promotes BDNF-dependent synaptic plasticity: potential implications for motor learning. *Neuron* 66, 198–204. doi: 10.1016/j.neuron.2010.03.035

Fujiyama, H., Hyde, J., Hinder, M. R., Kim, S. J., McCormack, G. H., Vickers, J. C., et al. (2014). Delayed plastic responses to anodal tDCS in older adults. *Front. Aging Neurosci*. 6:115. doi: 10.3389/fnagi.2014.00115

Gruart, A., Sciarretta, C., Valenzuela-Harrington, M., Delgado-García, J. M., and Minichiello, L. (2007). Mutation at the TrkB PLC{gamma}-docking site affects hippocampal LTP and associative learning in conscious mice. *Learn. Mem*. 14, 54–62. doi: 10.1101/lm.428307

Hariri, A. R., Goldberg, T. E., Mattay, V. S., Kolachana, B. S., Callicott, J. H., Egan, M. F., et al. (2003). Brain-derived neurotrophic factor val66met polymorphism affects human memory-related hippocampal activity and predicts memory performance. *J. Neurosci*. 23, 6690–6694.

Hector, A., Von Felten, S., and Schmid, B. (2010). Analysis of variance with unbalanced data: an update for ecology & evolution. *J. Anim. Ecol*. 79, 308–316. doi: 10.1111/j.1365-2656.2009.01634.x

Kennedy, K. M., Reese, E. D., Horn, M. M., Sizemore, A. N., Unni, A. K., Meerbrey, M. E., et al. (2015). BDNF val66met polymorphism affects aging of multiple types of memory. *Brain Res*. 1612, 104–117. doi: 10.1016/j.brainres.2014.09.044

Lu, B., Nagappan, G., Guan, X., Nathan, P. J., and Wren, P. (2013). BDNF-based synaptic repair as a disease-modifying strategy for neurodegenerative diseases. *Nat. Rev. Neurosci*. 14, 401–416. doi: 10.1038/nrn3505

Márquez-Ruiz, J., Leal-Campanario, R., Sánchez-Campusano, R., Molaee-Ardekani, B., Wendling, F., Miranda, P. C., et al. (2012). Transcranial direct-current stimulation modulates synaptic mechanisms involved in associative learning in behaving rabbits. *Proc. Natl. Acad. Sci. U.S.A*. 109, 6710–6715. doi: 10.1073/pnas.1121147109

McHughen, S. A., Rodriguez, P. F., Kleim, J. A., Kleim, E. D., Marchal, C. L., Procaccio, V., et al. (2010). BDNF val66met polymorphism influences motor system function in the human brain. *Cereb. Cortex* 20, 1254–1262. doi: 10.1093/cercor/bhp189

Moreira, F. P., Fabião, J. D., Bittencourt, G., Wiener, C. D., Jansen, K., Oses, J. P., et al. (2015). The Met allele of BDNF Val66Met polymorphism is associated with increased BDNF levels in generalized anxiety disorder. *Psychiatr. Genet*. 25, 201–207. doi: 10.1097/ypg.0000000000000097

Nitsche, M. A., and Paulus, W. (2000). Excitability changes induced in the human motor cortex by weak transcranial direct current stimulation. *J. Physiol.* 527(Pt 3), 633–639. doi: 10.1111/j.1469-7793.2000.t01-1-00633.x

Papenberg, G., Salami, A., Persson, J., Lindenberger, U., and Bäckman, L. (2015). Genetics and functional imaging: effects of APOE, BDNF, COMT, and KIBRA in aging. *Neuropsychol. Rev*. 25, 47–62. doi: 10.1007/s11065-015-9279-8

Patterson, S. L., Abel, T., Deuel, T. A., Martin, K. C., Rose, J. C., and Kandel, E. R. (1996). Recombinant BDNF rescues deficits in basal synaptic transmission and hippocampal LTP in BDNF knockout mice. *Neuron* 16, 1137–1145. doi: 10.1016/S0896-6273(00)80140-3

Pezawas, L., Verchinski, B. A., Mattay, V. S., Callicott, J. H., Kolachana, B. S., Straub, R. E., et al. (2004). The brain-derived neurotrophic factor val66met polymorphism and variation in human cortical morphology. *J. Neurosci*. 24, 10099–10102. doi: 10.1523/JNEUROSCI.2680-04.2004

Puri, R., Hinder, M. R., Fujiyama, H., Gomez, R., Carson, R. G., and Summers, J. J. (2015). Duration-dependent effects of the BDNF Val66Met polymorphism on anodal tDCS induced motor cortex plasticity in older adults: a group and individual perspective. *Front. Aging Neurosci*. 7:107. doi: 10.3389/fnagi.2015.00107

van der Kolk, N. M., Speelman, A. D., van, N. M., Kessels, R. P., IntHout, J., Hakobjan, M., et al. (2015). BDNF polymorphism associates with decline in set shifting in Parkinson's disease. *Neurobiol. Aging* 36, 1605–1606. doi: 10.1016/j.neurobiolaging.2014.08.023

Wagner, T., Valero-Cabre, A., and Pascual-Leone, A. (2007). Noninvasive human brain stimulation. *Annu. Rev. Biomed. Eng.* 9, 527–565. doi: 10.1146/annurev.bioeng.9.061206.133100

**Conflict of Interest Statement:** The authors declare that the research was conducted in the absence of any commercial or financial relationships that could be construed as a potential conflict of interest.

frontiers in Aging Neuroscience

GENERAL COMMENTARY
published: 19 February 2016
doi: 10.3389/fnagi.2016.00028

# Response: "Commentary: Duration-dependent effects of the BDNF Val66Met polymorphism on anodal tDCS induced motor cortex plasticity in older adults: a group and individual perspective"

*Rohan Puri* and Mark R. Hinder*

*Sensorimotor Neuroscience and Ageing Laboratory, Faculty of Health, School of Medicine, University of Tasmania, Hobart, TAS, Australia*

**Keywords: *BDNF*, Val66Met polymorphism, transcranial magnetic stimulation (TMS), transcranial direct current stimulation (tDCS), motor cortex, older adults, corticospinal excitability, plasticity**

**A response to**

**Commentary: Duration-dependent effects of the BDNF Val66Met polymorphism on anodal tDCS induced motor cortex plasticity in older adults: a group and individual perspective**
*by Shpektor, A., Bartrés-Faz, D., and Feurra, M. (2015). Front. Aging Neurosci. 7:183. doi: 10.3389/fnagi.2015.00183*

OPEN ACCESS

***Edited by:***
*Junfeng Sun,*
*Shanghai Jiao Tong University, China*

***Reviewed by:***
*Vincenzo Di Lazzaro,*
*Università Campus Biomedico di Roma, Italy*

****Correspondence:***
*Rohan Puri*
*rohan.puri@utas.edu.au*

***Received:*** *30 November 2015*
***Accepted:*** *05 February 2016*
***Published:*** *19 February 2016*

***Citation:***
*Puri R and Hinder MR (2016) Response: "Commentary: Duration-dependent effects of the BDNF Val66Met polymorphism on anodal tDCS induced motor cortex plasticity in older adults: a group and individual perspective". Front. Aging Neurosci. 8:28. doi: 10.3389/fnagi.2016.00028*

In a commentary on our recent paper (Puri et al., 2015), Shpektor et al. (2015) provide alternative interpretations on the effects of the *BDNF* Val66Met polymorphism on transcranial direct current stimulation (tDCS)-induced plasticity in older adults. Here we respond to several key issues raised in regard to our findings, and discuss broader implications for the field of non-invasive brain stimulation (NBS).

Shpektor et al. (2015) suggest that our findings, whereby older Met carriers (homozygous or heterozygous for the Met allele) exhibit a greater plastic response to 20 min of anodal tDCS compared to Val/Val homozygotes, may be seen as "controversial" as we reported an influence of the *BDNF* Val66Met polymorphism on plasticity at rest (i.e., not during task performance). However, a broader search of the extant literature suggests that the effects of the *BDNF* Val66Met polymorphism on tDCS-induced plasticity are varied, even before one considers the interaction of tDCS effects with neural activation resulting from performing a concurrent motor task (e.g., Fritsch et al., 2010). Specifically, Antal et al. (2010) reported a significant Genotype x Time interaction where greater motor evoked potential (MEP) amplitude was observed in Met allele carriers compared to Val/Val homozygotes at 25 and 60 min following anodal tDCS. Furthermore, Teo et al. (2014) reported a significant facilitation in MEPs post anodal stimulation only for Met carriers and not Val/Val homozygotes. Recently, Strube et al. (2015) reported a greater increase in MEPs for healthy Met carriers than Val/Val homozygotes after anodal tDCS (although this did not quite reach the *a-priori* level of statistical significance, $p = 0.072$, it was associated with a large effect size, $d = 0.799$). On the other hand, some studies do not report statistically significant differences between Met carriers and Val/Val homozygotes (Cheeran et al., 2008; Di Lazzaro et al., 2012; Fujiyama et al., 2014). However, as we alluded to in our paper, an absence of statistically significant effects should be interpreted with caution, especially when sample

sizes are small and studies are not primarily designed to investigate *BDNF* polymorphism effects (e.g., Fujiyama et al., 2014).

In addition, there appears to be some preliminary evidence to suggest that the specific polarity of tDCS may interact with BDNF to elicit different magnitude changes in plasticity. That is, putative LTD-like effects induced by cathodal tDCS appear to be somewhat less affected by the *BDNF* Val66Met polymorphism (Cheeran et al., 2008; Antal et al., 2010; Di Lazzaro et al., 2012; Strube et al., 2015) than purported LTP-like effects induced by way of anodal tDCS (Antal et al., 2010; Teo et al., 2014; Puri et al., 2015; Strube et al., 2015). Large sample studies which directly assess the effect of tDCS polarity on BDNF-mediated plasticity effects would help elucidate the extent of this interaction. Overall, it must be concluded that the role of *BDNF* Val66Met polymorphism on mediating tDCS-effects remains unclear, and, that further studies with significantly greater power (sample sizes) are needed to further elucidate a number of factors that may contribute to the divergent results across the existing literature.

Another important consideration is the role that altered brain states and processes may play in mediating plastic responses. Indeed, it has been suggested that in stroke patients, rather than being detrimental, the Met allele interferes with maladaptive brain plasticity such that Val/Val and Met carrier stroke patients may not differ in their absolute ability for recovery (Di Lazzaro et al., 2015, Di Pino et al., 2016). It is conceivable that changes that occur as a result of the natural (healthy) aging process could, at least in part, explain the "novel" results we recently reported. Despite the potential of tDCS (and NBS in general) to slow the undesired effects of aging, such as cognitive decline and degradation of fine motor skills, very few studies have specifically examined older cohorts. Given the scarcity of research considering *BDNF* Val66Met polymorphism effects on NBS-induced plasticity in older populations, it is worth reviewing extant research that has investigated the effects of this polymorphism on cognitive and motor function in young and aged populations.

In young adults, the Met allele is often associated with *impaired* cognitive functioning, particularly in the memory domain (for meta-analysis see Kambeitz et al., 2012). In contrast, the Met allele appears to be less detrimental in older adults, and may even protect against the deleterious effects of aging to some degree. Specifically, older Met carriers demonstrate *improved* performance compared to Val/Val homozygotes on an array of cognitive tasks (Harris et al., 2006; Gajewski et al., 2011, 2012)[1]. Moreover, a 10 year longitudinal study in healthy older adults reported that Val/Val homozygotes exhibited significant *decline* in task-switching over the 10 year period whereas Met carriers' performance remained unchanged (Erickson et al., 2008).

Comparable age-effects are observed in the motor domain: Fritsch et al. (2010) and McHughen et al. (2010) report degraded motor performance in young Met carriers, whereas no detrimental effect of the Met allele was observed in motor behavior, neurophysiology, or use-dependent plasticity mechanisms for older adults (McHughen and Cramer, 2013). Overall, these studies highlight that the effects of the *BDNF* polymorphism are dynamic in nature and change during the normal aging process. Moreover, these findings suggest that the positive effect of the Met allele on the extent of tDCS-induced plasticity in our study may be partly reflected by the aged status of our cohort.

Our paper, with its limitations acknowledged therein, is one of the largest sample sized studies aimed to provide preliminary insights into the effects of this polymorphism in an older population. In light of aging demographics it therefore assumes considerable importance. However, further systematic investigations are needed to develop a clearer and deeper understanding while also providing replication. First and foremost, future studies should employ larger participant numbers and – even though most research has employed unbalanced samples – seek equal sample sizes of all three genotypic distributions (Val/Val, Val/Met, Met/Met). Finally, in addition to probing the genetic effects on artificially induced-plasticity using NBS and use-dependent plasticity using motor/cognitive training paradigms, understanding how the interaction between these two forms of plasticity is mediated by genotype would provide a novel basis to extend research on the effects of this polymorphism.

## AUTHOR CONTRIBUTIONS

RP and MRH prepared, wrote, and revised the manuscript.

## FUNDING

This research was supported under the Australian Research Council's Discovery Projects funding scheme (DP130104317) and by a DECRA fellowship (DE120100729) awarded to MRH.

## ACKNOWLEDGMENTS

We would like to acknowledge Prof. Jeffery Summers for insightful conversations during the preparation of this manuscript.

[1] See Papenberg et al. (2015) for counter-argument.

## REFERENCES

Antal, A., Chaieb, L., Moliadze, V., Monte-Silva, K., Poreisz, C., Thirugnanasambandam, N., et al. (2010). Brain-derived neurotrophic factor (BDNF) gene polymorphisms shape cortical plasticity in humans. *Brain Stimul.* 3, 230–237. doi: 10.1016/j.brs.2009.12.003

Cheeran, B., Talelli, P., Mori, F., Koch, G., Suppa, A., Edwards, M., et al. (2008). A common polymorphism in the brain-derived neurotrophic factor gene (BDNF) modulates human cortical plasticity and the response to rTMS. *J. Physiol.* 586, 5717–5725. doi: 10.1113/jphysiol.2008.159905

Di Lazzaro, V., Manganelli, F., Dileone, M., Notturno, F., Esposito, M., Capasso, M., et al. (2012). The effects of prolonged cathodal direct current stimulation on

the excitatory and inhibitory circuits of the ipsilateral and contralateral motor cortex. *J. Neural Transm. (Vienna)* 119, 1499–1506. doi: 10.1007/s00702-012-0845-4

Di Lazzaro, V., Pellegrino, G., Di Pino, G., Corbetto, M., Ranieri, F., Brunelli, N., et al. (2015). Val66Met BDNF gene polymorphism influences human motor cortex plasticity in acute stroke. *Brain Stimul.* 8, 92–96. doi: 10.1016/j.brs.2014.08.006

Di Pino, G., Pellegrino, G., Capone, F., Assenza, G., Florio, L., Falato, E., et al. (2016). Val66Met BDNF polymorphism implies a different way to recover from stroke rather than a worse overall recoverability. *Neurorehabil. Neural Repair* 30, 3–8. doi: 10.1177/1545968315583721

Erickson, K. I., Kim, J. S., Suever, B. L., Voss, M. W., Francis, B. M., and Kramer, A. F. (2008). Genetic contributions to age-related decline in executive function: a 10-year longitudinal study of COMT and BDNF polymorphisms. *Front. Hum. Neurosci.* 2:11. doi: 10.3389/neuro.09.011.2008

Fritsch, B., Reis, J., Martinowich, K., Schambra, H. M., Ji, Y., Cohen, L. G., et al. (2010). Direct current stimulation promotes BDNF-dependent synaptic plasticity: potential implications for motor learning. *Neuron* 66, 198–204. doi: 10.1016/j.neuron.2010.03.035

Fujiyama, H., Hyde, J., Hinder, M. R., Kim, S. J., Mccormack, G. H., Vickers, J. C., et al. (2014). Delayed plastic responses to anodal tDCS in older adults. *Front. Aging Neurosci.* 6:115. doi: 10.3389/fnagi.2014.00115

Gajewski, P. D., Hengstler, J. G., Golka, K., Falkenstein, M., and Beste, C. (2011). The Met-allele of the BDNF Val66Met polymorphism enhances task switching in elderly. *Neurobiol. Aging* 32, 2327.e2327–2327.e2319. doi: 10.1016/j.neurobiolaging.2011.06.010

Gajewski, P. D., Hengstler, J. G., Golka, K., Falkenstein, M., and Beste, C. (2012). The Met-genotype of the BDNF Val66Met polymorphism is associated with reduced Stroop interference in elderly. *Neuropsychologia* 50, 3554–3563. doi: 10.1016/j.neuropsychologia.2012.09.042

Harris, S. E., Fox, H., Wright, A. F., Hayward, C., Starr, J. M., Whalley, L. J., et al. (2006). The brain-derived neurotrophic factor Val66Met polymorphism is associated with age-related change in reasoning skills. *Mol. Psychiatry* 11, 505–513. doi: 10.1038/sj.mp.4001799

Kambeitz, J. P., Bhattacharyya, S., Kambeitz-Ilankovic, L. M., Valli, I., Collier, D. A., and Mcguire, P. (2012). Effect of BDNF val(66)met polymorphism on declarative memory and its neural substrate: a meta-analysis. *Neurosci. Biobehav. Rev.* 36, 2165–2177. doi: 10.1016/j.neubiorev.2012.07.002

McHughen, S. A., and Cramer, S. C. (2013). The BDNF val(66)met polymorphism is not related to motor function or short-term cortical plasticity in elderly subjects. *Brain Res.* 1495, 1–10. doi: 10.1016/j.brainres.2012.12.004

McHughen, S. A., Rodriguez, P. F., Kleim, J. A., Kleim, E. D., Marchal Crespo, L., Procaccio, V., et al. (2010). BDNF val66met polymorphism influences motor system function in the human brain. *Cereb. Cortex* 20, 1254–1262. doi: 10.1093/cercor/bhp189

Papenberg, G., Salami, A., Persson, J., Lindenberger, U., and Backman, L. (2015). Genetics and functional imaging: effects of APOE, BDNF, COMT, and KIBRA in aging. *Neuropsychol. Rev.* 25, 47–62. doi: 10.1007/s11065-015-9279-8

Puri, R., Hinder, M. R., Fujiyama, H., Gomez, R., Carson, R. G., and Summers, J. J. (2015). Duration-dependent effects of the BDNF Val66Met polymorphism on anodal tDCS induced motor cortex plasticity in older adults: a group and individual perspective. *Front. Aging Neurosci.* 7:107. doi: 10.3389/fnagi.2015.00107

Shpektor, A., Bartrés-Faz, D., and Feurra, M. (2015). Commentary: Duration-dependent effects of the BDNF Val66Met polymorphism on anodal tDCS induced motor cortex plasticity in older adults: a group and individual perspective. *Front. Aging Neurosci.* 7:183. doi: 10.3389/fnagi.2015.00183

Strube, W., Nitsche, M. A., Wobrock, T., Bunse, T., Rein, B., Herrmann, M., et al. (2015). BDNF-Val66Met-polymorphism impact on cortical plasticity in schizophrenia patients: a proof of concept study. *Int. J. Neuropsychopharmacol.* 18:pyu040. doi: 10.1093/ijnp/pyu040

Teo, J. T., Bentley, G., Lawrence, P., Soltesz, F., Miller, S., Willé, D., et al. (2014). Late cortical plasticity in motor and auditory cortex: role of met-allele in BDNF Val66Met polymorphism. *Int. J. Neuropsychopharmacol.* 17, 705–713. doi: 10.1017/S1461145713001636

**Conflict of Interest Statement:** The authors declare that the research was conducted in the absence of any commercial or financial relationships that could be construed as a potential conflict of interest.

frontiers in Aging Neuroscience

ORIGINAL RESEARCH
published: 18 November 2015
doi: 10.3389/fnagi.2015.00210

# MicroRNAs 99b-5p/100-5p Regulated by Endoplasmic Reticulum Stress are Involved in Abeta-Induced Pathologies

*Xiaoyang Ye[1†], Hongxue Luo[1†], Yan Chen[2], Qi Wu[1], Yi Xiong[1], Jinyong Zhu[1], Yarui Diao[3], Zhenguo Wu[2], Jianting Miao[4] and Jun Wan[1,2*]*

[1] Shenzhen Key Laboratory for Neuronal Structural Biology, Biomedical Research Institute, Shenzhen Peking University – The Hong Kong University of Science and Technology Medical Center, Shenzhen, China, [2] Division of Life Science, The Hong Kong University of Science and Technology, Hong Kong, China, [3] Ludwig Institute for Cancer Research, San Diego, CA, USA, [4] Department of Neurology, Tangdu Hospital, Fourth Military Medical University, Xi'an City, China

Alzheimer's disease (AD) is the most common cause of dementia. Amyloid β (Abeta, Aβ) deposition and intracellular tangles are the pathological hallmarks of AD. MicroRNAs (miRNAs) are small non-coding RNAs, which have been found to play very important roles, and have the potential to serve as diagnostic markers during neuronal pathogenesis. In this study, we aimed to determine the roles of miR-99b-5p and miR-100-5p in Aβ-induced neuronal pathologies. We detected the expression levels of miR-99b-5p and miR-100-5p in the brains of APPswe/PS1ΔE9 double-transgenic mice (APP/PS1 mice) at different age stages and found that both miRNAs were decreased at early stages while increased at late stages of APP/PS1 mice when compared with the age-matched wild type (WT) mice. Similar phenomenon was also observed in Aβ-treated cultured cells. We also confirmed that mammalian target of rapamycin (mTOR) is one of the targets of miR-99b-5p/100-5p, which is consistent with previous studies in cancer. MiR-99b-5p/100-5p has been found to promote cell apoptosis with the Aβ treatment. This effect may be induced via the mTOR pathway. In our study, we find both miR-99b-5p and miR-100-5p affect neuron survival by targeting mTOR. We also speculate that dynamic change of miR-99b-5p/100-5p levels during Aβ-associated pathologies might be attributed to Aβ-induced endoplasmic reticulum stress (ER stress), suggesting the potential role of the "ER stress–miRNAs–mTOR" axis in Aβ-related AD pathogenesis.

**Keywords: microRNA-99b-5p, microRNA-100-5p, amyloid β, Alzheimer's disease, endoplasmic reticulum stress**

OPEN ACCESS

***Edited by:***
*Chunbo Li,*
*Shanghai Jiao Tong University School of Medicine, China*

***Reviewed by:***
*Catarina Oliveira,*
*University of Coimbra, Portugal*
*Robert Petersen,*
*Case Western Reserve University, USA*

****Correspondence:***
*Jun Wan*
*wanj@ust.hk*

*†Xiaoyang Ye and Hongxue Luo have contributed equally to this work.*

***Received:*** *24 August 2015*
***Accepted:*** *26 October 2015*
***Published:*** *18 November 2015*

***Citation:***
*Ye X, Luo H, Chen Y, Wu Q, Xiong Y, Zhu J, Diao Y, Wu Z, Miao J and Wan J (2015) MicroRNAs 99b-5p/100-5p Regulated by Endoplasmic Reticulum Stress are Involved in Abeta-Induced Pathologies. Front. Aging Neurosci. 7:210. doi: 10.3389/fnagi.2015.00210*

## INTRODUCTION

Alzheimer's disease (AD) is the most common human neurodegenerative disease in the elderly; more than 30 million people suffer from AD worldwide (Schonrock et al., 2012). The nosogenesis of AD is widely accepted as amyloid-β peptide (Aβ) deposition caused by abnormal protein metabolism

**Abbreviations:** Aβ, amyloid β; AD, Alzheimer's disease; APP, amyloid precursor protein; ER stress, endoplasmic reticulum stress; MiRNA, microRNA; mTOR, mammalian target of rapamycin; PI3K, phosphatidylinositol 3-kinase; PS1, presenilin 1; WT, wild type.

and tau protein precipitation in AD brains. The AD progress encompasses multiple alterations of gene expression and protein reactions related to Aβ deposition, tau hyperphosphorylation, inflammation, energy metabolism, cell cycle, and apoptosis (Ballard et al., 2009; Schonrock et al., 2012). Aβ is the main component of amyloid plaques, which trigger cascaded reaction, leading to synaptic dysfunction, disrupting neural connectivity and neuronal death (Murphy and LeVine, 2010). Recently, lots of studies have demonstrated that aberrant levels of microRNAs (miRNAs) are widely involved in AD brains, indicating a complicated regulatory network of miRNAs in the etiopathology of AD (Schratt et al., 2006; Cheng et al., 2009; Magill et al., 2010; Zhao et al., 2010).

MicroRNAs are non-coding RNAs with 21–25 nt, which originate from both intergenic and intronic regions, inhibiting protein expression in a post-transcriptional manner by interacting with the 3′-UTR of target mRNAs (Ambros, 2004). A single miRNA has the ability to target thousands of mRNA molecules. Moreover, there are hundreds of potential miRNA-binding sites in just one mRNA molecule. MiRNAs have been reported to be involved in a wide spectrum of human diseases, especially in cancer, infectious diseases, cardiac diseases, and many others (Ardekani and Naeini, 2010; Tufekci et al., 2014). Accumulating evidences show that miRNAs also participate in numerous neurodegenerative disorders, including AD, Amyotrophic lateral sclerosis, Parkinson's disease, and Huntington's disease (Kim et al., 2007). Recent studies of AD have demonstrated aberrant miRNA expression profile in AD via developed sequencing approach (Nunez-Iglesias et al., 2010; Shioya et al., 2010). The roles of miRNAs in APP and Aβ production, synaptic remodeling, neuron survival, and glia cell activation have also been identified (Kurosinski and Gotz, 2002; Kocerha et al., 2009; Schratt, 2009). Nevertheless, there are far more miRNAs remaining enigmatic as to their roles in AD etiology.

Our previous study found that miR-99b-5p and miR-100-5p were abnormally expressed in the brains of APPswe/PS1ΔE9 double-transgenic mice [APP/PS1 mice (Luo et al., 2014)], which have AD symptoms after 6 months of age, suggesting their pivotal roles in Aβ deposition-associated AD pathology. MiR-99b-5p and miR-100-5p belong to the same miR-99 family, which consists of three members, miR-99a, miR-99b, and miR-100. Studies have shown that miR-99 family regulates cell survival, cell stress response, proliferation, angiogenesis, DNA damage, and wound healing process (Zhang et al., 2009; Doghman et al., 2010; Sun et al., 2011; Chen et al., 2012; Zheng et al., 2012; Jin et al., 2013; Mueller et al., 2013). It has been reported that mammalian target of rapamycin (mTOR) is one of the targets of both miR-99 and miR-100 (Sun et al., 2011; Li et al., 2013; Xu et al., 2013).

Mammalian target of rapamycin is a conserved serine–threonine kinase, belonging to the phosphatidylinositol 3-kinase (PI3K)-related kinase protein family. This kinase family plays essential roles in cell apoptosis, proliferation and differentiation, cell senescence, cytoskeleton composition, angiogenesis, gene transcription, tumor formation, and development, mainly via PI3K/Akt/mTOR signaling pathway (Hassan et al., 2013; Maiese et al., 2013; Trigka et al., 2013). Interestingly, emerging evidences demonstrate that mTOR regulates neuron survival, neuronal protection, autophagy, synaptic development, and function in nerve system (Chen et al., 2010; Heras-Sandoval et al., 2014). Previous studies have illustrated that both in patient cases and mouse models of AD, Aβ can inhibit mTOR pathway, leading to dysregulation of tau, phosphatase and tensin homolog (PTEN), and neuronal survival as well as plasticity (Chen et al., 2010). In addition, mTOR is associated with clearance of Aβ, synaptic remodeling, long-term potentiation (LTP), and cognitive decline (Jaworski et al., 2005; Paccalin et al., 2006; Hoeffer and Klann, 2010; Ma et al., 2010), indicating its predominant roles in AD development. Therefore, the role of mTOR under the regulation of miR-99b-5p and miR-100-5p in Aβ-induced neuronal pathologies needs to be further illuminated.

In this study, we used APP/PS1 mice to determine the role of miR-99b-5p and miR-100-5p in Aβ-associated brain pathologies. Our work first demonstrated that miR-99b-5p/100-5p levels exhibited a dynamic change along the Aβ deposition, which could also be recapitulated in Aβ-treated cells *in vitro*. We presumed that this dynamic change of both miRNAs might be due to Aβ-induced endoplasmic reticulum stress (ER stress). Moreover, we found that miR-99b-5p/100-5p played a pivotal role via targeting mTOR, indicating that the ER stress–miRNAs–mTOR axis might give us a novel clue to understand Aβ-induced AD pathology.

## MATERIALS AND METHODS

### Animal Samples

The APP/PS1 mice [held by The Jackson Laboratory, stain name: "B6.Cg-Tg(APPswe, PSEN1dE9)85Dbo/Mmjax" (Borchelt et al., 1996)] were purchased from the Model Animal Research Center of Nanjing University. The non-carrier C57BL/6J mice were used as the wild type (WT) control. Six to eight pairs of APP/PS1 and WT mice at different age stages were included in this study. All the mice were anesthetized with pentobarbital (50 mg/kg). Then, 0.5 ml of peripheral whole blood was kept in anticoagulation tubes with EDTA. Cortexes of the brains were dissected and lysed for either RNA or protein extraction. All the animal experiments were performed in accordance with animal use guidelines approved by the Committee for the Ethics of Animal Experiment, Shenzhen-Peking University, The Hong Kong University of Science and Technology Medical Center (SPHMC). The protocol number is 2011-004.

### Reagents and Antibodies

Amyloid-β peptide 1–42 (Aβ1–42) was from AnaSpec (AS-20276). The ER stress inhibitor sodium phenylbutyrate (PBA) and inducer thapsigargin (TG) were both from Sigma. PBA and TG were dissolved in ethanol and used with the final concentration of 10 mM and 500 nM, respectively. MiRNA mimics and inhibitors were purchased from Invitrogen. Mouse monoclonal antibodies of GAPDH and β-actin were from Sangon, and rabbit polyclonal antibody of mTOR was from Cell Signaling Technology.

### Cell Culture and Aβ Treatment

Rat pheochromocytoma cells – PC12 (ATCC) were routinely cultured in DMEM (GIBCO) containing 6% fetal bovine serum (Hyclone), 6% horse serum (GIBCO), 50 U/ml penicillin, and 50 μg/ml streptomycin (GIBCO) in a humidified incubator at

37°C with 7.5% $CO_2$. PC12 cell differentiation was induced by NGF. Cells were plated 1 day before treatment with NGF. After incubating for 1 day, culture medium was changed to differentiation medium (DMEM with 50 ng/ml NGF, 0.5% fetal bovine serum, 0.5% horse serum and penicillin/streptomycin). Primary cortical neuron cultures were prepared from embryonic day 18 rat embryos (Wan et al., 2008). Cortical neurons were plated and cultured on poly-L-lysine (PLL)-precoated culture plates in Neurobasal A medium containing B27 supplement, 0.05 mM glucose, and 0.5 mM L-glutamine in a 37°C, 5% $CO_2$ incubator. Culture medium was half-changed every 2 days. Aβ1–42 oligomers were prepared by dissolving Aβ1–42 powder in 1% $NH_4OH$ followed by diluting to 0.2 mM in PBS, and incubating in 37°C water bath overnight. Aβ1–42 with different final concentrations was treated with cortical neurons cultured at 7-day *in vitro* (DIV7) or differentiated PC12 cells (NGF treatment for 48 h) for various time intervals as indicated.

## Plasma MicroRNAs Quantification Based on Taqman Probe qPCR

Whole blood samples from different ages of mice were centrifuged at 2,000 rpm for 10 min at room temperature. The separated plasma was stored at −80°C. RNA was isolated from 150 μl plasma by Trizol Reagent (Invitrogen) for Taqman probe-based (Invitrogen) qPCR analysis as described before (Wang et al., 2015). Both miR-99b-5p and miR-100-5p mimics were used to establish standard curves for the determination of the miRNAs copies in plasma. All probe-based qPCR was done using Lightcycler 480 probe Master (Roche) according to the manufacturer's instructions. For normalization of sample variation, 5 ng internal control Mmu-miR-486 and external miRNAs control Cel-miR-238 were added to each plasma sample for extraction and qRT-PCR. The statistical analyses were performed using the methods as described before (Wang et al., 2015). The probe sequences were listed in **Table 1**.

## RNA Extraction and Real-Time PCR

Total RNA was extracted by Trizol Reagent (Invitrogen) from either mice brains or cultured cells, followed by reverse transcription as described previously (Luo et al., 2014). CDNAs were then used as the templates in Real-time PCR using iQ™ SYBR® Green Supermix (BIO-RAD). The mRNA level of mTOR was normalized by the average levels of GAPDH, while miRNA was by the levels of snRNAU6. The delta–deltaCt method was used in this study to quantify the fold change of both mRNA and miRNAs. The primer sequences were listed in **Table 1**.

## Transient Transfection

PC12 cells were plated on PLL-coated culture plates in growth medium at 16 h before the transfection. One hundred nanomole miRNAs (Invitrogen) were transfected into PC12 cells using Lipofectamine 2000 Reagent (Invitrogen) according to the manufacturer's instruction. Immediately after isolated from the embryo cortexes, primary cortical neurons were transfected with the miRNAs using Neon™ MPK 5000S Transfection system (Invitrogen) according to the manufacturer's protocol. The transfected neurons were plated on PLL-coated plates and cultured for 7 days before different treatments.

**TABLE 1 | Sequence of the primers used for real-time PCR**.

| Primer/probe | Sequence |
|---|---|
| Has miR-R | 5′-GTGCGTGTCGTGGAGTC-3′ |
| snRNAU6-F | 5′-GCTTCGGCAGCACATATACTAAAAT-3′ |
| snRNAU6-R | 5′-CGCTTCACGAATTTGCGTGTCAT-3′ |
| miR-99b-5p-F | 5′-CACCCGTAGAACCGACCTT-3′ |
| miR-99b-5p-R | 5′-GTCGTATCCAGTGCGTGTCGTGGAGTCGGCAATTGC ACTGGATACGACCGCAAGG-3′ |
| miR-100-5p-F | 5′-AAGAGAACCCGTAGATCCG-3′ |
| miR-100-5p-R | 5′-GTCGTATCCAGTGCGTGTCGTGGAGTCGGCAATTGC ACTGGATACGACCACAAG-3′ |
| MsGAPDH-F | 5′-AACTTTGGCATTGTGGAAGG-3′ |
| MsGAPDH-R | 5′-AACTTTGGCATTGTGGAAGG-3′ |
| RatGAPDH-F | 5′-TGTGAACGGATTTGGCCGTA-3′ |
| RatGAPDH-R | 5′-TGTGAACGGATTTGGCCGTA-3′ |
| mTOR-F | 5′-CTTCTTCCGTTCTATCTCCTT-3′ |
| mTOR-R | 5′-CTTCTTCCGTTCTATCTCCTT-3′ |
| Mmu-miR-486-F | 5′-ACCGTCCTGTACTGAGCT-3′ |
| Mmu-miR-486-R | 5′-GTCGTATCCAGTGCGTGTCGTGGAGTCGGCAATTGC ACTGGATACGACCTCGGG-3′ |
| Cel-miR-238-F | 5′-AGCCTTTGTACTCCGATGC-3′ |
| Cel-miR-238-R | 5′-GTCGTATCCAGTGCGTGTCGTGGAGTCGGCAATTGC ACTGGATACGACTCTGAA-3′ |
| miR-99b-5p probe | 5′-CACTGGATACGACCGCAAGGTCG-3′ |
| miR-100-5p probe | 5′-CACTGGATACGACCACAAGTTCGGT-3′ |

## Western Blot Assay

Brain tissues or cultured cells were lysed in RIPA buffer [150 mM NaCl, 1% (v/v) Nonidet P-40, 0.5% deoxycholic acid, 0.1% (w/v) SDS] containing protease inhibitors (cocktail, Sangon) and 1 mM phenylmethanesulfonyl fluoride (Sigma). The lysate was centrifuged at 4°C, 14,000 rpm for 15 min to get the supernatants. The proteins separated by SDS-PAGE were transferred onto PVDF membranes. GAPDH, β-actin, and mTOR antibodies were used in this study.

## Cell Viability Assays

To evaluated the cell viability, CellTiter 96 AQueous (Promega) was added to PC12 cells or primary cortical neurons at 1/10 volume of the medium. Cells were incubated at 37°C for 4 h. Two hundred microliters of mixed medium was transferred into 96-well ELISA plate. The absorbance was measured at 490 nm using a Microplate reader (BIO-RAD). Cell viability was presented as the percentage of absorbance obtained in control cells.

## Statistical Analysis

Data are represented as mean ± SD. Statistical analysis of the data was performed with Student's *t* test using SPSS 13.0 software. A value of $p < 0.05$(*) was considered statistically significant.

# RESULTS

## miR-99b-5p and miR-100-5p Are Involved in Aβ-Induced Alzheimer's Disease

Our previous study demonstrated that miR-99b-5p/miR-100-5p was upregulated in 9-month-old APP/PS1 mice cortexes

via high-throughput sequencing (Luo et al., 2014). To further explore the association of miR-99b-5p/miR-100 with Aβ-associated pathologies, real-time PCR was performed to determine the expression pattern along the aging progress in six to eight pairs of APP/PS1 and WT mice at each indicated age stage (2-, 4-, 6-, 9-, 12-, and 15-month-old). The expression levels of miR-99b-5p and miR-100-5p were significantly decreased at early stages (6 and 9 months) but increased at late stages (12 and 15 months) of APP/PS1 mice when compared with age-matched WT mice (**Figure 1A**), indicating that miR-99b-5p and miR-100-5p are dynamically regulated and exert their functions in accordance with different stages of brain pathologies induced by Aβ deposition.

In order to verify whether miR-99b-5p and miR-100-5p were detectable in mice plasma and thus could be used as biomarkers for diagnosis of AD, we detected the plasmatic copy numbers of two miRNAs via Taqman probe-based qPCR. After the normalization and calculation by referring to standard curve, we found that APP/PS1 mice showed higher expression levels of miR-99b-5p and miR-100-5p at 2, 4, 6, and 9 months in plasma, but lower at 12 months as well as 15 months (**Figure 1B**). This trend is opposite to the results in cortex tissues, indicating that the biogenesis, circulation, and distribution of miR-99b-5p and miR-100-5p along the development of Aβ-induced pathologies might be regulated by complicated yet sophisticated machinery.

To further investigate the expression pattern of two miRNAs after Aβ-treatment, we also used PC12 cell model. At the early stage of Aβ-treatment (6 h), miR-99b-5p/miR-100-5p levels were declined. Afterwards, the expression of both miRNAs was elevated, especially in the high concentration groups (**Figure 1C**), which is consistent with the data from mice tissues.

## mTOR Is One of the Targets of miR-99b-5p and miR-100-5p in PC12 Cells

In order to shed light on the functionality of miR-99b-5p and miR-100-5p in Aβ-induced pathologies, we predicted the potential

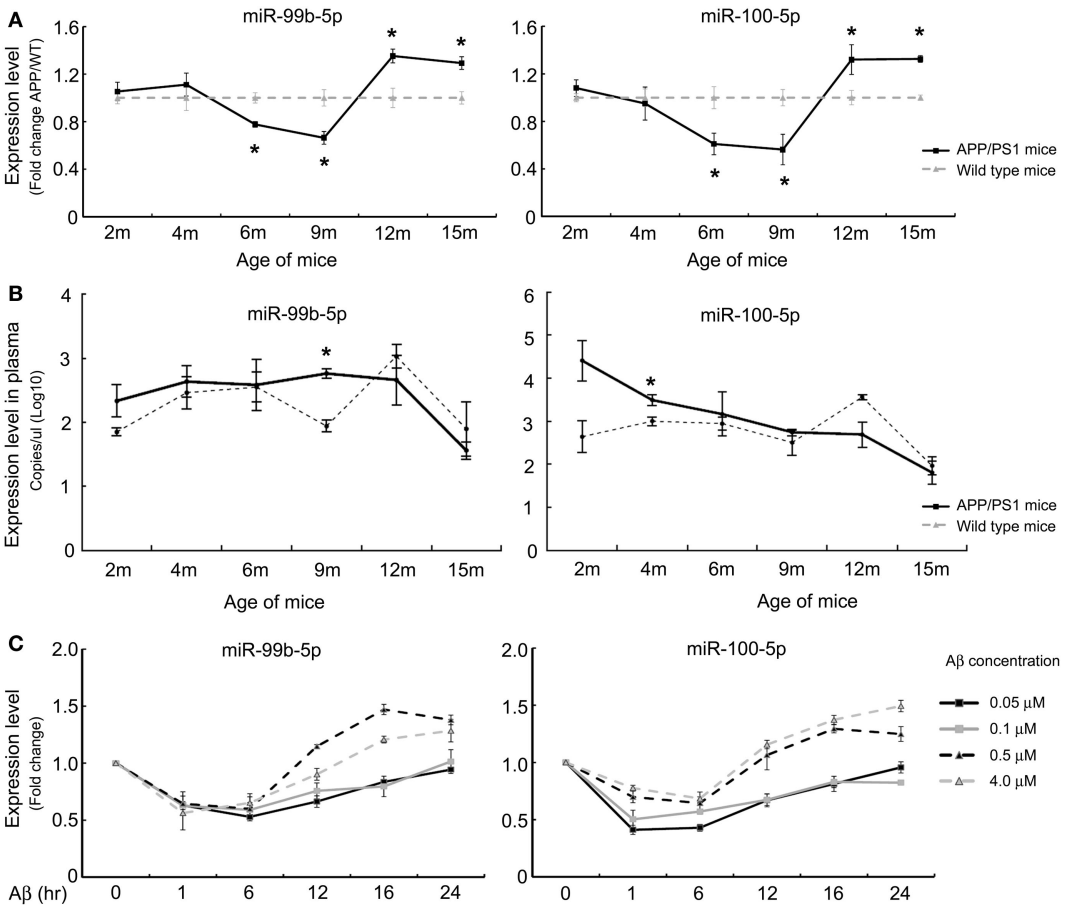


**FIGURE 1 | The expression levels of miR-99b-5p and miR-100-5p in APP/PS1 mice and Aβ-treated PC12 cells**. **(A)** Relative expression levels (presented as fold change) of miR-99b-5p/miR-100-5p were quantified in six to eight pairs of APP/PS1 and WT mice cortexes by real-time PCR. The levels were normalized to the expression of snRNAU6 using the delta–deltaCt methods. **(B)** The absolute copy number of plasma miRNAs were calculated by referring to the standard curve and normalized with the Ct of mmu-miR-486 and cel-miR-238. Data are represented as mean ± SD, results were analyzed with Student's *t* test (*$p < 0.05$, $n = 3$). **(C)** PC12 cells were differentiated for 48 h before the treatments with different concentrations of Aβ1–42 oligomers (0.05, 0.1, 0.5, and 4.0 μM) for various time intervals. Relative expression levels of miR-99b-5p and miR-100-5p are represented as fold change compared to vehicle controls. Data are expressed as mean ± SD and results were analyzed with Student's *t* test [*$p < 0.05$, compared with control ($n = 6$)].

targets of these two miRNAs using three online target prediction databases (miRDB, miRanda, and TargetScan) (Luo et al., 2014). Among the potential targets, mTOR was taken into consideration, which had been proved as one of the major targets of miR-99 family. Overexpression of miR-99b-5p and miR-100-5p dramatically reduced the mRNA and protein levels of mTOR in PC12 cells. In contrast, the miRNAs inhibitors only led to the upregulation effect on mTOR protein level but not mRNA level (**Figures 2A,B**). The expression level of mTOR protein in mice cortexes was also investigated. In 9-month-old APP/PS1 cortexes, mTOR level was higher than that in the age-matched WT mice cortex tissues, whereas it was lower in 12-month-old APP/PS1 cortexes than in the age-matched WT mice cortexes (**Figures 2C,D**). In Aβ-treated PC12 cells, the mTOR expression was also downregulated (**Figure 2E**). The inverse-correlated expression profile of miR-99b-5p/miR-100-5p and mTOR also indicates that miRNAs-regulated mTOR pathway may play different roles during the progression of brain injuries induced by Aβ deposition.

## miR-99b-5p and miR-100 Inhibit Cell Viability of Primary Neurons and PC12 Cells

To determine the role of miR-99b-5p and miR-100-5p in cell viability, we transfected the mimics or inhibitors of miR-99b-5p and miR-100-5p to primary rat cortical neurons or PC12 cells, respectively. Then the cells were treated with Aβ1–42 for 24 h. The viability of primary rat neurons was dramatically decreased when miR-99b-5p or miR-100-5p was overexpressed. On the contrary, cell viability was increased when miR-99b-5p or miR-100-5p was inhibited (**Figure 3A**). In PC12 cells, we also observed the similar results (**Figure 3B**), suggesting that either miR-99b-5p or

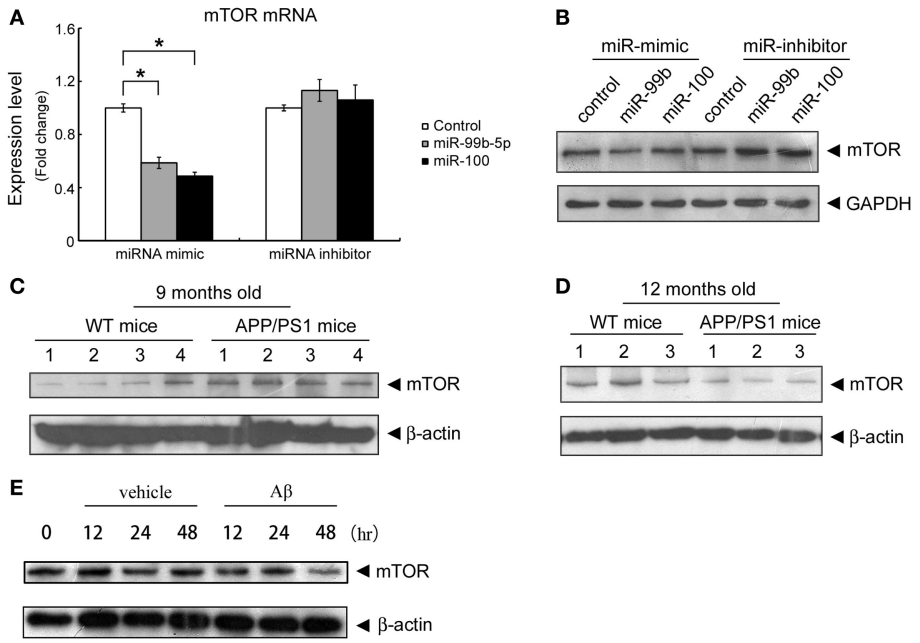


**FIGURE 2 | Both miR-99b-5p and miR-100-5p negatively regulate mTOR expression in PC12 cells as well as in APP/PS1 mice**. **(A,B)** MiR-99b-5p and miR-100-5p mimics or inhibitors were transfected in PC12 cells. mTOR mRNA or protein levels were analyzed by real-time PCR or western blot, respectively. Data are represented as mean ± SD and results were analyzed with Student's *t* test (*$p < 0.05$, $n = 4$). **(C,D)** Western blot analysis of mTOR protein level in cortex tissues from 9 and 12 months old APP/PS1 and WT mice. The housekeeping gene β-actin was taken as the internal reference. **(E)** Western blot of mTOR expression in PC12 at 0, 12, 24, and 48 h after the treatment of Aβ1-42.

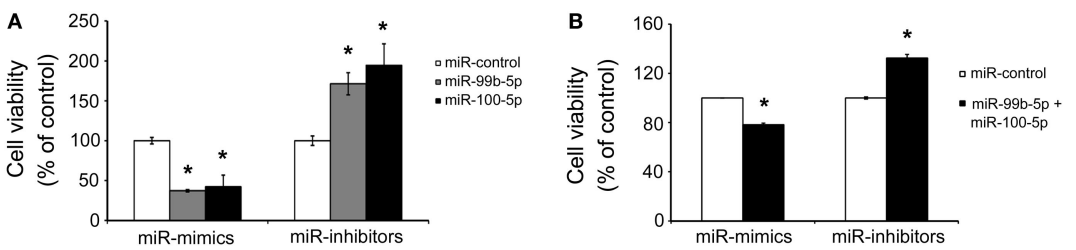


**FIGURE 3 | MiR-99b-5p and miR-100-5p reduce cell viability**. **(A)** Cell viability assay in primary neurons with the transfection of miR-99b-5p/miR-100-5p mimics or inhibitors. **(B)** Co-transfection of miR-99b-5p and miR-100-5p mimics or inhibitors varied the cell viability in PC12 cells. Data are represented as mean ± SD; $n = 3$. Results were analyzed with Student's *t* test (*$p < 0.05$).

miR-100-5p can further promote the neuronal cell death induced by Aβ1–42.

## The Expression Change of miR-99b-5p and miR-100-5p Induced by Aβ is Related to ER Stress

To determine whether the dynamic change of miR-99b-5p and miR-100-5p is related to Aβ-induced ER stress, we induced ER stress by TG in differentiated PC12 cells. Similar to Aβ treatment, TG also induced the decrease of two miRNAs at early stage but increase at late stage (**Figure 4A**). When we used ER stress inhibitor PBA to treat PC12 cells together with Aβ, the levels of miR-99b-5p and miR-100-5p after Aβ treatment were further upregulated (**Figure 4B**).

# DISCUSSION

Many studies have showed the importance of mTOR signaling in brain. Neurons utilize mTOR to modulate multiple brain functions, including regulation of feeding, synaptic plasticity, and memory formation (Garelick and Kennedy, 2011). The cross talk of mTOR pathway with other signaling pathways has been indicated in autophagy, Aβ clearance, and AD development (Godoy et al., 2014). It has been demonstrated that the miR-99 can repress three targets: mTOR, SMARCA5 (SWI/SNF-related, matrix-associated, actin-dependent regulator of chromatin, subfamily a, member 5), and SMARCD1 (SWI/SNF-related, matrix-associated, actin-dependent regulator of chromatin, subfamily d, member 1) (Sun et al., 2011). mTOR, PLK1 (Polo-like kinase 1), FKBP51 (FK506 binding protein 51), IGF1R (insulin-like growth factor 1 receptor), IGF2 (insulin-like growth factor 2), and HOXA1 (homeobox A1) have been proved as the target genes of miR-100 (Nagaraja et al., 2010; Li et al., 2011, 2013; Gebeshuber and Martinez, 2013; Xu et al., 2013; Xiao et al., 2014). Here, mTOR is a common target of miR-99 and miR-100, and it is also a pivotal molecule involved in neurodegenerative diseases. To date, the functional role of mTOR in AD development is still enigmatic. However, several studies have suggested that inhibition of mTOR by rapamycin improves cognitive deficits and rescues Aβ pathology and NFTs through increased autophagy (Caccamo et al., 2010; Santos et al., 2011; Cai et al., 2012). In our study, we found that mTOR level was decreased at late stages of Aβ deposition mouse model cortexes. It is worthwhile to scrutinize whether mTOR plays positive roles in preventing neuronal death as early onset of Aβ deposition, and downregulation of mTOR at late stage ultimately leads to apoptosis of neuronal cells.

MicroRNA-99 family was found to be deregulated in different cancer types (Zhang et al., 2009; Doghman et al., 2010; Sun et al., 2011; Chen et al., 2012; Zheng et al., 2012; Jin et al., 2013; Mueller et al., 2013), but the role of miR-99 family in neuronal cell differentiation or cell death is not clear. Recently, Denk et al. (2015) found that miR-100 in cerebrospinal fluid (CSF) from AD patients could serve as one of the reliable biomarkers to detect AD. In this study, we chose APP/PS1 mice to explore the link between miR-99b-5p/miR-100-5p and Aβ-induced pathological development. Interestingly, the expression levels of miR-99b-5p and miR-100 in APP/PS1 mice brains were decreased at early stages (6–9 months old) and increased at late stages (12–15 months old) when compared with age-matched WT mice. This result suggests that miR-99b-5p/miR-100-5p play distinct roles during different stages of Aβ deposition-induced brain pathologies. To explain the underlying mechanism that orchestrates dynamic change of two miRNAs during the progression of Aβ-associated pathologies, we speculated ER stress as the regulator of the two miRNAs.

ER stress is triggered by the loss of homeostasis in the ER, leading to the accumulation of misfolded proteins within the ER lumen. Aβ was found to induce mild ER stress (Chafekar et al., 2007). We hypothesized that the change of miR-99b-5p/100-5p induced by Aβ was through ER stress induction, and we confirmed it by both activator and inhibitor of ER stress. The unfolded protein response (UPR) is a highly conserved stress response, functioning as a short-term adaptive mechanism to reduce unfolded protein levels and restore balance to the ER. However, if the UPR is insufficient to clear the unfolded proteins, another pathway, CHOP pathway, is activated, and ER stress-induced cell death occurs (Logue et al., 2013). APP and its processing products were found to have potential role in UPR (Endres and Reinhardt, 2013). Aβ can induce ER stress in both cultured neurons and animal models (Lee et al., 2010; Costa et al., 2013; Kondo et al., 2013). In our APP/PS1 mice, we could detect ER stress markers (PERK, eIF2α, and CHOP) at different stages, which were correlated with the change of miRNAs (data not shown). At UPR stages (6–9 months), the levels of miR-99b-5p/miR-100-5p

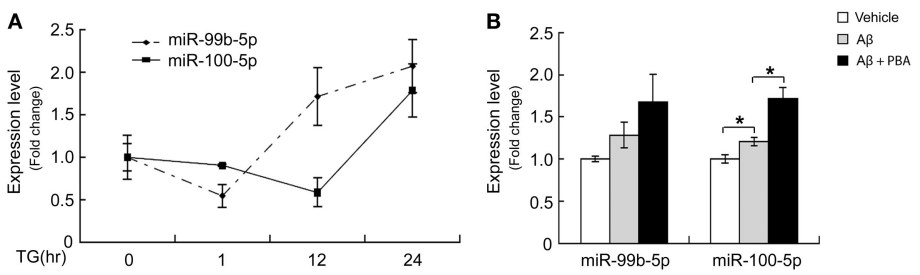


**FIGURE 4 | ER stress regulates miR-99b-5p and miR-100-5p**. **(A)** NGF-differentiated PC12 cells were treated with TG (500 nM) for different time intervals as indicated. Total RNA was extracted. MiR-99b-5p and miR-100-5p were half-quantified by real-time PCR. **(B)** Aβ was treated to differentiated PC12 cells with or without PBA for 24 h, and the qRT-PCR was performed as **(A)**. Data are expressed as mean ± SD and results were analyzed with Student's *t* test (*$p < 0.05$).

were decreased, which were beneficial for neuron survival and synaptic plasticity. However, at late stages, due to long exposure to Aβ, the ER stress-induced death signaling was activated, and two miRNAs were increased to induce neuronal apoptosis. Three signaling pathways, IRE1α, PERK, and ATF6 pathways, modulate UPR upon ER stress induction. The downstream signals of all three pathways regulate the transcription of their target genes. We hypothesized that miR-99b-5p/miR-100-5p might also be one of the target genes. However, we still need more studies to verify our hypothesis.

Taken together, increasing evidences suggest that mTOR pathway may be a critical regulator of Aβ-associated pathologies. Our findings about the dynamic alteration of miR-99b-5p/100-5p-mTOR pathway during the progression of Aβ injuries provide further insight toward our understanding of Aβ-related AD pathogenesis. Recently, many scientists in the field are taking effort to look for new biomarkers for AD diagnosis, and circulating miRNAs have been regarded as promising and feasible approach in clinical. In our study, we also investigated the expression levels of miR-99b-5p/100-5p in the plasma of APP/PS1 mice. The differences of their levels between APP/PS1 and WT mice were not significant at some stages. It might be due to the small sample size included in our study. However, we still saw an interesting trend that plasma miRNA levels were inversely correlated with that of cortexes. Further investigations on animal models as well as AD patients are needed to address the underlying mechanism of how the pathological progression of AD in central nervous system affects the copy numbers of miRNAs in peripheral plasma in order to provide novel insights into non-invasive diagnostic methodology for AD.

## AUTHOR CONTRIBUTIONS

XY, HL, ZW, JM, and JW conceived and designed the experiments. XY, HL, YC, QW, YX, JZ, and YD performed the experiments. XY, HL, YC, ZW, JM, and JW analyzed the data. XY, YC, JM, and JW wrote the paper.

## ACKNOWLEDGMENTS

We would like to thank the Shenzhen Biomedical Research Support Platform and the Shenzhen Molecular Diagnostic Platform of Dermatology for technical help.

## FUNDING

This work was supported by National Basic Research Program of China (973 Program) Grant 2014CB910204; by National Natural Scientific Foundation of China (Grant No. 81171017, 81300922 and 81571043); by Innovation Science and Technology Commission of Shenzhen Municipality for Peacock Plan Research Grant (Grant No. KQC201105300001A). The funders had no contribution in study design, data collection and analysis, decision to publish, or preparation of the manuscript.

## REFERENCES

Ambros, V. (2004). The functions of animal microRNAs. *Nature* 431, 350–355. doi:10.1038/nature02871

Ardekani, A. M., and Naeini, M. M. (2010). The role of microRNAs in human diseases. *Avicenna J. Med. Biotechnol.* 2, 161–179. doi:10.1007/978-1-62703-748-8_3

Ballard, C., Hanney, M. L., Theodoulou, M., Douglas, S., McShane, R., Kossakowski, K., et al. (2009). The dementia antipsychotic withdrawal trial (DART-AD): long-term follow-up of a randomised placebo-controlled trial. *Lancet Neurol.* 8, 151–157. doi:10.1016/S1474-4422(08)70295-3

Borchelt, D. R., Davis, J., Fischer, M., Lee, M. K., Slunt, H. H., Ratovitsky, T., et al. (1996). A vector for expressing foreign genes in the brains and hearts of transgenic mice. *Genet. Anal.* 13, 159–163. doi:10.1016/S1050-3862(96)00167-2

Caccamo, A., Majumder, S., Richardson, A., Strong, R., and Oddo, S. (2010). Molecular interplay between mammalian target of rapamycin (mTOR), amyloid-beta, and Tau: effects on cognitive impairments. *J. Biol. Chem.* 285, 13107–13120. doi:10.1074/jbc.M110.100420

Cai, Z., Zhao, B., Li, K., Zhang, L., Li, C., Quazi, S. H., et al. (2012). Mammalian target of rapamycin: a valid therapeutic target through the autophagy pathway for Alzheimer's disease? *J. Neurosci. Res.* 90, 1105–1118. doi:10.1002/jnr.23011

Chafekar, S. M., Hoozemans, J. J., Zwart, R., Baas, F., and Scheper, W. (2007). Abeta 1-42 induces mild endoplasmic reticulum stress in an aggregation state-dependent manner. *Antioxid. Redox Signal.* 9, 2245–2254. doi:10.1089/ars.2007.1797

Chen, L., Xu, B., Liu, L., Luo, Y., Yin, J., Zhou, H., et al. (2010). Hydrogen peroxide inhibits mTOR signaling by activation of AMPKalpha leading to apoptosis of neuronal cells. *Lab. Invest.* 90, 762–773. doi:10.1038/labinvest.2010.36

Chen, Z., Jin, Y., Yu, D., Wang, A., Mahjabeen, I., Wang, C., et al. (2012). Down-regulation of the microRNA-99 family members in head and neck squamous cell carcinoma. *Oral Oncol.* 48, 686–691. doi:10.1016/j.oraloncology.2012.02.020

Cheng, L. C., Pastrana, E., Tavazoie, M., and Doetsch, F. (2009). miR-124 regulates adult neurogenesis in the subventricular zone stem cell niche. *Nat. Neurosci.* 12, 399–408. doi:10.1038/nn.2294

Costa, R. O., Ferreiro, E., Oliveira, C. R., and Pereira, C. M. (2013). Inhibition of mitochondrial cytochrome c oxidase potentiates Abeta-induced ER stress and cell death in cortical neurons. *Mol. Cell. Neurosci.* 52, 1–8. doi:10.1016/j.mcn.2012.09.005

Denk, J., Boelmans, K., Siegismund, C., Lassner, D., Arlt, S., and Jahn, H. (2015). MicroRNA profiling of CSF reveals potential biomarkers to detect Alzheimer's disease. *PLoS ONE* 10:e0126423. doi:10.1371/journal.pone.0126423

Doghman, M., El Wakil, A., Cardinaud, B., Thomas, E., Wang, J., Zhao, W., et al. (2010). Regulation of insulin-like growth factor-mammalian target of rapamycin signaling by microRNA in childhood adrenocortical tumors. *Cancer Res.* 70, 4666–4675. doi:10.1158/0008-5472.CAN-09-3970

Endres, K., and Reinhardt, S. (2013). ER-stress in Alzheimer's disease: turning the scale? *Am. J. Neurodegener. Dis.* 2, 247–265.

Garelick, M. G., and Kennedy, B. K. (2011). TOR on the brain. *Exp. Gerontol.* 46, 155–163. doi:10.1016/j.exger.2010.08.030

Gebeshuber, C. A., and Martinez, J. (2013). miR-100 suppresses IGF2 and inhibits breast tumorigenesis by interfering with proliferation and survival signaling. *Oncogene* 32, 3306–3310. doi:10.1038/onc.2012.372

Godoy, J. A., Rios, J. A., Zolezzi, J. M., Braidy, N., and Inestrosa, N. C. (2014). Signaling pathway cross talk in Alzheimer's disease. *Cell Commun. Signal.* 12, 23. doi:10.1186/1478-811X-12-23

Hassan, B., Akcakanat, A., Holder, A. M., and Meric-Bernstam, F. (2013). Targeting the PI3-kinase/Akt/mTOR signaling pathway. *Surg. Oncol. Clin. N. Am.* 22, 641–664. doi:10.1016/j.soc.2013.06.008

Heras-Sandoval, D., Perez-Rojas, J. M., Hernandez-Damian, J., and Pedraza-Chaverri, J. (2014). The role of PI3K/AKT/mTOR pathway in the modulation of autophagy and the clearance of protein aggregates in neurodegeneration. *Cell. Signal.* 26, 2694–2701. doi:10.1016/j.cellsig.2014.08.019

Hoeffer, C. A., and Klann, E. (2010). mTOR signaling: at the crossroads of plasticity, memory and disease. *Trends Neurosci.* 33, 67–75. doi:10.1016/j.tins.2009.11.003

Jaworski, J., Spangler, S., Seeburg, D. P., Hoogenraad, C. C., and Sheng, M. (2005). Control of dendritic arborization by the phosphoinositide-3'-kinase-Akt-mammalian target of rapamycin pathway. *J. Neurosci.* 25, 11300–11312. doi:10.1523/JNEUROSCI.2270-05.2005

Jin, Y., Tymen, S. D., Chen, D., Fang, Z. J., Zhao, Y., Dragas, D., et al. (2013). MicroRNA-99 family targets AKT/mTOR signaling pathway in dermal wound healing. *PLoS ONE* 8:e64434. doi:10.1371/journal.pone.0064434

Kim, J., Inoue, K., Ishii, J., Vanti, W. B., Voronov, S. V., Murchison, E., et al. (2007). A microRNA feedback circuit in midbrain dopamine neurons. *Science* 317, 1220–1224. doi:10.1126/science.1140481

Kocerha, J., Kauppinen, S., and Wahlestedt, C. (2009). microRNAs in CNS disorders. *Neuromolecular Med.* 11, 162–172. doi:10.1007/s12017-009-8066-1

Kondo, T., Asai, M., Tsukita, K., Kutoku, Y., Ohsawa, Y., Sunada, Y., et al. (2013). Modeling Alzheimer's disease with iPSCs reveals stress phenotypes associated with intracellular Abeta and differential drug responsiveness. *Cell Stem Cell* 12, 487–496. doi:10.1016/j.stem.2013.01.009

Kurosinski, P., and Gotz, J. (2002). Glial cells under physiologic and pathologic conditions. *Arch. Neurol.* 59, 1524–1528. doi:10.1001/archneur.59.10.1524

Lee, J. H., Won, S. M., Suh, J., Son, S. J., Moon, G. J., Park, U. J., et al. (2010). Induction of the unfolded protein response and cell death pathway in Alzheimer's disease, but not in aged Tg2576 mice. *Exp. Mol. Med.* 42, 386–394. doi:10.3858/emm.2010.42.5.040

Li, B. H., Zhou, J. S., Ye, F., Cheng, X. D., Zhou, C. Y., Lu, W. G., et al. (2011). Reduced miR-100 expression in cervical cancer and precursors and its carcinogenic effect through targeting PLK1 protein. *Eur. J. Cancer* 47, 2166–2174. doi:10.1016/j.ejca.2011.04.037

Li, X. J., Luo, X. Q., Han, B. W., Duan, F. T., Wei, P. P., and Chen, Y. Q. (2013). MicroRNA-100/99a, deregulated in acute lymphoblastic leukaemia, suppress proliferation and promote apoptosis by regulating the FKBP51 and IGF1R/mTOR signalling pathways. *Br. J. Cancer* 109, 2189–2198. doi:10.1038/bjc.2013.562

Logue, S. E., Cleary, P., Saveljeva, S., and Samali, A. (2013). New directions in ER stress-induced cell death. *Apoptosis* 18, 537–546. doi:10.1007/s10495-013-0818-6

Luo, H., Wu, Q., Ye, X., Xiong, Y., Zhu, J., Xu, J., et al. (2014). Genome-wide analysis of miRNA signature in the APPswe/PS1DeltaE9 mouse model of Alzheimer's disease. *PLoS ONE* 9:e101725. doi:10.1371/journal.pone.0101725

Ma, T., Hoeffer, C. A., Capetillo-Zarate, E., Yu, F., Wong, H., Lin, M. T., et al. (2010). Dysregulation of the mTOR pathway mediates impairment of synaptic plasticity in a mouse model of Alzheimer's disease. *PLoS ONE* 5:e12845. doi:10.1371/journal.pone.0012845

Magill, S. T., Cambronne, X. A., Luikart, B. W., Lioy, D. T., Leighton, B. H., Westbrook, G. L., et al. (2010). microRNA-132 regulates dendritic growth and arborization of newborn neurons in the adult hippocampus. *Proc. Natl. Acad. Sci. U.S.A.* 107, 20382–20387. doi:10.1073/pnas.1015691107

Maiese, K., Chong, Z. Z., Shang, Y. C., and Wang, S. (2013). mTOR: on target for novel therapeutic strategies in the nervous system. *Trends Mol. Med.* 19, 51–60. doi:10.1016/j.molmed.2012.11.001

Mueller, A. C., Sun, D., and Dutta, A. (2013). The miR-99 family regulates the DNA damage response through its target SNF2H. *Oncogene* 32, 1164–1172. doi:10.1038/onc.2012.131

Murphy, M. P., and LeVine, H. III (2010). Alzheimer's disease and the amyloid-beta peptide. *J. Alzheimers Dis.* 19, 311–323. doi:10.3233/JAD-2010-1221

Nagaraja, A. K., Creighton, C. J., Yu, Z., Zhu, H., Gunaratne, P. H., Reid, J. G., et al. (2010). A link between mir-100 and FRAP1/mTOR in clear cell ovarian cancer. *Mol. Endocrinol.* 24, 447–463. doi:10.1210/me.2009-0295

Nunez-Iglesias, J., Liu, C. C., Morgan, T. E., Finch, C. E., and Zhou, X. J. (2010). Joint genome-wide profiling of miRNA and mRNA expression in Alzheimer's disease cortex reveals altered miRNA regulation. *PLoS ONE* 5:e8898. doi:10.1371/journal.pone.0008898

Paccalin, M., Pain-Barc, S., Pluchon, C., Paul, C., Besson, M. N., Carret-Rebillat, A. S., et al. (2006). Activated mTOR and PKR kinases in lymphocytes correlate with memory and cognitive decline in Alzheimer's disease. *Dement. Geriatr. Cogn. Disord.* 22, 320–326. doi:10.1159/000095562

Santos, R. X., Correia, S. C., Cardoso, S., Carvalho, C., Santos, M. S., and Moreira, P. I. (2011). Effects of rapamycin and TOR on aging and memory: implications for Alzheimer's disease. *J. Neurochem.* 117, 927–936. doi:10.1111/j.1471-4159.2011.07262.x

Schonrock, N., Matamales, M., Ittner, L. M., and Gotz, J. (2012). MicroRNA networks surrounding APP and amyloid-beta metabolism – implications for Alzheimer's disease. *Exp. Neurol.* 235, 447–454. doi:10.1016/j.expneurol.2011.11.013

Schratt, G. (2009). MicroRNAs at the synapse. *Nat. Rev. Neurosci.* 10, 842–849. doi:10.1038/nrn2763

Schratt, G. M., Tuebing, F., Nigh, E. A., Kane, C. G., Sabatini, M. E., Kiebler, M., et al. (2006). A brain-specific microRNA regulates dendritic spine development. *Nature* 439, 283–289. doi:10.1038/nature04367

Shioya, M., Obayashi, S., Tabunoki, H., Arima, K., Saito, Y., Ishida, T., et al. (2010). Aberrant microRNA expression in the brains of neurodegenerative diseases: miR-29a decreased in Alzheimer disease brains targets neurone navigator 3. *Neuropathol. Appl. Neurobiol.* 36, 320–330. doi:10.1111/j.1365-2990.2010.01076.x

Sun, D., Lee, Y. S., Malhotra, A., Kim, H. K., Matecic, M., Evans, C., et al. (2011). miR-99 family of MicroRNAs suppresses the expression of prostate-specific antigen and prostate cancer cell proliferation. *Cancer Res.* 71, 1313–1324. doi:10.1158/0008-5472.CAN-10-1031

Trigka, E. A., Levidou, G., Saetta, A. A., Chatziandreou, I., Tomos, P., Thalassinos, N., et al. (2013). A detailed immunohistochemical analysis of the PI3K/AKT/mTOR pathway in lung cancer: correlation with PIK3CA, AKT1, K-RAS or PTEN mutational status and clinicopathological features. *Oncol. Rep.* 30, 623–636. doi:10.3892/or.2013.2512

Tufekci, K. U., Oner, M. G., Meuwissen, R. L., and Genc, S. (2014). The role of microRNAs in human diseases. *Methods Mol. Biol.* 1107, 33–50. doi:10.1007/978-1-62703-748-8_3

Wan, J., Cheung, A. Y., Fu, W. Y., Wu, C., Zhang, M., Mobley, W. C., et al. (2008). Endophilin B1 as a novel regulator of nerve growth factor/TrkA trafficking and neurite outgrowth. *J. Neurosci.* 28, 9002–9012. doi:10.1523/JNEUROSCI.0767-08.2008

Wang, Y., Zhao, X., Ye, X., Luo, H., Zhao, T., Diao, Y., et al. (2015). Plasma microRNA-586 is a new biomarker for acute graft-versus-host disease. *Ann. Hematol.* 94, 1505–1514. doi:10.1007/s00277-015-2414-z

Xiao, F., Bai, Y., Chen, Z., Li, Y., Luo, L., Huang, J., et al. (2014). Downregulation of HOXA1 gene affects small cell lung cancer cell survival and chemoresistance under the regulation of miR-100. *Eur. J. Cancer* 50, 1541–1554. doi:10.1016/j.ejca.2014.01.024

Xu, C., Zeng, Q., Xu, W., Jiao, L., Chen, Y., Zhang, Z., et al. (2013). miRNA-100 inhibits human bladder urothelial carcinogenesis by directly targeting mTOR. *Mol. Cancer Ther.* 12, 207–219. doi:10.1158/1535-7163.MCT-12-0273

Zhang, H., Luo, X. Q., Zhang, P., Huang, L. B., Zheng, Y. S., Wu, J., et al. (2009). MicroRNA patterns associated with clinical prognostic parameters and CNS relapse prediction in pediatric acute leukemia. *PLoS ONE* 4:e7826. doi:10.1371/journal.pone.0007826

Zhao, C., Sun, G., Li, S., Lang, M. F., Yang, S., Li, W., et al. (2010). MicroRNA let-7b regulates neural stem cell proliferation and differentiation by targeting nuclear receptor TLX signaling. *Proc. Natl. Acad. Sci. U.S.A.* 107, 1876–1881. doi:10.1073/pnas.0908750107

Zheng, Y. S., Zhang, H., Zhang, X. J., Feng, D. D., Luo, X. Q., Zeng, C. W., et al. (2012). MiR-100 regulates cell differentiation and survival by targeting RBSP3, a phosphatase-like tumor suppressor in acute myeloid leukemia. *Oncogene* 31, 80–92. doi:10.1038/onc.2011.208

**Conflict of Interest Statement:** The authors declare that the research was conducted in the absence of any commercial or financial relationships that could be construed as a potential conflict of interest.

frontiers in Aging Neuroscience

MINI REVIEW
published: 08 July 2016
doi: 10.3389/fnagi.2016.00172

# Review of Sparse Representation-Based Classification Methods on EEG Signal Processing for Epilepsy Detection, Brain-Computer Interface and Cognitive Impairment

*Dong Wen*[1,2], *Peilei Jia*[1,2], *Qiusheng Lian*[1,2], *Yanhong Zhou*[3]* and *Chengbiao Lu*[4]*

[1] School of Information Science and Engineering, Yanshan University, Qinhuangdao, China, [2] The Key Laboratory for Computer Virtual Technology and System Integration of Hebei Province, Yanshan University, Qinhuangdao, China, [3] School of Mathematics and Information Science and Technology, Hebei Normal University of Science and Technology, Qinhuangdao, China, [4] School of Basic Medicine, Xinxiang Medical University, Xinxiang, China

At present, the sparse representation-based classification (SRC) has become an important approach in electroencephalograph (EEG) signal analysis, by which the data is sparsely represented on the basis of a fixed dictionary or learned dictionary and classified based on the reconstruction criteria. SRC methods have been used to analyze the EEG signals of epilepsy, cognitive impairment and brain computer interface (BCI), which made rapid progress including the improvement in computational accuracy, efficiency and robustness. However, these methods have deficiencies in real-time performance, generalization ability and the dependence of labeled sample in the analysis of the EEG signals. This mini review described the advantages and disadvantages of the SRC methods in the EEG signal analysis with the expectation that these methods can provide the better tools for analyzing EEG signals.

**Keywords: sparse representation-based classification, sparse representation, EEG signal, preclinical mild cognitive impairment, mild cognitive impairment, Alzheimer's disease, epilepsy, brain computer interface**

OPEN ACCESS

***Edited by:***
*Junfeng Sun,*
*Shanghai Jiao Tong University, China*

***Reviewed by:***
*Ramesh Kandimalla,*
*Emory University, USA*
*Wanzeng Kong,*
*Hangzhou Dianzi University, China*

***Correspondence:**
*Yanhong Zhou*
*zhouyanhong_02@126.com*
*Chengbiao Lu*
*johnlu9000@hotmail.com*

***Received:*** *20 January 2016*
***Accepted:*** *28 June 2016*
***Published:*** *08 July 2016*

***Citation:***
*Wen D, Jia P, Lian Q, Zhou Y and Lu C (2016) Review of Sparse Representation-Based Classification Methods on EEG Signal Processing for Epilepsy Detection, Brain-Computer Interface and Cognitive Impairment. Front. Aging Neurosci. 8:172. doi: 10.3389/fnagi.2016.00172*

## INTRODUCTION

Sparse representation (SR) is used to represent data with as few atoms as possible in a given overcomplete dictionary. By using the SR, we can concisely represent the data and easily extract the valuable information from the data. The sparse representation-based classification (SRC) methods have become a research hotspot for the data processing in many fields (Vialatte et al., 2009, 2012; Liu et al., 2012; Kaleem et al., 2013; Shin et al., 2015; Yuan et al., 2015), and can greatly simplify the processing of the multi-dimensional electroencephalograph (EEG) signals from epilepsy, mild cognitive impairment (MCI), Alzheimer's disease (AD) and brain computer interface (BCI).

Currently, studies on SRC methods used in the brain disorders and BCI involve mainly the preprocessing, SR and feature extraction, and have achieved accomplishments in computational accuracy, efficiency and robustness. Preclinical mild cognitive impairment (Pre-MCI) is a cognitive impairment status between normal aging and MCI, and also an earliest status of cognitive impairment which is more difficult to be diagnosed relative to MCI and AD (Sperling et al., 2011; Zhou et al., 2016). With the improvement of computational accuracy and efficiency, SRC methods may have potential to aid the diagnosis of Pre-MCI.

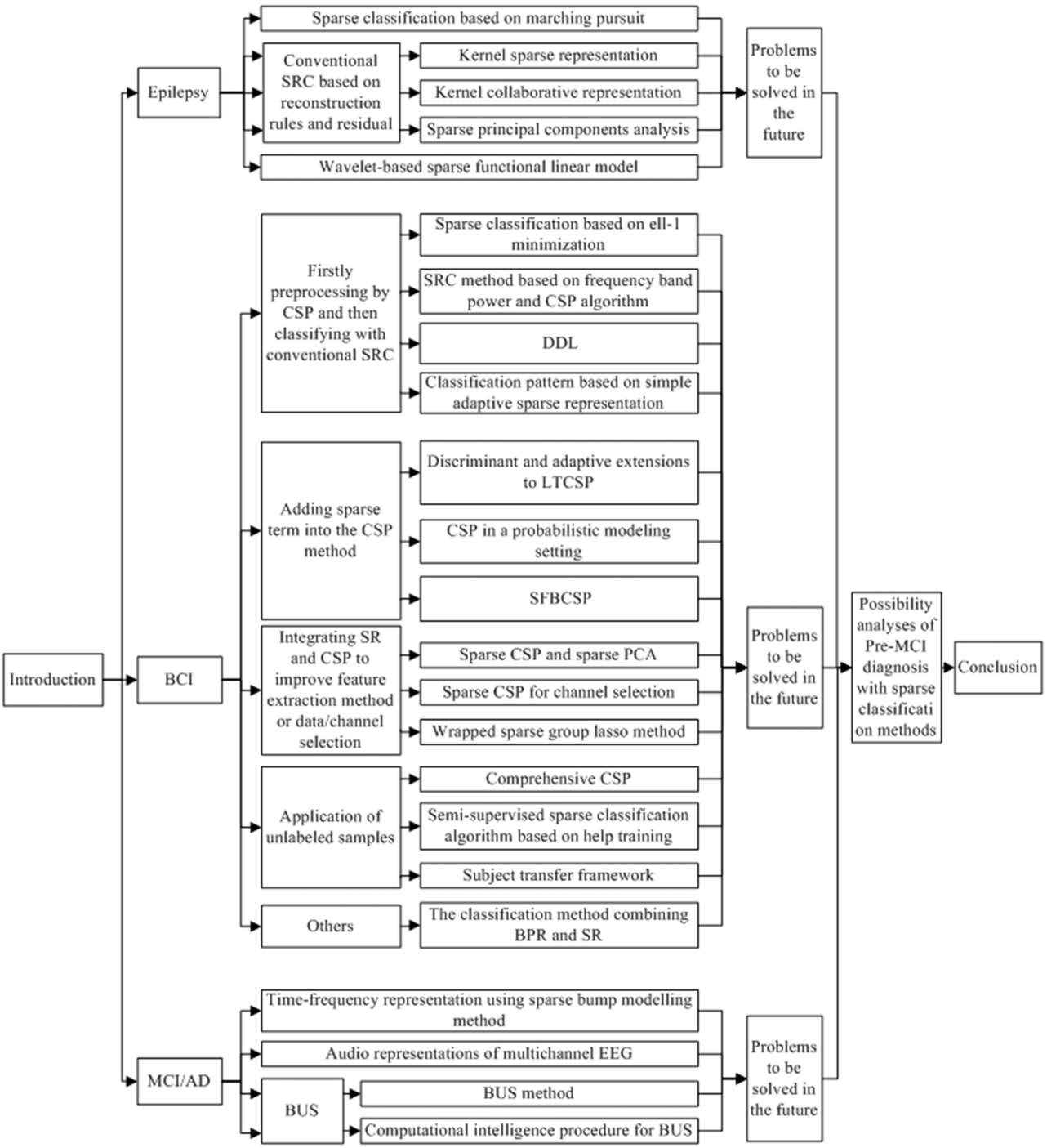


**FIGURE 1 | The frame of the contents in this review.** Abbreviations: SRC, sparse representation-based classification; BCI, brain computer interface; CSP, common spatial patterns; DDL, discriminative dictionary learning; LTCSP, local temporal common spatial patterns; SFBCSP, sparse filter bands common spatial pattern; PCA, principal component analysis; BPR, biomimetic pattern recognition; SR, sparse representation; MCI, mild cognitive impairment; AD, Alzheimer's disease; EEG, electroencephalograph; BUS, bump sonification.

However, there still exist some deficiencies needed to be solved.

This article reviewed the SRC methods in the analysis of EEG signals of epilepsy, MCI, AD and BCI, and discussed the possibility for the application of SRC methods in the diagnosis of Pre-MCI patients. The frame of this article was presented in **Figure 1**, and the main findings were listed in **Table 1**.

**TABLE 1 | Summary of studies for epilepsy, brain computer interface (BCI), mild cognitive impairment (MCI) and Alzheimer's disease (AD) detection using sparse representation-based classification (SRC) methods.**

**(A) Summary of studies for epilepsy detection using SRC**

| Fields | Methods | Literatures | Datasets | Accuracy (%) | Sensitivity (%) | Specificity (%) | Main findings |
|---|---|---|---|---|---|---|---|
| Epilepsy | | Wang and Guo (2011) | | 100 | 100 | 100 | Obtaining the highest accuracy and robust to noise |
| | Sparse classification based on marching pursuit | Guo et al. (2012) | Datasets Z (ictal) and S (healthy) | 100 | – | – | Reducing running time and feature dimension |
| | | Wang et al. (2013) | | 100 | – | – | Enhancing the classification accuracy and the efficiency simultaneously |
| | Kernel sparse representation | Yuan et al. (2014) | Set A (healthy), D (interictal) and E (ictal) | 98.63 ± 2.80 | 98.25 ± 4.37 | 99.00 ± 4.00 | |
| | Kernel collaborative representation | Yuan et al. (2015) | Interictal and ictal iEEG database | 99.99 | 100 | 100 | Avoiding the choice and calculation of EEG features |
| | Sparse principal components analysis | Xie et al. (2012) | Set A,B (healthy) and C,D (interictal) | 99.999 ± 0.0002 | – | – | Focusing on the extraction of signal features with high discrimination power |
| | Wavelet-based sparse functional linear model | Xie and Krishnan (2013) | Set A,B (healthy), C,D (interictal) and E (ictal) | 100 | | | Effective combination of feature extraction and classification methods |
| | | | EEG data from University of Freiburg | 99 | – | – | |

**(B) Summary of studies for BCI using SRC**

| | | | | | | | |
|---|---|---|---|---|---|---|---|
| BCI | Sparse classification based on ell-1 minimization | Shin et al. (2011) | Motor imagery (left and right hand) EEG from four healthy subjects | 91.67 | – | – | SRC based on ell-1 minimization |
| | SRC method based on frequency band power and CSP algorithm | Shin et al. (2012) | INFONET dataset from experiment and Dataset IVa from BCI competition III | 75.75/96.85 | – | – | SRC based on L1 minimization. |
| | | Shin et al. (2013) | Dataset Iva from BCI competition III | 96.85 | – | – | Dictionary based on the CSP filtering and the band power |
| | Discriminative dictionary learning (DDL) | Zhou et al. (2012) | Dataset IVa from BCI competition III | 70.5/94.9 | – | – | Lower computational complexity and higher accuracy than SRC |

*(Continued)*

**TABLE 1 | (Continued).**

| Fields | Methods | Literatures | Datasets | Accuracy (%) | Sensitivity (%) | Specificity (%) | Main findings |
|---|---|---|---|---|---|---|---|
| | Classification pattern based on simple adaptive sparse representation | Shin et al. (2015) | Motor imagery (left and right hand, foot) EEG from 10 healthy subjects and dataset IVc from BCI Competition III | 98.0/96.07 | – | – | Adaptive classification techniques based on sparse representation |
| | Discriminant and adaptive extensions to local temporal common spatial patterns | Wang (2013) | Dataset IVa from BCI competition III and Dataset IIa of BCI competition IV | 98.21/93.75 | – | – | Discriminant extension: combining the between-class and the within-class scatter information. Adaptive extension: defining the weights by utilizing the sparse representation |
| | CSP in a probabilistic modeling setting | Wu et al. (2015) | Dataset IIIa, IVa from BCI competition III | 90.68 ± 9.93 | – | – | Proposing probabilistic CSP (P-CSP) model |
| | Sparse filter bands common spatial pattern | Zhang et al. (2015) | Dataset IVa from BCI competition III and | 92.05 ± 2.45 | | | Automatically selecting the significant filter bands to |
| | | | Dataset IIb from BCI competition IV | 81.17 ± 3.55 | – | – | improve classification performance |
| | Sparse CSP and sparse PC A | Shi et al. (2011) | Dataset IIIa from BCI competition III | 90 | – | – | Sparse subspace learning technique |
| | Sparse CSP for channel selection | Arvaneh et al. (2011) | Dataset IIa from BCI competition IV and | 82.55 ± 12.8 | | | Improving performance in the case of noise |
| | | | Dataset IVa from BCI competition III | 73.5 ± 15.1 | – | – | interference and limited data |
| | | Goksu et al. (2011, 2013) | ECoG dataset of BCI competition 2005 | 90 | – | – | Extension of the greedy search based solution to multiple sparse filters |
| | | Tomida et al. (2015) | Dataset IVa from BCI competition III and Dataset I from BCI competition IV | 87.64/81.25 | – | – | Introducing weighted averaging with weight coefficients rejecting low quality trials |
| | Wrapped sparse group lasso method | Wang et al. (2015) | Dataset I from BCI competition IV | 84.72 | – | – | Simultaneously achieving channel and feature selection with a lower error rate |

*(Continued)*

**TABLE 1 | (Continued).**

| Fields | Methods | Literatures | Datasets | Accuracy (%) | Sensitivity (%) | Specificity (%) | Main findings |
|---|---|---|---|---|---|---|---|
| | Comprehensive CSP | Wang and Xu (2012) | Dataset IVa from BCI competition III and EEG motor movement/ Imagery dataset | 98.2/89.5 | – | – | Contributing a comprehensive CSP (cCSP) that learns on both labeled and unlabeled trials |
| | Semi-supervised sparse classification Jiaetal., algorithm based on 2014 help training | Jia et al. (2014) | Dataset I from BCI competition I and Dataset II-IV from BCI competition II | 97/82 | – | – | Selecting samples with high confidence according to sparse representation classifier |
| | Subject transfer framework | Tu and Sun (2012) | EEG data from the NIPS 2001 BCI workshop | 72.49 | – | – | Reducing the training sessions of the target subject by utilizing samples from other subjects |
| | The classification method combining BPR and SR | Ge and Wu (2012) | Dataset 1: Iva in 2005 BCIC III | 94 | – | – | |
| | | Ren et al. (2014) | Dataset 1: Iva in 2005 BCIC III | 97 | | | Utilizing SR to solve the overlapping coverage problem of BPR |
| | | | Dataset 2: from Tongji University | 82.6 | – | – | |
| | | | Dataset 3: from BCIC III | 88.03 | | | |
| **(C) Summary of studies for MCI/AD detection using SRC** | | | | | | | |
| MCI/AD | Time-frequency representation using sparse bump modeling method | Vialatte et al. (2005a,b) | Healthy control, MCI patients and AD patients | 93 | 86.4 | 97.4 | Compressing nformation contained in EEG time-frequency maps |
| | Bump sonification (BUS) method | Vialatte and Cichocki (2006) | | – | – | – | Perceiving simultaneously every channel, and analyzing more tractably the time dynamics of the signals |
| | Computational intelligence procedure for BUS | Vialatte et al. (2009) | Mildly impaired patients progression towards AD group and Control group | 89 | – | – | Applicating BUS to online sonification |
| | Audio representations of multichannel EEG | Vialatte et al. (2012) | MCI group and Control group | 89 | – | – | Presenting a physiologically inspired method for generating music scores from multi-channel EEG |

# THE EEG SIGNAL ANALYSIS METHODS BASED ON SRC

## Application and Performance Evaluation of SRC in Epilepsy Detection

### Method Description and Evaluation

Currently, there are three perspectives of SRC methods used in epileptic detection, including reconstruction rules and residual error classifications on the whole classification stage, overcomplete dictionary on the preprocessing stage, and wavelet-based sparse functional linear model on the feature extraction stage.

For the first perspective, as the reconstruction rule classifications do not need to extract features or to design a classifier, the applied range of the methods is therefore greatly improved, and is superior than the traditional epilepsy detection methods. Using the classification method based on kernel SR and kernel collaborative representation, the classification accuracy in analyzing the epilepsy EEG signals reached up to 98.63% and 99.99% respectively, and the fast speed in computation can help to monitor epilepsy in real-time (Yuan et al., 2014, 2015).

Using above methods, good performance in classifications were demonstrated between epileptic patients with ictal EEG normal control group, or between epileptic patients with interictal EEG and ictal EEG However, for the classification between epileptic patients with interictal EEG and normal control group, whether these methods can achieve the similar performance remains to be further verified. Recently, using sparse principal components analysis method with reconstruction rules, the performance of classification between epilepsy patients with interictal EEG and normal control group was demonstrated to be excellent (Xie et al., 2012; Xie and Krishnan, 2013).

For the second perspective, Wang and Guo (2011) initially proposed SR based on matching pursuit and selected decomposition coefficients and atom parameters as features. However, the computation complexity was relatively high. To reduce the computation complexity, they then proposed Harmony Search method to find the optimal atom parameters, and selected the decomposition coefficients, FR parameters and restructured error to constitute a feature vector (Guo et al., 2012). By constituting the feature vector using decomposition coefficients, atom parameters and FR parameters, the computing time was further reduced (Wang et al., 2013).

For the third perspective, using wavelet-based sparse functional linear model, the accuracy in classifying epilepsy patients with interictal EEG from normal control group was up to 100% (Xie et al., 2012; Xie and Krishnan, 2013). However, the computation efficiency of feature extraction needs to be improved by using the methods, such as signal decomposition algorithms (Kaleem et al., 2013).

### Problems to be Solved in the Future

A first problem is how to automatically determine the appropriate dictionary size and feature number of overcomplete dictionary. Secondly, the computation speed of SR needs to be improved. The aspects of the improvement may include dictionary learning algorithm and sparse coefficient solution algorithm. Thirdly, the difference between epileptic patients with interictal EEG and normal control group need to be analyzed in depth. It is the main reason why actual performance of different methods can be distinguished only when the difference between two kinds of signals is very small.

## Application and Performance Evaluation of SRC in BCI

### Method Description and Evaluation

Five perspectives of the SRC methods applied in BCI system were presented in this review. The main stream idea of the first three perspectives is to improve the classification performance, the feature extraction and data selection by combining SR with common spatial patterns (CSP). For the fourth perspective, researchers used unlabeled samples to improve the classification performance. As for the fifth perspective, some scholars proposed integrating SR with other traditional classification methods.

For the first perspective, some researchers used CSP and conventional SRC methods for signal preprocessing and classifying, respectively. SRC method based on ell-1 minimization has a classification accuracy of 91.67% (Shin et al., 2011), and the classification accuracy in constructing dictionary reached 96.85% when using the band power feature of signal filtered by CSP (Shin et al., 2012, 2013). However, it is difficult to select the appropriate number of CSP filters, and the computation complexity still needs to be reduced. In view of this, recently proposed discriminative dictionary learning (DDL) improved the classification accuracy and computational efficiency (Zhou et al., 2012). A new classification method based on simple adaptive SR also showed a relatively high classification accuracy (Shin et al., 2015).

For the second perspective, sparse term is often used to improve the performance of the CSP method. Wang (2013) integrated discriminant and adaptive extensions to local temporal CSP, which had better classification accuracy. CSP algorithm was cast in a probabilistic modeling setting to overcome overfitting problem of CSP by using of sparse Bayesian learning (Wu et al., 2015). Sparse filter bands common spatial pattern (SFBCSP) recently proposed by Zhang et al. (2015). showed an improved classification accuracy. However, the determination of the regularization parameter $\lambda$ in SFBCSP is time consuming, and SFBCSP is not suitable for the analysis of the data set with small samples.

For the third perspective, SR and CSP are often integrated to improve the effectiveness of feature extraction or data/channel selection. In respect of feature extraction, the sparse component analysis (SCA) and CSP were utilized to construct a combined feature vector (Li et al., 2005). The sparse CSP and sparse principal component analysis (PCA) were applied to select relevant EEG components and extract EEG features in BCI system, respectively (Shi et al., 2011). However, there exists a

vast improvement space in the classification accuracy of these methods.

The classification performance can be improved according to the selection of different data/channels. A sparsity-aware method was proposed in order to select and remove low-quality trial data (Tomida et al., 2015). When applying L1 regularization term to CSP, Yong et al. (2008) showed that the average number of electrodes was reduced to 11% with a slight decrease of classification accuracy. To ensure the lowest reduction degree of classification performance, the minimal subset of EEG channels was selected for the classification. When L1/L2 norm was combined with CSP, the performance of channel selection algorithm was improved in the case of noise interference and limited data (Arvaneh et al., 2011). A sparse CSP (sCSP) method proposed by Goksu et al. (2011, 2013) showed a low computation complexity. However, the performance may be decreased when the different samples were used or the number of training samples is low.

A wrapped sparse group lasso method to select mixed EEG channel feature is suitable for high dimensional feature fusion. Stability and computing speed in this method were high, but the classification accuracy needs to be improved (Wang et al., 2015). The channel selection methods with CSP likely were trapped in a local minimum due to the non convexity of the optimization problem in CSP, which resulted in a decline in classification accuracy (Goksu et al., 2013).

For the fourth perspective, the less training samples will lead to the generalization performance deterioration caused by over-fitting, and it is easy to obtain unlabeled samples. Therefore, some researchers studied comprehensive learning mode to combine the labeled with unlabeled data, and showed that the classification performance was largely improved compared to the traditional CSP. The comprehensive learning mode includes the comprehensive CSP and semi-supervised SRC algorithm (Wang and Xu, 2012; Jia et al., 2014). A subject transfer framework reduced the training sessions of the target subjects by utilizing samples from other subjects and improved the classification accuracy (Tu and Sun, 2012). However, the computation complexity of this method was high, and the number of samples must be equal, which limited its application in reality.

For the fifth perspective, biomimetic pattern recognition (BPR) and SR were combined to accomplish the task of classification (Ge and Wu, 2012). A new classification method which combined BPR and SR under the semi-supervised co-training framework was recently proposed (Ren et al., 2014). These methods utilized SR to solve the overlapping coverage problem of BPR, and the classification accuracy was greatly increased compared to traditional classification methods. Mixed alternating least squares based on nonnegative matrix factorization were proposed to analyze event-related potential and event related spectral perturbation features. As a consequence, the performance of the algorithm was increased (Sburlea et al., 2015).

### Problems to be Solved in the Future

Some problems remain to be solved in the field of BCI application. On account of channel selection in SRC, it is necessary not only to reduce channels, but also to maintain a high classification rate at the same time. Nevertheless, how to balance both is a challenge. It is still a research focus to determine the appropriate number of spatial filters in order to avoid over-fitting and meet the requirements of sparse coefficient solution. In addition to the principle based on the minimization of the reconstruction error, it is necessary to select new perspectives in the dictionary construction methods.

## Application and Performance Evaluation of SRC in Detection of MCI and AD

### Method Description and Evaluation

There are a few studies about SRC methods for the detection of MCI and AD. Most studies focused on the angle of sparse bump modeling. The classification accuracy was 93% when using the sparse bump modeling method in the analysis of the EEG signal (Vialatte et al., 2005a,b). However, it still needs validation with more datasets. A BUS method (Vialatte and Cichocki, 2006) and a computational intelligence procedure for online sonification were proposed by Vialatte et al. (2009, 2012). The results showed high identification accuracy and also confirmed the potential of these methods to be used in real-time diagnosis. In Vialatte et al. (2011) improved the classification specificity of clinical EEG by means of wavelet transform and sparse bump modeling. However, the application of sparse bump modeling method is limited to the analysis of the events at low frequency bands. And for the reason of using a low pass filter, gamma band activity did not suitable for the analysis in using this method.

### Problems to be Solved in the Future

When utilizing SRC for the analysis of EEG signals from MCI and AD patients, the classification performance of SRC can be improved by using sparse Bayesian learning method to extract coupling and synchronization feature. For the MCI classification, the space sparsity of the brain areas and time sparsity of channel samples need to be considered. Reducing the amount of data participating in the classification by selecting channels will promote the classification performance.

## Application of SRC Methods for the Analysis of EEG Signal of Pre-MCI Patients

Application of SRC method in the analysis of epilepsy, BCI, MCI and AD has achieved considerable achievements, however no relevant research literatures about Pre-MCI diagnosis using SRC methods can be found. We thus proposed to use SRC method for Pre-MCI diagnosis. The small difference in EEG signals between the Pre-MCI patients and normal control group makes the diagnosis of Pre-MCI difficult. However, if the accuracy, sensitivity, specificity and computing speed of SRC methods can be further improved, it is possible that these methods can be used for the diagnosis of the Pre-MCI. As the data dimension of Pre-MCI is high, we need to consider the space sparsity of brain areas and time sparsity of EEG signals of every channel, reduce the amount

of data used in the classification by selecting channels in order to improve classification performance and enhance the effectiveness in the dictionary design, feature extraction and SR.

## CONCLUSION

We evaluated the SRC methods in the analysis of EEG signals from epilepsy, BCI, MCI and AD and illustrated the characteristics, advantages and disadvantages of various methods. The SRC methods have become an effective tool in aiding the diagnosis of brain disorder. Further improving the current SRC methods by such as combining SR with CSP will largely increase the classification accuracy and efficiency as well as sensitivity, making it potential for the application in diagnosis of Pre-MCI.

## AUTHOR CONTRIBUTIONS

DW and YZ designed the study and wrote this article. PJ and QL wrote this article. CL designed the study and revised this article.

## ACKNOWLEDGMENTS

This research was funded in part by National Natural Science Foundation of China (61503326, 81271422), China Postdoctoral Science Foundation (2015M581317), Natural Science Foundation of Hebei Province in China (F2016203343), Doctorial Foundation of Yanshan University in China (B900), Science and Technology Support Programme of Hebei Province in China (13212003), and Test Bank Construction Foundation of Hebei Normal University of Science and Technology in China (JYTK201506).

## REFERENCES

Arvaneh, M., Guan, C., Ang, K. K., and Quek, H. C. (2011). "Spatially sparsed common spatial pattern to improve BCI performance," in *IEEE International Conference on Acoustics, Speech and Signal Processing*, Prague 2412–2415.

Ge, Y., and Wu, Y. (2012). A new hybrid method with biomimetic pattern recognition and sparse representation for EEG classification. *Emerg. Intell. Comput. Technol. Appl.* 304, 212–217. doi: 10.1007/978-3-642-31837-5_31

Goksu, F., Ince, N. F., and Tewfik, A. H. (2011). "Sparse common spatial patterns in brain computer interface applications," in *IEEE International Conference on Acoustics, Speech and Signal Processing*, Prague, 533–536.

Goksu, F., Ince, N. F., and Tewfik, A. H. (2013). Greedy solutions for the construction of sparse spatial and spatio-spectral filters in brain computer interface applications. *Neurocomputing* 108, 69–78. doi: 10.1016/j.neucom.2012.12.003

Guo, P., Wang, J., Gao, X. Z., and Tanskanen, J. (2012). "Epileptic EEG signal classification with marching pursuit based on harmony search method," in *IEEE International Conference on Systems, Man and Cybernetics*, Seoul, 283–288.

Jia, M., Wang, J., Li, J., and Hong, W. (2014). Application of semi-supervised sparse representation classifier based on help training in EEG classification. *Sheng Wu Yi Xue Gong Cheng Xue Za Zhi* 31, 1–6.

Kaleem, M., Guergachi, A., and Krishnan, S. (2013). EEG seizure detection and epilepsy diagnosis using a novel variation of empirical mode decomposition. *Conf. Proc. IEEE Eng. Med. Biol. Soc.* 2013, 4314–4317. doi: 10.1109/EMBC.2013.6610500

Li, Y., Guan, C., and Qin, J. (2005). Enhancing feature extraction with sparse component analysis for brain-computer interface. *Conf. Proc. IEEE Eng. Med. Biol. Soc.* 5, 5335–5338. doi: 10.1109/iembs.2005.1615686

Liu, M., Zhang, D., and Shen, D. (2012). Ensemble sparse classification of Alzheimer's disease. *Neuroimage* 60, 1106–1116. doi: 10.1016/j.neuroimage.2012.01.055

Ren, Y., Wu, Y., and Ge, Y. (2014). A co-training algorithm for EEG classification with biomimetic pattern recognition and sparse representation. *Neurocomputing* 137, 212–222. doi: 10.1016/j.neucom.2013.05.045

Sburlea, A. I., Montesano, L., and Minguez, J. (2015). Continuous detection of the self-initiated walking pre-movement state from EEG correlates without session-to-session recalibration. *J. Neural Eng.* 12:036007. doi: 10.1088/1741-2560/12/3/036007

Shi, L., Li, Y., Sun, R., and Lu, L. (2011). A sparse common spatial pattern algorithm for brain-computer interface. *Neural Inf. Process.* 7062, 725–733. doi: 10.1007/978-3-642-24955-6_86

Shin, Y., Lee, S., Ahn, M., Cho, H., Jun, S. C., and Lee, H. N. (2015). Simple adaptive sparse representation based classification schemes for EEG based brain-computer interface applications. *Comput. Biol. Med.* 66, 29–38. doi: 10.1016/j.compbiomed.2015.08.017

Shin, Y., Lee, S., Ahn, M., Jun, S. C., and Lee, H.-N. (2011). "Motor imagery based BCI classification via sparse representation of EEG signals," in *8th International Symposium on Noninvasive Functional Source Imaging of the Brain and Heart and 2011 8th International Conference on Bioelectromagnetism*, Banff, AB, 93–97.

Shin, Y., Lee, S., Lee, J., and Lee, H. N. (2012). Sparse representation-based classification scheme for motor imagery-based brain-computer interface systems. *J. Neural Eng.* 9:056002. doi: 10.1088/1741-2560/9/5/056002

Shin, Y., Lee, S., Woo, S., and Lee, H.-N. (2013). "Performance increase by using a EEG sparse representation based classification method," in *2013 IEEE International Conference on Consumer Electronics*, Las Vegas, NV, 201–203.

Sperling, R. A., Aisen, P. S., Beckett, L. A., Bennett, D. A., Craft, S., Fagan, A. M., et al. (2011). Toward defining the preclinical stages of Alzheimer's disease: recommendations from the National Institute on Aging-Alzheimer's Association workgroups on diagnostic guidelines for Alzheimer's disease. *Alzheimers Dement.* 7, 280–292. doi: 10.1016/j.jalz.2011.03.003

Tomida, N., Tanaka, T., Ono, S., Yamagishi, M., and Higashi, H. (2015). Active data selection for motor imagery EEG classification. *IEEE Trans. Biomed. Eng.* 62, 458–467. doi: 10.1109/TBME.2014.2358536

Tu, W., and Sun, S. (2012). A subject transfer framework for EEG classification. *Neurocomputing* 82, 109–116. doi: 10.1016/j.neucom.2011.10.024

Vialatte, F. B., and Cichocki, A. (2006). "Sparse bump sonification: a new tool for multichannel EEG diagnosis of mental disorders; application to the detection of the early stage of Alzheimer's disease," in *Neural Information Processing, Lecture Notes in Computer Science*, ed. I. King (Berlin, Heidelberg: Springer), 92–101.

Vialatte, F., Cichocki, A., Dreyfus, G., Musha, T., Rutkowski, T. M., and Gervais, R. (2005a). "Blind source separation and sparse bump modelling of time frequency representation of EEG signals: new tools for early detection of Alzheimer's disease," in *Proceedings of the IEEE Workshop on Machine Learning for Signal Processing* Mystic, CT, 27–32.

Vialatte, F., Cichocki, A., Dreyfus, G., Musha, T., Shishkin, S. L., and Gervais, R. (2005b). Early detection of Alzheimer's disease by blind source separation, time frequency representation and bump modeling of EEG signals. *Biol. Inspirations Artif. Neural Netw.* 3696, 683–692. doi: 10.1007/11550822_106

Vialatte, F. B., Dauwels, J., Musha, T., and Cichocki, A. (2012). Audio representations of multi-channel EEG: a new tool for diagnosis of brain disorders. *Am. J. Neurodegener. Dis.* 1, 292–304.

Vialatte, F.-B., Dauwels, J., Maurice, M., Musha, T., and Cichocki, A. (2011). Improving the specificity of EEG for diagnosing Alzheimer's disease. *Int. J. Alzheimers Dis.* 2011:259069. doi: 10.4061/2011/259069

Vialatte, F. B., Musha, T., and Cichocki, A. (2009). Sparse bump sonification: a new tool for multichannel EEG diagnosis of brain disorders. *Artif. Intell. Med.* 138–139.

Wang, H. (2013). Discriminant and adaptive extensions to local temporal common spatial patterns. *Pattern Recognit. Lett.* 34, 1125–1129. doi: 10.1016/j.patrec.2013.03.014

Wang, J., and Guo, P. (2011). "Epileptic electroencephalogram signal classification based on sparse representation," in *International Conference on Neural Computation Theory and Applications*, Seol 15–23.

Wang, J., Gao, X., and Guo, P. (2013). Feature extraction based on sparse representation with application to epileptic EEG classification. *Int. J. Imaging Syst. Technol.* 23, 104–113. doi: 10.1002/ima.22045

Wang, H., and Xu, D. (2012). Comprehensive common spatial patterns with temporal structure information of EEG data: minimizing nontask related EEG component. *IEEE Trans. Biomed. Eng.* 59, 2496–2505. doi: 10.1109/TBME.2012.2205383

Wang, J. J., Xue, F., and Li, H. (2015). Simultaneous channel and feature selection of fused EEG features based on sparse group lasso. *Biomed Res. Int.* 2015:703768. doi: 10.1155/2015/703768

Wu, W., Chen, Z., Gao, X., Li, Y., Brown, E. N., and Gao, S. (2015). Probabilistic common spatial patterns for multichannel EEG analysis. *IEEE Trans. Pattern Anal. Mach. Intell.* 37, 639–653. doi: 10.1109/TPAMI.2014.2330598

Xie, S., and Krishnan, S. (2013). Wavelet-based sparse functional linear model with applications to EEGs seizure detection and epilepsy diagnosis. *Med. Biol. Eng. Comput.* 51, 49–60. doi: 10.1007/s11517-012-0967-8

Xie, S., Krishnan, S., and Lawniczak, A. T. (2012). "Sparse principal component extraction and classification of long-term biomedical signals," in *25th International Symposium on Computer-Based Medical Systems*, Rome, 1–6.

Yong, X., Ward, R. K., and Birch, G. E. (2008). "Sparse spatial filter optimization for EEG channel reduction in brain-computer interface," in *IEEE International Conference on Acoustics, Speech and Signal Processing*, Las Vegas, NV, 417–420.

Yuan, Q., Zhou, W., Yuan, S., Li, X., Wang, J., and Jia, G. (2014). Epileptic EEG classification based on kernel sparse representation. *Int. J. Neural Syst.* 24:1450015. doi: 10.1142/S0129065714500154

Yuan, S., Zhou, W., Yuan, Q., Li, X., Wu, Q., Zhao, X., et al. (2015). Kernel collaborative representation-based automatic seizure detection in intracranial EEG. *Int. J. Neural Syst.* 25:1550003. doi: 10.1142/S0129065715500033

Zhang, Y., Zhou, G., Jin, J., Wang, X., and Cichocki, A. (2015). Optimizing spatial patterns with sparse filter bands for motor-imagery based brain-computer interface. *J. Neurosci. Methods* 255, 85–91. doi: 10.1016/j.jneumeth.2015.08.004

Zhou, Y., Tan, C., Wen, D., Sun, H., Han, W., and Xu, Y. (2016). The biomarkers for identifying preclinical Alzheimer's disease via structural and functional magnetic resonance imaging. *Front. Aging Neurosci.* 8:92. doi: 10.3389/fnagi.2016.00092

Zhou, W., Yang, Y., and Yu, Z. (2012). "Discriminative dictionary learning for EEG signal classification in Brain-computer interface", *12th International Conference on Control Automation Robotics and Vision*, Guangzhou, 1582–1585.

**Conflict of Interest Statement**: The authors declare that the research was conducted in the absence of any commercial or financial relationships that could be construed as a potential conflict of interest.

# Advantages of publishing in Frontiers

**OPEN ACCESS**
Articles are free to read, for greatest visibility

**COLLABORATIVE PEER-REVIEW**
Designed to be rigorous – yet also collaborative, fair and constructive

**FAST PUBLICATION**
Average 85 days from submission to publication (across all journals)

**COPYRIGHT TO AUTHORS**
No limit to article distribution and re-use

**TRANSPARENT**
Editors and reviewers acknowledged by name on published articles

**SUPPORT**
By our Swiss-based editorial team

**IMPACT METRICS**
Advanced metrics track your article's impact

**GLOBAL SPREAD**
5'100'000+ monthly article views and downloads

**LOOP RESEARCH NETWORK**
Our network increases readership for your article

**Frontiers**
EPFL Innovation Park, Building I • 1015 Lausanne • Switzerland
Tel +41 21 510 17 00 • Fax +41 21 510 17 01 • info@frontiersin.org
**www.frontiersin.org**

**Find us on**